



**UNIVERSIDADE FEDERAL DO PARÁ
CENTRO DE GEOCIÊNCIAS
PROGRAMA DE PÓS-GRADUAÇÃO EM GEOLOGIA E GEOQUÍMICA**

TESE DE DOUTORADO

**EVOLUÇÃO GEOLÓGICA DA PORÇÃO CENTRO-SUL DO ESCUDO DAS
GÜIANAS COM BASE NO ESTUDO GEOQUÍMICO, GEOCRONOLÓGICO
(EVAPORAÇÃO DE Pb E U-Pb ID-TIMS EM ZIRCÃO) E ISOTÓPICO (Nd-Pb)
DOS GRANITÓIDES PALEOPROTEROZOÍCOS DO SUDESTE DE
RORAIMA, BRASIL.**

Tese apresentada por:

MARCELO ESTEVES ALMEIDA

**BELÉM
2006**



Universidade Federal do Pará

Centro de Geociências

Programa de Pós-Graduação em Geologia e Geoquímica

**EVOLUÇÃO GEOLÓGICA DA PORÇÃO CENTRO-SUL DO ESCUDO DAS
GÜIANAS COM BASE NO ESTUDO GEOQUÍMICO, GEOCRONOLÓGICO
(EVAPORAÇÃO DE Pb E U-Pb ID-TMS EM ZIRCÃO) E ISOTÓPICO (Nd-Pb)
DOS GRANITÓIDES PALEOPROTEROZOÍCOS DO SUDESTE DE
RORAIMA, BRASIL.**

TESE APRESENTADA POR

MARCELO ESTEVES ALMEIDA

Como requisito parcial à obtenção do Grau de Doutor em Ciências
na Área de GEOQUÍMICA E PETROLOGIA.

Data de Aprovação: **17/11/2006**

Co-orientador: Franck Poitrasson (LMTGCNRS, TOULOUSE, FRANÇA)

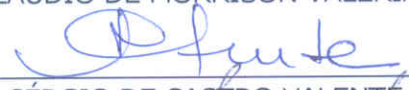
Comitê de Tese



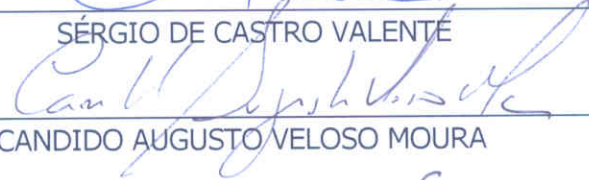
MOACIR JOSÉ BUENANO MACAMBIRA (Orientador)



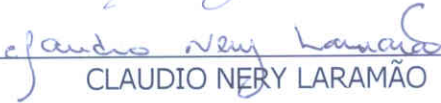
CLAUDIO DE MORRISON VALERIANO



SÉRGIO DE CASTRO VALENTE



CANDIDO AUGUSTO VELOSO MOURA



CLAUDIO NERY LARAMÃO

T ALMEIDA, Marcelo Esteves

≠ **Evolução geológica da porção centro-sul do Escudo das Guianas com base no estudo geoquímico, geocronológico (evaporação de Pb e U-Pb ID-TIMS em zircão) e isotópico (Nd-Pb) dos Granitóides Paleoproterozóicos do Sudeste de Roraima, Brasil.** / Marcelo Esteves Almeida; orientador, Moacir José Buenano Macambira. Belém: [s.n], 2006. 223f.; il.

Tese (Doutorado em Geoquímica e Petrologia) – Curso de Pós-Graduação em Geologia e Geoquímica, CG, UFPA, 2006.

1.GEOCRONOLOGIA 2. GEOQUÍMICA 3. ISÓTOPOS RADIOGÊNICOS 4. PETROLOGIA 5. EVOLUÇÃO CRUSTAL 6.ESCUDO DAS GUIANAS 7. PALEOPROTEROZÓICO 8. DOMÍNIO UATUMÃ-ANAUÁ 9. DOMÍNIO GUIANA CENTRAL 10. SUDESTE DE RORAIMA. I.MACAMBIRA, Moacir José Buenano, Orient. II. Título.

~~CDD:?~~

A meus pais,
À Adriana e à minha pequena Maria Júlia

AGRADECIMENTOS

Apesar da redação de uma tese de doutorado ser um produto de responsabilidade e “*stress*” de natureza individual, sem a o apoio contínuo e incondicional da família e a contribuição e a dedicação coletiva de várias colegas, certamente este trabalho não chegaria bom termo. A todos eles registro minha mais profunda gratidão.

Minha gratidão ao professor Dr. Moacir Macambira, meu orientador, que tive a oportunidade e a alegria de conhecer desde a minha primeira visita de trabalho ao Pará-Iso (há mais de 10 anos atrás). Desde essa época pude descobrir o grande profissional e a pessoa extremamente generosa que é, justificando a admiração de todos os seus colegas e alunos. Sua experiência de vida e profissional (muitas das vezes transmitidas on-line ou por e-mail!) foram determinantes ao longo da construção desta tese de doutorado. A sua disponibilidade irrestrita, sua forma crítica, inteligente e criativa de argüir as idéias apresentadas deram norte a este trabalho, facilitando o alcance de seus objetivos. Ao “Moa Mac Ambira”, e a seu clã (Cristina, Aline e Amanda), meus sinceros agradecimentos.

Aos professores Drs. Jean-Michel Lafon, Cândido Augusto Veloso Moura e Thomas Scheller, que com sua dedicação e paixão pela geologia isotópica conseguiram colocar a UFPA e o Pará-Iso num nível de reconhecida competência tanto no cenário nacional quanto internacional. O meu profundo agradecimento pelo aprendizado durante esse período de tese. Ao prof. Dr. Cândido Augusto Veloso Moura vale ainda o agradecimento pela gentileza de ter aceitado fazer parte da banca de tese.

Ao Professor Dr. e “comendador” Roberto Dall’Agnol, verdadeiro patrimônio da geologia brasileira e das geociências da UFPA, obrigado pelas suas reflexões sobre os granitóides do Escudo das Guianas e em especial aqueles do sudeste de Roraima, as quais muito nos ajudaram a compreendê-los e a realizar uma análise crítica sobre os mesmos. Nossos sinceros agradecimentos pela sua presença nesta banca de doutorado.

Ao Professor Dr. Sérgio de Castro Valente da Universidade Federal Rural do Rio de Janeiro, o mais talentoso professor e pesquisador que tive a oportunidade de conhecer durante minha vida acadêmica e figura humana das mais queridas, a minha profunda gratidão. O prof. Sérgio tem sido de uma disponibilidade irrestrita sempre que procurado para tratar de assuntos relacionados à petrologia e a geoquímica elementar e isotópica. Um mestre de verdade. Nossos

agradecimentos também pela sua participação nesta banca de doutorado, o que certamente enriquecerá nosso trabalho.

Ao Professor Dr. Cláudio de Morrison Valeriano da Universidade do Estado do Rio de Janeiro, geólogo de grande competência e paixão pelos estudos tectônicos, tem nos acompanhado desde os tempos de mestrado na UFRJ, onde pude constatar como suas sugestões e observações podem enriquecer uma tese. Manifesto aqui minha gratidão pelo aceite em compor novamente uma banca, agora neste novo desafio.

À secretaria do CPGG pelo apoio constante, aos colegas e estagiários bolsistas do Pará-Iso (Rose Brabo, Rosi Rocha, Elma, Roberta Florêncio, Roberta, Krymsky, Valter Avelar, Marco Antonio, Pablo Rolando, Pablo Monteiro, Keila, César) e a todos os colegas da turma de doutorado (Alex, Davis, Marivaldo) pelo ambiente amigável e fraterno durante o curso, amizades certamente que se perpetuarão.

Ao professor e jornalista Cláudio Pedro de Alcântara pela sua obstinação e paciência na árdua tarefa de ensinar a língua francesa a alunos com tanta dificuldade de aprendizagem (nos quais certamente eu me incluo).

A população dos municípios de Rorainópolis, São Luiz do Anauá, São João da Baliza, Caroebe, Caracaraí, incluindo todas as comunidades pertencentes aos assentamentos de terra do INCRA do SE de Roraima, o meu muito obrigado pela colaboração durante os trabalhos de campo.

Ao superintendente (Daniel Nava) e aos companheiros de trabalho da CPRM-Serviço Geológico do Brasil (Manaus) pelo incentivo, discussão dos dados e apoio constantes, incluindo a infra-estrutura de preparação de amostras (João Almeida e sua equipe), editoração e geoprocessamento (Amaro Luiz Ferreira e sua equipe) e laboratório petrográfico (René Luzardo). Agradeço ainda aos diretores passados (Luiz Augusto Bizzi) e presentes (Agamenon Dantas, Fernando Pereira de Carvalho e Manoel Barreto) que acreditaram e facilitaram, no que foi possível, a realização desta tese. A CPRM-Serviço Geológico do Brasil em conjunto com a UFPA (Pará-Iso), FINEP (Projeto CT Mineral 01/2001 "Geocronologia Aplicada ao modelamento metalogenético da Plataforma Amazônica"-2002-2004), Capes (Proc. BEX 1041/05-3), além do PRONEX/UFPA/CNPq/FADESP (662103/1998-0) e da Université Paul Sabatier e CNRS (LMTG), constituíram as fontes de financiamento desta pesquisa.

As mulheres da minha vida, Adriana e Maria Júlia (nascida durante a elaboração da tese), pelo amor, encorajamento e compreensão, que tanto me ajudaram nessa caminhada. Sem isso não teria forças para continuar. Só Deus sabe (e ele foi decisivo) o quanto foi difícil passar algumas temporadas longe de casa por conta dos trabalhos da tese. Aos meus doces pais João e Glória, ao meu querido irmão Sérgio, minha cunhada-irmã Selma, aos meus sobrinhos Pedro e João e aos meus maravilhosos sogros Adelino e Zilda, meus eternos agradecimentos. Vocês são simplesmente fundamentais na minha vida, responsáveis diretos pela minha saúde afetiva.

Aqueles não lembrados ou não citados me perdoem a injustiça do esquecimento.

CERTEZA

De tudo ficaram 3 coisas:

A certeza de que estamos sempre começando

A certeza de que precisamos continuar

A certeza de que seremos interrompidos antes de
terminar

Portanto devemos:

Fazer da interrupção um novo caminho

Da queda, um passo de dança

Do medo, uma escada

Do sonho, uma ponte

Da procura, um encontro

Fernando Pessoa

SUMÁRIO

| | |
|---|-----|
| DEDICATÓRIA | i |
| AGRADECIMENTOS | ii |
| EPÍGRAFE | v |
| RESUMO | 1 |
| ABSTRACT | 3 |
| 1 - INTRODUÇÃO | 5 |
| 2 - PROBLEMÁTICA GEOLÓGICA | 10 |
| 3 - MÉTODOS UTILIZADOS | 14 |
| 3.1 - LEVANTAMENTO E REVISÃO DO ACERVO GEOLÓGICO PRÉ-EXISTENTE | 14 |
| 3.2 - TRABALHOS DE CAMPO E CARTOGRAFIA GEOLÓGICA | 14 |
| 3.3 - TRABALHOS LABORATORIAIS | 15 |
| 3.3.1 - Análise Petrográfica e Geoquímica Multielementar | 15 |
| 3.3.2 - Análise Isotópica (Isótopos Radiogênicos) | 15 |
| 3.3.2.1 - Evaporação de Pb em monocristais de zircão | 15 |
| 3.3.2.2 - U-Pb em zircão por diluição isotópica (ID-TIMS ou Isotope Dilution–Thermal Ionization Mass Spectrometry) | 18 |
| 3.3.2.3 - Sm-Nd em Rocha Total | 18 |
| 3.3.2.4 - Pb-Pb em feldspato | 19 |
| 4 - ARTIGOS CIENTÍFICOS | 20 |
| 4.1 - NEW GEOLOGICAL AND SINGLE-ZIRCON PB-EVAPORATION DATA FROM THE CENTRAL GUYANA DOMAIN IN THE SOUTHEAST OF RORAIMA, BRAZIL: TECTONIC IMPLICATIONS FOR THE CENTRAL PORTION OF THE GUYANA SHIELD | 21 |
| 4.2 - GEOLOGY, PETROGRAPHY AND MINERALIZATIONS OF PALEOPROTEROZOIC GRANITOIDS FROM UATUMÃ-ANAUÁ DOMAIN (GUYANA SHIELD), SOUTHEAST OF RORAIMA, BRAZIL | 45 |
| 4.3 - GEOCHEMISTRY AND ZIRCON GEOCHRONOLOGY OF THE I-TYPE HIGH-K CALC-ALKALINE AND S-TYPE GRANITOIDS FROM SOUTHEAST OF RORAIMA STATE, BRAZIL: OROSIRIAN MAGMATISM EVIDENCE (1.97-1.96 Ga) IN CENTRAL PORTION OF GUYANA SHIELD | 79 |
| 4.4 - EVIDENCE OF THE WIDESPREAD 1.90-1.89 Ga I-TYPE, HIGH-K CALC-ALKALINE MAGMATISM IN SOUTHEAST OF RORAIMA, BRAZIL (CENTER-SOUTH REGION OF GUYANA SHIELD) BASED ON GEOCHEMISTRY AND ZIRCON GEOCHRONOLOGY | 122 |
| 4.5 - Nd-Pb ISOTOPIC CONSTRAINTS ON PALEOPROTEROZOIC GEODYNAMIC EVOLUTION OF THE CENTRAL PORTION OF GUYANA SHIELD, BRAZIL | 174 |
| 5 - CONCLUSÕES GERAIS | 211 |
| 5.1 - DOMÍNIO GUIANA CENTRAL | 211 |
| 5.2 - DOMÍNIO UATUMÃ-ANAUÁ | 212 |
| 5.2.1 - Setor Norte | 212 |
| 5.2.2 - Setor Sul | 214 |
| REFERÊNCIAS | 217 |
| Anexo 1 - Mapa de Estações Geológicas | |
| Anexo 2 - Mapa Geológico | |

RESUMO

Este estudo focaliza os granitóides da região centro-sul do Escudo das Guianas (sudeste de Roraima, Brasil), área caracterizada essencialmente por dois domínios tectono-estratigráficos denominados Guiana Central (DGC) e Uatumã-Anauá (DUA) e considerada limite entre províncias geocronológicas (Ventuari-Tapajós ou Tapajós-Parima, Amazônia Central e Maroni-Itacaiúnas ou Transamazônica). O objetivo principal deste trabalho é o estudo geoquímico, isotópico e geocronológico dos granitóides desta região, buscando ao mesmo tempo subsidiar a análise petrológica e lito-estratigráfica local e contribuir com as propostas e modelos evolutivos regionais.

O DGC é apenas localmente abordado na sua porção limítrofe com o DUA, tendo sido apresentados novos dados geológicos das rochas ortognáissicas e duas idades de zircão (evaporação de Pb) de biotita granodiorito milonítico (1,89 Ga) e de hastingsita-biotita granito foliado (1,72 Ga). Essas idades contrastam com as idades obtidas para os protólitos de outras áreas do DGC (1,96-1,93 Ga), sugerindo a existência de cenários litoestratigráficos distintos dentro do mesmo domínio.

Mapeamento geológico regional, petrografia, geoquímica, e geocronologia por evaporação de Pb e U-Pb ID-TIMS em zircão efetuadas nas rochas do DUA apontam para a existência de um amplo magmatismo granítico paleoproterozóico cálcio-alcálico. Estes granitóides estão distribuídos em diversas associações magmáticas com diferentes intervalos de idade – entre 1,97 e 1,89 Ga - estruturas e afinidades geoquímicas, individualizados em dois subdomínios no DUA, denominados de norte e sul.

No setor norte dominam granitos tipo-S (Serra Dourada) e tipo-I cálcio-alcálico com alto-K (Martins Pereira) mais antigos (1,97-1,96 Ga), ambos intrusivos em *inliers* do embasamento composto por associação do tipo TTG e seqüências meta-vulcanossedimentares de médio a alto grau (>2,03 Ga). No setor sul, xenólitos do Granito Martins Pereira e enclaves ricos em biotita são encontrados no Granito Igarapé Azul (1,89 Ga), que é caracterizado por seu quimismo cálcio-alcálico de alto-K, restrito a termos monzograníticos ricos em SiO₂. O Granito Caroebe (1,90-1,89 Ga) também apresenta quimismo cálcio-alcálico de alto-K, mas possui composição mais expandida e ocorre associado a rochas vulcânicas co-genéticas (1,89 Ga, vulcânicas Jatapu) e a charnoquitóides (1,89 Ga, p.ex. Enderbito Santa Maria). As características petrográficas similares, aliada à idade obtida em amostra do Granito Água Branca em sua área-tipo (1,90 Ga)

permite incluí-los numa mesma suíte (Suíte Água Branca). O setor sul é caracterizado apenas por discretas e localizadas zonas de cisalhamento dúctil-rúptil dextrais com direção NE-SW.

Duas gerações de granitos tipo-A (Moderna, 1,81 Ga; Mapuera, 1,87 Ga) cortam o DUA, embora sejam mais freqüentes no setor sul. Além disso, foram identificados três tipos diferentes de metalotectos nesta região: a) mineralização de ouro hospedada em granitóides Martins Pereira-Serra Dourada (setor norte), b) columbita-tantalita aluvionar assentada em região dominada por granitóides Igarapé Azul (setor sul), e c) ametista associada a pegmatitos hospedados em granitos do tipo Moderna.

Os dados isotópicos dos sistemas do Nd (rocha total) e do Pb (feldspato) sugerem que todos os granitóides do DUA analisados são produtos de fontes crustais mais antigas, sejam elas de natureza mais siálica (de idade sideriana-arqueana) e/ou juvenil (de idade transamazônica), afastando a possibilidade de participação de magmas mantélicos na sua geração. Embora o mecanismo de subducção tenha sido dominante no estágio inicial da evolução do setor norte do DUA, o magmatismo pós-colisional do setor sul teve significativa participação na adição de material crustal. É possível que após o fechamento do oceano do sistema de arco Anauá (2,03 Ga) e após a orogenia colisional (1,97-1,94 Ga?), líquidos basálticos tenham sido aprisionados na base da crosta (mecanismo de *underplating*). Estes líquidos basálticos puderam então interagir com a crosta inferior, fundi-la e gerar, subsequente em ambiente pós-colisional, imenso volume de granitos e vulcânicas observados entre 1,90 e 1,87 Ga.

Quadro similar é identificado no domínio Tapajós (DT), sugerindo que ambos domínios (DUA e DT) fazem parte de uma mesma província (Ventuari-Tapajós ou Tapajós-Parima). Apesar dessas semelhanças, o estágio colisional parece não ter sido tão efetivo no DT, como atestam os escassos indícios de granitos tipo-S e de rochas de alto grau metamórfico.

ABSTRACT

This study focuses the granitoids of center-southern portion of Guyana Shield, southeastern Roraima, Brazil. The region is characterized by two tectono-stratigraphic domains, named as Central Guyana (GCD) and Uatumã-Anauá (UAD) and located probably in the limits of geochronological provinces (e.g. Ventuari-Tapajós or Tapajós-Parima, Central Amazonian and Maroni-Itacaiúnas or Transamazon). The aim this doctoral thesis is to provide new petrological and lithostratigraphical constraints on the granitoids and contribute to a better understanding of the origin and geodynamic evolution of Guyana Shield.

The GCD is only locally studied near to the UAD boundary, and new geological data and two single zircon Pb-evaporation ages in mylonitic biotite granodiorite (1.89 Ga) and foliated hastingsite-biotite granite (1.72 Ga) are presented. These ages of the protholiths contrast with the lithostratigraphic picture in the other areas of CGD (1.96-1.93 Ga).

Regional mapping, petrography, geochemistry and zircon geochronology carried out in the UAD have showed widespread paleoproterozoic calc-alkaline granitic magmatism. These granitoids are distributed into several magmatic associations with different paleoproterozoic (1.97-1.89 Ga) ages, structural and geochemical affinities. Detailed mapping, petrographic and geochronological studies have distinguished two main subdomains in UAD. In the northern UAD, the high-K calc-alkaline Martins Pereira (1.97 Ga) and Serra Dourada S-type granites (1.96 Ga) are affected by NE-SW and E-W ductile dextral shear-zones, showing coexistence of magmatic and deformational fabrics related to heterogeneous deformation. Inliers of basement (2.03 Ga) crop out to northeastern part of this area, and are formed by metavolcano-sedimentary sequence (Cauarane Group) and TTG-like calc-alkaline association (Anauá Complex). Xenoliths of meta-diorites (Anauá Complex) and paragneisses (Cauarane Group) reinforce the intrusive character of Martins Pereira Granite. On the other hand, xenoliths of Martins Pereira and biotite-bearing enclaves are founded in the younger, undeformed, and SiO₂-rich Igarapé Azul Granite (1.89 Ga). This last and the high-K calc-alkaline Caroebe Granite (1.90-1.89 Ga, Água Branca Suite), including coeval volcanic rocks (1.89 Ga, Jatapu volcanics) and charnockitoids (1.89 Ga, e.g. Santa Maria Enderbite), crop out in the southern UAD. This subdomain is characterized only by local and slight NE-SW ductile-brittle dextral shear zones. A-type granites such as Moderna (ca. 1.81 Ga) and Mapuera (ca. 1.87 Ga) granites, cross cut both areas of UAD. Furthermore, the geological mapping also identified three main types of metalotects in this region. Gold

mineralization is observed in Martins Pereira-Serra Dourada granitoids (northern UAD), alluvial columbite-tantalite is related to Igarapé Azul granitoids (southern UAD), and amethyst is associated to pegmatites from Moderna A-type granites.

The Nd-Pb isotope data suggest that all granitoids of UAD are generated by reworking of older and pre-existence crustal sources (sialic Rhyacian-Archean and/or juvenile Transamazonian origin) and mantle input is not probably a viable model. Although the dominant process may be ~~one~~ subduction in the early stage of NUAD evolution, post-collisional magmatism may be a significant process in the production of new continental crust in the southern UAD. It is possible that, following oceanic closure in the Anauá arc system (2.03 Ga) and subsequent collisional orogeny (1.97-1.94 Ga?), underplated mantle melts (basalt liquids) were trapped below pre-existing lower crustal rocks of various compositions (e.g. granulites, metatonalites, amphibolites). The basalt liquids and subsequently melted lower crust could produced the immense volumes of granite (and volcanics) observed at 1.90-1.87 Ga. This geological picture is similar to the Tapajós Domain (TD) in the southern Amazonian Craton and suggest that both belongs to the same province (Ventuari-Tapajós or Tapajós-Parima). Nevertheless, the scarcity of S-type granites and high-grade metamorphic rocks show that the collisional stage is not so evident in TD.

1 - INTRODUÇÃO

A região sudeste do Estado de Roraima constitui o foco desta pesquisa, cuja área selecionada perfaz um total de aproximadamente 3500 km² (Fig. 01). Embora esteja delimitada por coordenadas fixas, a área selecionada foi algumas vezes ao longo do estudo reduzida ou ampliada em função do objeto geológico a ser analisado. Esta área está localizada na porção centro-sul do Escudo das Guianas (Fig. 01, Gibbs & Barron, 1993) e abriga uma extensa floresta tropical. Parte dela possui um acesso relativamente fácil para os padrões amazônicos, sendo comuns as estradas não pavimentadas, que servem de ligação entre os diversos assentamentos rurais patrocinados pelo INCRA. Partindo-se da cidade de Manaus (AM) pode-se acessá-la através da rodovia federal (Manaus-Boa Vista: BR-174), que corta a área investigada na direção aproximada N-S. Os principais povoados da região são a Vila Nova Colina, Rorainópolis, Martins Pereira, Vila Novo Paraíso, Vila Moderna, São Luis do Anauá, Serra Dourada, São João da Baliza, Caroebe e Entre Rios e constituíram importante suporte de apoio logístico.

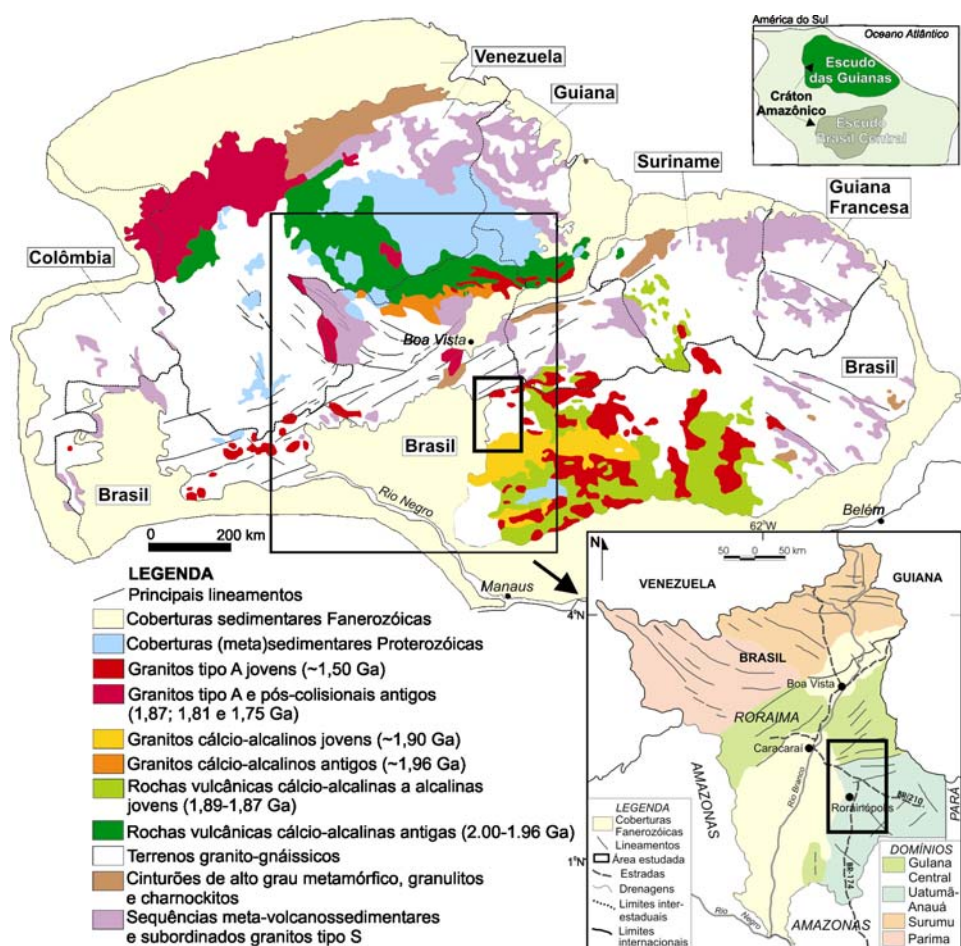


Figura 01. Mapa de localização da área estudada dentro do contexto do Escudo das Guianas (mod. Gibbs & Barron, 1993) e dos domínios tectono-estratigráficos (mod. CPRM, 2006).

O foco principal deste trabalho é o estudo geoquímico, isotópico e geocronológico dos granitóides do sudeste de Roraima, e tem como objetivo subsidiar a análise petrológica e litoestratigráfica, buscando contribuir assim com as propostas e modelos evolutivos regionais. Entretanto, apesar de ter obtido localmente nível de detalhamento (1:50.000), em geral difícil de ser alcançado em estudos amazônicos em função da acessibilidade, do elevado grau de intemperismo e da escassez de afloramentos, o mapa geológico resultante engloba informações na escala 1:250.000. Ou seja, longe de querer ter a pretensão de ser um trabalho de detalhe, a síntese apresentada aqui tem conotação essencialmente regional. Regiões montanhosas (região noroeste, divisa com a Guiana), sem acessibilidade por estradas ou legalmente demarcadas, como áreas indígenas ou de proteção ambiental (região leste e sudeste, divisa com o Pará), tiveram sua investigação restringida aos sensores remotos (imagem de radar JERS, Geocover, SRTM, Landsat 7, Modelo de Elevação de Terreno, e aerogeofísica).

Esta tese de doutorado é composta cinco artigos submetidos (ou em vias de submissão) a revistas com corpo editorial, além desta parte introdutória, e dos capítulos referentes ao ferramental metodológico e as conclusões gerais. Uma listagem das referências bibliográficas utilizadas nestes capítulos é disponibilizada no final do volume, enquanto as referências bibliográficas relativas aos artigos acompanham os mesmos.

Do ponto de vista geológico, alguns trabalhos pioneiros levados a cabo em Roraima (p.ex. Paiva 1929) foram decisivos para delinear os primeiros traços da geologia da região. Outros estudos pontuais retomados, sobretudo na primeira metade da década de 70, também constituem importantes fontes de consulta históricas (Arantes & Mandeta, 1970; Ramgrab & Damião, 1970, Ramgrab *et al.*, 1972; Braun, 1973; Bomfim *et al.*, 1974; Muniz & Dall'Agnol, 1974). Mas, somente a partir da década de 70, é que os levantamentos geológicos sistemáticos, baseados numa cartografia de natureza regional, foram iniciados no Estado de Roraima e também na porção nordeste do Estado do Amazonas. Estes foram conduzidos principalmente pelo convênio DNPM/CPRM (Santos *et al.*, 1974) e pelo projeto RADAMBRASIL (Montalvão *et al.*, 1975), culminando assim com o estabelecimento das primeiras grandes unidades geológicas.

Além dos trabalhos citados, diversos outros foram executados entre as décadas de 70 e 90 (Melo *et al.*, 1978; Araújo Neto & Moreira, 1976, Veiga Jr. *et al.*, 1979; Pinheiro *et al.*, 1981, Costi *et al.*, 1984). Mais recentemente grandes avanços no conhecimento geológico puderam ser sentidos através dos resultados dos projetos de mapeamento geológico executados pela CPRM-

SGB na escala 1:500.000 (CPRM, 1999, 2000) e alguns trabalhos de síntese e organização de dados nas escalas 1:2.500.000 e 1:1.000.000 (CPRM, 2003, 2004). Entretanto, em todo este conjunto bibliográfico nota-se uma grande carência (até mesmo ausência) de dados laboratoriais, principalmente aqueles de natureza geocronológica e isotópica. A maior parte deste escasso acervo de dados, relacionada especificamente ao sudeste de Roraima e nordeste do Amazonas, foi produzida e publicada apenas nos últimos dez anos (Sato & Tassinari, 1997, Almeida *et al.*, 1997, Santos *et al.*, 1997, Costi *et al.*, 2000, Macambira *et al.*, 2002, CPRM 2003, Valério, 2006), constituindo ainda um conjunto de informações limitado e de caráter pontual.

Estes trabalhos, sem exceção, sempre identificaram nesta porção do Escudo das Guianas grandes áreas de exposição granítica, sejam elas preservadas ou não por evento(s) deformacionais. A individualização dessas grandes massas continentais graníticas *sensu lato* e o avanço do conhecimento cartográfico e geológico dos últimos anos, tornou possível também a sua separação em grandes domínios (Reis *et al.*, 2003) tectono-estratigráficos e localmente sua subdivisão em “subdomínios” (Almeida *et al.*, 2002). Dois destes domínios ocorrem no sudeste de Roraima, sendo denominados de Guiana Central e Uatumã-Anauá.

O Domínio Guiana Central abrange apenas uma pequena parte da área estudada (porção nor-noroeste). O primeiro artigo aborda exatamente os litótipos graníticos e gnáissicos ortoderivados do Domínio Guiana Central junto ao limite com o Domínio Uatumã-Anauá. Além do contexto geológico local, são apresentadas duas idades pelo método Pb-Pb de evaporação de zircão em biotita granodiorito milonítico (1,89 Ga) e em hastingsita-biotita sienogranito com fluxo magmático (1,72 Ga), as quais contrastam com aquelas encontradas por outros autores no restante do domínio (1,96-1,93 Ga, Gaudette *et al.* 1996, Fraga, 2002, CPRM, 2003). Foliação NE-SW e mergulho subvertical associada a zonas de cisalhamento dúctil são as feições estruturais dominantes neste setor.

O restante do escopo da tese privilegia os granitóides do Domínio Uatumã-Anauá, ao quais tem suas características de campo e petrográficas descritas num segundo artigo. Além do mapeamento faciológico dos corpos graníticos, neste artigo foi abordada também a relação entre a granitogênese e as principais ocorrências minerais catalogadas na região. Este artigo reforça ainda a separação do Domínio Uatumã-Anauá em dois subdomínios distintos (norte e sul), ambos marcados por magmatismos com evolução petrológica e história tectono-estrutural distintas.

Estas diferenças foram reforçadas posteriormente pelo conjunto de dados geoquímico e geocronológico, este último utilizando-se os métodos Pb-Pb evaporação de zircão e U-Pb ID-TIMS. O terceiro artigo aborda exclusivamente o setor (ou subdomínio) norte do Domínio Uatumã-Anauá, onde dominam granitóides do tipo-S (Serra Dourada) e do tipo-I cálcio-alcálico com alto-K (Martins Pereira) mais antigos (1,97-1,96 Ga), ambos intrusivos em *inliers* do embasamento composto por associação do tipo TTG e seqüências meta-vulcanossedimentares de médio a alto grau (>2,03 Ga).

No quarto artigo, o mesmo procedimento foi adotado para tratar os granitóides do setor (ou subdomínio) sul. O panorama apresentado pelos dados geoquímicos e geocronológicos demonstrou amplo predomínio de uma granitogênese tipo-I cálcio-alcálica de alto-K mais jovem (1,90-1,89 Ga), representando pelos granitos Igarapé Azul e Caroebe, que, ao contrário do observado no setor norte, apresenta vulcanismo co-genético associado (1,89 Ga, vulcânica Jatapu). Charnoquito (1,89 Ga) e granitos tipo A (1,87 Ga) também têm seus resultados geocronológicos em zircão discutidos.

O quinto e último artigo apresenta um estudo isotópico baseado nos sistemas do Nd (rocha total) e do Pb (em feldspatos) que abrange os granitóides dos dois subdomínios. Os resultados reforçam uma origem eminentemente crustal, cujas fontes devem ser siálicas (de idade Sideriana-Arqueana) e/ou juvenis (de idade Rhiaciana-Transamazônica), com pouca ou nenhuma contribuição direta de magmas mantélicos. Estes dados isotópicos, associados às características de campo, petrográficas, geoquímicas e geocronológicas, permitem sugerir um modelo evolutivo baseado em 3 estágios distintos.

O primeiro estágio diz respeito à formação de um orógeno acrescionário relacionado ao sistema de arco Anauá (2,03 Ga), os quais devem estar associados a bacias do tipo retro-arco (?). Num segundo e subseqüente estágio, a fase acrescionária dá lugar a um orógeno colisional, causando espessamento crustal, aumento da temperatura e geração por fusão parcial dos granitóides Martins Pereira e Serra Dourada (1,97-1,96 Ga). Este estágio colisional pode ter evoluído ao longo do tempo, tendo sido responsável por alçar tectonicamente as rochas granulíticas a níveis crustais mais rasos e pela geração do Domínio Guiana Central (1,94-1,93 Ga?). O último estágio diz respeito aos granitóides do setor sul do DUA. A ausência de eventos tectono-deformacionais, de remanescentes de crosta oceânica ou de coberturas meta-vulcanossedimentares relacionadas a ambiente de arco, sugere que o setor sul não deve ter

evoluído a partir de um sistema acrescionário via subducção tipo-B. É possível que após o fechamento do oceano do sistema de arco Anauá (2,03 Ga) e após a orogenia colisional (1,97-1,94 Ga?), líquidos basálticos através do mecanismo de *underplating* tenham sido trapeados na base da crosta, fundindo esta última e gerando em seguida um grande volume magmas graníticos pós-colisionais do tipo I e do tipo A entre 1,90 e 1,87 Ga.

Ao final deste volume, em anexo, pode ser consultado o mapa geológico e de estações geológicas na escala 1:250.000, contendo ainda perfis esquemáticos que buscam traduzir o arranjo estrutural e a inter-relação entre as grandes unidades litoestratigráficas paleoproterozóicas.

2 - PROBLEMÁTICA GEOLÓGICA

Alguns aspectos da problemática geológica regional do ponto de vista litoestratigráfico, estrutural, petrológico e evolutivo serão listados abaixo, tendo como foco os domínios tectono-estratigráficos (Güiana Central e Uatumã-Anauá) estudados e suas respectivas associações graníticas e gnáissicas.

2.1 - DOMÍNIO GÜIANA CENTRAL (DGC)

- O DGC é composto por um terreno essencialmente granito-gnáissico afetado por ampla deformação regional, caracterizada por extensos lineamentos e uma ampla variação de protólitos, estilos de deformação e graus metamórficos. Esta variação, associada a escassez de dados, confere ao DGC um elevado grau de complexidade geológica.
- As rochas ortoderivadas, na sua maioria agrupadas na Suíte Metamórfica Rio Urubu (atual Complexo), atestam a existência de litótipos com significativa variedade textural (metagranitóides, milonitos e gnaisses) e importantes particularidades composicionais. Dados geoquímicos apontam protólitos com assinaturas distintas (p.ex. tipo A e tipo I) e com idades de cristalização variada (1,96 a 1,92 Ga; Gaudette *et al.*, 1996; Fraga, 2002; CPRM, 2003), tornando necessária uma investigação mais aprofundada na tentativa de identificar áreas ou domínios onde há predomínio espacial de cada tipo particular.
- Dentro deste intervalo de idade são descritas rochas charnoquíticas sin-cinemáticas (Suíte Serra da Prata) e granulíticas (Granulito Brauana). Ambas apresentam idades similares, apesar da escassez de dados não garantir uma perfeita correlação. No caso do Granulito Brauana (1,94 Ga), além do resultado geocronológico ser determinado a partir de zircões ígneos (idade do evento anatético?), o intrincado padrão estrutural indica deformação polifásica e a migmatização associada contrasta com o quadro apresentado pelos charnoquitos da Suíte Serra Prata (1,94-1,93 Ga; Fraga, 2002). A dificuldade de identificação deste evento metamórfico granulítico no tempo e o desconhecimento da sua evolução P-T-t trazem sérios prejuízos para entendimento da litoestratigrafia regional e dificulta a elaboração de um modelo evolutivo mais adequado para o DGC.
- Os termos paraderivados encontra-se agrupados no Grupo Cauarane e na Suíte Metamórfica Murupu, localmente contendo tipos migmatíticos gerando localmente bolsões leucograníticos (p.ex. região do Taiano) e granitos tipo S associados (p.ex.

Granito Curuxuim). Apenas uma idade de cristalização para esse magmatismo foi obtida (1,97 Ga, CPRM, 2003), sendo insuficiente para caracterizar um evento granítico tipo S em escala regional.

- A existência de granulitos e rochas paraderivadas de alto grau associadas com granitogênese tipo S, corroboram um modelo evolutivo colisional para o DGC (p.ex. Cordani & Brito Neves, 1982; Hasui *et al.*, 1984; Gibbs & Barron, 1993; Fraga & Reis, 1996; Sena Costa & Hasui; 1997, CPRM, 1999; Santos *et al.*, 2000, 2006a,b) Esse orógeno colisional seria resultado de sucessivos eventos deformacionais que contribuiriam para o espessamento crustal, caso a evolução PT obedeça um sentido anti-horário (p.ex. Ellis, 1987; Brown & Dallmeyer, 1996; Brown, 2001). Entretanto, se desconhece quais massas continentais teriam colidido e em qual contexto geodinâmico.
- A complexidade geológico-estrutural do DGC demanda uma análise na sua proximidade com o DUA, delimitada pelo sistema de falhas do Ita. Seria este limite apenas um limite estrutural ou este limite separa realmente associações petrotectônicas distintas? Em termos composicionais e geocronológicos estes domínios poderiam ser correlacionados?

2.2 - DOMÍNIO UATUMÃ-ANAUÁ (DUA)

- O DUA é caracterizado por um amplo predomínio de granitóides em geral pouco deformados, variando de tipos foliados a norte até tipos isótipos a sul, entretanto seu quadro litoestratigráfico está reduzido a um conjunto muito limitado de suítes graníticas (Suítes Igarapé Azul e Água Branca), cujas idades e petrogênese apresentam-se pouco esclarecidas.
- Apenas o setor norte é provido de algum resultado geocronológico, tendo apontado intervalo de idade entre 1,97 e 1,96 Ga para os granitóides (p.ex. Almeida *et al.*, 1997; CPRM, 2003), considerado equivocadamente como pertencente às suítes Igarapé Azul e Água Branca, respectivamente. Posteriormente, este conjunto de granitóides passou a ser agrupado no Granito Martins Pereira (Almeida *et al.*, 2002) e a continuidade dos estudos geocronológicos apontou idades de cristalização menores (1,90-1,89 Ga) para granitos relacionados ao magmatismo Igarapé Azul e Água Branca no setor sul do DUA.
- Entretanto, a gênese destes granitóides permanece em discussão. De acordo com alguns autores (Oliveira *et al.* 1996), a suíte Água Branca no DUA foi caracterizada como cálcio-

alcalina e tem como processo petrogenético dominante a cristalização fracionada (p.ex. plagioclásio e hornblenda). Processos alternativos como *magma mixing* e fusão parcial também foram recentemente postulados (Almeida & Macambira, 2003). Portanto, algumas questões permanecem: a) Qual seria o processo petrogenético (ou seria mais de um?) dominante na formação dos granitóides interpretados como Água Branca? b) Sua origem e fonte(s) seriam semelhantes aos dos demais granitóides gerados no mesmo intervalo de tempo?

- Parte da suíte Água Branca definida por Oliveira *et al.* (1996) com características químicas peraluminosas foi desmembrada dando origem a Suíte Igarapé Azul (Faria *et al.*, 1999). Além desses tipos peraluminosos à biotita, granitóides à muscovita, cordierita e silimanita aflorantes no setor norte do DUA foram adicionados a esta suíte. Entretanto, Sardinha (1999) através de análise petrográfica e de susceptibilidade magnética nos tipos peraluminosos da Suíte Igarapé Azul, não identificaram características compatíveis com granitos tipo S, sugerindo uma possível origem híbrida (fontes sedimentares e ígneas) para explicar sua geração. Posteriormente, Almeida *et al.* (2002) incluem os granitos tipo S *sensu stricto* (à cordierita) sob a denominação Granito Serra Dourada, retirando-os da suíte Igarapé Azul. Estes granitos estão localizados na parte norte do DUA em associação com seqüências meta-volcanosedimentares do Grupo Cauarane, distantes cerca de 80 km da área-tipo dos granitóides Igarapé Azul. Mesmo tendo sido desmembrado por apresentar localização e feições de campo e petrográficas distintas, teria o Granito Igarapé Azul gênese independente ou seria esta compatível aos dos demais granitóides Água Branca?
- Além dos granitos de natureza cálcio-alcalina, o DUA (em especial o setor sul) apresenta abundantes intrusões de granitóides tipo A correlacionados ao magmatismo Madeira-Água Boa (~1,81 Ga) e Abonari-Mapuera (~1,87 Ga) (CPRM, 2003). Entretanto estas correlações são definidas na maioria das vezes apenas por critérios petrográficos (p.ex. presença ou não de hastingsita), carecendo maciçamente de dados geoquímicos e geocronológicos, devendo esta correlação regional (embora possível) ser avaliada com cautela;
- Além disso, o vulcanismo da região do rio Jatapu (andesitos e dacitos dominantes e quimismo cálcio-alcalino) está espacial (CPRM, 2000a) e temporalmente (Macambira *et*

al., 2003) associado a granitogênese do setor sul do DUA. Estas vulcânicas são tradicionalmente vinculadas ao magmatismo Mapuera nessa região e, portanto, foram englobadas no Grupo Iricoumé numa tentativa de correlação com o vulcanismo Iricoumé (CPRM, 2000a), aflorante no nordeste do Amazonas e distante cerca de 150 km. Entretanto, os dados preliminares existentes apontam uma maior possibilidade de vinculação do vulcanismo Jatapu com os granitóides Água Branca, abrindo espaço para o questionamento a respeito da existência de diferentes tipos vulcânicos, penecontemporâneos, vinculados a magmatismos distintos (“aluminoso ou alcalino tipo A” e “cálcio-alcalino tipo I”). Situação semelhante é descrita também no Grupo Iriri na região do Tapajós (p.ex. CPRM, 2000b).

- A carência de dados que auxiliem no entendimento da cronologia dos eventos graníticos, além da sua petrogênese, têm complicado bastante a elaboração de modelos evolutivos para o DUA, gerando quase sempre controvérsia e debates acerca do tema. Um modelo evolutivo acrescionário baseado na existência de arcos magmáticos amalgamados sucessivamente a um núcleo estável arqueano tem sido o preferido da maioria dos autores (p.ex. Tassinari & Macambira, 1999, 2004; Santos *et al.*, 2006a,b). Proposta alternativa (underplating) é utilizada na região do Tapajós para explicar a geração dos granitóides mais jovens, considerados pós-colisionais (1,90-1,87 Ga; Lamarão *et al.*, 2001; Vasquez *et al.*, 2002).
- Tais dificuldades repercutem também fortemente na definição das rochas hospedeiras e metalotectos das mineralizações descritas na região, como por exemplo, as de ouro (garimpo Anauá) e ametista (Vila Moderna) primários e as de columbita-tantalita (bacia do Igarapé Azul) aluvionar (CPRM, 2000a).

Na visão dos modelos existentes, e de acordo com os diferentes limites entre Províncias propostos, a área em questão (DGC e DUA) pode estar englobada por duas (K´Mudku Shear Belt e Tapajós-Parima) ou três (Maroni-Itacaiúnas, Ventuari-Tapajós e Amazônia Central) províncias geocronológicas, demonstrando a sua real importância no contexto dos modelos evolutivos vigentes neste segmento do Escudo das Guianas. Apesar da inegável necessidade e aplicabilidade destes modelos, os mesmos têm como base um limitado acervo de dados geocronológicos e isotópicos (em que pesem o aporte recente de dados), devendo ser analisados, sobretudo do ponto de vista local, com prudência.

3 - MÉTODOS UTILIZADOS

A obtenção de dados desta pesquisa foi dividida basicamente em três fases principais: a) levantamento e revisão do acervo geológico existente, b) trabalhos de campo e c) laboratoriais. Estas fases, além dos recursos metodológicos empregados, são descritas a seguir.

3.1 - LEVANTAMENTO E REVISÃO DO ACERVO GEOLÓGICO PRÉ-EXISTENTE

Um conjunto significativo de dados e informações pré-existentes foi levantado e objeto de análise, a maioria deles provenientes de instituições como o Serviço Geológico do Brasil e de algumas universidades que atuam na região. Entre estes dados destacam-se:

- a) Análise e atualização de bancos de dados de afloramento, petrografia, geoquímica e geocronologia existentes e sua comparação com os dados gerados nesta pesquisa;
- b) Consulta e compilação de mapas geológicos pré-existentes, auxiliando na confecção do mapa geológico da área em questão;
- c) Consulta a banco de amostras de rochas e de lâminas petrográficas, implicando na reanálise e reavaliação das unidades litoestratigráficas pré-estabelecidas;
- d) Revisão da literatura geológica do tema específico (petrologia, geoquímica, geocronologia e evolução crustal) e da geologia regional, continuamente atualizada ao longo do período de execução da pesquisa.

3.2 - TRABALHOS DE CAMPO E CARTOGRAFIA GEOLÓGICA

Foram realizados mais de 2000 km de caminhamentos geológicos, sendo 180 km deles em vias fluviais, culminando com a análise e descrição de **352** afloramentos. Estes perfis geológicos permitiram, ao mesmo tempo, a individualização das grandes unidades litoestratigráficas (informações na escala 1:250.000) e o mapeamento faciológico dos granitóides Igarapé Azul, Caroebe e Martins Pereira (informações na escala 1:100.000), além da coleta sistemática de amostras de rocha (**447** amostras no total) e seleção posterior para estudos laboratoriais subseqüentes.

Este mapeamento geológico regional integrado teve o apoio cartográfico de sensores remotos como imagens (fundidas ou não) de radar (SRTM - Shuttle Radar Topography Mission; JERS - Japanese Earth Resources Satellite), de satélite (landsat TM7 - Thematic Mapper; Geocover) e aerogeofísicas (derivada 1^a., sinal analítico, contagem total e ternário U-Th-K). O

resultado final deste trabalho pode ser consultado nos anexos 1 (mapa geológico) e 2 (mapa de amostragem).

O acervo de dados materializados pelos mapas matriciais e vetoriais, assim como todo o conjunto de afloramentos e amostras de rocha coletadas encontram-se georrefrenciados e armazenados em plataforma SIG (ArcView 3.2a).

3.3 - TRABALHOS LABORATORIAIS

3.3.1 - Análise Petrográfica e Geoquímica Multielementar

A análise petrográfica detalhada de **234** seções delgadas (p.ex. classificação textural e composicional, descrição mineralógica, ordem aproximada de cristalização, caracterização de paragêneses minerais), integrada com as informações de campo, constituindo subsídio básico para a seleção de elenco de rochas representativo visando obtenção de análises químicas e geocronológicas.

Após avaliação petrográfica, os litótipos selecionados (**28** amostras) foram submetidos a análise química multielementar (rocha total) envolvendo método de espectrometria por ICP (*induced Coupled Plasma*) para determinação de elementos maiores, perda ao fogo, e mais 42 elementos traços, incluindo elementos terras raras (ACMELAB, Vancouver, Canadá).

A preparação das amostras individuais seguiu o procedimento inicial de fragmentação *in situ* (no campo). No laboratório de preparação de amostras da CPRM (Manaus) estes fragmentos foram britados (britador de mandíbula) e pulverizados (moinho de porcelana) visando a obtenção de uma granulometria da ordem de 200 mesh.

3.3.2 - Análise Isotópica (Isótopos Radiogênicos)

As análises geocronológicas e isotópicas foram realizadas no laboratório da UFPA (Pará-Iso), utilizando-se dois espectrômetros (Finnigan MAT262 e VG Isomass 54). A preparação química das amostras também foi efetuada nas dependências do Pará-Iso, assim como parte da preparação dos minerais a serem analisados (CPRM e UFPA). A seguir serão listados os métodos empregados durante a fase analítica.

3.3.2.1 - Evaporação de Pb em monocristais de zircão

O método de evaporação Pb em monocristais de zircão em rotina no Pará-Iso (UFPA) segue o mesmo princípio do método desenvolvido por Kober (1986; 1987), utilizando-se um

espectrômetro de massa de ionização termal (Finningan MAT262). Segundo esses autores, admite-se que a estrutura cristalina do zircão resista o suficiente para preservar as informações isotópicas da época de sua cristalização até o presente.

Os concentrados contendo os cristais de zircão para análise foram obtidos após processo prévio de britagem, moagem e pulverização das amostras de rocha, e subsequente peneiramento nas frações de 60, 80 mesh (rochas plutônicas) e 100 (rochas vulcânicas) mesh. Na fase final de preparação os minerais passam por uma separação magnética (ímã de mão e separador magnético Frantz) e por densidade (líquidos densos). Após o processo de preparação, procedeu-se a triagem manual através do uso de lupa binocular dos cristais de zircão. Os cristais selecionados têm ainda sua imagem capturada mediante equipamento fotográfico acoplado a microscópio petrográfico, visando assim uma melhor avaliação das condições físicas dos grãos. No total foram analisadas **16** amostras de rochas por este método.

O método de evaporação Pb utiliza um duplo filamento de rênio, sendo um deles utilizado para o processo de evaporação, e o outro para a ionização. Os cristais escolhidos são depositados individualmente nos filamentos de evaporação, introduzidos no espectrômetro de massa e, então, gradativamente aquecidos em diferentes etapas de evaporação. Com o aumento da temperatura o Pb presente no retículo cristalino do mineral é liberado (ou evaporado), ficando retido no filamento de ionização (desligado durante a etapa de evaporação). As temperaturas de evaporação utilizadas são normalmente de 1450°C, 1500°C e 1550°C (ou mais, como por exemplo, 1600°C), mas pode ser flexível e variável de acordo com as características dos zircões analisados, podendo ser efetuada ~~que~~ até que se esgote todo o Pb do cristal.

Numa etapa seguinte, desliga-se o filamento de evaporação e inicia-se o aquecimento do filamento de ionização, em geral a temperaturas entre 950°C e 1150°C, dependendo do comportamento de cada amostra. Em seguida, as intensidades dos diferentes isótopos são medidas com um contador de íons na seqüência de massa 206, 207, 208, 206, 207 e 204, gerando um bloco com 8 razões $^{207}\text{Pb}/^{206}\text{Pb}$ em cinco varreduras, em um máximo de cinco blocos por etapa de evaporação. Para cada etapa de evaporação é obtida uma idade a partir da média das razões $^{207}\text{Pb}/^{206}\text{Pb}$. A idade de uma amostra é então calculada a partir da média das razões $^{207}\text{Pb}/^{206}\text{Pb}$ obtidas, em geral, nas etapas de maior temperatura de evaporação de cada grão analisado. Nesse cálculo, são utilizadas apenas idades similares, sendo descartados as etapas ou

grãos com idades inferiores (p.ex. perda de Pb após a cristalização, Vanderhaeghe *et al.*, 1998) ou superiores (p.ex. zircão herdado proveniente de rochas mais antigas).

As razões $^{207}\text{Pb}/^{206}\text{Pb}$ são corrigidas por um fator de discriminação de massa de $0,12 \pm 0,03\%$ por u.m.a. (unidade de massa atômica), determinado a partir de análises repetidas do padrão de Pb NBS-982. Correções do Pb comum foram feitas através do modelo de evolução do Pb na Terra em dois estágios (Stacey & Kramers, 1975). As médias ponderadas e erros associados às determinações são calculados de acordo com Gaudette *et al.* (1998). Estimativas da razão Th/U inicial modelo foram feitas usando os valores atuais (medidos) corrigido do Pb comum da razão $^{208}\text{Pb}/^{206}\text{Pb}$ (Bartlett *et al.*, 1998): $\text{Th} = [({}^{208}\text{Pb}/{}^{206}\text{Pb})/(\lambda_{\text{Th}} * T) - 1] + ({}^{208}\text{Pb}/{}^{206}\text{Pb})$; $\text{U} = [({}^{208}\text{Pb}/{}^{206}\text{Pb})/(\lambda_{\text{U}} * T) - 1] + ({}^{208}\text{Pb}/{}^{206}\text{Pb})$; $\lambda_{\text{Th}} = 4.94750 * 10^{-12}$; $\lambda_{\text{U}} = 1.55125 * 10^{-11}$.

A idade dos cristais de zircão é calculada a partir das duas equações de desintegração dos isótopos, ^{235}U em ^{207}Pb e ^{238}U em ^{206}Pb : (a) $^{207}\text{Pb} = {}^{235}\text{U} * (e^{\lambda_{235} * t} - 1)$; (b) $^{206}\text{Pb} = {}^{238}\text{U} * (e^{\lambda_{238} * t} - 1)$. Onde, λ - constante de desintegração; t – tempo decorrido entre o fechamento do sistema U-Pb e a geração dos isótopos filhos intermediários; $\lambda_{235} = 1,55125 * 10^{-10}$ e $\lambda_{238} = 9,8485 * 10^{-10}$ (Steiger & Jäger 1977). A partir dessas equações fundamentais obtém-se a razão $^{207}\text{Pb}/^{206}\text{Pb}$ em função da idade: (c) $^{207}\text{Pb}/^{206}\text{Pb} = 1/137,88 * [(e^{\lambda_{235} * t} - 1)/(e^{\lambda_{238} * t} - 1)]$. Com base na equação (c), após a correção do Pb comum (^{204}Pb) e independente da determinação do U, é possível determinar a idade do mineral em questão (idade “aparente”). Em um diagrama de Concórdia, por exemplo, a idade obtida corresponde a uma determinada inclinação da discórdia, traçada entre o ponto na Concórdia e a origem dos eixos (vide item U-Pb em zircão por diluição isotópica).

No entanto, apesar da impossibilidade de avaliar se tal ponto é discordante ou concordante, (uma vez que qualquer ponto de natureza experimental localizado na discórdia, definida pela equação, fornece a mesma idade “aparente”), a repetitividade dos resultados comprova estatisticamente que o método de evaporação de Pb em monocristais de zircão fornece idades próximas, senão similares à idade de cristalização da rocha obtidas por outros métodos (p.ex. Macambira & Scheller, 1994; Söderlund, 1996; Gaudette *et al.*, 1998).

Em suma o método de evaporação de Pb em monocristais de zircão possui, entre outras vantagens, a capacidade de fornecer resultados rápidos, de baixo custo e de boa qualidade analítica, pois não há necessidade de tratamento químico prévio dos cristais. Além disso, os

valores absolutos mostram-se muitas vezes similares ao obtidos em outras metodologias, inclusive aquelas de alta resolução, conforme atestam, por exemplo, os resultados deste trabalho.

3.3.2.2 - U-Pb em zircão por diluição isotópica (ID-TIMS ou Isotope Dilution–Thermal Ionization Mass Spectrometry)

Duas amostras foram analisadas no Pará-Iso (espectrômetro de massa Finnigan MAT 262), utilizando-se o método U-Pb em zircão por diluição isotópica modificado por Krymsky (2002) a partir de Krogh (1973) e Parrish (1987). Os grãos de zircão após triagem inicial foram previamente pesados e submetidos a abrasão por 30 a 40 minutos sob pressão de 1,2 a 1,8 psi. Posteriormente foram lavados no ultra-som com metanol e uma mistura de HCl + HNO₃. Em seguida, as amostras foram dissolvidas em micro-cápsulas de teflon utilizando-se HF + HNO₃ e HCl em duas etapas distintas. Em cada etapa as micro-cápsulas foram colocadas em uma bomba de Parr e aquecidas em forno a temperatura a 245°C por cerca de 12 horas. Foi utilizado um traçador misto ²³⁵U-²⁰⁵Pb (10 µL) visando determinar as concentrações de urânio e chumbo.

O branco total medido foi de <30 pg para o chumbo e de <1 pg para o urânio e a repetição das análises no padrão NBS-982 forneceram as seguintes razões médias: ²⁰⁴Pb/²⁰⁶Pb = 0,0272162; ²⁰⁷Pb/²⁰⁶Pb = 0,467013; ²⁰⁸Pb/²⁰⁶Pb = 0,9998288. O fracionamento de massa para o Pb foi estabelecido em 0,12 u.m.a. e 0,18 u.m.a. 19 para o UO₂, enquanto os cálculos foram efetuados através dos programas PbDat (Ludwig, 1993) e Isoplot (Ludwig, 2001).

3.3.2.3 - Sm-Nd em Rocha Total

Foram analisadas **22** amostras de rocha pelo método Sm-Nd em rocha total. O processo de preparação das amostras seguiu o mesmo procedimento adotado para a realização das análises geoquímicas multielementares, gerando alíquotas com cerca de 200 mesh. Os procedimentos listados a seguir seguem a rotina desenvolvida por Oliveira (2002).

A abertura química dessas amostras (aproximadamente 100 mg) foi alcançada utilizando-se seqüencialmente os ácidos HNO₃, HF e HCl. Na solução resultante, o Sm e o Nd foram separados em duas etapas distintas através de cromatografia de troca iônica. A primeira etapa consistiu na separação dos ETR (Elementos Terras Raras) dos demais elementos, sendo a troca iônica realizada em colunas de teflon contendo resina Dowex 50Wx8. Nesta etapa são adicionados de modo seqüencial HCl e HNO₃ em diferentes concentrações.

Na segunda etapa de separação cromatográfica, Sm e Nd são separados dos demais ETR através da combinação HNO_3 + metanol. A troca iônica é realizada em resina Dowex AG1x4 eluída com HNO_3 -metanol, igualmente colocada em colunas de teflon. No processo analítico foi utilizado traçador misto ^{150}Nd - ^{149}Sm , de modo a identificar as razões isotópicas e o conteúdo de Sm e Nd. Na análise espectrométrica (Finnigan modelo MAT 262) na etapa de evaporação o Sm e o Nd são depositados em filamentos de tântalo, enquanto que a ionização é feita com filamentos de rênio.

Os dados de Nd foram normalizados para a razão $^{146}\text{Nd}/^{144}\text{Nd}$ de 0,7219. Durante o período de análises, uma razão $^{143}\text{Nd}/^{144}\text{Nd}$ média de $0,511843 \pm 12$ foi obtida para o padrão La Jolla e as concentrações de Sm e Nd para o padrão BCR-01 foram 6,56 e 28,58 ppm, respectivamente. Os brancos totais medidos foram <110 pg para o Sm e <240 pg para o Nd.

3.3.2.4 - Pb-Pb em feldspato

As amostras de feldspato analisadas foram obtidas, sobretudo de tipo porfíricos, tendo sido inicialmente fragmentadas no próprio afloramento e posteriormente pulverizadas em laboratório em frações granulométrica entre 1 e 2 mm. Foram selecionadas alíquotas com 30 a 50 mg de um total de 14 amostras. O método Pb-Pb feldspato por lixiviação seqüencial utilizado foi modificado de Ludwig & Silver (1977) e Housh & Bowring (1991).

Inicialmente os fragmentos de feldspato foram lavados com HCl e HNO_3 e em seguida lixiviados em várias etapas (de 3 a 8 etapas) com HF e HBr. A separação do Pb do restante dos outros elementos foi feita através da adição seqüencial monitorada de HBr e HCl em colunas de teflon contendo resina DOWEX AG 1x8 (200-400 mesh). O Pb separado obtido foi depositado em filamento de rênio com uma combinação de 1 μL de sílica gel + H_3PO_4 e a composição isotópica das amostras foi medida no espectrômetro de massa VG ISOMASS 54E com monocoletor. Foram considerados para o estudo isotópico os resultados das etapas com menor interferência de Pb estranho (em geral as últimas), e que conseqüentemente refletem o Pb inicial da rocha no tempo de sua formação. O tratamento dos dados e construção dos diagramas foi feito utilizando-se o programa Isoplot (Ludwig, 2001).

4 - ARTIGOS CIENTÍFICOS

Os resultados obtidos ao longo desta pesquisa encontram-se materializados nos artigos submetidos aos periódicos especializados. Estes serão apresentados a seguir, iniciando pelos litótipos do domínio Güiana Central, próximos ao limite com o Domínio Uatumã-Anauá, passando pelos resultados geológicos, petrográficos, geoquímicos e geocronológicos obtidos nos granitóides deste último domínio, culminando com a assinatura isotópica dos sistemas do Nd e Pb da crosta no sudeste de Roraima e elaboração de modelo de evolução geológica.

New Geological and Single-zircon Pb-evaporation data from the Central Guyana Domain, Southeastern Roraima State, Brazil: Tectonic Implications for the Central portion of Guyana Shield

Marcelo E. Almeida^{1,2*}, Moacir J.B. Macambira², Sérgio de C. Valente²

¹CPRM – Geological Survey of Brazil, Av. André Araújo 2160, Aleixo, CEP 69060-001, Manaus, Amazonas, Brazil

²Isotope Geology Laboratory, Center of Geosciences, Federal University of Pará, Rua Augusto Corrêa s/n, Guamá, CEP 66075-110, Belém, Pará, Brazil

³ Geosciences Department, Federal University Rural of Rio de Janeiro, Km 7 – BR-465, Seropédica, CEP 23890-000, Rio de Janeiro, Brazil

* Corresponding author; ph.: +55-92-2126-0301, fax: +55-92-2126-0319, e-mail adress: marcelo_almeida@ma.cprm.gov.br

ARTIGO SUBMETIDO AO CORPO EDITORIAL DA REVISTA “JOURNAL OF SOUTH-AMERICAN EARTH SCIENCES”

Words: summary (68), resumo (174), abstract (158), Body text (6093, including references), figure captions (270) and table caption (100).

Total: 1 table and 9 figures.

RESUMO

ABSTRACT

INTRODUCTION

GEOLOGY OF SOUTHEASTERN RORAIMA

THE CENTRAL GUYANA DOMAIN (CGD) IN SOUTHEASTERN RORAIMA

Barauana granulite

Itã mylonite and Igarapé Khalil orthogneiss

Amphibole-biotite foliated granitoids

SINGLE-ZIRCON Pb-EVAPORATION GEOCHRONOLOGY

Analytical procedures

Samples, results and interpretation

TECTONIC SETTING OF THE CENTRAL GUYANA DOMAIN IN SOUTHEASTERN RORAIMA: THE COLLISIONAL MODEL

CRUSTAL AMALGATION PROCESSES IN GLOBAL-SCALE: THE SUPERCONTINENT THEORY AND YOUR APPLICATION IN THE CENTRAL GUYANA DOMAIN

DISCUSSION AND CONCLUSIONS

References

RESUMO

Hornblenda e biotita (meta)granitóides, milonitos, leucognaisses e granulitos, com estruturas preferencialmente NE-SW e E-W, ocorrem no Domínio Guiana Central (DGC), próximo do limite com o Domínio Uatumã-Anauá (DUA), região central do Escudo das Guianas, sudeste de Roraima (Brasil). Os resultados fornecidos pelo método evaporação de Pb (zircão) apontam idades de 1.724 ± 14 Ma e 1.889 ± 4 Ma, respectivamente, para um hornblenda-biotita monzogranito foliado (granito sincinemático) e um granodiorito milonítico (Suíte Água Branca?). Desta forma, sugere-se, além dos eventos deformacionais marcados pelo intervalo de 1,94-1,93 Ga (pós-Transamazônico) e 1,35-0,98 Ga (K'Mudku), a existência de um outro evento deformacional em torno de 1,72 Ga (Evento Itã), provavelmente relacionado, nesta região, à evolução do Supercontinente Columbia. Além disso, os dados sugerem que o Sistema de Falhas do Itã pode ter sido gerado ou reativado pós-1,89 Ga e os protólitos ortoderivados estudados nesta porção do DGC não se mostraram correlacionáveis àqueles de áreas vizinhas (cujas idades variam de 1,96 a 1,93 Ga), indicando a necessidade de revisão das propostas litoestratigráficas e dos limites entre domínios vigentes.

Palavras-chave: Guiana Central, Roraima, Escudo das Guianas, Geologia, Geocronologia

ABSTRACT

Metagranitoids, mylonites, leucogneisses and granulites occur in the Central Guyana Domain (CGD) near to the Uatumã-Anauá Domain (UAD) boundary, southeastern Roraima (Brazil). In general these rocks show trend NE-SW to E-W and dip NW to N. Single-zircon Pb evaporation results yielded $1,724 \pm 14$ Ga and $1,889 \pm 3$ Ma to a synkinematic foliated hornblende-biotite monzogranite and a granodioritic mylonite, respectively. These results point to a new tectonic event (Itã Event) in the area in addition to the 1.94-1.93 Ga (late- to post-Transamazonian) and the 1.35-0.98 Ga (K'Mudku) thermal tectonic events. This new event may be related, at least locally, with the evolution of the Columbia Supercontinent. In addition, the Itã Fault System is younger than 1.89 Ga (granodioritic mylonite age), contrasting with the Barauana high grade lineament and 1.94 Ga polideformed rocks, pointing to the needs of a major revision in the present proposals for the lithostratigraphic column within the CGD and the CGD and UAD boundary.

Keywords: Central Guyana, Roraima State, Guyana Shield, Geology, Geochronology

INTRODUCTION

The Central Guyana Domain (Reis and Fraga, 2000a, Reis *et al.*, 2003) or K`Mudku Shear Belt (Santos *et al.*, 2000, 2006a,b) is considered the most important structural feature in central-western Guyana Shield (**Fig. 1**). This major NE-SW-trending tectonic domain spreads over Brazil, Guyana and Surinam. The domain has been interpreted as a collisional orogen (Hasui *et al.*, 1984, Gibbs and Barron, 1993), although no relicts of oceanic crust have been recorded, despite the subduction-related geochemical signature found in some orthogneisses (calc-alkaline crustal sources). According to CPRM (1999) this calc-alkaline signature is not directly associated with mantle partial melting in the subduction pre-collisional setting but may be reflecting an origin associated with an ensialic mobile belt (Cordani and Brito Neves, 1982). As such, those authors suggested that the Central Guyana Domain was generated during an earlier event in late-Transamazonian times as a result from an oblique movement along the limits of two collisional lithospheric plates (*ie.* intracollisional orogenic belt). Further tectonic events, such as the K`Mudku (Guyana) or the Nickerie (Surinam) events, obliterated the igneous and metamorphic protholiths and the actual northern and southern limits of the Central Guyana Domain.

This paper presents geological data for granulites, orthogneisses, mylonites and (meta)granitoids and new zircon Pb geochronological data for mylonites and granitoids from the Central Guyana Domain in southeastern Roraima State (Brazil). The aim is contribute for a better establishment of the southern limit of this domain and the understanding of the chronology of the major igneous, metamorphic and tectonic events in the central portion of Guyana Shield.

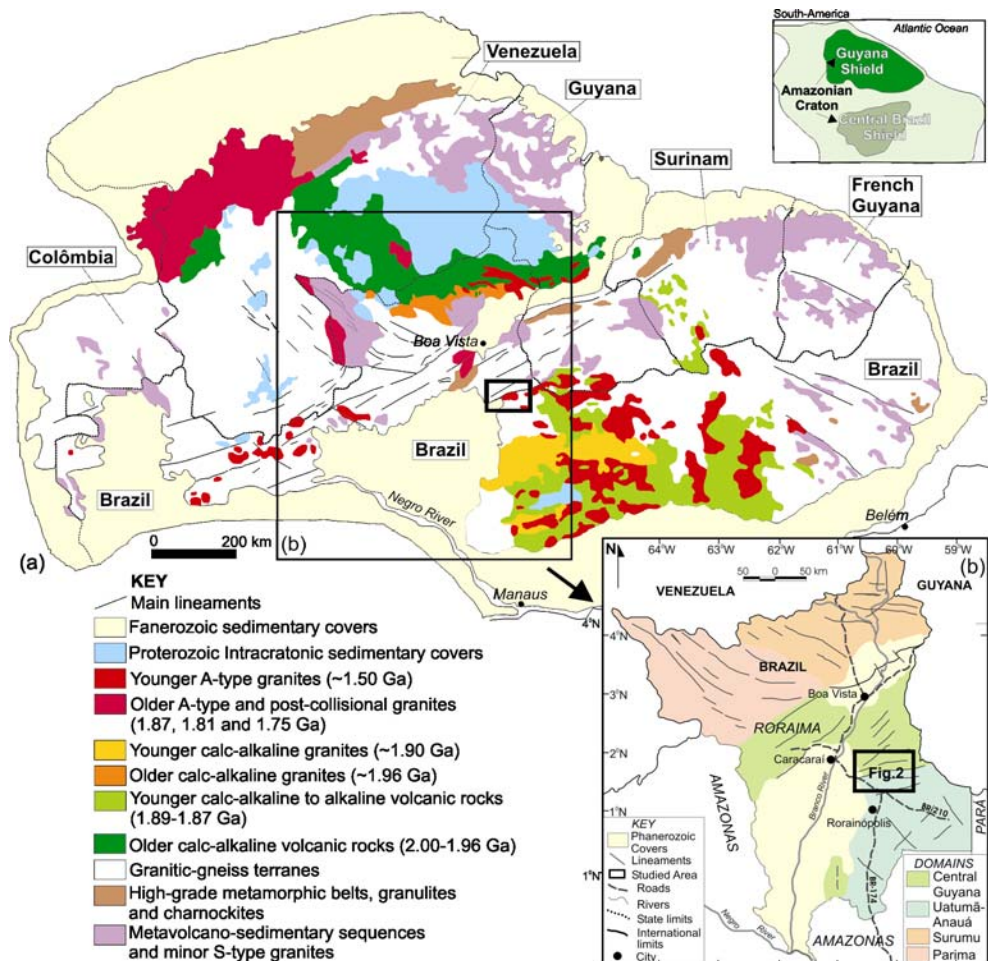
GEOLOGY OF SOUTHEASTERN RORAIMA

The southeastern Roraima State comprises two main lithostructural domains, the so-called Central Guyana and Uatumã-Anauá domains (**Fig. 1**, Reis *et al.*, 2003, CPRM, 2006). These two domains correspond, respectively, to the K`Mudku Shear Belt and the Tapajós-Parima Belt (Santos *et al.*, 2000, 2006a,b). According to CPRM (1999), the Central Guyana Domain (CGD) is essentially a shear belt with a strong NE-SW and E-W-trending (**Fig. 2**) dipping steeply to NW. Although the age and evolution of this shear-belt still remain uncertain, Fraga and Reis (1996) reinforced that its main tectonic feature can be related to oblique thrust structures with a main stress component from NW to SE. The most common rocks that crop out in southern CGD are orthogneisses, mylonites, metagranitoids and local lenses of granulites and leucogneisses (the Rio Urubu Metamorphic Suite; CPRM, 1999) associated with low- (Cauarane Group, CPRM, 1999)

to high-grade (Murupu Suite, Luzardo and Reis, 2001) metavolcano-sedimentary sequences and S-type granites (Curuxuim Granite, CPRM, 1999).

In this region, the Uatumã-Anauá Domain (UAD) is characterized by E-W to NE-SW-trending lineaments and an older metamorphic basement (**Fig. 2**) associated with an island arc environment (Faria *et al.*, 2002). Such basement is represented by TTG-like metagranitoids to orthogneisses, including meta-mafic to meta-ultramafic enclaves (the Anauá Complex). Metavolcano-sedimentary rocks (Caurane and Murupi related rocks) are also associated with the basement rocks in this area (CPRM, 2000).

The TTG and the supracrustal basement are intruded by S-type (the Serra Dourada Granite) and I-type calc-alkaline (Martins Pereira) granites (**Fig. 2**). Altogether, they comprise the Martins Pereira-Anauá Granitic Terrane (Almeida *et al.*, 2002) or the Northern Uatumã-Anauá Domain (NUAD, Almeida and Macambira, submitted). This terrane is 1.96 to 2.03 Ga old, and corresponds to the “deformed” portion of the UAD.



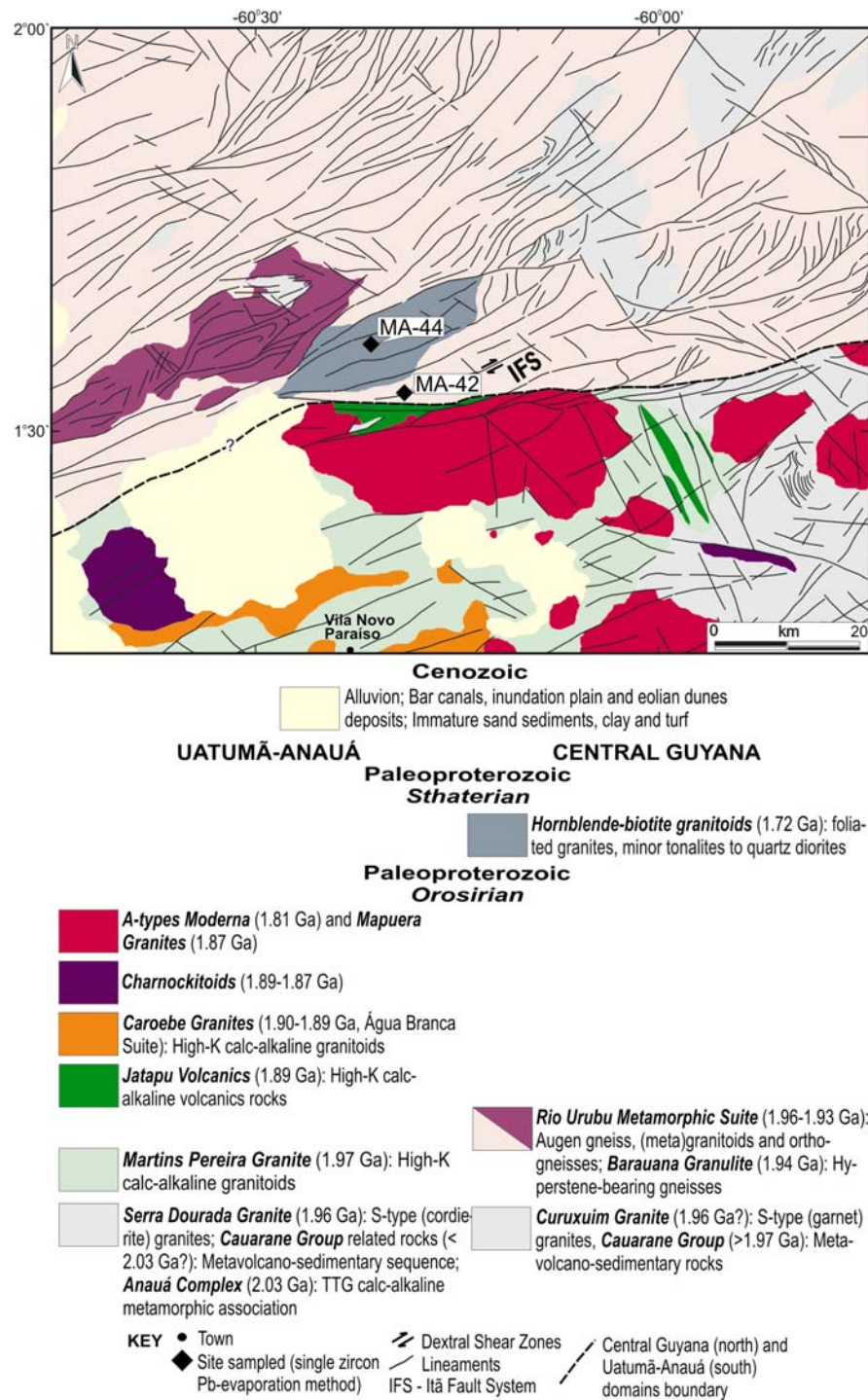


Fig. 2. Geological map of the Southeastern Roraima State modified from CPRM (2000) and Almeida *et al.* (2002).

The Caroebe (Água Branca Suite, **Fig. 2**) and the Igarapé Azul calc-alkaline granitoids bear younger ages being unmetamorphosed and undeformed rocks (Almeida and Macambira, submitted). The coeval Caroebe granitoids were associated with the Iricoumé volcanic rocks (Macambira *et al.*, 2002) on the basis of geochemical data (Reis *et al.*, 2000). Locally, igneous

charnockitic (Igarapé Tamandaré) and enderbititic (Santa Maria) plutons are also found in the area. These rocks comprise the “undeformed” Igarapé Azul-Água Branca Granitic Terrane (Almeida *et al.*, 2002) located on the Southern Uatumã-Anauá Domain (SUAD, Almeida and Macambira, submitted). Several A-type granites plutons (**Fig. 2**) represented by the Moderna and Madeira (1.81 Ga), and Mapuera and Abonari (1.87 Ga) granites are widespread in the UAD and cross cut both terranes.

THE CENTRAL GUYANA DOMAIN (CGD) IN SOUTHEASTERN RORAIMA

Metagranitoids, high-grade metamorphic rocks and several other metamorphic and granitoid rocks found within the CGD nearby the UAD were grouped into the Rio Urubu Metamorphic Suite (CPRM, 1999, 2000, Reis and Fraga, 2000b). The hypersthene-bearing gneisses (the Barauana granulite), leucogneisses (the Igarapé Khalil leucogneiss), epidote-rich biotite mylonites (the Itã mylonite) and hornblende-biotite gneisses to foliated granitoids of this suite were mapped in the southern limit of the CGD as part of the present work and will be described in the following sections.

Barauana granulite

High-grade metamorphic domains have been reported in the Imataca Complex (Venezuela), Kanuku Mountains (Guyana), Bakhuis Mountains and Coeroeni area (Suriname), and also in eastern Amapá and center-southern Roraima states (Brazil) in the Guyana Shield (**Fig. 1**; Gibbs and Barron, 1993). Among these terranes, the Barauana Mountain represents a major granulite-facies domain (CPRM, 2000) in southern Roraima (**Fig. 2**).

The Barauana Mountain is constituted by banded, polydeformed, locally migmatized hypersthene-bearing gneisses with charnockitic to enderbite composition and igneous textures have not been preserved in these rocks. (**Fig. 3**). The migmatites show anathetic mobilizates and stromatic, agmatic and schollen structures. The gneisses show grano-lepidoblastic textures and a mineral assemblage composed by plagioclase, alkaline feldspar, hypersthene, quartz and minor red brownish biotite, opaque minerals (mainly magnetite), apatite and zircon (**Fig. 4a-b**).

On a regional scale, the NE-SW foliation (N60°E/80°NW to N35°E/90°) dips steeply NW and generally parallel to the CGD trends. Similar trends are observed in the Kanuku Mountains, in Guyana (McConnel, 1962; Gibbs and Barron, 1993), as well as in the Bakhuis and Coeroeni Mountains, in Suriname (Bosma *et al.*, 1983, De Roever *et al.*, 2003).



Fig. 3. Outcrop of banded charnockitic gneiss (Barauana Granulite) with enderbite lenses (MA-207 outcrop).

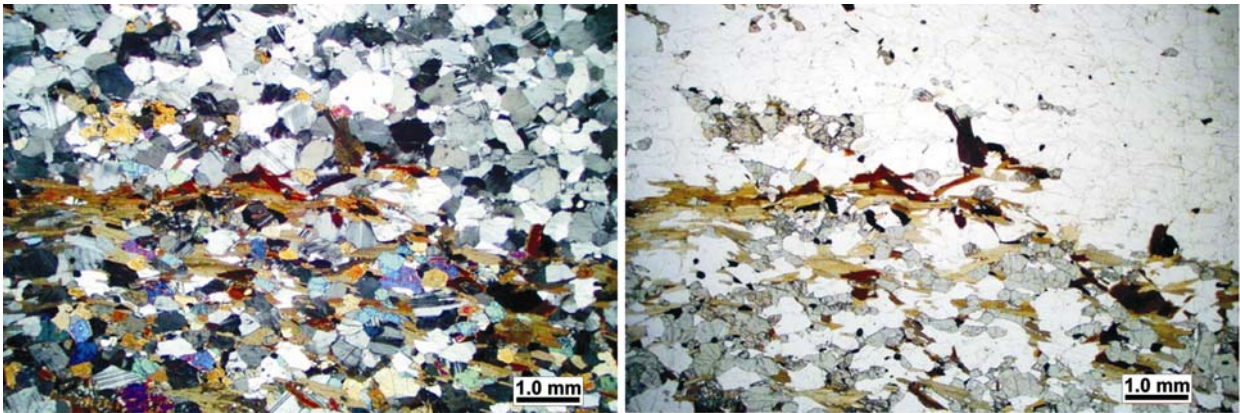


Fig. 4. Photomicrograph of charnockitic gneiss (Barauana Granulite) with bands of granoblastic charnockite (uppermost) and granolepidoblastic enderbite (lowermost). (a) Cross-polarized light and (b) plane-polarized light (1.25x).

Rims of zircon crystals in the Barauana granulite (anatexite sample) were interpreted as having a late metamorphic origin (1,818 Ma, U-Pb SHRIMP), while the cores (1,942 \pm 7-8 Ma, U-Pb SHRIMP) have been related to an anatectic event (igneous zircons) under PT granulitic conditions (CPRM, 2002, 2003). Synkinematic charnockites within the CGD (Serra da Prata Suite reviewed by Fraga, 2002), yielded ages between 1,934 and 1,943 Ma (single-zircon Pb-evaporation). These ages are in general agreement with those of the Barauana granulite and all these data suggest an important pyroxene-bearing rocks (anhydrous) generation event. Nevertheless, despite of their similar age range, their coeval origin (the Barauana and the Serra da Prata) is yet a debatable hypothesis. These ages are also much younger than the Amapá (2.06-2.05 Ga, Lafon *et al.*, 2001 and Avelar *et al.*, 2003) and Bakhuis (2.07-2.05 Ga and \sim 2.15 Ga inherited component, De Roeve *et al.*, 2003) ultra high-temperature (UHT) granulites, revealing the 140 to 110 Ma elapsed time and diachronous high-grade metamorphism episodes in the Guyana Shield (**Fig. 1**).

Itã mylonite and Igarapé Khalil orthogneiss

The Itã mylonite crops out near to RR-170 road, within the Itã Fault System, located on the boundary of the CGD and the UAD (**Fig. 2**). According to CPRM (2000) other mylonites are observed to the north, in the Lua Mountains (Vila Vilhena region), associated with fine grained biotite gneisses. Nevertheless, these types are older than the Itã mylonite (see the next chapter).

The Itã mylonite is medium to fine-grained, augen feldspar porphyroclast-bearing rocks with granodioritic to monzogranitic compositions (**Fig. 5**). These rocks display a $N75^{\circ}E$ to $N70^{\circ}E$ S-C foliation (dextral sense), steep NW dipping, and a mineral assemblage mainly composed by alkalifeldspar, plagioclase and biotite (and associated epidote). Epidote, quartz and feldspars are very fine grained, recrystallized and, locally, quartz and feldspar show granoblastic features (**Fig. 6a-b**). The other accessory minerals are sphene, allanite, opaque minerals (mainly magnetite), apatite and zircon. Secondary minerals are chlorite and local titanite. Relict igneous textures are scarcely observed in these rocks.

The Igarapé Khalil gneiss crops out along the BR-174 highway and shows leucocratic types with equigranular, fine-grained and grano-lepidoblastic to locally protomylonitic textures. It displays a $N80^{\circ}E$ to $N50^{\circ}E$ foliation and subvertical dipping and a mineral assemblage composed by quartz, microcline and plagioclase. Biotite and muscovite, shows low abundances in this rock (~3% vol.). Accessory minerals are rare and represented by allanite, primary epidote, zircon, apatite and opaque minerals. Epidote, chlorite and sericite are the main secondary minerals.



Fig. 5. Granodioritic to monzogranitic biotite mylonite showing a conspicuous mylonitic foliation with ENE-WSW trend and NW steep dip (MA-42 outcrop).

Amphibole-biotite foliated granitoids

The biotite-amphibole gneisses and metagranitoids are commonly found between the Barauana Mountain and Itã Fault System, along to RR-170 road (**Fig. 2**). They comprise a ENE-

WSW trending, lenses-shaped body with slightly higher radiometric features (CPRM, 1984). These rocks display a NW steeply dipping, N70°E to N75°E conspicuous foliation (**Fig. 7**) and S-C fabric as a result of emplacement under amphibolite-facies conditions and dextral transpressive regime.

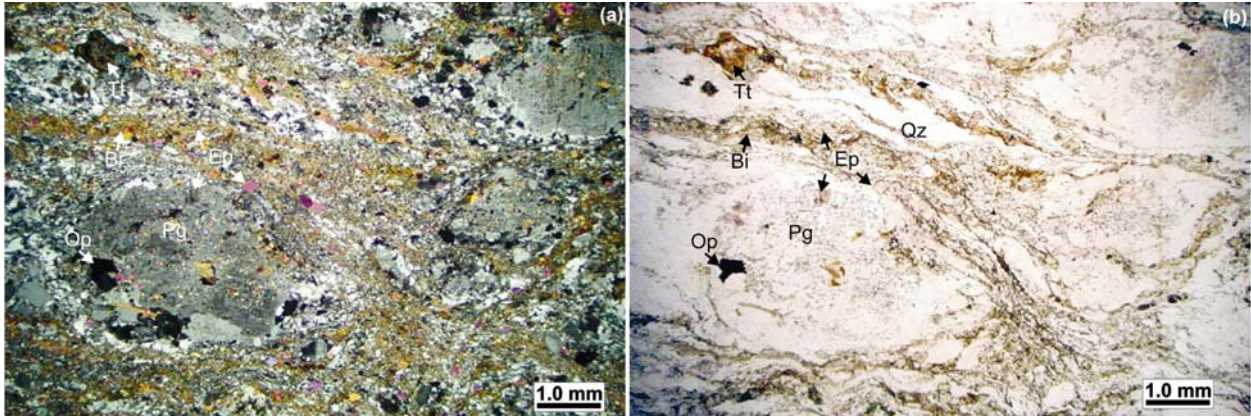


Fig. 6. Photomicrograph of porphyritic granodiorite with mylonitic texture and conspicuous foliation, as well as a local fine-grained matrix and feldspar relicts. (a) Cross-polarized light and (b) plane-polarized light (1.25x). Bi. Biotite; Ep. Epidote; Op. Opaque minerals; Pg. Plagioclase; Qz. Quartz. Tt- Titanite.

These rocks show monzogranitic to syenogranitic and rarely granodioritic to quartz dioritic compositions, with equigranular to slightly porphyritic textures, medium-grained matrix and a pale gray color. Biotite and amphibole (probably hastingsite) are the main mafic minerals, while the main accessory minerals are sphene, allanite-epidote, opaque minerals, apatite and zircon. In thin section, despite the conspicuous foliation and mineral lineation, these are generally strain free rocks, suggesting deformation in the presence of a melt phase (*ie.* syn-kinematic emplacement). There is no dynamic and/or static conspicuous recrystallization and the igneous mineralogy and texture are well preserved in these rocks (**Fig. 8a-b**). Only a few quartz crystals show local grain reduction (dynamic recrystallization) and undulatory extinction. On the other hand, CPRM (1999, 2000) have pointed out to similar highly deformed (solid state) rocks in the Barauana River and Lua Mountain, also suggesting that the granite had been partially crystalized at the time of deformation. According CPRM (1999) these rocks points to correlation with the Kusad and Corentyne (augen) gneisses in southern Guyana.

In general sense, the petrographic and field features described for the in biotite-amphibole granite “gneiss” suggest that granitic emplacement took place in a partially molten state in a tectonic active zone. Furthermore, according Brown and Solari (1999) granites with concordant to subconcordant, sheet-like body shape suggest magma transport in planar conduits through the AFZ (apparent flattening zone). This is corroborated by the $S > L$ fabrics observed in these

granites that record apparent flattening-to-plane strain, mainly in the case of “straight” belts (Brown and Solari, 1999).



Fig. 7. Foliated hornblende-biotite granite (“streaky gneiss”) showing strong foliation and mineral lineation by magma flow (MA-44 outcrop).

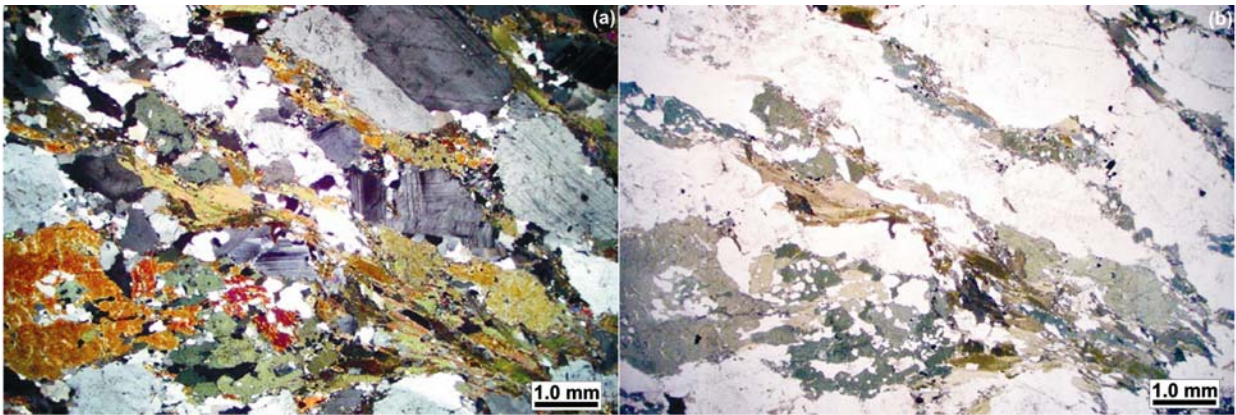


Fig. 8. Photomicrograph of foliated hornblende-biotite monzogranite with low dynamic recrystallization effects and abundant relicts of igneous texture. (a) Cross-polarized light and (b) plane-polarized light (1.25x).

SINGLE-ZIRCON Pb-EVAPORATION GEOCHRONOLOGY

Analytical procedures

Two to ten kg of each rock sample were crushed, washed and dried out for at least 12 hours, and milled under 60 to 80 mesh. After that, heavy mineral fractions were obtained by water mechanical concentration. Following, the samples were then processed by means of a hand-magnet and a Frantz Isodynamic Separator followed by mineral separation in dense liquid. The lowest magnetic zircon concentrates (from five magnetic fractions) were then selected for hand-picking. As much as possible, only alteration-free zircon grains with no metamictization features, inclusions and fractures were selected for analysis (see zircon descriptions below). In order to remove impurities, the zircon final concentrates were leached under HNO_3 on a hotplate (100°C for 10 minutes), cooled, submitted to a ultrasound cube (5 minutes) and finally washed in two

times distilled water. After drying, the concentrates were observed under the petrographic microscope and the zircon grains were selected by hand-picking.

In the Pb-evaporation method on the single zircon, the selected grains were tied in Re-filaments and charged into Finnigan MAT262 mass spectrometer for isotope analyses. The $^{207}\text{Pb}/^{206}\text{Pb}$ ratios were corrected for a mass discrimination factor of $0.12\% \pm 0.03 \text{ a.m.u}^{-1}$, determined by repeated measurements of the NBS-982 Pb-standard. In this technique, the $^{207}\text{Pb}/^{206}\text{Pb}$ ratio was measured in three evaporation steps at temperatures of 1450° , 1500° , and 1550°C . Usually, the average $^{207}\text{Pb}/^{206}\text{Pb}$ ratio obtained in the highest evaporation temperature was considered for age calculation. The data were dynamically acquired using the ion-counting system of the instrument. The Pb signal was measured by peak hopping in the 206, 207, 208, 206, 207, 204 mass order along 10 mass scans, defining one block of data with 18 $^{207}\text{Pb}/^{206}\text{Pb}$ ratios. Outliers were eliminated using the Dixon's test. The $^{207}\text{Pb}/^{206}\text{Pb}$ ratio average of each step was determined on the basis of five blocks, or until the intensity beam was sufficiently strong for a reliable analysis. The ages were calculated with 2 sigma error and common Pb correction. Appropriate age values derived from the Stacey and Kramers (1975) model were obtained for those blocks in which the $^{204}\text{Pb}/^{206}\text{Pb}$ ratios were lower than 0.0004. The data were processed using the DOS-based *Zircon* shareware (T. Scheller, 1998).

Samples, results and interpretation

Two fresh samples representing the Itã granodioritic mylonite (MA-42: $1^\circ 32' 50''\text{N}$; $60^\circ 19' 48''\text{W}$) and the foliated biotite-amphibole monzogranite (MA-44: $1^\circ 36' 35''\text{N}$; $60^\circ 21' 36''\text{W}$) were collected and analyzed by the single-zircon Pb evaporation method.

Six zircon crystals from sample MA-42 (porphyritic granodioritic mylonite), have been analyzed, but only three (crystals #2, #4 and #5) gave results that led to age calculations. The zircons were non-magnetic, euhedral, pale yellow to brown, transparent to translucent crystals showing some inclusions and fractures. The crystals were generally bipyramidal with preserved faces, 220-360 μm in length and length:width ratio around 3:1 to 2:1.

The analyzed crystals yielded a mean age of $1,889 \pm 4 \text{ Ma}$ (**Fig. 9a**, Table 1) and the $^{207}\text{Pb}/^{206}\text{Pb}$ individual ages obtained at the higher temperature steps were rather uniform, showing values between $1,889 \pm 4 \text{ Ma}$ (grain #2) and $1,892 \pm 2 \text{ Ma}$ (grain #5). Thus, the $1,889 \pm 4 \text{ Ma}$ was interpreted as the crystallization age and the time of emplacement of the igneous protholith of the

MA-42 mylonite. The lowest temperature steps were eliminated from the calculation of the mean age because they have spreaded out and yielded younger ages ($1,828 \pm 10$ Ma to $1,879 \pm 8$ Ma) and higher $^{204}\text{Pb}/^{206}\text{Pb}$ ratios. The Th/U ratios gave an uniform range of 0.51 to 0.58 (Table 1), similarly to the other magmatic rocks.

The mean age is, at least, 20 to 75 Ma younger than that of other igneous protholiths from orthogneisses and mylonites related to the Rio Urubu Metamorphic Suite in the CGD, such as the Vilhena mylonite, which yielded $1,950 \pm 9$ Ma (magmatism age) and $1,879 \pm 4$ Ma (metamorphism age) according to U-Pb zircon SHRIMP analyses (CPRM, 2002, 2003). Locally, mylonites with younger ages are described to the south, in the Alalaú and Jauaperi rivers (CPRM, 2000) yielding $1,869 \pm 9$ Ma by U-Pb zircon SHRIMP method (Santos *et al.*, 2002, CPRM, 2003). On the other hand, igneous ages of around 1.89 to 1.90 Ga were only observed on the Igarapé Dias (CPRM, 2003) and Caroebe granitoids (Água Branca Suite), both in the southeast of Roraima. Thus, despite of difficulties concerning the protholith identification, the 1.89 Ga age, associated with the mineral assemblage (e.g. biotite, epidote and calcic zoned plagioclase) and granodioritic to monzogranitic composition suggest that the igneous protholith of the Itã mylonite is a granitoid related with the Caroebe (Água Branca Suite) magmatism.

Twenty zircon crystals from sample MA-44 (foliated hornblende-bearing granite were analyzed, but only five crystals (crystals #6, #8, #12, #14 and #18) gave results that led to age calculations (**Fig. 9b**, Table 1). The zircons were euhedral, bipyramidal crystals with 180-370 μm in length and ratio dimensions around 2:1. They showed slightly rounded vertices and local irregular faces. The grains were pale yellow, transparent to translucent, with several inclusions, fractures, being also weakly magnetic.

The analyzed crystals yielded a mean age of $1,724 \pm 14$ Ma (**Fig. 9b**), but the $^{207}\text{Pb}/^{206}\text{Pb}$ individual ages obtained under the 1450°C to 1500°C evaporation steps were not well homogeneous giving high errors, and values between $1,707 \pm 16$ Ma (grain #8) to $1,755 \pm 10$ Ma (grain #12). Thus, this mean age is interpreted as a minimum crystallization age of the analyzed crystals. Grain #3 gave the oldest age ($1,827 \pm 23$ Ma) and has been taken as an inherited crystal, showing ages close to those of the Moderna Granite (Santos *et al.*, 1997). The Th/U ratios range from 0.36 to 0.50 (Table 1), resembling those found in magmatic systems.

The mean crystallization age of 1.72 Ga is at least 200 Ma younger than those of others orthogneisses and metagranitoids correlated to Rio Urubu Metamorphic Suite, in the CGD

(Gaudette *et al.*, 1996, Fraga, 2002). The Sm-Nd whole-rock data of these foliated granitoids were reviewed and yielded an Nd model age (T_{DM}) of 2.07 Ga and $\epsilon_{Nd} = -0.91$ (T_{crist} 1724 Ma), suggesting depleted crustal protholiths with late Transamazonic ages (with no appreciable mantle contribution).

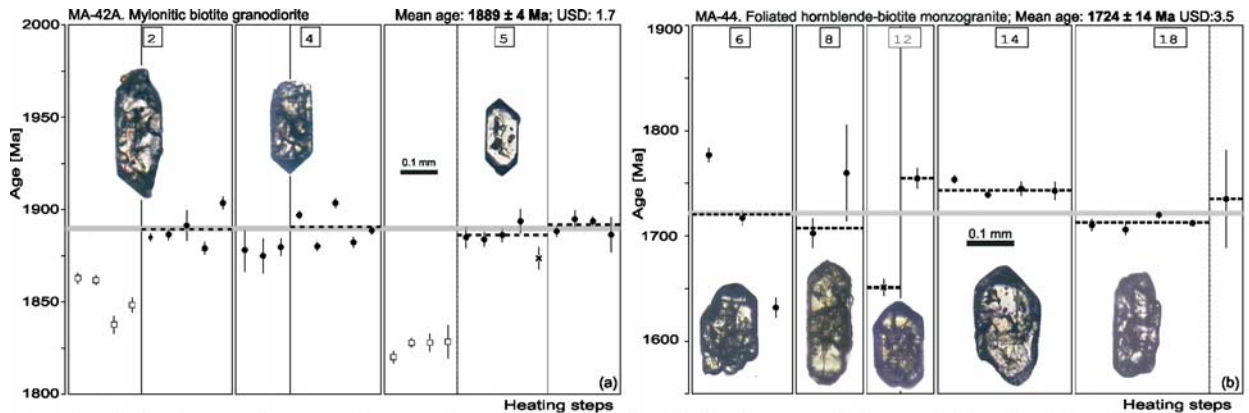


Fig. 9. Single zircon Pb-evaporation age diagram of (a) mylonitic biotite granodiorite and (b) foliated hornblende-biotite monzogranite. Filled circle - accepted blocks for age calculation. Square - blocks discarded due to their higher or lower values of the $^{207}\text{Pb}/^{206}\text{Pb}$ ratio in relation to the mean. X - rejected blocks due to show $^{204}\text{Pb}/^{206}\text{Pb} > 0.0004$. Crystal numbers are indicated (see table 1). The scale bar is the same for all diagrams.

Ar-Ar ages on a muscovite crystal from sheared granitoids within the UAD, near to the boundary with GCD, yielded ages between $1,656 \pm 4$ Ma and $1,710 \pm 4$ Ma (CPRM, 2002), recording an important thermal event (near 350°C Ar-Ar blocking temperature, Hodges, 1991) in southeastern Roraima. These Ar-Ar ages are in good agreement with the foliated amphibole-biotite granite age ($1,724 \pm 14$ Ma).

TECTONIC SETTING OF THE CENTRAL GUYANA DOMAIN IN SOUTHEASTERN RORAIMA: THE COLLISIONAL MODEL

The CGD has been taken as a major collisional orogen by many authors in the past years (e.g. Cordani and Brito Neves, 1982, Hasui *et al.*, 1984, Gibbs and Barron, 1993, Fraga and Reis, 1996, Sena Costa and Hasui, 1997, CPRM, 1999, Santos *et al.*, 2000, 2006a,b). In general, granulite terranes in collisional orogens follow a clockwise PT path (e.g. Ellis, 1987, Brown and Dallmeyer, 1996; Brown, 2001) and their exposure has been attributed to isostatic rebound as a result of crustal thickening during one or more tectonic events (Ellis, 1987).

Nevertheless, many granulite terranes seem to have been just too hot to have formed during continental collision and may represent thickened hot orogens associated with underplating processes within other tectonic settings (Collins, 2002a). For instance, granite generation in the Paleozoic-related Lachlan Folded Belt and Circum Pacific regions was assisted by heat advected

from the mantle during prolonged regional extension under low- to medium-P granulite facies (Collins, 2002b). These recent studies have pointed out that some granulites are unlikely to be related with a collisional orogen. Furthermore, collisional orogens develop when an ocean closes between continental blocks. However, many orogenic systems have not experienced collision, called accretionary (e.g. Coney, 1992), with the Lachlan orogen an excellent example.

Collisional orogens develop when an ocean basin closes up leading to continental collision, but accretionary orogens such as the Paleozoic Lachlan Folded Belt have not experienced collision (e.g. Coney, 1992). Even in classic collisional orogens such as the European Alps and Himalayas coeval granites and granulites are rare. On the contrary, broad zones of anomalously high heat flow occur in extensional and accretionary orogens leading to widespread silicic magmatism, as in the Basin and Range Province, the Taupo volcanic zone, the Circum-Pacific orogens and some Precambrian terranes (e.g. Central Australia) (Collins, 2002a). These orogens are characterized by voluminous granitic batholiths associated with repeated extensive-compressive events and are underlain by granulites. The latter are only scarcely exposed (e.g. Ducea, 2001) because crustal thickening rarely occurs. Even so, granulite xenoliths found in modern basalts in those orogens attest for the existence of a granulite basement (e.g. Chen *et al.*, 1998). Overall these data suggest that granulites would have been more commonly associated with accretionary orogens than collisional ones. Nevertheless other authors have argued that the association of granulite terranes with repeated tectonic events has only local application as in the case of the Lachlan orogen since it does not apply to other UHT and HP granulite terranes undoubtedly related to collisional tectonics as in the case of the Variscan, Brasilia and Grenville orogens (Brown, 2003).

CRUSTAL AMALGATION PROCESSES IN GLOBAL-SCALE: THE SUPERCONTINENT THEORY AND YOUR APPLICATION IN THE CENTRAL GUYANA DOMAIN

The Amazonian Craton evolution has been closely associated with those of the Laurentia and Baltic cratons in the northern hemisphere (e.g. Rogers, 1996). Lateral magmatic arc accretion seems to have taken place in those cratons in Statherian times (Paleoproterozoic: 1.80-1.60 Ga) as well as taphrogenic events within the pre-Statherian domains (e.g. Atlantica) onto the Columbia supercontinent (Rogers and Santosh, 2002; Brito Neves and Almeida, 2003). These Statherian events are well-recorded in the Yavapai (1.75-1.68 Ga; e.g. Duebendorfer *et al.*, 2001)

and Cheyenne (1.78-1.75 Ga. e.g. Sims and Stein, 2003) orogens within Laurentia as well as in the Rio Negro (1.82-1.52 Ga) and the Rondonian-Juruena (1.82-1.54 Ga) provinces within the Amazonian Craton (Santos *et al.*, 2000, 2006a).

In southern Roraima, central portion of Guyana Shield (**Fig. 1**), the Statherian granitic magmatism are unknown at this time, but could be represented by the synkinematic biotite-amphibole granite emplaced around 1.72 Ga, although arc-related meta-quartz diorites with ~ 1.70 Ga do also crop out westerwards the Guyana Shield (Rio Negro Province; $1,703 \pm 7$ Ma, zircon U-Pb ID TIMS; Tassinari *et al.*, 1996). This apparent Statherian magmatism scarcity in Roraima, contrasts with Laurentia and Baltic cratons.

For instance, in Laurentia block the zircon geochronology studies (U-Pb SHRIMP and ID TIMS) pointed out $1,721 \pm 15$ Ma for the Boulder Creek Batholith (Premo and Fanning, 2000) and $1,737 \pm 4.3$ Ma, $1,719 \pm 1.2$ Ma and $1,721 \pm 2.4$ Ma for the Big Wash, Diana and Chloride granites respectively (Duebendorfer *et al.*, 2001). Similarly, ~ 1.7 Ga syntectonic plutons (Wet Mountains; Siddoway *et al.*, 2000) and muscovite and biotite Ar-Ar plateau ages (~ 1.74 - 1.70 Ga) obtained for samples from the western Trans-Hudson Orogeny (Heizler *et al.*, 2000) closely resemble those in southeastern Roraima obtained for foliated hornblende- biotite granites (1.72 Ga, this paper) and some muscovites in shear zones (1.71-1.66 Ga, CPRM, 2002). These data suggest the involvement of the southeastern Roraima lithosphere in the Columbia supercontinent evolution at least on a local scale.

Accretionary and collisional orogens have also affected the Amazonas, Laurentia and Baltica cratons in late Mesoproterozoic times. Geochronological Rb-Sr and K-Ar data (Pinson *et al.*, 1962, Barron, 1966, Priem *et al.*, 1971, Amaral, 1974, Lima *et al.*, 1974, Basei and Teixeira, 1975, Tassinari, 1996) show that the K'Mudku (Barron, 1966) event took place within the 1.35-0.98 Ga range as confirmed by recent Rb-Sr and minor Ar-Ar geochronology (Fraga, 2002; Santos *et al.*, 2003). As such, the K'Mudku Event in Roraima can be interpreted as a far-field, intracratonic effect of the continental collision (Grenvillian-Sunsas belt) within the southwestern and northwestern Amazonas Craton. This event can also be related with the Rodinia supercontinent amalgamation according Brito Neves (1999).

In summary, the data presented in this section strongly suggest that the central portion of the Guyana Shield (northern Amazonian Craton) in southeastern Roraima has played a role in repeated episodes of supercontinental amalgamation as follows: the Atlantica (1.94-1.93 Ga, late-

collisional stage?), Columbia (1.72-1.66 Ga, accretionary stage?) and Rodinia (1.35-0.98 Ga – collisional stage) supercontinents.

DISCUSSION AND CONCLUSIONS

The gneissic and granitic rocks of the CGD in the studied area have been distinctly affected by varied petrogenetic processes. These rocks comprise high-grade polideformed granulitic rocks; leucogneisses and mylonitic rocks affected by a single deformation phase and medium- to low-grade metamorphism and hornblende-biotite granites with magma flow foliation and igneous relict fabric.

These rocks were originally taken as part of the Rio Urubu Metamorphic Suite (CPRM, 1999) but the ages obtained for the Itã mylonite (1.89 Ga) and the foliated hornblende-biotite granites (1.72 Ga) are respectively 40-70 Ma and 200-240 Ma younger than the magmatic protoliths found elsewhere within the Rio Urubu Metamorphic Suite (1.93 to 1.96 Ga). In addition, these rocks show post-1.89 Ga deformation episodes. The new geochronological data presented in this paper strongly indicate that proposed lithostratigraphy for the CGD has to be reviewed, including your boundary with the UAD.

The 1.72 Ga, synkinematic granitic magmatism (foliated hornblende-biotite granitoid) in the CGD as well as the Ar-Ar ages (~1.70 Ga, CPRM 2002) suggest that a tectonic event intermediate in age to the late-Transamazonic (~1.94 Ga, Fraga, 2002) and K'Mudku (~1.20 Ga, Fraga, 2002) events, probably related to the Macuxi Event (CPRM, 1999) took place in the studied area and renamed for the Itã Event.

The K'Mudku Event has been detected in the area by means of several Rb-Sr (e.g. Amaral, 1974, Santos *et al.*, 2000, Fraga, 2002), K-Ar (e.g. Amaral, 1974) and rarely Ar-Ar (Santos *et al.*, 2003) ages. These ages are normally related with low to medium temperatures shear zones, locally associated with pseudotachyllites (CPRM, 1999).

The 1.89 Ga Itã granodioritic mylonite is similar in composition with the Caroebe granitoids (Água Branca Suite), located in the Anaua-Jatapu Domain. The mylonite is probably resulted of Caroebe granite deformed under greenschist to epidote-amphibolite metamorphic facies within wide shear zones. Thus, the E-W Itã Fault System post-dates these 1.89 Ga granitoids (K'Mudku or Itã related events?), and the location of the CGD boundaries also need to be reviewed. This boundary probably would be displaced to the north and placed in older NE-

SW Barauana lineament trends, similar to that observed in the Mucajaí region that separates two regions of distinct ages and thermal-tectonic evolution.

In conclusion, the data presented in this paper indicate that the structural pattern observed in the CG D in southeastern Roraima can be related with a main 1.94-1.93 Ga tectonic event hinderly affected by decoupled younger events (reactivation processes), namely the Itã (1.72-1.66 Ga) and the K'Mudku (1.33-1.00 Ga) events. This implies that the studied area has been subjected to major, long-lived structures in the the CGD, possibly related with continental-scale processes in the central portion of the Guyana Shield.

Acknowledgments

Special thanks to E. Klein (CPRM-Geological Survey of Brazil), P. A. Rolando and M. A. Galarza (ParáIso/UFPA) for help during Pb analytical procedures, and N. J. Reis (CPRM-Geological Survey of Brazil) for geological discussions. The authors are also grateful to CPRM-Geological Survey of Brazil, FINEP (CT-Mineral 01/2001 Project) and Isotope Geology Laboratory of UFPA (Federal University of Pará) for support the field and laboratorial works. Thanks also to two anonymous referees for the critical analysis of the manuscript.

References

- Almeida, M.E, Macambira, M.J.B., Faria, M.S.G. de. 2002. A Granitogênese Paleoproterozóica do Sul de Roraima. *In: SBG, Cong. Bras. Geol.*, 41, João Pessoa, Anais..., pp. 434. (in portuguese)
- Almeida, M.E., Macambira, M.J.B. Geology, Petrography and Mineralizations of Paleoproterozoic Granitoids from Uatumã-Anauá Domain (Guyana Shield), Southeast of Roraima State, Brazil. *Revista Brasileira de Geociências*, submitted.
- Almeida, M.E, Macambira, M.J.B., Galarza, M.A., Silva, L. Evidence of the widespread 1.90-1.89 Ga I-type, high-K calc-alkaline magmatism in Southeastern Roraima State, Brazil (central portion of Guyana Shield) based on Geochemistry and Zircon Geochronology. *Lithos*, submitted.
- Amaral, G. 1974. Geologia Pré-Cambriana da região Amazônica. Tese de livre docência, Instituto de Geociências, Universidade de São Paulo, São Paulo. 212 pp.
- Avelar, V.G. de, Lafon, J.M., Delor, C., Guerrot, C., Lahondère, D. 2003. Archean crustal remnants in the easternmost part of the Guyana Shield: Pb-Pb and Sm-Nd geochronological

- evidence for Mesoarchean versus Neoproterozoic signatures. *Géologie de la France*, 2-3-4, 83-99.
- Barron, C.N. 1966. Notes on the Stratigraphy of Guyana. In: Guyana Geol. Conf., 7, Paramaribo, *Proceed.*, 6, 1-28.
- Basei, M.A.S., Teixeira, W. 1975. Geocronologia do Território de Roraima. In: Conf. Geol. Interguianas, 10, Belém, *Anais*, 453-473.
- Bosma, W., Kroonenberg, S.B., Maas, K., De Roever, E.W.F. 1983. Igneous and Metamorphic Complexes of the Guyana Shield in Suriname. *Geol. Mijnbouw*, 62, 241-254p.
- Brito Neves, B.B. 1999. América do Sul: quatro fusões, quatro fissões e o processo acrescionário andino. *Rev. Bras. Geoc.*, 29, 379-392.
- Brito Neves, B.B., Almeida, F.F.M. 2003. A Evolução dos Cratons Amazônico e São Francisco comparada com o dos seus homólogos do hemisfério norte – 25 anos depois. In: SBG-Núcleo Norte, Simp. Geol. Amaz., 8, Manaus. CD-ROM. (in portuguese).
- Brown, M., 2001. From microscope to mountain belt: 150 years of petrology and its contribution to understanding geodynamics, particularly the tectonics of orogens: *Journal of Geodynamics*, 32, 115–164.
- Brown, M. 2003. Hot orogens, tectonic switching, and creation of continental crust: Comment and reply. *Geology*, 31 (6), 9.
- Brown, M., Dallmeyer, R.D. 1996. Rapid Variscan exhumation and role of magma in core complex formation: Southern Brittany metamorphic belt, France: *Journal of Metamorphic Geology*, 14, 361–379.
- Brown, M., Solari, G.S. 1999. The mechanism of ascent and emplacement of granite magma during transpression: a syntectonic granite paradigm. *Tectonophysics*, 312 (1), 1-33.
- Chen, Y.D., O'Reilly, S.Y., Griffin, W.L., Krogh, T.E. 1998. Combined U-Pb dating and Sm-Nd studies on lower crustal and mantle xenoliths from the Delegate basaltic pipes, southeastern Australia. *Contrib. Miner. Petrol.*, 130, 154–161.
- Collins, W.J., 2002a. Nature of extensional accretionary orogens. *Tectonics*, 21 (4), 6-1.
- Collins, W.J., 2002b. Hot orogens, tectonic switching, and creation of continental crust. *Geology*, 30, 535–538.
- Coney, P.J., 1992. The Lachlan belt of eastern Australia and circum-Pacific tectonic evolution: *Tectonophysics*, 214, 1–25.

- Cordani, U.G., Brito Neves, B.B. 1982. The Geologic Evolution of South America During the Archean and Early Proterozoic. *Rev. Bras. Geoc.*, 12 (1-3), 78-88.
- CPRM. 1984. Projeto Aerogeofísico Rio Branco. Convênio CPRM/DNPM, Rio de Janeiro, volumes I e II. (in portuguese).
- CPRM. 1999. Programa Levantamentos Geológicos Básicos do Brasil. *Roraima Central, Folhas NA.20-X-B e NA.20-X-D (integrals), NA.20-X-A, NA.20-X-C, NA.21-V-A e NA.21-V-C (parciais)*. Escala 1:500.000. Estado de Roraima. Manaus, CPRM, 166 p. CD-ROM.
- CPRM. 2000. Programa Levantamentos Geológicos Básicos do Brasil. *Caracará, Folhas NA.20-Z-B e NA.20-Z-D (integrals), NA.20-Z-A, NA.21-Y-A, NA.20-Z-C e NA.21-Y-C (parciais)*. Escala 1:500.000. Estado de Roraima. Manaus, CPRM, 157 p. CD-ROM.
- CPRM. 2002. Field Workshop: Manaus (AM)-Pacaraima (RR) Transect. GIS Brasil Program. CPRM, Manaus, Internal Report. (in portuguese)
- CPRM. 2003. Programa Levantamentos Geológicos Básicos do Brasil. *Geologia, Tectônica e Recursos Minerais do Brasil : sistema de informações geográficas - SIG*. Rio de Janeiro : CPRM , 2003. Mapas Escala 1:2.500.000. 4 CDs ROM.
- CPRM. 2006. Programa Integração, Atualização e Difusão de Dados da Geologia do Brasil: Subprograma Mapas Geológicos Estaduais. *Geologia e Recursos Minerais do Estado do Amazonas*. Manaus, CPRM/CIAMA-AM, 2006. Mapa Escala 1:1.000.000. Texto explicativo, 148p. CD ROM.
- De Roeber, E.W.F., Lafon, J-M., Delor, C., Cocherie, A., Rossi, P., Guerrot, C., Potrel, A. 2003. The Bakhuis ultrahigh-temperature granulite belt (Surinam): I. petrological and geochronological evidence for a counterclockwise P-T path at 2.07-2.05 Ga. *Géologie de la France*, 2-3-4, 175-205.
- Ducea, M. 2001. The California arc: Thick granitic batholiths, eclogitic residues, lithospheric-scale thrusting and magmatic flare-ups: *GSA Today*, 11 (11), 4–10.
- Duebendorfer, E.M., Chamberlain, K.R., Jones, C.S. 2001. Paleoproterozoic tectonic history of the Cerbat Mountains, northwestern Arizona: Implications for crustal assembly in the southwestern United States. *Geol. Soc. Amer. Bull.*, 113 (5), 575–590.
- Ellis, D.J. 1987. Origin and evolution of granulites in normal and thickened crusts: *Geology*, 15 : 167–170.

- Faria, M.S.G. de, Santos, J.O.S. dos, Luzardo, R., Hartmann, L.A., McNaughton, N.J. 2002. The oldest island arc of Roraima State, Brazil – 2.03 Ga: zircon SHRIMP U-Pb geochronology of Anauá Complex. *In: SBG, Congr. Bras. Geol.*, 41, *Anais...*, pp. 306.
- Fraga, L.M.B. 2002. A Associação Anortosito–Mangerito–Granito Rapakivi (AMG) do Cinturão Guiana Central, Roraima e Suas Encaixantes Paleoproterozóicas: Evolução Estrutural, Geocronologia e Petrologia. DSc Thesis, CPGG/CG, Universidade Federal do Pará, Belém. 386 pp. (in portuguese)
- Fraga, L.M.B., Reis, N.J. 1996. A Reativação do Cinturão de Cisalhamento Guiana Central durante o Episódio K’Mudku. *In: SBG, Congr. Bras. Geol.*, 39, Salvador, BA, *Anais*, v. 1, pp. 424-426.
- Gaudette, H. E., Olszewski, W.J. Jr., Santos, J.O.S. 1996. Geochronology of Precambrian rocks from the northern part of Guiana Shield, State of Roraima, Brazil. *Journ. South Am. Earth Sci.*, 9, 183-195.
- Gibbs, A.K., Barron, C.N. 1993. *The geology of the Guyana Shield*. Oxford University Press, Oxford, N. York, 245 p.
- Hasui, Y., Haralyi., N.L.E., Schobbenhaus F°, C. 1984. Elementos geofísicos e geológicos da região amazônica: subsídios para o modelo geotectônico. *In: SBG-núcleo Norte, Symposium Amazonico*, 2, Manaus. *Anais...* v. 1, pp. 129-148. (in portuguese)
- Heizler, M.T., Kelley, S., Condie, K., Perilli, S., Bickford, M.E., Wortman, G.L., Lewry, J., Syme, R., Bailes, A., Corkery, T., Zwanzig, H. 2000. The thermal history of the Trans-Hudson Orogen, Canada. GeoCanada 2000, Calgary, AB, Program with abstracts CD-ROM.
- Hodges, K.V. 1991. Pressure-temperature-time paths. *Annu. Rev. Earth Planet. Sci.* 19 : 207-236.
- Klötzli, U.S. 1999. Th/U zonation in zircon derived from evaporation analysis: a model and its implications. *Chem. Geol.* **158**, 25-333.
- Lafon, J.-M., Delor, C., Barbosa, O.S. 2001. Granulitos tardi-Transamazônicos (2,06 Ga) na região norte do Estado do Amapá: o charnockito de Calçoene. *In: SBG-Núcleo Norte, Simp. Geol. Amaz.*, 7, Belém, pp. 39-42. CD-ROM (in portuguese)
- Lima, M.I.C. de, Montalvão, R.M.G. de, Issler, R.S., Oliveira, A. da S., Basei, M.A.S., Araújo, J.V.F., Silva, G.G. da 1974. Geologia da Folha NA/NB.22 - Macapá. *In: BRASIL, DNPM. Projeto RADAMBRASIL*, Rio de Janeiro, (Levantamento de Recursos Naturais, 6). (in portuguese)

- Luzardo, R., Reis, N.J. 2001. O Grupo Cauarane (Estado Roraima): uma breve revisão litoestratigráfica. In: SBG-Núcleo Norte, Simp. Geol. Amaz., 7, Belém. CD-ROM. (in portuguese).
- Macambira, M.J.B., Almeida, M.E., Santos, L.S. 2002. Idade de Zircão das Vulcânicas Iricoumé do Sudeste de Roraima: contribuição para a redefinição do Supergrupo Uatumã. In: SBG, Simpósio Sobre Vulcanismo e Ambientes Associados, 2, *Anais...*, pp. 22. (in portuguese)
- McConnel, R.B. 1962. Provisional geological map of British Guyana: 1:1.000.000. Geological Survey of British Guyana, Georgetown, Guyana.
- Pinson, W.H., Hurley, P.M., Mencher, E., Fairbain, H.W. 1962. K-Ar and Rb-Sr ages of biotites from Colombia, South America. *Geol. Soc. Amer. Bull.*, 73, 907-910.
- Premo, W.R., Fanning, C.M. 2000. SHRIMP U-Pb zircon ages for Big Creek gneiss, Wyoming and Boulder Creek batholith, Colorado: Implications for timing of Paleoproterozoic accretion of the northern Colorado province: *Rocky Mountain Geology*, 35, 31–50.
- Priem, H.N.A., Boelrijk, N.A.I.M., Hebeda, E.H., Verdurmen, E.A.Th., Verschure, R.H. 1971. Isotopic ages of the Trans-Amazonian acidic magmatism and the Nickerie Metamorphic Episode in the Precambrian Basement of Suriname, South America. *Geol. Soc. Amer. Bull.*, 82, 1667-1680.
- Reis, N.J., Fraga, L.M.B. 2000a. Geological and tectonic framework of Roraima State, Guyana Shield – An overview. In: Int. Geol. Congr., 31, Rio de Janeiro, *Expanded Abstract*. CD-ROM
- Reis N.J., Fraga, L.M.B. 2000b. The Kanuku Concept Review in That Portion of Central Guiana Domain, Guiana Shield. In: Int. Geol. Congr., 31, Rio de Janeiro, *Expanded Abstract*. CD-ROM
- Reis, N.R., Faria, M.S.G. de, Fraga, L.M.B., Haddad, R.C. 2000. Orosirian calc-alkaline volcanism from eastern portion of Roraima State – Amazon Craton. *Rev. Bras. Geoc.*, 30 (3), 380-383.
- Reis, N.J., Fraga, L.M., Faria, M.S.G. de, Almeida M.E. 2003. Geologia do Estado de Roraima. *Géologie de la France*, 2-3, 71-84. (in portuguese)
- Rogers, J.J.W. 1996. A history of continents in the past three billions years. *Journ. Geology*, 104, 91-107.

- Rogers, J.J.W., Santosh, M. 2002. Configuration of Columbia, a Mesoproterozoic supercontinent. *Gond. Res.* 5, 5–22.
- Santos, J.O.S. dos, Silva, L.C., Faria, M.S.G. de, Macambira, M.J.B. 1997. Pb-Pb single crystal, evaporation isotopic study on the post-tectonic, sub-alkalic, A-type Moderna granite, Mapuera intrusive suite, State of Roraima, northern Brazil. *In: SBG, Symposium of Granites and Associated Mineralizations, 2. Extended Abstract and Program., Brazil, pp. 273-275.*
- Santos, J.O.S. dos, Hartmann, L.A., Gaudette, H.E., Groves, D.I., McNaughton, N.J., Fletcher, I.R. 2000. A new understanding of the provinces of the Amazon Craton based on integration of field mapping and U-Pb and Sm-Nd geochronology. *Gond. Res.* 3 (4), 453-488.
- Santos, J.O.S. dos, Faria, M.S.G. de, Hartmann, L.A., McNaughton, N.J. 2002. Significant presence of the Tapajós-Parima Orogenic Belt in the Roraima region, Amazon Craton based on SHRIMP U-Pb zircon geochronology. *In: SBG, Cong. Bras. Geol., 51, João Pessoa, Anais... pp. 336.*
- Santos, J.O.S. dos, Potter, P.E., Reis, N.J., Hartmann, L.A., Fletcher, I.R., McNaughton, N.J. 2003. Age, source and Regional Stratigraphy of the Roraima Supergroup and Roraima-like Sequences in Northern South America, based on U-Pb Geochronology. *Geol. Soc. Amer. Bull.* 115 (3), 331-348.
- Santos, J.O.S. dos, Hartmann, L.A., Faria, M.S.G. de, Riker, S.R.L., Souza, M.M. de, Almeida, M.E., McNaughton, N.J. 2006a. A Compartimentação do Cráton Amazonas em Províncias: Avanços ocorridos no período 2000-2006. *In: SBG-Núcleo Norte, Simp. Geol. Amaz., 9, Belém, CD-ROM.*
- Santos, J.O.S. dos, Faria, M.S.G. de, Riker, S.R.L., Souza, M.M. de, Hartmann, L.A., Almeida, M.E., McNaughton, N.J., Fletcher, I.R. 2006b. A faixa colisional K'Mudku (idade Grenvilliana) no norte do Cráton Amazonas: reflexo intracontinental do Orógeno Sunsás na margem ocidental do cráton. *In: SBG-Núcleo Norte, Simp. Geol. Amaz., 9, Belém, CD-ROM.*
- Sena Costa, J.B., Hasui, Y. 1997. Evolução Geológica da Amazônia, in Costa, M.L., and Angelica, R.S. (eds), *Contribuições à Geologia da Amazônia*. FINEP, Sociedade Brasileira de Geologia, Núcleo Norte, Belém, Brazil, 1, pp. 15-90. abstract in english.
- Siddoway, C., Givot, R.M., Bodle, C.D., Heizler, M.T. 2000. Dynamic setting for Proterozoic plutonism: information from host rock fabrics, central and northern Wet Mountains,

- Colorado. Special issue: Proterozoic Magmatism of the Rocky Mountain Region, Carol Frost (ed.), *Rocky Mountain Geology*, 35 (1), 91-111.
- Sims, P.K., Stein, H.J. 2003. Tectonic evolution of the Proterozoic Colorado province, Southern Rocky Mountains. *Rocky Mountain Geology*, 38 (2), 183-204.
- Tassinari, C.C.G. 1996. O Mapa Geocronológico do Cráton Amazônico no Brasil: revisão dos dados isotópicos. Tese de Livre docência, Instituto de Geociências da Universidade de São Paulo. 139p. (in portuguese).
- Tassinari, C.C.G., Cordani, U.G., Nutman, A.P., Van Schmus, W.R., Bettencourt, J.S., Taylor, P.N. 1996. Geochronological systematics on Basement Rocks from the Rio Negro-Juruena Province (Amazonian Craton) and Tectonic Implications. *Intern. Geol. Rev.*, 38, 161-175.

Table 1. Single-zircon Pb-evaporation isotopic data from mylonitic biotite granodiorite (MA-042) and foliated hornblende-biotite monzogranite (MA-044) samples.

| sample / zircon number | Temp. (°C) | ratios | ²⁰⁴ Pb/ ²⁰⁶ Pb | 2σ | ²⁰⁸ Pb/ ²⁰⁶ Pb | 2σ | ²⁰⁷ Pb/ ²⁰⁶ Pb | 2σ | (²⁰⁷ Pb/ ²⁰⁶ Pb) _(c) | 2σ | age | 2σ | Th/U |
|---|---------------|--------|--------------------------------------|-----|--------------------------------------|------|--------------------------------------|-----|--|-----------------|------|------------------------|------|
| Mylonitic biotite granodiorite | | | | | | | | | | | | | |
| MA42/01 | *1450 | 0/8 | 0.000116 | 26 | 0.18932 | 213 | 0.11578 | 63 | 0.11578 | 72 | 1868 | 11 | 0.54 |
| MA42/02 | *1450 | 0/28 | 0.000112 | 23 | 0.17927 | 74 | 0.11535 | 25 | 0.11354 | 64 | 1857 | 10 | 0.51 |
| | 1500 | 36/36 | 0.000014 | 2 | 0.19437 | 71 | 0.11565 | 47 | 0.11559 | 50 | 1888 | 8 | 0.55 |
| MA42/03 | #1450 | 0/32 | 0.000651 | 41 | 0.20128 | 60 | 0.12094 | 23 | 0.11176 | 63 | 1828 | 10 | 0.58 |
| MA42/04 | 1450 | 18/18 | 0.000154 | 12 | 0.19439 | 168 | 0.11663 | 38 | 0.11490 | 50 | 1879 | 8 | 0.55 |
| | 1500 | 32/32 | 0.000016 | 9 | 0.20432 | 107 | 0.11578 | 49 | 0.11567 | 54 | 1891 | 8 | 0.58 |
| MA42/05 | *1450 | 0/20 | 0.000359 | 12 | 0.14187 | 189 | 0.11625 | 20 | 0.11159 | 26 | 1826 | 4 | 0.44 |
| | 1500 | 38/38 | 0.000063 | 9 | 0.17983 | 160 | 0.11622 | 28 | 0.11528 | 33 | 1885 | 5 | 0.51 |
| | 1550 | 26/26 | 0.000077 | 5 | 0.17843 | 63 | 0.11684 | 22 | 0.11575 | 22 | 1892 | 3 | 0.51 |
| MA42/06 | *1450 | 0/36 | 0.000157 | 26 | 0.18369 | 195 | 0.11334 | 39 | 0.11171 | 71 | 1828 | 12 | 0.57 |
| | *1500 | 0/8 | 0.000073 | 16 | 0.19334 | 296 | 0.11483 | 41 | 0.11385 | 47 | 1862 | 7 | 0.60 |
| 150 (282) | | | | | | | | | | mean age | | 1890 4 USD 1.7 | |
| Foliated hornblende-biotite monzogranite | | | | | | | | | | | | | |
| MA44/03 | *1450 | 0/16 | 0.000494 | 89 | 0.07691 | 73 | 0.10150 | 194 | 0.09526 | 110 | 1533 | 22 | 0.22 |
| | *1500 | 0/16 | 0.000086 | 2 | 0.17460 | 132 | 0.11172 | 139 | 0.11167 | 141 | 1827 | 23 | 0.50 |
| MA44/05 | *1450 | 0/8 | 0.000000 | 0 | 0.15711 | 169 | 0.10363 | 53 | 0.10363 | 53 | 1690 | 9 | 0.45 |
| MA44/06 | 1450 | 22/22 | 0.000079 | 26 | 0.16616 | 3523 | 0.10633 | 370 | 0.10534 | 222 | 1721 | 77 | 0.48 |
| MA44/07 | #1450 | 0/8 | 0.000521 | 44 | 0.15396 | 118 | 0.11148 | 41 | 0.10437 | 73 | 1703 | 13 | 0.44 |
| MA44/08 | 1500 | 14/14 | 0.000363 | 106 | 0.11318 | 224 | 0.10925 | 65 | 0.10459 | 179 | 1707 | 32 | 0.33 |
| MA44/11 | *1450 | 0/28 | 0.000375 | 3 | 0.13889 | 105 | 0.10778 | 30 | 0.10258 | 45 | 1672 | 8 | 0.40 |
| MA44/12 | #1450 | 0/8 | 0.001250 | 58 | 0.19704 | 106 | 0.11860 | 35 | 0.10153 | 88 | 1652 | 16 | 0.57 |
| | 1500 | 8/8 | 0.000136 | 34 | 0.17190 | 192 | 0.10918 | 108 | 0.10733 | 118 | 1755 | 20 | 0.50 |
| MA44/14 | 1450 | 26/26 | 0.000391 | 6 | 0.16686 | 70 | 0.11208 | 16 | 0.10666 | 26 | 1743 | 9 | 0.48 |
| MA44/16 | *1450 | 0/14 | 0.000314 | 6 | 0.15654 | 249 | 0.10736 | 16 | 0.10736 | 16 | 1684 | 6 | 0.45 |
| MA44/17 | *1450 | 0/28 | 0.000305 | 2 | 0.13550 | 37 | 0.10395 | 36 | 0.10395 | 28 | 1617 | 5 | 0.39 |
| MA44/18 | 1450 | 26/26 | 0.000277 | 21 | 0.13612 | 113 | 0.10872 | 37 | 0.10492 | 29 | 1713 | 5 | 0.39 |
| | 1500 | 8/8 | 0.000092 | 12 | 0.12460 | 670 | 0.10618 | 268 | 0.10618 | 268 | 1735 | 46 | 0.36 |
| 104 (230) | | | | | | | | | | mean age | | 1724 14 USD 3.5 | |

Notes: The total blocks analyzed are shown in brackets in the *number of blocks* column, but only first number (out of bracket) is utilized for age calculation. Values in italic were not included in the age calculation of the grain (# - step discarded due to scatter more than two standard deviations from the average age; * - step manually discarded due to higher or lower values of the ²⁰⁷Pb/²⁰⁶Pb ratio in relation to the mean). (c) ratios corrected for initial common Pb. Th/U ratios calcul: $Th = \frac{[(^{208}Pb/^{206}Pb)/(\lambda Th * T) - 1] + (^{208}Pb/^{206}Pb)}{[(^{208}Pb/^{206}Pb)/(\lambda U * T) - 1] + (^{208}Pb/^{206}Pb)}$; $\lambda Th = 4.94750 * 10^{-12}$; $\lambda U = 1.55125 * 10^{-11}$ (in Klotzli, 1999).

**Geology, petrography and mineralizations of Paleoproterozoic
granitoids from Uatumã-Anauá Domain, central portion of Guyana
Shield, southeast of Roraima, Brazil**

Marcelo Esteves Almeida^{1,2*}, Moacir José Buenano Macambira²

¹CPRM – Geological Survey of Brazil, Av. André Araújo 2160, Aleixo, CEP 69060-001, Manaus, Amazonas, Brazil

²Isotope Geology Laboratory, Center of Geosciences, Federal University of Pará, Rua Augusto Corrêa s/n, Guamá, CEP
66075-110, Belém, Pará, Brazil

* Corresponding author; ph.: +55-92-2126-0301, fax: +55-92-2126-0319, e-mail adress: marcelo_almeida@ma.cprm.gov.br

ARTIGO SUBMETIDO AO CORPO EDITORIAL DA REVISTA BRASILEIRA DE GEOCIÊNCIAS

Words: summary (80), resumo (233), abstract (191), body text (8003), table (269) and figure (755) captions.

Total: 3 tables and 11 figures.

RESUMO

ABSTRACT

INTRODUCTION

UATUMÃ-ANAUÁ DOMAIN

NORTHERN AREA

TTG-like Anauá Complex and Cauarane Group

S-Type Serra Dourada Granite

Martins Pereira Granitoids

GRANODIORITES AND MONZOGRANITES

PODS AND LENSES OF LEUCOGRANITES

ENCLAVES

Tonalitic Enclaves

Others Enclaves

SOUTHERN AREA

Caroebe and Água Branca Granitoids

JABURUZINHO FACIES

ALTO ALEGRE FACIES

Igarapé Azul Granitoids

SARAMANDAIA FACIES

VILA CATARINA FACIES

CINCO ESTRELAS FÁCIES

PETROGRAPHIC FEATURES IN COMMON

ENCLAVES

A-TYPE GRANITES

Moderna Granite and related granitoids

Mapuera Granite and related granitoids

MINERAL OCCURRENCES

DISCUSSION AND CONCLUSIONS

Acknowledgments

References

RESUMO

Mapeamentos geológicos na escala regional têm identificado no Domínio Uatumã-Anauá (DUA), sudeste do Estado de Roraima (Brasil), porção central do Escudo das Guianas, um amplo domínio de granitóides cálcio-alcálicos. Estes granitóides estão distribuídos em diferentes associações magmáticas com idades, estilos de deformação e afinidades químicas particulares. Neste trabalho, mapeamento geológico de maior detalhe, apoiado por estudo petrográfico, propiciou a distinção de algumas dessas associações e a sua separação em duas áreas distintas (norte e sul). Os granitóides do setor norte do DUA (1,97-1,96 Ga), representados pelos granitos Martins Pereira e Serra Dourada, ocorrem invariavelmente deformados, em geral associados a amplas zonas de cisalhamento dúctil de direções NE-SW a E-W. Ainda no setor norte do DUA, restos de rochas mais antigas do embasamento (2,03 Ga) são representadas por coberturas metavulcanossedimentares (Grupo Cauarane) e associações do tipo TTG (Complexo Anauá). Já os granitóides do setor sul do DUA (1,90-1,89 Ga), como os granitos Igarapé Azul e Caroebe (Suíte Água Branca), não estão deformados, sendo afetados apenas localmente por zonas de cisalhamento NE-SW. Além disso, dois eventos graníticos tipo-A estão representados em todo o DUA pelos granitóides Moderna (~1,81 Ga) e Mapuera-Abonari (~1,87 Ga). Em termos de mineralizações, ocorrências primárias de ouro estão hospedadas nos granitóides Martins Pereira (setor norte), enquanto ocorrências aluvionares de Nb-Ta são encontradas no Granito Igarapé Azul (setor sul) e pegmatitos com ametista estão presentes em corpos relacionados ao Granito Moderna.

Palavras-chaves: Roraima, Escudos das Guianas, Petrografia, Proterozóico, Granitóides

ABSTRACT

Regional mapping carried out in the Uatumã-Anauá Domain (UAD), Guiana Shield, Southeastern Roraima State (Brazil), has showed widespread calc-alkaline granitic magmatism. These granitoids are distributed into several magmatic associations with different Paleoproterozoic (1.97-1.89 Ga) ages, structural and geochemical affinities. In this paper, more detailed mapping and petrographic studies have distinguished two main subdomains in UAD. In the northern UAD, the Martins Pereira and Serra Dourada S-type granites (1.97-1.96 Ga) are deformed and affected by NE-SW and E-W shear-zones. Inliers of basement (2.03 Ga) outcrop to northeastern part of this area, and are formed by metavolcano-sedimentary sequence (Cauarane Group) and TTG-like calc-alkaline association (Anauá Complex). Younger and undeformed (with local discrete NE-

SW shear zones) Igarapé Azul (Igarapé Azul suite) and Caroebe (Água Branca suite) granites outcrop in the southern UAD. A-type granites such as Moderna (1.81 Ga) and Mapuera (1.87 Ga) granites, cross cut both areas of UAD. The geological mapping also identified three main types of metalotects in this region. Gold mineralization is observed in Martins Pereira-Serra Dourada granitoids (northern UAD), alluvial columbite-tantalite is related to Igarapé Azul granitoids (southern UAD), and amethyst is associated to pegmatites from Moderna A-type granites.

Keywords: Roraima, Guyana Shield, Petrography, Proterozoic, Granitoids

INTRODUCTION

Calc-alkaline I-type granitoids, including aluminous to alkaline A-type granites, charnockitic rocks and minor S-type granites (CPRM 1999, 2000), are widespread on the central portion of Guyana Shield, southeastern Roraima State, Brazil (**Fig. 1**). The geological setting incorporates strong differences between low- and high-grade terranes, where the tectonic regime is also complex (overprinting events) and the relationship between granitogenesis and the major orogeny is not well established. This uncertain geological picture is mainly resulted from scarce geological mapping.

Nevertheless, based on lithostructural and geochronological data (**Fig. 1**), CPRM (2006 modified of Reis *et al.* 2003) outlined different lithological associations in Roraima State according to the following four domains proposed for these authors:

- Surumu Domain (north-northeastern Roraima) exhibits WNW-ESE and E-W structural trends. Calc-alkaline granites and volcanic rocks (1.98-1.95 Ga) prevail and show local greenschist-facies deformational features. Intracratonic sedimentary sequences (1.87-1.78 Ga) partly cover the volcanic rocks. Late to post-Transamazonian supracrustal rocks (2.03-1.97 Ga) are exposed in the southwestern part.
- Central Guyana Belt (central Roraima) shows NE-SW structural trends. There, amphibole-facies gneiss (1.94-1.93 Ga) predominates over granulite-facies rocks. A typical Mesoproterozoic AMG association (1.56-1.53 Ga) of anorthosite (gabbro), mangerite and rapakivi granite intrudes the older units.
- Parima Domain (west-northwestern Roraima) has predominantly NW-SE to E-W foliation and extensive late to post-Transamazonian granite-greenstone terranes. Granitic plutons and volcanic rocks, similar to those exposed in the Surumu Domain, are subordinated. Batholiths

and stocks of rapakivi granite (1.55 Ga) as well as younger sedimentary sequences are also present.

→ Uatumã-Anauá Domain (southeastern Roraima, northeastern Amazonas and northwestern Pará) exhibits NW-SE and NE-SW structural trends and widespread granite magmatism (2.03-1.81 Ga). Gneissic and supracrustal rocks are deformed into greenschist to amphibolite facies.

The studied area encompass mainly calc-alkaline granitoids included in Uatumã-Anauá Domain - UAD, such as Martins Pereira (Almeida *et al.* 2002), Igarapé Azul (Faria *et al.* 1999, Almeida *et al.* 2002) and Caroebe (this paper) granites. Locally, they host mineral occurrences like as gold and columbite-tantalite.

In this paper, we summarize the results of field and petrographic studies and propose a new geological map based on granitoid rocks groups and mineralizations related for the north-western part of the UAD, providing new insights about the granitoids in southeastern Roraima. It represents the first approach to correlate the granite tipology and regional stratigraphy with tectonic setting for the central Guyana Shield.

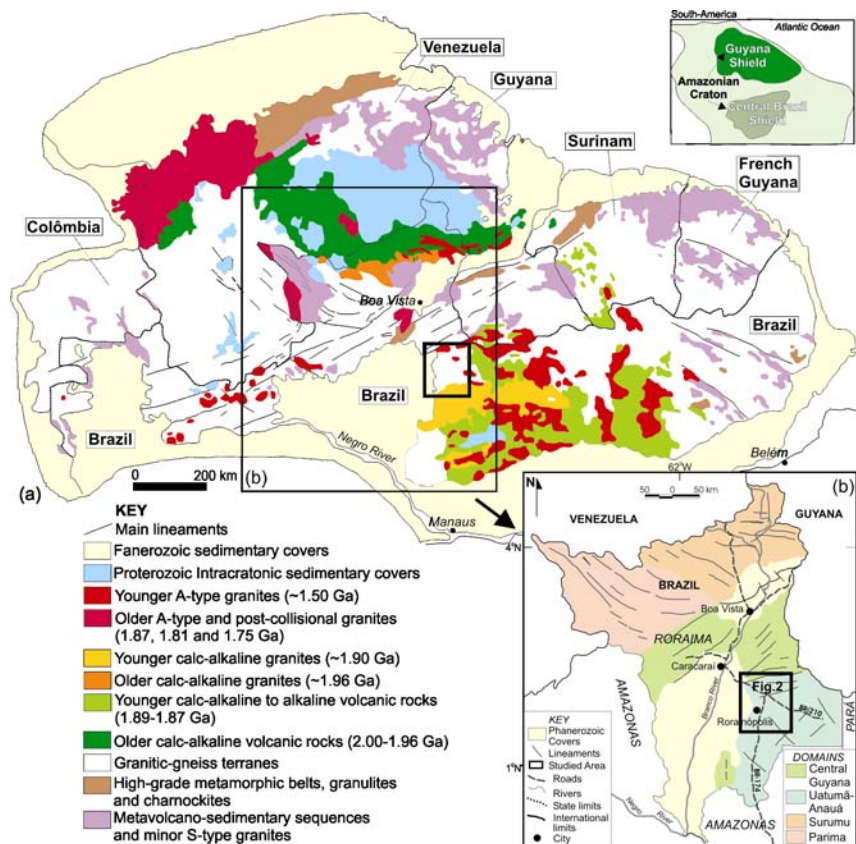


Fig. 1. Geological sketch map of (a) Guyana Shield (modified of Gibbs and Barron, 1993) and location of the studied area showing the (b) southeast of Roraima State and boundaries, including the lithostructural domains after CPRM (2006). For studied area details (small rectangle) see fig. 2.

UATUMÃ-ANAÚÁ DOMAIN

The Uatumã-Anauá Domain (UAD, CPRM 2006 modified of Reis and Fraga 2000, Reis *et al.* 2003), also named as northern Tapajós-Parima Belt (Uaimiri domain, Santos *et al.* 2000) or northern Ventuari-Tapajós Province (Tassinari and Macambira 1999), is characterized by old metamorphic basement and intrusive granitoids (**Fig. 2**).

According to Faria *et al.* (2002), in the northern Uatumã-Anauá Domain (NUAD) the basement is an island arc (Anauá Arc) represented by metagranitoids and TTG-like orthogneiss, including meta-mafic to meta-ultramafic enclaves (Anauá Complex), and inliers of metavolcano-sedimentary rocks (Cauarane Group). This basement occurs in the northern part of the studied area (**Fig. 2**), and is intruded by S-type (Serra Dourada) and I-type calc-alkaline (Martins Pereira) granites, which correspond to the 2.03 to 1.96 Ga Martins Pereira-Anauá Granitic Terrane (Almeida *et al.* 2002).

In the southern part of the Uatumã-Anauá Domain (SUAD, **Fig. 2**), Caroebe and Igarapé Azul calc-alkaline granitoids are ~70 M.y. younger than Martins Pereira and Serra Dourada granites, and do not show regional deformation and metamorphic features. The Caroebe granitoids are coeval to Iricoumé volcanic rocks (Macambira *et al.* 2002) and both have similar geochemical characteristics (Reis *et al.* 2000). Locally, it is also observed charnockitic (Igarapé Tamandaré) and enderbitic (Santa Maria) plutons. These rock set composes the Igarapé Azul-Água Branca Granitic Terrane (Almeida *et al.* 2002).

Several A-type granitic bodies, as the Moderna (1.81-1.82 Ga), correlated to Madeira Suite (Costi *et al.* 2000, 1.82-1.79 Ga), and the Mapuera and Abonari (1.87 Ga) granites, are widespread in the UAD (**Fig. 2**) and cross cut the rocks described above. They are considered as related to a “post-orogenic to anorogenic” setting.

NORTHERN AREA

TTG-like Anauá Complex and Cauarane Group related rocks

The Anauá Complex (CPRM 2000) outcrops along Anauá and Novo rivers, and is mostly composed by 2.03 Ga metagranitoids and metadiorites enclosing mafic and ultramafic enclaves (Faria *et al.* 2003). According to these authors, the metagranitoids and metadiorites are chemically comparable to calc-alkaline rocks from TTG terranes. They also show two deformational phases: a) D₁, dominant with N63°E/34°NW foliation, and b) D₂, represented by a mylonitic foliation.

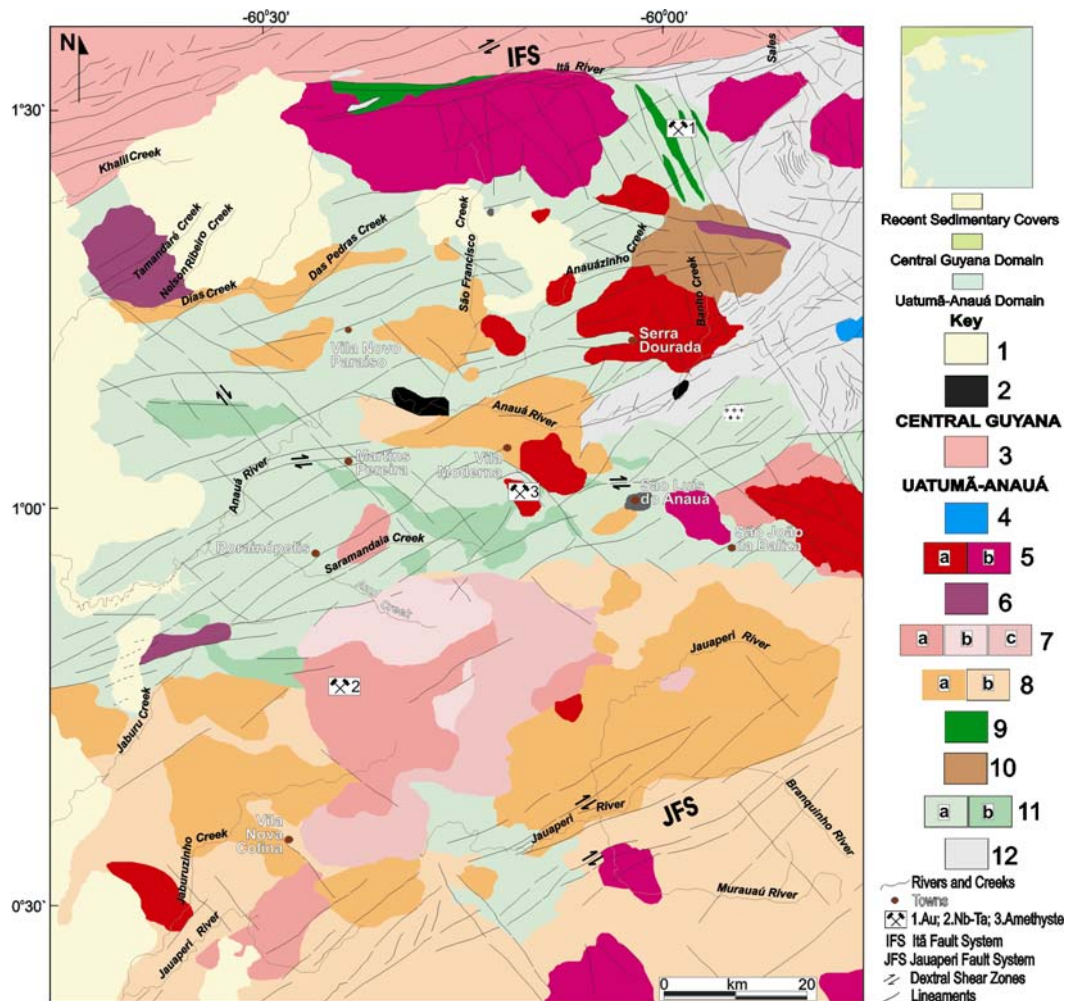


Fig. 2. Geological sketch map of southeastern Roraima modified from Almeida *et al.* (2002) and CPRM (2000). 1. Cenozoic sedimentary covers, 2. Undiscriminated plutonic mafic rocks, 3. Hornblende-biotite foliated granitoids (1.72 Ga), mylonitic granitoid (1.89 Ga), Barauana Granulite (1.94 Ga), augen gneisses, metagranitoids and orthogneisses (Rio Urubu Metamorphic Suite: 1.96-1.93 Ga), 4. Proterozoic sedimentary cover (Urupi Formation), 5. A-type Granites: a) Moderna (1.81 Ga) and b) Mapuera (1.87 Ga), 6. Santa Maria Enderbite, Tamandaré Charno-enderbite and undiscriminated charnockitoids, 7. Igarapé Azul granites (1.89 Ga): a) Vila Catarina, b) Estrela Guia, and c) Saramandaia facies, 8. Caroebe Granites (1.90-1.89 Ga): a) Jaburuzinho and b) Alto Alegre facies, 9. Calc-alkaline volcanic rocks (Iricoumé Group: 1.89 Ga), 10. S-type (cordierite) Serra Dourada Granite (1.96 Ga), 11. Martins Pereira Granite (1.97 Ga): a) High-K calc-alkaline granitoids b) granitoids with high U, Th, K contents, 12. Metavolcano-sedimentary sequence (Caurane Group related rocks: <2.03 Ga?) and TTG calc-alkaline association (Anauá Complex: 2.03 Ga).

The Caurane Group and related rocks are associated with the Anauá Complex and represents an important metavolcano-sedimentary sequence affected by low- to medium-grade metamorphism, locally in anatexis context, correlated to the Kwitaro Group, in South Guyana (Berrangé 1972). Detrital zircon crystals from the Caurane schist yielded two different populations: i) 2229 ± 8 Ma (U-Pb ID-TIMS, CPRM 2003 modified of Gaudette *et al.* 1996) and ii) 2074 ± 15 Ma (U-Pb SHRIMP, CPRM 2003), interpreted as the maximum age of the sedimentation.

The Caurane Group in this region comprises mica schists, quartzites, paragneisses, metacherts, phyllytes and amphibolites with at least two deformational phases (CPRM 2000): a)

S_n main foliation (N56°E/87°SE) and b) S_{n+1} foliation (N45°E/70°NW). According to CPRM (2000), the paragneisses are geochemically similar to immature clastic sedimentary rocks (graywackes and arkoses), whereas the amphibolitic rocks have high TiO_2 contents and MORB-REE pattern. Faria *et al.* (2002) suggest that these supracrustal rocks are a back-arc basin sequence, related to Anauá island arc, developed in the first accretionary orogenic event of the Tapajós-Parima Cycle (Santos *et al.* 2000).

S-type Serra Dourada Granite

The S-type granitoids of southeastern Roraima were initially described by Faria *et al.* (1999) and encompassed into the Igarape Azul Granite. However, Almeida *et al.* (2002) and Almeida and Macambira (2003), based on geochemical features and more detailed geological mapping in its type-area, subdivided the Igarape Azul Granite into three different granitic types: Serra Dourada Granite (“truly” S-type), Martins Pereira Granite (older and deformed I-type high-K calc-alkaline) and the Igarapé Azul Granite (younger and undeformed I-type high-K calc-alkaline).

The S-type Serra Dourada Granite has approximately 170 km², outcrops near to homonymous small town, and is associated with rocks from the Anauá Complex and Cauarane Group (**Fig. 2**). These granitoids are equigranular and coarse to medium-grained showing monzogranitic and minor syenogranitic and granodioritic compositions (**Fig 3a, table 1**) with diagnostic aluminous minerals such as biotite, muscovite and sometimes pinitized cordierite and sillimanite. Evidences of dynamic recrystallization and planar fabric are subordinated. The mineral assemblage these rocks is composed by alkalifeldspar (15.8-39.0 %), quartz (18.4-31.0 %), plagioclase (19.0-39.3 %), biotite (0.9-20.8 %), muscovite (1.7-6.4 %), and minor cordierite, monazite, xenotime, opaque minerals, apatite, zircon and sillimanite, including secondary minerals such as epidote, titanite, chlorite and leucoxene (**table 1**).

In general quartz is modally higher than feldspars and show commonly embayment contacts. The slight red-brown biotite is intergrown with muscovite (sub-solidus) or as subhedral isolated crystals showing several metamict mineral inclusions. Muscovite rarely occurs as large separate (primary?) crystals. Cordierite appears as crystals around 2 mm long with sillimanite inclusions, commonly having a crude rectangular tabular habit and is always partly to totally altered (pinitization and sericitization). Ilmenite and magnetite are also observed. Monazite and

xenotime are the main accessory minerals, showing pale yellow colours and wide pleochroic haloes in the mineral host.

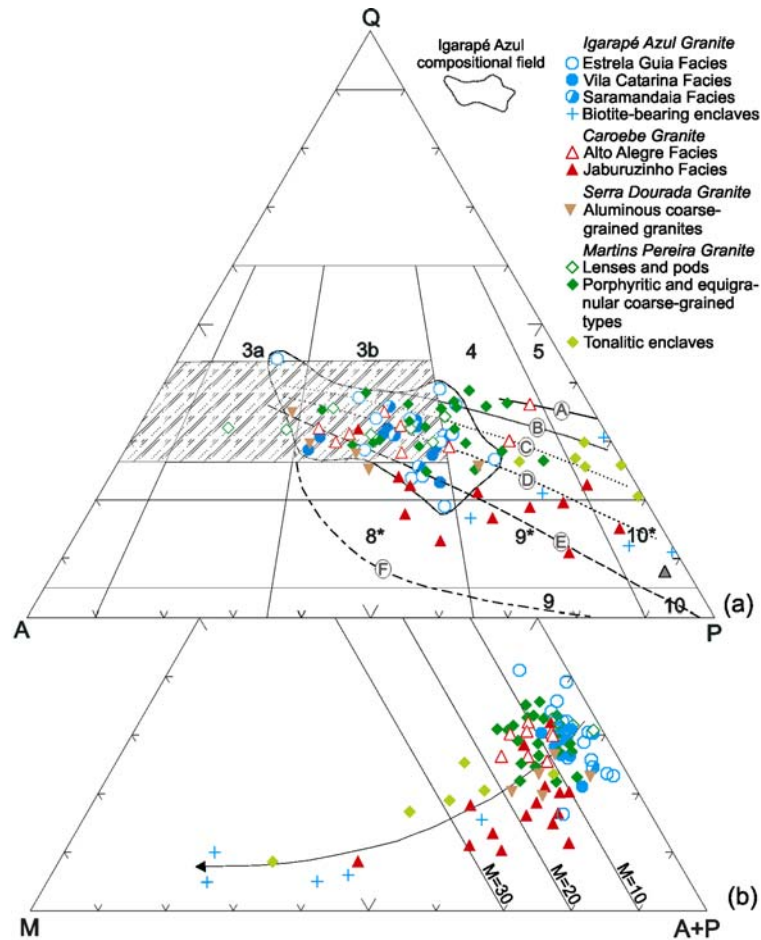


Fig. 3. QAP (a) and QM(A+P) (b) diagrams (Streckeisen, 1976) for samples from Martins Pereira, Serra Dourada, Caroebe and Igarapé Azul granitoids (including enclaves). For modal contents see the tables 1, 2 and 3. Q - Quartz, A - Alkalifeldspar, P - Plagioclase, M - Mafic minerals. The average trends of some plutonic suites was taken of Lameyre *et al.* (1982) and Lameyre and Bonin (1991). Fields: 3a. syenogranite; 3b. monzogranite; 4. granodiorite; 5. tonalite; 9. Monzodiorite/monzogabbro; 10. diorite/gabbro; 8*. quartz monzonite; 9*. quartz monzodiorite/quartz monzogabbro; 10*. quartz diorite/quartz gabbro. Calc-alkaline trends: Tonalitic-trondhjemitic from (A) SW Finland; and granodioritic from (B) Corsica-Sardinia, (C) Chile, (D) Peru and (E) Sierra Nevada. Monzonitic trend: (F) Vosges and Corsica. Granites of crustal origin: shaded area.

The existence of associated supracrustal rocks and aluminous paragenesis suggests a paraderived origin for Serra Dourada Granite, involving anatexis in low (cordierite crystallization) to moderate H_2O -activity (minor magnetite and biotite crystallization), and low to medium pressure (cordierite crystallization) condition (White 1992). Similar S-type granite was dated in Guiana Central Domain by CPRM (2003) by zircon U-Pb SHRIMP method, and yielded 1668 ± 3.5 Ma (crystallization age) and 2.05 to 2.07 Ga ages (late-Transamazonian inheritance).

Martins Pereira Granite

The Martins Pereira granitic batholith (up to 3780 km²) occurs to south of the Itã System Fault and its main outcrops have been recorded around the Martins Pereira (type-area), Rorainópolis and São Luís do Anauá towns. This granitic batholith is composed by medium-grained porphyritic gray granodiorites to monzogranites and locally by fine to medium-grained dark gray tonalites showing a calc-alkaline granodioritic trend (Chile related, Lameyre and Bowden 1982, Lameyre and Bonin 1991) in QAP diagram (**Fig 3a, table 1**). Intrusive small pods and lenses of leucogranites are also associated.

GRANODIORITES AND MONZOGRANITES

In general, the granodiorites and monzogranites are locally slight bluish and have conspicuous porphyritic (locally equigranular) texture with feldspar megacrystals (**Fig. 4a and 4b**), medium to coarse-grained matrix and 10% to 18% of mafic mineral (**Fig 3b, table 1**). Foliation with local banding and subparallel (N75°E/80°SE) mylonitic foliation are common in these granitoids (**Fig. 5a**) but, despite of heterogeneous solid-state deformation, only locally quartz shows high dynamic recrystallization features in thin section (**Fig. 5b**). Exceptionally, in ductile narrow mylonitic zones, feldspars and quartz with granoblastic polygonal texture are observed (indicating static recrystallization), which suggests temperatures over ca. 350°–400°C (e.g. Passchier and Trouw 1996). The mineral assemblage these rocks is composed by alkali-feldspar (9.7-36.6 %), quartz (20.5-35.3 %), plagioclase (22.7-52.5 %), biotite (4.3-12.1 %), muscovite (0.1-4.4 %) and minor epidote, opaque minerals, titanite, allanite, apatite, zircon and rare tourmaline (**table 1**).

The feldspar megacrystals (mainly alkali-feldspar) have ovoid and tabular shapes (**Fig. 4a**), with large size ranging from 2 to 8 cm and white to slightly pink colors. They are enclosed by weakly to highly deformed and foliated matrix. Many times these megacrystals are parallel to foliation, including also the types which the matrix does not have strong anisotropic fabric (magma flow?). Plagioclase is weakly zoned and locally shows obliterated multiple twinning. Highly altered calcic cores are uncommon. Anhedral to subhedral quartz shows undulatory extinction or partially recrystallized grains. Quartz inclusions (drop-like) are common in alkali-feldspar megacrystals.

Subhedral biotite has brown-greenish to straw-yellow colors, medium grain size and is associated with epidote, opaque minerals, allanite, titanite and rarely with tourmaline prismatic crystals. Biotite crystals are frequently parallel, overcoat in highly deformed types. In this case,

the biotite cleavages are iron-titanium oxides full, locally wick and folded (kink). In different stages, biotite also occurs partially replaced by muscovite and chlorite. Muscovite is commonly irregular grain, mostly associated with biotite. Prismatic or irregular muscovite crystals also replace plagioclase and alkalifeldspar megacrystals.

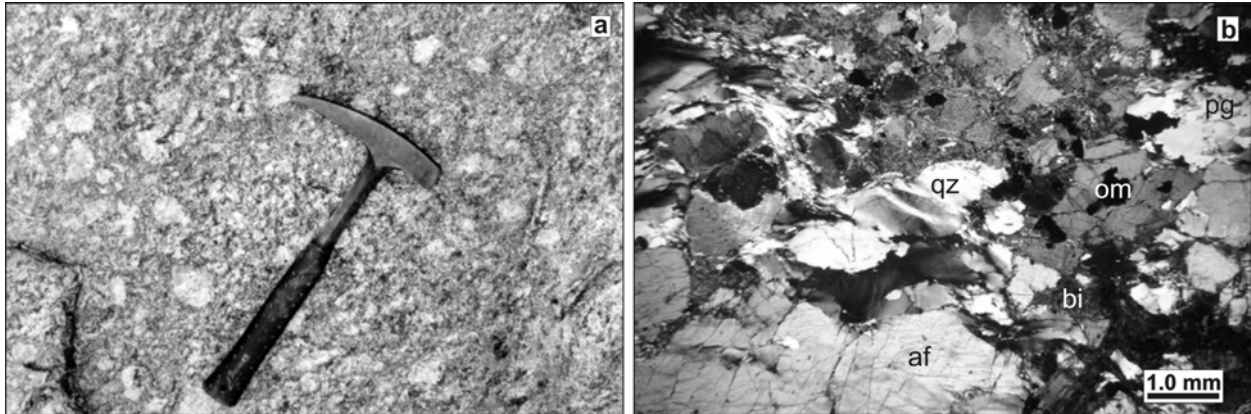


Fig. 04. Features of Martins Pereira Granite: a) Isotropic porphyritic biotite monzogranite (outcrop MA-218), showing ovoid alkalifeldspar megacrystals (< 80 mm in diameter). b) Photomicrography of porphyritic biotite monzogranite showing slightly orientated biotite, dynamically recrystallized quartz and fractured alkalifeldspar (Cross-polarized light, 1.25x). Obs: af. alkalifeldspar, pg. plagioclase, qz. quartz, biotite, om. opaque mineral.

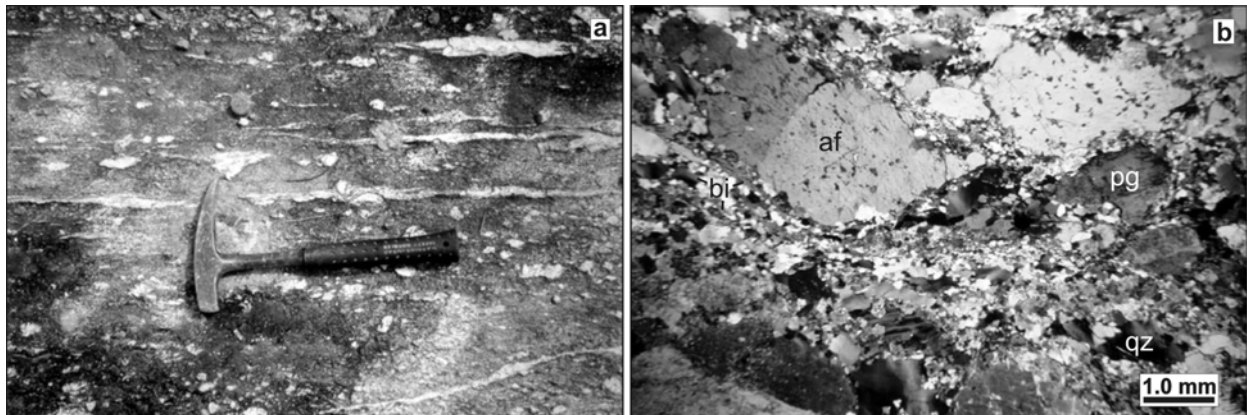


Fig. 05. Features of deformed Martins Pereira Granite: a) Biotite monzogranite (porphyritic facies) showing mylonitic foliation (N75°E/90° to N82°E/90°), rounded megacrystals with pressure shadows and locally quartz ribbons in dextral shear zone (outcrop MA-61). b) Photomicrography showing protomylonitic texture. Note the local matrix grain reduction by dynamic recrystallization (including core-and-mantle texture) and orientated mafic minerals contouring rounded alkalifeldspar megacrystals (Cross-polarized light, 1.25x). Obs: af. alkalifeldspar, pg. plagioclase, qz. quartz, bi. biotite.

LEUCOGRANITIC PODS AND LENSES

The leucogranites are very restricted and occur such as pods, veins and lenses subconcordant to foliation of host-rock, with increasing abundance around Igarapé Azul and Martins Pereira granites geological contacts. They have few centimeters (rarely 5 meters) in thickness and show syenogranitic to granodioritic composition, equigranular and medium to coarse-grained texture. The contacts between leucogranites and foliated granodiorite and

monzogranite hosts are lobate to irregular (occasionally diffuse) and progressively change to regular and concordant style (**Fig 6**).



Fig. 06. Outcrop (MA-07) of Martins Pereira Granite showing pods and lenses of leucogranite (1) and monzogranite (2) in porphyritic biotite granodiorite (3) with N80°W/18°NE strike foliation locally disrupted by NS normal faults (F).

The rocks are characterized by grayish white colour, generally with sugar-like and isotropic fabric, locally showing dynamic recrystallization and cataclastic features. The mineral assemblage is composed by alkali feldspar (21.1-54.6 %), quartz (27.1-32.5 %), plagioclase (8.4-41.7 %), biotite (1.2-4.9 %), muscovite (0.1-3.2 %), and minor epidote, opaque minerals, titanite, allanite, apatite and zircon (**table 1**).

The alkali feldspar is locally microperthite and is medium to coarse grained, subhedral to anhedral and tabular. It encloses several minerals, such as plagioclase, quartz and muscovite. Eventually, it also shows sericitization, fractures and undulatory extinction. Plagioclase shows slight compositional zoning, locally raised by cores submitted to secondary alteration (epidote, carbonate and sericite). It is tabular, subhedral, locally embayed with alkali feldspar grains and shows slight undulatory extinction.

The quartz has also undulatory extinction, is partially recrystallized, subhedral to anhedral and fine to medium-grained with abundant embayment features. The biotite has moderate pleochroism, straw yellow color, slightly undulatory extinction, medium to fine-grain size. It is partially to totally transformed into muscovite. Muscovite occasionally occurs as isolated crystals with undulatory extinction and associated with biotite and plagioclase. Tourmaline and igneous garnet are uncommon.

ENCLAVES

Tonalitic Enclaves

Tonalitic rocks in the Martins Pereira Granite (and minor granodiorites) are subordinated and occur like oblate and ellipsoidal enclaves concordant with the granodiorites and monzogranites foliation's (**Fig. 7a**). Furthermore, these enclaves have an internal structure which is visible at naked eye, emphasized by biotite crystals, systematically parallel to the host foliation. These elongated biotite-bearing tonalitic enclaves, and the leucogranitic pods and lenses are concordant to subconcordant with host structures, generating local banding.

The tonalitic enclaves are characterized by equigranular, medium to fine grained and lepidoblastic texture (**Fig. 7b**) and local and slight undulatory extinction in quartz and feldspar crystals. However, higher recrystallization stage or mineral stretching is not observed. They show also high mafic mineral contents (**Fig. 3b, table 1**), represented by epidote (0.1-12.5 %), titanite (1.0-3.8 %) and biotite (3.4-42.4 %), this last one partially replaced by muscovite (1.0-5.8 %) and chlorite (0.1-14.0 %). Other important accessory minerals are allanite, apatite, magnetite and zircon.

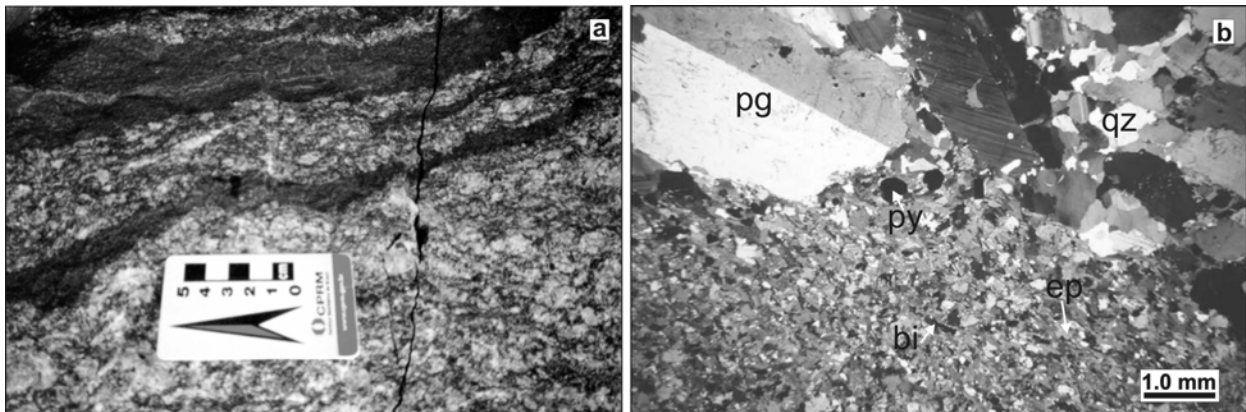


Fig. 07. Features of Martins Pereira Granite: a) Outcrop (MA-07) of deformed biotite granodiorite (porphyritic facies) showing lenses of mafic tonalitic gneiss. b) Photomicrography showing porphyritic granodiorite host (uppermost) and biotite-bearing tonalite enclave (lowermost) contact (Cross-polarized light, 1.25x). Obs: pg. plagioclase, qz. quartz, bi. biotite, ep. epidote, py. pyrite.

Others Enclaves

Other enclaves (xenoliths) represented by amphibolites, hornblende-rich igneous rocks (Anauá Complex) and paragneisses (Cauarane Group) are rare. The (meta)dioritic and (meta)quartz-monzodioritic enclaves are quite angular with slightly rounded vertices, greenish and isotropic to foliated that is locally disrupted by tonalitic veins network, but both (dioritic and tonalitic types) are enclosed by Martins Pereira granitoids. These xenoliths are equigranular, medium to coarse grained and have high mafic contents (biotite 25% and hornblende 20 %). The felsic minerals, such as quartz (10 %) and plagioclase (40 %), show just undulatory extinction

and local dynamic recrystallization features. The accessory minerals are mainly opaque (3 %), epidote (1 %) and apatite. Paragneissic xenoliths with cm-scale, angular shape and fine to medium-grained are very rare. They have an internal structure which is visible through the micaceous bands and metasedimentary relicts.

SOUTHERN AREA

Caroebe and Água Branca Granitoids

Several calc-alkaline granitic bodies in southern Roraima (Costi *et al.* 1984, Oliveira *et al.* 1996, CPRM 2000, Almeida *et al.* 2002) were by long time associated to the Água Branca Suite (Araújo Neto and Moreira 1976, Veiga *et al.* 1979, Jorge-João *et al.* 1985). The main granitic body of Água Branca Suite in this region, named as Caroebe Granite, is located to south of Rorainópolis, São Luiz do Anauá, São João da Baliza and Caroebe towns in the Jauaperi and Caroebe rivers region, including the Jaburuzinho creek basin.

The Caroebe batholith has around 65000 km² (CPRM 2003) and extend to northwestern Pará and northeastern Amazonas states, however, only the northwestern part (near to 4000 km²) of it is studied up to now. This granitic batholith was emplaced along EW to ENE-WNW structures, parallel to Martins Pereira metagranitoid host foliation, which is observed in other minor and similar granitic bodies (**Fig. 2**).

The Caroebe granitoids in southeastern Roraima occur in contact with coeval “Iricoumé” volcanics (Reis and Fraga 1996; Reis *et al.* 2000, Macambira *et al.* 2002) and intrude the Martins Pereira meta-granitoids. The Igarapé Azul Granite is quite younger than the Caroebe granitoids, and occurs locally cross-cutting the latter. Neogene sediments recover the western side of this granitic batholith. The Caroebe granitoids are characterized by extended compositional granitic association and calc-alkaline granodioritic serie (Peru and Sierra Nevada trends, Lameyre and Bowden 1982, Lameyre and Bonin 1996, **Fig. 3a**), subdivided in two main petrographic facies: Alto Alegre and Jaburuzinho (**Fig. 2**).

JABURUZINHO FACIES

The Jaburuzinho facies is represented by hornblende-bearing granitoids, such as granodiorites, monzogranites and tonalites, with minor diorites, quartz monzodiorites and quartz diorites (**Fig. 3a, table 2**). The main outcrops are located in Anauá (Jaburuzinho creek), Caroebe and Jauaperi river basins. They show homogeneous textures, equigranular to porphyritic types

(10% to 15% megacrystals content), medium to coarse-grain and gray colour. The scarce tabular alkalifeldspar megacrystals show white to slightly pinkish color and 15 to 25 mm in length, locally 50 mm (ratio 1:3). These megacrystal are frequently ENE-WSW orientated, suggesting magma flow process.

These granitoids have also abundant mafic clots and rounded circular autholits (**Fig. 8a**), including variable mafic mineral contents (12% to 65%, **Fig. 3b**). The mafic clots are sometimes interlinked and slightly orientated, without solid-state deformation and point out also magma flow. On the other hand, granitoids submitted to solid-state deformation are very rare, related with a strong ENE-WSW shear-zone (Jauaperi Fault System), located in Jauaperi and Branquinho rivers. The mineral assemblage (**table 2**) is formed by plagioclase (23.0-54.0 %), quartz (4.1-30.0 %), alkalifeldspar (1.9-34.5 %), biotite (6.0-19.9 %), hornblende (0.3-37.0 %), opaque minerals (mainly magnetite: 0.7-4.0 %), titanite (0.2-5.0 %), epidote, apatite, zircon and allanite. Muscovite and clinopyroxene are uncommon.

Plagioclase crystals are subhedral to euhedral, tabular, medium to coarse grained and shows strong normal to oscillatory zoning (**Fig. 8b**). In this last case, the An-enriched portions are raised by local saussuritization process. Polysynthetic twinning is very common and eventually also occurs combined with Carlsbad twinning. Disequilibrium features are locally present in partially corroded (irregular and embayment) rims. In these plagioclase megacrystals it is observed a quite linear flow, with similar strikes to the mafic minerals (ENE-WSW to NE-SW). A younger plagioclase generation is observed in matrix. It is subhedral, fine grained and shows subtle normal compositional zoning and several inclusions-like alkalifeldspar megacrystals.

Two quartz types are observed: a) interstitial, anhedral, medium grained, and b) subhedral, fine to medium grained with slight undulatory extinction. Under solid-state deformation, the quartz shows variable recrystallization stages. Normally, it shows fine grained subgrains outlining preserved ones, but granoblastic texture is also observed. Quartz ribbons are uncommon.

Microperthitic alkalifeldspar megacrystals (**Fig. 8b**) are anhedral (locally interstitial), tabular and show several inclusions (plagioclase, quartz drop-like, biotite, apatite, opaque minerals). Like as plagioclase megacrystals, they show a subtle ENE-WSW flow. Tartan twinning, occasionally combined with Carlsbad twinning, is very common. Microfractures and mirmequite are rare. The alkalifeldspar is not very abundant in matrix and shows subhedral, tabular (1:1 to 1:2), weak Tartan twinning and rare inclusions. In the deformed types, the feldspar megacrystals are

contoured by orientated mafic minerals and, in general, show (especially in alkalifeldspar) static recrystallization restrict to the rims (granoblastic texture). Furthermore, they can also show microfractures and dynamic recrystallization features. These fractures have orthogonal angle with twinning and are normally filled by quartz.

Biotite is straw yellow to yellow greenish and subhedral to euhedral, and shows strong to moderate pleocroism. It normally occurs in mafic clots associated with hornblende, titanite, epidote, opaque minerals and apatite (**Fig. 8b**). Apatite, zircon and epidote inclusions are very common. Biotite crystals occasionally are orientated, produced either by magma flow (most common) and solid-state flow, both with similar direction (ENE-WSW). Muscovite is uncommon and partially replaces biotite.

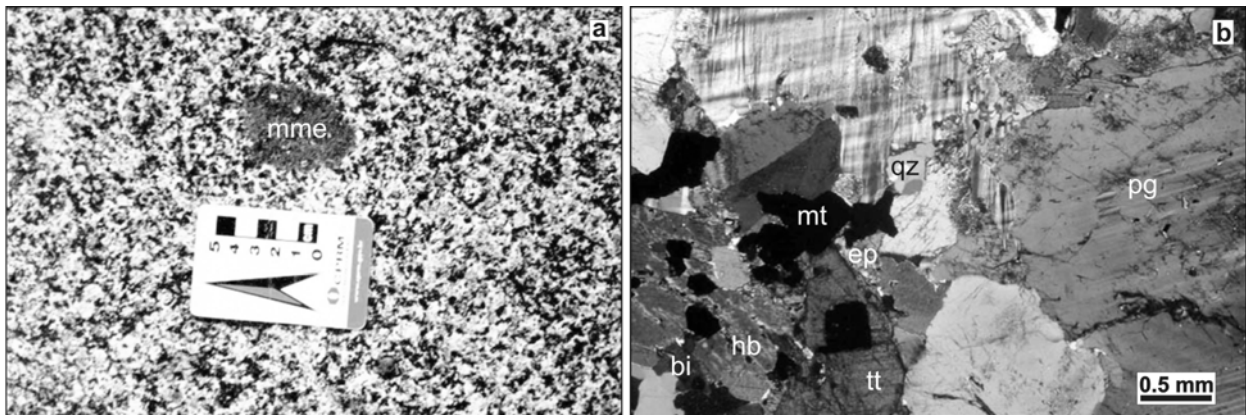


Fig. 8. Features of Jaburuzinho facies from the Caroebe Granite (outcrop MA-33): a) Hornblende-bearing tonalite showing rounded mafic clots and mafic microgranular enclave (mme); b) Photomicrography of mafic clots (bi. biotite, hb. hornblende, mt. magnetite, tt. titanite and ep. epidote) and coarse feldspars and fine-medium quartz grained (af. alkalifeldspar, pg. plagioclase, qz. quartz, my. myrmekite) in quartz-monzodiorite (Cross-polarized light, 2.5x).

Hornblende is subhedral to euhedral, straw yellow, dark olive green to dark green and strongly to moderate pleocroic. Few inclusions are observed, such as apatite, opaque minerals and minor titanite. Preserved clinopyroxene cores are very rare in some hornblende crystals. Biotite and hornblende appear as quite rounded aggregates (clots). Titanite is the most important accessory mineral in the Jaburuzinho facies. It is euhedral to subhedral crystals, medium to coarse grained (**Fig. 8b**), and generally perfect lozenge-like, associated to biotite, hornblende, opaque minerals and epidote in mafic clots (tt1). It also occurs like euhedral crystals, fine grained, included in biotite (tt2) and anhedral grains bordering opaque minerals (tt3).

ALTO ALEGRE FACIES

The Alto Alegre facies is mainly composed by biotite monzogranites (around 80%) with subordinated granodiorites (**Fig. 3a; table 2**) and minor sienogranites and tonalites. These

granitoids are generally isotropic, equigranular, medium- to coarse-grained and eventually porphyritic. The tabular alkali-feldspar megacrystals are white to grayish and pale pinkish, showing 1 to 4 cm in length (ratio 3:1), 5 to 30% (locally 50%) in volume and ENE-WSW orientated (magma flow). The Alto Alegre granitoids show mineral assemblage (**Table 2**) composed by plagioclase (23.3-45.6 %), quartz (19.2-31.2 %), alkali-feldspar (15-38 %), biotite (5.0-12.0 %), and minor titanite, opaque minerals, epidote, apatite, allanite and zircon. In some samples muscovite was also recorded replacing biotite.

The mafic mineral content is quite variable (**Fig. 3b**) and has biotite like the main varietal mineral. Biotite occurs associated with opaque minerals, titanite and minor epidote, locally like circular or irregular mafic clots. Similarly to the Jaburuzinho facies, the Alto Alegre facies has some portions with anisotropic texture. Two anisotropic features are observed: a) orientated tabular megacrystals and lenticular mafic enclaves (magma flow), and b) solid-state deformed mineral, including moderate recrystallization and mineral stretching. Both structures have ENE-WSW to NE-SW strikes, parallel to the regional trends.

The Alto Alegre granitoids also occur enclosing hornblende-bearing microgranular enclaves (dioritic to granodioritic) mainly near to the Jaburuzinho facies boundaries. These enclaves have 5 cm to 20 m in length and are elliptical, slightly rounded (**Fig. 9a**) and elongate (**Fig. 9g**), locally with irregular and wispy terminations (**Fig. 9c**).

Beyond hornblende-bearing enclaves, the Alto Alegre granitoids also enclose felsic and coarse grained monzogranite. These enclaves are equigranular, pale gray and, circular and rounded (**Figs. 9a, b and c**) to irregular (or elongate) and angular (**Figs. 9d, f and h**), locally also with linear orientation (**Figs. 9b and f**). These three magmatic phases (Alto Alegre granitoids, hornblende-bearing enclaves correlated to Jaburuzinho facies and felsic “coarse” monzogranite enclaves) show a complex physical interaction (**Fig. 9h**), but chemical effects are not discarded (Almeida and Macambira 2003).

The angular and rounded forms observed in felsic monzogranite enclaves (**Figs. 9a, b, c, d, e, f and h**) suggest more advanced crystallization stage (or much higher viscosity) in relation to the host granitoid, however, the contacts are sharp and chilled margins are not recorded. On the other hand, the hornblende-bearing tonalite enclaves show lobate to crenulate (flame-like) contacts with host monzogranite to granodiorite (**Fig. 9c**), locally with “dropped” megacrystals, which suggests that the amount of liquid was substantial at the time of emplacement. In detail, the

boundaries of these enclaves reproduce the overall contacts with the host granitoid (mimetization or ghost structures), suggesting a probable incomplete mingling/mixing process. Furthermore, the abundance of elongate to rounded enclaves and net veining in the mafic enclaves by the host granitoid, both suggest mingling/mixing of magmas at the site of emplacement.

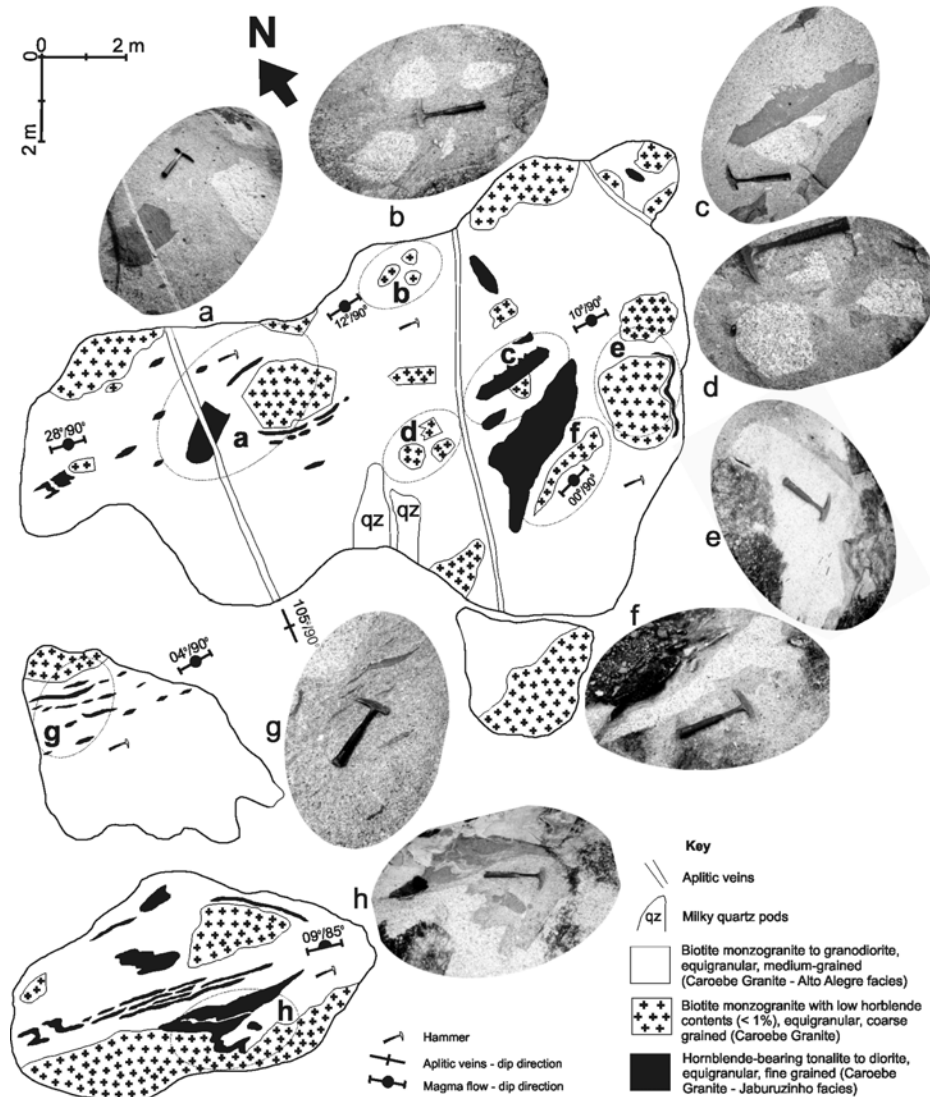


Fig. 09. Foliated (magma flow) Alto Alegre facies of Caroebe Granite enclosing enclaves from Jaburuzinho granitoid with different stages of chemical-physical interaction (outcrop MA-53). For details see text.

As a preliminary conclusion, the Alto Alegre facies granitoids could be partially resulted (hybrid magma) from felsic and coarse-grained monzogranite and fine-grained hornblende-bearing tonalite (commingled magmas) blended, but some authors (Chappell and McCulloch 1990, Chappell 1996), argue that large granitic bodies can not be generated by this kind of petrogenetic model due the large viscosity contrast between two magmas, inhibiting the mixing.

According them, the magma mixing petrogenetic model has local character in the most granitoids evolution.

Others authors believe that large granitic batholith are produced mainly by magma mixing process, such as Itaporanga Batholith in northeastern Brazil (Mariano and Sial 1990) and H-type granitoids in Spain (Castro *et al.* 1990, 1991). They are based on the geochemical and experimental constraints mainly observed in the volcanic rocks (e.g. Turner and Campbell 1986, Gourgaud *et al.* 1989) and their application to plutonic rocks (e.g. Blake and Koyaguchi 1991). According Blake and Koyaguchi (1991), if hybrid volcanic magmas are produced in the magma chambers (that are the precursors of plutonic rocks) then, the plutonic analogues of these same chambers should contain hybrid facies. But, like the volcanic types, areas of hybrid rock within pluton could record mixing events related to the intermittent generations of batch melts.

In this sense, only one outcrop of Alto Alegre facies has possible field features of magma mixing, recording a local mixing event in the Caroebe Granite. The possible mixing magma conduit may be inferred in outcrop. It has near of 2 m length and show strong to extreme elongation of enclaves (**Fig. 9g and h**) in which, the distortion has been accomplished by magmatic flow without solid state deformation, as evidenced by strong orientation of the minerals, coupled with lack of microstructural evidence of intergranular plastic strain (Vernon *et al.* 1988).

The plagioclase is tabular, subhedral to euhedral, medium to coarse grained, locally like megacrystals with combined polissintetic and Carlsbad twinning. These crystals exhibit evident normal (mainly) to oscillatory compositional zoning, raised by secondary alteration (saussuritization) in calcium-enriched portions. Some megacrystals are eventually irregular and show embayed rims in contact with alkalifeldspar grains. Quartz is heterogranular (fine to coarse grained), anhedral, and sometimes occurs like monocrystalline aggregates (qz1). Inclusions of drop-like quartz are also very common in alkalifeldspar megacrystals (qz2). Locally, it shows undulatory extinction and dynamic (fine grained subgrains) to static recrystallization (granoblastic texture) effects in solid-state deformed types (qz3).

The alkalifeldspar shows two main generations. The first type (af1) is characterized by fine grained crystals with euhedral to subhedral shapes and Tartan twinning (matrix occurrence and inclusions). The second generation (af2) is marked by anedral perthitic and poikilitic megacrystals encompassing several inclusions (biotite, drop-like quartz, plagioclase and first

generation alkalifeldspar). In solid-state deformed types, the alkalifeldspar megacrystals are contoured by biotite trails, showing marginal dynamic recrystallization (subgrains) and eventually granoblastic-poligonalized contacts.

The biotite is subhedral, medium grained, moderately pleocroic and yellow straw to yellow greenish. Normally, it forms crystal aggregates and has apatite, epidote, allanite, zircon and opaque mineral inclusions. Locally, it is slightly to strongly orientated and some crystals are partially altered into muscovite. Euhedral titanite is medium to fine grained, lozenge-like (tt1), anhedral and bordering opaque minerals (tt2).

Igarapé Azul Granitoids

Based on petrographic (e.g. muscovite presence) and chemical (peraluminous character) parameters, Faria *et al.* (1999) has individualized a portion of the Água Branca Suite as a new granitic body called Igarapé Azul Granite, interpreted as S-type. The Igarapé Azul Granite was revisited by Almeida *et al.* (2002) who noted that S-type granitoids in southeast of Roraima are restricted to the Serra Dourada region (see S-type Serra Dourada Granite description) and not in the Igarapé Azul type-area.

In the type-area the Igarapé Azul Granite is characterized only by (muscovite)-biotite leucomonzogranites and monzogranites to scarce syenogranites and granodiorites, generally with low mafic contents (**Fig. 3b**), showing a compositional field in QAP diagram similar those granites of crustal origin (Lameyre and Bowden 1982, Lameyre and Bonin 1996, **Fig. 3a, table 3**). The main granitic body shows 1120 km² and has also an important textural asymmetric zoning with three granitic facies describe below: Vila Catarina, Saramandaia and Cinco Estrelas (**Fig. 2**). Other minor correlated granitic bodies have around 30 km² to 125 km² in surface.

VILA CATARINA FACIES

The Vila Catarina facies (nearly 340 km²) occurs in the center-western portion of the Igarapé Azul batholith and shows several Nb-Ta alluvial mineral occurrences and high abundance of aplitic to pegmatitic dikes. It has also similar structural trend (NE-SW) that was observed in Cinco Estrelas facies (see below).

The Vila Catarina granitoids (mainly monzogranites and restrict syenogranite, see **Fig. 3a**) are pale gray to pale pink, equigranular to slightly porphyritic (<5% alkalifeldspar megacrystals), medium to coarse-grained and show variable mafic content (always <10%). In thin section, the

matrix is granular, xenomorphic and, locally, encompasses alkalifeldspar megacrystals (1.5 to 2.0 cm) and mafic clots.

The Vila Catarina facies mineral assemblage (**Table 3**) is composed by plagioclase (24.0-44.7 %), quartz (21.2-38.1 %), alkalifeldspar (20.1-40.5 %), biotite (0.6-7.9 %), locally transformed into muscovite (0.2-1.6 %), and opaque minerals, epidote, allanite, zircon and apatite. The most important secondary minerals in this facies are epidote, chlorite and titanite.

SARAMANDAIA FACIES

The Saramandaia facies has nearly 735 km² in area and occurs in northern batholith portion. This granitoid is cross-cut by Cinco Estrelas and Vila Catarina facies dykes and pods. In Saramandaia facies, the granitoids have porphyritic texture showing alkalifeldspar megacrystals (5% to 20%) with heterogeneous size (<1 to 5 cm) and spatial distribution (**Figs. 10a,b**), similar to those of Vila Catarina facies. These megacrystals are microperthitic, tabular, euhedral, white to slightly pinkish and eventually are orientated (magma flow). They are enveloped by homogeneous and medium grained matrix with monzogranitic to granodioritic composition.

The megacrystal direction is locally outlined by ellipsoidal biotite-bearing enclaves, following ENE-WSW to NE-SW-trendings. Similar trends are observed in megacrystal direction of Caroebe granitoids (see below) and are also subparallel to the regional foliation strikes observed in the host Martins Pereira granitoid. However, the low content of megacrystals makes this flow very often almost imperceptible.

In this facies, the monzogranites are dominant with subordinated granodiorites (**Fig. 3a**) and minor leucogranitic types. The mineral assemblage (**Table 3**) is composed by plagioclase (26.4-44.1 %), quartz (24.3-33.0 %), alkalifeldspar (23.3-28.6 %), biotite (0.4-5.7 %), muscovite (0.2-1.0 %), opaque minerals, epidote, allanite and minor zircon and apatite. Epidote, chlorite and, exceptionally titanite, are the main secondary minerals in the Saramandaia facies.

CINCO ESTRELAS FACIES

The Cinco Estrelas facies (445 km²), easternmost portion of Igarapé Azul batholith, shows granitoids with very low mafic contents and equigranular, homogeneous and fine to medium-grained texture (**Figs. 10c,d**). These granitoids are also gray whitish, monzogranitic in composition with subordinated syenogranite, granodiorite and quartz monzonite (**Fig. 3a**). They are emplaced according to a NE-SW structural direction and locally also occur like pods and

dikes subconcordant with magma flow direction as observed in porphyritic types (Saramandaia facies).

The Cinco Estrelas facies mineral assemblage (**Table 3**) is composed by plagioclase (11.3-52.0 %), quartz (16.0-38.0 %), alkalifeldspar (17.7-36.4 %), biotite (1.3-4.5 %), totally or partially transformed into muscovite (0.1-4.6 %), and opaque minerals, allanite, epidote, zircon and apatite. The most important secondary minerals are epidote, chlorite and leucoxene.

PETROGRAPHIC FEATURES IN COMMON

Despite of local textural variations, these three facies have similar granitic composition (mainly monzogranite and minor granodiorite to syenogranite) and mineral assemblages, including accessory (epidote-allanite, opaque minerals, zircon and apatite) and secondary minerals (epidote, chlorite and muscovite).

Subhedral and tabular plagioclase shows medium to fine-grain, polysintetic twinning and normal zoning. Locally, its nucleus is partially altered to epidote and minor sericite and chlorite. Euhedral megacrystals are rare and eventually show oscillatory zoning, biotite inclusion and preferred orientation. Anhedral crystals with embayment are also observed and sometimes they show obliterated zoning and twinning. Quartz is fine to coarse-grained, anhedral, sometimes interstitial and locally with undulatory extinction, partially recrystallized (subgrains) and fractured.

Alkalifeldspar is partially altered to sericite and muscovite, and occurs in two different types: a) subhedral to anhedral, fine to coarse grained (3-8 mm), tabular crystals showing Tartan twinning, rarely combined with Carlsbad twinning (af1); b) tabular, anhedral and microperthitic megacrystals (25-40 mm), locally with embayed rims and quartz (drop-like), plagioclase (very altered), biotite and locally opaque minerals and epidote inclusions (af2). Myrmekite intergrowth is also common.

The subhedral biotite is fine to coarse grained, moderate to strongly pleocroic and yellow straw to brown greenish. Biotite with red brownish color is very uncommon. Eventually it occurs like mafic clots associated with epidote (and/or allanite), opaque mineral, zircon and apatite. In general, it is slightly orientated and some crystals are partially or totally replaced by muscovite and/or chlorite.

The epidote is the main accessory mineral in Igarapé Azul Granite. It shows fine to medium grain, subhedral to euhedral shapes, pale yellow to pale green colors, low pleocroism (ep1) and

zoned, with cores of allanite. Anhedral crystals are commonly observed like inclusions in plagioclase (ep2). Metamitic allanite shows pale brown to brown orangeish colors and local intergrowth with epidote. Twinned crystals are uncommon. Opaque minerals (sulfides and oxides) are subhedral to euhedral, fine to medium-grained and show hexagonal and square habits, normally associated with biotite. Rarely do they show anhedral and interstitial forms.

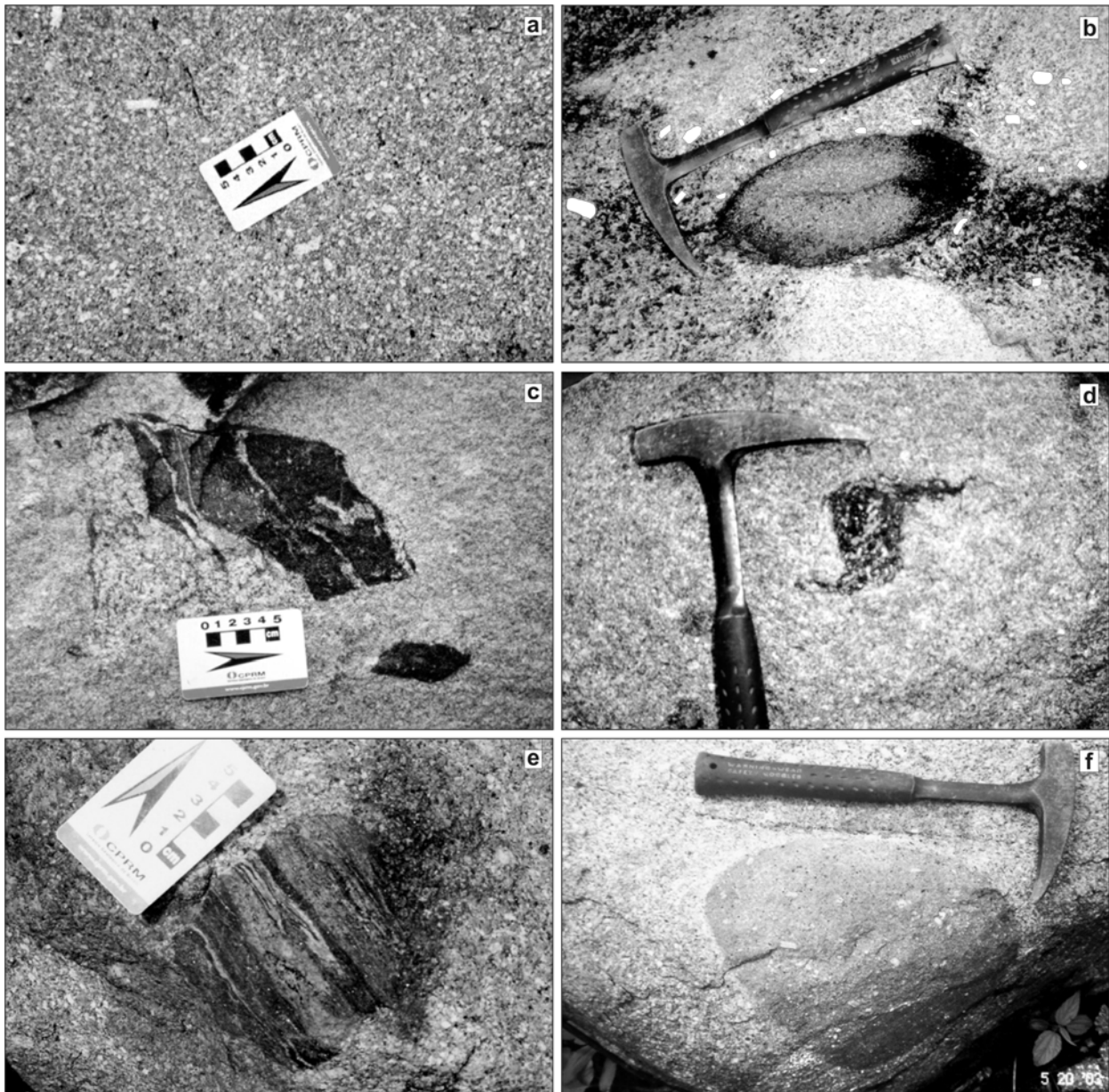


Fig. 10. Igarapé Azul Granite outcrops: a) Slightly porphyritic biotite monzogranite (Saramandaia facies) showing tabular alkali feldspar megacrystals with approximately N60°W strike magma flow (outcrop MA-322); b) Tabular alkali feldspar megacrystals in leucogranodiorite (Saramandaia facies) turning around elliptical tonalite gneiss enclave (outcrop MA-213); c) Irregular biotite-rich diorite gneiss enclave showing fine grained (equigranular) texture surrounded by biotite leucomonzogranite (Cinco Estrelas facies). Note that the host granite fill the enclave foliation planes (outcrop MA-147); d) Porphyritic biotite granodiorite enclave (Martins Pereira Granite) enclosed by Igarapé Azul Granite (Cinco Estrelas facies). The enclave is rotated and biotite trails are observed in its extremities (outcrop MA-99). e) Rounded paragneiss enclave showing strong compositional layering and local growing of biotite and muscovite (outcrop MA-322). f) Rounded and circular mafic microgranular enclave with porphyritic texture (outcrop MA-322).

ENCLAVES

The enclaves founded in Igarapé Azul granitoids are dominantly biotite-rich (**Table 3**) with fine to coarse-grained muscovite crystals. These enclaves show heterogeneous deformation, locally with gneissic texture, and sharp and irregular (**Fig. 10c**) to elliptical (**Fig. 10b**) shapes. Several enclaves have also elongated shapes and biotite trails and schlieren. In general, these enclaves are parallel to the magma flow defined by alkalifeldspar megacrystals in host granitoids (**Fig. 10b**). The contact enclaves-host granitoid is normally sharp; however, sometimes it shows transitional and gradational features (mainly in mafic mineral content rocks). It is difficult to determine the nature of the protholith, but locally some enclaves show similar textural features to the Martins Pereira granitoids. These xenoliths are rotated and partially modified, eventually with migmatitic features (**Fig. 10d**). Paragneiss enclaves (**Fig. 10e**) are rare and mafic (porphyritic) microgranular enclaves (**Fig 10f**) are observed only locally.

The biotite-bearing enclaves show quartz dioritic, tonalitic and quartz monzodioritic compositions (**Fig. 3a, Table 3**), equigranular fine to coarse grained texture and black to gray colors. They also show foliation defined by biotite and muscovite direction (**Fig. 11**), but it is not always observed at naked eye. Its mineral assemblage is composed by biotite (27.6-57.7 %), plagioclase (12.5-40.0 %), muscovite (2.0-10.0 %), quartz (4.4-12.9 %), alkalifeldspar (0.1-12.9 %), epidote (0.4-4.7 %) and opaque minerals (1.0-6.7 %). Other minerals are rare, such as titanite, apatite, zircon and allanite. Secondary epidote and sericite are common.

Subhedral biotite is fine to coarse grained, brown greenish to straw yellow, locally brown reddish, and moderately pleocroic. Inclusions such as zircon, apatite, epidote and occasionally allanite are common. Muscovite is also subhedral, fine to medium-grained and aligned at the same direction of biotite. Rarely it shows large individual crystals and replaces biotite rims and cleavages.

Plagioclase shows two crystal generations: a) coarse grained (eventually megacrystals), subhedral to anhedral (embayed contacts are very common), slight undulatory extinction, normal zoning (rarely oscillatory) with calcic zones steeply replaced by epidote, carbonate and minor sericite (pg1); b) fine to medium grained, subhedral to euhedral, tabular, clear polissintetic twinning and rarely replaced by secondary minerals (pg2). Fine to medium-grained subhedral quartz has undulatory extinction and locally dynamic recrystallization features. Subhedral to anhedral alkalifeldspar is very uncommon.

Subhedral epidote-allanite (compositional zoning) occurs like inclusion in biotite and plagioclase crystals. Opaque minerals show euhedral and tabular crystals. Titanite is rare and replaces calcic portions in plagioclase cores and biotite cleavages. Locally, titanite occurs like subhedral, fine to medium-grained and isolate crystals.

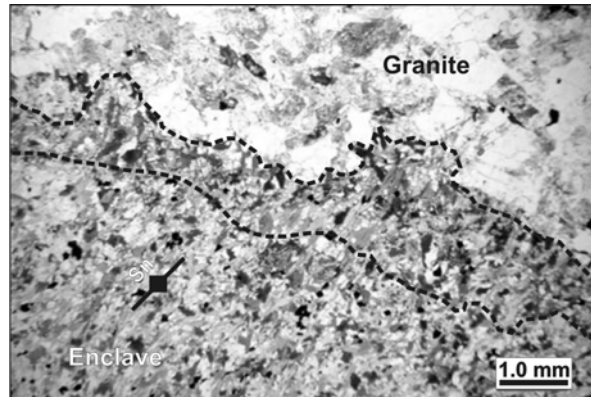


Fig. 11. Photomicrography showing contact between isotropic leucomonzogranite (Igarapé Azul Granite, Cinco Estrelas facies) and biotite-bearing gneissic enclave (quartz dioritic). Note the growing and high concentration of biotite crystals in the enclave near to the contact. The enclave foliation (Sn) is also showed. Parallel-polarized light (1.25x).

A-TYPE GRANITES

In general, the A-type granites in southern Roraima and northern Amazonas states cross-cut the basement rocks in two main magmatic events (Costi *et al.* 2000, CPRM 2000, 2003): Abonari-Mapuera (1.88-1.86 Ga) and Moderna-Madeira (1.82-1.79 Ga) granitic episodes.

Moderna granites and correlated granitoids

The Moderna (Santos *et al.* 1997) and correlated granitoids (**Fig. 2**) show monzogranite to syenogranite composition (rarely alkalifeldspar granite), pale pink to pale gray colors, equigranular to slightly porphyritic texture, coarse grain and mineral assemblage composition including amphibole and biotite like mafic clots. Paragneissic xenoliths (Caurane Group) and pegmatitic and quartz veins with amethyst are also observed.

At least, four granitic bodies related to Moderna-Madeira episode were mapped by aerogeophysical airborne and radar images: 1) Moderna Granite (type-area) occurs near to Moderna town and has 2 main plutonic bodies (51 km² and 15 km²) structurally controlled by NW-SE trend; 2) Serra da Tentativa Granite has 58 km² (NW-SE elongate) and outcrops in the Jaburuzinho river; 3) Itã Granitic Batholith with 560 km² was emplaced following E-W trend. It

is located near to the Itã Fault Zone, and headwaters of Anauá, Dias and Pedras rivers; and 4) Northern Caroebe Batholith has 330 km² and is structurally controlled by NW-SE trend.

Mapuera granites and related granitoids

Mapuera A-type granites (CPRM 2000, 2003) and correlated granitoids occur in the south and southeast of the studied area (**Fig. 2**), in the Jauaperi and Murauá rivers, showing biotite like the only varietal mineral. Two main granitic bodies were recorded. The first one has 44 km² and occurs near to the São João da Baliza and São Luís do Anauá towns (Jauaperi river basin). It shows monzogranitic to syenogranitic composition, wide porphyritic texture (locally with ovoid megacrystals) and coarse to medium grain. The second granitic body has 49 km² and occurs along Murauá River, composed by monzogranites with equigranular to slightly porphyritic texture, medium grain. Locally (northern portion) it is steeply deformed by NE-SW dextral shear zones.

MINERAL OCCURRENCES

Until few years ago, all mineral occurrences in southern Roraima were associated to “Água Branca” and “Igarapé Azul” granitoids (CPRM 2000). However, the results of field works and petrographic analyses yielded by this study demonstrated that amethyst, columbite-tantalite and gold occurrences are related to three different granitic host types.

In the northern area, the host rocks of Anauá small gold mine (Faria *et al.* 1996) are highly deformed (quartz vein shear zones related) and hydrothermally altered (muscovitization and tourmalinization) that mask the igneous features. Despite the difficulty to recognize the primary rocks, the Martins Pereira Granite is probably the host of mineralization, because relationship between gold occurrences and S-type granites, such as Serra Dourada, is very uncommon (*e.g.* Neiva 2000).

In the southern area, several columbite-tantalite occurrences in alluvial sediments have been described (CPRM 2000), all of them are located in Igarapé Azul Granite region. The main Nb-Ta occurrences are related to the central facies (Vila Catarina), which is characterized by abundant pegmatites. Also in this area, the amethyst crystals occur in veins and pegmatites, hosted by younger A-type Moderna granitoids and associated with abundant metasedimentary xenoliths.

DISCUSSION AND CONCLUSIONS

Geological mapping and petrographic constraints of granitoids in Uatumã-Anauá Domain (north and south areas) yielded a new geological picture of the geology of the central portion of Guyana Shield (**Fig. 1**), including mineralization occurrences relationship and tectonic evolution implications.

The Martins Pereira and Serra Dourada granites in NUAD are normally characterized by penetrative deformation and dextral shear zones associated with NE-SW to E-W-trendings. The Serra Dourada Granite, associated with metavolcano-sedimentary covers and older basement inliers (Anauá Complex and Cauarane Group), represents the only S-type magmatic event in this area, suggesting, at least locally, a widespread anatexis of dominant sedimentary sources. The Martins Pereira Granite has a granodioritic calc-alkaline trend (QAP diagram) with mainly monzogranites and granodiorites (porphyritic types) and minor biotite-bearing tonalitic enclaves, and leucogranitic lenses and pods. The petrographic similarities point out that granitoid host-rocks (monzogranites and granodiorites) and biotite-bearing enclaves (tonalites) are cogenetic. The origin of leucogranitic pods is not well understood, but two explanations can be considered: a) highly fractionated types from Martins Pereira calc-alkaline association, or b) new granitic magmas from small-scale remelting of Martins Pereira granitoids (local anatexis).

The tectonic evolution the NUAD granitoids is yet debatable, but its relationship with Anauá Arc (Faria *et al.* 2002) is envisageable. The I-type calc-alkaline (granodioritic trend) and S-type character suggest that they could be related to the final stages of Anauá Arc development.

On the other hand, in the SUAD area, only undeformed calc-alkaline granitoids (e.g. Caroebe and Igarapé Azul granites) and local coeval volcanic rocks (Iricoumé Group) are recorded. The Caroebe granitoids (Água Branca Suite) show calc-alkaline character with wide extended compositional serie and granodioritic trends in the QAP diagram. The petrogenetic evolution following fractional crystallization process was regarded by Oliveira *et al.* (1996), however, at least locally, other petrogenetic processes can be involved in Caroebe Granite genesis, such as partial melting, magma mixing or assimilation fractional crystallisation (AFC). The magma mixing hypothesis is based on field observations, where two end-members, represented by felsic monzogranite and hornblende-bearing tonalite (commingled magmas), produced an intermediate homogeneous granodioritic member (hybrid magma?). However, some authors argue that this petrogenetic process is related only to the small-scale granite generation and do not support large bodies generation. Others authors show that magma mixing is an

important petrogenetic model for granitoids generation, but only mixing events could be recorded in the pluton, generating local hybrid rocks. Meanwhile, a geochemical evaluation is necessary for a better discussion.

The Igarapé Azul Suite also shows calc-alkaline affinity (Almeida and Macambira 2003), but it is almost restrict to monzogranites types, which are characterized by very homogeneous texture and mineralogical assemblage. These granitoids show similar field and petrographic features to felsic granites occurring as lenses or pods in Martins Pereira Suite, such as: a) monzogranitic composition, b) textural homogeneity, c) low modal content of mafic minerals, d) biotite and late muscovite as the varietal minerals, and e) epidote and opaque minerals (major magnetite) as the main accessory minerals. The biotite-bearing enclaves enclosed by Igarapé Azul granitoids are also very similar to the (meta)tonalite types observed in Martins Pereira basement and suggests that fragments from basement were captured and partially modified by the Igarapé Azul magma during crustal ascension.

The magmatic flow and shape of granitic bodies with NE-SW to E-W-trendings observed in the Igarapé Azul and Caroebe granites suggest that the emplacement was probably structural-controlled by older lineaments, maybe related to NE-SW and E-W foliations observed in Martins Pereira meta-granitoids.

Two generations of A-type granite are widespread in UAD, probably related to a post-orogenic (1.87 Ga) to anorogenic (1.81 Ga) setting. They are marked by minor bodies, with circular to ellipsoidal forms, sharp contacts, and establishing the starting of the tectonic and magmatic stability period in the southeastern Roraima. The emplacement these A-types granites also shows E-W and NW-SE-trending structural-control, filling mainly brittle to brittle-ductile structures.

Furthermore, the envisaged relationship between mineralization and the granitoid hosts in the UAD, as a whole, open new metalotect perspectives, emphasizing the mineral potential of this region for gold (Martins Pereira granitoids), columbite-tantalite (mainly in the central facies of Igarapé Azul Granite) and amethyste (Moderna Granite).

Acknowledgments

Special thanks to M.S.G. de Faria (MJ-DPF-Manaus), N. J. Reis, S. da S. Pinheiro and R. Luzardo (CPRM-Geological Survey of Brazil) for geological discussions. The authors are grateful also to the CPRM-Geological Survey of Brazil and UFPA for support to this research.

References

- Almeida M.E., Macambira M.J.B., Faria M.S.G. de. 2002. A Granitogênese Paleoproterozóica do Sul de Roraima. *In: SBG, Cong. Bras. Geol.*, 41, Anais, p 434 (in portuguese).
- Almeida M.E. & Macambira M.J.B. 2003. Aspectos geológicos e litoquímicos dos granitóides cálcio-alcalinos Paleoproterozóicos do sudeste de Roraima. *In: SBGq, Cong. Brasil. Geoq.*, 9, Anais, p. 775-778 (in portuguese).
- Araújo Neto H. & Moreira H.L. 1976. *Projeto Estanho do Abonari*. Manaus, Convênio DNPM/CPRM, Relatório Final. 2v (in portuguese).
- Berrangé J.P. 1972. The Tectonic/Geological Map of Southern Guyana. *In: Ministerio de Minas e Hidrocarburos, Conferencia Geológica Inter-Guayanas*, 9, Boletín de Geología, Publicación Especial 6, p. 161-174.
- Blake S. & Koyaguchi T. 1991. Insights on the magma mixing model from volcanic rocks. *In: J. Didier and B. Barbarin (eds) Enclaves and granite petrology*, Elsevier, p.403-413.
- Castro A., de la Rosa J.D., Stephens W.E. 1990. Magma mixing in the subvolcanic environment. Petrology of the Gerena interaction zone near Seville, Spain. *Contrib. Mineral. Petrol.*, **105**: 9-26.
- Castro A., Moreno-Ventas I., de la Rosa J.D. 1991. H-type (Hybrid) granitoids: A proposed revision of the granite-type classification and nomenclature. *Earth Science Rev.*, 31: 237-253.
- Chappell B.W. & McCulloch M.T. 1990. Possible mixed source rocks in the Bega Batholith: constraints provided by combined chemical and isotopic studies. *Abstracts Geological Society of Australia*, **27**: 17.
- Chappell B.W. 1996. Magma mixing and the production of compositional variation within granite suites: evidence from the granites of southeastern Australia. *Journal of Petrology*, **37** : 449-470.
- Costi H.T., Santiago A.F., Pinheiro S.S. 1984. *Projeto Uatumã-Jatapu*. Manaus, CPRM, Relatório Final. 133p. (in portuguese).
- Costi H.T., Dall'Agnol R., Moura, C.A.V. 2000. Geology and Pb-Pb geochronology of Paleoproterozoic volcanic and granitic rocks of the Pitinga Province, Amazonian craton, northern Brazil. *Int. Geol. Rev.*, **42**: 832-849.
- CPRM. 1999. Programa Levantamentos Geológicos Básicos do Brasil. *Roraima Central, Folhas NA.20-X-B e NA.20-X-D (integrais), NA.20-X-A, NA.20-X-C, NA.21-V-A e NA.21-V-C*

- (*parciais*). Escala 1:500.000. Estado de Roraima. Manaus, CPRM, 166 p. CD-ROM. (abstract in english)
- CPRM. 2000. Programa Levantamentos Geológicos Básicos do Brasil. *Caracarái, Folhas NA.20-Z-B e NA.20-Z-D (integrais), NA.20-Z-A, NA.21-Y-A, NA.20-Z-C e NA.21-Y-C (parciais)*. Escala 1:500.000. Estado de Roraima. Manaus, CPRM, 157 p. CD-ROM. (abstract in english)
- CPRM. 2003. Programa Levantamentos Geológicos Básicos do Brasil. *Geologia, Tectônica e Recursos Minerais do Brasil: sistema de informações geográficas - SIG*. Rio de Janeiro : CPRM, 2003. Mapas Escala 1:2.500.000. 4 CDs ROM. (abstract in english)
- CPRM. 2006. Programa Integração, Atualização e Difusão de Dados da Geologia do Brasil: Subprograma Mapas Geológicos Estaduais. *Geologia e Recursos Minerais do Estado do Amazonas*. Manaus, CPRM/CIAMA-AM, 2006. Escala 1:1.000.000. Texto explicativo, 148p. CD ROM. (in portuguese)
- Faria M.S.G. de, Oliveira M.J.R., Luzardo R, Pinheiro S. da S. 1996. Garimpo do Anauá, Sudeste do Estado de Roraima: dados preliminares sobre ocorrência aurífera associada à zona de cisalhamento. *In: SBG, Cong. Bras. Geol., 39, Anais, v. 3 p. 316-319* (in portuguese).
- Faria M.S.G.de, Luzardo R., Pinheiro S. da S. 1999. Litoquímica e petrogênese do Granito Igarapé Azul. *In: SBG, Simp. Geol. Amaz., 6, Anais, p. 577-580* (in portuguese).
- Faria M.S.G. de, Santos J.O.S.dos, Luzardo R., Hartmann L.A., McNaughton N.J. 2002. The oldest island arc of Roraima State, Brazil – 2.03 Ga: zircon SHRIMP U-Pb geochronology of Anauá Complex. *In: SBG, Congr. Brasil. Geol., 41, Anais, p. 306*.
- Faria M.S.G. de, Almeida M.E., Santos J.O.S. dos, Chemale Jr. F. 2003. Evolução Geológica da Região do Alto Rio Anauá - Roraima. *In: SBG, Simp. Geol. Amaz., 8, Anais, CD-ROM* (in portuguese).
- Gaudette H.E., Olszewski W.J. Jr., Santos J.O.S.dos. 1996. Geochronology of Precambrian rocks from the northern part of Güiana Shield, State of Roraima, Brazil. *Journ. South Am. Earth Sci., 9*: 183-195.
- Gibbs A.K., Barron C.N. 1993. The geology of the Guyana Shield. Oxford University Press, Oxford, N. York, 245 p.
- Gourgaud A, Fichaut M, Joron J -L 1989. Magmatology of Mt. Pelee (Martinique, F.W.I.). I: Magma mixing and triggering of the 1902 and 1929 Pelean nuees ardentes. *J Volc Geotherm Res, 38*: 143-169.

- Jorge-João X.S., Santos C.A., Provost A. 1985. Magmatismo adamelítico Água Branca (Folha Rio Ma puera, NW do Estado do Pará). *In: SBG, Simp. Geol. Amaz., 2, Anais, v.2, p. 93-109* (in portuguese).
- Lameyre J. & Bowden P., 1982. Plutonic rock type series: discrimination of various granitoids series and related rocks. *Journal of Volcanology and Geothermal Research*, 14, 169-186.
- Lameyre J. & Bonin B., 1991. Granites in the main plutonic series. *In: J. Didier and B. Barbarin (eds.), Enclaves and Granite Petrology. Development in Petrology*, 13, 3-17.
- Macambira M.J.B., Almeida M.E., Santos L.S. 2002. Idade de Zircão das Vulcânicas Iricoumé do Sudeste de Roraima: contribuição para a redefinição do Supergrupo Uatumã. *In: SBG, Simpósio Sobre Vulcanismo e Ambientes Associados, 2, Anais, p. 22* (in portuguese).
- Mariano G. & Sial A.N. 1990. Coexistence and Mixing of Magmas in the Late Precambrian Itaporanga Batholith, State of Paraíba, Northeastern Brazil. *Revista Brasileira de Geociências*, **20** (1-4): 101-110.
- Neiva A.M.R. 2000. Comparison between Portuguese granites associated with Sn-W mineralizations and with Au mineralization. *In: SBG, Intern. Geol. Cong., 31 Abstr. Vol. CD-ROM*.
- Oliveira M.J.R., Almeida M.E., Luzardo R., Faria M.S.G. de. 1996. Litogeoquímica da Suíte Intrusiva Água Branca - SE de Roraima. *In: SBG, Congr. Brasil. Geol., 39, Anais, v.2, p. 213-216* (in portuguese).
- Passchier C.W. & Trouw R.A.J. 1996. *Microtectonics*. Springer Verlag, London, 326p.
- Reis N.R. & Fraga L.M.B. 1996. Vulcanismo Surumu - Estado de Roraima: Caracterização de seu comportamento químico à luz de novos dados. *In: SBG, Congr. Brasil. Geol., 39, Anais..., v. 2, p. 88- 90* (in portuguese).
- Reis N.J. & Fraga L.M.B. 2000. Geological and tectonic framework of Roraima State, Guyana Shield – An overview. *In: SBG, Intern. Geol. Cong., 31, Abstr. Vol., Gen. Simp. 9. CD-ROM*.
- Reis N.R., Faria M.S.G. de, Fraga L.M.B., Haddad R.C. 2000. Orosirian calc-alkaline volcanism from eastern portion of Roraima State – Amazon Craton. *Revista Brasileira de Geociências*, **30** (3): 380-383.
- Reis N.J., Fraga L.M., Faria M.S.G. de, Almeida M.E. 2003. Geologia do Estado de Roraima. *Géologie de la France*, **2-3**: 71-84 (in portuguese).

- Santos J.O.S. dos, Silva L.C., Faria M.S.G. de, Macambira, M.J.B. 1997. Pb-Pb single crystal, evaporation isotopic study on the post-tectonic, sub-alkalic, A-type Moderna granite, Mapuera intrusive suite, State of Roraima, northern Brazil. *In: SBG, Symposium of Granites and Associated Mineralizations*, 2, Extended Abstract, p.273-275.
- Santos, J.O.S. dos, Hartmann, L.A., Gaudette, H.E., Groves, D.I., McNaughton, N.J., Fletcher, I.R. 2000. A new understanding of the provinces of the Amazon Craton based on integration of field mapping and U-Pb and Sm-Nd geochronology. *Gond. Res.* 3 (4), 453-488.
- Sardinha A.S. 1999. *Petrografia do Granito Igarapé Azul, Sudeste do Estado de Roraima*. Trabalho de Conclusão de Curso, Centro de Geociências, Universidade Federal do Pará, 32p (in portuguese).
- Streckeisen A.C. 1976. To each plutonic rock its proper name. *Earth Sci. Rev.*, 12: 1-33.
- Turner J.S. & Campbell I.H., 1986. Convection and mixing in magma chambers. *Earth Sci. Rev.*, 23: 255-52.
- Veiga Jr. J.P., Nunes A.C.B., Souza E.C. de, Santos J.O.S. dos, Amaral J.E., Pessoa M.R., Souza S.A. de S. 1979. *Projeto Sulfetos do Uatumã*. Manaus, DNPM/CPRM, Relatório Final, 6 v. (in portuguese).
- Vernon R.H., Etheridge M.A., Wall V.J. 1988. Shape and microstructure of microgranitoid enclaves: indicators of magma mingling and flow. *Lithos* 22: 1-11.

Table 1. Modal mineral contents of samples from Martins Pereira and Serra Dourada granitoids and associated rocks.

| samples | classification | facies | qz | af | pg | bi | ms | tt | al | ep | zi | ap | om | cd | gr | si | tu | mz-xt | cl | lx | ss | my | ph | cb | ref. |
|-----------|---------------------|--------|------|------|------|------|-----|-----|-----|------|-----|-----|-----|-----|----|-----|-----|-------|------|-----|------|-----|-----|-----|------|
| MF-151 | syenogranite | A | 31.0 | 39.0 | 19.0 | 5.0 | 3.0 | - | - | tr | tr | tr | 1.0 | 2.0 | - | tr | - | tr | tr | - | tr | - | - | - | 2 |
| MF-156 | monzogranite | A | 24.0 | 35.5 | 20.6 | 7.8 | 5.0 | - | - | - | 0.2 | tr | 1.8 | 2.8 | - | 0.4 | - | 0.5 | 0.2 | - | 1.2 | - | - | - | 3 |
| MF-157 | monzogranite | A | 21.0 | 29.0 | 27.0 | 13.0 | 5.0 | - | - | tr | 1.0 | 1.0 | 2.0 | 1.0 | - | - | - | tr | tr | tr | tr | - | - | - | 2 |
| MF-155 | granodiorite | A | 19.1 | 15.8 | 39.3 | 20.8 | 1.7 | - | - | - | 0.3 | tr | 1.3 | 0.3 | - | - | - | tr | 0.0 | - | 0.7 | 0.7 | - | - | 3 |
| MF-154 | monzogranite | A | 18.4 | 29.8 | 28.8 | 0.9 | 6.4 | 1.2 | 0.0 | 12.0 | tr | tr | 0.3 | - | - | - | - | - | 2.1 | - | - | - | - | - | 3 |
| MJ-013B | granodiorite | B | 35.3 | 14.8 | 41.0 | 6.1 | 0.1 | 0.6 | - | 1.6 | 0.1 | 0.1 | 0.2 | - | - | - | - | - | 0.1 | - | - | - | - | - | 1 |
| MF-011B | monzogranite | B | 34.5 | 28.4 | 27.1 | 6.1 | 3.1 | 0.1 | 0.1 | 0.1 | 0.1 | 0.1 | 0.2 | - | - | - | - | - | 0.1 | - | - | - | - | - | 1 |
| MJ-055B | meta-granodiorite | B | 32.8 | 10.6 | 46.3 | 7.2 | 1.0 | 0.3 | - | 0.4 | 0.1 | 0.2 | 0.7 | - | - | - | - | - | 0.1 | - | 0.3 | - | - | - | 1 |
| MJ-024B2 | monzogranite gneiss | B | 32.7 | 36.6 | 23.3 | 4.3 | 1.4 | 0.1 | - | - | 0.1 | 0.1 | 0.8 | - | - | - | - | - | 0.1 | 0.2 | 0.3 | - | - | - | 1 |
| RL-137B | granodiorite | B | 32.3 | 20.0 | 38.6 | 6.0 | 1.1 | 0.1 | - | 0.9 | 0.1 | 0.1 | 0.3 | - | - | - | - | - | - | - | 0.5 | - | - | - | 1 |
| MF-007B | meta-granodiorite | B | 32.2 | 17.1 | 38.3 | 8.3 | 2.2 | 0.1 | 0.1 | 0.5 | 0.1 | 0.1 | 0.6 | - | - | - | - | - | 0.1 | 0.1 | 0.2 | - | - | - | 1 |
| MA-007A | meta-monzogranite | B | 31.4 | 22.8 | 32.2 | 9.7 | 0.8 | 0.5 | 0.2 | 0.7 | 0.1 | 0.3 | 1.3 | - | - | - | - | - | - | - | - | - | - | - | 3 |
| MJ-213A | monzogranite | B | 31.0 | 28.0 | 29.0 | 5.0 | 2.0 | - | 1.0 | 0.1 | 1.0 | 1.0 | 1.0 | - | - | - | - | - | 0.4 | - | 0.5 | - | - | - | 2 |
| PT-006A | monzogranite | B | 31.0 | 28.0 | 29.0 | 5.0 | 2.0 | 1.0 | - | 0.1 | 1.0 | 1.0 | 1.0 | - | - | - | - | - | 0.4 | - | 0.5 | - | - | - | 2 |
| MA-045 | meta-granodiorite | B | 30.2 | 13.1 | 35.9 | 11.4 | 1.0 | 1.0 | 1.0 | 1.7 | 0.0 | 1.0 | 1.7 | - | - | - | - | - | 0.0 | - | 0.7 | 0.3 | 1.0 | - | 3 |
| MF-011A | granodiorite | B | 30.0 | 16.4 | 37.4 | 12.0 | 2.1 | 0.1 | - | 1.1 | 0.1 | 0.3 | 0.3 | - | - | - | - | - | 0.2 | - | - | - | - | - | 1 |
| MJ-055A | meta-monzogranite | B | 29.7 | 23.7 | 38.2 | 5.5 | 1.2 | 0.2 | - | 0.5 | 0.1 | 0.1 | 0.6 | - | - | - | - | - | 0.1 | - | 0.1 | - | - | - | 1 |
| RL-016 | meta-granodiorite | B | 28.6 | 19.4 | 41.2 | 8.8 | - | 0.4 | - | 0.2 | 0.1 | 0.1 | 0.8 | - | - | - | - | - | - | - | 0.4 | - | - | - | 1 |
| PT-007 | monzogranite | B | 28.4 | 31.6 | 34.0 | 4.6 | 0.1 | 0.1 | 0.1 | 0.1 | 0.1 | 0.1 | 0.8 | - | - | - | - | - | - | - | - | - | - | - | 1 |
| MF-132A | meta-monzogranite | B | 28.0 | 26.0 | 26.0 | 10.0 | 5.0 | 1.0 | - | 0.3 | 0.2 | 1.0 | 1.0 | - | - | - | - | - | 0.5 | - | 1.0 | - | - | - | 2 |
| RL-013(2) | monzogranite | B | 27.3 | 26.5 | 39.7 | 4.3 | 0.3 | 0.2 | 0.1 | 0.4 | 0.1 | 0.1 | 1.0 | - | - | - | - | - | - | - | - | - | - | - | 1 |
| RL-046 | granodiorite | B | 27.0 | 12.0 | 42.0 | 10.0 | 4.0 | - | - | 0.1 | 1.0 | 0.3 | 3.0 | - | - | - | - | - | 0.3 | - | 0.3 | - | - | - | 2 |
| MA-061A | monzogranite | B | 26.9 | 22.6 | 24.7 | 10.1 | 1.3 | 0.6 | 0.0 | 3.4 | 0.2 | 0.6 | 0.9 | - | - | - | - | - | - | - | 7.1 | 1.1 | 0.4 | - | 3 |
| RL-050 | granodiorite | B | 26.5 | 22.0 | 43.0 | 5.0 | 1.0 | - | - | 0.2 | - | 1.0 | 0.3 | - | - | - | - | - | 0.5 | - | 0.5 | - | - | - | 2 |
| MF-010A | meta-granodiorite | B | 26.1 | 18.8 | 43.2 | 5.0 | 4.4 | 0.1 | 0.1 | 1.2 | 0.1 | 0.1 | 0.7 | - | - | - | - | - | 0.1 | 0.1 | - | - | - | - | 1 |
| MA-172A | monzogranite | B | 25.2 | 32.6 | 22.7 | 9.9 | 0.4 | 1.1 | 0.4 | 0.4 | 0.4 | 1.4 | 1.1 | - | - | - | - | - | 0.4 | - | 4.3 | - | - | - | 3 |
| PT-010 | granodiorite | B | 25.0 | 22.0 | 42.0 | 6.0 | 3.0 | - | - | 0.1 | - | 0.8 | 0.9 | - | - | - | - | - | 0.1 | - | 0.1 | - | - | - | 2 |
| MJ-013A | granodiorite | B | 24.7 | 14.6 | 48.1 | 7.8 | 0.1 | 0.9 | 0.1 | 3.3 | 0.1 | 0.1 | 0.1 | - | - | - | - | - | 0.1 | - | - | - | - | - | 1 |
| MA-119 | monzogranite | B | 24.1 | 27.6 | 23.9 | 12.1 | - | 2.0 | - | 2.9 | 0.3 | tr | 0.9 | - | - | - | - | - | 0.5 | - | 4.6 | 1.1 | - | - | 3 |
| NR-018 | meta-monzogranite | B | 22.7 | 27.1 | 41.9 | 5.9 | 0.2 | 0.3 | 0.1 | 0.4 | 0.1 | 0.2 | 0.7 | - | - | - | - | - | - | - | 0.4 | - | - | - | 1 |
| RL-139 | granodiorite | B | 22.6 | 9.7 | 52.5 | 10.7 | - | 2.3 | - | 0.4 | 0.1 | 0.3 | 0.9 | - | - | - | - | - | 0.1 | - | 0.4 | - | - | - | 1 |
| MA-261B | meta-granodiorite | B | 20.5 | 23.4 | 40.2 | 9.2 | - | 1.6 | - | 1.1 | 0.2 | 0.4 | 1.1 | - | - | - | 0.7 | - | - | - | 0.4 | 1.1 | - | - | 3 |
| MJ-013C | leucogranodiorite | C | 32.5 | 21.1 | 41.7 | 3.0 | 0.3 | 0.1 | 0.1 | 0.7 | 0.1 | 0.1 | 0.2 | - | - | - | - | - | 0.1 | - | - | - | - | - | 1 |
| MF-011C2 | leucomonzogranite | C | 31.4 | 27.4 | 38.7 | 1.2 | 0.1 | 0.1 | - | 0.3 | 0.1 | 0.1 | 0.1 | - | - | - | - | - | 0.2 | - | 0.3 | - | - | - | 1 |
| MA-246C2 | leucosyenogranite | C | 30.8 | 54.6 | 8.4 | tr | 0.3 | - | - | 1.0 | 0.1 | tr | tr | - | - | - | - | - | - | - | 4.4 | - | - | 0.5 | 3 |
| MA-46B | monzogranite | C | 30.2 | 34.3 | 20.9 | 4.9 | 3.2 | - | - | 0.2 | tr | tr | 1.4 | - | tr | - | - | - | 0.2 | - | 4.3 | 0.4 | - | - | 3 |
| RL-138 | leucomonzogranite | C | 30.2 | 33.4 | 33.3 | 1.3 | 0.1 | 0.1 | 0.1 | 0.8 | 0.1 | 0.1 | 0.5 | - | - | - | - | - | - | - | - | - | - | - | 1 |
| MA-007B | leucosyenogranite | C | 29.8 | 43.1 | 20.1 | 1.9 | 2.8 | 0.2 | 0.6 | 0.6 | 0.1 | 0.1 | 0.6 | - | - | - | - | - | 0.1 | - | - | - | - | - | 3 |
| MF-012 | monzogranite | C | 27.1 | 23.5 | 40.1 | 4.4 | 1.8 | 0.4 | - | 1.4 | 0.1 | 0.2 | 0.6 | - | - | - | - | - | 0.1 | - | 0.3 | - | - | - | 1 |
| MA-246C1 | tonalite gneiss | D | 21.6 | 2.7 | 26.4 | 3.4 | 5.8 | 3.8 | 0.3 | 5.5 | 0.3 | 0.3 | 1.7 | - | - | - | - | - | 14.0 | - | 13.7 | - | - | 0.3 | 3 |

Table1 (Continued)

| samples | classification | facies | qz | af | pg | bi | ms | tt | al | ep | zi | ap | om | cd | gr | si | tu | mz-xt | cl | lx | ss | my | ph | cb | ref. |
|----------|-------------------|--------|------|------|------|------|-----|-----|-----|------|-----|-----|-----|----|----|----|----|-------|-----|-----|-----|----|----|----|------|
| MA-176B | meta-granodiorite | D | 20.5 | 15.1 | 42.8 | 8.8 | 1.6 | tr | tr | 3.1 | 0.3 | tr | 0.5 | - | - | - | - | - | 0.3 | 5.4 | 1.6 | - | - | - | 3 |
| MF-073B2 | tonalite | D | 20.0 | 5.0 | 50.0 | 15.0 | 1.0 | 1.0 | - | 2.0 | - | 2.0 | 3.0 | - | - | - | - | - | 1.0 | - | - | - | - | - | 2 |
| RL-040B | tonalite gneiss | D | 18.0 | 4.0 | 48.0 | 20.0 | 1.0 | - | - | 2.0 | - | 2.0 | 3.0 | - | - | - | - | - | 1.0 | - | 1.0 | - | - | - | 2 |
| MA-009B | tonalite gneiss | D | 17.0 | - | 48.0 | 29.9 | - | 1.0 | - | 0.1 | 0.1 | 0.5 | 3.4 | - | - | - | - | - | - | - | - | - | - | - | 3 |
| MA-007C | tonalite gneiss | D | 8.5 | - | 32.1 | 42.4 | - | 2.2 | 0.8 | 12.5 | 0.2 | 0.4 | 0.8 | - | - | - | tr | - | 0.1 | - | - | - | - | - | 3 |

Modal analysis from (1) Sardinha (1999), (2) CPRM (2000) and (3) this paper. Serra Dourada Granite: A. aluminous coarse-grained granites. Martrins Pereira Granite: B. porphyritic and equigranular coarse-grained, C. pods and lenses, D. biotite-bearing enclaves. Abbreviations: qz. quartz, af. alkalifeldspar, pg. plagioclase, bi. biotite, ms. muscovite, tt. titanite, al. allanite, ep. epidote, zi. zircon, ap. apatite, om. opaque minerals, cd. cordierite, gr. garnet, si. sillimanite, tu. tourmaline, mz-xt. monazite and/or xenotime, cl. chlorite, lx. leucoxene, ss. saussurite, cb. carbonate, ph. prehnite. Note: tr. trace; ref. references.

Table 2. Modal mineral contents of samples from Caroebe Granite.

| samples | classification | facies | qz | af | pg | bi | amp | ms | tt | al | ep | zi | ap | om | cl | cpx | ss | my | ph | Ref |
|---------|---------------------|--------|------|------|------|------|------|-----|-----|-----|-----|-----|-----|-----|-----|-----|-----|-----|-----|-----|
| MA-276 | granodiorite | A | 31.2 | 7.8 | 45.6 | 7.5 | - | 0.3 | 1.5 | 0.6 | 0.9 | 0.3 | 0.3 | 0.9 | 0.3 | - | 2.7 | - | - | 3 |
| MA 130A | monzogranite | A | 30.0 | 27.0 | 34.3 | 7.0 | - | - | 0.6 | 0.1 | 0.2 | 0.1 | 0.1 | 0.5 | 0.1 | - | - | - | - | 3 |
| MA 124A | monzogranite | A | 29.5 | 38.0 | 23.3 | 8.0 | - | - | 0.2 | 0.1 | 0.1 | 0.1 | 0.1 | 0.5 | 0.1 | - | - | - | - | 3 |
| MA-150 | granodiorite | A | 26.1 | 12.2 | 44.8 | 6.5 | - | 0.3 | 1.6 | 0.0 | 2.2 | 0.3 | 0.0 | 1.6 | 0.5 | - | 3.0 | 0.5 | 0.3 | 3 |
| MA 120 | monzogranite | A | 26.0 | 35.0 | 25.5 | 12.0 | - | - | 0.5 | 0.1 | 0.3 | 0.1 | 0.1 | 0.3 | 0.1 | - | - | - | - | 3 |
| MA 123 | monzogranite | A | 25.0 | 28.0 | 35.7 | 10.0 | - | 0.1 | - | - | 0.2 | 0.1 | 0.1 | 0.7 | 0.1 | - | - | - | - | 3 |
| MJ 061C | monzogranite | A | 25.0 | 30.0 | 25.0 | 5.0 | - | 2.0 | 3.0 | - | 3.0 | - | 1.0 | 3.0 | 3.0 | - | - | - | - | 2 |
| MA 053A | granodiorite | A | 23.6 | 20.3 | 38.9 | 9.9 | - | 0.8 | 0.4 | 0.3 | 1.7 | - | - | 1.1 | - | - | 1.9 | 1.1 | - | 3 |
| MA-144A | granodiorite | A | 19.2 | 20.0 | 43.7 | 7.0 | - | - | 1.2 | 0.4 | 1.9 | 0.4 | 0.2 | 1.2 | - | - | 4.5 | 0.3 | - | 3 |
| MA 104 | monzogranite | B | 30.0 | 34.5 | 23.0 | 6.0 | 5.0 | - | 0.1 | - | 0.1 | 0.1 | 0.1 | 1.0 | 0.1 | - | - | - | - | 3 |
| MA 112 | monzogranite | B | 26.0 | 28.4 | 26.0 | 11.0 | 7.0 | - | 0.2 | 0.1 | 0.1 | 0.1 | 0.1 | 1.0 | - | - | - | - | - | 3 |
| RL 006 | monzogranite | B | 20.6 | 29.2 | 36.2 | 11.8 | 0.6 | - | 0.4 | - | 0.1 | 0.1 | 0.2 | 0.7 | - | 0.1 | - | - | - | 1 |
| HM-181* | monzogranite | - | 19.1 | 27.4 | 34.1 | 8.4 | 2.7 | - | 0.3 | - | 2.1 | 0.5 | 0.2 | 1.0 | - | - | 3.3 | 0.5 | - | 3 |
| MA 053C | tonalite | B | 16.3 | 4.9 | 42.7 | 19.9 | 7.0 | 0.4 | 0.8 | 0.1 | 1.5 | 0.1 | 0.1 | 1.2 | 0.1 | - | 4.7 | 0.2 | - | 3 |
| MA 121 | quartz monzodiorite | B | 15.8 | 14.5 | 54.0 | 9.7 | 2.3 | 0.1 | 1.1 | 0.1 | 0.8 | 0.2 | 0.2 | 1.1 | 0.1 | - | - | - | - | 3 |
| MA 103 | granodiorite | B | 15.0 | 12.0 | 43.0 | 10.0 | 12.0 | - | 0.6 | - | 0.6 | 0.1 | 0.1 | 1.7 | 0.1 | 4.8 | - | - | - | 3 |
| MA-187 | quartz monzodiorite | B | 14.9 | 9.5 | 48.9 | 11.2 | 3.4 | 0.0 | 3.2 | 0.0 | 1.7 | 0.0 | 0.3 | 2.3 | 0.6 | - | 3.2 | 0.9 | - | 3 |
| MA 053B | quartz monzonite | B | 14.2 | 30.4 | 38.3 | 12.1 | 0.3 | 0.3 | 0.4 | - | 0.6 | 0.1 | 0.2 | 1.9 | 0.2 | - | 0.6 | 0.4 | - | 3 |
| MF 068A | quartz monzodiorite | B | 10.0 | 14.0 | 35.0 | 10.0 | 8.0 | 2.0 | 2.0 | - | 2.0 | - | 3.0 | 4.0 | 2.0 | 7.0 | 1.0 | - | - | 2 |
| MJ 061B | quartz monzonite | B | 9.0 | 23.0 | 37.0 | 6.0 | 16.0 | 1.0 | 2.0 | - | 1.0 | - | 2.0 | 1.0 | 2.0 | - | - | - | - | 2 |
| MA-178B | quartz monzodiorite | B | 7.2 | 9.3 | 42.5 | 14.7 | 9.3 | - | 1.8 | - | 4.8 | 0.7 | 0.9 | 3.6 | - | - | 3.8 | 1.4 | - | 3 |
| MF 073C | quartz diorite | B | 5.0 | 2.0 | 26.0 | 14.0 | 37.0 | 2.0 | 5.0 | - | 2.0 | - | 2.0 | 4.0 | 1.0 | - | - | - | - | 2 |
| MA-144B | quartz diorite | B | 4.1 | 1.9 | 44.2 | 18.0 | 13.5 | - | 4.4 | - | 3.3 | 0.6 | 0.6 | 3.0 | - | - | 6.6 | - | - | 3 |

Modal analysis from (1) Sardinha (1999), (2) CPRM (2000) and (3) this paper. Obs: A. Alto Alegre and B. Jaburuzinho facies. Modal analysis from (1) Sardinha (1999), (2) CPRM (2000) and (3) this paper. Obs: A. Alto Alegre and B. Jaburuzinho facies. Abbreviations: qz. quartz, af. alkalifeldspar, pg. plagioclase, bi. biotite, amp. amphibole, ms. muscovite, tt. titanite, al. allanite, ep. epidote, zi. zircon, ap. apatite, om. opaque minerals, cpx. clinopyroxene, cl. chlorite, ss. saussurite, my. myrmecite, ph. prehnite. Note: ref. references. * Água Branca Granite (type-area).

Table 3. Modal mineral contents of Igarapé Azul Granite and their enclaves.

| samples | classification | facies | qz | af | pg | bi | ms | tt | al | ep | zi | ap | om | cl | lx | ss | my | Ref |
|---------|---------------------|--------|------|------|------|------|------|-----|-----|-----|-----|-----|-----|-----|-----|------|-----|-----|
| MA 088 | syenogranite | A | 38.0 | 36.4 | 11.3 | 4.5 | 4.6 | 0.2 | 1.0 | 1.1 | 0.1 | - | 0.7 | 0.6 | - | 1.5 | - | 3 |
| MJ 018 | leucomonzogranite | A | 35.3 | 31.1 | 27.9 | 3.0 | 1.4 | 0.1 | 0.1 | 0.3 | 0.1 | 0.1 | 0.5 | 0.1 | - | - | - | 1 |
| RL 010 | leucogranodiorite | A | 33.7 | 18.2 | 41.5 | 4.0 | 0.1 | 0.2 | 0.1 | 0.4 | 0.1 | 0.1 | 1.0 | 0.1 | - | 0.5 | - | 1 |
| NR 013 | leucomonzogranite | A | 32.2 | 30.8 | 32.1 | 2.2 | - | 0.1 | 0.1 | 0.6 | 0.1 | 0.1 | 1.4 | 0.2 | 0.2 | - | - | 1 |
| RL 007B | leucomonzogranite | A | 32.0 | 26.1 | 36.6 | 3.6 | - | 0.1 | 0.1 | 0.4 | 0.1 | 0.1 | 0.9 | 0.1 | 0.1 | 0.3 | - | 1 |
| MF 014 | leucogranodiorite | A | 30.0 | 21.6 | 44.5 | 2.3 | 0.9 | - | - | 0.1 | 0.1 | - | 0.1 | 0.3 | 0.1 | - | - | 1 |
| RL 009B | leucomonzogranite | A | 28.5 | 24.0 | 43.1 | 2.8 | - | 0.1 | - | 0.4 | 0.1 | 0.1 | 0.5 | 0.1 | 0.2 | 0.5 | - | 1 |
| MF 006C | leucogranodiorite | A | 25.6 | 17.7 | 52.0 | 3.5 | 0.2 | 0.2 | 0.1 | 0.1 | 0.1 | 0.1 | 0.4 | 0.3 | - | - | - | 1 |
| MA 147A | monzogranite | A | 24.6 | 31.8 | 24.2 | 1.3 | 1.9 | 0.1 | 0.1 | 4.6 | 0.1 | 0.1 | 1.0 | 3.4 | - | 6.1 | 0.7 | 3 |
| MF 006B | leucomonzogranite | A | 23.0 | 31.3 | 42.7 | 1.4 | - | 0.1 | - | 0.1 | 0.1 | 0.1 | 0.7 | 0.6 | - | - | - | 1 |
| MA 079 | quartz monzonite | A | 16.0 | 25.0 | 33.7 | 9.5 | 2.4 | 0.3 | - | 1.5 | - | - | 1.0 | 0.2 | - | 9.5 | 0.9 | 3 |
| RL 011 | monzogranite | B | 33.0 | 27.0 | 32.0 | 5.7 | 0.6 | 0.3 | 0.1 | 0.4 | 0.1 | 0.1 | 0.6 | 0.1 | - | - | - | 1 |
| MJ 014 | monzogranite | B | 30.6 | 25.2 | 37.3 | 4.8 | 0.6 | 0.1 | 0.1 | 0.4 | 0.1 | 0.1 | 0.7 | - | - | - | - | 1 |
| MJ 017B | leucogranodiorite | B | 30.2 | 23.3 | 44.1 | 0.4 | 0.2 | 0.1 | - | 0.7 | 0.1 | 0.1 | 0.4 | 0.4 | - | - | - | 1 |
| MA 186A | monzogranite | B | 29.0 | 27.9 | 26.4 | 4.6 | 1.0 | - | - | 1.1 | - | - | 0.9 | 0.2 | - | 7.9 | 1.0 | 3 |
| MA 201A | monzogranite | B | 25.8 | 25.1 | 31.6 | 3.9 | 0.3 | - | - | 1.5 | 0.1 | 0.2 | 0.3 | 0.2 | - | 10.5 | 0.5 | 3 |
| MJ 017A | leucomonzogranite | B | 24.3 | 28.6 | 41.5 | 3.6 | 0.2 | 0.1 | 0.1 | 0.2 | 0.1 | 0.1 | 0.5 | 0.8 | - | - | - | 1 |
| MF 006A | leucogranodiorite | C | 38.1 | 20.1 | 39.6 | 1.4 | tr | - | - | 0.1 | 0.1 | 0.1 | 0.3 | 0.1 | 0.1 | - | - | 1 |
| MA 002 | leucomonzogranite | C | 30.5 | 29.1 | 33.0 | 2.5 | 0.4 | 0.2 | 0.2 | 0.6 | 0.1 | - | 0.8 | 0.3 | - | 1.2 | 1.1 | 3 |
| RL 008 | monzogranite | C | 30.3 | 24.0 | 35.9 | 7.9 | 0.5 | 0.1 | - | 0.6 | 0.1 | 0.1 | 0.5 | - | - | - | - | 1 |
| RL 009A | monzogranite | C | 29.2 | 30.5 | 33.7 | 4.5 | 0.2 | 0.1 | 0.1 | 0.5 | 0.1 | 0.1 | 0.7 | 0.1 | 0.1 | 0.1 | - | 1 |
| MF 010B | monzogranite | C | 27.5 | 37.7 | 24.3 | 7.2 | 1.6 | 0.1 | - | 0.4 | 0.1 | 0.2 | 0.6 | 0.3 | - | - | - | 1 |
| MJ 012 | monzogranite | C | 26.4 | 23.7 | 41.0 | 6.9 | 0.5 | 0.2 | 0.1 | 0.4 | 0.1 | 0.1 | 0.3 | - | - | 0.3 | - | 1 |
| MJ 015B | monzogranite | C | 25.8 | 40.5 | 24.0 | 6.0 | 1.5 | 0.1 | - | 0.3 | 0.1 | 0.1 | 0.4 | 0.2 | - | 1.0 | - | 1 |
| MA 102A | leucomonzogranite | C | 22.9 | 28.7 | 36.8 | 0.6 | 0.7 | 0.1 | 0.3 | 1.0 | 0.1 | - | 1.1 | 0.2 | - | 6.4 | 1.1 | 3 |
| MF 079 | monzogranite | C | 21.2 | 26.1 | 44.7 | 6.2 | tr | 0.1 | 0.4 | 0.1 | 0.1 | 0.1 | 1.0 | - | - | - | - | 1 |
| MA-085B | granodiorite | D | 12.9 | 8.8 | 34.1 | 27.6 | - | 0.6 | - | 1.2 | 0.6 | 1.2 | 4.7 | 1.2 | - | 5.9 | 1.2 | 3 |
| MA 186B | tonalite | D | 9.0 | 0.1 | 20.0 | 55.0 | 10.0 | - | - | 4.7 | 0.1 | 0.1 | 1.0 | - | - | - | - | 3 |
| MA 213B | quartz monzodiorite | D | 6.0 | 3.0 | 40.0 | 46.0 | 2.0 | - | - | tr | tr | 0.1 | 2.9 | - | - | - | - | 3 |
| MA 147B | quartz diorite | D | 5.0 | 0.1 | 39.0 | 49.7 | 2.0 | 0.1 | 0.1 | 1.1 | 0.1 | 0.1 | 2.7 | - | - | - | - | 3 |
| MA 201B | quartz diorite | D | 4.4 | 7.0 | 12.5 | 57.7 | 6.3 | 0.2 | - | 0.4 | 0.7 | 1.5 | 6.7 | 0.4 | - | 2.1 | 0.1 | 3 |

Modal analysis from (1) Sardinha (1999), (2) Faria & Luzardo (2000) and (3) this paper. Obs: A. Cinco Estrelas, B. Saramandaia, C. Vila Catarina, D. biotite-bearing enclave. Abbreviations: qz. quartz, af. alkali-feldspar, pg. plagioclase, bi. biotite, ms. muscovite, tt. titanite, al. allanite, ep. epidote, zi. zircon, ap. apatite, om. opaque minerals, cl. chlorite, lx. leucoxene, ss. saussurite, my. myrmequite. Note: ref. references.

Geochemistry and Zircon Geochronology of the I-type High-K Calc-alkaline and S-Type Granitoids from Southeastern Roraima State, Brazil: Orosirian Collisional Magmatism Evidence (1.97-1.96 Ga) in central portion of Guyana Shield

Marcelo E. Almeida^{1,2*}, Moacir J.B. Macambira², Elma C. Oliveira²

¹CPRM – Geological Survey of Brazil, Av. André Araújo 2160, Aleixo, CEP 69060-001, Manaus, Amazonas, Brazil

²Isotope Geology Laboratory, Center of Geosciences, Federal University of Pará, CP. 8608, CEP 66075-110, Belém, Pará, Brazil

* Corresponding author; ph.: +55-92-2126-0301, fax: +55-92-2126-0319, e-mail address: marcelo_almeida@ma.cprm.gov.br

ARTIGO SUBMETIDO AO CORPO EDITORIAL DA REVISTA *PRECAMBRIAN RESEARCH*

Words: summary (76), abstract (121), body text (10356), table (446) and figure (933) captions.

Total: 6 tables and 12 figures.

ABSTRACT

INTRODUCTION

GEOLOGICAL SETTING

ANALYTICAL PROCEDURES

Whole-rock Geochemistry Analysis

Zircon Isotope Analysis

WHOLE-ROCK GEOCHEMICAL RESULTS

Major and Minor Oxides, and Trace Elements Geochemistry

Rare Earth Element (REE) Geochemistry

MARTINS PEREIRA AND SERRA DOURADA GRANITES: PETROGENETIC CONSIDERATIONS

ZIRCON GEOCHRONOLOGY

Martins Pereira Granite (MA-172A, 061A and 007A samples)

S-type Serra Dourada Granite (MF-156 sample)

Lense of Leucogranite (MA-246C2 sample)

TAPAJÓS AND UATUMÃ-ANAUÁ DOMAINS: CHRONOSTRATIGRAPHY AND IMPLICATIONS FOR GEOLOGICAL EVOLUTION OF THE TAPAJÓS-PARIMA OR VENTUARI-TAPAJÓS PROVINCES

CONCLUSIONS

Acknowledgments

References

ABSTRACT

The understanding of the geological evolution of the Uatumã-Anauá Domain in southeastern Roraima, central region of Guyana Shield, is of major significance in the study of the Amazonian craton, because this region lies between some Paleoproterozoic geological-geochronological provinces: Tapajós-Parima or Ventuari-Tapajós (dominant), Maroni-Itacaiunas (northwest) and Central Amazonian or Central Amazon (southeast and east). Geological mapping of the northern area of Uatumã-Anauá Domain, integrated with previous and new Pb-evaporation and U-Pb zircon geochronological, and whole rock geochemistry data suggest a plutonic collisional magmatism (1975-1968 Ma) represented by I-type high-K calc-alkaline granitoids (Martins Pereira) and S-type granites (Serra Dourada), both probably generated during amalgamation of TTG-like Anauá magmatic arc (2028 Ma) with Transamazonian (2.2-2.0 Ga) and Central Amazonian (older than 2.3 Ga) terranes.

Keywords: Paleoproterozoic, Granitoids, Guyana Shield, Zircon geochronology, Geochemistry

INTRODUCTION

The Guyana Shield, with a surface area of nearly 1.5 million km², represents the northernmost section of the Amazonian craton. This shield was predominately formed during protracted periods of intense granitic magmatism, bracketed between 2.1 and 1.9 Ga (**Fig. 1a-b**). Despite representing an intricate component of the Amazonian craton, the Guyana shield has seen only limited attention among the scientific community. Geological maps of the region are scarce (*e.g.* CPRM, 1999, 2000a; Delor *et al.*, 2003), and only few petrographical, geochemical and geophysical studies are available. Comparison between previous studies from the Guyana shield has been hampered by a lack of confident age determinations, implying large errors (\pm 50-100 Ma), which preclude any attempt to establish a fine chronology of the magmatic and metamorphic events.

The study area in this research project concentrates on the central portion of Guyana Shield, located in the southeastern Roraima State (Brazil). Recent zircon geochronology data demonstrates that outcropping igneous rocks from this region (near to 4970 km², Fig. 2) show ages of 2.03 Ga (Faria *et al.*, 2002) and 1.97-1.96 Ga (Almeida *et al.*, 1997, CPRM, 2003), similarly to the Tapajós Domain in Central Brazil Shield (Santos *et al.*, 2000, Lamarão *et al.*, 2002). The characteristics and significance of these events and ages is, however, not fully understood (CPRM, 2000a; Almeida and Macambira, 2003). An example of this can be seen in

the 2.03-1.96 Ga magmatic event which, unlike the 1.90 Ga calc-alkaline magmatism, is uncommon in other regions of the world. Besides in the Tapajós Domain in Central Brazil Shield (southern Amazonian craton), Paleoproterozoic tectonic and magmatic activity older than 1.90 Ga is recorded in Western Australia (Gascoigne Complex, Dalgaringa Supersuite, 2005-1970 Ma) by Sheppard *et al.* (2004) and southern Australia (Gawler Craton, Miltalie Gneiss, ca. 2000 Ma) by Daly *et al.* (1998). The Taltson Magmatic Zone of northern Canada (McDonough *et al.*, 1993) and Kora-Karelian orogen of northern of Baltic Shield (Daly *et al.*, 2001) also show 2.0-1.9 Ga magmatic events.

The aim this paper is to provide new geochemical and geochronological constraints on the Martins Pereira and Serra Dourada granitoids (Almeida *et al.*, 2002). It is hoped that such studies will contribute to a better understanding of the lithostratigraphy, origin and geodynamic evolution of the northern part of the Uatumã-Anauá Domain, central portion of Guyana Shield (**Fig. 1**). These data will be integrated with previous geochemical and geochronological data for other magmatic associations, mainly calc-alkaline granitoids older than 1.90 Ga. Particular focus will be placed on comparative geochemical and geochronology data from previous studies in the same region and the southern part of the Amazonian craton.

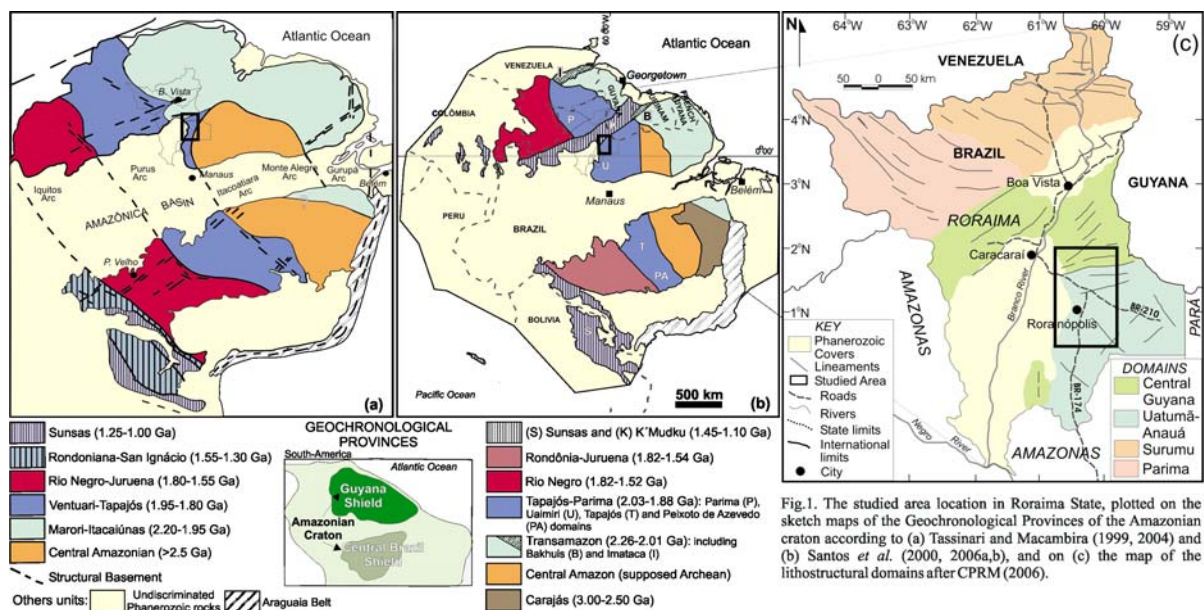


Fig.1. The studied area location in Roraima State, plotted on the sketch maps of the Geochronological Provinces of the Amazonian craton according to (a) Tassinari and Macambira (1999, 2004) and (b) Santos *et al.* (2000, 2006a,b), and on (c) the map of the lithostratigraphic domains after CPRM (2006).

GEOLOGICAL SETTING

Regional geological maps (CPRM 2000a, Almeida *et al.*, 2002) and zircon geochronological data (Almeida *et al.*, 1997, Santos *et al.*, 1997, Macambira *et al.*, 2002, CPRM,

2003) have shown that Paleoproterozoic granitoids and volcanic rocks (1.97 to 1.81 Ga) are widespread in southeastern Roraima. These intrusive and extrusive rocks are emplaced within minor basement rocks that have maximum ages of around 2.03 Ga (Faria *et al.*, 2002).

According to recent evolutionary models proposed for the Amazonian craton, the study area can be divided into different provinces. According to the work of Tassinari and Macambira (1999, 2004), the study area is largely enclosed by Ventuari-Tapajós and Central Amazonian provinces, with a subordinate northeastern section falling within the Maroni-Itacaiúnas province. Santos *et al.* (2000, 2006) argue that all provinces were collectively affected by the K'Mudku Shear Belt in this same region (**Fig. 1 a-b**). These models point out that Paleoproterozoic orogenic belts or magmatic arcs (*e.g.*, Ventuari-Tapajós or Tapajós-Parima, and Maroni-Itacaiúnas or Transamazon provinces) accreted to the Archean craton with time and/or represent a set of rocks produced from melting of Archean crust (Fig. **1a-b**; Cordani *et al.*, 1979, Teixeira *et al.*, 1989, Tassinari 1996, Tassinari and Macambira, 1999, 2004; Santos *et al.*, 2000, 2004, 2006).

The Tapajós-Parima (or Ventuari-Tapajós) Province is a Paleoproterozoic orogenic belt shows north-northwest trends and includes geological units which range from ~2.10 to 1.87 Ga in age (Santos *et al.*, 2000, 2006; Tassinari and Macambira 1999, 2004). This province was subdivided into four domains by Santos *et al.* (2000): Parima and Uaimiri, to north, and Peixoto Azevedo and Tapajós, to south. The southeastern Roraima belongs to the Uaimari Domain. The Central Amazonian Province (**Fig. 1a-b**) has granitoids and volcanic rocks (1.88 to 1.70 Ga) with no regional metamorphism and compressional folding (Santos *et al.*, 2000, Tassinari and Macambira 1999), and its basement rarely outcrops. The age for this basement has been estimated by some Nd-model ages at around 2.3-2.5 Ga (Tassinari and Macambira, 1999, 2004). According to these authors, the recorded Archean rocks in the Amazonian craton are only exposed in Imataca (Venezuela), Carajás and southern Amapá-northwestern Pará (Brazil) regions. The Maroni-Itacaiúnas (or Transamazon) Province is also characterized by an orogenic belt with Rhyacian ages (2.25 to 2.00 Ga, **Fig. 1a-b**) and is correlated to Birimian belt in West Africa (Tassinari and Macambira, 1999, 2004; Santos *et al.*, 2000; Delor *et al.*, 2003). The K'Mudku Shear Belt is characterized by mylonitic zones with ca. 1.20 Ga (low grade) and cross-cut at least three provinces (Rio Negro, Tapajós-Parima and Transamazon, Santos *et al.*, 2000).

Reis *et al.* (2003) and CPRM (2006), taking into account lithological associations and geochronological data, divided the Roraima State into four major domains – Surumu, Parima,

Central Guyana and Uatumã-Anauá (**Fig. 1c**). Each of these domains contains a wide range of rock types and stratigraphic units. The southeastern Roraima is composed of the Central Guyana and Uatumã-Anauá lithostructural domains, that correspond to the K`Mudku Shear Belt and Uaimiri Domain (northern Tapajós-Parima Province) respectively proposed by Santos *et al.* (2000).

The Central Guyana Domain (CGD) primarily consists of granulites, orthogneiss, mylonites and metagranitoids (Rio Urubu Metamorphic Suite) associated with low to high metamorphic grade metavolcanosedimentary covers (Cuarane Group) and S-type granite (Curuxuim Granite). The lineaments are strongly NE-SW trends. The Uatumã-Anauá Domain (UAD) is characterized by E-W to NE-SW lineaments and the northern part of the domain (NUAD) shows an older metamorphic basement (**Figs. 1 and 2**) formed in a presumed island arc environment (Faria *et al.*, 2002). This basement is composed by TTG-like metagranitoids to orthogneisses (Anauá Complex), enclosing meta-mafic to meta-ultramafic xenoliths, and is associated with some inliers of metavolcano-sedimentary rocks. The basement rocks are intruded by S-type (Serra Dourada Granite) and high-K, I-type calc-alkaline (Martins Pereira) granitic magmatism of around 1.97-1.96 Ga (see zircon geochronology section).

In the southern area of Uatumã-Anauá domain (SUAD), intrusive younger granites (with no regional deformation and metamorphism) are most common. The most prominent magmatism is related to the calc-alkaline Caroebe and Igarapé Azul granitoids (Água Branca Suite) with coeval Iricoumé volcanic rocks. Locally igneous charnockitic (Igarapé Tamandaré) and enderbitic (Santa Maria) plutons were also recorded. Several A-type granitic bodies are widespread in the Uatumã-Anauá Domain (**Fig. 2**) represented by Moderna-Água Boa (1.81 Ga) and Mapuera-Abonari (1.87 Ga) granites.

ANALYTICAL PROCEDURES

Whole-rock Geochemistry Analysis

Whole-rock chemical analyses of 11 samples (milled under 200 mesh) were done at the Acme Analytical Laboratories Ltd in Vancouver, British Columbia, Canada. The analytical package include inductively coupled plasma-atomic emission spectrometer (ICP-AES) analyses after LiO₂ fusion for all major oxides (SiO₂, TiO₂, Al₂O₃, MnO, MgO, CaO, K₂O, Na₂O, P₂O₅) and LOI. Total iron concentration is expressed as Fe₂O₃. The trace elements were analyzed by inductively coupled plasma-mass spectrometer (ICP-MS), with rare-earth and incompatible

elements determined from a LiBO₂ fusion and precious and base metals determined from an aqua regia digestion. An additional 16 samples were compiled (and partially reinterpreted) from CPRM (2000a). These last whole-rock chemical analyses were done at the Geosol Laboratories S.A. in Belo Horizonte, Minas Gerais, Brazil.

Zircon Isotope Analysis

For the isotope analysis, the crystals of zircon were obtained from samples with 2 to 10 kg. After crushing (milled to 60-80 mesh) and sieving, heavy mineral fractions were obtained by water-mechanical and dense liquid concentrations, and processed under hand magnet and Frantz Isodynamic Separator. In order to remove impurities, the zircon concentrates were washed with HNO₃ at 100^o C (10 minutes), submitted to ultrasound cube (5 minutes) and finally washed on bidistilled H₂O. The less magnetic zircon concentrates (from five magnetic fractions) were preferred for hand-picking. Only zircon grains free of alteration, metamictization features, inclusions and fractures were selected for analysis, however it was not always possible (see zircon descriptions below). All selected grains for analysis were photomicrographed via a conventional optical microscope.

The single-zircon dating by Pb-evaporation and U-Pb isotopic dilution in thermal ionization mass spectrometer (ID-TIMS) methods were performed at the Isotope Geology Laboratory (Pará-Iso), Federal University of Pará (UFPA), Brazil. The U decay constants are those recommended by IUGS (Steiger and Jäger 1977), and errors are given at the 95% confidence level. Ages of 5 samples were obtained by the Pb-evaporation technique established by Kober (1986, 1987), and only one sample is obtained by the U-Pb ID-TIMS. All the isotope analyses were carried out on a Finnigan MAT 262 mass spectrometer in dynamic mode using the ion counting detector.

In the Pb-evaporation method on a single zircon, the selected grains were tied in Re-“evaporation”-filament and introduced in the mass spectrometer. The Pb was normally extracted from the crystals by heating in three evaporation steps at temperatures of 1450^o, 1500^o and 1550^oC. The evaporated Pb was load on an “ionization” filament, which is heated for the isotope analyses. In this technique, the data were dynamically acquired using the ion counting system of the instrument. Pb signal was measured by peak hopping in the 206, 207, 208, 206, 207, 204 mass order along 10 scans, defining one block of data with 18 ²⁰⁷Pb/²⁰⁶Pb ratios. The ²⁰⁷Pb/²⁰⁶Pb ratio average of each step was based on five blocks or less, till the intensity beam was sufficiently high for a reliable analysis. Usually, the average ²⁰⁷Pb/²⁰⁶Pb ratio obtained in the highest

temperature step was taken for age calculation, but the other steps are also considered. Outliers were eliminated using Dixon's test. The $^{207}\text{Pb}/^{206}\text{Pb}$ ratios were corrected for a mass discrimination factor of $0.12\% \pm 0.03 \text{ a.m.u}^{-1}$, and results with $^{204}\text{Pb}/^{206}\text{Pb}$ ratios higher than 0.0004 were, in general, discarded. The ages were calculated with 2 sigma error and common Pb correction was done using appropriate age values derived from the two-stage model of Stacey and Kramers (1975). The obtained data were processed in shareware *Zircon* program (T. Scheller, 1998), DOS system version.

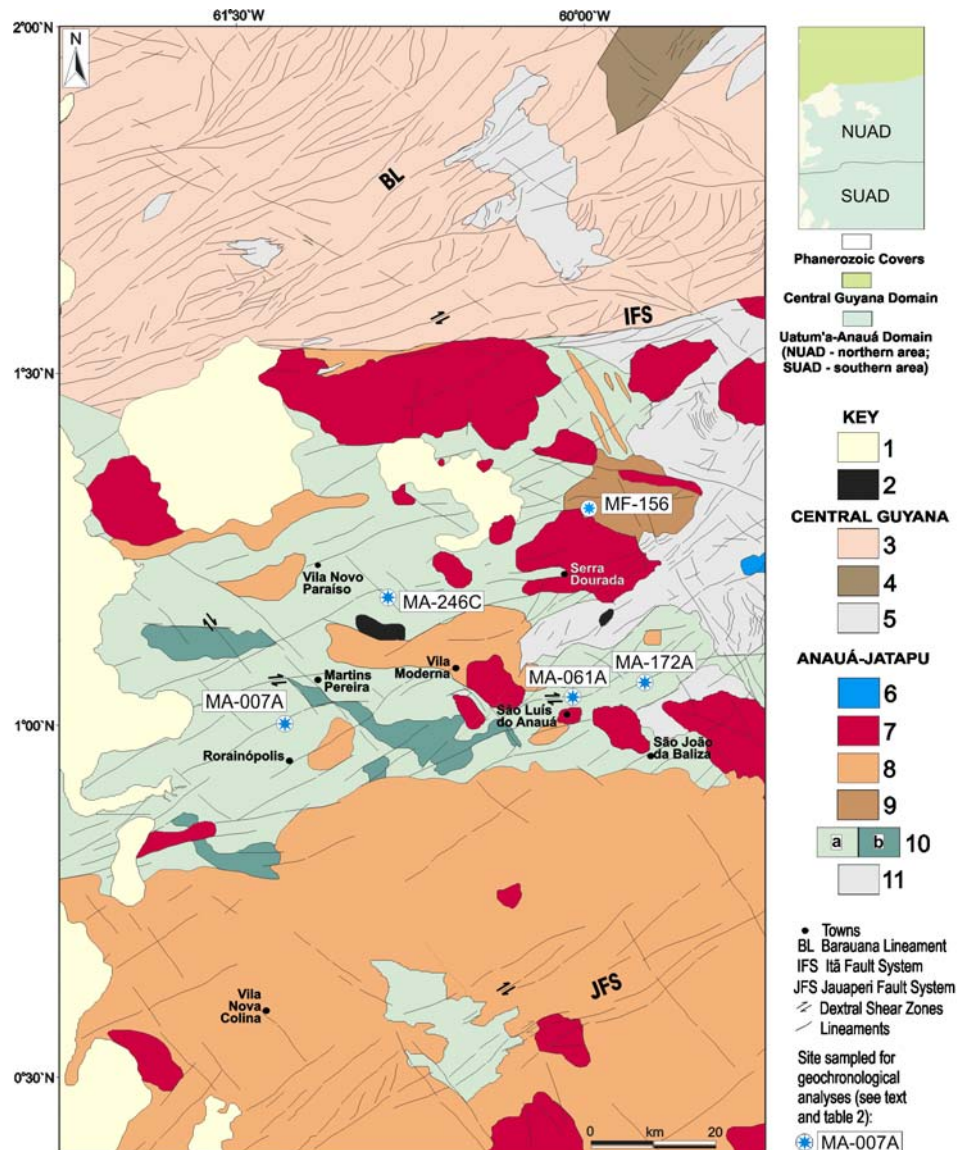


Fig.2. Simplified geological map of Southeastern Roraima State modified from Almeida *et al.* (2002) and CPRM (2000a, 2005): 1. Plio-Pleistocene sedimentary covers, 2. Caracará Gabbro (1.52 Ga?), 3. Foliated granitoids (1.72 Ga), mylonitic granites (1.89 Ga), granulites, augen gneisses, metagranitoids and orthogneisses from Rio Urubu Complex (1.96-1.93 Ga), 4. S-type Curuxuim (garnet) Granite (1.97 Ga?), 5. Metavolcano-sedimentary sequence (Cauarane Group), 6. Proterozoic sedimentary cover (Urupi Formation), 7. a) A-type Moderna (1.81 Ga) and Mapuera granites (1.87 Ga), and minor charnockitoids (1.89 Ga), 8. Igarapé Azul and Caroebe granites and minor Jatapu volcanic rocks (1.90-1.89 Ga), 9. S-type Serra Dourada (cordierite) Granite (1.96 Ga), 10. High-K calc-alkaline granitoids with normal (a) to high U, Th, K (b) contents (Martins Pereira Granite, 1.97 Ga), 11. Metavolcano-sedimentary sequence (Cauarane Group related rocks) and TTG calc-alkaline association (Anauá Complex, 2.03 Ga).

The Pb-evaporation on a single zircon method yields apparent $^{207}\text{Pb}/^{206}\text{Pb}$ ages and the degree of concordance of the analytical points is not possible to assess. Furthermore, zircons exhibiting a complex history, often furnish mixed ages with no geological meaning (Dougherty-Page and Bartlett, 1999). With these uncertainties in mind, the age obtained for a single grain is considered as a minimum age. This being the case, as has been proposed in several studies (Kober, 1986; Andsell and Kyser, 1991; Macambira and Scheller, 1994; Söderlund, 1996), if a set of magmatic grains from the same sample yields similar ages, it is possible to suggest that such similarities indicate the time of the magmatic crystallization.

The U-Pb ID-TIMS procedure undertaken in the Pará-Iso Laboratory followed those presented by Krymsky (2002). All zircon fractions selected for analysis were previously air abraded with pyrite crystals (20 mg and 0.1-0.5 mm diameter) in 1.2-1.8 p.s.i. pressure for 30-40 minutes. After abrasion the zircon grains were washed with HNO_3 and HCl (100^o C, 30 minutes) and H_2O -Millipore (3 times). The grains were then washed with metanol, weighed, spiked with ^{235}U - ^{205}Pb tracer and dissolved with a mixture of HF and HCl in PTFE Teflon[®] bombs. Uranium and lead were separated with anion-exchange resin (Dowex[®] 1x8 200-400 mesh) in HCl medium in 50-70 μL columns. Uranium and Lead were loaded with Si-gel and H_3PO_4 (1N) onto the same out-gassed Re-filament and analyzed at 1400^o-1600^o C. For zircon analyses, blanks are <30 pg Pb and <1 pg U. The obtained data were processed in ISOPLOT/Excel program version 2 (Ludwig, 1999). The $^{208}\text{Pb}/^{206}\text{Pb}$ ratios were corrected for common Pb using also Stacey and Kramers (1975) model.

WHOLE-ROCK GEOCHEMICAL RESULTS

Major and Minor Oxides, and Trace Elements Geochemistry

Analytical results of representative samples from Martins Pereira, Serra Dourada and Anauá granitoids of the NUAD, including leucogranite pods and lenses, are presented in **table 1** and plotted in diagrams in **Figs. 3 to 7**. Serra Dourada and Anauá results are extracted from CPRM (2000a). The Creporizão (CPRM, 2000b) and Old São Jorge (Lamarão *et al.*, 2002) granitoids data from Tapajós region are also plotted in some diagrams for comparison with Martins Pereira granitoids.

The Martins Pereira Granite consist of a compositionally wide series of rocks with SiO_2 contents between 49.3 to 74.6 wt.% (**table 1**). The associated leucogranite pods and lenses have high SiO_2 contents (72.9 to 73.9 wt. %), but in the Harker diagrams show no correlation with the

Martins Pereira Granite. For instance, leucogranites with the same SiO₂ contents as Martins Pereira granatoids, have low Na₂O (**Fig. 3g**), MnO (**Fig. 3d**), Fe₂O₃+FeO (**Fig. 3c**) and very high K₂O (**Fig. 4a**) values.

The rock samples from Martins Pereira Granite is also characterized by linear trends in the all Harker diagrams (**Fig. 3a-h**). In these diagrams, excluding Na₂O vs. SiO₂, the statistic parameters show negative linear correlations with regression agreement between 99% and 99.9%. Linear trends can be resulted from several petrogenetic processes, such as contamination, mixing and partial melting (*e.g.* Cox *et al.*, 1979). The lack of significant compositional gaps in Harker diagrams for Martins Pereira samples suggests that the main petrogenetic process is likely related to partial melting. Fractional crystallization, by comparison, usually results in curvilinear Harker-plot trends (*e.g.* Cox *et al.*, 1979, Wilson, 1989) that are not observed for Martins Pereira samples.

In contrast to the Martins Pereira samples, the Anauá Complex and related rocks show lower SiO₂ contents ranging from 41.3% to 59.8% (**table 1**), and dispersion in the Harker diagrams (*e.g.* TiO₂, MnO, Al₂O₃, Na₂O and Fe₂O_{3t}). When compared to the Martins Pereira granitoids, the Anauá samples are characterized by lower K₂O and P₂O₅ contents (**Fig. 4a, 3h**) while having higher Na₂O and MgO (**Fig. 3e-g**) contents. The Serra Dourada Granite shows remarkable Na₂O (**Fig. 3g**) and K₂O lower contents (**table 1**).

Compared to the Martins Pereira granitoids, the 1.99-1.96 Ga Old São Jorge and Creporizão granites from Tapajós Domain have lower TiO₂ (**Fig. 3a**), MnO (**Fig. 3d**) and P₂O₅ (**Fig. 3h**), and higher Na₂O (**Fig. 3g**) contents. The corresponding Harker diagrams demonstrate that the Creporizão granites have a shorter range and higher contents of SiO₂ (65.2 % to 73.4%, **table 1**), as well as lower MnO (**Fig. 3d**), Al₂O₃ (**Fig. 3b**) and K₂O (**Fig. 4b**) contents.

In the log [CaO/(Na₂O+K₂O)] vs. SiO₂ diagram (**Fig. 4a**), all the studied granitoids (excluding Serra Dourada Granite) indicate calc-alkaline affinity, with the samples plotting in the normal calc-alkaline andesitic field. Only the Old São Jorge Granite shows exclusive transitional character between normal and mature arc series. Most of the granitoid samples also plot in the high-K field (K₂O vs. SiO₂ diagram, **Fig. 4b**), however, the Martins Pereira and Old São Jorge granites have a transitional high-K to slightly shoshonitic character. It is also apparent from the K₂O vs SiO₂ diagram that samples from the Creporizão Granite display a transitional high-K to locally medium-K trend, whereas Anauá types are medium-K to slightly low-K. The

leucogranites are highly fractionated and show high K contents (>7%).

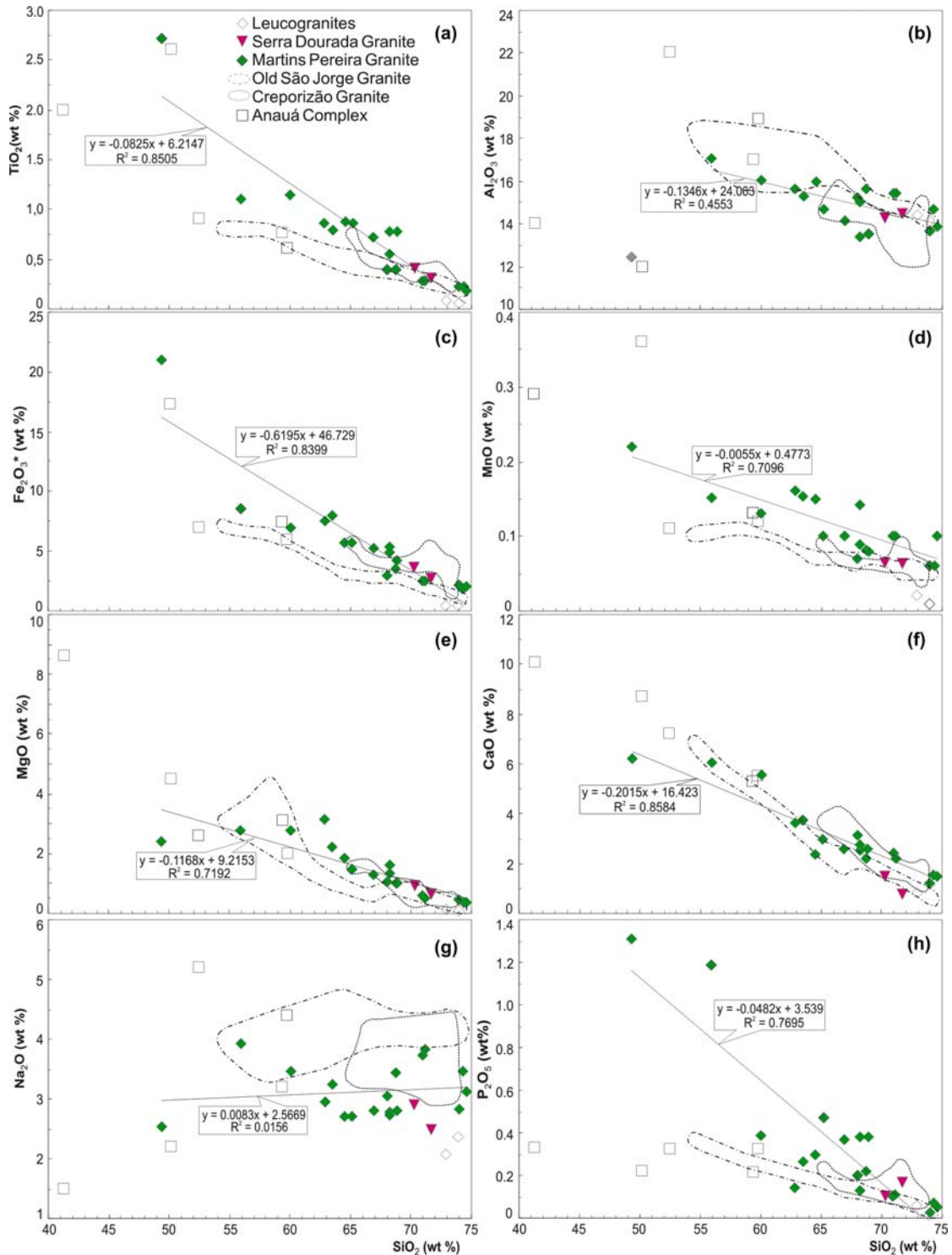


Fig. 3. (a-h) Selected Harker variation diagrams for Martins Pereira and Serra Dourada Granites, leucogranites and Anauá Complex. For references see table 1. Fields representing Creporizão (CPRM, 2000b) and Old São Jorge granites (Lamarão *et al.*, 2002) of the Tapajós Domain are plotted for comparison. For the linear regression are used only the Martins Pereira Granite samples.

The Martins Pereira and Creporizão granite compositions are transitional between

metaluminous to peraluminous, while the Old São Jorge granite is metaluminous to slightly peraluminous (**Fig. 5a**). Almost all these granites show A/NK molar ratios < 2 . Only the Anauá Complex rocks (A/NK molar > 2) and the leucogranite veins are metaluminous and peraluminous. The Serra Dourada Granite is broadly peraluminous, plotting in the S-type granite compositions. This granitic body shows A/CNK molar ratios of 1.1 and 1.3, while some samples of the Martins Pereira Granite also show locally high A/CNK values. In the Na_2O vs. K_2O diagram, the Martins Pereira granitoids plot on the I-type field, but several samples also plot near to the S-type field boundary (**Fig. 5b**) showing, as well as the Serra Dourada Granite samples, the lowest $\text{Na}_2\text{O}/\text{K}_2\text{O}$ ratios.

In the Rb vs. (Y+Nb) tectonic discriminator diagrams (**Fig. 5c**), the Martins Pereira granite samples show transitional VAG (granites to granodiorites) to WPG (biotite-rich tonalites) trends. Anauá rock-types generally plot in the VAG field, with correspondingly low Rb contents. The Creporizão and Old São Jorge granites samples dominantly plot in the VAG field, falling near to the WPG boundary. Thus, excluding Anauá rocks, most of the analyzed samples fall in the postcollisional field of Pearce (1996), which suggests an increasing in arc maturity (Brown *et al.*, 1984, see **Fig. 4a**) or the beginning of the transition from calc-alkaline to alkaline magmatic series in orogenic to post-orogenic tectonic settings (Bonin, 1990; Barbarin, 1999).

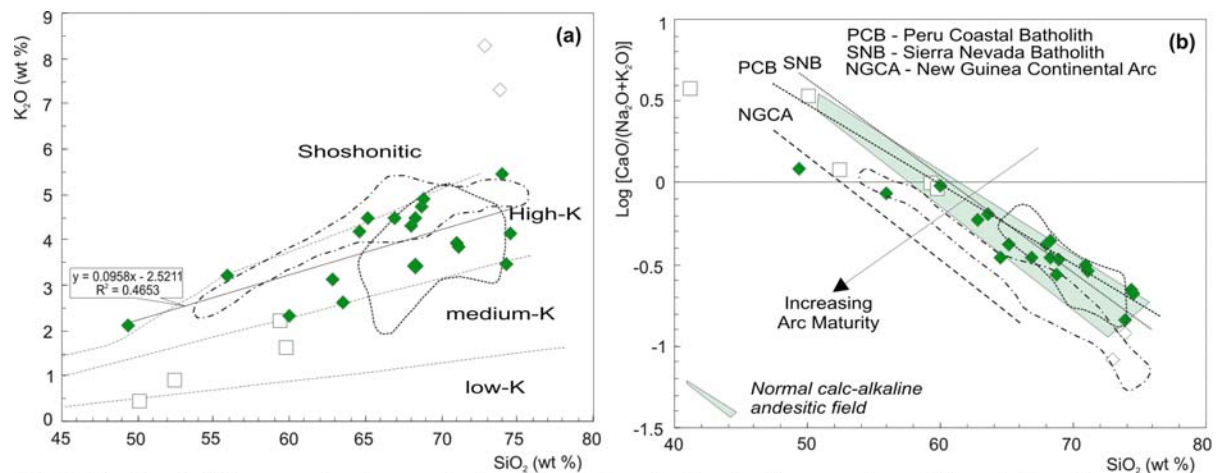


Fig.4. Geochemical diagrams showing results from Martins Pereira Granite, leucogranites and Anauá Complex rocks (for references see table 1). Fields representing Creporizão (CPRM, 2000b) and Old São Jorge granites (Lamarão *et al.*, 2002) are plotted for comparison: (a) K_2O vs. SiO_2 contents displaying the shoshonite, high-K, medium-K and low-K fields (from Peccerilo and Taylor, 1976; modified by Rickwood, 1989). For the linear regression are used only the Martins Pereira Granite samples. (b) $\log[\text{CaO}/(\text{Na}_2\text{O}+\text{K}_2\text{O})]$ vs. SiO_2 contents (from Brown *et al.*, 1984). Symbols as in Fig. 3.

In the $(\text{K}_2\text{O} + \text{Na}_2\text{O})/\text{CaO}$ vs. $(\text{Zr} + \text{Nb} + \text{Ce} + \text{Y})$ diagram (**Fig. 5d**), the calc-alkaline Martins Pereira, Creporizão and Old São Jorge granites plot on the unfractionated S- and I-type granites to transitional A-type fields. Concerning the Martins Pereira granitoids, the higher Zr, Y

and Ce contents are probably related to the presence of accessory minerals such as epidote, allanite and zircon, mainly in biotite-rich tonalite types. However, their metaluminous to peraluminous nature (**Fig. 5a**) and VAG character (**Fig. 5c**) point to I-type granite affinity. Samples from Anauá Complex display on the unfractionated S- and I-type granites field with low $(K_2O + Na_2O)/CaO$ ratios. Only the pods of leucogranites and few Creporizão Granite samples plot on the fractionated felsic granites field (**Fig. 5d**).

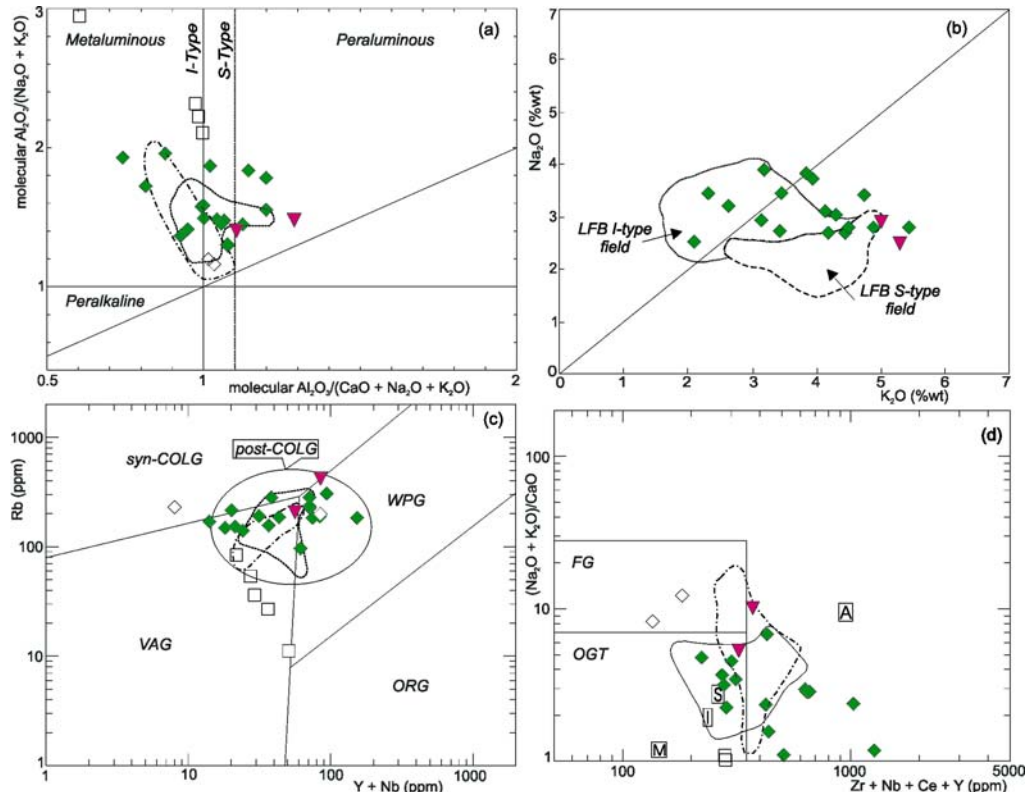


Fig.5. Martins Pereira and Serra Dourada granites, leucogranites and Anauá Complex samples plotted in the diagrams (for references see table 1): (a) Molecular $Al_2O_3/(Na_2O+K_2O)$ vs. molecular $Al_2O_3/(CaO+Na_2O+K_2O)$ (Maniar and Piccoli, 1989; mod. Shand, 1927) and (b) Na_2O vs. K_2O plots showing S-type and I-type granites compositional data from Lachlan Folded Belt (LFB); (c) Rb vs. $(Y+Nb)$ and (d) $(K_2O+Na_2O)/CaO$ vs. $(Zr+Nb+Ce+Y)$. Fields representing Creporizão (CPRM, 2000b) and Old São Jorge granites (Lamarão *et al.*, 2002) are plotted for comparison. In (c), VAG (Volcanic Arc Granites), ORG (Ocean Ridge Granites), syn-COLG (Syn-collisional Granites) and WPG (Within-Plate Granites) fields are from Pearce *et al.* (1984) and post-COLG (post-collisional granites) from Pearce (1996); In (d), OGT (Orogenic granite types: unfractionated I- and S-type granites) and FG (Fractionated felsic I- and S-type granites) fields are taken from Whalen *et al.* (1987). Compositional average of A-, M-, I-, S- and I-type are also represented. Symbols as in Fig. 3.

In the primordial mantle-normalized spidergrams, the Martins Pereira Granite (**Fig. 6a**) exhibits depleted trace element patterns for some HFSE such as Ta, Nb, P, and Ti, and does not show significant LILE depletion (*e.g.* Sr and Ba), as observed for alkali-calcic granitoids of more mature arcs (Brown *et al.*, 1984). This pattern is somewhat similar to those of the calc-alkaline granitoids from normal arcs (*cf.* Brown *et al.*, 1984), though some samples of the Martins Pereira Granite show deep Ti and P depletion, like the media of mature arc granitoids. This geochemical

behavior suggests that Martins Pereira Granite belongs to transitional granitic magmatism, from normal to mature continental arcs (see also **Fig. 4a**).

The Anauá spidergram pattern (**Fig. 6b**) displays coherent Rb, Ba and K contents with primitive arcs (Brown *et al.*, 1984), however, U, Ta, Zr, Sm, Ti and Y are enriched in relation to the primitive arc pattern. All other elements (Th, Nb, La, Ce, Sr, and P) in the Anauá rocks show primitive to mature arcs transitional values. The spidergram pattern of the pods and lenses of leucogranite (**Fig. 6c**) displays the higher Nb, Ta, La, Ce and Hf fractionated values and steeply negative P and Ti anomalies. The leucogranites also show moderate to high Rb, Ba, Th and K contents in relation to chondrite values. The Serra Dourada Granite (**Fig. 6d**) has Rb, Ba, Sr, P and Ti (locally Rb, Nb and P) pattern remarkably similar to the normal S-type media and La, Ce and Y display more enriched contents than normal S-type granites (*e.g.* Chappell and White 1992).

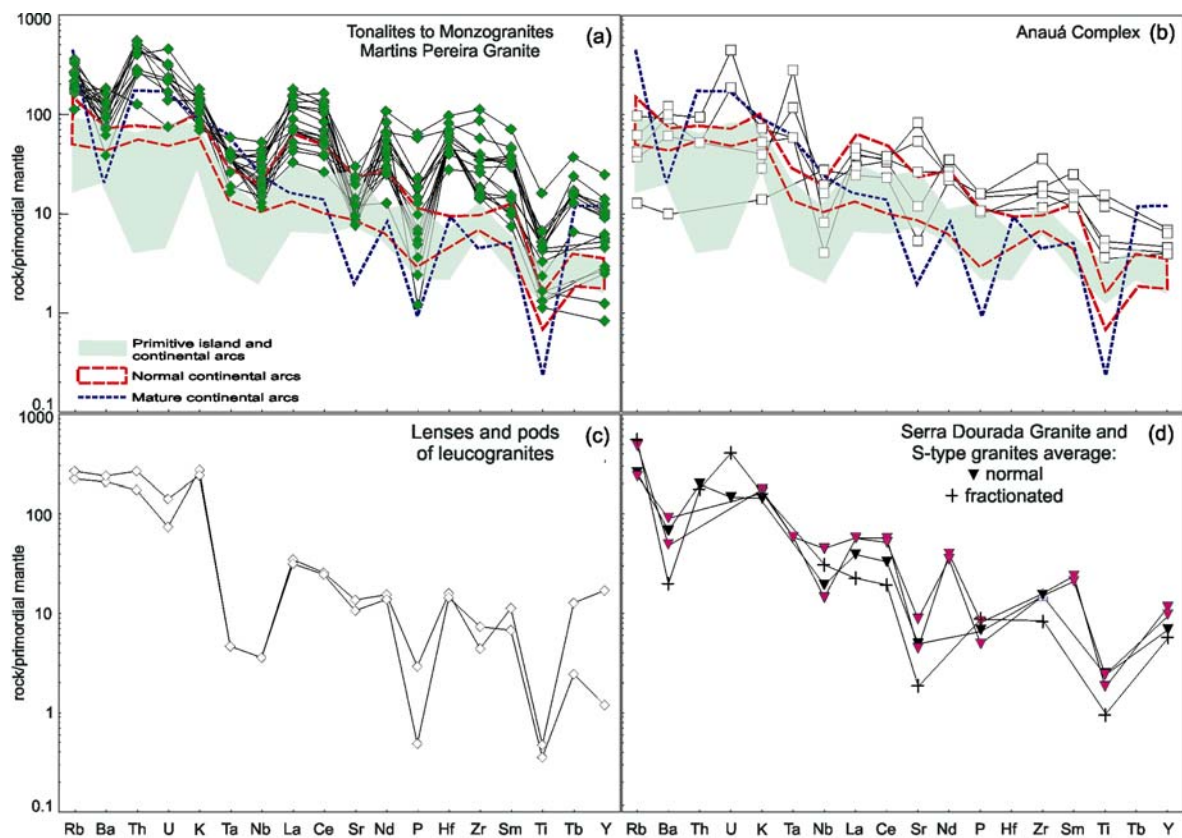


Fig.6. Primitive mantle-normalized spidergram (Wood *et al.*, 1979) for (a) Martins Pereira granitoids (tonalites to monzogranites); (b) Anauá Complex; (c) Pods and lenses of leucogranites, and (d) Serra Dourada Granite. Data from granitoids of primitive, normal and mature arcs (Brown *et al.*, 1984) are also plotted for comparison. Symbols as in Fig. 3.

Rare Earth Element (REE) Geochemistry

The total REE contents of the studied granitoids are relatively similar (**table 1**), except in

the Anauá Complex (138 to 148 ppm) and leucogranites (100 to 153 ppm) samples. Martins Pereira (97 to 624 ppm) and Creporizão granites (104 to 541 ppm) show some REE enriched samples, contrasting with Old São Jorge Granite which displays moderate to low REE contents (52 to 244 ppm).

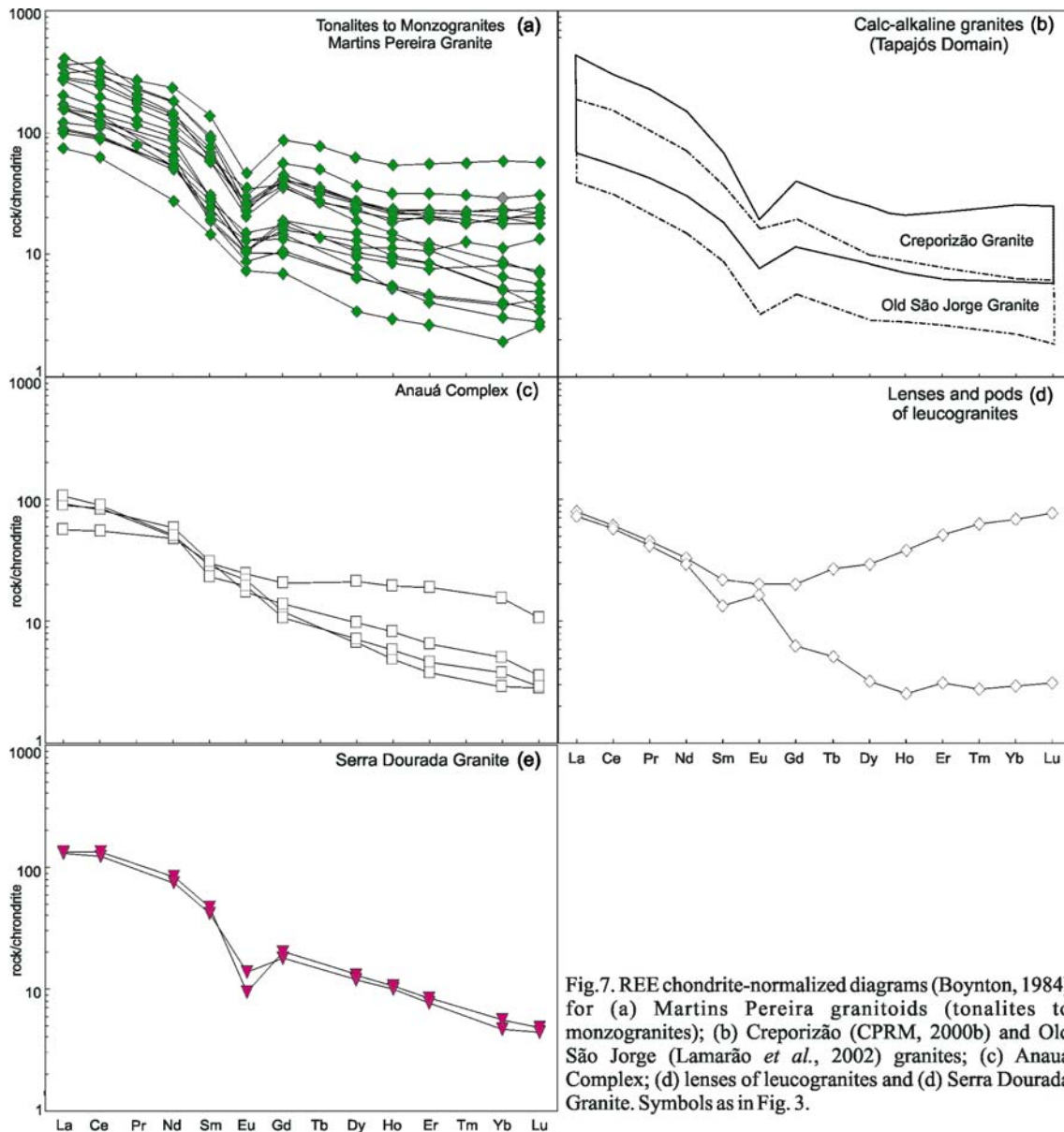
The REE chondrite-normalized pattern of the Martins Pereira Granite (**Fig. 7a**) is enriched in the LREE (*e.g.* La with 80x to 400x the chondrite values), but the LREE fractionation [(La/Sm)_n ratios range from 3.4 to 6.7, exceptionally 8.0] is similar to the Creporizão and Old São Jorge granites (**Fig 7b**). By contrast, the Anauá Complex (**Fig 6c**) shows lower LREE contents (*e.g.* La with 50x to 100x the chondrite values) and low (La/Sm)_n ratios (1.9 to 4.6). The Anauá REE pattern is probably controlled by the hornblende and allanite-epidote fractionation.

The Martins Pereira Granite shows variable HREE contents (*e.g.* Yb and Lu ranging 3x to 60x the chondrite values) and the degree of HREE fractionation [(Gd/Yb)_n] is similar to the Creporizão, Old São Jorge and Anauá granites (1.1 to 4.5). In the more HREE enriched granites, the HREE patterns are normally flat. The wide HREE range in the Martins Pereira types is probably associated to the variable residual zircon retention during partial melting process and the different Zr saturation level of magma (Watson and Harrison 1983). The same is observed in the highly fractionated leucogranitic samples, though these samples have atypical REE patterns, including no positive or negative Eu anomaly (**Fig 7d**). These REE patterns may be related to the high hydrothermal activity in the final stages of crystallization or chemical heterogeneities related to source(s). The Old São Jorge (**Fig 7b**) and Anauá (**Fig 7c**) granitoids exhibit the most HREE depleted patterns.

The Anauá types show discrete negative to positive Eu anomaly, with Eu_n/Eu* ratios ranging from 0.8 to 1.2 (**table 1; Fig. 7c**), suggesting occurrence of plagioclase cumulatic and/or hornblende fractionation. The Old São Jorge Granite (**Fig. 6b**) has slight to no Eu anomalies (Eu_n/Eu* = 0.4 to 1.0), whereas Martins Pereira (**Fig. 7a**) and Creporizão (**Fig. 7b**) granites show moderate negative Eu anomalies, with Eu_n/Eu* ratios ranging from 0.4 to 0.7 and 0.3 to 0.8, respectively (**table 1**). In the case of Martins Pereira, the moderate to discrete negative Eu anomaly probably demonstrates variable residual plagioclase retention in the melt. Overall, the REE patterns are similar among Martins Pereira, Creporizão and Old São Jorge granites.

The Serra Dourada S-type granite (**table 1; Fig. 7e**) shows moderate total REE content (205 to 223 ppm) and moderate to high negative Eu anomaly (Eu_n/Eu* = 0.5 and 0.3). The LREE

fractionation is moderate $[(La/Sm)_n = 3.2 \text{ and } 2.8]$ and HREE fractionation is moderate to high $[(Gd/Yb)_n = 3.6 \text{ and } 3.8]$.



MARTINS PEREIRA AND SERRA DOURADA GRANITES: PETROGENETIC CONSIDERATIONS

The Martins Pereira Granite is of the most prominent examples of Orosirian high-K calc-alkaline plutonism in southern Roraima State, outcropping in the NUAD. The geological literature shows that the high-K calc-alkaline granitoids are very common in orogenic belts since Proterozoic times, corresponding to 35%-40% of all post-Archean metaluminous granitoids seen around the world. The two main tectonic environments envisaged for high-K magma generation

are (Roberts and Clemens, 1993): a) continental arc (Andean-type), and b) postcollisional (Caledonian-type) settings.

In general, the tectonic setting discrimination diagrams (e.g. Pearce *et al.*, 1984) diagnose the settings in which the protoliths were formed better than the environment where the magma was generated (e.g. Barbarin, 1999). This implies that these diagrams could denote geochemical (and isotopic) characteristics of the sources (inheritance), irrespective of the residual minerals components. In the hornblende-free Martins Pereira high-K calc-alkaline granitoids, for instance, the linear and continuous trends in Harker diagrams suggest that the rocks were generated by partial melting processes. However, the sources are not yet fully understood, despite a number of geochemical features (e.g. K, U, Th, Rb and REE enrichment) pointing towards the importance of crustal rocks in the magma source.

Experimental data on the potential sources for high-K cal-alkaline granitoids have suggested several crustal source possibilities (e.g. Roberts and Clemens, 1993). These partial melting hypotheses yield compositional differences among magmas produced by partial melting of common crustal rocks, such as amphibolites, tonalitic gneisses, metagreywackes and metapelites under variable melting conditions (e.g. Patiño-Douce, 1996, 1999). This compositional variation can be visualized in terms of major oxides ratios (**fig. 8a-c**) or molar oxide ratios (**Fig. 8d**). It can be seen in these plots that partial melts derived from mafic to intermediate source rocks have lower $\text{Al}_2\text{O}_3/(\text{FeO}+\text{MgO}+\text{TiO}_2)$, $(\text{Na}_2\text{O}+\text{K}_2\text{O})/(\text{FeO}+\text{MgO}+\text{TiO}_2)$ and molar $\text{Al}_2\text{O}_3/(\text{MgO}+\text{FeO}_{\text{tot}})$ ratios relative to those originated from metapelites and metagreywackes (**Fig 8a-d**).

The most Martins Pereira Granite samples generally plot in the amphibolite and metabasalt-metatonalite fields (**Fig 8a-d**), showing low $\text{Al}_2\text{O}_3/(\text{FeO}+\text{MgO}+\text{TiO}_2)$, $(\text{Na}_2\text{O}+\text{K}_2\text{O})/(\text{FeO}+\text{MgO}+\text{TiO}_2)$ and molar $\text{Al}_2\text{O}_3/(\text{MgO}+\text{FeO}_{\text{tot}})$ ratios, but exhibit relatively high $\text{CaO}/(\text{FeO}+\text{MgO}+\text{TiO}_2)$. This feature, associated with relatively high Mg# values (32.5-45.3), precludes a derivation from felsic pelite and/or metagreywacke for Martins Pereira Granite, particularly the low-SiO₂ samples (<70%). The most SiO₂-rich samples (>70%), however, have lower Mg# values (24.7-30.7), higher $\text{Al}_2\text{O}_3/(\text{FeO}+\text{MgO}+\text{TiO}_2)$ and $(\text{Na}_2\text{O}+\text{K}_2\text{O})/(\text{FeO}+\text{MgO}+\text{TiO}_2)$ ratios, and lower $\text{Al}_2\text{O}_3+\text{FeO}+\text{MgO}+\text{TiO}_2$ (15-18%) and $\text{Na}_2\text{O}+\text{K}_2\text{O}+\text{FeO}+\text{MgO}+\text{TiO}_2$ (8-10%) contents. These Martins Pereira SiO₂-rich samples, as well as the Serra Dourada Granite samples, also show low $\text{CaO}+\text{FeO}+\text{MgO}+\text{TiO}_2$ contents (2-

4%) and plot in the metagreywacke field (**Fig 8a-d**), suggesting metasedimentary source contribution (at least locally) in the Martins Pereira magma genesis. The most suitable metasedimentary source rocks available in the NUAD are related to the Cauarane Group.

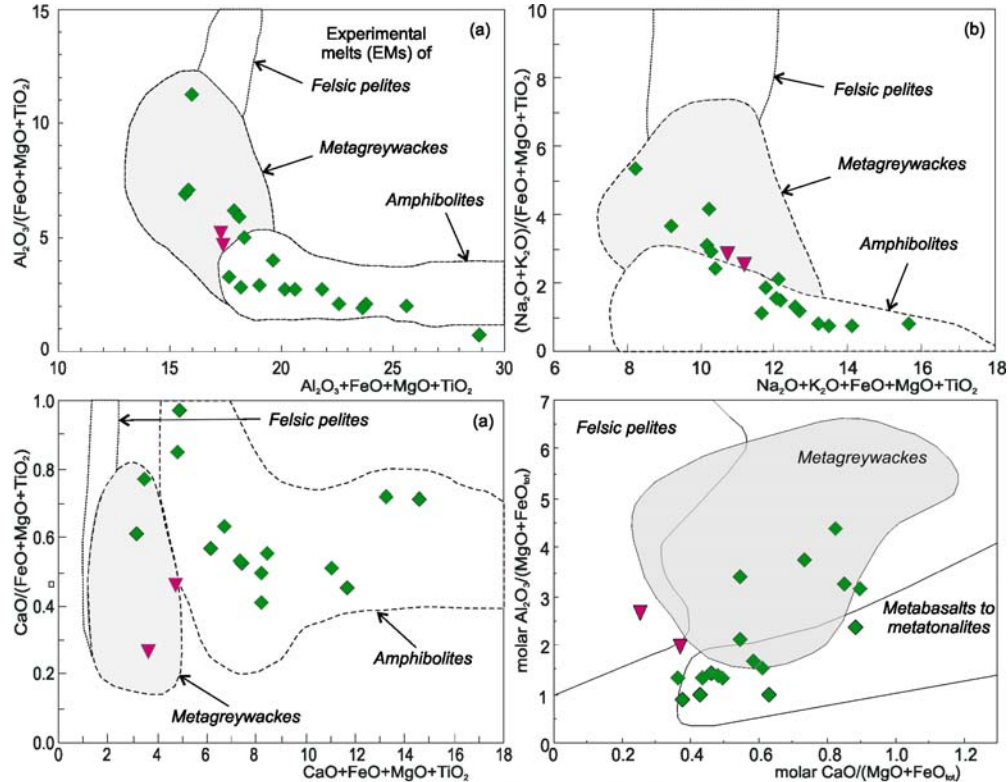


Fig.8. Martins Pereira and Serra Dourada Granites samples plotted on the (a) $Al_2O_3/(FeO+MgO+TiO_2)$ vs. $Al_2O_3+FeO+MgO+TiO_2$, (b) $(Na_2O+K_2O)/(FeO+MgO+TiO_2)$ vs. $Na_2O+K_2O+FeO+MgO+TiO_2$, (c) $CaO/(FeO+MgO+TiO_2)$ vs. $CaO+FeO+MgO+TiO_2$ and (d) molar $Al_2O_3/(MgO+FeO_{wt})$ vs. molar $CaO/(MgO+FeO_{wt})$ diagrams. Outlined fields denote compositions of partial melts obtained in experimental studies by dehydration melting of felsic pelites, metagreywackes, amphibolites-metabasalts and metatonalites sources (Wolf and Wyllie, 1994; Patiño-Douce, 1999; Patiño-Douce and Beard, 1996; Thompson, 1996, and references therein). Symbols as in fig. 03. See text for discussion.

By combining the above, mentioned geochemical features with petrographic and other geochemical parameters, the Serra Dourada Granite is dominantly derived from a metagreywacke source by a partial melting process. In contrast to the Serra Dourada Granite, the Martins Pereira granitic magma could be linked with the partial melting of amphibolite sources, and further input of metagreywacke sources, either by partial melting or contamination-assimilation processes. A similar hybrid origin was proposed by Sardinha (1999) the 1.89 Ga Igarapé Azul Granite (Almeida *et al.*, 2002). Similarly, an origin for high-K, calc-alkaline I-type granitoids by partial melting of metagreywacke-sources was also proposed by Barker *et al.* (1992), Altherr *et al.* (2000) and Thuy Nguyen *et al.* (2004), in Alaska, Germany and Vietnam, respectively.

ZIRCON GEOCHRONOLOGY

Five fresh granitic rocks of NUAD were sampled and analyzed by Pb-evaporation and U-Pb ID-TIMS methods (**table 2**). Three samples from Martins Pereira Granite and one from leucogranite lenses were analyzed by zircon Pb-evaporation, whereas the same sample from Serra Dourada Granite was analyzed by both methods.

Martins Pereira Granitoids (MA-172A, 061A and 007A samples)

In the general sense, hornblende-free Martins Pereira metagranitoids are composed of porphyritic coarse- to medium-grained granodiorites, monzogranites and rare fine- to medium-grained (epidote)-biotite-rich tonalites (calc-alkaline granodioritic trend in QAP diagram), locally associated with very small bodies (lenses and pods) of leucogranites. Three samples from the Martins Pereira Granite were analyzed by single-zircon Pb-evaporation method (**table 2**): cataclastic porphyritic monzogranite (MA-172A), mylonitic granodiorite (MA-61A) and porphyritic metamonzogranite (MA-007A).

The sample of cataclastic coarse-grained monzogranite (MA-172A) shows translucent crystals with local opaque portions, pale brown to pale yellow colours, prismatic (length/width ratios between 2.9:1 to 1.8:1) and 90-400 μm in length, exhibiting well-defined faces and vertices. Mineral inclusions (such as apatite and Fe-Ti oxides) and fractures are common. A total of 6 crystals were analyzed yielding a mean age of 1975 ± 6 Ma age (USD: 2.9) from 162 isotopic ratios (**table 3, Fig. 9a**). Individual ages of these analyses vary from 1988 Ma to 1962 Ma.

The MA-61A mylonitic biotite granodiorite was sampled along an ENE-WSW mylonitic zone to north of São Luiz do Anauá town. Two different zircon populations were described in this sample: a) prismatic (length/width ratios between 2.4:1 and 1.6:1), translucent and brown to pale brown crystals showing fractures and rounded vertices; b) prismatic (length/width ratios between 3.8:1 and 2:1), transparent, pale yellow crystals showing few fractures and vertices, and well-defined faces. Both zircon populations showed scarce mineral inclusions, crystals with 140-360 μm in length and local irregular internal zoning, this last observation suggesting igneous overgrowth and/or older inherited cores. The mean age of analyses of 8 crystals (264 isotopic ratios) from both populations by the Pb-evaporation method yielded 1973 ± 2 Ma (USD: 2.1) (**table 3, Fig. 9b**), exhibiting individual ages varying of 1978 Ma to 1962 Ma. Locally, an anomalous age was observed in crystals # 4 (2042 ± 20 Ma, 1450°C and 1500°C step-heatings) and # 9 (1994 ± 4 Ma, 1500°C step-heating), which could represent an inherited component.

The sample of the porphyritic metamonzogranite facies (MA-007A) selected for dating is locally foliated and banded. The zircon crystals are pale brown, transparent to translucent, prismatic and bypyramidal, with 190-450 μm in length (3.5:1 to 2.2:1 length/width ratios). They show fractures, sometimes radial-like, well-defined faces and rounded vertices. Inclusions are very rare in these zircon samples. A total of 4 crystals were analyzed yielding individual ages varying of 1973 Ma to 1967 Ma, and a mean age of 1971 ± 2 Ma age (**table 3, Fig. 9c**). The 25 blocks and 180 isotopic ratios show a very homogeneous pattern, yielding a well-defined mean age with good statistical level (USD: 1.1).

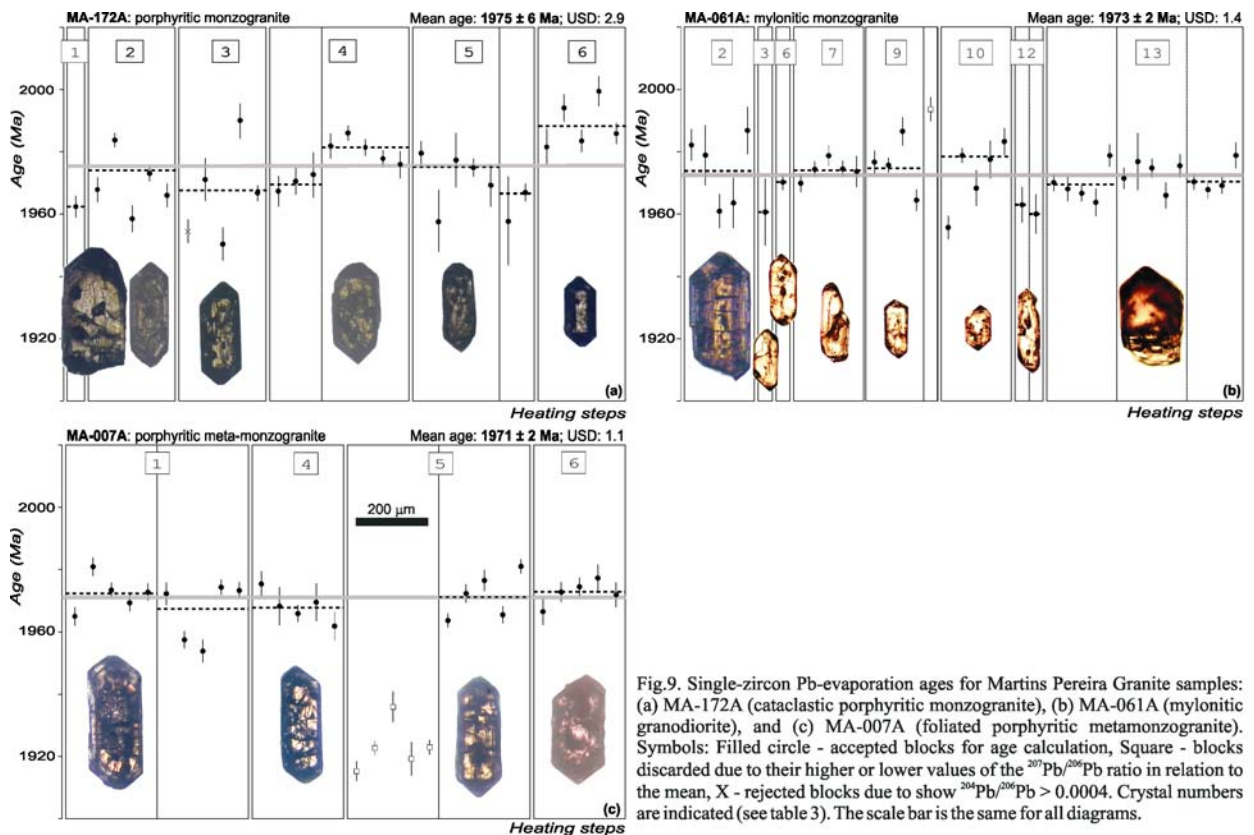


Fig.9. Single-zircon Pb-evaporation ages for Martins Pereira Granite samples: (a) MA-172A (cataclastic porphyritic monzogranite), (b) MA-061A (mylonitic monzogranite), and (c) MA-007A (foliated porphyritic metamonzogranite). Symbols: Filled circle - accepted blocks for age calculation, Square - blocks discarded due to their higher or lower values of the $^{207}\text{Pb}/^{206}\text{Pb}$ ratio in relation to the mean, X - rejected blocks due to show $^{204}\text{Pb}/^{206}\text{Pb} > 0.0004$. Crystal numbers are indicated (see table 3). The scale bar is the same for all diagrams.

The results obtained from Martins Pereira Granite show a small interval age (1980-1968 Ma) and local 1.99 Ga and 2.04 Ga inheritances, these last probably related to Anauá Complex. Other granitoids from Martins Pereira Granite area, and equivocally related to Água Branca Suite and Igarapé Azul Granite, were dated by Almeida *et al.* (1997) and CPRM (2003) yielding 1960 ± 21 Ma and 1972 ± 8 Ma respectively (**Table 5**). These ages are in agreement with the results obtained in this paper (see **Fig. 9a-c**) and mark an important magmatic event in southeastern Roraima State, here named as Rorainópolis event. In general sense, these results are uniform, homogeneous and establish a 1.97-1.96 Ga age range, despite the observed heterogeneous

textures (*e.g.* igneous, mylonitic and cataclastic), different geographical site sampling, and different applied methodologies (**tables 2 and 5, Fig. 2**).

Serra Dourada Granite (MF-156 samples)

The S-type granitoids in southeastern Roraima State were initially described by Faria *et al.* (1999) and incorporated into the Igarapé Azul Granite. However, Almeida *et al.* (2002) subdivided the Igarapé Azul Granite into three different types: Serra Dourada Granite (true S-type), Martins Pereira Granite (I-type high-K calc-alkaline) and the proper Igarapé Azul Granite (I-type felsic high-K calc-alkaline).

A syenogranite sample of Serra Dourada Granite (MF-156) with biotite, muscovite and cordierite (**table 2**), including monazite and xenotime as accessory minerals, was analyzed by single-zircon Pb-evaporation method. This sample shows two zircon populations with different features. The first group is scarce and shows rounded vertices, irregular faces (corrosion?), light yellow colour, 310-500 μm in length (length/width ratios between 2.3:1 to 1.5:1), translucent to transparent opacity, and is generally free of inclusions. The second type of zircon shows crystals with slightly rounded vertices, is light brown to brown colour, 170-340 μm in length (length/width ratios between 3.1:1 to 1.5:1), transparent and locally with few inclusions and fractures. This second type of zircon is characterized by well-developed {211} pyramid, similar to zircons crystallized from the peraluminous melt (Pupin, 1980).

In the Pb-evaporation method, the zircon fractions yielded two different age patterns, irrespective of the few analyzed grains and isotopic ratios obtained (**table 3**). The lower age (1948 ± 11 Ma) was obtained from two blocks from two crystals. The higher age (2138 ± 3 Ma) was obtained by nine blocks of isotopic ratios from two zircon crystals (**Fig. 10a**), and is interpreted as an age of inherited origin.

U-Pb ID-TIMS was carried out on the same sample with the aim of interpreting the ages obtained by the Pb-evaporation method. The regression of four experimental points yields a discordia line which indicates an upper intercept at 1962 ± 2 Ma (**table 4, Fig. 10b**), interpreted as the crystallization age of the analyzed crystals and, similarly, that of the Serra Dourada Granite. This age is very close to the age yielded any the Pb-evaporation method for the same sample which, taking into account the errors, almost overlap one another.

The geological similarities between Serra Dourada (Uatumã-Anauá Domain) and Taiano (Central Guyana Domain) S-type granites are also pointed out by our U-Pb and Pb-evaporation

zircon ages. The Taiano anatectic leucogranite yields 1969 ± 3.5 Ma (zircon U-Pb SHRIMP, CPRM, 2003) and the minimum crystallization age yielded by single-zircon Pb-evaporation (1948 ± 11 Ma) and U-Pb ID-TIMS ($1962 \pm 2/-6$ Ma) methods for the Serra Dourada type are quite similar (**Table 5**), confirming an important anatectic process in the center-southern Roraima State occurred 1.97-1.96 B.y. ago. Others S-type granitoids in the Roraima State, such as Curuxuim and Amajari granites (CPRM, 1999), could be also related to this same event, however they yet are not dated.

The inherited ages in both S-type granites also show Eo- to Neo-Transamazonian ages, ranging from 2138 ± 3 Ma (Serra Dourada Granite) to 2047 ± 7 Ma and 2072 ± 3 Ma (Taiano Granite), probably related to sedimentary contribution. This hypothesis is partially confirmed by Transamazonian detrital zircon crystals detected in the metavolcanosedimentary rocks from Cauarane Group (**Table 6**), where two paragneiss samples were dated by U-Pb ID-TIMS (2223 ± 19 Ma, Gaudette *et al.*, 1996) and U-Pb SHRIMP (2038 ± 17 Ma and 2093 ± 62 Ma, CPRM, 2003) methods.

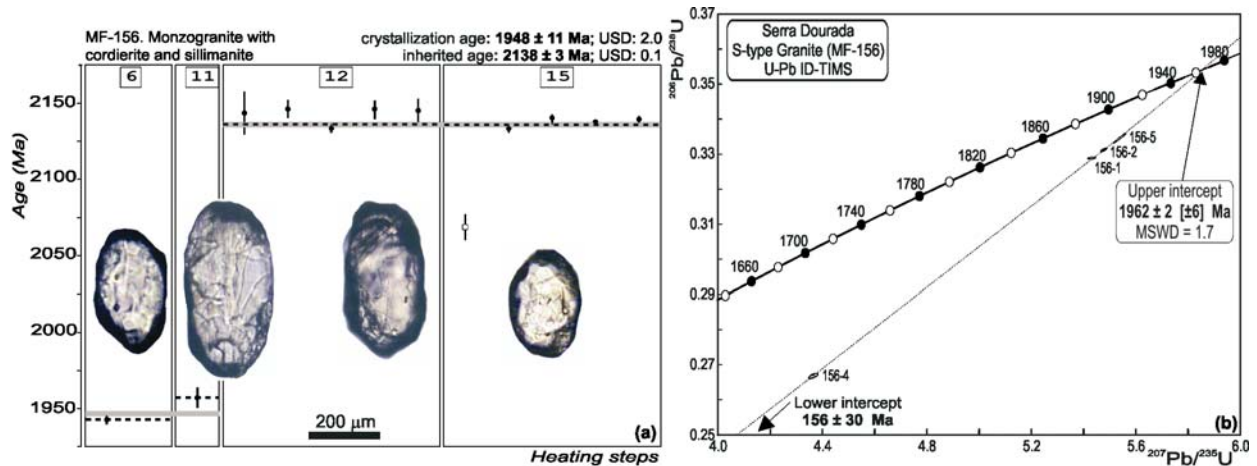


Fig.10. Single-zircon ages for Serra Dourada Granite (sample MF-156) yielded by (a) Pb-evaporation and (b) U-Pb ID-TIMS (concordia diagram) methods. Crystal numbers are indicated (see tables 3 and 4). Symbols: Filled circle - accepted blocks for age calculation; Square - blocks discarded due to too low value of the $^{207}\text{Pb}/^{206}\text{Pb}$ ratio in relation to the average.

Lenses of Leucogranite (MA-246C2 sample)

The leucosyenogranite lense sample (MA-246C2) associated with Martins Pereira granitoids showed a complex set of results. Five groups were displayed in this sample in decreasing age order (**table 5, Fig. 11a-b**):

The group I is represented by only one pale brown, transparent to translucent zircon with $265 \mu\text{m}$ in length (length/width ratio 1.9:1), showing regular internal zoning, well-defined faces

and dark inclusions into the core. It yielded an age of 2354 ± 6 Ma (crystal #1).

The group II exhibits pale yellow and transparent grains (locally translucent to opaque) being 250-330 μm in length (length/width ratios between 3.2:1 and 2.5:1). Cracks are common, but inclusions are rare. This group comprises 3 zircon crystals with individual ages varying from 2148 Ma to 2126 Ma, and yielded a mean age of 2134 ± 15 Ma (crystals #10, 14, and 16).

The group III encompass colorless to pale yellow crystals which are 166-180 μm in length (length/width ratios around 2.7:1), with crystals locally exhibiting internal zoning and cracks in the core. This group yielded 1997 ± 8 Ma as a mean age (crystals #17 and 21).

In general, the crystals of the group IV are characterized by brown to pale brown and translucent grains with well-defined faces (locally broken) and 210-260 μm in length (length/width ratios around 2.6:1). This group consists of 4 crystals with individual ages varying from 1968 Ma to 1952 Ma, and yielded a mean age of 1959 ± 5 Ma (crystals #7, 9, 13, and 23).

The crystals of the group V are 164-330 μm in length (length/width ratios between 3.1:1 and 1.8:1), are pale yellow to pale brown in colour, transparent, and show local cracks and inclusions. This group displays a mean age of 1906 ± 4 Ma from 5 crystals (# 5, 6, 8, 18, and 19), with individual ages varying from 1913 Ma to 1894 Ma. This lowest age (group V) is interpreted as the crystallization age, whereas the higher ages (groups I, II, III and IV) probably represent inherited zircon of different origins.

Despite the wide variety of zircon populations from the sample MA246C2, including grains with internal complexity or zoning (“mixing age”) or partial resetting, the results obtained by the single-zircon Pb-evaporation method give rise to a comprehensible interpretation, which follows:

a) The 1906 ± 4 Ma (group V) is interpreted as the minimum crystallization age of leucosyenogranite. Other ages, around 1.89 to 1.90 Ga, which are related to Igarapé Azul and Água Branca granitoids (*e.g.* CPRM, 2003; Almeida *et al.*, 2002) are described in this region, mainly in the southern Uatumã-Anauá Domain. These leucogranitic lenses also show some petrographic similarities with Igarapé Azul granitoids and were both likely generated in the same magmatic event;

b) The 1997 ± 8 Ma (group III) and 1959 ± 5 Ma (group IV) ages probably correspond to inherited components from the Surumu volcanics and Martins Pereira granitoids (or Urubu orthogneisses?), respectively, however the first rocks do not outcrop in Uatumã-Anauá Domain and correlated igneous rocks are not founded there.

c) The 2354 ± 6 Ma (Siderian, group I) and 2134 ± 15 Ma (Sthaterian, group II) ages suggest local inheritance from older crust (not outcropping), respectively related to the pre-Transamazonian and Transamazonian magmatic events. Transamazonian rocks with 2.26-2.01 Ga (Santos *et al.*, 2003a) have been described ~600 km northeast from the sampled site, in the Maroni-Itacaiúnas or Transamazon Province (**Fig. 1**). Transamazonian rocks mainly occur in Brazil (Amapá State; Avelar *et al.*, 2001, Rosa Costa *et al.*, 2003), French Guyana (Vanderhaerghe *et al.*, 1998, Delor *et al.*, 2003), São Luis Craton (Klein and Moura, 2001) and (its extension) in the West Africa craton (Boher *et al.*, 1992; Milési *et al.*, 1992; Gasquet *et al.*, 2003). In the last case, they are related to Birimian (2185-2150 Ma) and Bandamian (2115-2100 Ma) events.

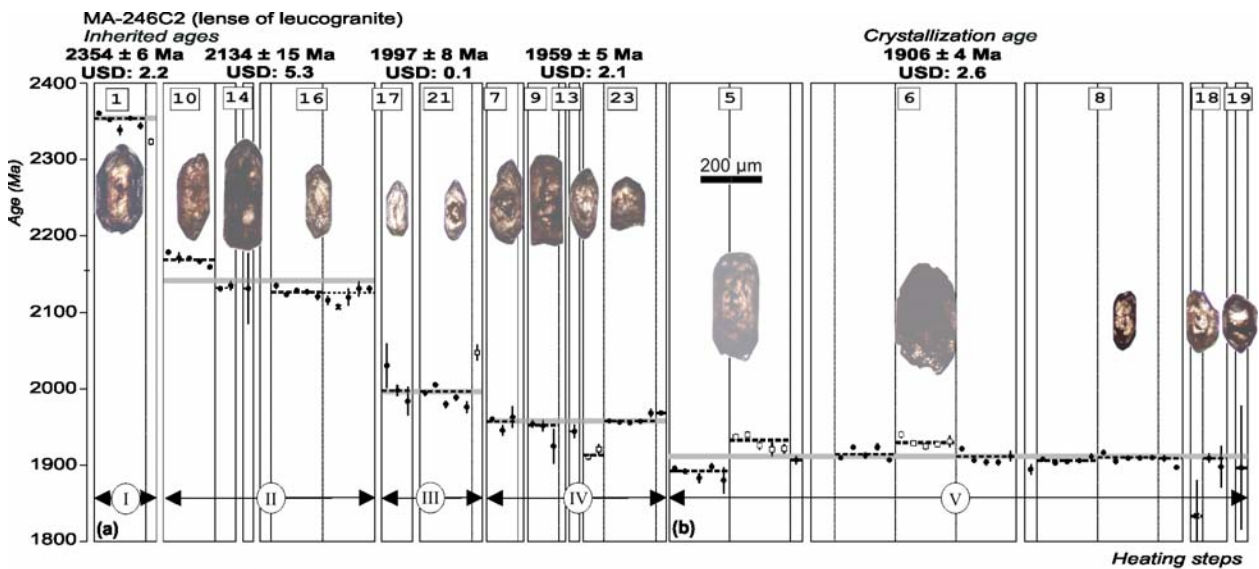


Fig.11. Single-zircon Pb-evaporation ages of lenses of leucogranite in association with Martins Pereira Granite. (a) Inherited ages: I - Pre-Transamazonian (Siderian); II - Transamazonian; III - Late-Transamazonian (Anauá Complex?); IV - Martins Pereira, and (b) V - Minimum crystallization age (Igarapé Azul and Caroebe magmatic event?). Symbols: Filled circle - accepted blocks for age calculation; Square - blocks discarded due their higher or lower values of the $^{207}\text{Pb}/^{206}\text{Pb}$ ratio in relation to the mean; X - rejected blocks due to $^{204}\text{Pb}/^{206}\text{Pb} > 0.0006$. Crystal numbers are indicated (see table 3). The scale bar is the same for all diagrams.

In West Africa, pre-Birimian ages (Burkinian, according to Lemoine *et al.*, 1990) are described by Gasquet *et al.* (2003) in Dabakala (Ivory Coast). The 2312 ± 17 Ma age has seen two interpretations by the prementioned authors. The first interpretation has this age representing an Archean inheritance (and not Siderian) based on the complex model of Lead loss in the analyzed zircon crystals. The second interpretation holds that this age is related to the ca. 2.3 Ga pre-Birimian crust. According to these authors, the second hypothesis is more consistent due to the systematically well-defined age patterns, around 2.2-2.3 Ga (without evidence of older Archean ages). This second hypothesis gains additional support from the fact that these rocks are

not spatially close to the Archean nucleus.

The Siderian age in Uatumã-Anauá Domain (Tapajós-Parima Province) is the first zircon data reported in any section of the centre-western Guyana Shield and suggest reworking of pre-Transamazonian and post-Archean crust. The proximity with Central Amazonian Province (older than 2.3 Ga) is uncertain, because provincial boundaries are not precise. In the central Guyana Shield, this province remains poorly investigated, while the U-Pb and Pb-Pb geochronological data is scarce, showing ages systematically lower than 2.3 Ga.

Other Siderian ages have been found in Amazonian Craton, but not in the Guyana Shield. Additionally, the Siderian age (2354 Ma) in Uatumã-Anauá is lower than the Siderian inheritance (2380-2483 Ma) obtained by Santos *et al.* (2001) in Cuiú-Cuiú rocks from Tapajós Domain (Brazil Central Shield). Other Siderian ages are reported in the Transamazonian terrane (2.20 to 1.99 Ga, Vasquez *et al.*, 2003) of Bacajá domain (to North-Northwestern of Carajás Province) where zircon dating from Vasquez *et al.* (2003), Santos *et al.* (in Faraco *et al.*, 2003), and Macambira *et al.* (2004) yielded 2.44-2.30 Ga, 2.47-2.31 Ga, and 2.36 Ga, respectively.

TAPAJÓS AND UATUMÃ-ANAUÁ DOMAINS: CHRONOSTRATIGRAPHY AND IMPLICATIONS FOR GEOLOGICAL EVOLUTION OF THE TAPAJÓS-PARIMA OR VENTUARI-TAPAJÓS PROVINCES

Previous and new geochronological data have shown several similarities among granitoids from the NUAD and Tapajós Domain (orogenic subdomain, CPRM, 2000b) (**tables 5 and 6**). The Orosirian primitive arc inliers, for example, are represented by the Anauá (NUAD) and Cuiú-Cuiú (Tapajós) TTG-like complexes and are the oldest rocks outcropping in these regions.

In NUAD, the Anauá Tonalite is 2028 ± 9 Ma old (**Table 5, Fig. 12**), but does not have inheritance evidence and shows ϵ_{Nd} of -0.20 . This is interpreted as being of juvenile origin (Faria *et al.*, 2002), although only one sample had been analyzed. The Cuiú-Cuiú Complex of the Tapajós Domain shows a age range of 2033-2005 Ma and the older types are coeval to the Anauá granitoids from the NUAD (**Table 5, Fig. 12**). In contrast to Anauá types, the Cuiú-Cuiú Complex yields several zircon inherited components (**Table 6, Fig 12**), in which, the main inheritance is from Transamazonian (2040-2100 Ma), with minor Siderian to Archean records (2380-2483 Ma).

The well-defined interval age of Martins Pereira Granite (1980-1969 Ma) in the NUAD is also very similar to that showed by the Creporizão Suite (1980-1951 Ma) from Tapajós Domain

(Table 5, Fig. 12, CPRM, 2000b, Santos *et al.*, 2000, 2001). Similarly, the Old São Jorge Granite (Lamarão *et al.*, 2002) of the Tapajós Domain is nearly 10 Ma older than Creporizão Suite, but both high-K calc-alkaline granites are related to the Creporizão Orogeny (1.98-1.96 Ga), according to Santos *et al.* (2004). The Pedra Pintada granitoids (Fraga *et al.*, 1996) in the Surumu Domain (Orocaina event, Reis *et al.*, 2000) are also coeval (1958 Ma, CPRM, 2003) to the calc-alkaline Martins Pereira Granite.

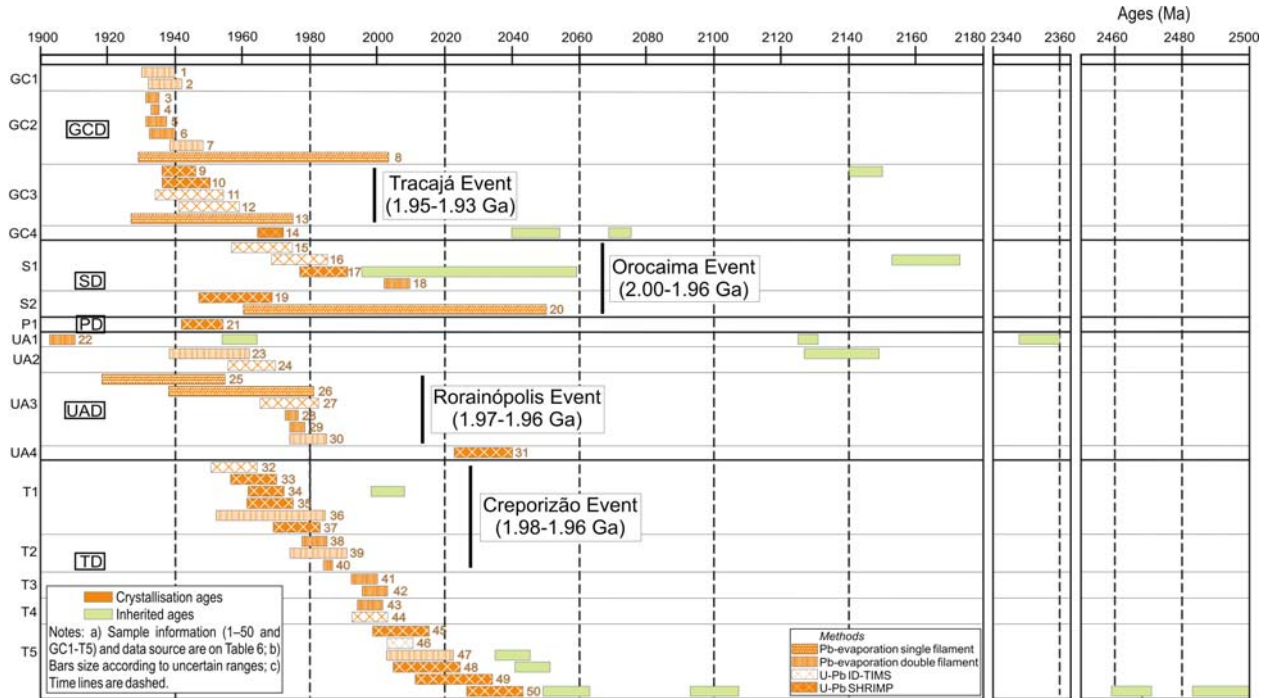


Fig. 12. Temporal distribution of main magmatic rocks older than 1900 Ma of Ventuari-Tapajós (or Parima-Tapajós) Province, grouped by geological domains: CGD - Central Guyana; S - Surumu; PD - Parima; UAD - Uatumã-Anauá; TD - Tapajós.

In NUAD, lenses of leucosyenogranite are ~70 Ma younger than the Martins Pereira host-rock and show crystallization age (1906 ± 4 Ma) similar those of the Igarapé Azul-Caroebe granitoids (Água Branca magmatism: 1906-1885 Ma) describe in the SUAD. Some similar inherited ages are also observed in both granitic types, such as Martins Pereira granitoids and Transamazonian inheritances (table 6). Siderian inheritance yielded by the leucogranites is localized, whereas in SUAD, this is only recorded in the Murauá Granite. The same 1.90-1.88 Ga interval age corresponds also to the Tropas and Parauari magmatism, in the Tapajós Domain (table 5).

In contrast with Roraima region - where the S-type granitic rocks (e.g. Serra Dourada, Curuxuim and Amajari), granulites (e.g. Barauana) and charnockites are relatively common - these respective rock types are scarce in the Tapajós Domain. They are locally described as small

garnet leucogranitic bodies (not mapped on the 1:250.000 scale) associated with Cuiú-Cuiú metagranitoids (Almeida *et al.*, 2001) and have not been dated previously. This scarcity of S-type granites and granulite metamorphism suggests that the collisional processes were less intense in the Tapajós domain.

CONCLUSIONS

The geological, geochronological and geochemical data available for granitoids from southeastern Roraima State (Brazil) suggest a Paleoproterozoic evolution in, at least, two stages: the Anauá orogeny is related to 2.03 Ga TTG granitoids (*accretionary phase* generating the Anauá granitoids and Cauarane metavolcanosedimentary cover), followed by crustal thickening and anatexis around 1.97-1.96 Ga (*collisional phase* generating Martins Pereira and Serra Dourada granitoids). The Anauá juvenile origin is envisaged, but scarce Nd isotopic data do not make this hypothesis conclusive. The NUAD crust, characterized by Orosirian granitoids, is mainly thought to have been generated by reworking of older Transamazonian and minor Siderian crust, according to inherited zircon records.

The following magmatic events can be listed as had occurred in NUAD:

A) 2.03 Ga - crystallization of Anauá Tonalite within the TTG association, representing a primitive arc (?) in southeastern Roraima State with related back arc basins;

B) 1.97-1.96 Ga - Martins Pereira high-K calc-alkaline granitoids and Serra Dourada S-type granite showing similar crystallization ages. These granitoids are probably related to crustal thickening and anatexis in the latest (or after) stage of Anauá arc evolution;

C) ca. 1.90 Ga - meter to centimeter scale leucogranite pods and lenses (low degree of partial melting?). It is thought that these pods in-filled older, planar structures in the Martins Pereira metagranitoids. A regional-scale magmatic event (1.90-1.89 Ga) is mentioned in the southern Uatumã-Anauá Domain, and is believed to be related to the Igarapé Azul and Água Branca granitoids and coeval volcanism.

Furthermore, two main periods are also recorded in inherited zircon:

A) Siderian (2.35 Ga) - only one zircon crystal with this age was detected in the lenses of leucogranite, but it represents the first indicative of Siderian crust (host or material source) in the Central Guyana Shield. Alternatively, this Siderian age could be the result of an isotopic mixing between “Transamazonian” and “Archean” components of the same zircon or a partial resetting of an older grain. On the other hand, similar ages are also recorded in West African craton (2312

Ma, Gasquet *et al.*, 2003), Bacajá (2359 ± 3 Ma, Macambira *et al.*, 2004) and Tapajós domains (2483-2380 Ma, Santos *et al.*, 2001) in Amazonian craton.

B) Syn- to Late-Transamazonian (2.14-2.13 Ga) - this interval age is yielded by the oldest zircon crystals from the Serra Dourada S-type granite (two crystals) and group II from the lenses of leucogranite (three crystals). Similar inheritance (2163-2100 Ma) was observed in Surumu, Central Guyana and Tapajós domains (CPRM, 2003, Santos *et al.*, 2001, 2003b).

Neoproterozoic inheritances are absent in the NUAD, but they are locally recorded in other domains of Tapajós-Parima Province, such as Tapajós (2852-2591 Ma, Lamarão *et al.*, 2002) and Parima (2872-2781 Ma, Santos *et al.*, 2003c) domains.

Previous works had been recognized three geochronological provinces in southeastern Roraima State, but our new geological, geochronological and geochemical data have been showed that this region is very similar to the Tapajós Domain (Santos *et al.*, 2004) and reinforce the Ventuari-Tapajós or Parima-Tapajós provinces prolongation in the southeastern Roraima, taking into account that rocks older than 2.03 Ga do not outcrop in the studied region. However, the Central Amazonian and Maroni-Itacaiúnas provinces seem to be important crustal sources for the rocks of the NUAD, suggesting partial or total crustal recycling.

In summary, the I-type high-K calc-alkaline granitoids (Martins Pereira) and S-type granites (Serra Dourada) has been generated in the NUAD (Ventuari-Tapajós or Tapajós-Parima provinces), probably during amalgamation of TTG-like Anauá magmatic arc (2028 Ma) with Transamazon (2.2-2.0 Ga) and Central Amazonian (older than 2.3 Ga) terranes.

Some authors argue that most collision orogenic systems have a prior accretion history (*e.g.* Van Staal *et al.*, 1998), so it is easy to confuse the accretion and collision histories in the ancient examples, such as the Ventuari-Tapajós or Tapajós-Parima provinces. This makes hard to rebuild the Anauá orogeny and the hypothesis presented in this paper is only an outline of the tectonic evolution of the central portion of Guyana Shield.

Acknowledgments

Special thanks to the colleagues of CPRM (Geological Survey of Brazil) for geological discussions and Nicholas Tailby (Australian National University) for the english review. The authors are also grateful to CPRM-Geological Survey of Brazil for the research grants and FINEP (CT-Mineral 01/2001 Project) and Isotope Geology Laboratory of Federal University of Pará for support of laboratorial works.

References

- Almeida, M.E., Macambira, M.J.B. 2003. Aspectos geológicos e litoquímicos dos granitóides cálcio-alcálicos Paleoproterozóicos do sudeste de Roraima. In: SBGq, Cong. Brasil. Geoq., 9, Anais, p. 775-778 (in portuguese).
- Almeida, M.E., Fraga, L.M.B., Macambira, M.J.B. 1997. New geochronological data of calc-alkaline granitoids of Roraima State, Brazil. In: IG/USP, South-American Symposium on Isotope Geology, 1, Abstract, p.34-37.
- Almeida, M.E., Brito, M.F.L., Ferreira, A.L., Monteiro, M.A.S. 2001. Evolução Tectono-estrutural da região do médio-alto curso do rio Tapajós. In: N.J. Reis and M.A.S. Monteiro (Orgs), Contribuições à Geologia da Amazônia, 2, , Belém, SBG, p.57-112. (in portuguese).
- Almeida, M.E., Macambira, M.J.B., Faria, M.S.G. de. 2002. A Granitogênese Paleoproterozóica do Sul de Roraima. In: SBG, Congresso Brasileiro de Geologia, 41, Anais, p 434 (in portuguese).
- Altherr, R., Holl, A., Hegner, E., Langer, C., Kreuzer, H. 2000. High-potassium, calc-alkaline I-type plutonism in the European Variscides: northern Vosges (France) and northern Schwarzwald (Germany). *Lithos* 50, 51–73.
- Andsell, K.M., Kyser, T.K. 1991. Plutonism, deformation and metamorphism in the Proterozoic Flin Flon greenstone belt, Canada: Limits on timing provided by single-zircon Pb-evaporation technique. *Geology*, **19**, p. 518-521.
- Avelar, V.G. de, Lafon, J.-M., Delor, C. 2001. Geocronologia Pb-Pb em zircão e Sm-Nd em rocha total da porção centro-norte do Amapá. Implicações para a evolução geodinâmica do Escudo das Guianas. In: SBG, Simpósio de Geologia da Amazônia, 7, Belém, Resumos Expandidos (CD-ROM) (in portuguese).
- Barbarin, B. 1999. A review of the relationships between granitoid types, their origins and their geodynamic environments. *Lithos* 46, 605–626.
- Barker, F., Farmer, G.L., Ayuso, R.A., Plafker, G., Lull, J.S. 1992. The 50 Ma granodiorites of the eastern Gulf of Alaska: melting in an accretionary prism in the forearc. *J. Geophys. Res.* **97**, 6757–6778.
- Boher, M., Abouchami, W., Michard, A., Albarède, F., Arndt, N. 1992. Crustal growth in West Africa at 2.1 Ga. *Journal of Geophysical Research* **97**, 345–369.
- Bonin, B. 1990. From orogenic to anorogenic settings: evolution of granitoid suites after a major

- orogenesis. *Geol. J.* 25, 261–270.
- Boynton, W.V. 1984. Cosmochemistry of the rare earth elements: meteorite studies. In: Henderson, P. (ed), Rare earth element geochemistry, Elsevier Publ. p. 63-114.
- Brown, G.C., Thorpe, R.S., Webb, P.C. 1984. The geochemical characteristics of granitoids in contrasting arcs and comments on magma sources. *Journal of Geological Society of London* **141**, 413-426.
- Chappell, B.W., White, A.J.R. 1992. I- and S-type granites in the Lachalan Fold Belt. *Transactions of Royal Society of Edinburg: Earth Sciences* **83**, 1-26.
- Cordani, U.G., Tassinari, C.C.G., Teixeira, W., Basei, M.A.S., Kawashita, K. 1979. Evolução tectônica da Amazônia com base nos dados geocronológicos. In: Congresso Geológico Chileno, 2, 1979, Arica, Anais, v.4, p.177-148 (in portuguese).
- Costa, J.A.V., Costa, J.B.S., Macambira, M.J.B. 2001. Grupo Surumu e Suíte Intrusiva Saracura, RR - Novas Idades Pb-Pb em Zircão e Interpretação Tectônica. In: SBG, Simpósio de Geologia da Amazônia, 7, Belém, Pará, Resumos Expandidos, CD-ROM. p. 16- 19 (in portuguese).
- Cox, K.G.; Bell, J.D., Pankhurst, R.J. 1987. The interpretation of igneous rocks. George Allen and Unwin ltd., 5th ed., London. 450p.
- CPRM. 1999. Programa Levantamentos Geológicos Básicos do Brasil. *Roraima Central, Folhas NA.20-X-B e NA.20-X-D (integrais), NA.20-X-A, NA.20-X-C, NA.21-V-A e NA.21-V-C (parciais)*. Escala 1:500.000. Estado de Roraima. Manaus, CPRM. 166 p. [CD-ROM]. (in portuguese)
- CPRM. 2000a. Programa Levantamentos Geológicos Básicos do Brasil. *Caracarái, Folhas NA.20-Z-B e NA.20-Z-D (integrais), NA.20-Z-A, NA.21-Y-A, NA.20-Z-C e NA.21-Y-C (parciais)*. Escala 1:500.000. Estado de Roraima. Manaus, CPRM, 157 p. CD-ROM. (abstract in english)
- CPRM. 2000b. Programa Levantamentos Geológicos Básicos do Brasil. Projeto Especial Província Mineral do Tapajós. Geologia e Recursos Minerais. *Vila Riozinho, Folha SB.21-Z-A*. Escala 1:250.000. Estado do Pará. Nota Explicativa. CPRM/Serviço Geológico do Brasil [CD-ROM] (in portuguese).
- CPRM. 2003. Programa Levantamentos Geológicos Básicos do Brasil. *Geologia, Tectônica e Recursos Minerais do Brasil: sistema de informações geográficas - SIG*. Rio de Janeiro :

- CPRM, 2003. Mapas Escala 1:2.500.000. 4 CDs ROM. (abstract in english)
- CPRM. 2005. Programa Levantamentos Geológicos Básicos do Brasil. *Mapa Geológico do Brasil*. Escala 1:1000.000. 41 mapas Brasília, MME. Edição 2004. CD-ROM. (in portuguese)
- CPRM. 2006. Programa Integração, Atualização e Difusão de Dados da Geologia do Brasil: Subprograma Mapas Geológicos Estaduais. *Geologia e Recursos Minerais do Estado do Amazonas*. Manaus, CPRM/CIAMA-AM, 2006. Escala 1:1.000.000. Texto explicativo, 148p. CD ROM. (in portuguese)
- Daly, S.J., Fanning, C.M., Fairclough, M.C., 1998. Tectonic evolution and exploration potential of the Gawler Craton, South Australia. *AGSO J. Aust. Geol. Geophys.* 17, 145–168.
- Daly, J.S., Balagansky, V.V., Timmerman, M.J., Whitehouse, M.J., de Jong, K., Guise, P., Bogdanova, S., Gorbatshev, R., Bridgewater, D., 2001. Ion microprobe U–Pb zircon geochronology and isotopic evidence for a trans-crustal suture in the Lapland–Kola Orogen, northern Fennoscandian Shield. *Pecamb. Res* 105,289–314.
- Delor, C., Lahondère, D., Egal, E., Lafon, J.-M., Cocherie, A., Guerrot, C., Rossi, P., Truffert, C., Théveniaut, H., Phillips, D., Avelar, V.G. de. 2003. Transamazonian crustal growth and reworking as revealed by the 1:500,000-scale geological map of French Guiana (2nd edition). *Géologie de la France* **2-3-4**, 5-57.
- Dougherty-Page, J.S., Bartlett, J. M. 1999. New analytical procedures to increase the resolution of zircon geochronology by the evaporation technique. *Chem. Geol.* **153**, 227-240.
- Faraco, M.T.L., Vale, A.G., Santos, J.O.S. dos, Luzardo, R., Ferreira, A.L., Oliveira, M.A., Marinho, P.A.C. 2003. Levantamento geológico na região a norte do Bloco Carajás: Notícias preliminares. In: SBG, Simpósio de Geologia da Amazônia, 8, Manaus, AM, Anais (CD-ROM) (in portuguese).
- Faria, M.S.G. de, Luzardo, R., Pinheiro, S.S. 1999. Litoquímica e petrogênese do Granito Igarapé Azul. In: SBG, Simpósio de Geologia da Amazônia, 6, Anais, p. 577-580 (in portuguese).
- Faria, M.S.G. de, Santos, J.O.S. dos, Luzardo, R., Hartmann, L.A., McNaughton, N.J. 2002. The oldest island arc of Roraima State, Brazil – 2.03 Ga: zircon SHRIMP U–Pb geochronology of Anauá Complex. In: SBG, Congresso Brasileiro de Geologia, 41, Anais, p. 306.
- Fraga, L.M.B. 2002. A Associação Anortosito–Mangerito–Granito Rapakivi (AMG) do Cinturão Guiana Central, Roraima e Suas Encaixantes Paleoproterozóicas: Evolução Estrutural, Geocronologia e Petrologia. CPGG, UFPA, Tese de Doutorado. 386p (inédito) (in

- portuguese).
- Fraga, L.M.B., Reis, N.J., Araújo, R.V., Haddad, R.C. 1996. Suíte Intrusiva Pedra Pintada - Um Registro do Magmatismo Pós-colisional no Estado de Roraima. In: SBG, Simpósio de Geologia da Amazônia, 5, Belém, PA. Anais, 76-78 (in portuguese).
- Fraga, L.M.B., Almeida, M.E., Macambira, J.B. 1997. First lead-lead zircon ages of charnockitic rocks from Central Güiana Belt (CGB) in the state of Roraima, Brazil. In: South-American Symposium on Isotope Geology, Campos do Jordão, Resumo, p. 115-117.
- Fraga, L.M.B., Macambira, M.J.B., Dall'Agnol, R., Costa, J.B.S. 2003. The age of the charnockitic rocks of the Serra da Prata Intrusive Suite, Central Guyana Belt, Guyana Shield. In: SBG, Simpósio de Geologia da Amazônia, 8, Manaus, AM, Anais. (CD-ROM).
- Gasquet, D., Barbey, P., Adoua, M., Paquette, J.L. 2003. Structure, Sr–Nd isotope geochemistry and zircon U–Pb geochronology of the granitoids of the Dabakala area (Cote d'Ivoire): evidence for a 2.3 Ga crustal growth event in the Palaeoproterozoic of West Africa? *Precamb. Res.* **127**, 329–354.
- Gaudette, H.E., Olszewski, W.J. Jr., Santos, J.O.S. dos. 1996. Geochronology of Precambrian rocks from the northern part of Güiana Shield, State of Roraima, Brazil. *Journal of South-American Earth Sciences* **9**, 183-195.
- Klein, E.L., Moura, C.A.V. 2001. Age constrains on the granitoids and metavolcanics rocks of the São Luís Craton and Gurupi Belt, Northern Brazil: Implications for lithostratigraphy and geological evolution. *Intern. Geol. Rev.* **43**, 237-253.
- Klötzli, U.S. 1999. Th/U zonation in zircon derived from evaporation analysis: a model and its implications. *Chem. Geol.* **158**, 25-333.
- Kober, B. 1986. Whole grain evaporation for $^{207}\text{Pb}/^{206}\text{Pb}$ age investigations on single zircons using a double filament source. *Contrib. Mineral. Petrol.* **93**, 82-490.
- Kober, B. 1987. Single-grain evaporation combined with Pb+ emitter bedding for $^{207}\text{Pb}/^{206}\text{Pb}$ investigations using thermal ion mass spectrometry, and implications for zirconology. *Contrib. Mineral. Petrol.* **96**, 63-71.
- Krymsky, R. 2002. Metodologia de análise de U-Pb em mono zircão com traçador ^{235}U - ^{205}Pb . Universidade Federal do Pará, Laboratório de Geologia Isotópica. 7p. (in portuguese).
- Lamarão, C.N., Dall'Agnol, R., Lafon, J.-M., Lima, E.F., 2002. Geology, geochemistry and Pb–Pb zircon geochronology of the Paleoproterozoic magmatism of Vila Riozinho, Tapajós gold

- province, Amazonian craton, Brazil. *Precamb. Res.* 119 (1-4), 189–223.
- Lemoine, S., Tempier, P., Bassot, J.-P., Caen-Vachette, M., Vialette, Y., Toure, S., Wenmenga, U., 1990. The Burkinian, an orogenic cycle, precursor of the Eburnean. *Geol. Journal* **25**, 171–188.
- Ludwig, K.R. 1999. Using ISOPLOT/Ex, version 2: a geochronological toolkit for Microsoft Excel. Berkeley Geochronological Center Special Publication 1a, 47 pp.
- Macambira, M.J.B., Scheller, T. 1994. Estudo comparativo entre métodos geocronológicos aplicados em zircões: o caso do Granodiorito Rio Maria. In: Simpósio de Geologia da Amazônia., 4, Belém, 1994. Bol. Res. Exp., Belém/SBG. p. 343-346.
- Macambira, M.J.B., Almeida, M.E., Santos, L.S. 2002. Idade de Zircão das Vulcânicas Iricoumé do Sudeste de Roraima: contribuição para a redefinição do Supergrupo Uatumã. In: SBG, Simpósio Sobre Vulcanismo Ambientes Associados, 2, Anais, p.22 (in portuguese).
- Macambira, M.J.B.; Silva, D.C.C.; Vasquez, M.L.; Barros, C.E.M. 2004. Investigação do limite arqueano-paleoproterozóico ao norte da Província de Carajás, Amazônia Oriental. In: Congresso Brasileiro de Geologia, 42, Araxá. Anais. CD-ROM.
- Maniar, P.D., Piccoli, P.M. 1989. Tectonic discrimination of granitoids. *Geol. Soc. Am. Bull.* **101**, 635-643.
- McDonough, M.R., Grover, T.W., McNicoll, V.J., Lindsay, D.D. 1993. Preliminary geology of the southern Taltson magmatic zone, Canadian Shield, northeastern Alberta. *Geol. Surv. Can. Pap.* 93-1C, 221–231.
- Milési, J.P., Ledru, P., Feybesse, J.L., Dommangeat, A., Marcoux, E. 1992. Early Proterozoic ore deposits and tectonics of the Birimian orogenic belt, West Africa. *Precamb. Res.* **58**, 305–344.
- Patiño-Douce, A.E. 1996. Effects of pressure and H₂O content on the composition of primary crustal melts. *Trans. R. Soc. Edinburgh: Earth Sci.* 87, 11–21.
- Patiño-Douce, A.E. 1999. What do experiments tell us about the relative contributions of crust and mantle to the origin of granitic magmas? In: Castro, A., Fernandez, C., Vigneresse, J.L. (Eds.), *Understanding Granites: Integrating New and Classical Techniques*, 168. *Geol. Soc. London*, Special Publication 168, pp. 55–75.
- Patiño-Douce, A.E., Beard, J.S. 1996. Effects of P, fO₂ and Mg/Fe ratio on dehydration melting of model metagreywackes. *J. Petrol.* **37**, 999–1024.

- Pearce, J.A. 1996. Sources and settings of granitic rocks. *Episodes* **19**, 120-125
- Pearce, J.A., Harris, N.B., Tindle, A.G. 1984. Trace element discrimination diagrams for the tectonic interpretation of granitic rocks. *J. Petrol.* **25**, 956–983.
- Peccerillo, A., Taylor, S.R. 1976. Geochemistry of Eocene calc-alkaline rocks from Kastamonu area, Northern Turkey. *Contrib. Mineral. Petrol.* **58**, 63-81.
- Pupin, J. P. 1980. Zircon and granite petrology. *Contrib. Min. Petrol.* **73**, 207–220.
- Reis, N.J., Faria, M.S.G. de, Fraga, L.M.B., Haddad, R.C. 2000. Orosirian Calc-Alkaline Volcanism and the Orocaima Event in the Northern Amazonian Cráton, Eastern Roraima State, Brazil. *Rev. Bras. Geoc.* **30** (3), 380-383.
- Reis, N.J., Fraga, L.M.B., Faria, M.S.G. de, Almeida, M.E. 2003. Geologia do Estado de Roraima. *Géologie de la France* **2-3-4**, 71-84 (in portuguese).
- Rickwood, P. 1989. Boundary lines within petrologic diagrams which use oxides of major and minor elements. *Lithos* **22**, 247-263.
- Roberts, M.P., Clemens, J.D. 1993. The origin of high-K, calc-alkaline, I-type granitoid magmas. *Geology* **21**, 825-828.
- Rosa-Costa L.T., Ricci P.S.F., Lafon J.M., Vasquez M.L., Carvalho J.M.A., Klein E.L., Macambira E.M.B. 2003. Geology and geochronology of Archean and Paleoproterozoic domains of the southwestern Amapá and Northwestern Pará, Brazil, southeastern Guiana Shield. *Géologie de la France* **2-3-4**, 101-120.
- Santos, J.O.S. dos. 2002. Field Workshop: Manaus (AM)-Pacaraima (RR) Transect. GIS Brasil Program. CPRM, Manaus, Internal Report. (in portuguese)
- Santos, J.O.S. dos, Olszewski, W. 1988. Idade dos granulitos tipo Kanuku em Roraima. In: SBG/DNPM, Congresso Latino-Americano de Geologia, 7, Belém, Anais, p. 378-388 (in portuguese).
- Santos, J.O.S. dos, Silva, L.C., Faria, M.S.G. de, Macambira, M.J.B. 1997. Pb-Pb single crystal, evaporation isotopic study on the post-tectonic, sub-alkalic, A-type Moderna granite, Mapuera intrusive suite, State of Roraima, northern Brazil. In: SBG, Symposium of Granites and Associated Mineralizations, 2, Extended Abstract and Program. p. 273-275.
- Santos, J.O.S. dos, Hartmann, L.A., Gaudette, H.E., Groves, D.I., McNaughton, N.J., Fletcher, I.R. 2000. A new understanding of the provinces of the Amazon Craton based on integration of field mapping and U-Pb and Sm-Nd geochronology. *Gond. Res.* **3** (4), 453-488.

- Santos, J.O.S. dos, Groves, D.I., Hartmann, L.A., McNaughton, N.J., Moura, M.B., 2001. Gold deposits of the Tapajós and Alta Floresta domains, Tapajós–Parima orogenic belt, Amazon Craton, Brazil. *Mineralium Deposita* **36**, 278–299.
- Santos, J.O.S dos, Hartmann, L.A., Bossi, J., McNaughton, N.J., Fletcher, I.R. 2003a. Duration of the Trans-Amazon Cycle and its correlation within South America based on U–Pb SHRIMP geochronology of the La Plata Craton, Uruguay. *Intern. Geol. Rev.* **45** (1), 27–48.
- Santos, J.O.S. dos, Potter, P.E., Reis, N.J., Hartmann, L.A., Fletcher, I.R., McNaughton, N.J. 2003b. Age, source and Regional Stratigraphy of the Roraima Supergroup and Roraima-like Sequences in Northern South America, based on U-Pb Geochronology. *Geol. Soc. Am. Bull.* **115** (3), 331-348.
- Santos, J.O.S. dos, Reis, N.J., Chemale, F., Hartmann, L.A., Pinheiro, S. da S., McNaughton, N.J. 2003c. Paleoproterozoic Evolution of Northwestern Roraima State – Absence of Archean Crust, Based on U-Pb and Sm-Nd Isotopic Evidence. In: Simposium of South-American on Isotope Geology, 4, Pucon, Chile.
- Santos, J.O.S. dos, Van Breemen, O.B., Groves, D.I., Hartmann, L. A., Almeida, M.E., McNaughton, N.J., Fletcher, I.R. 2004. Timing and evolution of multiple Paleoproterozoic magmatic arcs in the Tapajós Domain, Amazon Craton: constraints from SHRIMP and TIMS zircon, baddeleyite and titanite U–Pb geochronology. *Precamb. Res.* vol. 131, 1-2, **10**, 73-109.
- Santos, J.O.S. dos, Hartmann, L.A., Faria, M.S.G. de, Riker, S.R.L., Souza, M.M. de, Almeida, M.E., McNaughton, N.J. 2006. A Compartimentação do Cráton Amazonas em Províncias: Avanços ocorridos no período 2000-2006. In: SBG, Simpósio de Geologia da Amazônia, 9, Belém, CD-ROM. (in portuguese)
- Sardinha, A.S. 1999. Petrografia do Granito Igarapé Azul, Sudeste do Estado de Roraima. Trabalho de Conclusão de Curso, UFPA, Belém, 32p. (in portuguese).
- Schobbenhaus, C., Hoppe, A., Lork, A., Baumann, A. 1994. Idade U/Pb do Magmatismo Uatumã no Norte do Cráton Amazônico, Escudo das Guianas (Brasil): Primeiros Resultados. In: SBG, Congresso Brasileiro de Geologia, 38, Camboriú, Anais, 2, 395-397 (in portuguese).
- Shand, S.J., 1927. *Eruptive Rocks*, D. Van Nostrand Company, New York, pp. 360.
- Sheppard, S., Occhipinti, S.A., Tyler, I.M. 2004. A 2005–1970 Ma Andean-type batholith in the southern Gascoyne Complex, Western Australia. *Precamb. Res.* **128**, 257–277.

- Söderlund, U. 1996. Conventional U-Pb dating vs. single-zircon Pb evaporation dating of complex zircons from a pegmatite in the high-grade gneisses of southwestern Sweden. *Lithos* **38**, 93-105.
- Stacey, J.S., Kramers, J.D. 1975. Approximation of terrestrial lead isotope evolution by a two-stage model. *Earth Plan. Sci. Letters* **26**, 207-221.
- Steiger, R.H., Jager, J. 1977. Convention of the use of decay constants in geo- and cosmochronology. *Earth Plan. Sci. Letters*, **36**:359-362.
- Tassinari, C.C.G. 1996. O Mapa Geocronológico do Cráton Amazônico no Brasil: revisão dos dados isotópicos. Tese de Livre docência, Instituto de Geociências da Universidade de São Paulo. 139p. (in portuguese).
- Tassinari, C.C.G., Macambira M.J.B. 1999. Geochronological Provinces of the Amazonian Craton. *Episodes* **22** (3), 174-182.
- Tassinari, C.C.G., Macambira M.J.B. 2004. A Evolução Tectônica do Cráton Amazônico. In: Mantesso-Neto, Virginio, Bartoreli, Andrea, Carneiro, Celso Dal Ré, Brito-Neves, Benjamin Bley de (eds), *Geologia do Continente Sul-Americano - Evolução da Obra de Fernando Flávio Marques de Almeida*, São Paulo, Ed. Beca, p. 471-485 (in portuguese).
- Teixeira, W., Tassinari, C.C.G., Cordani, U.G., Kawashita, K. 1989. A review of the Geochronology of the Amazonian Craton tectonic implications. *Precamb. Res.* **42**, 213-227.
- Thompson, A.B., 1996. Fertility of crustal rocks during anatexis. *Trans. Royal Society of Edinburgh. Earth Sci.* **87**, 1-10.
- Thuy Nguyen, T.B., Satir, M., Siebel, W., Venneman, T., van Long, T. 2004. Geochemical and isotopic constraints on the petrogenesis of granitoids from Dalat zone, southern Vietnam. *Journal of Asian Earth Sciences* **23**, 467-482.
- Vanderhaeghe, O., Ledru, D., Thiéblemont, D., Egal, E., Cocherie, A., Tegye, M. and Milési, J.P. (1998) Contrasting mechanisms of crustal growth. Geodynamic evolution of the Paleoproterozoic granite-greenstone belts of French Guiana. *Precamb. Res.* **92**, 165-193.
- Van Staal, C.S., Dewey, J.F., MacNiocaill, C., McKerrow, W.S. 1998. The Cambrian-Silurian tectonic evolution of the northern Appalachians and British Caledonides: History of a complex, west and southwest Pacific-type segment of Iapetus, in Blundell, D., and Scott, A.C., eds., *Lyell: The past is the key to the present: Geol. Soc. London, Special Publication* **143**, 199-242.

- Vasquez, M.L., Macambira, M.J.B., Galarza, M.A. 2003. Granitóides Transamazônicos da Região Iriri-Xingu – Estado do Pará. In: SBG, Simpósio de Geologia da Amazônia, 8, Manaus, Resumos Expandidos (CD-ROM) (in portuguese).
- Watson, E.B., Harrison, T.M. 1983. Zircon saturation revisited: temperature and composition effects in a variety of crustal magma types. *Earth Plan. Sci. Letters* **64**, 295-304.
- Whalen, J.B., Currie, K.L., Chappell, B.W. 1987. A-type granites: geochemical characteristics, discrimination and petrogenesis. *Contrib. Mineral. Petrol.* **95**, 407-419.
- Wilson, M., 1991. *Igneous Petrogenesis: a global tectonic approach*. Harper Collins Acad., 2nd ed., London. 466p.
- Wolf, M.B., Wyllie, J.P., 1994. Dehydration-melting of amphibolite at 10 kbar: the effects of temperature and time. *Contrib. Mineral. Petrol.* **115**, 369–383.
- Wood, D.A., 1979. A variably veined suboceanic upper mantle*/genetic significance for mid-ocean ridge basalts from geochemical evidence. *Geology* **7**, 499-503.

Table 1. Chemical compositions of main plutonic associations of Northern Uatumã-Anauá Domain (NUAD), such as Martins Pereira granitoids, lenses and pods of leucogranites, Serra Dourada Granite and Anauá Complex. The geochemical data were obtained from this study¹ and CPRM (2000a)².

| Martins Pereira Granite | | | | | | | | | | | | | | | | | Pods and lenses | | Serra Dourada Granite | | Anauá Complex | | | | | | | |
|----------------------------------|----------------------|----------------------|----------------------|-----------------------|---------------------------------|----------------------|----------------------|----------------------|---------------------|----------------------|---------------------|----------------------|----------------------|---------------------|---------------------|----------------------|---------------------|----------------------|-----------------------|----------------------|---------------------|---------------------|-------------------------------|----------------------|----------------------|---------------------|----------------------|--|
| Tonalites | | | | | Granodiorites and Monzogranites | | | | | | | | | | | | Leucogranites | | Granites | | Enclave | | TTG-like plutonic association | | | | | |
| Sample | MA-009B ¹ | MA-176B ¹ | MA-007C ¹ | MA-246C1 ¹ | MF-011B ² | MF-011A ² | MA-172A ¹ | MA-261B ¹ | MA-119 ¹ | MA-061A ¹ | PT-010 ² | MF-132A ² | MA-007A ¹ | RL-050 ² | RL-046 ² | MJ-213A ² | RL-013 ² | PT-006A ² | MA-246C2 ¹ | MA-007B ¹ | MF-157 ² | MF-151 ² | MF-131B ² | MF-129C ² | MF-051B ² | RL-116 ² | RL-119A ² | |
| Rock Type | BTnGn | bTn | EbTnGn | MbTnGn | bMgr | bGd | BMGrP | BMtGd | BMtMgr | BMtMgrP | bGd | mbMtMgr | BMtMgrP | bGd | bGd | bMgr | Mgr | bMgr | LcSgr | LcSgr | BMgr | MB | AGbN | AMP | MtD | MtTn | MtTn | |
| <i>Major elements (wt %)</i> | | | | | | | | | | | | | | | | | | | | | | | | | | | | |
| SiO ₂ | 49.33 | 55.91 | 60.04 | 64.55 | 62.85 | 63.52 | 65.16 | 66.91 | 68.03 | 68.23 | 68.24 | 68.72 | 68.87 | 70.95 | 71.14 | 73.96 | 74.33 | 74.60 | 72.92 | 73.92 | 70.30 | 71.70 | 41.30 | 50.20 | 52.50 | 59.40 | 59.80 | |
| TiO ₂ | 2.71 | 1.11 | 1.15 | 0.88 | 0.86 | 0.80 | 0.86 | 0.72 | 0.40 | 0.78 | 0.56 | 0.39 | 0.78 | 0.28 | 0.28 | 0.22 | 0.22 | 0.19 | 0.08 | 0.06 | 0.41 | 0.31 | 2.00 | 2.60 | 0.90 | 0.77 | 0.61 | |
| Al ₂ O ₃ | 12.44 | 17.09 | 16.05 | 15.96 | 15.61 | 15.27 | 14.71 | 14.13 | 15.25 | 13.38 | 15.06 | 15.66 | 13.55 | 15.42 | 15.46 | 13.70 | 14.66 | 13.89 | 14.42 | 14.15 | 14.30 | 14.50 | 14.00 | 12.00 | 22.00 | 17.00 | 18.90 | |
| Fe ₂ O ₃ * | 20.96 | 8.61 | 7.01 | 5.76 | 7.50 | 7.96 | 5.70 | 5.27 | 2.96 | 4.87 | 5.73 | 3.78 | 4.23 | 2.66 | 2.68 | 2.26 | 1.92 | 2.20 | 0.49 | 0.50 | 3.87 | 2.99 | 19.87 | 18.74 | 7.90 | 6.26 | 3.27 | |
| MnO | 0.22 | 0.15 | 0.13 | 0.15 | 0.16 | 0.15 | 0.10 | 0.10 | 0.07 | 0.09 | 0.14 | 0.08 | 0.08 | 0.10 | 0.10 | 0.06 | 0.06 | 0.10 | 0.02 | 0.01 | 0.07 | 0.07 | 0.29 | 0.36 | 0.11 | 0.13 | 0.12 | |
| MgO | 2.42 | 2.77 | 2.78 | 1.84 | 3.14 | 2.22 | 1.48 | 1.30 | 1.05 | 1.36 | 1.62 | 1.01 | 1.03 | 0.60 | 0.52 | 0.44 | 0.36 | 0.36 | 0.15 | 0.07 | 0.94 | 0.66 | 8.60 | 4.50 | 2.60 | 3.10 | 2.00 | |
| CaO | 5.66 | 6.07 | 5.54 | 2.39 | 3.65 | 3.74 | 3.00 | 2.56 | 3.12 | 2.55 | 2.73 | 2.22 | 2.59 | 2.42 | 2.22 | 1.21 | 1.53 | 1.51 | 0.85 | 1.17 | 1.50 | 0.77 | 10.10 | 8.70 | 7.20 | 5.30 | 5.50 | |
| Na ₂ O | 2.54 | 3.91 | 3.47 | 2.70 | 2.94 | 3.24 | 2.70 | 2.80 | 3.05 | 2.79 | 2.73 | 3.44 | 2.81 | 3.73 | 3.84 | 2.82 | 3.46 | 3.12 | 2.07 | 2.37 | 2.90 | 2.50 | 1.50 | 2.20 | 5.20 | 3.20 | 4.40 | |
| K ₂ O | 2.10 | 3.19 | 2.31 | 4.17 | 3.14 | 2.63 | 4.46 | 4.49 | 4.31 | 4.50 | 3.44 | 4.75 | 4.89 | 3.93 | 3.84 | 5.44 | 3.46 | 4.13 | 8.31 | 7.31 | 5.00 | 5.30 | 1.20 | 0.42 | 0.87 | 2.20 | 1.60 | |
| P ₂ O ₅ | 1.31 | 1.19 | 0.39 | 0.30 | 0.14 | 0.26 | 0.47 | 0.37 | 0.20 | 0.38 | 0.13 | 0.22 | 0.38 | 0.10 | 0.11 | 0.03 | 0.07 | 0.05 | 0.06 | 0.01 | 0.10 | 0.17 | 0.33 | 0.22 | 0.32 | 0.21 | 0.32 | |
| LOI | 0.10 | 0.90 | 0.70 | 1.10 | 0.95 | 0.87 | 1.10 | 0.90 | 0.90 | 0.90 | 0.58 | 0.64 | 0.60 | 0.42 | 0.47 | 0.28 | 0.21 | 0.38 | 0.80 | 0.60 | 0.33 | 0.67 | 0.65 | 0.01 | 0.33 | 0.45 | 0.23 | |
| TOTAL | 99.79 | 100.90 | 99.57 | 99.80 | 100.95 | 100.67 | 99.74 | 99.55 | 99.34 | 99.83 | 100.95 | 100.92 | 99.81 | 100.60 | 100.67 | 100.42 | 100.29 | 100.54 | 100.17 | 100.17 | 99.72 | 99.64 | 99.84 | 99.95 | 99.93 | 98.02 | 96.75 | |
| <i>Trace element (ppm)</i> | | | | | | | | | | | | | | | | | | | | | | | | | | | | |
| Ni | 21 | 16 | 26 | 26 | - | - | 14 | 12 | 7 | 20 | - | - | 20 | - | - | - | - | - | 2.11 | 2.61 | - | - | - | 31 | 5 | 14 | 5 | |
| Cr | 821 | - | 753 | 547 | - | - | 274 | 342 | 68 | 274 | - | - | 342 | - | - | - | - | - | 205.26 | 68.42 | - | - | - | 138 | 34 | 90 | 48 | |
| Rb | 184 | 97 | 183 | 228 | 296 | 280 | 307 | 282 | 157 | 233 | 186 | 191 | 187 | 140 | 149 | 216 | 153 | 169 | 192.92 | 229.09 | 204 | 414 | 32 | 11 | 53 | 83 | 36 | |
| Cs | 5.72 | 0.91 | 8.50 | 4.98 | - | - | 14.60 | 13.68 | 6.40 | 8.10 | 9.10 | 2.53 | 6.10 | 2.52 | 2.53 | 2.52 | 7.13 | 10.07 | 1.01 | 2.01 | 9.0 | 9.0 | 2.5 | - | 36.0 | 2.5 | 2.5 | |
| Ba | 563 | 1374 | 536 | 749 | 292 | 465 | 865 | 967 | 710 | 853 | 695 | 841 | 1025 | 952 | 1372 | 1217 | 959 | 961 | 1576.94 | 1807.77 | 684 | 373 | 460 | 75 | 908 | 679 | 757 | |
| Sr | 456 | 683 | 494 | 284 | 176 | 327 | 200 | 199 | 298 | 180 | 225 | 291 | 217 | 544 | 517 | 290 | 448 | 277 | 313.58 | 246.16 | 203 | 103 | 272 | 123 | 1887 | 601 | 1221 | |
| Ga | 31.30 | 25.86 | 25.59 | 26.72 | 13.18 | 12.14 | 22.81 | 23.42 | 17.57 | 20.40 | 17.19 | 16.17 | 18.70 | 11.09 | 5.05 | 5.04 | 5.09 | 5.03 | 12.28 | 13.46 | 12 | 20 | 16 | - | 31 | 19 | 19 | |
| Ta | 2.51 | 0.71 | 1.82 | 1.12 | 2.50 | 2.50 | 1.52 | 1.72 | 0.81 | 1.60 | 2.50 | 2.50 | 1.70 | 2.50 | 2.50 | 2.50 | 2.50 | 2.50 | 0.20 | 0.20 | 2.50 | 2.50 | 5.00 | - | 12.00 | 2.50 | 2.50 | |
| Nb | 32.50 | 17.95 | 26.90 | 21.74 | 14.19 | 16.18 | 25.14 | 19.56 | 9.24 | 23.20 | 13.14 | 12.13 | 23.40 | 11.09 | 12.13 | 8.06 | 7.13 | 10.07 | 2.21 | 2.21 | 9.0 | 28.0 | 12.0 | 17.0 | 5.0 | 2.5 | 10.0 | |
| Hf | 33.70 | 19.98 | 9.20 | 11.48 | 20.00 | 20.00 | 16.32 | 10.75 | 9.24 | 11.30 | 20.00 | 20.00 | 10.90 | 20.00 | 20.00 | 20.00 | 20.00 | 20.00 | 2.31 | 2.91 | - | - | - | - | - | - | - | |
| Zr | 1239 | 956 | 320 | 379 | 155 | 284 | 626 | 383 | 286 | 434 | 167 | 169 | 383 | 182 | 200 | 180 | 177 | 158 | 48.61 | 81.15 | 166 | 174 | 206 | 126 | 392 | 190 | 177 | |
| Y | 120 | 44 | 48 | 50 | 25 | 22 | 69 | 52 | 28 | 47 | 30 | 19 | 60 | 13 | 6 | 12 | 14 | 4 | 82.62 | 5.82 | 47 | 56 | 31 | 33 | 22 | 19 | 19 | |
| Th | 42 | 12 | 26 | 53 | 25 | 25 | 49 | 53 | 47 | 27 | 25 | 25 | 39 | 25 | 25 | 25 | 25 | 25 | 16.60 | 25.61 | - | - | - | - | - | 5.00 | 9.00 | |
| U | 9 | 2 | 5 | 4 | 5 | 5 | 8 | 8 | 6 | 6 | 5 | 5 | 12 | 5 | 5 | 5 | 5 | 5 | 2.01 | 3.82 | - | - | - | - | - | 5.00 | 12.00 | |
| La | 94.19 | 128.19 | 48.55 | 86.56 | 37.24 | 52.83 | 111.72 | 86.47 | 48.05 | 63.50 | 33.18 | 32.59 | 82.60 | 30.29 | 48.05 | 107.61 | 48.12 | 23.04 | 24.66 | 22.50 | 40.62 | 40.89 | 21.57 | 17.32 | 28.22 | 27.64 | 32.40 | |
| Ce | 260.21 | 251.93 | 114.39 | 211.72 | 90.40 | 113.18 | 309.61 | 196.35 | 101.18 | 130.20 | 75.72 | 73.21 | 160.20 | 71.87 | 95.07 | 229.33 | 101.90 | 50.05 | 49.11 | 46.60 | 98.52 | 107.80 | 71.35 | 44.01 | 65.33 | 67.84 | 72.09 | |
| Pr | 33.00 | 24.63 | 13.96 | 22.52 | - | - | 28.64 | 21.18 | 9.66 | 15.79 | - | - | 18.84 | - | - | - | - | - | 5.53 | 5.05 | - | - | - | - | - | - | - | |
| Eu | 3.28 | 2.52 | 1.89 | 1.68 | 0.79 | 0.96 | 2.19 | 1.71 | 1.11 | 1.52 | 0.95 | 0.80 | 1.95 | 0.63 | 0.77 | 1.87 | 0.75 | 0.54 | 1.46 | 1.20 | 1.02 | 0.70 | 2.49 | 1.79 | 1.60 | 1.28 | 1.42 | |
| Gd | 22.44 | 9.77 | 10.59 | 11.67 | 4.86 | 3.78 | 14.67 | 10.69 | 4.48 | 9.16 | 3.49 | 4.16 | 10.76 | 2.76 | 2.65 | 9.55 | 4.68 | 1.80 | 5.27 | 1.61 | 4.60 | 5.18 | 7.07 | 5.27 | 3.11 | 3.59 | 2.75 | |
| Tb | 3.65 | 1.29 | 1.49 | 1.64 | - | - | 2.35 | 1.69 | 0.65 | 1.27 | - | - | 1.58 | - | - | - | - | - | 1.27 | 0.24 | - | - | - | - | - | - | - | |

Table 1. (continued)

| | | | | | | | | | | | | | | | | | | | | | | | | | | | |
|----------------------|--------|--------|--------|--------|--------|--------|--------|--------|--------|--------|--------|--------|--------|--------|--------|--------|--------|-------|--------|--------|--------|--------|--------|--------|--------|--------|--------|
| Dy | 19.84 | 7.26 | 8.31 | 8.81 | 4.86 | 2.52 | 11.73 | 8.79 | 3.60 | 7.61 | 3.38 | 4.14 | 8.50 | 2.11 | 2.05 | 6.04 | 3.10 | 1.10 | 9.49 | 1.03 | 3.89 | 4.16 | 5.35 | 6.89 | 2.13 | 3.16 | 2.25 |
| Ho | 3.88 | 1.41 | 1.53 | 1.68 | 0.97 | 0.38 | 2.27 | 1.63 | 0.82 | 1.32 | 0.67 | 0.71 | 1.59 | 0.38 | 0.40 | 1.09 | 0.61 | 0.22 | 2.71 | 0.18 | 0.72 | 0.77 | 1.07 | 1.41 | 0.35 | 0.59 | 0.42 |
| Er | 11.75 | 4.15 | 4.66 | 4.86 | 2.63 | 0.94 | 6.69 | 4.39 | 2.23 | 4.29 | 1.77 | 1.79 | 4.89 | 0.85 | 0.99 | 2.37 | 1.58 | 0.55 | 10.71 | 0.65 | 1.61 | 1.76 | 2.90 | 3.94 | 0.80 | 1.37 | 0.96 |
| Tm | 1.86 | 0.59 | 0.69 | 0.72 | - | - | 0.99 | 0.64 | 0.42 | 0.58 | - | - | 0.72 | - | - | - | - | - | 2.04 | 0.09 | - | - | - | - | - | - | - |
| Yb | 12.28 | 4.08 | 4.23 | 4.65 | 1.83 | 0.80 | 6.10 | 3.70 | 2.38 | 4.16 | 1.07 | 1.08 | 4.94 | 0.63 | 0.85 | 1.37 | 1.72 | 0.41 | 14.13 | 0.62 | 0.97 | 1.18 | 1.82 | 3.20 | 0.60 | 1.04 | 0.79 |
| Lu | 1.85 | 0.70 | 0.65 | 0.79 | 0.22 | 0.14 | 0.99 | 0.58 | 0.43 | 0.58 | 0.16 | 0.12 | 0.71 | 0.09 | 0.11 | 0.18 | 0.23 | 0.08 | 2.48 | 0.10 | 0.14 | 0.16 | 0.27 | 0.35 | 0.09 | 0.12 | 0.09 |
| ETR total | 633.94 | 534.38 | 278.29 | 455.85 | 194.69 | 217.16 | 623.67 | 430.78 | 212.38 | 312.28 | 156.55 | 153.05 | 380.08 | 146.18 | 193.66 | 483.34 | 219.13 | 97.18 | 153.10 | 100.36 | 205.24 | 222.64 | 171.79 | 117.95 | 137.72 | 146.96 | 148.14 |
| Mg# | 18.61 | 38.91 | 43.99 | 38.75 | 45.34 | 35.64 | 33.96 | 32.82 | 41.26 | 35.61 | 35.85 | 34.64 | 32.53 | 30.71 | 27.96 | 27.95 | 26.82 | 24.58 | 37.74 | 21.71 | 32.50 | 30.41 | 46.16 | 32.23 | 43.73 | 38.77 | 36.54 |
| Rb/Sr | 0.40 | 0.14 | 0.37 | 0.80 | 1.68 | 0.86 | 1.54 | 1.42 | 0.53 | 1.29 | 0.83 | 0.66 | 0.86 | 0.26 | 0.29 | 0.74 | 0.34 | 0.61 | 0.62 | 0.93 | 1.00 | 4.02 | 0.12 | 0.09 | 0.03 | 0.14 | 0.03 |
| Rb/Ba | 0.33 | 0.07 | 0.34 | 0.30 | 1.01 | 0.60 | 0.36 | 0.29 | 0.22 | 0.27 | 0.27 | 0.23 | 0.18 | 0.15 | 0.11 | 0.18 | 0.16 | 0.18 | 0.12 | 0.13 | 3.35 | 0.90 | 14.38 | 6.82 | 17.13 | 8.18 | 21.03 |
| Eu(n)/Eu* | 0.39 | 0.69 | 0.52 | 0.38 | 0.45 | 0.58 | 0.4 | 0.42 | 0.68 | 0.44 | 0.74 | 0.53 | 0.5 | 0.58 | 0.71 | 0.41 | 0.44 | 0.68 | 0.93 | 1.66 | 0.47 | 0.29 | 0.85 | 0.98 | 1.07 | 0.78 | 1.15 |
| (La/Sm) _n | 2.16 | 6.74 | 2.67 | 3.70 | 4.15 | 5.61 | 3.89 | 4.03 | 5.72 | 3.53 | 5.00 | 4.24 | 4.09 | 5.12 | 7.98 | 3.93 | 5.41 | 5.10 | 3.58 | 5.42 | 3.15 | 2.83 | 1.33 | 1.89 | 3.19 | 2.89 | 4.55 |
| (Gd/Yb) _n | 1.47 | 1.93 | 2.02 | 2.02 | 2.14 | 3.83 | 1.94 | 2.33 | 8.31 | 1.78 | 2.62 | 3.11 | 1.76 | 3.51 | 2.52 | 5.62 | 2.20 | 3.56 | 0.3 | 2.08 | 3.82 | 3.55 | 3.13 | 1.33 | 4.18 | 2.79 | 2.82 |
| (La/Yb) _n | 5.17 | 21.2 | 7.74 | 12.54 | 13.69 | 44.69 | 12.34 | 15.76 | 4.58 | 10.29 | 20.87 | 20.32 | 11.27 | 32.17 | 38.17 | 52.90 | 18.85 | 38.01 | 1.18 | 24.36 | 28.20 | 23.40 | 7.99 | 3.65 | 31.71 | 17.94 | 27.72 |

Abbreviations: a. amphibole; b. biotite; e. epidote; m. muscovite; D. diorite; Gb. gabbro; Gd. granodiorite; Mgr. monzogranite; N. norite; Sgr. syenogranite; Tn. tonalite; Gn. gneiss; Lc. leuco; Mt. meta; P. porphyritic.

Table 2. Petrography summary and geographic coordinates of analyzed samples by the single-zircon Pb-evaporation and U-Pb ID-TIMS methods.

| sample code | stratigraphic unit | geog coord N | geog coord W | sample description | U-Pb ID TIMS | MSWD | Pb-evap | USD |
|-------------|----------------------------------|--------------|--------------|---|----------------|------|---------------|-----|
| MA-172A | Martins Pereira Granite | 01° 02' 49" | 59° 55' 51" | Biotite porphyritic monzogranite with abundant tabular and ovoid alkalifeldspar megacrystals. The matrix is isotropic, coarse grained with local cataclastic texture. | - | - | 1975 ± 6 (6) | 2.9 |
| MA-61A | Martins Pereira Granite | 01° 01' 43" | 60° 01' 29" | Biotite mylonitic granodiorite, fine-to medium grained matrix with protomylonitic to mylonitic textures and NE-SW foliation (granolepidoblastic). Titanite and epidote are the main accessory minerals. | - | - | 1973 ± 2 (8) | 1.4 |
| MA-007A | Martins Pereira Granite | 00° 59' 39" | 60° 24' 21" | Biotite porphyritic metamonzogranite, medium to coarse grained matrix and accessory minerals such as epidote, magnetite and minor apatite, titanite, allanite and zircon. ENE-WSW foliation locally filled by subconcordant pods and lenses of leucogranite. | - | - | 1971 ± 2 (4) | 1.1 |
| MF-156 | Serra Dourada Granite | 01° 18' 03" | 54° 00' 20" | Equigranular monzogranite coarse to medium-grained showing aluminous minerals such as biotite, muscovite and locally cordierite (pinitized) and sillimanite. Dynamic recrystallization and planar fabrics are subordinated. | upper 1962 ± 6 | 1.7 | 1948 ± 11 (2) | 2.0 |
| | | | | | lower 156 ± 30 | - | 2138 ± 3 (2) | 0.1 |
| MA-246C2 | Pods and lenses of leucogranites | 01° 11' 11" | 60° 17' 38" | White graysh, equigranular, leucogranite in lenses and pods with isotropic fabrics, locally showing dynamic recrystallization and cataclasis. The mineral assemblage is composed by alkalifeldspar, quartz, plagioclase, biotite, muscovite, epidote, and rare opaque minerals, allanite, titanite, apatite and zircon. | - | - | 2354 ± 6 (1) | 2.2 |
| | | | | | - | - | 2134 ± 15 (3) | 5.3 |
| | | | | | - | - | 1997 ± 8 (2) | 0.1 |
| | | | | | - | - | 1959 ± 5 (4) | 2.1 |
| - | - | - | - | 1906 ± 4 (5) | 2.6 | | | |

Notes: In parenthesis the number of zircon analyses used to calculate the age. Key: U-Pb ID TIMS. Conventional U-Pb results, Pb-evap. Pb-evaporation results.

Table 3. Zircon single-crystal Pb-evaporation isotopic data from Martins Pereira Granite (MA-172A, 061A and 007A), Serra Dourada Granite (MF-156), and lenses of leucogranite (MA-246C2) samples.

| sample/zircon number | Temp. (°C) | ratios | $^{204}\text{Pb}/^{206}\text{Pb}$ | 2σ | $^{208}\text{Pb}/^{206}\text{Pb}$ | 2σ | $^{207}\text{Pb}/^{206}\text{Pb}$ | 2σ | $(^{207}\text{Pb}/^{206}\text{Pb})_c$ | 2σ | age | 2σ | Th/U |
|---|------------|--------|-----------------------------------|-----------|-----------------------------------|-----------|-----------------------------------|-----------|---------------------------------------|-----------|-------------|-----------|------|
| Martins Pereira Granite - Porphyritic (ovoids) biotite monzogranite | | | | | | | | | | | | | |
| MA-172A/1 | 1550 | 8/8 | 0.000110 | 14 | 0.17363 | 181 | 0.12186 | 15 | 0.12186 | 15 | 1984 | 2 | 0.49 |
| MA-172A/2 | 1500 | 34/34 | 0.000019 | 2 | 0.12364 | 21 | 0.12141 | 26 | 0.12119 | 29 | 1974 | 4 | 0.35 |
| MA-172A/3 | 1450 | 30/38 | 0.000402 | 3 | 0.12353 | 30 | 0.12674 | 60 | 0.12094 | 40 | 1971 | 6 | 0.35 |
| MA-172A/4 | 1450 | 20/20 | 0.000155 | 16 | 0.11822 | 39 | 0.12336 | 39 | 0.12089 | 20 | 1970 | 3 | 0.33 |
| | 1500 | 34/34 | 0.000068 | 5 | 0.15392 | 19 | 0.12260 | 15 | 0.12169 | 12 | 1981 | 2 | 0.44 |
| MA-172A/5 | 1500 | 36/36 | 0.000120 | 2 | 0.12514 | 28 | 0.12290 | 14 | 0.12131 | 14 | 1976 | 2 | 0.35 |
| | 1550 | 16/16 | 0.000000 | 0 | 0.11807 | 95 | 0.12070 | 19 | 0.12070 | 19 | 1967 | 3 | 0.33 |
| MA-172A/6 | 1500 | 30/30 | 0.000116 | 4 | 0.17099 | 111 | 0.12372 | 16 | 0.12216 | 21 | 1988 | 3 | 0.48 |
| | | | 208 (216) | | usd: 2.9 | | | | mean age | | 1975 | 6 | |
| Martins Pereira Granite - Mylonitic biotite monzogranite | | | | | | | | | | | | | |
| MA-061A/02 | 1550 | 40/40 | 0.000251 | 3 | 0.10772 | 23 | 0.12506 | 17 | 0.12117 | 36 | 1974 | 11 | 0.30 |
| MA-061A/03 | 1450 | 8/8 | 0.000000 | 1 | 0.09694 | 97 | 0.12028 | 73 | 0.12028 | 73 | 1961 | 22 | 0.27 |
| MA-061A/04 | #1450 | 0/24 | 0.000456 | 44 | 0.10745 | 26 | 0.12590 | 11 | 0.12590 | 11 | 2042 | 2 | 0.30 |
| | *1500 | 0/6 | 0.000000 | 1 | 0.10825 | 112 | 0.12591 | 72 | 0.12590 | 72 | 2042 | 10 | 0.31 |
| MA-061A/05 | #1450 | 0/30 | 0.000647 | 15 | 0.22820 | 963 | 0.12116 | 23 | 0.12116 | 23 | 1848 | 21 | 0.65 |
| MA-061A/06 | 1450 | 8/8 | 0.000052 | 6 | 0.16154 | 101 | 0.12162 | 15 | 0.12162 | 15 | 1970 | 6 | 0.46 |
| MA-061A/07 | 1450 | 32/32 | 0.000085 | 3 | 0.14130 | 56 | 0.12211 | 15 | 0.12119 | 9 | 1974 | 3 | 0.40 |
| MA-061A/09 | 1450 | 26/26 | 0.000267 | 8 | 0.11054 | 20 | 0.12485 | 17 | 0.12123 | 25 | 1975 | 7 | 0.31 |
| | *1500 | 0/8 | 0.000115 | 4 | 0.13236 | 32 | 0.12406 | 26 | 0.12253 | 27 | 1994 | 4 | 0.37 |
| MA-061A/10 | 1450 | 28/28 | 0.000191 | 5 | 0.13814 | 32 | 0.12331 | 26 | 0.12117 | 33 | 1978 | 5 | 0.39 |
| MA-061A/11 | *1450 | 0/28 | 0.000168 | 6 | 0.11267 | 89 | 0.12126 | 31 | 0.12126 | 31 | 1941 | 9 | 0.32 |
| MA-061A/12 | 1450 | 8/8 | 0.000361 | 26 | 0.21707 | 24 | 0.12526 | 15 | 0.12526 | 15 | 1963 | 11 | 0.61 |
| | 1500 | 8/8 | 0.000075 | 1 | 0.19636 | 48 | 0.12124 | 43 | 0.12124 | 43 | 1960 | 13 | 0.56 |
| MA-061A/13 | 1450 | 36/36 | 0.000129 | 1 | 0.16711 | 105 | 0.12264 | 14 | 0.12088 | 15 | 1969 | 5 | 0.47 |
| | 1500 | 40/40 | 0.000121 | 2 | 0.23122 | 489 | 0.12259 | 10 | 0.12109 | 12 | 1973 | 3 | 0.67 |
| | 1550 | 30/30 | 0.000170 | 13 | 0.15605 | 181 | 0.12312 | 21 | 0.12094 | 13 | 1970 | 4 | 0.44 |
| | | | 264 (360) | | usd: 2.9 | | | | mean age | | 1973 | 2 | |
| Martins Pereira Granite - Porphyritic biotite metamonzogranite | | | | | | | | | | | | | |
| MA-007A/01 | 1540 | 38/38 | 0.000071 | 5 | 0.14894 | 18 | 0.12198 | 34 | 0.12107 | 34 | 1972 | 5 | 0.42 |
| | 1550 | 36/36 | 0.000082 | 10 | 0.15636 | 141 | 0.12195 | 66 | 0.12074 | 57 | 1967 | 8 | 0.43 |
| MA-007A/02 | *1450 | 0/34 | 0.000102 | 27 | 0.16074 | 447 | 0.12040 | 54 | 0.11883 | 89 | 1939 | 13 | 0.46 |
| MA-007A/04 | 1500 | 36/36 | 0.000081 | 4 | 0.24268 | 34 | 0.12158 | 43 | 0.12076 | 30 | 1968 | 4 | 0.69 |
| MA-007A/05 | *1450 | 0/28 | 0.000098 | 13 | 0.13021 | 20 | 0.11918 | 27 | 0.11773 | 32 | 1922 | 5 | 0.37 |
| | 1500 | 32/32 | 0.000045 | 7 | 0.16279 | 18 | 0.12159 | 39 | 0.12099 | 48 | 1971 | 7 | 0.46 |
| MA-007A/06 | 1500 | 38/38 | 0.000030 | 6 | 0.14321 | 283 | 0.12146 | 22 | 0.12110 | 22 | 1973 | 3 | 0.41 |
| | | | 180 (242) | | usd: 0.1 | | | | mean age | | 1971 | 2 | |
| Serra Dourada Granite - Muscovite-biotite monzogranite with cordierite and sillimanite | | | | | | | | | | | | | |
| MF156/12 | 1450 | 26/34 | 0.000000 | 0 | 0.12405 | 18 | 0.13301 | 23 | 0.13301 | 23 | 2138 | 3 | 0.35 |
| MF156/15 | 1450 | 36/36 | 0.000037 | 2 | 0.08816 | 21 | 0.13360 | 13 | 0.13299 | 11 | 2138 | 1 | 0.25 |
| | | | 62 (70) | | usd: 0.1 | | | | mean age | | 2138 | 3 | |
| MF156/06 | 1550 | 4/8 | 0.000078 | 7 | 0.47918 | 1656 | 0.12012 | 17 | 0.11907 | 19 | 1943 | 3 | 0.14 |
| MF156/11 | 1550 | 6/6 | 0.000073 | 28 | 0.54277 | 132 | 0.12102 | 24 | 0.12004 | 44 | 1957 | 7 | 0.15 |
| | | | 10 (14) | | usd: 2.0 | | | | mean age | | 1948 | 11 | |
| Pods and lenses - Leucogranite | | | | | | | | | | | | | |
| MA-246C2/01 | 1500 | 24/24 | 0.000038 | 2 | 0.04358 | 104 | 0.15111 | 46 | 0.15066 | 52 | 2354 | 6 | 0.12 |
| | *1550 | 0/8 | 0.000044 | 2 | 0.04139 | 58 | 0.14857 | 78 | 0.14800 | 78 | 2323 | 9 | 0.11 |
| | | | 24 (32) | | usd: 2.2 | | | | mean age (Group I) | | 2354 | 6 | |
| MA-246C2/10 | 1500 | 36/36 | 0.000233 | 13 | 0.06005 | 30 | 0.13863 | 40 | 0.13533 | 56 | 2169 | 7 | 0.17 |
| | 1550 | 8/8 | 0.000246 | 106 | 0.05694 | 47 | 0.13545 | 143 | 0.13254 | 47 | 2132 | 6 | 0.16 |
| MA-246C2/14 | 1450 | 8/8 | 0.000423 | 26 | 0.10097 | 44 | 0.13804 | 694 | 0.13248 | 699 | 2131 | 92 | 0.28 |
| MA-246C2/16 | 1500 | 38/38 | 0.000464 | 12 | 0.06177 | 32 | 0.13868 | 42 | 0.13209 | 31 | 2126 | 4 | 0.17 |
| | 1550 | 24/32 | 0.000515 | 28 | 0.06177 | 26 | 0.13899 | 29 | 0.13207 | 60 | 2126 | 8 | 0.17 |
| | | | 114 (122) | | usd: 5.3 | | | | mean age (Group II) | | 2134 | 15 | |
| MA-246C2/17 | 1500 | 20/20 | 0.000116 | 102 | 0.05330 | 396 | 0.12487 | 87 | 0.12280 | 93 | 1998 | 13 | 0.15 |
| MA-246C2/21 | 1500 | 34/34 | 0.000119 | 28 | 0.03507 | 14 | 0.12453 | 31 | 0.12273 | 68 | 1997 | 10 | 0.10 |
| | *1550 | 0/6 | 0.000000 | 0 | 0.03531 | 29 | 0.12630 | 148 | 0.12630 | 148 | 2047 | 21 | 0.10 |
| | | | 54 (60) | | usd: 0.1 | | | | mean age (Group III) | | 1997 | 8 | |
| MA-246C2/07 | 1500 | 20/20 | 0.000270 | 15 | 0.05075 | 55 | 0.12369 | 53 | 0.12004 | 56 | 1957 | 8 | 0.14 |
| MA-246C2/09 | 1500 | 22/22 | 0.000236 | 9 | 0.10952 | 280 | 0.12285 | 87 | 0.11972 | 57 | 1952 | 9 | 0.31 |
| | | | 90 (104) | | usd: 2.1 | | | | mean age (Group IV) | | 1959 | 5 | |

Table 3 (Continued)

| sample/zircon number | Temp. (°C) | ratios | ²⁰⁴ Pb/ ²⁰⁶ Pb | 2σ | ²⁰⁸ Pb/ ²⁰⁶ Pb | 2σ | ²⁰⁷ Pb/ ²⁰⁶ Pb | 2σ | (²⁰⁷ Pb/ ²⁰⁶ Pb) _c | 2σ | age | 2σ | Th/U |
|----------------------|--------------|-------------|--------------------------------------|------------|--------------------------------------|------------|--------------------------------------|------------|--|------------|-------------|-----------|-------------|
| MA-246C2/13 | 1450 | 8/8 | 0.000099 | 4 | 0.04017 | 313 | 0.12051 | 117 | 0.11918 | 118 | 1944 | 18 | 0.11 |
| MA-246C2/23 | <i>*1450</i> | <i>0/14</i> | <i>0.000551</i> | 22 | <i>0.04188</i> | <i>34</i> | <i>0.12441</i> | <i>74</i> | <i>0.11713</i> | <i>57</i> | <i>1913</i> | <i>9</i> | <i>0.12</i> |
| | 1500 | 34/34 | 0.000408 | 4 | 0.11232 | 105 | 0.12535 | 27 | 0.12009 | 21 | 1958 | 3 | 0.32 |
| | 1550 | 6/6 | 0.000392 | 18 | 0.10542 | 57 | 0.12604 | 30 | 0.12080 | 39 | 1968 | 6 | 0.30 |
| MA-246C2/05 | 1500 | 36/36 | 0.000340 | 28 | 0.06289 | 153 | 0.12044 | 21 | 0.11578 | 29 | 1892 | 4 | 0.18 |
| | <i>*1550</i> | <i>0/36</i> | <i>0.000111</i> | <i>45</i> | <i>0.04114</i> | <i>280</i> | <i>0.11986</i> | <i>30</i> | <i>0.11842</i> | <i>49</i> | <i>1933</i> | <i>7</i> | <i>0.12</i> |
| | 1580 | 8/8 | 0.000430 | 20 | 0.06177 | 158 | 0.12252 | 67 | 0.11674 | 72 | 1907 | 11 | 0.18 |
| MA-246C2/06 | <i>#1450</i> | <i>0/16</i> | <i>0.001815</i> | <i>73</i> | <i>0.09369</i> | <i>108</i> | <i>0.13676</i> | <i>209</i> | <i>0.10994</i> | <i>108</i> | <i>1799</i> | <i>18</i> | <i>0.27</i> |
| | 1500 | 38/38 | 0.000413 | 39 | 0.06081 | 62 | 0.12311 | 27 | 0.11721 | 45 | 1914 | 7 | 0.17 |
| | <i>*1550</i> | <i>0/36</i> | <i>0.000398</i> | <i>17</i> | <i>0.07336</i> | <i>570</i> | <i>0.12357</i> | <i>31</i> | <i>0.11822</i> | <i>33</i> | <i>1930</i> | <i>5</i> | <i>0.21</i> |
| | 1580 | 32/32 | 0.000455 | 8 | 0.06004 | 19 | 0.12307 | 41 | 0.11703 | 50 | 1912 | 8 | 0.17 |
| MA-246C2/08 | 1450 | 8/8 | 0.000579 | 40 | 0.04980 | 93 | 0.12373 | 66 | 0.11594 | 86 | 1895 | 13 | 0.14 |
| | 1480 | 30/30 | 0.000147 | 4 | 0.05632 | 54 | 0.11870 | 22 | 0.11668 | 16 | 1906 | 3 | 0.17 |
| | 1500 | 38/38 | 0.000164 | 11 | 0.06134 | 160 | 0.11910 | 24 | 0.11694 | 19 | 1910 | 3 | 0.19 |
| | 1550 | 12/12 | 0.000179 | 2 | 0.05614 | 162 | 0.11889 | 100 | 0.11623 | 61 | 1899 | 9 | 0.17 |
| MA-246C2/18 | <i>#1450</i> | <i>0/8</i> | <i>0.001175</i> | <i>176</i> | <i>0.07656</i> | <i>957</i> | <i>0.12798</i> | <i>513</i> | <i>0.11209</i> | <i>576</i> | <i>1834</i> | <i>93</i> | <i>0.24</i> |
| | 1500 | 16/16 | 0.000368 | 148 | 0.05822 | 30 | 0.12204 | 143 | 0.11686 | 75 | 1909 | 12 | 0.18 |
| MA-246C2/19 | 1500 | 8/8 | 0.000590 | 574 | 0.19248 | 833 | 0.12400 | 688 | 0.11607 | 1043 | 1897 | 162 | 0.60 |
| | | | 254 (286) | | usd: 2.6 | | | | mean age (Group V) 1906 | 4 | | | |

Notes: Crystal numbers are indicated. The column number of ratios shows the total of isotopic ratios used to the age calculation and, in parenthesis, the total isotopic ratios measured. Evaporation steps in italics were not included in the age calculation of each grain due to: * too much higher or lower values of the ²⁰⁷Pb/²⁰⁶Pb ratio in relation to the average of the zircon, and # ²⁰⁴Pb/²⁰⁶Pb > 0.0004 (and ²⁰⁴Pb/²⁰⁶Pb > 0.0006 for the leucogranite sample). Th/U ratios calcul: Th = [(²⁰⁸Pb/²⁰⁶Pb)/(lTh * T)-1] + (²⁰⁸Pb/²⁰⁶Pb); U = [(²⁰⁸Pb/²⁰⁶Pb)/(lU * T)-1] + (²⁰⁸Pb/²⁰⁶Pb); lTh = 4.94750 * 10⁻¹²; lU = 1.55125 * 10⁻¹¹ (in Klotzli, 1999).

Table 4. U-Pb isotopic zircon data (ID-TIMS) from Serra Dourada granitoid (sample MF-156).

| Zircon Number | Sample Weight (mg) | Concentrations | | | | Atomic ratios | | | | | Ages (Ma) | | | | |
|---------------|--------------------|----------------|--------|--|-------|--|-------|--|-------|--|-----------|--------------------------------------|--------------------------------------|---|-----|
| | | ppm U | ppm Pb | ²⁰⁶ Pb/ ²⁰⁴ Pb ^{c1} | %err | ²⁰⁷ Pb*/ ²³⁵ U ^{c2} | %err | ²⁰⁶ Pb*/ ²³⁸ U ^{c2} | %err | ²⁰⁷ Pb*/ ²⁰⁶ Pb* ^{c2} | %err | ²⁰⁶ Pb*/ ²³⁸ U | ²⁰⁷ Pb*/ ²³⁵ U | ²⁰⁷ Pb*/ ²⁰⁶ Pb* ^d | (%) |
| MF-156-1 | 0.144 | 35.20 | 12.33 | 129.714 | 1.040 | 543.181 | 0.225 | 0.328881 | 0.079 | 0.119786 | 0.204 | 1833 | 1890 | 1953 | 94 |
| MF-156-2 | 0.304 | 12.16 | 4.42 | 818.679 | 0.459 | 547.834 | 0.152 | 0.331237 | 0.118 | 0.119952 | 0.088 | 1844 | 1897 | 1956 | 94 |
| MF-156-4 | 0.213 | 18.01 | 5.29 | 683.428 | 0.366 | 436.517 | 0.324 | 0.266823 | 0.223 | 0.118652 | 0.234 | 1525 | 1706 | 1936 | 79 |
| MF-156-5 | 0.166 | 34.19 | 12.01 | 233.930 | 0.793 | 553.956 | 0.354 | 0.334560 | 0.347 | 0.120088 | 0.068 | 1860 | 1907 | 1958 | 95 |
| MF-156-6 | 0.770 | 5.51 | 1.90 | 816.957 | 0.700 | 536.251 | 0.457 | 0.326122 | 0.394 | 0.119258 | 0.231 | 1820 | 1879 | 1945 | 94 |

Notes: Maximum total blanks for zircon analyses are 10 pg for Pb and 2 pg for U. Stacey and Kramers (1975) values were used.

^{c1} Measure ratios corrected for mass fractionation; ^{c2} Ratios corrected for spike, fractionation, blank and initial common Pb following Stacey and Kramers (1975) model. Errors are at 2 s; ^d Concordance in relation to Concordia curve: 100t(²⁰⁶Pb/²³⁸U)/t(²⁰⁷Pb/²⁰⁶Pb).

Table 5. Summary of new and previous Pb-Pb and U-Pb (ID-TIMS and SHRIMP) ages yielded by zircon from volcano-plutonic rocks older than 1900 Ma of the Ventuari-Tapajós (or Tapajós-Parima) Province.

| Symbol | Reference Number | Rock Type | Lithostratigraphic Unit | Age (Ma) | Reference | Method |
|------------------------------|------------------|---|-----------------------------|-----------------------|---|------------------------------|
| <i>Guiana Central Domain</i> | | | | | | |
| GC1 | 1 | Hornblende-biotite gneiss with titanite (Miracélia Gneiss) | Rio Urubu "A-type" gneisses | 1935 ± 5 | Fraga (2002) | B |
| | 2 | Hornblende-biotite gneiss with allanite (Igarapé Branco Gneiss) | Rio Urubu "A-type" gneisses | 1937 ± 5 | Fraga (2002) | B |
| GC2 | 3 | Quartz jotunite | Serra da Prata C-type | 1933 ± 2 | Fraga <i>et al.</i> (2003) | B |
| | 4 | Clinopyroxene porphyritic charnockite | Serra da Prata C-type | 1934 ± 1 | Fraga <i>et al.</i> (2003) | B |
| | 5 | Hypersthene quartz syenite | Serra da Prata C-type | 1934 ± 3 | Fraga <i>et al.</i> (2003) | B |
| | 6 | Clinopyroxene porphyritic charnockite | Serra da Prata C-type | 1936 ± 4 | Fraga <i>et al.</i> (2003) | B |
| | 7 | Charnockite hydrothermalized | Serra da Prata C-type | 1943 ± 5 | Fraga <i>et al.</i> (2003) | B |
| | 8 | Quartz jotunite gneiss | Serra da Prata C-type | 1966 ± 37 | Fraga <i>et al.</i> (2003) | A |
| GC3 | 9 | Vilhena Mylonite | Rio Urubu "I-type" gneisses | 1932 ± 10 | CPRM (2003) | D |
| | 10 | Mucajai Metagranite | Rio Urubu "I-type" gneisses | 1938 ± 9 | CPRM (2003) | D |
| | 11 | Granitic gneiss | Rio Urubu "I-type" gneisses | 1943 ± 7 | Gaudette <i>et al.</i> (1996) | C |
| | 12 | Granitic gneiss | Rio Urubu "I-type" gneisses | 1944 ± 10 | Santos & Olszewski (1988) | C |
| | 13 | Tonalite orthogneiss | Rio Urubu "I-type" gneisses | 1951 ± 24 | Fraga <i>et al.</i> (1997) | A |
| GC4 | 14 | S-type leucogranite | Taiano S-type | 1969 ± 4 | CPRM (2003) | D |
| <i>Surumu Domain</i> | | | | | | |
| S1 | 15 | Tabaco Mountain Dacite | Surumu Group | 1966 ± 9 | Schobbenhaus <i>et al.</i> (1994) | C |
| | 16 | Tabaco Mountain Dacite | Surumu Group | 1977 ± 8 | Schobbenhaus <i>et al.</i> (1994) mod. by CPRM (2003) | C |
| | 17 | Ururicáa Rhyodacite | Surumu Group | 1984 ± 7 | Santos <i>et al.</i> (2003b) | D |
| | 18 | Cavalo Mountain Rhyodacite | Surumu Group | 2006 ± 4 | Costa <i>et al.</i> (2001) | B |
| S2 | 19 | Orocaima Granodiorite | Pedra Pintada Suite | 1956 ± 5 | CPRM (2003) | D |
| | 20 | Pedra Pintada Monzogranite | Pedra Pintada Suite | 2005 ± 45 | Almeida <i>et al.</i> (1997) | A |
| <i>Parima Domain</i> | | | | | | |
| P1 | 21 | Prainha meta-andesite | Parima Group | 1948 ± 6 | Santos <i>et al.</i> (2003c) | D |
| <i>Uatumã-Anauá Domain</i> | | | | | | |
| UA1 | 22 | Leucosyenogranite (ma246c2) | Pods of leucogranite | 1906 ± 4 | This paper | B |
| UA2 | 23 | Monzogranite (mf156) | S-type Serra Dourada | 1948 ± 11 | This paper | B |
| | 24 | Monzogranite (mf156) | S-type Serra Dourada | 1962 ± 6 | This paper | C |
| | 25 | Metamonzogranite | Martins Pereira Granite | 1938 ± 17 | Almeida <i>et al.</i> (1997) | A |
| UA3 | 26 | Metamonzogranite | Martins Pereira Granite | 1960 ± 21 | Almeida <i>et al.</i> (1997) | A |
| | 27 | Metamonzogranite | Martins Pereira Granite | 1972 ± 7 | CPRM (2003) | C |
| | 28 | Metamonzogranite (ma007a) | Martins Pereira Granite | 1971 ± 2 | This paper | B |
| | 29 | Mylonitic monzogranite (ma061a) | Martins Pereira Granite | 1973 ± 2 | This paper | B |
| | 30 | Monzogranite (ma172a) | Martins Pereira Granite | 1975 ± 6 | This paper | B |
| UA4 | 31 | Metatonalite | Anauá Complex | 2028 ± 9 | Faria <i>et al.</i> (2002) | D |
| <i>Tapajós Domain</i> | | | | | | |
| T1 | 32 | Granite | Creporizão Suite | 1957 ± 6 | Santos <i>et al.</i> (2000) | C |
| | 33 | Creporizão Monzogranite | Creporizão Suite | 1963 ± 6 | Santos <i>et al.</i> (2001) | D |
| | 34 | JL Monzogranite | Creporizão Suite | 1966 ± 5 | Santos <i>et al.</i> (2001) | D |
| | 35 | Joel Monzogranite | Creporizão Suite | 1968 ± 7 | Santos <i>et al.</i> (2004) | D |
| | 36 | km130 Monzogranite | Creporizão Suite | 1968 ± 16 | CPRM (2000b) | B |
| | 37 | Ouro Roxo Metandesite II | Creporizão Suite | 1974 ± 6 | Santos <i>et al.</i> (2001) | D |
| | T2 | 38 | Biotite leucomonzogranite | Old São Jorge Granite | 1981 ± 2 | Lamarão <i>et al.</i> (2002) |
| 39 | | Hornblende-biotite monzogranite | Old São Jorge Granite | 1983 ± 8 | Lamarão <i>et al.</i> (2002) | B |
| 40 | | Granite | Old São Jorge Granite | 1984 ± 1 | CPRM (2000b) | B |
| T3 | 41 | Trachyte | Vila Riozinho Volcanics | 1998 ± 3 | Lamarão <i>et al.</i> (2002) | B |
| | 42 | Trachyte | Vila Riozinho Volcanics | 2000 ± 4 | Lamarão <i>et al.</i> (2002) | B |
| T4 | 43 | Rio Claro Monzogranite | - | 1997 ± 3 | CPRM (2000b) | B |
| | 44 | Jamansim Rapakivi Monzogranite | - | 1997 ± 5 | Santos <i>et al.</i> (1997) | C |
| T5 | 45 | Cabruá Tonalite | Cuiu-Cuiu Complex | 2005 ± 7 | Santos <i>et al.</i> (2001) | D |
| | 46 | Conceição Tonalite | Cuiu-Cuiu Complex | 2006 ± 3 | Santos <i>et al.</i> (1997, 2004) | C |
| | 47 | Ouro Roxo Andesite | Cuiu-Cuiu Complex | 2012 ± 8 | Santos <i>et al.</i> (2001) | D |
| | 48 | JL Tonalite | Cuiu-Cuiu Complex | 2015 ± 9 | Santos <i>et al.</i> (2001) | D |
| | 49 | Amana Monzogranite | Cuiu-Cuiu Complex | 2020 ± 12 | Santos <i>et al.</i> (2001) | D |
| | 50 | Cuiu-Cuiu Meta-tonalite | Cuiu-Cuiu Complex | 2033 ± 7 | Santos <i>et al.</i> (2001) | D |

Notes: A. Pb-evaporation on single filament; B. Pb-evaporation on double filament; C. U-Pb ID-TIMS; D. U-Pb SHRIMP. Reference Number 1 to 50 and symbols GC1-T5 are the same as in Fig. 12.

Table 6. Summary of ages and possible sources of the inherited zircons from volcano-plutonic and (meta)sedimentary rocks older than 1900 Ma of the Ventuari-Tapajós (or Tapajós-Parima) Province.

| Domain | Reference Number | Rock Type | Lithostratigraphic Unit | Age (Ma) | Interpretation | Reference | Method |
|------------------------------|------------------|-----------------------------|-------------------------------------|-----------|----------------------|-------------------------------|--------|
| <i>Guiana Central Domain</i> | | | | | | | |
| GC4 | 14 | Leucogranite | S-type Taiano Granite | 2047 ± 7 | Late Transamazonian | CPRM (2003) | D |
| | - | Taiano Paragneiss | Cuarane Group | 2072 ± 3 | Late Transamazonian | CPRM (2003) | D |
| | | | | 2093 ± 62 | | | |
| | | | | 2223 ± 19 | Early Transamazonian | Gaudette <i>et al.</i> (1996) | C |
| GC3 | 9 | Vilhena Mylonite | Rio Urubu "I-type" gneisses | 2145 ± 5 | Early Transamazonian | CPRM (2003) | D |
| <i>Surumu Domain</i> | | | | | | | |
| | - | Uiramutã Quartz sandstone | Arai Formation (Roraima Supergroup) | 1958 ± 19 | Pedra Pintada/Surumu | Santos <i>et al.</i> (2003b) | D |
| | | | | 2123 ± 14 | Early Transamazonian | | |
| | | | | 2718 ± 18 | Archean | | |
| S1 | 17 | Uraricáa Rhyodacite | Surumu Group | 2027 ± 32 | Late Transamazonian | Santos (2002) | D |
| | 16 | Surumu Rhyodacite | Surumu Group | 2163 ± 10 | Early Transamazonian | | |
| <i>Parima Domain</i> | | | | | | | |
| P | - | Uatátás Quartzite | Parima Group | 1971 ± 9 | Pedra Pintada/Surumu | Santos <i>et al.</i> (2003c) | D |
| | | | | 2098 ± 16 | Late Transamazonian | | |
| | | | | 2201 ± 10 | Early Transamazonian | | |
| | | | | 2781 ± 6 | Archean | | |
| | | | | 2872 ± 6 | Archean | | |
| <i>Uatumã-Anauá Domain</i> | | | | | | | |
| UA2 | 23 | S-type monzogranite (mf156) | S-type Serra Dourada Granite | 2138 ± 11 | Early Transamazonian | This paper | B |
| UA1 | 22 | Leucogranite (ma246c2) | Pods and lenses of leucogranite | 1959 ± 5 | Martins Pereira | This paper | B |
| | | | | 1997 ± 8 | Anauá? | | |
| | | | | 2128 ± 3 | Early Transamazonian | | |
| | | | | 2354 ± 6 | Siderian | | |
| <i>Tapajós Domain</i> | | | | | | | |
| T1 | 34 | JL Monzogranite | Creporizão Suite | 2003 ± 5 | Cuiu-Cuiu | Santos <i>et al.</i> (2001) | D |
| T3 | 41 | Trachyte | Vila Riozinho Volcanic Rocks | 2852 ± 4 | Archean | Lamarão <i>et al.</i> (2002) | B |
| | | | | 2591 ± 3 | Late Archean | | |
| T5 | 47 | Ouro Roxo Andesite | Cuiu-Cuiu Complex | 2040 ± 5 | Late Transamazonian | Santos <i>et al.</i> (2001) | D |
| | 50 | Cuiu-Cuiu Metatonalite | Cuiu-Cuiu Complex | 2056 ± 7 | Late Transamazonian | | |
| | | | | 2046 ± 5 | Late Transamazonian | | |
| | 48 | JL Tonalite | Cuiu-Cuiu Complex | 2100 ± 7 | Early Transamazonian | | |
| | | | | 2380 ± 8 | Siderian | | |
| | | | 2483 ± 19 | Siderian | | | |

Notes: A. Pb-evaporation on single filament; B. Pb-evaporation on double filament; C. U-Pb ID-TIMS; D. U-Pb SHRIMP. Reference Number 1 to 50 and symbols GC1-T5 are the same as in fig. 12.

Evidence of the widespread 1.90-1.89 Ga I-type, high-K calc-alkaline magmatism in Southeastern Roraima State, Brazil (center-southern region of Guyana Shield) based on Geochemistry and Zircon Geochronology

M.E. Almeida^{1,2*}, M.J.B. Macambira², M.A.G. Toro², L.S. dos Santos²

¹CPRM – Geological Survey of Brazil, Av. André Araújo 2160, Aleixo, CEP 69060-001 – Manaus, Amazonas, Brazil

²Isotope Geology Laboratory, Center of Geosciences, Federal University of Pará, Rua Augusto Corrêa s/n, Guamá, CEP 66075-110 - Belém, Pará, Brazil

Corresponding author; ph.: +55-92-2126-0301, fax: +55-92-2126-0319, e-mail address: marcelo_almeida@ma.cprm.gov.br

ARTIGO A SER SUBMETIDO

Words: summary (76), abstract (374), body text (12009), table (411) and figure (971) captions.

Total: 15 tables and 6 figures.

ABSTRACT

INTRODUCTION

GEOLOGICAL SETTING

ANALYTICAL PROCEDURES

Whole-rock Geochemistry Analyses

Zircon Geochronology Analyses

WHOLE-ROCK GEOCHEMICAL RESULTS

Major oxides and trace elements

Rare-earth element (REE) geochemistry

ZIRCON GEOCHRONOLOGY RESULTS (Pb-EVAPORATION AND U-Pb ID-TIMS)

Caroebe (MA-121 and 053A samples) and Água Branca Granitoids (HM-181 sample)

Igarapé Azul Granitoids (MA-147A and 186A samples) and Biotite-bearing Enclave (MA-201b sample)

Jatapu Volcanics (MA-208 sample)

Santa Maria Enderbite (MA-198 sample)

Murauaú Granite (Mapuera Suíte, MA-226 sample)

ZIRCON AGES AND GEOLOGICAL IMPLICATIONS

Zircon Geochronology constraints

Tapajós and Uatumã-Anauá domains: Lithostratigraphy and Tectonic Evolution

CONCLUSIONS

Acknowledgments

References

ABSTRACT

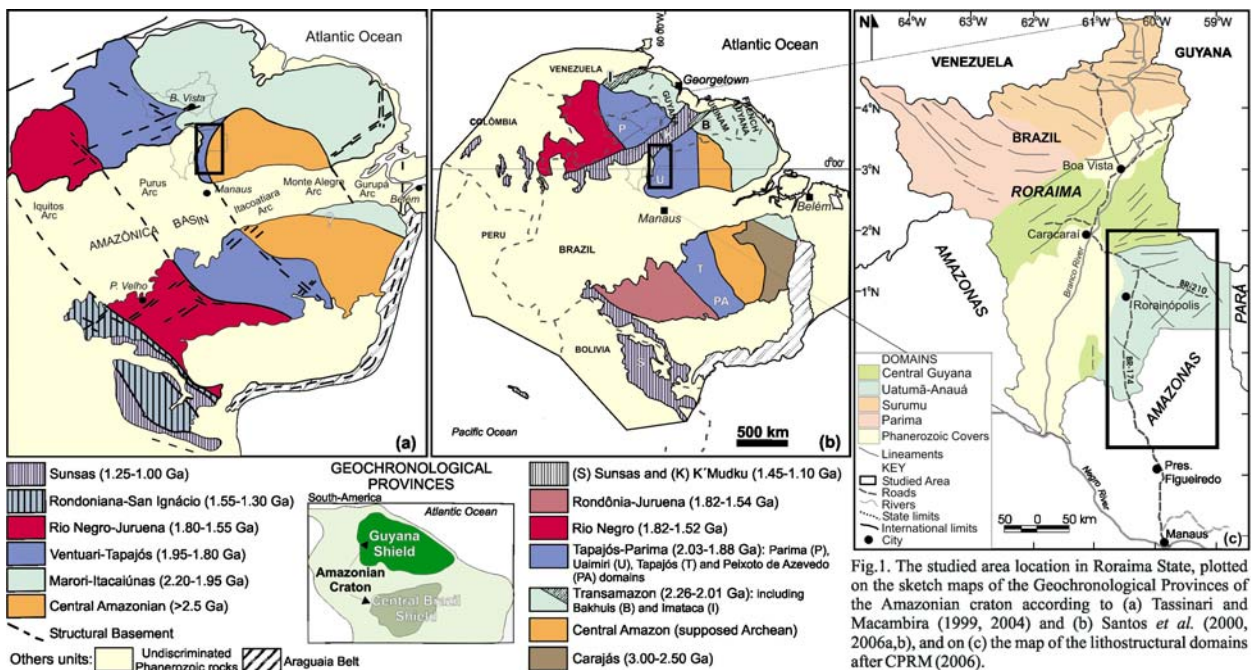
The southern Uatumã-Anauá Domain (SUAD) in the SE Roraima State (Brazil), center-southern portion of the Guyana Shield, is characterized by a widespread ca. 1.90 Ga calc-alkaline magmatism, represented by the Água Branca (1901 ± 5 Ma), Caroebe (1898 ± 2 Ma and 1891 ± 2 Ma) and Igarapé Azul (1891 ± 6 Ma and 1889 ± 2 Ma) granitoids (Água Branca Suite), Jatapu volcanic rocks (1893 ± 4 Ma) and most rarely by the Santa Maria hypersthene-bearing Tonalite (1890 ± 2 Ma). A-type granitoids are represented by the Murauaú Granite (1871 ± 5 Ma), probably related to 1.88-1.87 Ga Mapuera and Abonari magmatism. Beyond of crystallization ages, some zircons from the analyzed rocks also yielded three main inherited interval ages: a) 1972 ± 3 Ma to 1963 ± 4 Ma (Martins Pereira metagranitoids) and subordinated b) 2142 ± 10 Ma (Transamazonian) and 2359 ± 7 Ma (Siderian). The zircon geochronology results of SUAD show that crystallization age range (and inheritances) is very similar to the calc-alkaline Parauari-(Tropas)-Irirí magmatism (1898-1879 Ma) in the Tapajos domain (Brazil Central Shield). In general sense, these two domains record an important period of Orosirian crustal growth in Amazonian craton, but their origin is still a matter of debate. The Caroebe and Igarapé Azul granites (and coeval Jatapu volcanics) have I-type, high-K calc-alkaline affinities, chondrite-normalized REE patterns moderately fractionated and small negative Eu anomalies. For the hornblende-bearing facies of Caroebe granitoids, the low $Al_2O_3/(FeO+MgO+TiO_2)$ and $(Na_2O+K_2O)/(FeO+MgO+TiO_2)$ ratios, including relatively high Mg# values, suggest an origin through dehydration melting of amphibolites to metabasaltic-metatonalitic source rocks. The biotite-bearing facies shows local chemical overlap composition with the Igarapé Azul granitoids. These last exhibit normally restricted rich-SiO₂ range and moderate to very low contents of $Al_2O_3+FeO+MgO+TiO_2$, $Na_2O+K_2O+FeO+MgO+TiO_2$ and $CaO+FeO+MgO+TiO_2$, suggesting that additional input of metagreywacke source play a role in their genesis. The magmatic evolution picture is maybe compatible with volcanic arc setting, but the trace element compositions are strongly dependent of protholith composition and, therefore, not necessarily indicative of the tectonic setting of magma formation. The inherited zircons also suggest an crustal (older basement) involvement during the emplacement these granitoids, however, isotopic data (e.g. Nd, Pb and Sr) are not available for these rocks, making difficult a better evaluation of the evolutionary models.

Keywords: Geochemistry, Geochronology, Paleoproterozoic, Granitoids, Guyana Shield

INTRODUCTION

The Guyana Shield represents the northern segment of the Amazonian Craton in South America (with a surface area of nearly 1.5 million km²) and was partially formed during protracted periods of intense granitic magmatism, bracketed between 2.1 and 1.9 Ga (**Fig. 1a-b**). However, scarce geological mapping and only few petrographical, geochemical and geophysical studies are available (*e.g.* CPRM, 1999, 2000a; Delor *et al.*, 2003).

The studied area in this paper is located in the southeastern Roraima State (Brazil), central portion of Guyana Shield, and shows expressive ca. 1.90 Ga magmatism (up to 64000 m², **Fig. 2**), but its characteristic and significance are not fully understood (Oliveira *et al.*, 1996; Almeida *et al.*, 2002; CPRM, 2003). Although only recently discovered in this region, magmatism with 1.90-1.80 Ga is commonly recorded in the southern segment of Amazonian Craton (Tapajós domain, Brazil Central Shield) and has been interpreted of different ways for explain its tectonic evolution. The first hypothesis argues that this magmatism is generated in subduction-related setting (Santos *et al.*, 2000, 2004) but, in contrast, Almeida *et al.* (2001), Vasquez *et al.* (2002) and Lamarão *et al.* (2002) pointed out an alternative post-collisional and intracontinental evolution.



Magmatism with 1.90-1.80 Ga is describe also in many other parts of the world, such as northern Australia (*e.g.* Page, 1988, Griffin *et al.*, 2000), northern America (Dunphy and Ludden, 1998; St-Onge *et al.*, 1999) and Sweden (*e.g.* Billström and Weihed, 1996; Lahtinen and Huhma,

1996). This time interval is recognized like an important period of episodic crustal growth and supercontinent formation (Condie 1998).

This paper focuses the discussion on the origin of this widespread calc-alkaline magmatism younger than 1.90 Ga in the central portion of Guyana Shield (**Fig. 1**; Southeastern Roraima), using geochemical and zircon geochronology results to further constraint its petrogenesis and tectonostratigraphic history. The possible tectonic setting of these rocks is also discussed.

GEOLOGICAL SETTING

In the last years, regional geological mapping (CPRM 2000a, 2005, Almeida *et al.*, 2002, Almeida and Macambira submitted) and few zircon geochronological data (Almeida *et al.*, 1997, Santos *et al.*, 1997a, Macambira *et al.*, 2002, CPRM, 2003) have showed that Paleoproterozoic granitoids and volcanic rocks (1.97-1.81 Ga) are widespread in southeastern Roraima, intruding subordinated basement rocks with maximum ages around 2.03 Ga (Faria *et al.*, 2002).

According to recent evolutionary models proposed for the Amazonian craton, the study area can be divided into different provinces. According to Tassinari and Macambira (1999, 2004), the study area is largely enclosed by Ventuari-Tapajós and Central Amazonian provinces, with a subordinate northeastern section falling within the Maroni-Itacaiúnas province. Santos *et al.* (2000, 2006) argue that all provinces were collectively affected by the K´Mudku Shear Belt in this same region (**Fig. 1 a-b**). These models point out that Paleoproterozoic orogenic belts or magmatic arcs (*e.g.*, Ventuari-Tapajós or Tapajós-Parima, and Maroni-Itacaiúnas or Transamazon provinces) accreted to the Archean craton with time and/or represent a set of rocks produced from melting of Archean crust (Fig. **1a-b**; Cordani *et al.*, 1979, Teixeira *et al.*, 1989, Tassinari 1996, Tassinari and Macambira, 1999, 2004; Santos *et al.*, 2000, 2004, 2006).

The Ventuari-Tapajós (or Tapajós-Parima) Province is a Paleoproterozoic orogenic belt shows north-northwest trends and includes geological units which range from ~2.10 to 1.87 Ga in age (Santos *et al.*, 2000, 2006; Tassinari and Macambira 1999, 2004). This province was subdivided into four domains by Santos *et al.* (2000): Parima and Uaimiri, to north, and Peixoto Azevedo and Tapajós, to south. The southeastern Roraima belongs to the Uaimari Domain. The Central Amazonian Province (**Fig. 1a-b**) has granitoids and volcanic rocks (1.88 to 1.70 Ga) with no regional metamorphism and compressional folding (Santos *et al.*, 2000, Tassinari and Macambira 1999), and its basement rarely crops out. The age for this basement has been estimated by some Nd-model ages at around 2.3-2.5 Ga (Tassinari and Macambira, 1999, 2004).

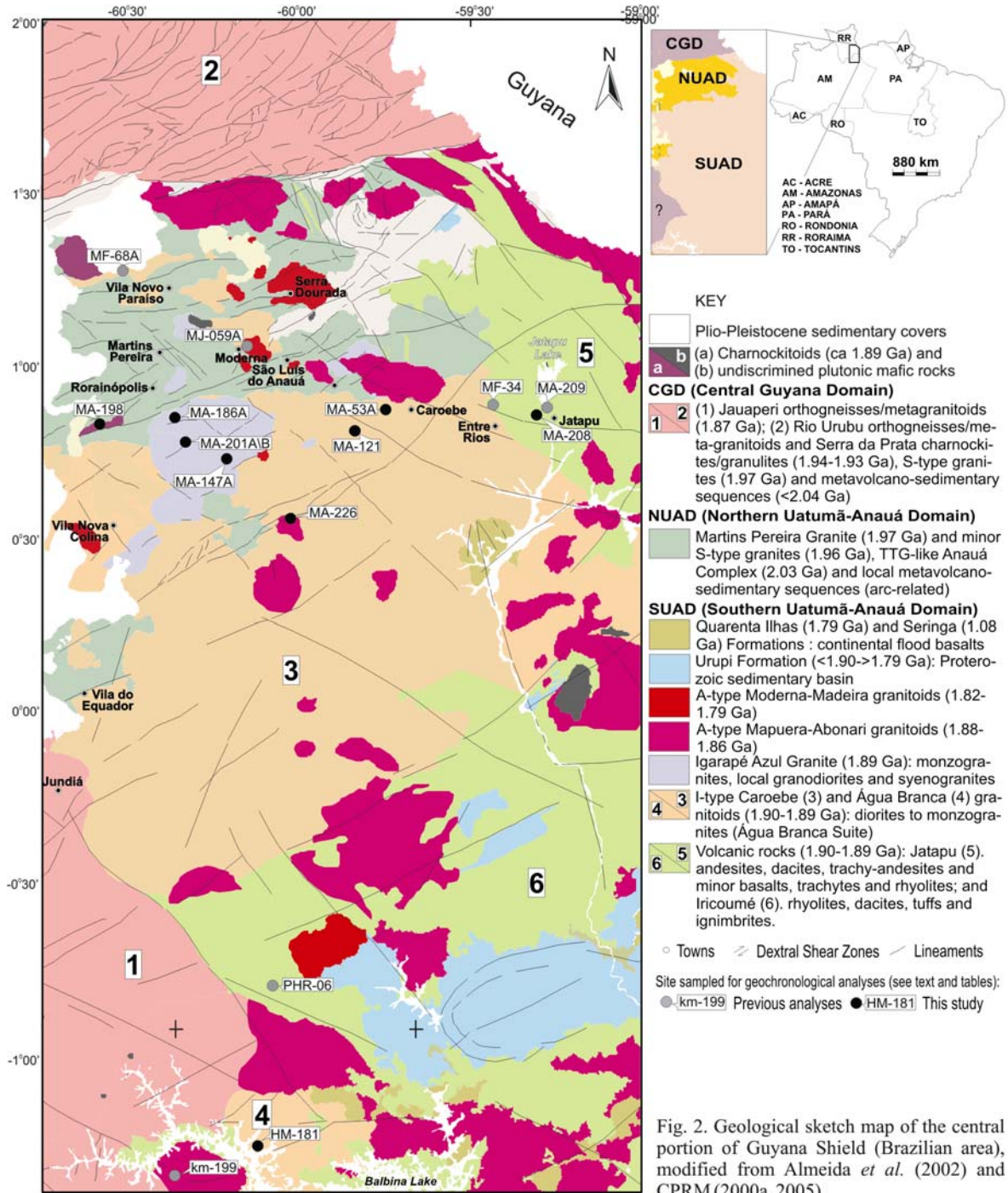
According to these authors, the recorded Archean rocks in the Amazonian craton are only exposed in Imataca (Venezuela), Carajás and southern Amapá-northwestern Pará (Brazil) regions. The Maroni-Itacaiúnas (or Transamazon) Province is also characterized by an orogenic belt with Rhyacian ages (2.25 to 2.00 Ga, **Fig. 1a-b**) and is correlated to Birimian belt in West Africa (Tassinari and Macambira, 1999, 2004; Santos *et al.*, 2000; Delor *et al.*, 2003). The K'Mudku Shear Belt is characterized by mylonitic zones with ca. 1.20 Ga (low grade) and cross-cut at least three provinces (Rio Negro, Tapajós-Parima and Transamazon, Santos *et al.*, 2000).

Reis *et al.* (2003) and CPRM (2006), taking into account lithological associations and geochronological data, divided the Roraima State into four major domains – Surumu, Parima, Central Guyana and Uatumã-Anauá (**Fig. 1c**). Each of these domains contains a wide range of rock types and stratigraphic units. The southeastern Roraima is composed of the Central Guyana and Uatumã-Anauá lithostructural domains, that correspond to the K'Mudku Shear Belt and Uaimiri Domain respectively (northern Tapajós-Parima Province) proposed by Santos *et al.* (2000).

The Central Guyana Domain (CGD) primarily consists of granulites, orthogneiss, mylonites and metagranitoids (Rio Urubu Metamorphic Suite) associated with low to high metamorphic grade metavolcanosedimentary covers (Cauarane Group) and S-type granite (Curuxuim Granite). The lineaments are strongly NE-SW trends (**Figs. 1c and 2**). The Uatumã-Anauá Domain (UAD) is characterized by E-W to NE-SW lineaments and the northern part of the domain (NUAD) shows an older metamorphic basement (**Figs. 1 and 2**) formed in a presumed island arc environment (Faria *et al.*, 2002). This basement is composed by TTG-like metagranitoids to orthogneisses (Anauá Complex), enclosing meta-mafic to meta-ultramafic xenoliths, and is associated with some inliers of metavolcano-sedimentary rocks (Uai-Uai Group) and intruded by S-type (Serra Dourada Granite) and high-K, I-type calc-alkaline (Martins Pereira) granitic magmatism of around 1.97-1.96 Ga (Almeida *et al.* 2002).

In the southern area of Uatumã-Anauá domain (SUAD), intrusive younger granites (with no regional deformation and metamorphism) are most common. The most prominent magmatism is related to the calc-alkaline Caroebe and Igarapé Azul granitoids (Água Branca Suite) with coeval Jatapu volcanic rocks. Locally igneous charnockitic (Igarapé Tamandaré) and enderbitic (Santa Maria) plutons were also recorded. Several A-type granitic bodies are widespread in the Uatumã-Anauá Domain (**Fig. 2**) represented by Moderna-Água Boa (1.81 Ga) and Mapuera-Abonari

(1.87 Ga) granites.



Some geochemical and geochronological data for the magmatism from SUAD will be showed below, including a petrogenesis and evolution models discussion. The data was obtained from Caroebe, Água Branca and Igarapé Azul granites, including coeval Jatapu volcanics, and Murauá (Mapuera type) and Santa Maria hypersthene granites.

ANALYTICAL PROCEDURES

Whole-rock Geochemistry Analyses

Whole-rock chemical analyses of 18 samples (milled under 200 mesh) were done at the Acme Analytical Laboratories Ltd in Vancouver, British Columbia, Canada. The analytical package include inductively coupled plasma - atomic emission spectrometer (ICP-AES) analysis after LiO_2 fusion for all major oxides (SiO_2 , TiO_2 , Al_2O_3 , MnO , MgO , CaO , K_2O , Na_2O , P_2O_5) and LOI. Total iron concentration is expressed as Fe_2O_3 . The trace elements were analyzed by inductively coupled plasma - mass spectrometer (ICP-MS), with rare earth and incompatible elements determined from a LiBO_2 fusion and, precious and base metals determined from an aqua regia digestion. Results from other 16 samples were compiled (and partially reinterpreted) from CPRM (2000a). These whole-rock chemical analyses were done at the Geosol Laboratories S.A. in Belo Horizonte, Minas Gerais, Brazil.

Zircon Geochronology Analyses

Samples of two to ten kg were crushed, powered and milled under 60 to 80 mesh, washed and dried out. After that, heavy mineral fractions were obtained by water mechanical concentration. These samples were then processed by means of a hand-magnet and a Frantz Isodynamic Separator followed by mineral separation in dense liquid. The lowest magnetic zircon concentrates (from five magnetic fractions) were then selected for hand-picking. As much as possible, only alteration-free zircon grains with no metamictization features, inclusions and fractures were selected for analysis (see zircon descriptions below).

In order to remove impurities, the zircon final concentrates were leached under HNO_3 on a hotplate (100°C for 10 minutes), submitted to a ultrasound cube (5 minutes) and finally washed in two times distilled water. After drying, the concentrates were observed under stereomicroscope and the selected zircon grains by hand-picking were photographed under petrographic microscope.

The zircon single-grain dating by U-Pb isotopic dilution in thermal ionization mass spectrometer (1 sample) - ID-TIMS - and step-wise Pb-evaporation (nine samples) analyses were performed at the Finnigan MAT262 multicollector mass spectrometer in dynamic mode using the ion counting detector at the Laboratory of Isotope Geology - Pará-Iso, Federal University of Pará, Brazil. The U decay constants are those recommended by IUGS (Steiger and Jäger, 1977) and errors are given at the 95% confidence level. In the Pb-evaporation method on single zircon

(Kober, 1986; 1987), the selected grains were tied in Re-filaments and charged into mass spectrometer for isotope analyses. The ages were calculated with 2 sigma error and initial common Pb corrected according to appropriate age values derived from the Stacey and Kramers (1975) model for those blocks of isotopic ratios (maximum of 18 ratios in 10 mass scans) in which the $^{204}\text{Pb}/^{206}\text{Pb}$ ratios were lower than 0.0004. Those blocks which presented values higher than 0.0004 were discarded. The data were processed using the DOS-based *Zircon* shareware (T. Scheller, 1998). The Pb-evaporation technique, including the complete procedures, is available in Klein and Moura (2002).

The U-Pb ID-TIMS procedures are developed at the Pará-Iso by Krymsky (2002). All zircon fractions selected for analysis were air abraded in 1.2-1.8 psi pressure for 30-40 minutes. These grains were abraded together with pyrite crystals (20 mg and 0.1-0.5 mm diameter). After the abrasion, the zircon crystals were washed in HNO_3 and HCl (100°C , 30 minutes) and after rinsed with H_2O -Millipore (3 times). The crystals were washed with metanol, weighted, spiked with ^{235}U - ^{205}Pb tracers solution (10 μL) and dissolved with a mixture of HF and HCl which were carried out in Teflon bombs.

Uranium and lead were isolated from zircon solution with anion-exchange resin (BioRad 1x8 200-400 mesh Cl^- form) in HCl medium in 50-70 μl columns and collected in different beakers. In order to obtain the lowest possible Pb blank, all reagents were purified by sub-boiling distillation. Uranium and lead from zircon were loaded onto the same outgassed Re-filament with SiO_2 -gel and 1N H_3PO_4 and analyzed at 1400 - 1600°C . For zircon analyses, blanks are <30 pg Pb and <1 pg U. The obtained data are processed in ISOPLOT/Excel program version 2 (Ludwig, 1998). The $^{208}\text{Pb}/^{206}\text{Pb}$ ratios were corrected for common Pb using also Stacey and Kramers (1975) model.

WHOLE-ROCK GEOCHEMICAL RESULTS

Major oxides and trace elements

Representative chemical analyses of samples of Caroebe, Igarapé Azul granites (this study, CPRM, 2000a) and Jatapu volcanics (CPRM, 2000a) are listed in **table 1**. The bulk-rock concentrations of Caroebe and Igarapé Azul granitoids are characterized by the higher and smaller range of $\text{SiO}_2\%$ contents, respectively. The Jaburuzinho facies (with hornblende and biotite) of Caroebe granite shows the lowest contents of SiO_2 (49.50%-61.85%), whereas the Alto Alegre facies (biotite granitoids) shows 65.95%-69.14% of SiO_2 and there is a compositional gap

of 4% of SiO₂ between them. The higher SiO₂ contents are observed in the Igarapé Azul granites (67.87%-72.25%). In Harker diagrams, the regression lines show the same mean trend for these two granitoid types (Caroebe and Igarapé Azul), which exhibit TiO₂, Al₂O₃, F₂O₃, MgO, CaO and P₂O₅ abundances decrease (**fig. 3a-f**) and K₂O increase (**Fig. 4a**) with SiO₂ increasing. In the Na₂O vs. SiO₂ diagram, the samples remain nearly constant but, in general, the data are scattered (**fig. 3g**).

All samples are of subalkaline affinity (**Fig. 4b**) and belong to the calc-alkaline series (**Fig. 4c**; *e.g.* Irvine and Baragar, 1971), showing high-K affiliation (*e.g.* Peccerillo and Taylor, 1985), locally plotting in the shoshonitic field, near to the high-K boundary (**Fig. 4a**). These rocks also show similar patterns to the normal calc-alkaline andesites (*e.g.* Brown *et al.*, 1984) of continental margin in the log[CaO/(Na₂O+K₂O)] vs. SiO₂ plot (**Fig. 4d**).

The molar A/CNK vs. A/NK diagram (Maniar and Piccoli, 1989, mod. Shand, 1927) defines the Caroebe and Igarapé Azul as metaluminous to slightly peraluminous, and of I-type character (**Fig. 5a**), although some samples of Igarapé Azul plots on the S-type and I-type boundary. The Jaburuzinho facies of Caroebe Granite confirm its I-type character on the Na₂O vs. K₂O diagram (**Fig. 5b**), plotting in the field outlined for typical I-type granite of the Lachlan Fold Belt (White and Chappell, 1983), however, several samples plot out of the fields. Compared to typical S-types (White and Chappell, 1983), the Alto Alegre facies shows also higher Na₂O in the same K₂O contents (Na₂O/K₂O < 1), and the Igarapé Azul Granite presents types more enriched in K₂O (**Fig. 5b**). The Na₂O vs. K₂O diagram suggests a transitional increasing of K₂O contents (with Na₂O nearly constant) from Caroebe Granite (Jaburuzinho facies) to Igarapé Azul types. There is also a compositional overlap between the Alto Alegre facies and Igarapé Azul granite in this diagram, as well as in other diagrams based on major elements (see **Fig. 3a-h, 4a-d and 5a**).

The coeval volcanic rocks of Jatapu region commonly exhibit chemical similarities with the Caroebe granites (**Fig. 3a-h, 4a-d and 5a-b**), except for the lowest Na₂O and highest MnO contents. This geochemical affinity has been also discussed by Reis *et al.* (2000). The calc-alkaline granitoids from Tapajós Domain, such as Tropas granite, demonstrate several similarities with Caroebe granites, mainly the Fe₂O₃tot, MgO and CaO contents (**Figs 3 c, e and f**), but Na₂O is normally lower (**Fig. 3g**) in the same SiO₂ contents. On the other hand, the Parauari Granite shows higher SiO₂ (59%-76%) and Fe₂O₃tot (**Fig. 3c**), and lower Al₂O₃ (**Fig. 3b**) and MgO (**Fig. 3e and 4c**) contents.

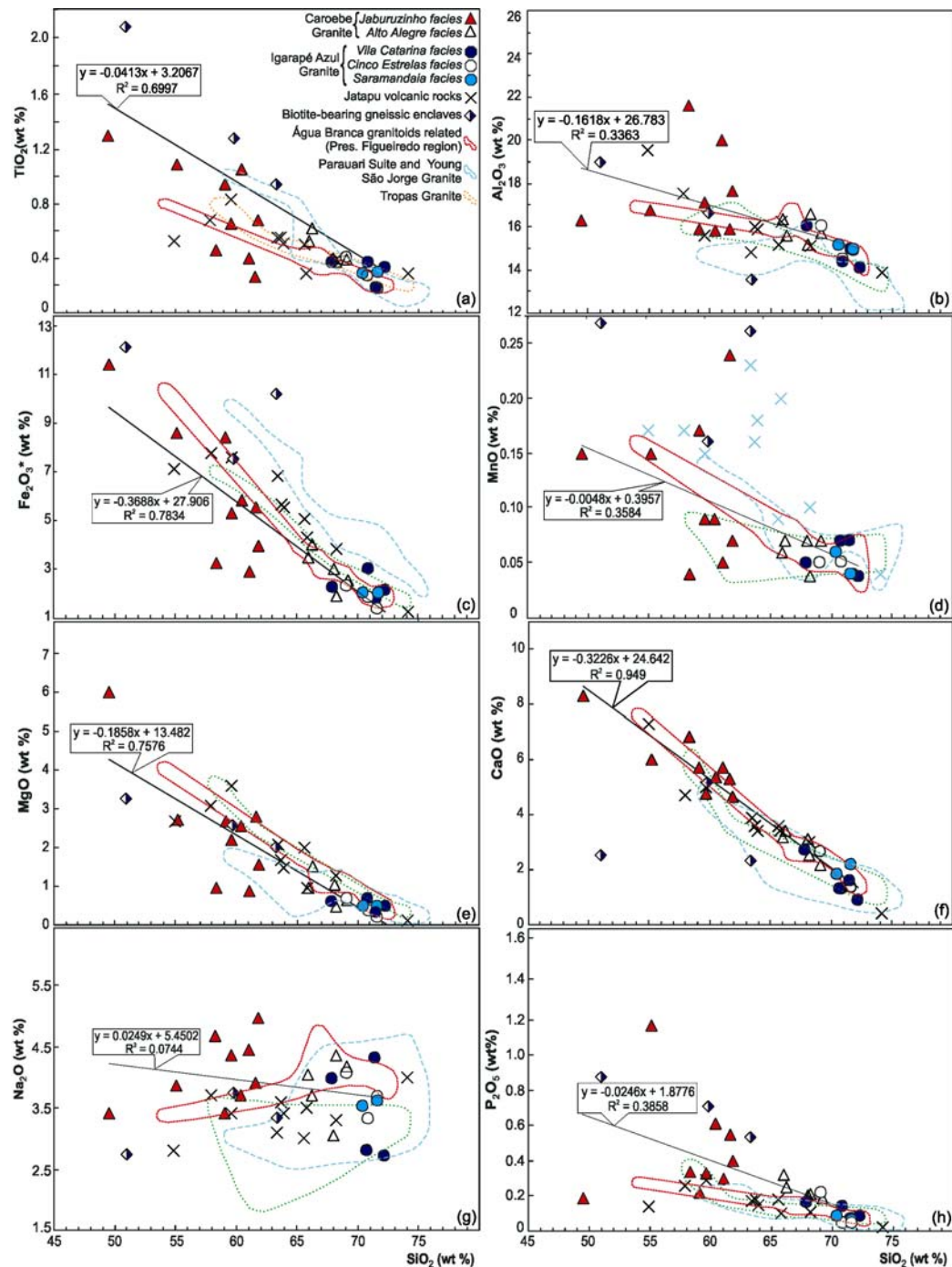


Fig. 3. (a-h) Selected Harker variation diagrams of major elements for the Caroebe and Igarapé Azul granites, including coeval Jatapu volcanics (SUAD). For references see table 1. For the linear regression are used only the Caroebe and Igarapé Azul granite samples. Compositional fields of Tropas (Santos *et al.*, 2004), Parauari (Vasquez *et al.*, 2002; Santos *et al.*, 2004) and Young São Jorge (Lamarão *et al.*, 2002) granites from Tapajós Domain and Água Branca related granitoids (Valério, 2006) are also plotted for comparison.

In the FeO*/MgO vs. Zr+Nb+Ce+Y diagram (Fig. 5c, Whalen *et al.*, 1987), the Caroebe Granite samples plot partially on the OGT field, showing types with higher Zr+Nb+Ce+Y (*e.g.* MA-178B, diorite). The Igarapé Azul granites plot out of OGT and FG fields (except the MA-88, muscovite-bearing syenogranite), exhibiting subtle higher FeO*/MgO ratios and enrichment in

Zr+Nb+Ce+Y. On the Rb vs. Y+Nb diagram (**Fig. 5d**, Pearce *et al.*, 1984) almost all Caroebe, Igarapé Azul and Jatapu samples plot in the VAG field, suggesting chemical affinity with volcanic arc magmatism. However, local magmatic differentiation and hydrothermal processes (Pearce *et al.*, 1984) could explain the crossing of VAG and syn-COLG (MF-10B) and WPG (MA-88) boundaries by some samples of Igarapé Azul Granite. The same is not true for the samples of Caroebe Granite. This one cross over the VAG and WPG boundary, because the more Y-rich samples are not the most differentiated types (*e.g.* MA-178B, diorite). The probable explanation in this case could be related to the source composition and/or anomalous enrichment in accessory minerals (*e.g.* allanite inclusions in hornblende and biotite crystals).

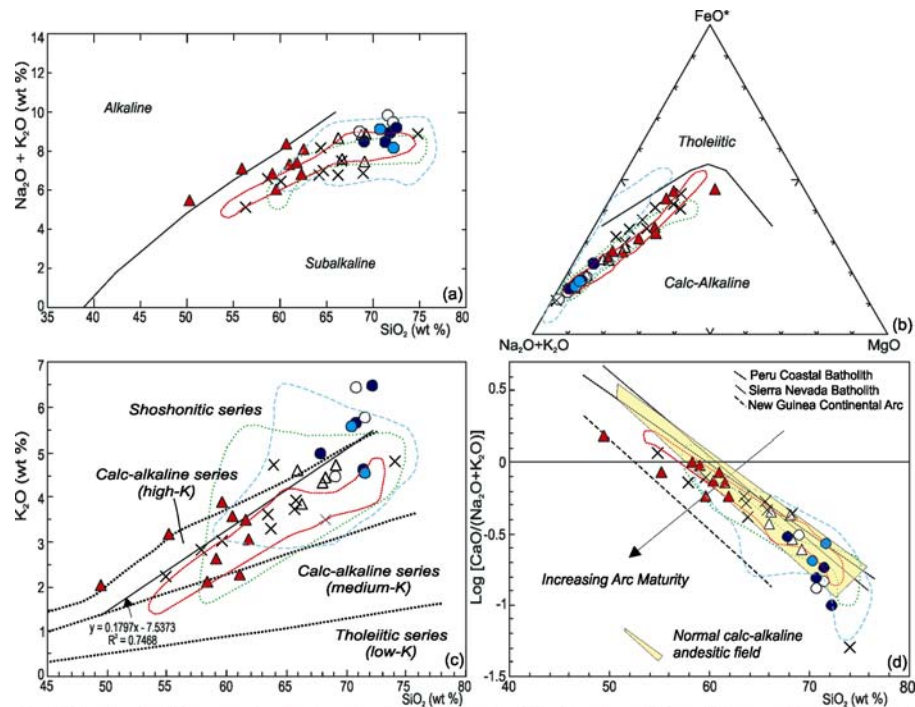


Fig. 4. Geochemical diagrams showing the calc-alkaline character of the Caroebe and Igarapé Azul granites (and coeval Jatapu volcanic rocks): (a) $\text{Na}_2\text{O} + \text{K}_2\text{O}$ vs. SiO_2 (for the linear regression are used only the Caroebe and Igarapé Azul granite samples) and (b) AFM diagrams (Irvine and Baragar, 1971); (c) K_2O vs. SiO_2 plot displaying the shoshonite, high-K, medium-K and low-K fields (from Peccerillo and Taylor, 1976 mod. by Rickwood, 1989); and (d) $\log [\text{CaO}/(\text{Na}_2\text{O} + \text{K}_2\text{O})]$ vs. SiO_2 (from Brown *et al.*, 1984). Compositional fields of Tropas, Parauari, Young São Jorge (Tapajós Domain) and and Água Branca related granitoids are also plotted for comparison. References and symbols as in Fig. 3.

In this sense, the trace elements in the Caroebe and Igarapé Azul granites are considerably more scattered than major elements, particularly for Ba, Sr, Zr and Nb Harker diagrams (**Fig. 6b-e**). However, Rb plots a positive correlation with increasing SiO_2 contents (**Fig. 6a**). Contrasting with this scattered pattern, the Jatapu volcanic rocks exhibit a linear trend in almost all these diagrams. The volcanic rocks show Sr in negative linear trend and Nb, Zr, Ba and Rb in positive correlation with increasing SiO_2 contents (**Fig. 6a-e**). The $\text{Mg}\#$ deeply decreases with the SiO_2 increasing (**Fig. 6f**). The Jaburuzinho facies exhibits the highest values (37.5-46.8, only one

sample with 51.5) comparatively to the Alto Alegre facies (34.1-43.0) and Igarapé Azul (21.5-37.8) granitoids.

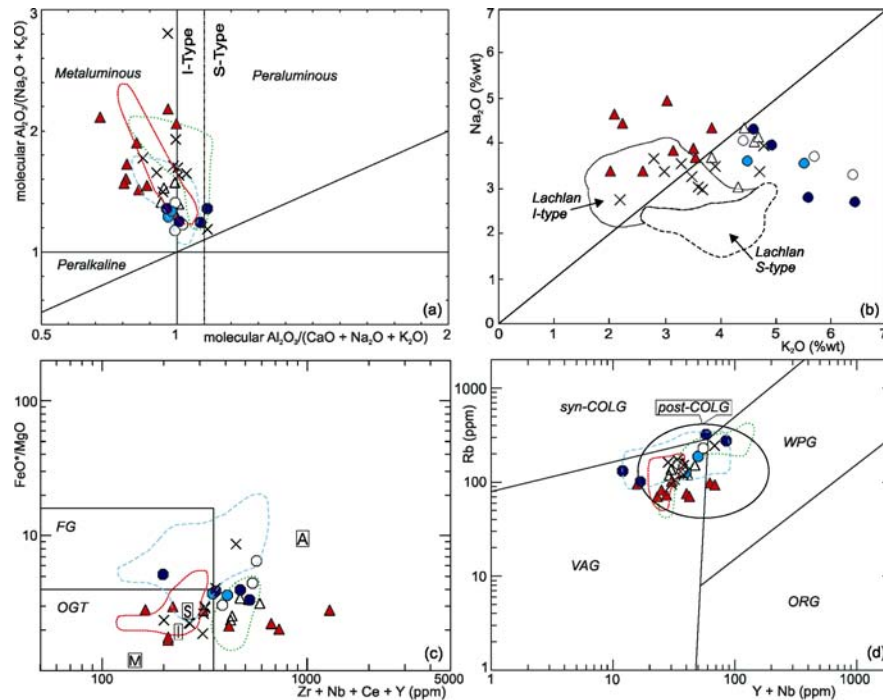


Fig. 5. Caroebe and Igarapé Azul granites and, coeval Jatapu volcanic rocks samples plotted in the diagrams (for references see table 1): (a) Molecular $Al_2O_3/(Na_2O+K_2O)$ vs. molecular $Al_2O_3/(CaO+Na_2O+K_2O)$ (Maniar and Piccoli, 1989; mod. Shand, 1927) and (b) Na_2O vs. K_2O plots showing S-type and I-type granites compositional data from Lachlan Folded Belt (LFB); (c) Rb vs. $(Y+Nb)$ and (d) $(K_2O+Na_2O)/CaO$ vs. $(Zr+Nb+Ce+Y)$. Fields representing Tropas, Parauari, Young São Jorge (Tapajós Domain) and Água Branca related granitoids are plotted for comparison. In (c), VAG (Volcanic Arc Granites), ORG (Ocean Ridge Granites), syn-COLG (Syn-collisional Granites) and WPG (Within-Plate Granites) fields are from Pearce *et al.* (1984) and post-COLG (post-collisional granites) from Pearce (1996); In (d), OGT (Orogenic granite types: unfractionated I- and S-type granites) and FG (Fractionated felsic I- and S-type granites) fields are taken from Whalen *et al.* (1987). Compositional average of A-, M-, I-, S- and I-type are also represented. References and symbols as in Fig. 3.

The primitive mantle-normalized spidergrams of the Caroebe and Igarapé Azul granites show discrete differences (**Fig. 7a-d**). The Jaburuzinho facies exhibits wider range contents and moderate enrichment in some large-ion lithophile elements (LILE), such as Ba (50-400x), Th (50-150x) and U (25-120x), contrasting with low Rb (70-100x) and K (60-100x) contents (**Fig. 7a**). This facies is also characterized by negative anomalies for high field strength elements (HFSE: *e.g.* Nb, Ta and Ti). The Alto Alegre facies shows spidergram patterns with narrow range (**Fig. 7b**) and, in general, exhibits similar patterns of Jaburuzinho facies, except for a more enrichment in Rb (100-200x) and K (110-120x), and for the moderately negative anomaly of P (7-15x) and Ti (0.4-3x).

The Saramadaia and Cinco Estelas facies of Igarapé Azul Granite (**Fig. 7c**) exhibit stronger Sr (3-30x), P (3-10x), Ti (1.5-2x) negative anomalies in the spidergrams. In contrast, they are more enriched in Rb (150-300x) and Th (150-550x) and show less pronounced Nb (20-35x) and Ta (20-45x) negative anomalies. The Vila Catarina facies (**Fig. 7d**) presents the most

heterogeneous spidergram patterns. For example, the samples range from low to high Nb, La, P, Sm and Tb contents.

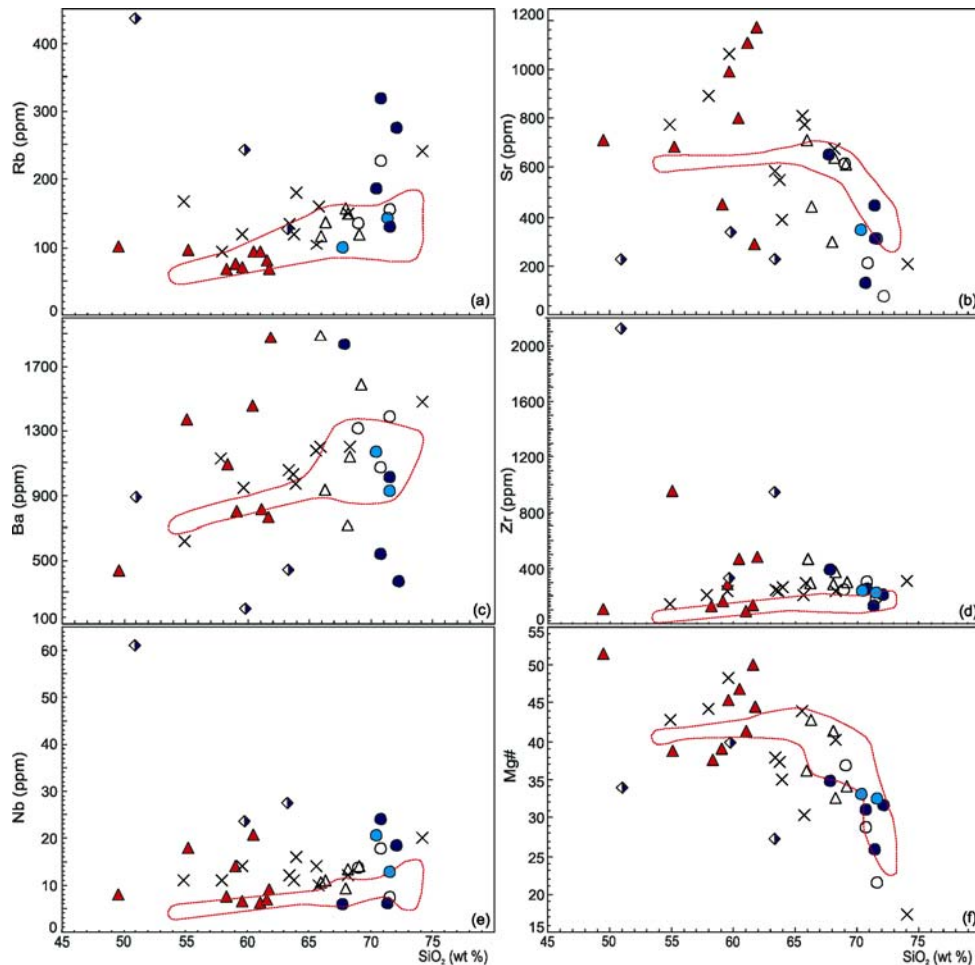


Fig. 6. (a-f) Selected Harker variation diagrams of trace elements and Mg# for the Caroebe and Igarapé Azul granites, including coeval Jatapu volcanics. Obs: $Mg\# = [100 \times \text{molar MgO} / (\text{MgO} + 0.9\text{FeO}_w)]$. Symbols as in Fig. 3.

Similarly to the Caroebe granites, the Jatapu volcanic rocks present spidergram patterns (**Fig. 7e**) with low to moderate enrichment in Rb, Ba, K, Zr and Y and less pronounced Nb, Sr and P negative anomalies, except for the MF-144B sample. The spidergrams of Caroebe types and Jatapu volcanics (**Fig. 7a-b, e**) are also chemical compatible with the granitoids from primitive to normal continental arcs (Brown *et al.*, 1984), showing locally HFSE enrichment (*e.g.* Nd, P, Hf, Zr and Sm). The more heterogeneous patterns make the Igarapé Azul spidergrams have a transitional behavior from normal (*e.g.* Rb, K, Th, U, Nb and Ta) to mature (*e.g.* Ba, Sr, P, Hf) arc granitoids (**Fig. 7c-d**).

Contemporaneous calc-alkaline granitoids from other areas of SUAD (*e.g.* NE of Amazonas, Presidente Figueiredo region) and from Tapajós Domain (Tropas and Parauari granitoids) has showed chemical similarities mainly with the Caroebe Granite. The granitoids of

Presidente Figueiredo (Valério, 2006) and Tropas (Santos *et al.*, 2004) regions yielded Ti, Al, Fe, Mg, Ca (**Fig. 3a-e**) and spidergram envelope (**Fig. 7f**) similar to the Caroebe Granite, including locally lower values of P (**Fig. 3h**) and $\text{Na}_2\text{O}+\text{K}_2\text{O}$ (**Fig. 4a**). Contrasting pattern is observed in the Parauari granitoids (Vasquez *et al.*, 2002), that shows higher Ti and Fe, and lower contents of Al, Mg, Ca and P.

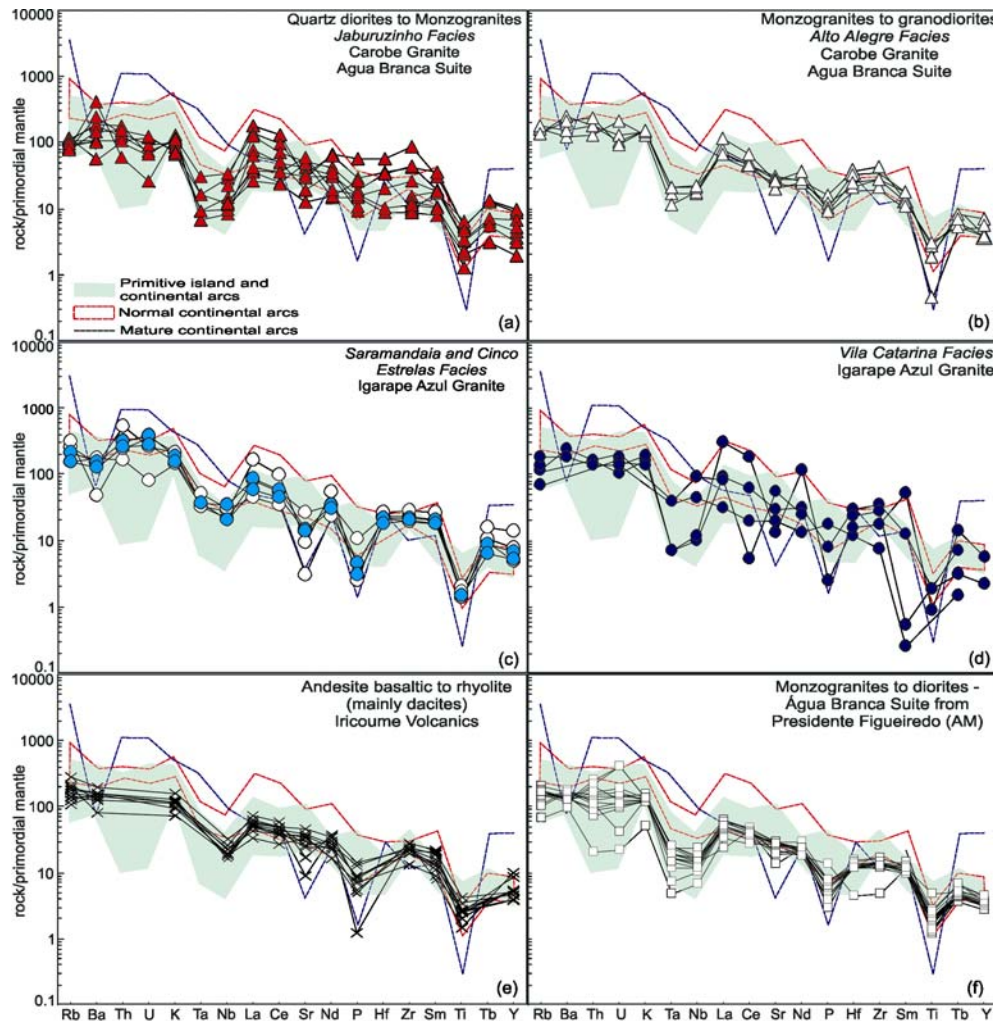


Fig. 7. Primitive mantle-normalized spidergrams (Wood *et al.*, 1979) from *Caroebe Granite*: (a) Jaburuzinho and (b) Alto Alegre facies, *Igarapé Azul Granite*: (c) Saramandaia and Cinco Estrelas facies; (d) Vila Catarina facies; and (e) coeval Jatapu volcanic rocks. References and symbols as in Fig. 3.

Rare-earth element (REE) geochemistry

The chondrite-normalized (Boynnton, 1984) REE patterns are plotted in **Fig. 8** and all analyzed samples show fractionation between the light (LREE) and heavy (HREE) rare-earth elements. Similarly to the spidergrams, the Jaburuzinho facies of Caroebe Granite is characterized by wide range of REE contents, reflecting its broad compositional spectrum, but the degree of REE fractionation is the same of Alto Alegre facies (**Fig. 8a-b**). Both granitic facies

demonstrate strong to moderate REE fractionation $[(La/Yb)_n = 11.26-29.32]$, nearly flattened HREE pattern $[(Gd/Yb)_n = 1.52-2.26]$ and low to moderate Eu negative anomalies ($Eu/Eu^* = 0.60-0.78$).

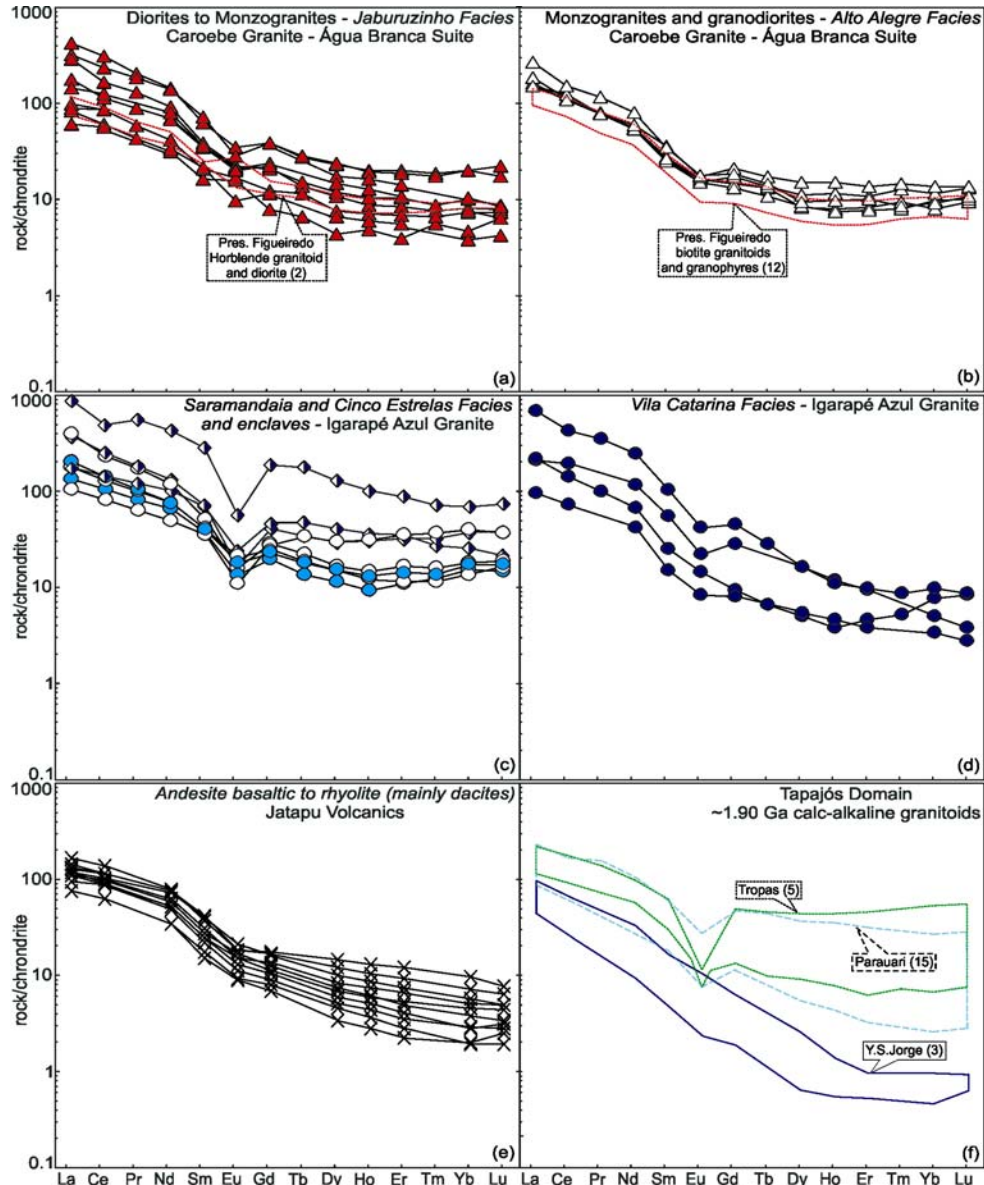


Fig. 8. REE chondrite-normalized diagrams (Boynton *et al.*, 1984) from (a) Jaburuzinho and (b) Alto Alegre facies (Caroebe Granite); (c) Saramandaia and Cinco Estrelas facies and (d) Vila Catarina facies (Igarapé Azul Granite); (e) Jatapu volcanic rocks and (f) REE-pattern envelope of Tropas, Parauari and Younger São Jorge granites. References and symbols as in Fig. 3.

Sometimes, the middle REE (MREE) are depleted relative to HREE, inducing a mildly concave-upwards in HREE patterns (**Fig. 8a-b**), mainly in the Jaburuzinho facies (MA-103, MF-068A and MJ-061B samples). Furthermore, the Jaburuzinho facies also exhibit REE patterns (**Fig. 8a**) with no anomalies (MA-053C) to positive Eu anomalies (MA-053B).

All petrographic facies of Igarapé Azul also exhibit moderate to discrete negative Eu

anomalies ($\text{Eu}/\text{Eu}^* = 0.48\text{-}0.86$), locally strong ($\text{Eu}/\text{Eu}^* = 0.36\text{-}0.39$). Mildly concave-upward HREE pattern [$(\text{Gd}/\text{Yb})_n = 1.27\text{-}1.81$] and moderate fractionated patterns [$(\text{La}/\text{Yb})_n = 8.69\text{-}21.94$] are observed in the Saramandaia and Cinco Estrelas facies (**Fig. 8c**). Only one sample (MA-88) exhibit flatted HREE and wing-bird pattern (strong LREE depleted), but no amphibole occurrence is described for these granites. In contrast, the REE patterns of Vila Catarina facies (**Fig. 8d**) are highly fractionated [$(\text{La}/\text{Yb})_n = 27.05\text{-}40.65$], although the sample MA-02 also shows concave-upward HREE pattern. In general sense, chemical changes caused by post-magmatic processes (hydrothermal alteration) could be at least partially affected the REE system, generating heterogeneous patterns in the Igarapé Azul Granite.

The Jatapu volcanic rocks (**Fig. 8e**) are characterized by REE patterns similar to those for Caroebe granitoids, such as negative Eu anomaly ($\text{Eu}/\text{Eu}^* = 0.62\text{-}0.83$) and REE total contents, but the formers are slightly most REE fractionated [$(\text{La}/\text{Yb})_n = 22.63\text{-}60.09$], mainly in HREE [$(\text{Gd}/\text{Yb})_n = 2.45\text{-}4.20$].

The contemporaneous calc-alkaline granitoids suites from Tapajós Domain and NE of Amazonas taken for comparison exhibit wide range of REE total contents, moderate REE fractionation, discrete (Parauari) to strong (Tropas) negative Eu anomalies and flat (Tropas) to fractionated (Parauari) HREE patterns (**Fig. 8f**). Further the major and trace elements geochemistry similarities, the Tropas and mainly the Água Branca granitoids from Presidente Figueiredo region shows several REE patterns similarities with the Caroebe granites (**Fig. 8a-b, f**). Such as the Jaburuzinho facies (Caroebe Granite), the Água Branca type from Presidente Figueiredo show also sample (“hornblende facies”) with positive Eu anomaly and similar total range of ETR. However, despite of similarities with the REE-pattern of Alto Alegre facies (Caroebe Granite), hornblende-free samples of Água Branca Suite in the Presidente Figueiredo show lower total contents of REE.

The Younger São Jorge Granite (Lamarão *et al.*, 2002) shows contrasting REE patterns (**Fig. 8f**) to those showed by Caroebe and Igarapé Azul granites (**Fig. 8a-d**). The former exhibits low REE contents, strong fractionated REE patterns, low HREE abundances, very discrete negative Eu anomaly, locally with no Eu anomaly (**Fig. 8f**). In addition to highly fractionated REE patterns, the Younger São Jorge Granite also shows low Y (10 to 11 ppm) and moderate to high Sr/Y ratios (25.5 to 122.7). These characteristics are shared by leucogranodiorites in the Cordillera Blanca Batholith (Andean-type, Cenozoic in age), which were generated by partial

melting of mafic rock in the stability field of garnet (Petford and Atherton, 1996).

PETROGENETIC CONSIDERATIONS

Two broad petrogenetic concepts are extensively evoked in the geological literature for explain the origin of calc-alkaline felsic magmas: 1) Derivation from basaltic parent magmas by fractional crystallization or AFC processes (*e.g.* Grove and Donnelly-Nolan, 1986; Bacon and Druitt, 1988); 2) Derivation from crustal rocks by partial melting (*e.g.* Bullen and Clynne, 1990; Roberts and Clemens, 1993; Tepper *et al.*, 1993; Guffanti *et al.*, 1996).

The first concept requires high volumes of mafic mantle-derived magmas for generate, by fractional crystallization, the extensive volume of rocks observed in southeastern Roraima and northwestern Amazonas states (up to 64000 km², see **Fig. 2**). In this region, rocks with basaltic composition are also scarce, identified locally in the Jatapu region (CPRM 2000a). Plutonic mafic counterparts are represented only by some diorites (SiO₂ 49.5%-55.1%) in the Caroebe Granite, which is dominated by granodiorites and monzogranites. More than 85% of Caroebe granitoids samples have up to 58% SiO₂ content (**Fig. 5, table 1**).

Furthermore, the fractional crystallization concept is normally associated to curvilinear trends in the Harker diagrams (*e.g.* El-Sayed *et al.*, 2002, 2004, Bakhit *et al.*, 2005) but, in contrast, all studied calc-alkaline granitoidsexhibit well-defined linear trends (**Fig. 3a-h**). The restite unmixing model of White and Chappell (1977) has been widely used to explain linear trends on variation diagrams for granite suites by variable separation of residuum from melt (*e.g.* Scambos *et al.*, 1986; Wyborn and Chappell, 1986; Chappell *et al.*, 1987; Barbero and Villaseca, 1992; Burnham, 1992; Barton and Sidle, 1994).

On the other hand, how widely the restite unmixing model can be applied, however, is highly controversial. For instance, Wall *et al.* (1987), Clemens (1989) and Bateman (1988) argue that, in many granite suites, linear variations are better explained by fractionation, accumulation and magma mixing, and restite unmixing will usually result in linear trends only if the restites are chemically homogeneous (Wall *et al.*, 1987), which is improbable given the large volumes of most granites and the likelihood of disequilibrium partial melting in the source (Barbero *et al.*, 1995).

The subtle compositional gap (4.10%) in SiO₂ observed in the Harker diagramsbetween Jaburuzinho (more mafic end-member) and Alto Alegre (more felsic end-member) facies of Caroebe Granite, associated to local field evidence (Almeida and Macambira submitted), could

suggest only subordinated participation of magma mixing/mingling process in the granites genesis. Thus, the fractional crystallization and mixing processes probably do not play important role in the Caroebe and Igarapé Azul granitogenesis and, partial melting could be dominantly process. In the most of chemical diagrams, the Igarapé Azul samples show good agreement with the Caroebe Granite, concerning linear trends. Furthermore, in several plots, the Alto Alegre facies and Igarapé Azul Granite samples exhibit commonly compositional overlap. Except for the Vila Catarina facies, there are similarities in the spidergrams and REE patterns. These features and the close spatial and temporal association (see zircon ages discussion below), suggest that Caroebe (and Jatapu volcanics) and Igarapé Azul granites can be linked to the same magmatic source by partial melting.

For the Caroebe Granite and Jatapu volcanics some chemical features suggest that amphibole (local MREE depletion in relation to HREE) and titanite (*e.g.* negative Ti anomalies) played a dominant role during the magma segregation. In contrast, the relative higher abundances of Sr and local positive Eu anomaly point out for a smaller amount of plagioclase in their residues. The petrographic facies of Igarapé Azul shows negative Eu anomalies that support the plagioclase restrict presence in the residue of melting. Concave-upward HREE pattern is observed in the Saramandaia and Cinco Estrelas facies of Igarapé Azul granite, with only one sample exhibiting flattened HREE and wing-bird pattern (strong LREE depleted), but no amphibole occurrence is described in these granites. In contrast, the REE patterns of Vila Catarina facies (Igarapé Azul) are highly fractionated; suggesting participation of residual garnet (?) during the role of magma segregation, but also no garnet is described in these rocks. The sample MA-02 shows concave-upward HREE pattern, suggesting possibly titanite and/or amphibole (Hoskin *et al.*, 2000) like residual phases, however titanite is very scarce and amphibole is not present in this facies.

In the Igarapé Azul Granite, chemical exchanges caused by post-magmatic processes (hydrothermal alteration) could be at least partially disturbed the REE system, generating heterogeneous patterns. The local high K/Ba (310-413) and low K/Rb (23-35) ratios observed in the Igarapé Azul types also suggest that this granite was affected by hydrothermal alteration, supporting the observed field and petrographic relationships (Almeida and Macambira submitted).

However, the magmatic evolution of these granites (mainly Igarapé Azul type) seems more

complex, suggesting that other parameters, such as a source of different composition, variable melting conditions and crustal contamination (*e.g.*, Zorpi *et al.*, 1989, 1991; Patiño-Douce, 1996, 1999; Petford *et al.*, 1996; Poli *et al.*, 1996), could be involved in their genesis. For example, the three different petrographic facies of Igarapé Azul Granite provided two main REE patterns and, in general, their chemical patterns are not so homogeneous in comparison with the Caroebe types.

Tepper *et al.* (1993) and Jonasson (1994) argue, for example, that a variety of granitoid and rhyolite can be generated by partial melting under different H₂O contents of lower crustal metabasalts. Based on experimental data, Roberts and Clemens (1989) stated that I-type and high-K calc-alkaline granitoid magmas can be generated from hydrous, calc-alkaline mafic to intermediate sources in the crust by partial melting. Several others experimental constrains are available (*e.g.* Patiño-Douce, 1996, 1999, and references therein), yielding compositional differences of magmas produced by partial melting of common crustal rocks, such as amphibolites, tonalitic gneisses, metagreywackes and metapelites under variable melting conditions. This compositional variation can be visualized in terms of major oxides ratios and molar oxide ratios in figures **9a-c** and **9d**, respectively.

Some these experimental results (*e.g.* Patiño-Douce, 1999) reveal that melts obtained from partial melting of three important crustal sources: felsic pelites, metagreywackes and amphibolites, including metabasalts and metatonalites. For example, in these plots, partial melts derived from mafic to intermediate rocks have lower $Al_2O_3/(FeO+MgO+TiO_2)$, $(Na_2O+K_2O)/(FeO+MgO+TiO_2)$ and molar $Al_2O_3/(MgO+FeO_{tot})$ ratios than those originated from metapelites and metagreywackes (**Fig 9a-d**).

The Caroebe Granite and Jatapu volcanic samples plot generally on the amphibolite and metabasalt-metatonalite fields, showing low $Al_2O_3/(FeO+MgO+TiO_2)$, $(Na_2O+K_2O)/(FeO+MgO+TiO_2)$ and molar $Al_2O_3/(MgO+FeO_{tot})$ ratios, but exhibit relatively higher $CaO/(FeO+MgO+TiO_2)$ ratios. This feature, associated with relatively high Mg# values (37.5-51.4), precludes a derivation by felsic pelite or metagreywacke for Caroebe granitoids, mainly the Jaburuzinho types. Only two samples of Jaburuzinho facies have higher $Al_2O_3/(FeO+MgO+TiO_2)$ ratios (MA-053B and C) and few mafic members of Caroebe Granite present low-silica (<58%) and dioritic composition. Regardless of the degree of partial melting, such dioritic melts are generally characterized by Mg# < 44 and Na₂O >4.3% and derived by dehydration melting of metabasaltic sources in excess of ca. 1100° C (Wolf and Wyllie, 1994,

Rapp, 1995, Rapp and Watson, 1995, and references therein). However, the unfractionated HREE patterns and moderate to high Sr/Y showed by Caroebe diorites preclude the involvement of substantial amounts of residual garnet and that the melting temperatures could have been lower.

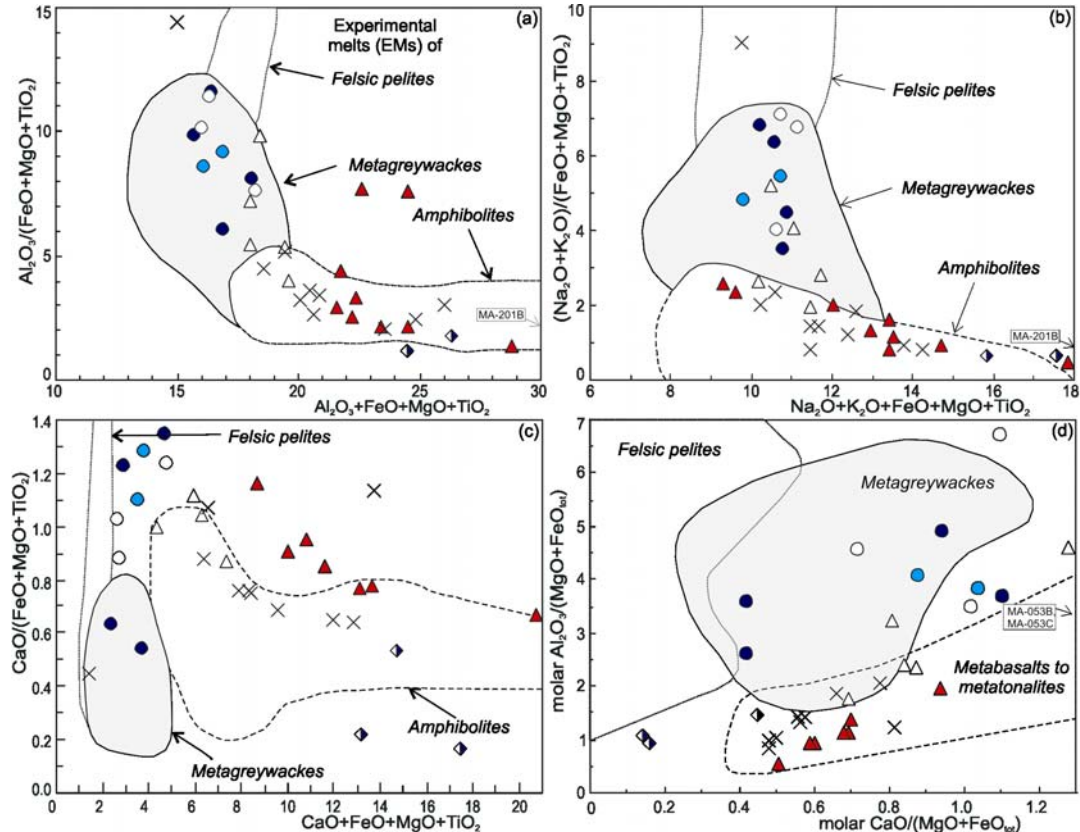


Fig. 9. Caroebe and Igarape Azul granites (and coeval volcanic rocks) samples plotted on the (a) $\text{Al}_2\text{O}_3/(\text{FeO}+\text{MgO}+\text{TiO}_2)$ vs. $\text{Al}_2\text{O}_3+\text{FeO}+\text{MgO}+\text{TiO}_2$, (b) $(\text{Na}_2\text{O}+\text{K}_2\text{O})/(\text{FeO}+\text{MgO}+\text{TiO}_2)$ vs. $\text{Na}_2\text{O}+\text{K}_2\text{O}+\text{FeO}+\text{MgO}+\text{TiO}_2$, (c) $\text{CaO}/(\text{FeO}+\text{MgO}+\text{TiO}_2)$ vs. $\text{CaO}+\text{FeO}+\text{MgO}+\text{TiO}_2$ and (d) molar $\text{Al}_2\text{O}_3/(\text{MgO}+\text{FeO}_{\text{wt}})$ vs. molar $\text{CaO}/(\text{MgO}+\text{FeO}_{\text{wt}})$ diagrams. Outlined fields denote compositions of partial melts obtained in experimental studies by dehydration melting of felsic pelites, metagreywackes, amphibolites-metabasalts and metatonalites sources (Wolf and Wyllie, 1994; Patino-Douce, 1996, 1999; Patiño-Douce and Beard, 1996; Singh and Johannes, 1996; Thompson, 1996, and references therein). Symbols as in fig. 03. See text for discussion.

The Alto Alegre facies (Caroebe Granite) show some samples plotting out of amphibolite and metabasalt-metatonalite fields, overlapping locally the Igarapé Azul Granite compositions. The Igarapé Azul Granite plots preferentially on the metagreywacke field (**Fig. 9a-d**), however, the samples distribution is sometimes scattered, implying a local heterogeneous geochemical pattern (**Fig. 9d**) and higher $\text{CaO}/(\text{FeO}+\text{MgO}+\text{TiO}_2)$ ratios. These granitoids exhibit also normally restricted range and moderate to very low contents of $\text{Al}_2\text{O}_3+\text{FeO}+\text{MgO}+\text{TiO}_2$, $\text{Na}_2\text{O}+\text{K}_2\text{O}+\text{FeO}+\text{MgO}+\text{TiO}_2$ and $\text{CaO}+\text{FeO}+\text{MgO}+\text{TiO}_2$ (**Fig. 9a-c**). This geochemical pattern suggests that the input of metagreywacke source play important role in the Igarapé Azul Granite genesis, reflecting probably the compositional heterogeneity in the metasedimentary source and

post-magmatic alterations. The Uai-Uai and Cauarane metavolcanosedimentary sequences, which crops out in the Southeastern Roraima, represent the most suitable sources. Further, metagraywackes with igneous parentage are also reported by CPRM (2000a) in the Cauarane Group, suggesting an original heterogeneity in these sources. Records of probable restites (surmicaceous enclaves?) in the Igarapé Azul granitoids are represented by (muscovite)-biotite-rich gneissic enclaves (Almeida and Macambira submitted).

In these sense, combining these features with REE patterns, at least two origins can be pointed out for the Igarapé Azul granitoids: a) similar REE patterns to those of Caroebe granitoids, showing low to moderate fractionated REE, flat HREE and low negative Eu anomalies, which could be linked with amphibolite sources, and further input of metagreywacke sources (Saramandaia and Vila Catarina facies); b) most fractionated total REE and HREE, with local high negative Eu anomaly, suggesting retention of residual garnet in the source (higher input of melts from metagreywacke sources), although no garnet was observed in the petrographic studies (Vila Catarina facies).

Thus, the original melt of Igarapé Azul granitoids was probably generated by partial melting of amphibolite and metasedimentary sources in different and unknown proportions, representing the most affected Caroebe member by the metasedimentary sources. This hypothesis is in agreement with the hybrid origin proposed by Sardinha (1999, 2001) for the Igarapé Azul granites. The final product of Igarapé Azul melt was also affected by important hydrothermal activity in the final stages of crystallization, according with the field (pegmatite abundance), petrographic (epidote, sericite, minor carbonate secondary minerals) and chemical (K/Rb and Ba/Rb ratios) relationships. In addition, assimilation of host metagranitoids of Martins Pereira is suggested for the Igarapé Azul genesis, in agreement with the evidence of host-rock xenoliths (Almeida and Macambira submitted) and several 1.97-1.96 Ga inherited zircon age records (see zircon ages discussion below).

The plots with experimental melts data suggest that the origin of Caroebe granitoids (and Jatapu volcanics) involves partial melting of amphibolite source under water-rich conditions, with low input of melt from metagreywacke source, in this last case represented by some samples of Alto Alegre facies. As well as the Igarapé Azul granitoids, the 1.96-1.97 Ga inherited zircon yielded by Alto Alegre facies (see below) also implies local possibly of assimilation of host Martins Pereira metagranitoids.

The origin of high-K, calc-alkaline I-type granites generated by partial melting of metagreywacke-sources (reflecting sometimes largely your igneous parentage) are also supported by Barker *et al.* (1992), Altherr *et al.* (2000) and Thuy Nguyen *et al.* (2004) in the Alaska, Germany and Vietnam granitoids, respectively.

ZIRCON GEOCHRONOLOGY RESULTS (Pb-EVAPORATION AND U-Pb ID-TIMS)

A total of 4 samples of Caroebe and Igarapé Azul granitoids were selected for dating, including a biotite-rich enclave. Thus, Jatapu andesite, Água Branca Granite (type area), Murauaú Granite and Santa Maria hypersthene tonalite samples were analyzed.

Caroebe (MA-121 and 053A samples) and Água Branca Granitoids (HM-181 sample)

Two samples of Caroebe Granite (MA-121: Jaburuzinho facies; MA-053A: Alto Alegre facies), correlated to the Água Branca granitic magmatism, were analyzed by the single-zircon Pb-evaporation technique. One sample from Agua Branca granitoid (HM-181) of type-area was also dated for comparison. The samples location and summary of petrographic description are available, respectively, in the **Fig. 2** and **table 2**. The Pb isotopic data are showed in **table 3**.

The zircon crystals of HM-181 sample are brown, with well-defined faces, locally with rounded vertices, showing inclusions in the cores and some cracks on the borders. They are transparent to translucent, exhibiting 120-310 μm in long and length/width 3.1:1 to 1.6:1 ratios. Four crystals yielded individual ages varying from 1905 Ma to 1885 Ma (Th/U: 0.50-0.80), resulting a mean age of 1901 ± 5 Ma and USD: 1.2 (**table 3; Fig. 10a**). Another one revealed to be an inherited zircon with an age of 2142 ± 10 Ma yielded for just one isotopic block of 8 isotopic ratios (Th/U: 0.65).

The crystallization age obtained in hornblende-biotite granodiorite sample (HM-181) from Água Branca Suite (**table 2**) was similar to that of Jaburuzinho facies of the Caroebe Granite (sample MA-121). Zircon crystals from hornblende-biotite quartz monzodiorite sample (MA-121) of Jaburuzinho facies (Caroebe Granite, **table 2**) has typical magmatic origin (Th/U: 0.49-0.64, see **table 3**), showing euhedral elongated prismatic shapes and parallel oscillatory zoning. The crystals are pale yellow to pale brown, transparent, but locally few crystals are turbid and have inclusions (apatite and Fe-Ti oxide minerals) in the core domains. Fractures are scarce. They are 140-290 μm long and length/width ratios are between 3.3:1 and 2.1:1. A total of 6 crystals were analyzed yielding individual ages varying from 1905 Ma to 1888 Ma, and a mean

age of 1895 ± 3 Ma and USD: 2.1 (**table 3; Fig. 10b**).

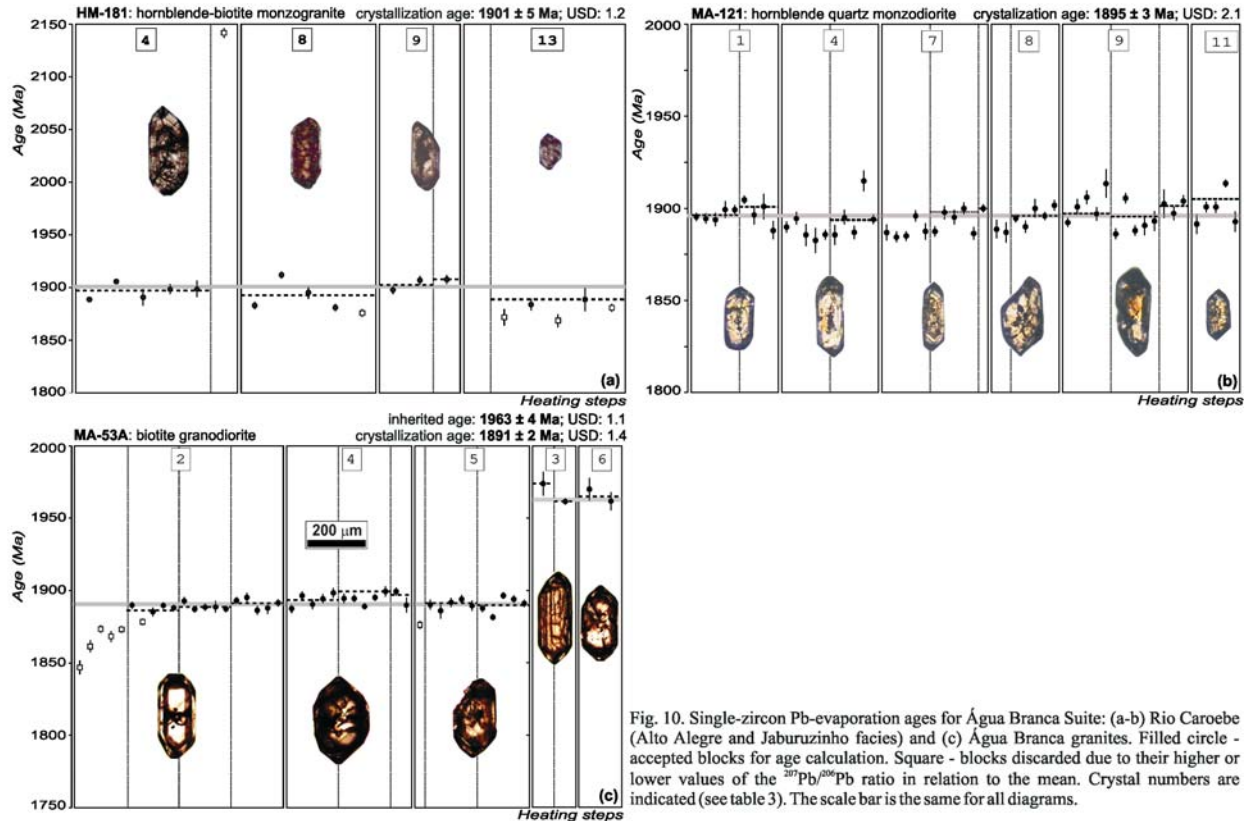


Fig. 10. Single-zircon Pb-evaporation ages for Água Branca Suite: (a-b) Rio Caroebe (Alto Alegre and Jaburuzinho facies) and (c) Água Branca granites. Filled circle - accepted blocks for age calculation. Square - blocks discarded due to their higher or lower values of the $^{207}\text{Pb}/^{206}\text{Pb}$ ratio in relation to the mean. Crystal numbers are indicated (see table 3). The scale bar is the same for all diagrams.

The crystals from the biotite granodiorite sample (MA-053A) of Alto Alegre facies (Caroebe Granite, **table 2**) are brown to pale brown, with well-defined faces and slightly rounded vertices, with few inclusions and scarce cracks. They are transparent to translucent, showing 100-320 μm in long and length/width ratios between 3.2:1 and 1.3:1. The individual ages from 3 zircon crystals are between 1905 Ma and 1885 Ma (Th/U: 0.51-0.85), defining a mean age of 1891 ± 2 Ma and USD: 1.4 (**table 3; Fig. 10c**), which is slightly lower than the ages of two samples previously presented. Inherited zircon ages are recorded in 2 crystals, yielding a mean age of 1963 ± 4 Ma (**table 3, Fig. 10c**). Despite of different ages and locally lower Th/U (0.16-0.17) in the inherited zircon crystals, they show similar optical features in comparison with the other analyzed ones.

Igarapé Azul Granitoids (MA-147A and 186A samples) and Biotite-bearing Enclave (MA-201b sample)

Two samples of Igarapé Azul Granite (MA-147A: Cinco Estrelas facies; MA-186A: Saramandaia facies) and one biotite-bearing quartz diorite (MA-210B: enclave) were analyzed by

the single-zircon Pb-evaporation technique. One sample of Igarapé Azul Granite was also selected for U-Pb TIMS analysis. (See **Fig.2** and **tables 2** and **3**).

Zircon crystals from fine-grained leucocratic monzogranite sample (MA-147A) of Cinco Estrelas facies (**fig. 2, table 2**) show euhedral prismatic shapes, locally with bypyramidal edges, exhibiting 270-360 μm in long and length/width ratios between 2.8:1 and 1.3:1. Some crystals display oscillatory zoning, parallel to external faces. They are pale brown to brown, transparent but, locally in few crystals, cracks and inclusions are common (apatite and Fe-Ti oxide minerals). A total of 6 crystals were analyzed yielding individual ages varying from 1902 Ma to 1882 Ma (Th/U: 0.43-1.08), and a mean age of 1889 ± 5 Ma and USD: 3.0 (**table 3; Fig. 11a**). Only one zircon recorded higher age (1 isotopic block of 4 isotopic ratios) of 1964 ± 4 Ma (Th/U: 0.40).

The zircon crystals from the porphyritic monzogranite sample (MA-186A) of Saramandaia facies are brown, with well-defined faces, in general with rounded vertices, containing some inclusions in the cores and scarce cracks. They are transparent to translucent, prismatic to stubby, showing 90-350 μm in long and length/width ratios between 4.1:1 and 1.2:1. Three crystals from this sample (**fig. 2, table 2**) showed individual ages varying from 1897 Ma to 1887 Ma (Th/U: 0.55-0.68), resulting a mean age of 1889 ± 2 Ma and USD: 1.4 (**table 3; Fig. 11b**) which is in good agreement with the age yielded by the Cinco Estrelas facies sample. The Samandaia facies sample shows more evident inheritance record, exhibiting 2 inherited crystals that yielded a mean age of 1972 ± 3 Ma (Th/U:0.38-0.48).

One enclave sample (MA-201B, foliated biotite-bearing quartz diorite) was also selected for single zircon Pb-evaporation analysis (**fig. 2, table 2**). The zircon crystals of MA-201B are transparent to translucent and prismatic, showing 80-330 μm in long and length/width ratios between 4.1:1 and 1.9:1. They are also pale yellow to brown, showing locally inclusions in the cores and scarce cracks. This sample yielded 2 different mean ages. The first one was yielded for four crystals which individual ages varying from 1890 Ma to 1900 Ma (Th/U: 0.43-0.70), resulting in a mean age of 1891 ± 3 Ma and USD: 1.3 (**table 3; Fig. 11c**). This age is identical to those obtained in the host granitoids, yielded by zircon from the granitic veins that cross-cut the enclave. The second mean age was obtained from 2 crystals and is 1967 ± 6 Ma (Th/U: 0.27-0.61). It probably represents the protolith age of foliated enclave (**table 3; Fig. 11c**).

In function of the ambiguous results obtained in the sample MA-186A, more four zircon crystals were analyzed by the U-Pb ID-TIMS method. In spite of the grains had been abraded, the

analytical points are very discordant and the discordia line yielded a superior intercept at 1913 ± 4 Ma (**fig. 11d, table 4**). This comparatively higher U-Pb age (ca. 20 Ma) could be related to the small amounts of the inherited isotopic component (observed in the Pb-evaporation analysis), resulting in a discrete mixing age, or due to the interference of common Pb.

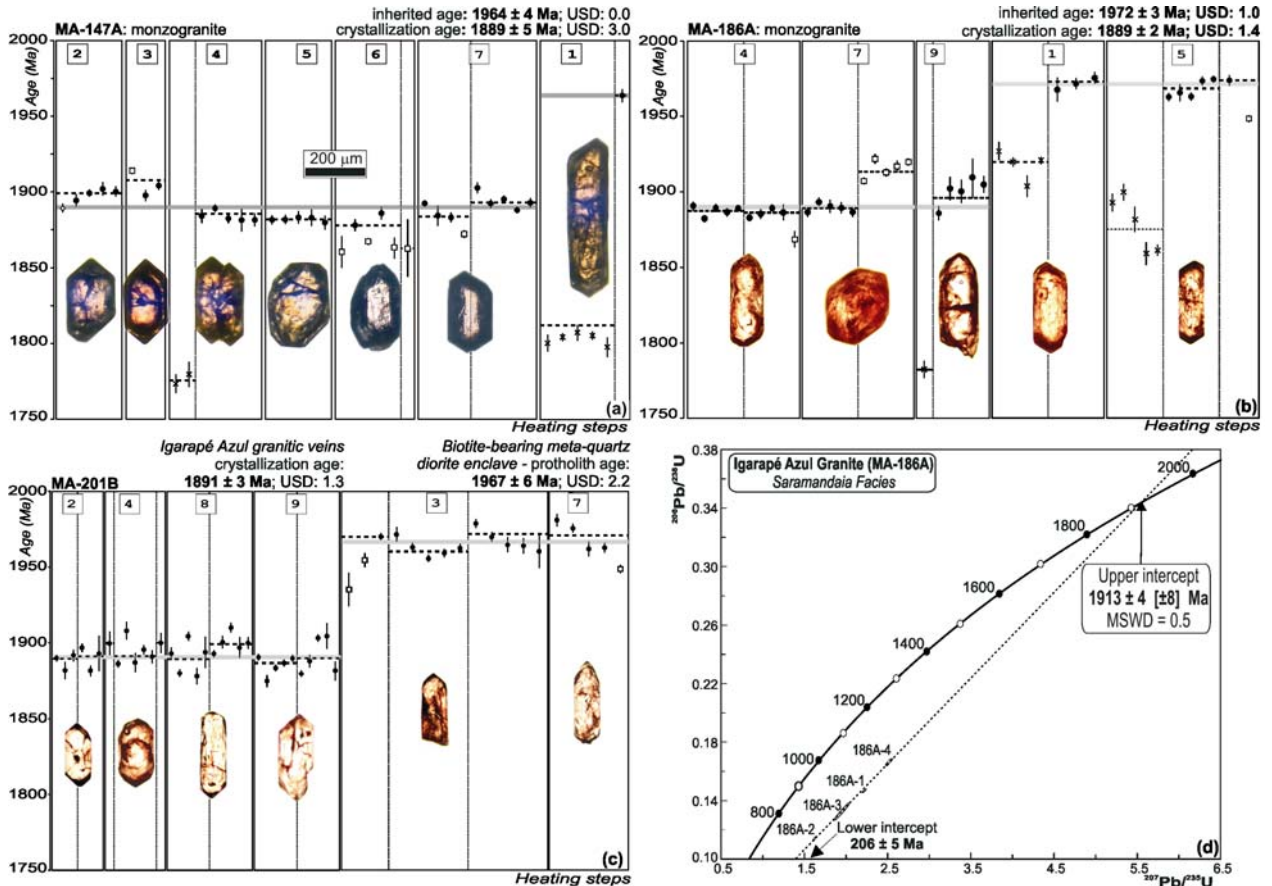


Fig. 11. Single-zircon Pb-evaporation ages (a-c) and U-Pb Concordia diagram (d) for Igarapé Azul Granite samples. Filled circle - accepted blocks for age calculation. Square - blocks discarded due to their higher or lower values of the $^{207}\text{Pb}/^{206}\text{Pb}$ ratio in relation to the mean. X - rejected blocks due to show $^{207}\text{Pb}/^{206}\text{Pb} > 0.0004$. Crystal numbers are indicated (see table 3). The scale bar is the same for all diagrams.

Jatapu Volcanics (MA-208 sample)

Zircon from andesite (MA-208) sampled in the Jatapu river region (**table 2**) shows euhedral bipyramidal crystals, locally with broken edges and/or rounded vertices. They are colorless, transparent and some crystals have inclusions, such as apatite and Fe-Ti oxide minerals, exhibiting 70-390 μm in long and length/width ratios between 3.7:1 and 2:1. The inherited crystals show also corroded and rounded borders and lower $^{208}\text{Pb}/^{206}\text{Pb}$ (< 0.15) and Th/U (0.15-0.57) ratios in comparison with the younger crystals ($^{208}\text{Pb}/^{206}\text{Pb} > 0.15$, Th/U: 0.43-0.98), reinforcing their distinct origin.

The zircon from the andesite was analyzed by the single-crystal Pb-evaporation technique,

yielding a mean age of 1893 ± 5 Ma and USD: 2.2 (**table 3; Fig. 12**) from four crystals with individual ages ranging from 1898 to 1886 Ma. This age is in good agreement with the results obtained in dacite porphyry of this same region also by single-zircon Pb-evaporation (1893 ± 2 Ma; Macambira *et al.*, 2002). But, in contrast, some zircons analyzed in the andesite sample have showed strong evidences of inherited age. For instance, others 4 crystals analyzed yielded individual ages varying from 1970 Ma to 1960 Ma, and a mean age of 1966 ± 3 Ma with a USD: 1.3 (**table 3; Fig. 12**).

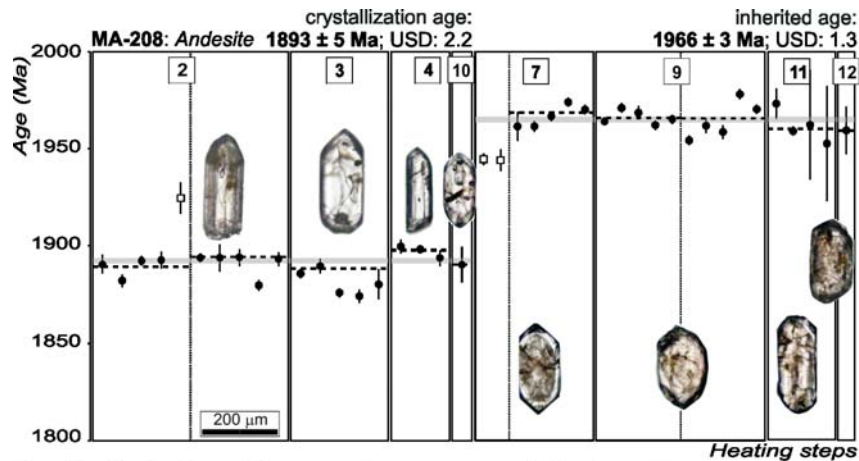


Fig. 12. Single-zircon Pb-evaporation ages for andesite from Jatapu region. Filled circle - accepted blocks for age calculation. Square - blocks discarded due to their higher or lower values of the $^{207}\text{Pb}/^{206}\text{Pb}$ ratio in relation to the mean. Crystal numbers are indicated (see table 3).

Santa Maria Enderbite (MA-198 sample)

The undeformed hypersthene tonalite sample (MA-198) from ENE-WSW elongated Santa Maria body (**Fig. 2** and **table 2**) was analyzed by the single-zircon Pb-evaporation technique. The sample exhibit prismatic to stubby crystals with 120-480 μm in long and length/width ratios between 2:1 and 1.3:1, generally showing brown colors (colorless and pale yellow crystal are rare), transparent to translucent and well-defined faces and vertices. They have also commonly apatite and opaque minerals inclusions, and scarce fractures.

A mean age of 1891 ± 1 Ma and USD: 1.2 (**table 3; Fig. 13**) was obtained from 6 individual crystals with homogeneous age range from 1894 to 1889 Ma (Th/U: 0.48-0.68, see **table 3**). This crystallization age fall down in the same age range of the others studied granitoids of SUAD (*e.g.* Caroebe and Igarapé Azul granites).

Murauaú Granite (Mapuera Suite, MA-226 sample)

A circular-like body of pale pink porphyry granite intrudes the Caroebe Granite in the

Murauaú river region (**table 2**), but the northern area of this granite was strongly deformed by dextral NE-trending brittle-ductile shear zones related to the Jauaperi Fault System (**Fig. 2**), obliterating the intrusion field relationships. The granite from deformed area was sampled (MA-226) for analysis with the objective of determines the crystallization age and the maximum age of the shear zone.

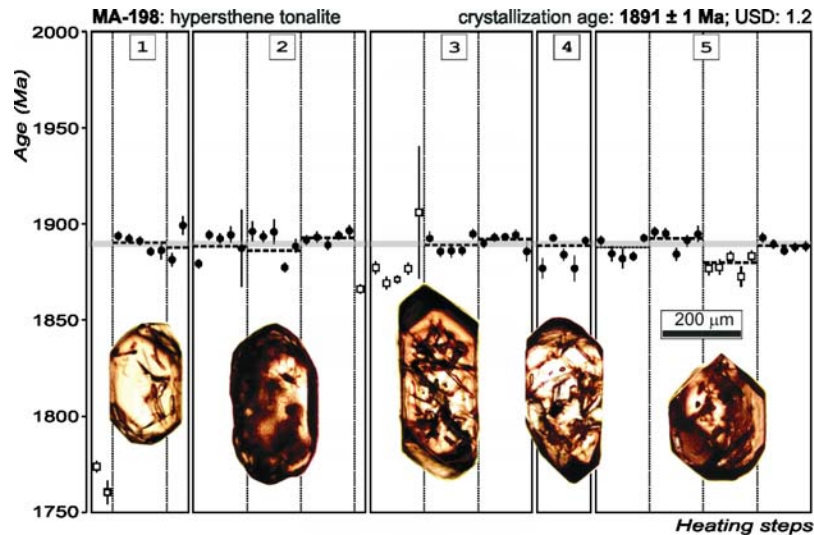


Fig. 13. Single-zircon Pb-evaporation ages for hypersthene tonalite (Santa Maria Enderbite). Filled circle - accepted blocks for age calculation. Square - blocks discarded due to their higher or lower values of the $^{207}\text{Pb}/^{206}\text{Pb}$ ratio in relation to the mean. Crystal numbers are indicated (see table 3).

Seven zircon crystals analyzed by single-zircon Pb-evaporation technique, yielding three main age patterns showing individual crystals ages ranging from 2366 to 1866 Ma (Th/U: 0.35-0.37, **table 3**). The younger population (two zircon crystals) resulted in a mean age of 1871 ± 5 Ma and USD: 2.6 (**table 3; Fig. 14**), interpreted as the crystallization age of Murauaú Granite (Th/U:0.35-0.44). This crystallization age is ~ 20 Ma lower in relation to the Caroebe and Água Branca granites (1901-1892 Ma), but fall down in the Mapuera granitoids interval age (1880-1860 Ma, see **table 5**).

Initially, based on the petrographic and field characteristics and mode of intrusion, the Murauaú Granite was tentatively correlated to the Mapuera magmatism (CPRM, 2000a, 2003). In addition, 2 other crystal populations yielded a higher mean age of 1888 ± 3 Ma with USD: 1.8 (Th/U:0.35-0.42) and 2359 ± 7 Ma with USD: 4.1 (Th/U:0.31-0.37), interpreted as inherited origin (**table 3**). No optical difference among these 3 populations of zircon was detected in the binocular microscopic. These crystals are prismatic, showing 110-250 μm (in long) and length/width ratios between 3.1:1 and 1.7:1. Generally, they are pale brown to colorless,

transparent to translucent, with well-defined faces and vertices. Apatite and opaque minerals inclusions and fractures are scarce.

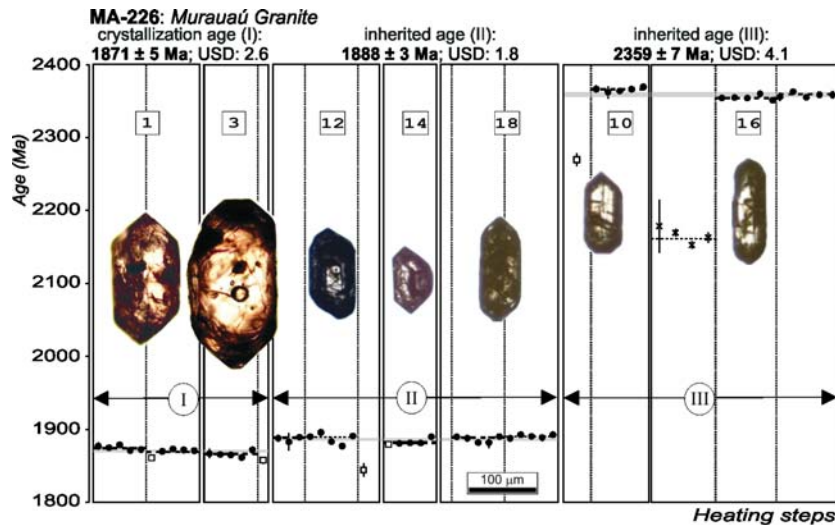


Fig. 14. Single-zircon Pb-evaporation ages for biotite sheared monzogranite (Murauá Granite, Mapuera Suite?). Filled circle - accepted blocks for age calculation. Square - blocks discarded due to their higher or lower values of the $^{207}\text{Pb}/^{206}\text{Pb}$ ratio in relation to the mean. X - rejected blocks due to show $^{204}\text{Pb}/^{206}\text{Pb} > 0.0004$. Crystal numbers are indicated (see table 3).

ZIRCON AGES AND GEOLOGICAL IMPLICATIONS

Zircon Geochronology constraints

Several authors have utilized field, petrographic and geochemical criteria (*e.g.* Costi *et al.*, 1984, Jorge-Joao *et al.*, 1985, Oliveira *et al.*, 1996, CPRM, 2000a, Almeida and Macambira, 2003) for correlate the undeformed hornblende-bearing granitoids of southeastern Roraima State (and northwestern of Pará State) to the Água Branca Granite (Araújo Neto and Moreira, 1976, Veiga Jr. *et al.*, 1979) in the northeastern Amazonas State (nearly 400 km far away to south).

Furthermore, the 1972 ± 7 Ma (U-Pb SHRIMP) to 1960 ± 21 Ma (Pb-evaporation) zircon ages (informar os desvios dessas idades) obtained by CPRM (2003) and Almeida *et al.* (1997) in the southeastern Roraima, were respectively misleading interpreted as “Igarapé Azul” and “Água Branca” ages. New geological mapping and preliminary geochronological data (Almeida *et al.*, 2002) pointed out that these ages were obtained from samples of Martins Pereira granitoids and not from the Água Branca and Igarapé Azul types. At this time, only two WR Rb-Sr isochronic ages were available for the Água Branca granitoids (and correlated rocks). These isochronic ages were taken by Santos and Reis Neto (1982) and Jorge-João *et al.* (1985), yielding respectively $1942 \text{ Ma} \pm 32 \text{ Ma}$ and $1910 \pm 23 \text{ Ma}$ ($\text{Sr}_i: 0.70225 \pm 0.00031$, MSWD: 1.26). The last one was

obtained in hornblende granitoids of northwestern of Pará State (**table 5, Fig. 15**).

More recently, the undeformed and ENE-trending elongated hornblende-bearing granitoid body, with 105 km² (Igarapé Dias quartz monzodiorite) and located on the southeastern Roraima, was dated by U-Pb SHRIMP on zircon (CPRM, 2003), yielding concordant analytical points with mean age of 1891 ± 6 Ma (**table 5, Fig. 15**). This one and Caroebe ages are in good agreement (within error limits) with the WR Rb-Sr isochronic age of 1910 ± 23 Ma.

In the present study, the Igarapé Dias quartz monzodiorite age (1891 Ma) is included in same interval age (1889-1901 Ma) of the Caroebe, Água Branca and Igarapé Azul granites, suggesting that all these granitoids of the southeastern Roraima could be correlated to the Água Branca magmatic event. The ages obtained by Valério (2006) in (hornblende)-biotite granitoids of the northeastern of Amazonas (1898-1890 Ma) are also very similar those of Caroebe and Água Branca granites (**table 5**). The same is true for the volcanic events. The zircon ages of the andesite (1893 ± 5 Ma, this paper) and dacite (1893 ± 2 Ma, Macambira *et al.*, 2002) from the Jatapu region are in agreement (within error limits) with the ages of volcanic samples of Iricoumé Group from the other regions (e.g. 1896 ± 7 Ma, CPRM, 2003) (see **table 5, Fig. 15**). However, in northeastern Amazonas some authors pointed out that the Iricoumé volcanics are coeval and cogenetic with Mapuera and Abonari granitoids, showing 1888 ± 3 Ma (Costi *et al.*, 2000) and 1883 ± 4 Ma (Valério *et al.*, 2005), including more acid composition (rhyolites) and alkaline chemical affinities. These data suggest at least two main volcano-plutonic event in the center-south Guyana Shield: a) I-type, calc-alkaline magmatism with 1901-1889 Ma interval age, enclosing Água Branca, Caroebe, Igarapé Azul granites and Jatapu volcanic rocks, and b) A-type, alkaline magmatism showing 1888-1871 Ma interval age, represented by Mapuera-Abonari granitoids and Iricoumé volcanic rocks.

Locally, charnockitic rocks also belong to this important volcano-plutonic event. Hypersthene tonalites, represented by the Santa Maria Enderbite exhibit similar age (1891 ± 1 Ma), suggesting more dry conditions and highest temperatures on the granites formation in the SUAD. The Santa Maria type (**table 5, Fig. 15**) shows higher age in comparison with the charnockitoids from the Jaburu river (1873 ± 6 Ma, zircon U-Pb ID-TIMS, Santos *et al.*, 2001a). In the Central Guyana Domain, two generation events of the charnockites are described: a) charnockites of Mucajai Suite (AMG association revisited by Fraga 2002) with 1564 ± 21 Ma (single-zircon Pb evaporation, Fraga *et al.*, 1997); and b) older and locally deformed charnockites

of Serra da Prata Suite (1934-1943 Ma, single-zircon Pb evaporation, Fraga, 2002). All these data pointed out for at least three charnockite generation events in the center-southern Roraima State: 1.94-1.93 Ga, 1.89-1.87 Ga (**table 5, Fig. 15**) and 1.54 Ga.

The Murauaú Granite (1871 ± 5 Ma) is correlated to the younger granites from Mapuera Suite, which belongs to the 1.87 Ga A-type magmatism event recognized in the southeastern Roraima, northeastern Amazonas and northwestern of Para states (**fig. 15, table 5**, Santos *et al.*, 2002; CPRM, 2003). This A-type event is related to the final stage of magmatic activity of the Água Branca-Iricoumé magmatism and delimits the start of the more crustal stability period of the UAD. However, the Murauaú and Mapuera types correlation must be regarded with care because key data to identifying the type and the origin these granites (*e.g.* isotopic-geochemical data) were not sufficiently available. The younger A-type ~ 1.81 Ga Moderna (Santos *et al.*, 1997a) and Madeira (*e.g.* Costi *et al.*, 2000) granitoids are also showed at the **fig. 15**.

All these geochronological data support that the granitoids and volcanic rocks of SUAD belongs to the same magmatic event, responsible for a widespread calc-alkaline 1.90 Ga volcano-plutonism (**Fig. 15**), showing a high magma volume generated on the relative little interval time (1901-1873 Ma). The same is observed in the southern region of Tapajos-Parima belt or Ventuari-Tapajos Province (**table 5**; *e.g.* Santos *et al.*, 1997b, 2000, 2004; CPRM, 2000b,c; Lamarão *et al.*, 2002), located on the Tapajos domain (see discussion below).

The older and inherited ages (1972-1962 Ma) observed in all granitoids and volcanics dated (except for Jaburuzinho facies and hypersthene granite), are very similar to the crystallization interval ages (1975-1962 Ma) of Martins Pereira and Serra Dourada granitoids from NUAD (Almeida *et al.*, 2002). These abundant inherited records in the SUAD granitoids (**table 6, fig. 15**) pointed out a strong participation of the metagranitoids of NUAD in their genesis (partial melting or assimilation/contamination?). Minor evidences of Transamazonian (2142 ± 10 Ma) and Siderian (2359 ± 7 Ma) zircons are also identified, respectively, in the Água Branca and Murauaú granites (**table 6, fig. 15**), suggesting, at least locally in the SUAD, the presence of the Transamazonian and Central Amazonian crusts.

The magmatic rocks of Tapajos domain (TD) also present several inheritances from several sources (**table 6, fig. 15**). The Iriri volcanics show 2.66-2.46 Ga, 2.01 Ga and 1.96 Ga inherited zircons, suggesting, respectively, Central Amazonian craton, Cuiú-Cuiú and Creporizão provenances. The Younger São Jorge also exhibit Archean (2.73 Ga) and Creporizão (1.96 Ga)

inheritance ages and coeval Ingarana mafic rocks show Cuiú-Cuiú inherited zircons ages (2.00 Ga). The Maloquinha granitoids are the most important example of the inherited zircon in the TD, showing 4 generations (**table 6**, Santos *et al.*, 2001b): 2.84-2.46 Ga (Central Amazonian Province), 2.21 Ga (Transamazon or Maroni-Itacaiúnas Province), 2.00 Ga (Cuiú-Cuiú arc) and 1.98 Ga (Creporizão granitoids).

Tapajós and Uatumã-Anauá domains: Lithostratigraphy and Tectonic Evolution

The SUAD granitoids and volcanics (1901-1873 Ma) show important chronological similarities with the Tapajós Domain ones in the southern Tapajós-Parima orogenic belt or Ventuari-Tapajós Province. However, the charnockites and high-K calc-alkaline Igarapé Azul granitoids-like are not described in the Tapajós domain (TD). In the Tapajós region, the 1898-1870 Ma granitoids (see **table 5**, **Fig. 15**) crop out in the post-orogenic domain (*e.g.* CPRM, 2000b, c), represented by Tropas, Parauari, Younger São Jorge and Maloquinha granitoids, Ingarana mafic rocks and coeval volcanics. The origin of this magmatism has been attributed to large-scale taphrogenesis that marked the break up of a large Paleoproterozoic continent (Vasquez *et al.*, 2002, Lamarão *et al.*, 2002, 2005), contrasting with a arc-related orogenic origin (Tropas Orogeny, Santos *et al.*, 2000).

For instance, in the SUAD, some chemical discriminant diagrams (**Fig. 4, 5 and 7**) pointed out that Caroebe and Igarapé Azul granitoids belong to the “active continental margin” setting with variable crustal contributions. In the special case of Caroebe granitoids, they contain hornblende and biotite, are metaluminous to weakly peraluminous, and have the characteristics of I-type granites and high-K calc-alkaline series. This picture is compatible with volcanic arc setting, but the trace element compositions are strongly dependent of protolith composition and, therefore, can not necessarily be indicative of the tectonic setting of magma formation (*e.g.* Roberts and Clemens, 1989).

High-K calc-alkaline granitoids (KCG) are present in various geodynamic settings (*e.g.* Roberts and Clemens, 1989, Barbarin, 1999). According Barbarin (1999), these granitoids indicate much more a variation of the tectonic regimes than a specific geodynamic environment and generally are good indicators of major changes in the geodynamic environment. They are normally abundant in the orogenic belts related to continental collision, mostly when the collision is ending, either during periods of relaxation (separating periods of culmination of collisional events) or transition from a compressional regime to a tensional regime (*e.g.* Lameyre, 1988;

Bonin, 1990).

Thus, the younger 1.90-1.89 Ga high-K calc-alkaline granitoids (Caroebe, Água Branca and Igarapé Azul, as well as Tropas and Parauari types) could be associated with the latest subduction related processes (?) or, alternatively, represent an intracontinental tectonic evolution (*e.g.* Vasquez *et al.*, 2002; Lamarão *et al.*, 2002, 2005), suggesting a transition for more stable tectonic crustal conditions, characterized by the 1.88-1.87 Ga A-type Mapuera and Abonari granitoids.

CONCLUSIONS

The geochemical data support that Caroebe and Igarapé Azul granitoids origin can be linked to partial melting of crustal protoliths with different compositions (amphibolite or metatonalites and metagreywacke sources), leaving restites with variable proportions of amphibole, titanite and plagioclase as result of melting under variable H₂O contents. This H₂O variation can locally generate coeval hypersthene granitoids (*e.g.* Igarapé Tamandaré and Santa Maria), suggesting dry conditions and high temperatures on the granite formation.

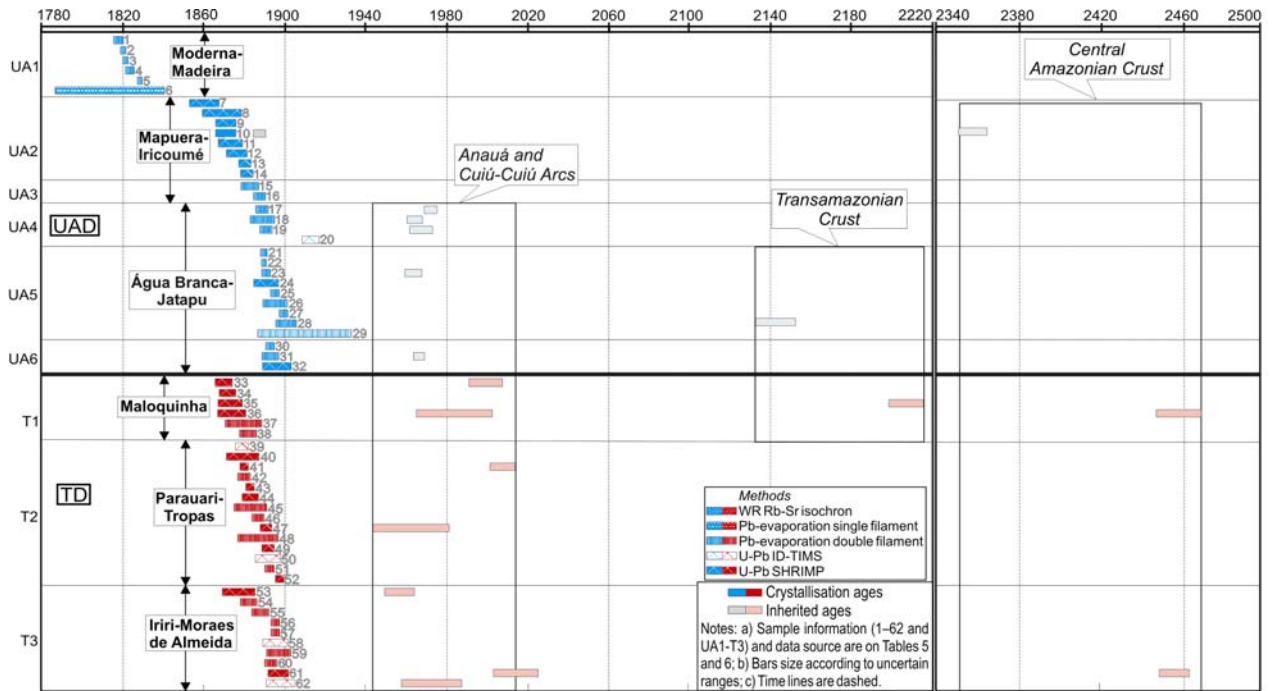


Fig. 15. Temporal distribution of main magmatic rocks younger than 1900 Ma (and respective inheritances) of the Parima-Tapajós or Ventuari-Tapajós Province, grouped by Uatamã-Anauá (UAD) and Tapajós (TD) geological domains. For references see tables 5 and 6.

The geochronological constraints, based on the inherited zircon ages (1.97-1.96 Ga), show that the Martins Pereira granites from NUAD are strongly related to the Caroebe (Alto Alegre facies) and mainly of Igarapé Azul origin. In addition, the Igarapé Azul Granite shows (muscovite)-biotite-rich enclaves and Martins Pereira xenoliths, suggesting that contamination

effects of host rock also could be play a role in the magma evolution. Local evidence of inherited zircon with Transamazonian and Siderian ages, suggest, at least partially, the involvement of Maroni-Itacaiúnas (or Transamazon) and Central Amazonian (or Amazon) Provinces in the generation of some granites (*e.g.* Água Branca and Murauaú granites).

In the SUAD, the zircon geochronology results pointed out that several granitoids (Água Branca, Caroebe, Igarapé Azul and Santa Maria) and the Iricoumé Volcanics belong to the same magmatic event (1901-1889 Ma). This age range is very similar to that of the calc-alkaline Parauari-(Tropas)-Irirí magmatism (1898-1879 Ma) in the Tapajos domain; despite of this last one, the high-K calc-alkaline granitoids with metasedimentary source contributions (*e.g.* Igarapé Azul Granite) and charnockitic rocks are absent. In general sense, The Água Branca-(Caroebe-Igarapé Azul)-Iricoumé (SUAD) and Parauari-Irirí (TD) magmatism represent an important period of Orosirian crustal growth in the Ventuari-Tapajos (or Tapajós-Parima) Province and their origin is still a matter of debate.

The magmatic evolution picture is maybe compatible with volcanic arc setting, but metaturbiditic and ophiolite sequences are not observed in association with the calc-alkaline granitoids (and coeval volcanism) in the SUAD. Furthermore, the trace element compositions are strongly dependent of source composition and, therefore, not necessarily indicative of the tectonic setting of magma formation. The several inherited ages yielded by the SUAD granitoids also suggest an important crustal involvement during the emplacement these granitoids and a juvenile origin on the magmatic arc setting is unlike for this portion of Guyana Shield. However isotopic data (Nd, Pb and Sr) are not available for these rocks, making difficult a better evaluation of the evolutionary models.

Acknowledgments

Special thanks to the colleagues of CPRM (Geological Survey of Brazil) and Para-Iso (UFPA) for geological discussions and helpful during isotopic analyses, respectively. The authors are also grateful to CPRM-Geological Survey of Brazil for the research grants and FINEP (CT-Mineral 01/2001 Project) and Isotope Geology Laboratory of Federal University of Pará for support of laboratorial works.

References

Almeida, M.E., Macambira, M.J.B. 2003. Aspectos geológicos e litoquímicos dos granitóides

- cálcio-alcálicos Paleoproterozóicos do sudeste de Roraima. In: SBGq, Congresso Brasileiro de Geoquímica, 9, Anais, p. 775-778 (in portuguese).
- Almeida, M.E., Macambira, M.J.B. Geology, Petrography and Mineralizations of Paleoproterozoic Granitoids from Uatumã-Anauá Domain (Guyana Shield), Southeast of Roraima State, Brazil. *Revista Brasileira de Geociências*. submitted.
- Almeida, M.E., Fraga, L.M.B., Macambira, M.J.B. 1997. New geochronological data of calc-alkaline granitoids of Roraima State, Brazil. In: IG/USP, South-American Symp. on Isotope Geology, 1, Extend Abst., p.34-37.
- Almeida, M.E., Brito, M.F.L., Ferreira, A.L., Monteiro, M.A.S. 2001. Evolução Tectono-estrutural da região do médio-alto curso do rio Tapajós. In: N.J. Reis and M.A.S. Monteiro (Orgs), *Contribuições à Geologia da Amazônia*, 2, , Belém, SBG, p.57-112. (in portuguese).
- Almeida, M.E., Macambira, M.J.B., Faria, M.S.G. de. 2002. A Granitogênese Paleoproterozóica do Sul de Roraima. In: SBG, Congresso Brasileiro de Geologia, 41, Anais, p 434 (in portuguese).
- Altherr, R., Holl, A., Hegner, E., Langer, C., Kreuzer, H. 2000. High-potassium, calc-alkaline I-type plutonism in the European Variscides: northern Vosges (France) and northern Schwarzwald (Germany). *Lithos* **50**, 51–73.
- Araújo Neto, H., Moreira, H.L. 1976. Projeto Estanho de Abonari: Relatório Final. BRASIL. Departamento Nacional da Produção Mineral, Manaus, Convênio DNPM/CPRM, relat. inédito. 2v (in portuguese).
- Bacon, C.R., Druitt, T.H. 1988. Compositional evolution of the zoned calcalkaline magma chamber of mount Mazama, crater Lake, Oregon. *Contrib. Miner. Petrol.* **98**, 224–256.
- Bakhit, F., El-Nisr,S., Saleh, G., El-Afandy, A. 2005. Geochemistry and Petrogenesis of Neoproterozoic Granitoids in Kilkbob Area, Southeastern Desert, Egypt. *Mineralogical Society Of Poland – Special Papers* **26**, 121-125.
- Barbarin, B. 1999. A review of the relationships between granitoid types, their origins and their geodynamic environments. *Lithos* **46**, 605–626.
- Barbero, L., Villaseca, C. 1992. The Layos Granite. Hercynian complex of Toledo (Spain): An example of parautochthonous restite-rich granite in a granulitic area. *Trans. R. Soc. Edinburgh Earth Sci.* **83**, 127-138.
- Barbero, L., Villaseca, C., Rogers, G., Brown, P.E. 1995. Geochemical and isotopic

- disequilibrium in crustal melting: An insight from the anatectic granitoids from Toledo, Spain. *J. Geophys. Res. Solid Earth* **100**, 15745- 15765.
- Barker, F., Farmer, G.L., Ayuso, R.A., Plafker, G., Lull, J.S. 1992. The 50 Ma granodiorites of the eastern Gulf of Alaska: melting in an accretionary prism in the forearc. *J. Geophys. Res.* **97**, 6757–6778.
- Barton, M., Sidle, W.C. 1994. Petrological and geochemical evidence for granitoid formation: The Waldoboro pluton complex, Maine. *J. Petrol.* **35**, 1241-1274.
- Bateman, R. 1988. The Center Pond pluton: The restite of the story (phase separation and melt evolution in granitoid genesis). Comment. *Am. J. Sci.* **288**, 282-287.
- Billström, K., Weihed, P. 1996. Age and provenance of host rocks and ores in the Palaeoproterozoic Skellefte district, northern Sweden. *Econ. Geol.* **91**, 1054–1072.
- Bonin, B. 1990. From orogenic to anorogenic settings: evolution of granitoid suites after a major orogenesis. *Geol. J.* **25**, 261–270.
- Boynton, W.V. 1984. Cosmochemistry of the rare earth elements: meteorite studies. In: Henderson, P.(ed), *Rare earth element geochemistry*, Elsevier Publ. p. 63-114.
- Brown, G.C., Thorpe, R.S., Webb, P.C. 1984. The geochemical characteristics of granitoids in contrasting arcs and comments on magma sources. *Journ. Geol. Soc. London* **141**, 413-426.
- Bullen, T.D., Clyne, M.A. 1990. Trace element and isotopic constraints on magmatic evolution at Lassen volcanic center. *J. Geophys. Res.* **95**, 19671–19691.
- Burnham, C.W. 1992. Calculated melt and restite compositions of some Australian granites. *Trans. R. Soc. Edinburgh Earth Sci.* **83**, 387-397.
- Chappell, B.W., White, A.J.R., Wyborn, D. 1987. The importance of residual source material (restite) in granite petrogenesis. *J. Petrol.* **28**, 111-138.
- Clemens, J.D. 1989. The importance of residual source material (restite) in granite petrogenesis: A comment. *J. Petrol.* **30**, 1313-1316.
- Condie, K.C. 1998. Episodic continental growth and super-continent: a mantle avalanche connection? *Earth Planet. Sci. Lett.* **163**, 97–108.
- Cordani, U.G., Tassinari, C.C.G., Teixeira, W., Basei, M.A.S., Kawashita, K. 1979. Evolução tectônica da Amazônia com base nos dados geocronológicos. In: Congresso Geológico Chileno, 2, 1979, Arica, Anais, v.4, p.177-148 (in portuguese).
- Costi, H.T., Dall’Agnol, R., Moura, C.A.V. 2000. Geology and Pb-Pb geochronology of

- Paleoproterozoic volcanic and granitic rocks of the Pitinga Province, Amazonian craton, northern Brazil. *Intern. Geol. Rev.* **42**, 832-849.
- Costi, H.T.; Santiago, A.F., Pinheiro, S. da S. 1984. Projeto Uatumã – Jatapu; Relatório Final. Manaus: CPRM, SUREG-MA. 133p (in portuguese).
- CPRM. 1999. Programa Levantamentos Geológicos Básicos do Brasil. Roraima Central, Folhas NA.20-X-B e NA.20-X-D (integrais), NA.20-X-A, NA.20-X-C, NA.21-V-A e NA.21-V-C (parciais). Escala 1:500.000. Estado de Roraima. Superintendência Regional de Manaus, 166 p. CD-ROM. Abstract in english (in portuguese)
- CPRM. 2000a. Programa Levantamentos Geológicos Básicos do Brasil. Caracaraí, Folhas NA.20-Z-B e NA.20-Z-D (integrais), NA.20-Z-A, NA.21-Y-A, NA.20-Z-C e NA.21-Y-C (parciais). Escala 1:500.000. Estado de Roraima. Superintendência Regional de Manaus, 157 p. CD-ROM. Abstract in english (in portuguese)
- CPRM. 2000b. Programa Levantamentos Geológicos Básicos do Brasil. Projeto Especial Província Mineral do Tapajós. Geologia e recursos minerais da folha Vila Riozinho, Folha SB.21-Z-A. Escala 1:250.000. Estado do Pará. Nota Explicativa. CPRM/Serviço Geológico do Brasil [CD-ROM] (in portuguese).
- CPRM. 2000c. Programa Levantamentos Geológicos Básicos do Brasil. Projeto Especial Província Mineral do Tapajós. Geologia e recursos minerais da folha Rio Novo, Folha SB.21-Z-C. Escala 1:250.000. Estado do Pará. Nota Explicativa. CPRM/Serviço Geológico do Brasil [CD-ROM] (in portuguese).
- CPRM. 2003. Programa Levantamentos Geológicos Básicos do Brasil. Geologia, Tectônica e Recursos Minerais do Brasil: Sistema de Informações Geográficas - SIG. Rio de Janeiro : CPRM, 2003. Mapas Escala 1:2.500.000. 4 CDs ROM. (in portuguese, abstract in english)
- CPRM. 2005. Programa Levantamentos Geológicos Básicos do Brasil. Escala 1:1000.000. Mapa Geológico do Brasil. 41 mapas Brasília, MME. CD-ROM. (in portuguese)
- CPRM. 2006. Programa Levantamentos Geológicos Básicos do Brasil. Escala 1:1000.000. Mapa Geológico do Estado do Amazonas. Manaus, MME. Text and CD-ROM. (in portuguese)
- Delor, C., Lahondère, Egal, E., Lafon, J.-M., Cocherie, A., Guerrot, C., Ross, P., Truffert, C., Théveniaut, H., Phillips, D., Avelar, W.G. de. 2003. Transamazonian crustal growth and reworking as revealed by the 1:500,000-scale geological map of French Guiana (2nd edition). *Géologie de la France* **2-3-4**, 5-57.

- Dunphy, J.M., Ludden, J.N. 1998. Petrological and geochemical characteristics of a Paleoproterozoic magmatic arc (Narsajuaq Terrane, Ungawa Orogen, Canada) and comparisons to Superior Province granitoids. *Precamb. Res.* **91**, 109-142.
- El-Sayed, M.M., Mohamed, F.H., Furnes, H., Kanisawa, S. 2002. Geochemistry and Petrogenesis of the Neoproterozoic Granitoids in the Central Eastern Desert, Egypt. *Chemie der Erde/Geochemistry* **62** (4), 317-346.
- El-Sayed, M.M., Obeid, M.A., Furnes, H., Moghazi, A.M. 2004. Late Neoproterozoic volcanism in the southern Eastern Desert, Egypt: petrological, structural and geochemical constraints on the tectonic-magmatic evolution of the Allaqi Dokhan volcanic suite. *Neues Jahrbuch für Mineralogie - Abhandlungen* **180** (3), 261-286.
- Faria, M.S.G. de, Santos, J.O.S. dos, Luzardo, R., Hartmann, L.A., McNaughton, N.J. 2002. The oldest island arc of Roraima State, Brazil - 2,03 Ga: zircon SHRIMP U-Pb geochronology of Anauá Complex. *In: SBG, Congresso Brasileiro de Geologia*, 41, Anais, p. 306.
- Fraga, L.M.B. 2002. A Associação Anortosito–Mangerito–Granito Rapakivi (AMG) do Cinturão Güiana Central, Roraima e Suas Encaixantes Paleoproterozóicas: Evolução Estrutural, Geocronologia e Petrologia. Tese de Doutorado, CPGG/CG, Universidade Federal do Pará. 386p. (in portuguese)
- Fraga, L.M.B., Almeida, M.E., Macambira, J.B. 1997. First lead-lead zircon ages of charnockitic rocks from Central Güiana Belt (CGB) in the state of Roraima, Brazil. *In: South-American Symp. on Isotope Geology*, 1997, Campos do Jordão. Resumo, Campos do Jordão [s.n.], 1997. p. 115- 117.
- Griffin, T.J., Page, R.W., Sheppard, S., Tyler, I.M. 2000. Palaeoproterozoic post-collisional, high-K felsic igneous rocks from the Kimberley region of northwestern Australia. *Precamb. Res.* **101**, 1–23.
- Grove, T.L., Donnelly-Nolan, J.M. 1986. The evolution of young silicic lavas at Medicine lake Volcano, California: implications for the origin of compositional gaps in calc-alkaline series lavas. *Contrib. Min. Petrol.* **92**, 281–302.
- Guffanti, M., Clyne, M.A., Muffler, L.J.P. 1996. Thermal and mass implications of magmatic evolution in the Lassen volcanic region, California, and constraints on basalt influx to the lower crust. *J. Geophys. Res.* **101**, 3001–3013.
- Hoskin, P.W.O., Kinny, P.D., Wyborn, D., Chappell, B.W. 2000. Identifying accessory mineral

- saturation during differentiation in granitoid magmas: An integrated approach. *J. Petrol.* **41**, 1365–1395.
- Irvine, T.N., Baragar, W.R.A. 1971. A guide to the chemical classification of the common volcanic rocks. *Can. J. Earth Sci.* **8**, 523-548.
- Jonasson, K. 1994. Rhyolite volcanism in the Krafla central volcano, northeast Iceland. *Bulletin of Volcanology* **56**, 516–528.
- Jorge-João, X.S.; Santos, C.A., Provost, A. 1985. Magmatismo adamelítico Água Branca (Folha Rio Mapuera, NW do Estado do Pará). Simp. de Geol. da Amaz., 2, Belém. *Anais...* Belém, Pará, SBG, v.2, p. 93-109 (in portuguese).
- Klein, E.L., Moura, C.A.V. 2001. Age constraints on granitoids and metavolcanic rocks of the São Luis Craton and Gurupi Belt, northern Brazil: implications for lithostratigraphy and geological evolution. *Int. Geol. Rev.* **43**, 237–253.
- Kober, B. 1986. Whole grain evaporation for $^{207}\text{Pb}/^{206}\text{Pb}$ age investigations on single zircons using a double filament source. *Cont. Min. Petrol.* **93**, 482-490.
- Kober, B. 1987. Single grain evaporation combined with Pb^+ emitter bedding for $^{207}\text{Pb}/^{206}\text{Pb}$ investigations using thermal ion mass spectrometry, and implications for zirconology. *Cont. Min. Petrol.* **96**, 63-71.
- Krymsky, R. 2002. Metodologia de análise de U-Pb em mono zircão como traçador $^{235}\text{U}-^{205}\text{Pb}$. Universidade Federal do Pará, Laboratório de Geologia Isotópica. 7p. (in portuguese).
- Lahtinen, R., Huhma, H. 1996. Isotopic and geochemical constrains on the evolution of the 1.93-1.79 Ga Svecofennian crust and mantle in Finland. *Precamb. Res.* **82**, 13-34.
- Lamarão, C.N., Dall’Agnol, R., Lafon, J.-M., Lima, E.F. 2002. Geology, geochemistry and Pb–Pb zircon geochronology of the Paleoproterozoic magmatism of Vila Riozinho, Tapajós gold province, Amazonian craton, Brazil. *Precamb. Res.* **119** (1-4), 189–223.
- Lamarão, C.N., Dall’Agnol, R., Pimentel, M.M. 2005. Nd isotopic composition of Paleoproterozoic volcanic and granitoid rocks of Vila Riozinho: implications for the crustal evolution of the Tapajós gold province, Amazon craton. *J. South Am. Earth Sci.* **18**, 277–292.
- Lameyre, J. 1988. Granite settings and tectonics. *Rend. Soc. It. Mineral. Petrol.* **43**, 215–236.
- Macambira, M.J.B., Almeida, M.E., Santos, L.S. 2002. Idade de Zircão das Vulcânicas Iricoumé do Sudeste de Roraima: contribuição para a redefinição do Supergrupo Uatumã. In: Simpósio Sobre Vulcanismo Ambientes Associados, 2, 2002, Belém. *Anais...* p.22 (in portuguese).

- Maniar, P.D., Piccoli, P.M. 1989. Tectonic discrimination of granitoids. *Geol Soc.Am.Bull.* **101**, 635-643.
- Oliveira, M.J.R., Almeida, M.E., Luzardo, R., Faria, M.S.G. de. 1996. Litogeoquímica da Suíte Intrusiva Água Branca - SE de Roraima. Congr. Brasil. de Geol., 39, Salvador, 1996. *Anais...* Salvador, Bahia, SBG, v.2, p. 213-216 (in portuguese).
- Page, R.W. 1988. Geochronology of early to middle Proterozoic fold belts in northern Australia: a review. *Precamb. Res.* **40/41**, 1–20.
- Patiño-Douce, A.E. 1996. Effects of pressure and H₂O content on the composition of primary crustal melts. *Trans. R. Soc. Edinburgh: Earth Sci.* **87**, 11–21.
- Patiño-Douce, A.E. 1999. What do experiments tell us about the relative contributions of crust and mantle to the origin of granitic magmas? In: Castro, A., Fernandez, C., Vigneresse, J.L. (Eds.), *Understanding Granites: Integrating New and Classical Techniques*, 168. *Geological Society of London*, Special Publication **168**, 55–75.
- Patiño-Douce, A.E., Beard, J.S. 1996. Effects of P, fO₂ and Mg/Fe ratio on dehydration melting of model metagreywackes. *J. Petrol.* **37**, 999–1024.
- Pearce, J.A. 1996. Sources and settings of granitic rocks. *Episodes* **19**, 120-125.
- Pearce, J.A., Harris, N.B., Tindle, A.G. 1984. Trace element discrimination diagrams for the tectonic interpretation of granitic rocks. *J. Petrol.* **25**, 956–983.
- Peccerillo A., Taylor S.R. 1976. Geochemistry of Eocene calc-alkaline rocks from Kastamonu area, Northern Turkey. *Contrib. Miner. Petrol.* **58**, 63-81.
- Petford, N., Atherton, M. 1996. Na-rich partial melts from newly underplated basaltic crust: the Cordillera Blanca Batholith, Peru. *J. Petrol.* **37**, 1491–1521.
- Petford, N., Paterson, B., McCaffrey, K., Pugliese, S. 1996. Melt infiltration and advection in microdioritic enclaves. *Eur. J. Mineral.* **8**, 405–412.
- Poli, G., Tommasini, S., Halliday, A.N. 1996. Trace element isotopic exchange during acid–basic magma interaction processes. *Trans. R. Soc. Edinburgh: Earth Sci.* **87**, 225–232.
- Rapp, R.P. 1995. Amphibole-out phase boundary in partially melted metabasalt, its control over liquid fraction and composition, and source permeability. *J. Geophys. Res.* **100**, 15601–15610.
- Rapp, R.P., Watson, E.B. 1995. Dehydration melting of metabasalt at 8–32 kbar: implications for continental growth and crust mantle recycling. *J. Petrol.* **36**, 891–931.
- Reis, N.R., Faria, M.S.G. de, Fraga, L.M.B., Haddad, R.C. 2000. Orosirian calc-alkaline

- volcanism from eastern portion of Roraima State – Amazon Craton. *Rev. Bras. Geoc.* **30** (3), 380-383.
- Reis, N.J., Fraga, L.M.B., Faria, M.S.G. de, Almeida, M.E. 2003. Geologia do Estado de Roraima. *Géologie de la France* **2-3-4**, 71-84. Abstract in english (in portuguese)
- Rickwood, P. 1989. Boundary lines within petrologic diagrams which use oxides of major and minor elements. *Lithos* **22**, 247-263.
- Roberts, M.P., Clemens, J.D. 1993. Origin of high-potassium, calc-alkaline, I-type granitoids. *Geology* **21**, 825–828.
- Santos, J.O.S., Reis Neto, J.M. 1982. Algumas idades de rochas graníticas do Cráton Amazônico. Congr. Brasil. de Geol., 32, Salvador, 1982. Anais... Salvador, BA, SBG, v.1, 339-348. (in portuguese)
- Santos J.O.S., Silva L.C., Faria M.S.G. de, Macambira, M.J.B. 1997a. Pb-Pb single crystal, evaporation isotopic study on the post-tectonic, sub-alkalic, A-type Moderna granite, Mapuera intrusive suite, State of Roraima, northern Brazil. In: Symposium of Granites and Associated Mineralizations, 2. Extended Abstract and Program. Salvador, Brasil: p. 273-275.
- Santos J.O.S., Hartmann L.A., Gaudette H.E. 1997b. Reconnaissance U-Pb in Zircon, Pb-Pb in Sulphides and Review of Rb-Sr Geochronology in the Tapajós Gold Province, Pará-Amazonas States, Brazil. In: South American Symp. on Isotope Geol., 1, Campos do Jordão-SP, Extended Abstracts: 280-282.
- Santos J.O.S, Hartmann L.A., Gaudette H.E., Groves D.I., McNaughton N.J., Fletcher I.R. 2000. A new understanding of the provinces of the Amazon Craton based on integration of field mapping and U-Pb and Sm-Nd geochronology: *Gondwana Research*, **3** (4): 453-488.
- Santos J.O.S., Faria M.S.G de, Hartmann L.A., McNaughton N., Fletcher I.R. 2001a. Oldest charnockitic magmatism in the Amazon Craton: zircon U-Pb SHRIMP geochronology of the Jaburu Charnockite, southern Roraima, Brazil. In: SBG/Norte, Simp. de Geol. da Amaz., 7, Belém. Anais..., p.70-72.
- Santos, J.O.S. dos, Groves, D.I., Hartmann, L.A., McNaughton, N.J., Moura, M.B., 2001b. Gold deposits of the Tapajós and Alta Floresta domains, Tapajós–Parima orogenic belt, Amazon Craton, Brazil. *Mineralium Deposita* **36**, 278–299.
- Santos J.O.S., Faria M.S.G. de, Hartmann L.A., McNaughton N.J. 2002. Significant Presence of the Tapajós – Parima Orogenic Belt in the Roraima Region, Amazon Craton based on

- SHRIMP U-Pb zircon Geochronology. In: SBG, Cong. Bras. Geol., 41, João Pessoa, PB, Anais: 336.
- Santos, J.O.S., Van Breemen, O.B., Groves, D.I., Hartmann, L. A., Almeida, M.E., McNaughton, N.J., Fletcher, I.R. 2004. Timing and evolution of multiple Paleoproterozoic magmatic arcs in the Tapajós Domain, Amazon Craton: constraints from SHRIMP and TIMS zircon, baddeleyite and titanite U–Pb geochronology. *Precamb. Res.*, vol. 131, 1-2, **10** : 73-109.
- Santos, J.O.S. dos, Hartmann, L.A., Faria, M.S.G. de, Riker, S.R.L., Souza, M.M. de, Almeida, M.E., McNaughton, N.J. 2006. A Compartimentação do Cráton Amazonas em Províncias: Avanços ocorridos no período 2000-2006. In: SBG, Simpósio de Geologia da Amazônia, 9, Belém, CD-ROM. (in portuguese)
- Sardinha, A.S. 1999. Petrografia do Granito Igarapé Azul, Sudeste do Estado de Roraima. Trabalho de Conclusão de Curso, UFPA, Belém, 32p.
- Sardinha, A.S. 2001. Estudo dos minerais opacos do Granito Igarapé Azul, sudeste de Roraima. Relatório de Pesquisa Orientada. UFPA, Centro de Geociências, CPGG, Belém, 37p.
- Scambos, T.A., Loisel, M.C., Wones, D.R. 1986. The Center Pond pluton: The restite of the story (phase separation and melt evolution in granitoid genesis). *Am. J. Sci.* **116**, 77-103.
- Shand, S.J. 1927. Eruptive Rocks, D. Van Nostrand Company, New York, pp. 360.
- Singh, J., Johannes, W. 1996. Dehydration melting of tonalites: Part II. Composition of melts and solids. *Contrib. Mineral. Petrol.* **125**, 26–44.
- Stacey, J.S., Kramers, J.D. 1975. Approximation of terrestrial lead isotope evolution by a two-stage model. *Earth Planetary Science Letters* **26**, 207-221.
- Steiger, R.H., Jager, J. 1977. Convention of the use of decay constants in geo- and cosmochronology. *Earth Planetary Science Letters* **36**, 359- 362.
- St-Onge, M.R., Lucas, S.B., Scott, D.J., Wodicka, N. 1999. Upper and lower plate juxtaposition, deformation and metamorphism during crustal convergence, Trans-Hudson Orogen (Quebec-Baffin segment), Canada. *Precambrian Res.* **93**, 27–49.
- Tassinari, C.C.G., Macambira, M.J.B. 1999. Geochronological Provinces of the Amazonian Craton. *Episodes*, **22** (3), 174-182.
- Tassinari, C.C.G., Macambira, M.J.B. 2004. A Evolução Tectônica do Cráton Amazônico. In: Mantesso-Neto, V., Bartoreli, A., Carneiro, C.D.R., Brito-Neves, B.B. de (eds), Geologia do Continente Sul-Americano - Evolução da Obra de Fernando Flávio Marques de Almeida, São

- Paulo, Ed. Beca, p. 471-485. Abstract in english (in portuguese).
- Teixeira, W., Tassinari, C.C.G., Cordani, U.G., Kawashita, K. 1989. A review of the Geochronology of the Amazonian Craton tectonic implications. *Precamb. Res.* **42**, 213-227.
- Tepper, J.H., Nelson, B.K., Bergantz, G.W., Irving, A.J. 1993. Petrology of the Chilliwack batholith, North Cascades, Washington: generation of calc-alkaline granitoids by melting of mafic lower crust with variable water fugacity. *Contrib. Miner. Petrol.* **113**, 333–351.
- Thompson, A.B. 1996. Fertility of crustal rocks during anatexis. *Transactions of the Royal Society of Edinburgh. Earth Sciences* **87**, 1–10.
- Thuy Nguyen, T.B., Satir, M., Siebel, W., Venneman, T., van Long, T. 2004. Geochemical and isotopic constraints on the petrogenesis of granitoids from Dalat zone, southern Vietnam. *Journal of Asian Earth Sciences* **23**, 467-482.
- Valério, C.S. 2006. Magmatismo Paleoproterozóico do extremo sul do Escudo das Guianas, município de Presidente Figueiredo (AM): geologia, geoquímica e geocronologia Pb-Pb em zircão. Universidade Federal do Amazonas, Dissertação de Mestrado, Manaus. (in portuguese)
- Valério, C.S., Souza, V.S., Macambira, M.J.B., Milliotti, C.A., Carvalho, A.S. 2005. Geoquímica e Idade Pb-Pb de zircão no Grupo Iricoumé na região da borda norte da bacia do Amazonas, município de Presidente Figueiredo (AM). In: SBG-Núcleo Norte, Simp. Vulc. Amb. Relac., 3, Belém, *Anais*: 47-52. (in portuguese)
- Vasquez, M.V., Ricci, P.S.F., Klein, E.L. 2002. Granitóides pós-colisionais da porção leste da Província Tapajós. In: Klein, E.L., Vasquez, M.L., Rosa-Costa, L.T. (orgs), *Contribuições à Geologia da Amazônia*, 3, Belém, SBG, p. 63-83. Abstract in english (in portuguese).
- Veiga Jr., J.P.; Nunes, A.C.B.; Souza, E.C. de; Santos, J.O.S.; Amaral, J.E., Pessoa, M.R., Souza, S.A. de S. 1979. Projeto Sulfetos do Uatumã; Relat. Final. Manaus, DNPM/CPRM, 6v (in portuguese).
- Wall, V.J., Clemens, J.D., Clarke, D.B. 1987. Models for granitoid evolution and source compositions. *J. Geol.* **95**, 731-749.
- Whalen, J.B., Currie, K.L., Chappell, B.W. 1987. A-type granites: Geochemical characteristics and discrimination. *Contrib. Miner. Petrol.* **95**, 420–436.
- White, A.J.R., Chappell, B.W. 1977. Ultrametamorphism and granitoid genesis. *Tectonophysics* **43**, 7-22.

- White, A.J.R., Chappell, B.W. 1983. Granitoid types and their distribution in the Lachlan Fold Belt, southeastern Australia. *Geol. Soc. Am. Memoir* **159**, 21–34.
- Wolf, M.B., Wyllie, J.P., 1994. Dehydration-melting of amphibolite at 10 kbar: the effects of temperature and time. *Contrib. Mineral. Petrol.* **115**, 369–383.
- Wyborn, D., Chappell, B.W. 1986. The petrogenetic significance of chemically related plutonic and volcanic rock units. *Geol. Mag.* **123**, 619-628.
- Zorpi, M.J., Coulon, C., Orisini, J.B. 1991. Hybridization between felsic and mafic magmas in calc-alkaline granitoids — a case study in northern Sardinia, Italy. *Chem. Geol.* **92**, 45–86.
- Zorpi, M.J., Coulon, C., Orisini, J.B., Cocirta, C. 1989. Magma mingling, zoning and emplacement in calc-alkaline granitoid plutons. *Tectonophysics* **157**, 315–329.

Table 1. Chemical compositions of main calc-alkaline associations of Southern Uatumã-Anauá domain, such as Caroebe and Igarapé Azul granitoids and volcanic rocks of Jatapu region. The geochemical data were obtained from this study¹ and CPRM (2000a)².

| Caroebe Granite | | | | | | | | | | | | | | |
|----------------------------------|----------------------|----------------------|----------------------|----------------------|---------------------|---------------------|----------------------|----------------------|---------------------|----------------------|----------------------|----------------------|---------------------|---------------------|
| Sample | Jaburuzinho Facies | | | | | | | | | Alto Alegre Facies | | | | |
| | MF-073C ² | MA-178B ¹ | MA-053C ¹ | MF-068A ² | MA-103 ¹ | MA-112 ¹ | MA-053B ¹ | MJ-061B ² | MA-121 ¹ | MA-144A ¹ | MA-053A ¹ | MA-119A ¹ | MA-150 ¹ | MA-276 ¹ |
| Rock Type | QD | QMzD | Tn | QMzD | Gd | Mgr | QMz | QMz | QMzD | Gd | Gd | Mgr | Gd | Gd |
| <i>Major elements (wt %)</i> | | | | | | | | | | | | | | |
| SiO ₂ | 49.50 | 55.13 | 58.31 | 59.09 | 59.60 | 60.44 | 61.04 | 61.60 | 61.85 | 65.95 | 66.24 | 68.03 | 68.22 | 69.14 |
| TiO ₂ | 1.29 | 1.09 | 0.46 | 0.93 | 0.65 | 1.05 | 0.40 | 0.26 | 0.68 | 0.53 | 0.62 | 0.40 | 0.37 | 0.39 |
| Al ₂ O ₃ | 16.39 | 16.85 | 21.66 | 16.00 | 17.19 | 15.94 | 20.06 | 16.00 | 17.74 | 16.42 | 15.70 | 15.25 | 16.70 | 15.81 |
| Fe ₂ O ₃ * | 11.38 | 8.61 | 3.21 | 8.40 | 5.29 | 5.84 | 2.88 | 5.53 | 3.93 | 3.45 | 4.00 | 3.01 | 1.85 | 2.53 |
| MnO | 0.15 | 0.15 | 0.04 | 0.17 | 0.09 | 0.09 | 0.05 | 0.24 | 0.07 | 0.06 | 0.07 | 0.07 | 0.05 | 0.07 |
| MgO | 6.00 | 2.73 | 0.96 | 2.70 | 2.19 | 2.57 | 0.90 | 2.80 | 1.57 | 0.98 | 1.51 | 1.05 | 0.49 | 0.66 |
| CaO | 8.30 | 5.98 | 6.85 | 5.70 | 4.75 | 5.33 | 5.69 | 5.30 | 4.66 | 3.19 | 3.42 | 3.12 | 2.54 | 2.18 |
| Na ₂ O | 3.40 | 3.86 | 4.66 | 3.40 | 4.36 | 3.70 | 4.44 | 3.90 | 4.95 | 4.04 | 3.71 | 3.05 | 4.35 | 4.17 |
| K ₂ O | 2.00 | 3.15 | 2.09 | 2.60 | 3.86 | 3.55 | 2.25 | 3.50 | 3.06 | 4.60 | 3.84 | 4.31 | 4.43 | 4.70 |
| P ₂ O ₅ | 0.18 | 1.17 | 0.34 | 0.22 | 0.33 | 0.61 | 0.30 | 0.55 | 0.40 | 0.32 | 0.25 | 0.20 | 0.21 | 0.19 |
| LOI | 1.38 | 0.90 | 0.80 | 0.76 | 1.20 | 0.50 | 1.80 | 0.54 | 0.60 | 0.80 | 0.50 | 0.90 | 0.80 | 0.60 |
| TOTAL | 100.02 | 99.62 | 99.38 | 99.97 | 99.51 | 99.62 | 99.81 | 100.22 | 99.51 | 100.34 | 99.86 | 99.39 | 100.01 | 100.44 |
| <i>Trace elements (ppm)</i> | | | | | | | | | | | | | | |
| Ni | - | 16 | 8 | - | 20 | 25 | 8.2 | - | 20 | 5 | 23 | 7 | 3 | 4 |
| Cr | - | 26 | 17 | - | 22 | 22 | 17 | - | 13 | 4 | 22 | 4 | 4 | 4 |
| Rb | 101 | 97 | 69 | 75 | 72 | 93 | 93.7 | 82 | 69 | 117 | 136 | 157 | 150 | 120 |
| Cs | - | 0.91 | 2.13 | - | 1.20 | 1.00 | 3.90 | - | 1.20 | 1.31 | 5.50 | 6.40 | 1.71 | 1.60 |
| Ba | 433 | 1374 | 1088 | 803 | 3220 | 1457 | 813 | 764 | 1881 | 1893 | 937 | 710 | 1140 | 1582 |
| Sr | 714 | 683 | 1394 | 447 | 987 | 800 | 1105.6 | 288 | 1172 | 713 | 444 | 298 | 638 | 612 |
| Ga | 12 | 26 | 25 | 13 | 23 | 21 | 22.4 | 5 | 21 | 19 | 22 | 18 | 21 | 19 |
| Ta | - | 0.71 | 0.71 | - | 0.30 | 1.30 | 0.40 | - | 0.40 | 0.70 | 0.50 | 0.81 | 0.91 | 0.90 |
| Nb | 8.0 | 18.0 | 7.5 | 14.0 | 5.2 | 20.8 | 6.2 | 7.0 | 9.0 | 10.6 | 11.1 | 9.2 | 13.3 | 13.9 |
| Hf | - | 19.98 | 3.65 | - | 7.00 | 12.80 | 3.10 | - | 11.70 | 12.66 | 7.30 | 9.24 | 11.19 | 8.61 |
| Zr | 109 | 956 | 128 | 169 | 290 | 470 | 95.3 | 139 | 486 | 470 | 300 | 286 | 379 | 305 |
| Y | 22 | 44 | 15 | 26 | 22 | 47 | 9 | 18 | 33 | 18 | 19 | 28 | 33 | 27 |
| Th | - | 12.17 | 14.82 | - | 5.70 | 17.10 | 10.40 | - | 13.20 | 17.68 | 12.10 | 47.24 | 17.04 | 22.34 |
| U | - | 2.03 | 3.35 | - | 0.70 | 1.80 | 3.20 | - | 2.50 | 2.81 | 5.70 | 6.40 | 3.43 | 2.50 |
| La | 27.55 | 128.19 | 30.44 | 44.59 | 54.70 | 99.10 | 25.40 | 18.58 | 88.90 | 50.44 | 57.10 | 48.05 | 47.48 | 83.63 |
| Ce | 67.78 | 251.93 | 67.59 | 100.08 | 91.20 | 186.20 | 48.50 | 45.55 | 132.50 | 87.52 | 91.10 | 101.18 | 87.60 | 124.40 |
| Pr | 0.00 | 24.63 | 6.97 | 0.00 | 10.79 | 21.97 | 5.10 | 0.00 | 15.54 | 9.58 | 9.71 | 9.66 | 9.52 | 14.03 |
| Nd | 40.50 | 85.90 | 24.56 | 47.50 | 41.60 | 82.30 | 18.90 | 20.31 | 54.50 | 33.26 | 32.40 | 32.10 | 35.89 | 48.08 |
| Sm | 6.81 | 11.97 | 4.06 | 7.06 | 6.90 | 13.80 | 3.10 | 4.13 | 7.50 | 5.33 | 4.90 | 5.28 | 6.96 | 6.91 |
| Eu | 1.51 | 2.52 | 1.22 | 1.48 | 1.56 | 2.08 | 1.15 | 0.71 | 1.64 | 1.18 | 1.10 | 1.11 | 1.28 | 1.30 |
| Gd | 6.08 | 9.77 | 3.16 | 5.74 | 5.53 | 10.05 | 2.00 | 2.90 | 5.26 | 3.81 | 3.46 | 4.48 | 5.52 | 4.82 |
| Tb | 0.00 | 1.29 | 0.54 | 0.00 | 0.65 | 1.35 | 0.31 | 0.00 | 0.72 | 0.62 | 0.51 | 0.65 | 0.83 | 0.69 |
| Dy | 5.58 | 7.26 | 2.44 | 4.71 | 3.37 | 7.55 | 1.39 | 2.13 | 3.84 | 2.70 | 2.75 | 3.60 | 4.80 | 2.99 |
| Ho | 1.14 | 1.41 | 0.50 | 0.91 | 0.61 | 1.36 | 0.34 | 0.43 | 0.73 | 0.58 | 0.53 | 0.82 | 1.07 | 0.70 |
| Er | 2.91 | 4.15 | 1.40 | 2.24 | 1.74 | 3.92 | 0.80 | 1.14 | 2.13 | 1.74 | 1.65 | 2.23 | 2.90 | 2.12 |
| Tm | 0.00 | 0.59 | 0.21 | 0.00 | 0.24 | 0.55 | 0.18 | 0.00 | 0.28 | 0.31 | 0.26 | 0.42 | 0.47 | 0.28 |
| Yb | 2.17 | 4.08 | 1.53 | 1.54 | 1.66 | 4.08 | 0.96 | 0.77 | 2.09 | 1.65 | 2.02 | 2.38 | 2.84 | 1.92 |
| Lu | 0.27 | 0.70 | 0.23 | 0.20 | 0.25 | 0.56 | 0.20 | 0.13 | 0.28 | 0.30 | 0.33 | 0.43 | 0.43 | 0.35 |
| ETR total | 162.30 | 534.38 | 144.84 | 216.05 | 220.80 | 434.87 | 108.33 | 96.79 | 315.91 | 199.02 | 207.82 | 212.38 | 207.59 | 292.24 |
| Mg# | 51.45 | 38.91 | 37.48 | 39.08 | 45.48 | 46.78 | 41.26 | 50.15 | 44.42 | 36.14 | 42.96 | 41.27 | 34.53 | 34.06 |
| Rb/Sr | 0.14 | 0.14 | 0.05 | 0.17 | 0.07 | 0.12 | 0.08 | 0.28 | 0.06 | 0.16 | 0.31 | 0.53 | 0.24 | 0.20 |
| Ba/Rb | 4.29 | 14.19 | 15.76 | 10.71 | 45.03 | 15.70 | 8.68 | 9.32 | 27.14 | 16.19 | 6.89 | 4.53 | 7.60 | 13.18 |
| Eu _(n) /Eu* | 0.70 | 0.69 | 1.00 | 0.69 | 0.75 | 0.52 | 1.32 | 0.60 | 0.76 | 0.76 | 0.78 | 0.68 | 0.61 | 0.66 |
| (La/Sm) _n | 2.54 | 6.74 | 4.72 | 3.97 | 4.99 | 4.52 | 5.15 | 2.83 | 7.46 | 5.96 | 7.33 | 5.72 | 4.29 | 7.61 |
| (Gd/Yb) _n | 2.26 | 1.93 | 1.66 | 3.01 | 2.69 | 1.99 | 1.68 | 3.03 | 2.03 | 1.86 | 1.38 | 1.52 | 1.57 | 2.02 |
| (La/Yb) _n | 8.56 | 21.20 | 13.39 | 19.52 | 22.22 | 16.38 | 17.84 | 16.18 | 28.68 | 20.64 | 19.06 | 13.63 | 11.26 | 29.32 |

Table1 (Continued)

| Igarapé Azul Granite | | | | | | | | | | | | |
|----------------------------------|----------------------|----------------------|----------------------|-----------------------|---------------------|----------------------|---------------------|----------------------|----------------------|-----------------------------------|---------|---------|
| | Vila Catarina Facies | | | Cinco Estrelas Facies | | | | Saramandaia Facies | | Biotite-bearing gneiss (enclaves) | | |
| Sample | MA-002 ¹ | MF-010B ² | MF-006A ² | MA-102A ¹ | MA-079 ¹ | MA-147A ¹ | MA-088 ¹ | MA-186A ¹ | MA-201A ¹ | MA-201B | MA-213B | MA-085B |
| RockType | LcMgr | Mgr | LcGd | LcMgr | QMz | Mgr | Sgr | MgrP | MgrP | QD | QMzD | Gd |
| <i>Major elements (wt %)</i> | | | | | | | | | | | | |
| SiO ₂ | 67.87 | 70.80 | 71.50 | 71.63 | 69.09 | 70.86 | 72.25 | 70.44 | 71.64 | 50.94 | 59.77 | 63.33 |
| TiO ₂ | 0.37 | 0.37 | 0.19 | 0.18 | 0.41 | 0.27 | 0.33 | 0.29 | 0.30 | 2.11 | 1.28 | 0.95 |
| Al ₂ O ₃ | 16.13 | 14.50 | 15.10 | 15.04 | 16.16 | 14.61 | 14.24 | 15.27 | 14.45 | 18.97 | 16.63 | 13.56 |
| Fe ₂ O ₃ * | 2.25 | 3.02 | 1.79 | 1.38 | 2.31 | 1.80 | 2.12 | 1.98 | 2.01 | 12.20 | 7.56 | 10.28 |
| MnO | 0.05 | 0.07 | 0.07 | 0.04 | 0.05 | 0.05 | 0.05 | 0.06 | 0.04 | 0.27 | 0.16 | 0.26 |
| MgO | 0.60 | 0.68 | 0.31 | 0.19 | 0.68 | 0.36 | 0.49 | 0.49 | 0.48 | 3.28 | 2.54 | 1.98 |
| CaO | 2.68 | 1.30 | 1.60 | 1.36 | 2.62 | 1.27 | 0.91 | 1.83 | 2.16 | 2.52 | 5.16 | 2.33 |
| Na ₂ O | 3.97 | 2.80 | 4.30 | 3.68 | 4.06 | 3.31 | 2.71 | 3.53 | 3.61 | 2.75 | 3.76 | 3.34 |
| K ₂ O | 4.93 | 5.60 | 4.60 | 5.73 | 4.44 | 6.42 | 6.45 | 5.55 | 4.50 | 5.70 | 2.40 | 3.36 |
| P ₂ O ₅ | 0.16 | 0.14 | 0.07 | 0.05 | 0.22 | 0.05 | 0.09 | 0.09 | 0.06 | 0.87 | 0.69 | 0.52 |
| LOI | 0.70 | 0.51 | 0.31 | 0.60 | 0.70 | 0.70 | 0.80 | 0.30 | 0.50 | 2.20 | 0.90 | 1.10 |
| TOTAL | 99.72 | 99.79 | 99.84 | 99.88 | 100.74 | 99.70 | 100.44 | 99.83 | 99.75 | 101.80 | 93.28 | 90.73 |
| <i>Trace elements (ppm)</i> | | | | | | | | | | | | |
| Ni | 19 | - | - | 20 | 3 | 20 | 5 | 20 | 20 | 17 | 26 | 9 |
| Cr | 4 | - | - | 4 | 4 | 9 | 4 | 9 | 9 | 4 | 9 | 4 |
| Rb | 100 | 318 | 143 | 154 | 133 | 226 | 274 | 186 | 130 | 437 | 244 | 127 |
| Cs | 1.00 | 2.50 | 2.50 | 2.42 | 2.00 | 1.60 | 10.14 | 2.80 | 2.00 | 8.26 | 10.48 | 2.32 |
| Ba | 1834 | 526 | 1009 | 1377 | 1303 | 1064 | 363 | 1166 | 921 | 897 | 196 | 436 |
| Sr | 649 | 122 | 444 | 307 | 612 | 211 | 69 | 340 | 307 | 218 | 329 | 221 |
| Ga | 19 | 12 | 5 | 17 | 19 | 19 | 17 | 19 | 17 | 38 | 22 | 26 |
| Ta | 0.30 | - | - | 0.30 | 1.40 | 1.40 | 2.11 | 1.60 | 1.60 | 1.45 | 1.31 | 1.61 |
| Nb | 5.9 | 24.0 | 6.00 | 7.4 | 13.5 | 17.6 | 18.3 | 20.5 | 12.7 | 61.8 | 24.0 | 27.7 |
| Hf | 10.30 | - | - | 5.34 | 7.90 | 9.30 | 7.33 | 7.50 | 6.30 | 50.79 | 8.46 | 25.02 |
| Zr | 389 | 256 | 131 | 186 | 247 | 304 | 209 | 242 | 224 | 2127 | 326 | 949 |
| Y | 11 | 34 | 7 | 27 | 24 | 37 | 67 | 33 | 25 | 193 | 73 | 69 |
| Th | 15.60 | - | - | 12.99 | 15.69 | 50.60 | 23.28 | 29.20 | 23.90 | 108.70 | 11.89 | 31.88 |
| U | 2.70 | - | - | 3.73 | 2.20 | 6.90 | 9.53 | 10.40 | 7.60 | 9.60 | 2.82 | 9.58 |
| La | 65.80 | 63.31 | 29.90 | 213.36 | 54.88 | 117.80 | 31.11 | 61.00 | 40.20 | 277.80 | 54.79 | 116.53 |
| Ce | 114.20 | 155.04 | 59.32 | 342.20 | 102.56 | 178.40 | 63.53 | 111.40 | 81.70 | 400.12 | 116.04 | 204.50 |
| Pr | 12.09 | - | - | 42.29 | 11.77 | 20.78 | 7.52 | 12.36 | 9.81 | 67.19 | 14.86 | 22.39 |
| Nd | 40.10 | 68.50 | 25.20 | 147.88 | 44.28 | 68.90 | 29.00 | 44.10 | 38.50 | 254.57 | 60.74 | 79.90 |
| Sm | 4.80 | 10.50 | 2.88 | 19.64 | 7.80 | 9.70 | 6.72 | 7.70 | 6.90 | 56.05 | 13.40 | 13.72 |
| Eu | 1.07 | 1.74 | 0.61 | 3.02 | 1.51 | 1.13 | 0.80 | 1.32 | 0.96 | 4.16 | 1.79 | 1.21 |
| Gd | 2.43 | 7.38 | 2.08 | 11.44 | 6.23 | 7.29 | 6.98 | 5.85 | 4.90 | 48.50 | 12.18 | 10.72 |
| Tb | 0.31 | - | - | 1.34 | 0.88 | 1.04 | 1.56 | 0.83 | 0.62 | 8.37 | 2.25 | 1.64 |
| Dy | 1.62 | 5.26 | 1.71 | 5.20 | 4.83 | 5.19 | 9.47 | 4.79 | 3.66 | 41.03 | 13.16 | 9.63 |
| Ho | 0.27 | 0.84 | 0.33 | 0.80 | 0.86 | 1.02 | 2.17 | 0.91 | 0.65 | 7.24 | 2.61 | 2.16 |
| Er | 0.96 | 1.95 | 0.81 | 2.02 | 2.39 | 3.36 | 7.15 | 2.91 | 2.29 | 18.45 | 7.48 | 6.78 |
| Tm | 0.17 | - | - | 0.28 | 0.36 | 0.51 | 1.14 | 0.43 | 0.39 | 2.31 | 0.89 | 1.04 |
| Yb | 1.64 | 1.05 | 0.69 | 2.06 | 2.78 | 3.62 | 8.23 | 3.50 | 3.12 | 14.57 | 5.34 | 7.78 |
| Lu | 0.27 | 0.12 | 0.09 | 0.28 | 0.51 | 0.59 | 1.15 | 0.54 | 0.47 | 2.35 | 0.69 | 1.23 |
| ETRtotal | 245.73 | 315.69 | 123.63 | 791.81 | 241.62 | 419.33 | 176.54 | 257.64 | 194.17 | 1202.72 | 306.21 | 479.24 |
| Mg# | 34.76 | 30.98 | 25.70 | 31.41 | 36.84 | 28.60 | 21.51 | 33.00 | 32.33 | 34.05 | 39.76 | 27.41 |
| Rb/Sr | 0.15 | 2.61 | 0.32 | 0.50 | 0.22 | 1.07 | 3.95 | 0.55 | 0.42 | 2.00 | 0.74 | 0.58 |
| Ba/Rb | 18.34 | 1.65 | 7.06 | 8.92 | 9.77 | 4.71 | 1.33 | 6.27 | 7.07 | 2.05 | 0.81 | 3.42 |
| Eu _(n) /Eu* | 0.86 | 0.58 | 0.73 | 0.57 | 0.64 | 0.39 | 0.36 | 0.58 | 0.48 | 1.08 | 1.91 | 1.35 |
| (La/Sm) _n | 8.62 | 3.79 | 6.53 | 6.83 | 4.43 | 7.64 | 2.91 | 3.66 | 4.28 | 3.12 | 2.57 | 5.34 |
| (Gd/Yb) _n | 1.20 | 5.67 | 2.42 | 4.49 | 1.81 | 1.63 | 0.68 | 1.35 | 1.27 | 2.69 | 1.84 | 1.11 |
| (La/Yb) _n | 27.05 | 40.65 | 29.13 | 70.00 | 13.31 | 21.94 | 2.55 | 11.75 | 8.69 | 12.86 | 6.92 | 10.10 |

Table 1 (Continued)

| Jatapu Volcanics | | | | | | | | | | |
|----------------------------------|----------------------|----------------------|---------------------|----------------------|----------------------|---------------------|----------------------|----------------------|----------------------|----------------------|
| Andesite Basaltic to Rhyolite | | | | | | | | | | |
| Sample | MF-135A ² | MJ-164A ² | SR-13C ² | MJ-134A ² | MF-142A ² | SR-13D ² | MF-129B ² | MJ-133A ² | MF-144A ² | MF-144B ² |
| RockType | And Bas | Tch And | And | Dac | Dac | Tch | Dac Ph | Dac | Dac Ph | Rhy |
| <i>Major elements (wt %)</i> | | | | | | | | | | |
| SiO ₂ | 54.90 | 57.90 | 59.60 | 63.40 | 63.70 | 63.90 | 65.60 | 65.80 | 68.20 | 74.10 |
| TiO ₂ | 0.53 | 0.68 | 0.83 | 0.55 | 0.55 | 0.51 | 0.50 | 0.29 | 0.39 | 0.29 |
| Al ₂ O ₃ | 19.60 | 17.60 | 15.70 | 14.90 | 16.10 | 16.00 | 15.30 | 16.30 | 15.20 | 14.00 |
| Fe ₂ O ₃ * | 7.13 | 7.76 | 7.59 | 6.80 | 5.62 | 5.50 | 5.04 | 4.29 | 3.82 | 1.23 |
| MnO | 0.17 | 0.17 | 0.15 | 0.23 | 0.16 | 0.18 | 0.09 | 0.20 | 0.10 | 0.04 |
| MgO | 2.70 | 3.10 | 3.60 | 2.10 | 1.70 | 1.50 | 2.00 | 0.95 | 1.30 | 0.13 |
| CaO | 7.30 | 4.70 | 5.00 | 3.90 | 3.60 | 3.40 | 3.60 | 3.40 | 3.00 | 0.44 |
| Na ₂ O | 2.80 | 3.70 | 3.40 | 3.10 | 3.60 | 3.40 | 3.00 | 3.50 | 3.30 | 4.00 |
| K ₂ O | 2.20 | 2.80 | 3.00 | 3.60 | 3.30 | 4.70 | 3.70 | 3.90 | 3.50 | 4.80 |
| P ₂ O ₅ | 0.14 | 0.26 | 0.29 | 0.17 | 0.18 | 0.15 | 0.18 | 0.10 | 0.11 | 0.03 |
| LOI | 2.17 | 0.97 | 0.40 | 0.91 | 1.14 | 0.46 | 0.57 | 0.85 | 0.64 | 0.65 |
| TOTAL | 99.64 | 99.64 | 99.56 | 99.66 | 99.65 | 99.70 | 99.58 | 99.58 | 99.56 | 99.70 |
| <i>Trace elements (ppm)</i> | | | | | | | | | | |
| Ni | 40 | 26 | 59 | 47 | 24 | 21 | 16 | 22 | 18 | 5 |
| Cr | 80 | 59 | 103 | 120 | 63 | 57 | 36 | 70 | 34 | 5 |
| Rb | 168 | 93 | 118 | 135 | 120 | 180 | 105 | 160 | 150 | 241 |
| Cs | - | - | - | - | - | - | - | - | - | - |
| Ba | 611 | 1129 | 939 | 1052 | 1029 | 973 | 1179 | 1195 | 1199 | 1476 |
| Sr | 770 | 886 | 1058 | 585 | 547 | 384 | 810 | 775 | 672 | 206 |
| Ga | - | - | - | - | - | - | - | - | - | - |
| Ta | - | - | - | - | - | - | - | - | - | - |
| Nb | 11.0 | 11.0 | 14.0 | 12.0 | 11.0 | 16.0 | 14.0 | 10.0 | 12.0 | 20.0 |
| Hf | - | - | - | - | - | - | - | - | - | - |
| Zr | 142 | 212 | 238 | 244 | 242 | 267 | 210 | 296 | 238 | 308 |
| Y | 22 | 19 | 24 | 25 | 26 | 42 | 18 | 18 | 26 | 48 |
| Th | - | - | - | - | - | - | - | - | - | - |
| U | - | - | - | - | - | - | - | - | - | - |
| La | 23.05 | 36.83 | 39.02 | 41.43 | 34.30 | 50.88 | 29.67 | 36.99 | 34.55 | 44.59 |
| Ce | 51.37 | 83.16 | 91.92 | 93.58 | 78.52 | 111.60 | 71.06 | 72.30 | 69.60 | 91.30 |
| Pr | - | - | - | - | - | - | - | - | - | - |
| Nd | 20.60 | 34.26 | 44.23 | 37.68 | 31.11 | 46.41 | 30.65 | 20.61 | 28.89 | 44.60 |
| Sm | 3.39 | 5.46 | 7.77 | 6.02 | 4.84 | 7.20 | 4.83 | 2.94 | 4.25 | 8.14 |
| Eu | 0.69 | 1.26 | 1.57 | 1.11 | 0.95 | 1.32 | 1.09 | 0.67 | 0.83 | 1.34 |
| Gd | 2.06 | 3.19 | 4.23 | 3.52 | 2.69 | 4.60 | 2.85 | 1.81 | 2.30 | 4.46 |
| Tb | - | - | - | - | - | - | - | - | - | - |
| Dy | 1.46 | 2.35 | 3.19 | 2.71 | 1.93 | 3.88 | 2.20 | 1.08 | 1.66 | 4.60 |
| Ho | 0.26 | 0.44 | 0.61 | 0.53 | 0.36 | 0.76 | 0.43 | 0.20 | 0.31 | 0.92 |
| Er | 0.58 | 1.01 | 1.53 | 1.37 | 0.84 | 1.96 | 1.09 | 0.46 | 0.73 | 2.49 |
| Tm | - | - | - | - | - | - | - | - | - | - |
| Yb | 0.40 | 0.78 | 1.18 | 1.07 | 0.60 | 1.52 | 0.94 | 0.41 | 0.58 | 1.99 |
| Lu | 0.06 | 0.11 | 0.16 | 0.16 | 0.09 | 0.21 | 0.14 | 0.08 | 0.10 | 0.25 |
| ETRtotal | 103.92 | 168.85 | 195.41 | 189.18 | 156.23 | 230.34 | 144.95 | 137.55 | 143.80 | 204.66 |
| Mg# | 42.84 | 44.18 | 48.44 | 37.95 | 37.45 | 35.07 | 44.02 | 30.49 | 40.24 | 17.35 |
| Rb/Sr | 0.22 | 0.10 | 0.11 | 0.23 | 0.22 | 0.47 | 0.13 | 0.21 | 0.22 | 1.17 |
| Ba/Rb | 3.64 | 12.14 | 7.96 | 7.79 | 8.58 | 5.41 | 11.23 | 7.47 | 7.99 | 6.12 |
| Eu _(n) /Eu* | 0.74 | 0.75 | 0.76 | 0.68 | 0.73 | 0.66 | 0.83 | 0.82 | 0.73 | 0.62 |
| (La/Sm) _n | 4.28 | 4.24 | 3.16 | 4.33 | 4.45 | 4.44 | 3.86 | 7.92 | 5.11 | 3.45 |
| (Gd/Yb) _n | 4.20 | 3.32 | 2.90 | 2.66 | 3.62 | 2.45 | 2.46 | 3.52 | 3.20 | 1.81 |
| (La/Yb) _n | 34.39 | 31.96 | 22.31 | 26.15 | 38.67 | 22.63 | 21.39 | 60.09 | 40.16 | 15.11 |

Abbreviations: Lc. leuco; P. porphyritic; Ph. porphyry; And. andesite; AndBas.andesite basaltic; Dac. dacite; Gd. granodiorite; Mgr. monzogranite; QD. Quartz diorite; QzM. Quartz monzonite; QMzD. Quartz monzodiorite; Sgr. syenogranite; Tn. tonalite; Tch. trachyte; TchAnd. trachyandesite; Rhy. rhyolite.

Table 2. Petrography summary and geographic coordinates of analyzed samples by the single-zircon Pb-evaporation and U-Pb ID-TIMS methods.

| sample | stratigraphic unit | Geog. coord. | | sample description | zi U-Pb ID TIMS | MSWD | zi Pb evap | USD | | |
|---------|--|---------------|---------------|---|-----------------|------|----------------------|-----|----------------|-----|
| HM-181 | Água Branca Intrusive Suite (Água Branca Granite; type-area) | 01° 09' 10" S | 60° 20' 35" W | Hornblende-biotite granodiorite mildly porphyritic (feldspar megacrystals) with medium grained matrix and mafic-rich clots. Accessory minerals: titanite, epidote, magnetite, apatite and minor allanite and zircon. | - | - | 2142 ± 10 (1zi) | - | | |
| | | | | | | | - | - | 1901 ± 5 (4zi) | 1.2 |
| MA-121 | Água Branca Intrusive Suite (Carobe Granite; Jaburuzinho facies) | 00° 48' 48" N | 59° 50' 58" W | Hornblende-biotite quartz monzodiorite showing equigranular, medium grained texture and mafic-rich clots. Accessory minerals: titanite, epidote, magnetite, apatite and minor allanite and zircon. | - | - | 1895 ± 2 (6zi) | 2.1 | | |
| MA-053A | Água Branca Intrusive Suite (Carobe Granite; Alto Alegre facies) | 00° 51' 55" N | 59° 45' 56" W | Biotite monzogranite showing equigranular, medium grained texture and mafic-rich clots. Accessory minerals: titanite, magnetite, apatite and minor epidote, allanite and zircon. | - | - | 1963 ± 4 (2zi) | 1.1 | | |
| | | | | | | | - | - | 1891 ± 2 (3zi) | 1.4 |
| MA-147A | Igarapé Azul Granite (Estrela Guia facies) | 00° 43' 59" N | 60° 13' 12" W | Leucomonzogranite with biotite (1.3%) and muscovite (1.9%) showing equigranular and fine to medium-grained texture. Enriched in secondary minerals such as epidote (4.6%), chlorite (3.4%) and saussurite (6.1%). Accessory minerals: ilmenite, magnetite, epidote, allanite, zircon and apatite. | - | - | 1964 ± 4 (1zi) | - | | |
| MA-186A | Igarapé Azul Granite (Saramandaia facies) | 00° 51' 03" N | 60° 21' 45" W | Monzogranite with biotite (4.6%) and muscovite (1.0%) showing porphyritic and medium-grained texture. Enriched in secondary minerals such as epidote (1.1%), saussurite (7.9%) and minor chlorite (0.2%). Accessory minerals: ilmenite, magnetite, epidote, zircon and apatite. | lower 206 ± 5 | - | 1972 ± 3 (2zi) | 1.0 | | |
| | | | | | | | upper 1913 ± 4 (4zi) | 0.5 | 1889 ± 2 (3zi) | 1.4 |
| MA-201B | Enclave in Igarapé Azul Granite host (Vila Catarina facies) | 00° 46' 21" N | 60° 20' 03" W | Biotite-bearing quartz diorite with muscovite (1.0%), showing equigranular, medium- to coarse-grained texture. Accessory minerals: magnetite (6.7%), apatite (1.5%) and minor zircon, epidote and titanite. Secondary minerals: saussurite (2.1%) and chlorite (0.4%). | - | - | 1967 ± 6 (2zi) | 2.2 | | |
| MA-208 | Jatapu Volcanic | 00° 50' 02" N | 59° 18' 14" W | Andesite with aphanitic texture enclosing some plagioclase (<50% An), amphibole and pyroxene phenocrystals. The plagioclase and amphibole could be replaced respectively by fine-grained and xenomorphic crystals of saussurite and epidote, chlorite and opaque minerals. | - | - | 1966 ± 3 (4zi) | 1.3 | | |
| | | | | | | | - | - | 1893 ± 5 (4zi) | 2.2 |
| MA-198 | Santa Maria Enderbite | 00° 50' 05" N | 60° 34' 36" W | Pyroxene-bearing tonalite showing equigranular, coarse grained texture and caramelish dark green colour. Corona texture is also common (pyroxenes surrounded by overgrowth of reddish brown biotite). Accessory minerals: magnetite, titanite, zircon and apatite. | - | - | 1891 ± 1 (6zi) | 1.2 | | |
| MA-226 | Murauá Granite (Mapuera Intrusive Suite?) | 00° 33' 39" N | 60° 02' 49" W | Biotite monzogranite with equigranular and fine to medium-grained texture, deeply sheared (dynamic recrystallization, quartz ribbon) and local banding. Relicts of zoned plagioclase grains are founded. Accessory minerals: titanite, epidote, local magnetite and minor allanite, zircon and apatite. | - | - | 2359 ± 7 (2zi) | 4.1 | | |
| | | | | | | | - | - | 1888 ± 3 (3zi) | 1.8 |
| | | | | | | | - | - | 1871 ± 5 (2zi) | 2.6 |

Notes: In parenthesis the number of zircon analyses used to calculate the age. Key: U-Pb ID TIMS - Conventional U-Pb results. Pb-evap - Pb-evaporation results.

Table 3. Zircon single-crystal Pb-evaporation isotopic data for Água Branca (HM-181), Caroebe (MA-121, 053A), Igarapé Azul (MA-186A, 147A), Murauaú (MA-226) and Santa Maria (MA-198) granitoids, biotite-bearing quartz diorite enclave (MA-210B) and Jatapu volcanic rock (MA-209) samples.

| sample/zircon number | Temp.(°C) | ratios | ²⁰⁴ Pb/ ²⁰⁶ Pb | 2σ | ²⁰⁸ Pb/ ²⁰⁶ Pb | 2σ | ²⁰⁷ Pb/ ²⁰⁶ Pb | 2σ | (²⁰⁷ Pb/ ²⁰⁶ Pb) _c | 2σ | age | 2σ |
|---|-----------|------------------|--------------------------------------|-----|--------------------------------------|------|--------------------------------------|-----|--|-----|----------------------|-----------|
| Hornblende-biotite granodiorite (Água Branca Intrusive Suite, Água Branca Granite, type-area) | | | | | | | | | | | | |
| HM181/04 | 1540 | 8/8 | 0.000000 | 2 | 0.22991 | 2885 | 0.13326 | 73 | 0.13326 | 73 | 2142 | 10 |
| | | 8 (8) | | | | | USD: 0.0 | | | | mean age 2142 | 10 |
| HM181/04 | 1500 | 32/32 | 0.000039 | 4 | 0.22878 | 213 | 0.11669 | 47 | 0.11609 | 51 | 1897 | 8 |
| HM181/08 | 1500 | 28/32 | 0.000170 | 5 | 0.20347 | 104 | 0.11822 | 75 | 0.11581 | 101 | 1893 | 16 |
| HM181/09 | 1500 | 16/16 | 0.000059 | 10 | 0.22804 | 113 | 0.11683 | 36 | 0.11643 | 59 | 1902 | 9 |
| | 1550 | 6/6 | 0.000000 | 2 | 0.28207 | 147 | 0.11677 | 56 | 0.11677 | 56 | 1908 | 9 |
| HM181/13 #1450 | | 0/8 | 0.000834 | 648 | 0.16652 | 216 | 0.11759 | 247 | 0.10625 | 927 | 1736 | 160 |
| | 1500 | 8/40 | 0.000059 | 2 | 0.17693 | 88 | 0.11635 | 144 | 0.11555 | 144 | 1889 | 22 |
| | | 90 (144) | | | | | USD: 1.2 | | | | mean age 1901 | 5 |
| Biotite-hornblende quartz diorite (Água Branca Intrusive Suite, Caroebe Granite, Jaburuzinho facies) | | | | | | | | | | | | |
| MA121/01 | 1500 | 34/34 | 0.000046 | 7 | 0.20714 | 210 | 0.11666 | 11 | 0.11604 | 8 | 1896 | 1 |
| | 1550 | 28/28 | 0.000057 | 2 | 0.17310 | 96 | 0.11725 | 16 | 0.11647 | 14 | 1901 | 7 |
| MA121/04 | 1450 | 36/36 | 0.000008 | 4 | 0.18134 | 48 | 0.11604 | 22 | 0.11593 | 22 | 1889 | 4 |
| | 1500 | 32/32 | 0.000011 | 1 | 0.22198 | 72 | 0.11592 | 23 | 0.11587 | 24 | 1894 | 4 |
| MA121/07 | 1500 | 36/36 | 0.000054 | 10 | 0.22016 | 64 | 0.11673 | 15 | 0.11601 | 20 | 1896 | 3 |
| | 1550 | 36/36 | 0.000030 | 2 | 0.22078 | 49 | 0.11646 | 12 | 0.11614 | 14 | 1893 | 4 |
| | 1560 | 8/8 | 0.000000 | 0 | 0.21366 | 75 | 0.11629 | 14 | 0.11629 | 14 | 1900 | 2 |
| MA121/08 | 1450 | 14/14 | 0.000125 | 9 | 0.20966 | 67 | 0.11717 | 31 | 0.11549 | 34 | 1888 | 6 |
| | 1500 | 36/36 | 0.000037 | 1 | 0.22480 | 31 | 0.11648 | 10 | 0.11602 | 11 | 1896 | 2 |
| MA121/09 | 1450 | 36/36 | 0.000071 | 4 | 0.18868 | 62 | 0.11707 | 21 | 0.11614 | 20 | 1898 | 3 |
| | 1500 | 34/34 | 0.000053 | 2 | 0.23310 | 52 | 0.11668 | 31 | 0.11599 | 30 | 1896 | 5 |
| | 1550 | 22/22 | 0.000031 | 6 | 0.22544 | 114 | 0.11671 | 13 | 0.11636 | 15 | 1901 | 2 |
| MA121/10 *1450 | | 0/34 | 0.000251 | 18 | 0.17284 | 223 | 0.11851 | 27 | 0.11504 | 15 | 1881 | 2 |
| | *1500 | 0/4 | 0.000000 | 1 | 0.16259 | 314 | 0.11871 | 35 | 0.11871 | 35 | 1937 | 5 |
| MA121/11 | 1500 | 34/34 | 0.000038 | 3 | 0.21466 | 59 | 0.11690 | 15 | 0.11660 | 26 | 1905 | 4 |
| | | 434 (470) | | | | | USD: 2.1 | | | | mean age 1895 | 3 |
| Biotite monzogranite (Água Branca Intrusive Suite, Caroebe Granite, Alto Alegre facies) | | | | | | | | | | | | |
| MA53A/03 | 1450 | 8/8 | 0.000067 | 1 | 0.05674 | 16 | 0.12207 | 56 | 0.12118 | 56 | 1974 | 8 |
| | 1500 | 4/4 | 0.000000 | 1 | 0.06020 | 43 | 0.12034 | 15 | 0.12034 | 15 | 1962 | 2 |
| MA53A/06 | 1550 | 14/14 | 0.000000 | 0 | 0.21336 | 99 | 0.12057 | 33 | 0.12057 | 34 | 1965 | 5 |
| | | 26 (26) | | | | | USD: 1.1 | | | | mean age 1963 | 4 |
| MA53A/02 *1430 | | 0/30 | 0.000236 | 7 | 0.16696 | 20 | 0.11731 | 8 | 0.11429 | 25 | 1869 | 4 |
| | 1500 | 26/32 | 0.000042 | 2 | 0.18518 | 43 | 0.11615 | 8 | 0.11555 | 8 | 1889 | 1 |
| | 1550 | 32/32 | 0.000021 | 1 | 0.18057 | 38 | 0.11584 | 7 | 0.11555 | 7 | 1889 | 1 |
| | 1580 | 38/38 | 0.000021 | 1 | 0.17945 | 24 | 0.11599 | 9 | 0.11571 | 10 | 1891 | 1 |
| MA53A/04 | 1450 | 36/36 | 0.000296 | 4 | 0.19825 | 56 | 0.11989 | 8 | 0.11586 | 13 | 1893 | 2 |
| | 1500 | 36/36 | 0.000404 | 8 | 0.26129 | 107 | 0.1214 | 8 | 0.11587 | 10 | 1894 | 2 |
| | 1550 | 16/16 | 0.000345 | 3 | 0.2999 | 78 | 0.12078 | 11 | 0.11609 | 25 | 1897 | 4 |
| MA53A/05 #1430 | | 0/8 | 0.000257 | 1 | 0.17002 | 46 | 0.11822 | 17 | 0.11476 | 17 | 1876 | 3 |
| | 1500 | 38/38 | 0.000045 | 1 | 0.20056 | 23 | 0.11632 | 10 | 0.11571 | 10 | 1891 | 2 |
| | 1550 | 30/30 | 0.000053 | 5 | 0.20114 | 24 | 0.11632 | 17 | 0.11563 | 18 | 1890 | 3 |
| | | 252 (296) | | | | | USD: 1.4 | | | | mean age 1891 | 2 |
| Epidote leucogranite with biotite and muscovite (Igarapé Azul Granite, Estrela Guia facies) | | | | | | | | | | | | |
| MA147/01 #1450 | | 0/36 | 0.000675 | 8 | 0.17537 | 35 | 0.11932 | 14 | 0.11027 | 10 | 1804 | 2 |
| | 1500 | 4/4 | 0.000080 | 8 | 0.14060 | 43 | 0.12155 | 27 | 0.12048 | 29 | 1964 | 4 |
| | | 4 (40) | | | | | USD: 0.0 | | | | mean age 1964 | 4 |
| MA147/02 #1450 | | 0/10 | 0.001202 | 158 | 0.18253 | 433 | 0.12223 | 25 | 0.10487 | 246 | 1712 | 43 |
| | 1500 | 28/36 | 0.000041 | 4 | 0.23647 | 76 | 0.11677 | 10 | 0.11622 | 11 | 1899 | 2 |
| MA147/03 | 1500 | 12/18 | 0.000000 | 0 | 0.15104 | 156 | 0.11639 | 21 | 0.11639 | 21 | 1902 | 3 |
| MA147/04 #1450 | | 0/12 | 0.001020 | 19 | 0.20180 | 40 | 0.12254 | 30 | 0.10855 | 29 | 1776 | 5 |
| | 1500 | 36/36 | 0.000043 | 4 | 0.20913 | 26 | 0.11601 | 12 | 0.11534 | 11 | 1885 | 2 |
| MA147/05 #1450 | | 0/36 | 0.002973 | 9 | 0.34956 | 147 | 0.13919 | 25 | 0.09836 | 40 | 1594 | 8 |
| | 1500 | 90/90 | 0.000188 | 5 | 0.37980 | 43 | 0.11783 | 10 | 0.11511 | 11 | 1882 | 2 |
| MA147/06 | 1450 | 12/32 | 0.000154 | 7 | 0.21765 | 146 | 0.11657 | 22 | 0.11448 | 24 | 1882 | 4 |
| | *1500 | 0/8 | 0.000084 | 17 | 0.26827 | 89 | 0.11505 | 117 | 0.11391 | 120 | 1863 | 19 |
| MA147/07 | 1450 | 26/30 | 0.000085 | 5 | 0.23781 | 173 | 0.11666 | 12 | 0.11555 | 20 | 1889 | 3 |

Table 3 (Continued)

| sample/zircon number | Temp.(°C) | ratios | ²⁰⁴ Pb/ ²⁰⁶ Pb | 2σ | ²⁰⁸ Pb/ ²⁰⁶ Pb | 2σ | ²⁰⁷ Pb/ ²⁰⁶ Pb | 2σ | (²⁰⁷ Pb/ ²⁰⁶ Pb) _c | 2σ | age | 2σ |
|---|-----------|------------------|--------------------------------------|---------|--------------------------------------|-----------------|--------------------------------------|-----------------|--|-------------|-------------|----------|
| | 1500 | 32/32 | 0.000055 | 4 | 0.29694 | 36 | 0.11666 | 20 | 0.11583 | 14 | 1893 | 2 |
| | | 240 (380) | | | | | USD: 3.0 | | mean age | | 1891 | 6 |
| Biotite monzogranite with muscovite and epidote (Igarapé Azul Granite, Saramandaia facies) | | | | | | | | | | | | |
| MA186/1 #1450 | 0/28 | 0.001232 | 7 | 0.14034 | 23 | 0.13406 | 11 | 0.11765 | 18 | 1921 | 3 | |
| | 1500 | 24/24 | 0.000169 | 8 | 0.13142 | 37 | 0.12330 | 16 | 0.12111 | 17 | 1973 | 3 |
| MA186/5 #1450 | | | | | | | | | | | | |
| | 0/36 | 0.000873 | 26 | 0.16921 | 23 | 0.12502 | 22 | 0.11472 | 53 | 1876 | 8 | |
| | 1500 | 38/38 | 0.000180 | 10 | 0.16757 | 19 | 0.12337 | 9 | 0.12081 | 19 | 1969 | 3 |
| | 1550 | 6/10 | 0.000177 | 7 | 0.16723 | 75 | 0.12354 | 22 | 0.12117 | 24 | 1974 | 3 |
| | | 68 (136) | | | | USD: 1.0 | | mean age | | 1972 | 3 | |
| MA186/4 | 1450 | 30/36 | 0.000091 | 2 | 0.21450 | 224 | 0.11673 | 8 | 0.11557 | 8 | 1889 | 1 |
| | 1500 | 30/38 | 0.000094 | 1 | 0.20894 | 78 | 0.11665 | 10 | 0.11539 | 11 | 1886 | 2 |
| MA186/7 | 1450 | 40/40 | 0.000435 | 7 | 0.23793 | 94 | 0.12132 | 8 | 0.11558 | 10 | 1889 | 2 |
| | *1500 | 0/40 | 0.000195 | 10 | 0.21916 | 115 | 0.11976 | 9 | 0.11714 | 19 | 1913 | 3 |
| MA186/9 #1450 | 0/8 | 0.001829 | 11 | 0.20094 | 48 | 0.13380 | 29 | 0.10896 | 34 | 1782 | 6 | |
| | 1500 | 40/40 | 0.000288 | 12 | 0.19396 | 79 | 0.11973 | 18 | 0.11606 | 29 | 1897 | 4 |
| | | 140 (286) | | | | USD: 1.4 | | mean age | | 1889 | 2 | |
| Muscovite-biotite quartz diorite (biotite-bearing enclave in Igarapé Azul Granite host, Vila Catarina facies) | | | | | | | | | | | | |
| MA201B/3 | 1450 | 6/20 | 0.000000 | 0 | 0.13700 | 85 | 0.12092 | 32 | 0.12092 | 32 | 1970 | 5 |
| | 1500 | 40/40 | 0.000023 | 3 | 0.09448 | 27 | 0.12053 | 27 | 0.12026 | 29 | 1960 | 4 |
| | 1550 | 36/36 | 0.000024 | 7 | 0.09473 | 36 | 0.12134 | 38 | 0.12104 | 43 | 1972 | 6 |
| MA201B/7 | 1450 | 26/34 | 0.000065 | 15 | 0.13976 | 143 | 0.12184 | 52 | 0.12098 | 60 | 1971 | 9 |
| | | 108 (130) | | | | USD: 2.2 | | mean age | | 1967 | 6 | |
| MA201B/2 | 1500 | 16/16 | 0.000012 | 8 | 0.17761 | 99 | 0.11576 | 28 | 0.11560 | 25 | 1890 | 4 |
| | 1550 | 24/24 | 0.000034 | 7 | 0.18071 | 71 | 0.11614 | 67 | 0.11570 | 66 | 1891 | 10 |
| MA201B/4 | 1450 | 8/8 | 0.000000 | 0 | 0.15066 | 128 | 0.11625 | 100 | 0.11625 | 100 | 1900 | 15 |
| | 1500 | 34/34 | 0.000010 | 3 | 0.16836 | 146 | 0.11583 | 34 | 0.11571 | 40 | 1891 | 6 |
| | 1550 | 8/8 | 0.000000 | 0 | 0.16394 | 81 | 0.11629 | 88 | 0.11629 | 88 | 1900 | 14 |
| MA201B/8 | 1450 | 32/32 | 0.000072 | 4 | 0.19673 | 85 | 0.11661 | 69 | 0.11559 | 70 | 1889 | 11 |
| | 1500 | 34/34 | 0.000039 | 5 | 0.19779 | 87 | 0.11668 | 39 | 0.11622 | 43 | 1899 | 7 |
| MA201B/9 | 1500 | 36/36 | 0.000035 | 15 | 0.22993 | 53 | 0.11587 | 29 | 0.11542 | 28 | 1887 | 4 |
| | 1550 | 28/28 | 0.000043 | 11 | 0.24776 | 167 | 0.11620 | 61 | 0.11563 | 70 | 1890 | 11 |
| | | 220 (220) | | | | USD: 1.3 | | mean age | | 1891 | 3 | |
| Andesite (Jatapu Volcanic rock) | | | | | | | | | | | | |
| MA208/7 *1450 | 0/14 | 0.000081 | 7 | 0.15664 | 12 | 0.12037 | 35 | 0.1192 | 35 | 1945 | 5 | |
| | 1500 | 34/34 | 0.00005 | 35 | 0.11339 | 10 | 0.12123 | 32 | 0.12082 | 31 | 1969 | 5 |
| MA208/9 | 1450 | 28/28 | 0.000022 | 2 | 0.02024 | 19 | 0.12095 | 24 | 0.12063 | 21 | 1966 | 3 |
| | 1480 | 28/36 | 0.000082 | 11 | 0.05157 | 139 | 0.12193 | 55 | 0.12089 | 56 | 1970 | 8 |
| MA208/11 | 1450 | 16/22 | 0.000118 | 8 | 0.05429 | 216 | 0.12181 | 35 | 0.12025 | 37 | 1960 | 5 |
| MA208/12 | 1450 | 8/8 | 0.00007 | 24 | 0.12551 | 61 | 0.12114 | 161 | 0.1202 | 164 | 1960 | 24 |
| | | 114 (142) | | | | USD: 1.3 | | mean age | | 1966 | 3 | |
| MA208/2 | 1450 | 32/36 | 0.000178 | 17 | 0.33144 | 982 | 0.11784 | 62 | 0.11558 | 34 | 1889 | 5 |
| | 1500 | 38/38 | 0.000035 | 6 | 0.34356 | 378 | 0.11642 | 22 | 0.11587 | 22 | 1894 | 3 |
| MA208/3 | 1500 | 30/36 | 0.000059 | 47 | 0.24595 | 483 | 0.1161 | 45 | 0.1154 | 25 | 1886 | 4 |
| MA208/4 | 1500 | 22/22 | 0.000031 | 3 | 0.27797 | 88 | 0.11663 | 33 | 0.11612 | 22 | 1898 | 3 |
| MA208/5 *1500 | 0/8 | 0.000000 | 2 | 0.34995 | 724 | 0.11357 | 179 | 0.11357 | 179 | 1858 | 28 | |
| MA208/6 *1450 | 0/4 | 0.000000 | 2 | 0.22383 | 372 | 0.11465 | 29 | 0.11465 | 29 | 1875 | 5 | |
| MA208/10 | 1450 | 8/8 | 0.000032 | 38 | 0.15001 | 72 | 0.11608 | 106 | 0.11565 | 118 | 1890 | 18 |
| | | 130 (152) | | | | USD: 2.2 | | mean age | | 1893 | 5 | |
| Pyroxene-bearing tonalite (Santa Maria Enderbite) | | | | | | | | | | | | |
| MA198/1 *1450 | 0/16 | 0.000239 | 11 | 0.15289 | 215 | 0.11188 | 42 | 0.1083 | 31 | 1830 | 7 | |
| | 1500 | 36/36 | 0.000042 | 3 | 0.21636 | 110 | 0.11624 | 13 | 0.11564 | 10 | 1890 | 2 |
| | 1550 | 14/14 | 0.000067 | 8 | 0.21481 | 46 | 0.1163 | 37 | 0.11549 | 55 | 1888 | 9 |
| MA198/2 | 1450 | 36/36 | 0.000036 | 5 | 0.17197 | 75 | 0.11597 | 24 | 0.11554 | 22 | 1889 | 3 |
| | 1500 | 32/32 | 0.000012 | 1 | 0.19441 | 154 | 0.11545 | 27 | 0.11539 | 25 | 1886 | 4 |
| | 1550 | 32/32 | 0.000024 | 2 | 0.20493 | 41 | 0.11609 | 8 | 0.11581 | 8 | 1893 | 1 |
| | *1600 | 0/4 | 0.000038 | 6 | 0.21786 | 88 | 0.11462 | 14 | 0.1141 | 16 | 1874 | 2 |

Table 3 (Continued)

| sample/zircon number | Temp.(°C) | ratios | ²⁰⁴ Pb/ ²⁰⁶ Pb | 2σ | ²⁰⁸ Pb/ ²⁰⁶ Pb | 2σ | ²⁰⁷ Pb/ ²⁰⁶ Pb | 2σ | (²⁰⁷ Pb/ ²⁰⁶ Pb) _c | 2σ | age | 2σ |
|---|--------------|------------------|--------------------------------------|----|--------------------------------------|-----|--------------------------------------|----|--|-----------------|-------------|----------|
| MA198/3 | <i>*1450</i> | <i>0/36</i> | <i>0.000047</i> | 2 | <i>0.13994</i> | 50 | <i>0.11539</i> | 18 | <i>0.11456</i> | 11 | 1886 | 3 |
| | 1500 | 40/40 | 0.000027 | 1 | 0.16674 | 64 | 0.11592 | 11 | 0.11557 | 13 | 1889 | 2 |
| | 1550 | 32/32 | 0.000027 | 4 | 0.17937 | 84 | 0.11608 | 8 | 0.11577 | 8 | 1892 | 1 |
| MA198/4 | 1450 | 28/28 | 0.000058 | 5 | 0.19464 | 275 | 0.11627 | 16 | 0.11556 | 16 | 1889 | 3 |
| MA198/5 | 1450 | 36/36 | 0.000041 | 2 | 0.23494 | 36 | 0.11609 | 12 | 0.1155 | 14 | 1888 | 2 |
| | 1500 | 32/32 | 0.000088 | 2 | 0.23966 | 43 | 0.11701 | 11 | 0.1159 | 9 | 1894 | 1 |
| | <i>*1550</i> | <i>0/34</i> | <i>0.000115</i> | 6 | <i>0.23739</i> | 85 | <i>0.11647</i> | 13 | <i>0.11498</i> | 11 | 1880 | 2 |
| | 1600 | 34/34 | 0.000072 | 2 | 0.23677 | 29 | 0.11657 | 8 | 0.11555 | 7 | 1889 | 1 |
| | | 232 (392) | | | | | USD: 1.2 | | | mean age | 1891 | 1 |
| Mylonitic monzogranite (Murauá Granite) | | | | | | | | | | | | |
| MA226/10 | <i>*1450</i> | <i>0/6</i> | <i>0.000123</i> | 49 | <i>0.08105</i> | 57 | <i>0.14506</i> | 22 | <i>0.14347</i> | 67 | 2270 | 8 |
| | 1500 | 32/32 | 0.000022 | 9 | 0.11179 | 77 | 0.15176 | 14 | 0.15176 | 14 | 2366 | 2 |
| MA226/16 | <i>#1450</i> | <i>0/32</i> | <i>0.004657</i> | 51 | <i>0.27911</i> | 164 | <i>0.19585</i> | 49 | <i>0.13479</i> | 34 | 2161 | 4 |
| | 1480 | 36/36 | 0.000029 | 1 | 0.11560 | 36 | 0.15111 | 10 | 0.15073 | 11 | 2355 | 1 |
| | 1510 | 38/38 | 0.000009 | 1 | 0.13326 | 18 | 0.15129 | 14 | 0.15118 | 14 | 2360 | 2 |
| | | 106 (144) | | | | | USD: 4.1 | | | mean age | 2359 | 7 |
| MA226/12 | 1450 | 20/20 | 0.000221 | 1 | 0.13016 | 37 | 0.11840 | 11 | 0.11552 | 13 | 1888 | 2 |
| | 1500 | 28/28 | 0.000080 | 3 | 0.12844 | 88 | 0.11667 | 14 | 0.11558 | 17 | 1889 | 3 |
| | <i>#1550</i> | <i>0/12</i> | <i>0.000349</i> | 37 | <i>0.14478</i> | 68 | <i>0.11744</i> | 19 | <i>0.11272</i> | 54 | 1844 | 9 |
| MA226/14 | 1500 | 22/28 | 0.000086 | 2 | 0.12237 | 53 | 0.11623 | 8 | 0.11510 | 9 | 1882 | 1 |
| MA226/17 | <i>*1450</i> | <i>0/40</i> | <i>0.000280</i> | 2 | <i>0.14414</i> | 72 | <i>0.11794</i> | 11 | <i>0.11420</i> | 12 | 1868 | 2 |
| | <i>*1500</i> | <i>0/28</i> | <i>0.000038</i> | 2 | <i>0.14879</i> | 40 | <i>0.11782</i> | 27 | <i>0.11734</i> | 27 | 1916 | 4 |
| MA226/18 | 1500 | 38/38 | 0.000039 | 2 | 0.12377 | 14 | 0.11606 | 10 | 0.11552 | 10 | 1888 | 2 |
| | 1550 | 38/38 | 0.000048 | 2 | 0.12261 | 14 | 0.11626 | 8 | 0.11563 | 8 | 1890 | 1 |
| | | 146 (232) | | | | | USD: 1.8 | | | mean age | 1888 | 3 |
| MA226/01 | 1500 | 36/36 | 0.000145 | 3 | 0.12202 | 14 | 0.11660 | 7 | 0.11463 | 9 | 1874 | 1 |
| | 1550 | 32/32 | 0.000165 | 3 | 0.12276 | 46 | 0.11660 | 7 | 0.11430 | 13 | 1869 | 2 |
| MA226/02 | <i>#1450</i> | <i>0/34</i> | <i>0.000365</i> | 7 | <i>0.11253</i> | 17 | <i>0.11742</i> | 15 | <i>0.11238</i> | 11 | 1839 | 2 |
| | <i>*1500</i> | <i>0/36</i> | <i>0.000261</i> | 11 | <i>0.10639</i> | 48 | <i>0.11677</i> | 11 | <i>0.11341</i> | 11 | 1855 | 2 |
| MA226/03 | 1500 | 38/38 | 0.000216 | 3 | 0.15026 | 63 | 0.11688 | 11 | 0.11410 | 12 | 1866 | 2 |
| | <i>*1550</i> | <i>0/4</i> | <i>0.000251</i> | 2 | <i>0.15427</i> | 148 | <i>0.11697</i> | 30 | <i>0.11359</i> | 30 | 1858 | 5 |
| | | 106 (180) | | | | | USD: 2.6 | | | mean age | 1871 | 5 |

Notes: Crystal numbers are indicated. The column number of ratios shows the total of isotopic ratios used to the age calculation and, in parenthesis, the total isotopic ratios measured. Evaporation steps in italics were not included in the age calculation of each grain due to: * too much higher or lower values of the ²⁰⁷Pb/²⁰⁶Pb ratio in relation to the average of the zircon, and # ²⁰⁴Pb/²⁰⁶Pb > 0.0004.

Table 4. U-Pb isotopic data (ID-TIMS) for zircon from Igarapé Azul granite sample (MA-186A).

| Sample | Weight (mg) | Concentrations | | | | Atomic ratios | | | | | | Ages (Ma) | | | |
|-----------|-------------|----------------|--------|--|-------|--|-------|--|-------|---|----------|--------------------------------------|--------------------------------------|--|----|
| | | ppm U | ppm Pb | ²⁰⁶ Pb/ ²⁰⁴ Pb ^{c1} | %err | ²⁰⁷ Pb*/ ²³⁵ U ^{c2} | %err | ²⁰⁶ Pb*/ ²³⁸ U ^{c2} | %err | ²⁰⁷ Pb*/ ²⁰⁶ Pb ^{c2} | %err | ²⁰⁶ Pb*/ ²³⁸ U | ²⁰⁷ Pb*/ ²³⁵ U | ²⁰⁷ Pb*/ ²⁰⁶ Pb* (%) | |
| MA-186A-1 | 0.56 | 13.90 | 2.49 | 418.134 | 0.263 | 2.19649 | 0.272 | 0.146600 | 0.241 | 0.899070 | 0.108666 | 882 | 1180 | 1777 | 50 |
| MA-186A-2 | 0.465 | 59.51 | 8.76 | 300.536 | 0.099 | 1.62097 | 0.402 | 0.114056 | 0.377 | 0.938852 | 0.103076 | 696 | 978 | 1680 | 41 |
| MA-186A-3 | 0.92 | 9.33 | 1.49 | 344.142 | 1.610 | 1.93824 | 2.970 | 0.132913 | 2.870 | 0.974348 | 0.105764 | 804 | 1094 | 1728 | 47 |
| MA-186A-4 | 0.273 | 92.60 | 18.53 | 488.003 | 0.210 | 2.51441 | 0.422 | 0.166274 | 0.417 | 0.988353 | 0.109676 | 992 | 1276 | 1794 | 55 |

Notes: Maximum total blanks for zircon analyses are 10 pg for Pb and 2 pg for U. Stacey and Kramers (1975) values were used.

^{c1} Measure ratios corrected for mass fractionation; ^{c2} Ratios corrected for spike, fractionation, blank and initial common Pb following Stacey and Kramers (1975) model. Erros are at 2 σ; ^d Concordance in relation to Concordia curve: 100(²⁰⁶Pb/²³⁸U)/(²⁰⁷Pb/²⁰⁶Pb).

Table 5. Summary of new and previous Pb-Pb and U-Pb (ID-TIMS and SHRIMP) ages yielded by zircon from volcano-plutonic rocks younger than 1900 Ma of the Ventuari-Tapajós (or Tapajós-Parima) Province. Local WR Rb-Sr isochron is also showed.

| Symbol | Reference Number | Rock type (sample code) | Stratigraphic unit | Age (Ma) | Reference | Method |
|--|------------------|---|---|-----------|---------------------------------|--------|
| Uatumã-Anauá Domain (Southern Area) | | | | | | |
| UA1 | 1 | Madeira Granite (PHR-178) | Madeira Suite | 1817 ± 2 | Costi <i>et al.</i> (2000) | C |
| | 2 | Madeira Granite (PHR-191) | Madeira Suite | 1820 ± 1 | Costi <i>et al.</i> (2000) | C |
| | 3 | Madeira Granite (PHR-193) | Madeira Suite | 1822 ± 2 | Costi <i>et al.</i> (2000) | C |
| | 5 | Madeira Granite (PHR-125) | Madeira Suite | 1824 ± 2 | Costi <i>et al.</i> (2000) | C |
| | 5 | Europa Granite (PHR-192) | Madeira Suite | 1829 ± 1 | Costi <i>et al.</i> (2000) | C |
| | 6 | Moderna Granite (MJ-59A) | Madeira Suite | 1814 ± 27 | Santos <i>et al.</i> (1997b) | B |
| UA2 | 7 | Weathered gneiss (JO-05) | Mapuera Suite? | 1868 ± 8 | Santos <i>et al.</i> (2002) | E |
| | 8 | Mylonitic granite (MF-17) | Meretxa Granite (Mapuera Suite?) | 1869 ± 10 | CPRM (2003) | E |
| | 9 | Hastingsite syenogranite (km 199) | Abonari Granite (Mapuera Suite) | 1871 ± 5 | Santos <i>et al.</i> (2002) | E |
| | 10 | Mylonitic monzogranite (MA-226) | Murauá Granite (Mapuera Suite?) | 1871 ± 5 | This paper | C |
| | 11 | Charnockite (MF-99) | Jaburu Charnockite | 1873 ± 6 | Santos <i>et al.</i> (2001a) | E |
| | 12 | Mylonite (JO-08) | Alalaú Granite (Mapuera Suite?) | 1876 ± 4 | Santos <i>et al.</i> (2002) | E |
| | 13 | Weathered granitoid (JO-07) | Mapuera Suite? | 1879 ± 3 | Santos <i>et al.</i> (2002) | E |
| | 14 | Weathered granitoid (JO-06) | Mapuera Suite? | 1880 ± 3 | Santos <i>et al.</i> (2002) | E |
| UA3 | 15 | Epizonal rhyolite | Iricoumé Volcanics (Presidente Figueiredo region) | 1883 ± 4 | Valério <i>et al.</i> (2005) | C |
| | 16 | Rhyolite (PHR-06) | Iricoumé Volcanics (Pitinga region) | 1888 ± 3 | Costi <i>et al.</i> (2000) | C |
| UA4 | 17 | Monzogranite (MA-186A) | Igarapé Azul Granite (Saramandaia Facies) | 1889 ± 2 | This paper | C |
| | 18 | Monzogranite (MA-147A) | Igarapé Azul Granite (Cinco Estrelas Facies) | 1889 ± 5 | This paper | C |
| | 19 | Granitic veins in biotite-bearing enclave (MA-201B) | Igarapé Azul Granite (Vila Catarina facies) | 1891 ± 3 | This paper | C |
| | 20 | Monzogranite (MA-186A) | Igarapé Azul Granite (Saramandaia Facies) | 1913 ± 4 | This paper | D |
| UA5 | 21 | Mylonitic biotite granite | Água Branca Suite (Presidente Figueiredo region) | 1890 ± 2 | Valério (2006) | C |
| | 22 | Enderbite (MA-198) | Santa Maria Enderbite | 1891 ± 1 | This paper | C |
| | 23 | Monzogranite (MA-53A) | Água Branca Suite (Caroebe Granite, Alto Alegre Facies) | 1891 ± 2 | This paper | C |
| | 24 | Quartz Monzodiorite (MF-68A) | Água Branca Suite (Igarapé Dias Quartz Monzodiorite) | 1891 ± 6 | CPRM (2003) | E |
| | 25 | Quartz Monzodiorite (MA-121) | Água Branca Suite (Caroebe Granite, Jaburuzinho Facies) | 1895 ± 3 | This paper | C |
| | 26 | Porphyritic biotite granite | Água Branca Suite (Presidente Figueiredo region) | 1895 ± 6 | Valério (2006) | C |
| | 27 | Mylonitic hornblende-biotite granite | Água Branca Suite (Presidente Figueiredo region) | 1898 ± 3 | Valério (2006) | C |
| | 28 | Granodiorite (HM-181) | Água Branca Suite (Água Branca Granite, type-area) | 1901 ± 5 | This paper | C |
| | 29 | - | Água Branca Suite (Northwestern of Pará) | 1910 ± 23 | Jorge-João <i>et al.</i> (1985) | A |
| UA6 | 30 | Porphyry Dacite (MA-209) | Jatapu Volcanics (Jatapu River) | 1893 ± 2 | Macambira <i>et al.</i> (2002) | C |
| | 31 | Andesite (MA-208) | Jatapu Volcanics (Jatapu River) | 1893 ± 4 | This paper | C |
| | 32 | Canoas Rhyodacite (MF-34) | Jatapu Volcanics (BR-174, km 164) | 1896 ± 7 | Santos <i>et al.</i> (2002) | E |
| Tapajós Domain | | | | | | |
| T1 | 33 | Caroçal Granite | Maloquinha Suite | 1870 ± 4 | Santos <i>et al.</i> (2001b) | E |
| | 34 | Pepita Alaskitic Granite | Maloquinha Suite | 1872 ± 2 | Santos <i>et al.</i> (2001b) | E |
| | 35 | Barro Vermelho Granite | Maloquinha Suite | 1873 ± 6 | Santos <i>et al.</i> (2001b) | E |
| | 36 | Santa Rita Granite | Maloquinha Suite | 1874 ± 7 | Santos <i>et al.</i> (2001b) | E |
| | 37 | Leucomonzogranite | Maloquinha Suite | 1880 ± 9 | Lamarão <i>et al.</i> (2002) | C |
| | 38 | Syenogranite | Maloquinha Suite | 1882 ± 4 | CPRM (2000b) | C |
| T2 | 39 | Rosa de Maio Granite | Parauari Suite | 1879 ± 3 | Santos <i>et al.</i> (1997a) | D |
| | 40 | Anortosite | Ingarana Gabbro | 1879 ± 3 | Santos <i>et al.</i> (2001b) | E |
| | 41 | Gabbro | Ingarana Gabbro | 1880 ± 2 | Santos <i>et al.</i> (2004) | E |
| | 42 | Monzogranite | Jardim do Ouro Granite | 1880 ± 3 | Lamarão <i>et al.</i> (2002) | C |
| | 43 | Creporei River Granite | Parauari Suite | 1883 ± 2 | CPRM (2000b) | E |
| | 44 | Penedo Granite | Parauari Suite | 1883 ± 4 | Santos <i>et al.</i> (2001b) | E |
| | 45 | Cumaru Rapakivi Granite | Parauari Suite | 1883 ± 8 | Brito <i>et al.</i> (1999) | C |
| | 46 | Gabbro | Ingarana Gabbro | 1887 ± 3 | CPRM (2000b) | C |
| | 47 | Sao Jorge Monzogranite | Younger São Jorge Granite? | 1887 ± 10 | Santos <i>et al.</i> (2004) | E |
| | 48 | Monzogranite | Younger São Jorge Granite | 1891 ± 3 | Lamarão <i>et al.</i> (2002) | C |
| | 49 | Ouro Roxo Tonalite | Tropas Granite | 1892 ± 3 | Santos <i>et al.</i> (2004) | E |

Table 5 (continued)

| Symbol | Reference Number | Rock type (sample code) | Stratigraphic unit | Age (Ma) | Reference | Method |
|--------|------------------|-------------------------|-----------------------------|----------|---------------------------------|--------|
| | 50 | Abacaxis Monzogranite | Tropas Granite | 1892 ± 6 | Santos <i>et al.</i> (1997a) | D |
| | 51 | Granite | Parauari Suite | 1893 ± 2 | CPRM (2000b) | C |
| | 52 | Tropas Tonalite | Tropas Granite | 1898 ± 2 | Santos <i>et al.</i> (2000) | E |
| T3 | 53 | Pacu Rhyodacite Tuff | Iriri Volcanics | 1870 ± 8 | Santos <i>et al.</i> (2001b) | E |
| | 54 | Ignimbrite | Moraes de Almeida Volcanics | 1875 ± 4 | Lamarão <i>et al.</i> (2002) | C |
| | 55 | Trachyte | Moraes de Almeida Volcanics | 1881 ± 4 | Lamarão <i>et al.</i> (2002) | C |
| | 56 | Rhyolite | Iriri Volcanics | 1888 ± 2 | CPRM (2000b) | C |
| | 57 | Alkali-rhyolite | Iriri Volcanics | 1888 ± 2 | Dall'Agnol <i>et al.</i> (1999) | C |
| | 58 | Rhyolite | Iriri Volcanics | 1888 ± 6 | Moura <i>et al.</i> (1999) | D |
| | 59 | Rhyolite | Moraes de Almeida Volcanics | 1890 ± 6 | Lamarão <i>et al.</i> (2002) | C |
| | 60 | Dacite | Iriri Volcanics | 1893 ± 3 | CPRM (2000c) | C |
| | 61 | Uruá Tuff | Iriri Volcanics | 1897 ± 5 | Santos <i>et al.</i> (2004) | E |
| | 62 | Basalt | Iriri Volcanics | 1898 ± 7 | Santos <i>et al.</i> (1997a) | D |

Notes: A. WR Rb-Sr isochron; B. Pb-Pb evaporation on single filament; C. Pb-Pb evaporation on double filament; D. U-Pb ID TIMS; E. U-Pb SHRIMP. Numbers 1-62 are the same of fig. 15.

Table 6. Summary of ages and possible sources of the inherited zircon crystals from volcano-plutonic rocks younger than 1900 Ma of the Ventuari-Tapajós (or Tapajós-Parima) Province.

| Domain | Reference Number | Rock type | Stratigraphic unit | Age (Ma) | Inheritance Interpretation | Reference | Method |
|---|------------------|---|---|-----------|------------------------------|------------------------------|----------|
| <i>Utumã-Anauá Domain (Southern Area)</i> | | | | | | | |
| UA6 | 31 | Andesite (Jatapu river) | Jatapu Volcanic | 1966 ± 3 | Martins Pereira Granite | This paper | C |
| UA4 | 18 | Monzogranite (Cinco Estrelas Facies) | Igarapé Azul Granite | 1964 ± 4 | Martins Pereira Granite | This paper | C |
| | | Biotite-bearing meta-quartz diorite enclave | Igarapé Azul Granite | 1967 ± 6 | Martins Pereira Granite | This paper | C |
| | 17 | Monzogranite (Saramandaia Facies) | Igarapé Azul Granite | 1972 ± 3 | Martins Pereira Granite | This paper | C |
| UA5 | 23 | Monzogranite (Alto Alegre Facies) | Água Branca Suite (Caroebe Granite) | 1963 ± 4 | Martins Pereira Granite | This paper | C |
| | | Granodiorite | Água Branca Suite (Água Branca Granite) | 2142 ± 10 | Early Transamazonian | This paper | C |
| UA2 | 10 | Murauá Granite | Mapuera Suite | 1888 ± 3 | Água Branca Suite? | This paper | C |
| | | | | 2359 ± 7 | Siderian (Central Amazonian) | This paper | C |
| <i>Tapajós Domain</i> | | | | | | | |
| T3 | 53 | Pacu Rhyodacite Tuff | Iriri Volcanic | 1956 ± 7 | Creporizão Suite | Santos <i>et al.</i> (2001b) | E |
| T2 | 47 | Monzogranite | Younger São Jorge Granite? | 1962 ± 19 | Creporizão Suite | Santos <i>et al.</i> (2004) | E |
| | | | | 2733 ± 9 | Archean | | E |
| | 41 | Gabbro | Ingarana Gabbro | 2007 ± 6 | Cuiú-Cuiú Complex | Santos <i>et al.</i> (2004) | E |
| T3 | 62 | Basalt | Iriri Volcanic | 1972 ± 15 | Creporizão Suite | Santos <i>et al.</i> (1997a) | D |
| | | | | 2014 ± 11 | Cuiú-Cuiú Complex | Santos <i>et al.</i> (2004) | E |
| | | | | | | 2457 ± 7 | Siderian |
| | | | | 2662 ± 18 | Archean | E | |
| T1 | 36 | Santa Rita Granite | Maloquinha Suite | 1983 ± 19 | Creporizão Suite | Santos <i>et al.</i> (2001b) | E |
| | | | | 2459 ± 11 | Siderian | E | |
| | | | | 2849 ± 10 | Archean | E | |
| | 33 | Caroçal Granite | Maloquinha Suite | 1999 ± 8 | Cuiú-Cuiú Complex | Santos <i>et al.</i> (2001b) | E |
| | | | | 2634 ± 9 | Archean | E | |
| | | | | 2679 ± 10 | Archean | E | |
| | | | | 2714 ± 8 | Archean | E | |
| | 35 | Barro Vermelho Granite | Maloquinha Suite | 2207 ± 8 | Early Transamazonian | Santos <i>et al.</i> (2001b) | E |

Notes: Method references as in table 5. Reference Number 1 to 62 and symbols UA1-T3 are as in Fig. 15.

Nd-Pb isotopic constraints on Paleoproterozoic geodynamic evolution of the central portion of Guyana Shield, Brazil

Marcelo E. Almeida^{1,2*}, Moacir J. B. Macambira², Franck Poitrasson³, Cândido A.V. Moura², Elma C. Oliveira²

¹ CPRM – Geological Survey of Brazil, Av. André Araújo 2160, Aleixo, CEP 69060-001, Manaus, Amazonas, Brazil

² Isotope Geology Laboratory, Center of Geosciences, Federal University of Pará, Rua Augusto Corrêa s/n, Guamá, CEP 66075-110, Belém, Pará, Brazil

³ Laboratoire des Mécanismes et Transferts en Géologie, CNRS, Université Paul Sabatier, Av. Edouard Belin 14, 31000 - Toulouse, France

* Corresponding author; ph.: +55-92-2126-0301, fax: +55-92-2126-0319, e-mail adress: marcelo_almeida@ma.cprm.gov.br

ARTIGO A SER SUBMETIDO

Words: summary (91), abstract (320 words), body text (9452 words, including references), figure captions (698 words) and table caption (292 words)

Total: 4 tables and 8 figures

ABSTRACT

INTRODUCTION

REGIONAL GEOLOGY AND PREVIOUS GEOCHRONOLOGICAL DATA

ANALYTICAL PROCEDURES

Nd AND Pb ISOTOPE RESULTS

Sm-Nd isotopes on whole-rock

Pb isotopes on leached feldspars

DISCUSSION

Nd isotope signatures of the Ventuari-Tapajós (or Tapajós-Parima), Maroni-Itacaiúnas (or Transamazonic) and Central Amazonian (or Amazon) Geochronological Provinces and their boundaries in the Southeastern Roraima

Crustal formation ages and constraints on sources based on integrated use of the Pb-Nd isotopes: Martins Pereira, Igarapé Azul and Caroebe granitoids examples

An outline of geodynamic evolution of central portion of Guyana Shield at the Orosirian times

CONCLUSIONS

ACKNOWLEDGMENTS

REFERENCES

ABSTRACT

Previous zircon geochronology and new Nd-Pb isotopic data in SE Roraima, central portion of Guyana Shield, show that the granitoids from northern and southern areas of Uatumã-Anauá domain exhibits different magmatic events with distinct interval ages, yielding important evidences of crustal origin. In the Northern Uatumã-Anauá domain, the 1.97 Ga Martins Pereira Granite shows Nd_{DM} model ages with 2.67-2.33 Ga range, including negative ϵNd (-0.92 to -4.74) and high $^{207}Pb/^{204}Pb$ (15.58-15.70) ratios. This renders the Martins Pereira granitoids a good example of high-K calc-alkaline magmatism generated by reworking-recycling of pre-existing older crust (e.g. Archean Central Amazonian province sources), related probably to the final stages of Anauá Arc evolution (collisional event). The S-type Serra Dourada Granite is related to the early collisional stage (1962 Ma) and their Nd_{DM} model ages (2.53-2.39 Ga) and ϵNd (-1.08 to -4.34) imply also in older crustal-derived sources. The most suitable sources are the 1.96 Ga metavolcano-sedimentary sequence (Caurane Group related) that shows similar Nd_{DM} model ages (2.46-2.27 Ga, local 2.64 Ga) and ϵNd +1.23 to -4.16. In the southern Uatumã-Anauá domain, the 1.90-1.89 Ga Caroebe Granite presents very homogeneous $^{207}Pb/^{204}Pb$ ratios (ca. 15.54). The ϵNd (+0.46 to -2.05, locally -2.60 to -4.27) and Nd_{DM} model ages (2.29-2.16 Ga, locally 2.47-2.37 Ga) are similar to the 1.89 Ga Igarapé Azul granitoids (ϵNd -0.02 to -1.61 and Nd_{DM} 2.28-2.14 Ga), however this last shows more scattered $^{207}Pb/^{204}Pb$ ratios (15.42-15.65). Thus, no conspicuous juvenile pattern is identified and mantle-derived origin is not probably a viable model for these granitoids. Furthermore, the crystallization and model ages show a gap of at least 240 Ma, and their origin involves probably Transamazonian TTG metagneous rocks (juvenile crust?) and Orosirian metavolcano-sedimentary sources by partial melting in association with older sialic crustal sources (e.g. Central Amazonian and Archean sources) in the extensional setting driven by underplating mechanism. This geological picture pointed out similarities with other domains of the Ventuari-Tapajós (or Tapajós-Parima) geochronological province.

Keywords: Nd-Pb isotopes, granitoids, high-K calc-alkaline, Guyana Shield, geodynamic evolution

INTRODUCTION

The Guyana Shield, with a surface area of nearly 1.5 million km², represents the northern segment of the Amazonian Craton in South America and was partially formed during dominantly protracted periods of intense granitic magmatism between 2.1 and 1.9 Ga (**Fig. 1a-b**). There, geochronological and isotopic studies were scarce, which make hard to establish a refined timing of the lithostructural and, magmatic and metamorphic events up until the last decade, as well as, to draw more realistic tectonic models for the Guyana Shield, mainly in the central and westernmost regions. The main crustal evolution models for this region (**Fig. 1a-b**; Cordani *et al.*, 1979, Teixeira *et al.*, 1989, Tassinari 1996, Tassinari and Macambira, 1999, 2004; Santos *et al.*, 2000, 2004) pointed out that several Paleoproterozoic orogenic

belts (e.g. Ventuari-Tapajós or Tapajós-Parima and Maroni-Itacaiúnas or Transamazon) provinces are accreted along the time to an older Archean craton (Central Amazonian Province).

The study area is located in the southeastern Roraima State (Brazil), central portion of the Guyana Shield and, despite of recent geological, geochemical and geochronological data (e.g. Oliveira *et al.*, 1996, Santos *et al.*, 2000, Almeida *et al.*, 2002, Almeida and Macambira, 2003, CPRM 2000, 2003), its characteristic and significance are not fully understood. This paper focuses the discussion on the crustal formation of the central portion of the Guyana Shield (**Fig. 1**), using previous zircon geochronological data and new Nd-Pb isotopic signatures of granitoids to further constraints their lithostratigraphy, sources (mainly unexposed basement terranes) and geodynamic evolution. Thus, the studied granitoids and suitable sources could allow the construction of tectonic models, using isotope tracers in order to more clearly define the nature of the crust and relative contributions of crustal-derived and/or mantle-derived melts.

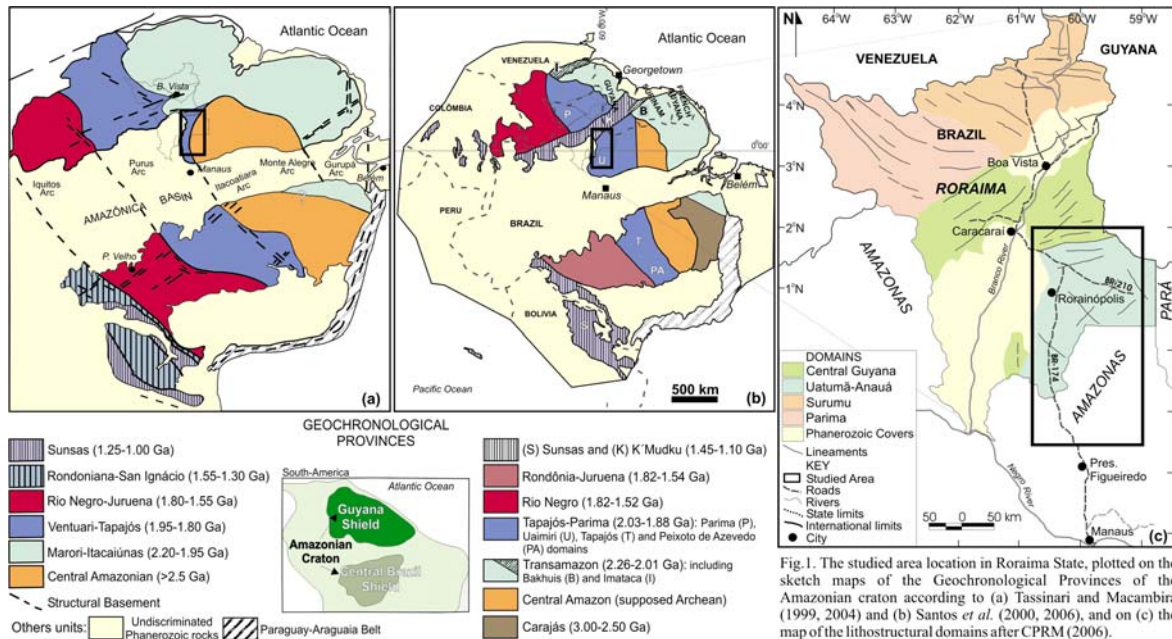


Fig. 1. The studied area location in Roraima State, plotted on the sketch maps of the Geochronological Provinces of the Amazonian craton according to (a) Tassinari and Macambira (1999, 2004) and (b) Santos *et al.* (2000, 2006), and on (c) the map of the lithostratigraphic domains after CPRM (2006).

REGIONAL GEOLOGY AND PREVIOUS GEOCHRONOLOGICAL DATA

Regional geological maps (CPRM 2000, Almeida and Macambira, submitted) and some few zircon geochronological data (Almeida *et al.*, 1997, Santos *et al.*, 1997, Macambira *et al.*, 2002, CPRM, 2003) have showed that paleoproterozoic granitoids and volcanic rocks (1.97-1.81 Ga) are widespread in southeastern Roraima, intruding inliers of basement rocks with maximum ages around 2.03 Ga (Faria *et al.*, 2002). According to the geochronological provinces models (e.g. Tassinari and Macambira 1999, 2004, Santos *et al.*, 2000, 2004, 2006) the study area is part of the Ventuari-Tapajós (western part) or Tapajós-Parima and Central Amazonian (eastern part) provinces, and probably of the Maroni-Itacaiúnas Province and K'Mudku Shear Belt (northernmost portion) (**Fig. 1a-b**).

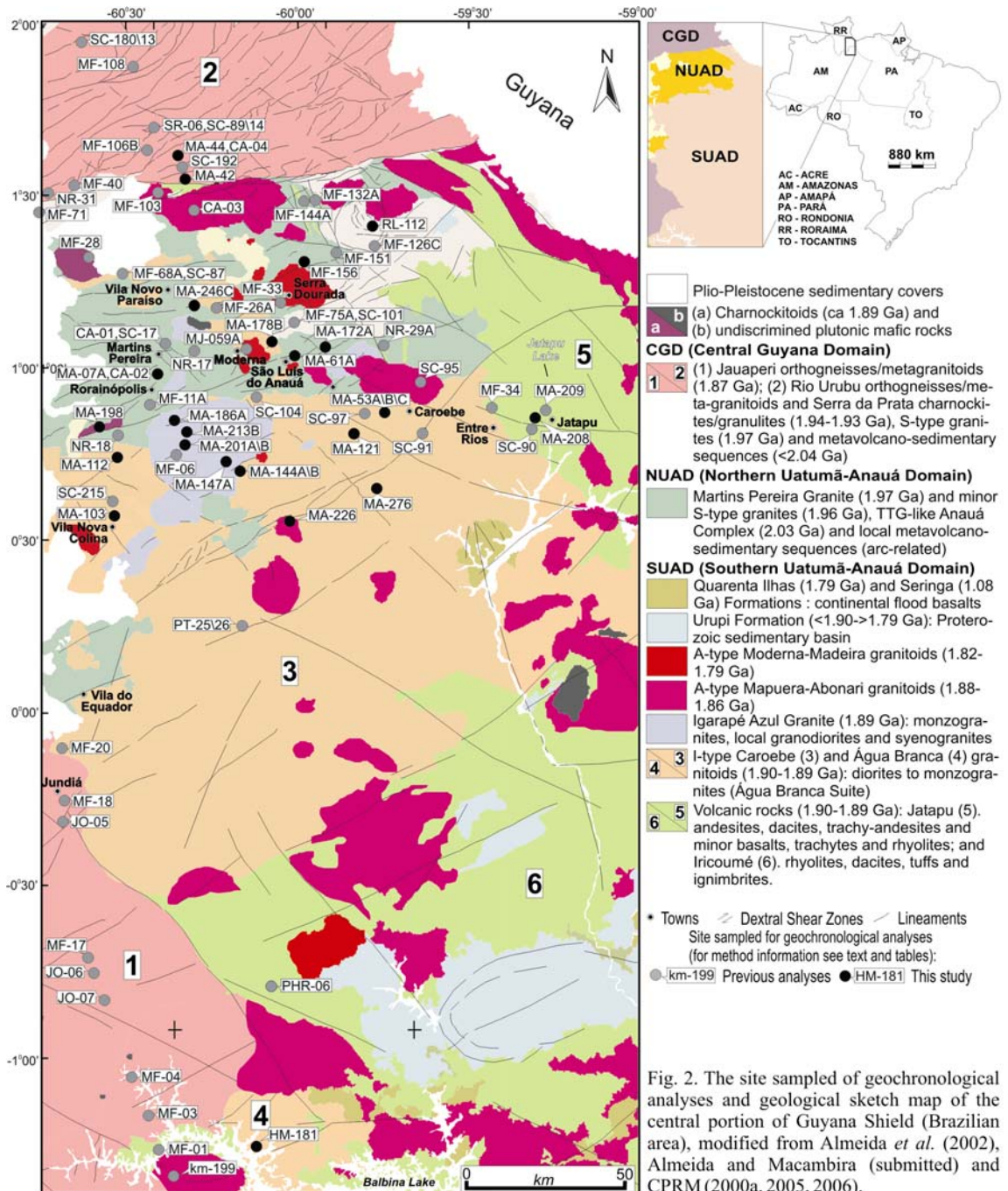
The Ventuari-Tapajós or Tapajós-Parima provinces are paleoproterozoic orogenic belts with north-northwest trends and include geological units which range from ca. 2.10 to 1.87 Ga in age (Santos *et al.*, 2000; Tassinari and Macambira 1999, 2004). The Central Amazonian Province (**Fig. 1a-b**) includes granitoids and volcanic rocks with no regional metamorphism and compressional folding (Tassinari and Macambira, 1999, Santos *et al.*, 2000), the basement rarely crops out and is poorly studied. The estimation of its formation age, as yielded by some Nd model ages, is ca. 2.3-2.5 Ga and older (Tassinari and Macambira, 1999, 2004), but the Archean rocks are only exposed in the Carajás region (southeastern Pará State, Brazil). The Maroni-Itacaiúnas (or Transamazon) Province is characterized as an orogenic belt with Rhyacian ages (2.25-2.00 Ga, **Fig. 1a-b**) and is correlated to Birimian belt in West Africa (Tassinari and Macambira, 1999, 2004; Santos *et al.*, 2000; Delor *et al.*, 2003). The K'Mudku Shear Belt (low grade) is characterized by mylonitic zones with ca. 1.20 Ga and cross-cut at least three provinces including Tapajós-Parima and Transamazon provinces.

The model of Reis *et al.* (2003) modified by CPRM (2006) is based only on lithostructural features, taking into account the different lithological associations and geochronological data for the Roraima and northwestern Amazonas states. These authors subdivided this region into four major domains with roughly estimated limits, each of one containing a wide range of rock types and stratigraphic units: Surumu, Parima, Central Guyana and Uatumã-Anauá domains (**Fig. 1c**). The last one was subdivided in the northern and southern areas by Almeida and Macambira (submitted).

According to Reis *et al.* (2003), the Central Guyana Domain (**Figs 1c and 2**) shows essentially granulites, orthogneiss, mylonites and metagranitoids (Rio Urubu Metamorphic Suite) associated with low (Cauarane Group) to high (Murupu Metamorphic Suite) metamorphic grade metavolcano-sedimentary sequences, S-type granite (Curuxuim Granite) and a strongly NE-SW trends. The Uatumã-Anauá Domain in the northern area (NUAD, **Fig. 2**) is characterized by E-W to NE-SW lineaments and old metamorphic basement, presumably formed in an island arc environment (Faria *et al.*, 2002). This basement is composed by metagranitoids to orthogneisses TTG-like (2028 Ma; Anauá Complex), enclosing meta-afic to meta-ultramafic xenoliths, in association with inliers of metavolcano-sedimentary rocks (Cauarane Group), and is intruded by S-type (Serra Dourada Granite) and high-K, I-type calc-alkaline (Martins Pereira) granitoids of 1975-1962 Ma (**table 1**).

In the southern area of Uatumã-Anauá domain (SUAD, **Fig. 2**), younger intrusive granites with no regional deformation and metamorphism are most common. The most expressive magmatism is related to the calc-alkalines Caroebe, Água Branca and Igarapé Azul granitoids (**table 1**) associated with coeval Iricoumé volcanic rocks (1906-1891 Ma), but locally it was also observed igneous charnockitic (Igarapé Tamandaré) and enderbitic (Santa Maria) plutons (1890 Ma). Several A-type granitic bodies are

widespread in the Uatumã-Anauá Domain represented by Moderna-Água Boa (1.81 Ga) and Mapuera-Abonari (1.87 Ga) granitic events (*e.g.* Costi *et al.*, 2000, Santos *et al.*, 1997, CPRM, 2003).



ANALYTICAL PROCEDURES

The isotopic ratios of Nd from whole-rock and Pb from feldspar were measured respectively in a Finnigan Mat 262 and VG Sector 54 mass spectrometers at the Isotope Geology Laboratory (Pará-Iso) of the Federal University of Pará, Belém, Brazil. For the Sm-Nd analysis, rock powders (ca. 100mg under milled of 200 mesh) were dissolved in teflon vials at 220°C for one week under HF+HNO₃, further with

HCl 6N and finally under HCl 2N at 145°C. After evaporation, the REE were separated from other elements of sample by cation exchange chromatography (Dowex 50WX-8 resin), after that, Sm and Nd were separated from the others REE by anion exchange chromatography (Dowex AG1-X4 resin). A mixed $^{150}\text{Nd} - ^{149}\text{Sm}$ spike was used and the Nd data were normalized to a $^{146}\text{Nd}/^{144}\text{Nd}$ ratio of 0.7219. Procedural blanks were <110 pg for Sm and <240 pg for Nd. The La Jolla Nd standard yielded a $^{143}\text{Nd}/^{144}\text{Nd}$ ratio of 0.511843 ± 12 and the Sm and Nd concentrations for BCR-01 standard were 6.56 ppm and 28.58 ppm, respectively. The crustal residence ages were calculated using the model of De Paolo (1988) for the depleted mantle (T_{DM}).

Other isotopes systems, such as Pb, also play important role in the discussion about the granite origin. Pb is a common trace element in feldspars (Heier *et al.*, 1967; Patterson and M. Tatsumoto, 1964), and it is well known that the U/Pb and Th/Pb ratios of feldspar (especially K-feldspar) are low (*e.g.* Doe, 1970). These attributes allow feldspar to record the isotopic composition of Pb that was incorporated at the time of its formation and, although multiple intracrustal processes produce scatter in the initial Pb isotopic compositions of rocks that formed at the same age, the variations are understandable. So, in order to assess the initial Pb isotope composition of a rock, the feldspar mineral is currently selected (see references above), because it normally contains Pb but no U. In this case, for initial Pb isotope composition analyses, low U is essential because any U present will have decayed to an 'excess' Pb radiogenic component.

Progressive leaching of feldspar grains shows a decrease in the amount of radiogenic Pb that may indicate the preferential leaching of the more radiogenic reservoirs (Housh and Bowring, 1991, McCulloch and Woodhead, 1993). Indigenous Pb vs. Pb introduced after crystallization may be evaluated partially using leach/residue pairs (Hemming *et al.*, 1996). Sinha (1969) has founded a general agreement between the least radiogenic isotope composition of feldspars and the Pb isotope composition of associated sulfides, suggesting that this method of severe leaching will be furnish a good estimate of initial Pb.

For the Pb isotopic system, the evolution of lead in the Earth's crust has been modeled on the basis of the U/Th/Pb ratios in the different bulk reservoirs (Doe and Zartman, 1979, Zartman and Doe, 1981; Zartman and Haines, 1988) and stages of isotopic homogenization (Stacey and Kramers, 1975; Cumming and Richards, 1975). Despite these models have limited application at the local and district scale, they are powerful tools for global and regional-scale studies, helping to identify the main geochemical reservoirs.

The feldspar grains were picked under a stereomicroscope and a qualitative selection was made taking into account the grain clarity, lack of inclusions, and absence of cracks. An initial mass between 30 to 50 mg of pure feldspar grains was weighed for each sample. According to Tomascak (1995), a single

analysis by thermal ionization mass spectrometry (TIMS) requires 50–100ng of Pb. Based on the expected concentration of Pb in the feldspars, only 10 to 20mg of feldspar is needed.

The used method for Pb feldspar leaching is based on the Housh and Bowering (1991) and Ludwig and Silver (1977), but was partially modified in this work. In the first stage of chemical preparation, the grains are transferred into clean Teflon vials and a cleaning solution of HNO₃** 7.5N (20 drops) is added. Vials are capped and transferred to a hot plate (100°C) for at least 20 minutes to remove surface contaminants and labile lead. This step is to help ensure that any lead ~~that had been~~ introduced after crystallization, either from the environment or through the actions of fluids moving through the pluton, is removed before leaching. The grains are then rinsed with Milli-Q water two times. The same process is repeated, now with HCl** 6N.

In the second step, HF** 1N is added to the grains and the vial is leaved in ultrasonic bath for 5 minutes. After, the solution is heated for 30 minutes (100°C) in the hot plate, and an aliquot of 0.5 ml is collected and HBr*** 0.5 N is added (50 drops). This procedure is performed a number of times until the grains are gradual and totally dissolved. In general, 10 to 15 aliquots are collected by sample. Each sample solution was processed through anion exchange column chemistry to isolate lead, that was loaded onto a Re-filament for TIMS analysis. Procedural blanks are processed using the same chemical preparation techniques as were used for the grains to assess the ambient amount of lead introduced during sample processing. In order to obtain de isotope composition of the part of the grains not contaminated by external lead, a total of 50 analyses were performed on 14 selected samples (2 to 6 analyses per sample). After a preliminary analysis for all samples, the choice of a new leached solution of each sample ever took into consideration the previous isotopic results obtained on the same sample. The results showed in **table 2** are those considered from the least contaminated parts of the grains for external lead.

Nd AND Pb ISOTOPE RESULTS

The initial Nd and Pb ratios are widespread used for granitoid rocks as the main indicator of the source material. This indicator is used together with some other geological criteria (geochronological, petrogenetic, structural) in order to estimate the relative amount of continental crust accreted or recycled during each time interval of geological time, for the area studied in the Guyana Shield. The association of the Sm-Nd and Pb measurements with the available geochronological data obtained by other methods permitted an improved interpretation for the origin of the granitoid rocks under examination.

Table 2 shows new (22) and previous (36) Sm-Nd isotopic results for UAD (mainly granitoids), further new 14 Pb isotope results from leached feldspars of Martins Pereira, Caroebe and Igarapé Azul granitoids. In the **table 3** are available Sm-Nd isotopic data (96 results were compiled or modified) from several other geochronological provinces (Ventuari-Tapajós or Tapajós-Parima, Maroni-Itacaiúnas or Transamazon and Central Amazonian) and domains of the Amazonian Craton (Carajás, Imataca, Central

Amapá, French Guyana, Tapajós, Surumu and Central Guyana). The summary of main geological features of UAD granitoids rocks are also available in the **table 4**.

Sm-Nd on whole-rock

Northern Uatumã-Anauá Domain (NUAD): Martins Pereira and Serra Dourada granitoids

The main granitoids studied in the NUAD belongs to the Martins Pereira (1.97 Ga) and the Serra Dourada (1.96 Ga) granites, including small bodies of younger leucogranites with 1.90 Ga (lenses and pods with meter to centimeter-scale) filling the Martins Pereira NNE-SSW trending foliation. The oldest rocks in this region are represented by the Anauá Complex (2.03 Ga TTG-like association).

The Anauá Complex and the metavolcano-sedimentary rocks correlated to the Cauarane Group (low to medium metamorphism grade) and the Murupu Metamorphic Suite (high metamorphism grade) are the oldest basement units known in the southeastern Roraima. For the Anauá Complex only two samples has been analyzed (see **tables 2 and 4**), yielding coherent T_{DM} model ages (2.37-2.33 Ga) and low to moderate negative $\epsilon Nd_{2.03 Ga}$ (-0.19 and -2.21). In the NUAD, no Nd data are available for the metavolcano-sedimentary sequence, but the related rocks of Cauarane Group (see **table 3**) in other areas (e.g. Guyana Central Domain) exhibits two main isotopic patterns. The first is related to paragneiss samples (e.g. garnet gneiss) with results showing moderate negative $\epsilon Nd_{2.07 Ga}$ (-1.12 to -4.16) values and higher NdT_{DM} model ages (2.46-2.41 Ga) including a Neoproterozoic NdT_{DM} age (2.64 Ga). The second gneissic type shows $\epsilon Nd_{2.07 Ga}$ near to zero to positive (+0.35 to +1.23) and lower NdT_{DM} ages (2.32-2.27 Ga), probably related to the volcanic protholith signatures (juvenile sources).

The Serra Dourada and Martins Pereira granitoids (1.97-1.96 Ga event) intrude this older basement in the NUAD. The S-type Serra Dourada granitoids confirms its wide crustal origin from partial melting of metavolcano-sedimentary sequence, showing negative $\epsilon Nd_{1.96 Ga}$ values (-1.08 and -4.34) and NdT_{DM} of 2.53-2.39 Ga for its sources, which are 420 to 560 Ma older than the crystallization age of these granites (**tables 1, 2 and 4, Fig. 3**).

The same is true for the I-type, high-K Martins Pereira granitoids (**tables 2 and 4, Fig. 3**), whose the results show T_{DM} ages of 2.43-2.38 Ga and slightly negative $\epsilon Nd_{1.97 Ga}$ (-1.42 to -2.17), including samples with higher T_{DM} ages (2.67-2.64 Ga) and ϵNd negative values (-4.74 and -3.89). The 1.90 Ga intrusive lenses of leucogranite (one sample) yielded negative ϵNd (-3.48) and NdT_{DM} model age (2.38 Ga). These data are in agreement with Martins Pereira host results and reflect the zircon inheritance origin recorded (at least 3 older populations) in the single-zircon Pb evaporation for the leucogranite sample (**table 1**). CPRM (unpubl.) Sm-Nd data present a similar isotope pattern for the Martins Pereira granitoids (**table 2**). The Nd data pointed out moderate negative $\epsilon Nd_{1.97 Ga}$ values (-0.92 to -3.20) and NdT_{DM} ages with 2.36-2.33 Ga range (locally 2.57 Ga).

In summary, all of early Orosirian rocks of NUAD (2.03 to 1.96 Ga) show similar behaviour in the Sm-Nd isotopic system. The ϵNd is negative (-0.92 to -4.74) and the dominantly Siderian NdT_{DM} model ages (2.47-2.33 Ga), with subordinated Neoproterozoic ages (2.67-2.57 Ga), suggest an input of mainly older crustal sources for the Serra Dourada and Martins Pereira genesis.

Southern Uatumã-Anauá Domain (SUAD): Caroebe and Igarapé Azul granitoids

The granitoids of the SUAD are intrusive in the older NUAD rocks. They are represented mainly by the I-type Caroebe, Igarapé Azul, Água Branca granitoids and coeval Iricoumé volcanism (1.90-189 Ga), including locally minor A-type plutonic bodies of Mapuera (1.88-1.86 Ga) and Moderna (1.82-1.79 Ga) granitoids related (**table 1**). The Caroebe Granite and related plutons show two main facies named as Alto Alegre (with biotite and hornblende-free) and Jaburuzinho (with biotite and hornblende) and both facies exhibit two different Nd isotopic patterns. The first pattern is characterized by moderate to high negative $\epsilon\text{Nd}_{1.89 \text{ Ga}}$ values (-2.05 to -4.27) and NdT_{DM} model ages of 2.29 to 2.47 Ga. This pattern is most common in the Alto Alegre facies, although it is also observed in the Jaburuzinho facies. The Água Branca Granite in the type-area, far 300 km to the south of Caroebe Granite, also shows moderate to high negative $\epsilon\text{Nd}_{1.90 \text{ Ga}}$ values (-3.00) and Siderian NdT_{DM} model age (2.39 Ga). Although petrographically similar to the Jaburuzinho facies, the Água Branca Granite Nd results are in agreement with those the Alto Alegre facies (**tables 2 and 4, Fig. 3**).

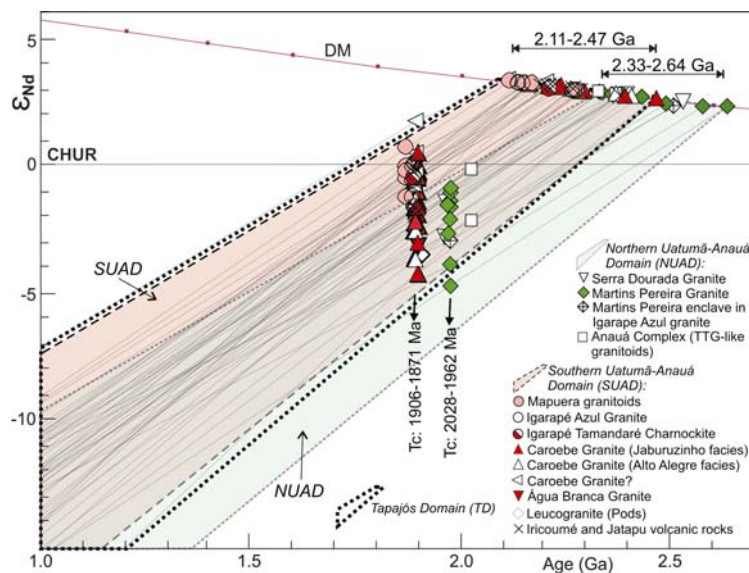


Fig 3. ϵNd vs. time diagram for the rocks from NUAD (Anauá Complex, Martins Pereira and Serra Dourada granitoids) and SUAD (Caroebe, Água Branca, Igarapé Azul, Mapuera granitoids, Igarapé Tamarandé charnockite, Iricoumé and Jatapu volcanic rocks). The Nd evolution field of Tapajós domain is also plotted for comparison. For details, see text and tables. Tc: crystallization ages range.

The second pattern is dominant in the Jaburuzinho types (**tables 2 and 4, Fig. 3**) showing $\epsilon\text{Nd}_{1.89 \text{ Ga}}$ values close to zero (+0.46 to -1.18) and relatively low NdT_{DM} model ages (2.16 to 2.26 Ga). The Igarapé Azul granitoids have a felsic character and only biotite (locally muscovite) as varietal, but their

Nd signature (**tables 2 and 4, Fig. 3**) is particularly similar to the Jaburuzinho types (hornblende-bearing), exhibiting $\epsilon\text{Nd}_{1.89\text{ Ga}}$ close to zero (-0.02 to -1.61) and Rhyacian NdT_{DM} model ages (2.14-2.28 Ga). Such as the Igarapé Azul and Caroebe granitoids (mainly the Jaburuzinho facies), the coeval Iricoumé volcanic rocks (**table 2, Fig. 3**) show slight negative ϵNd values (-0.27 to -1.76) and Rhyacian NdT_{DM} model ages (2.19-2.28 Ga).

Despite of differences in the crystallization ages, the A-type Mapuera (1.88-1.86 Ga), Moderna and Madeira (1.82-1.79 Ga) granitoids and related rocks show Nd signatures based on the Rhyacian NdT_{DM} model ages and low negative ϵNd values (**table 3**). The Mapuera samples yielded $\epsilon\text{Nd}_{1.87\text{ Ga}}$ between -0.56 and -1.22 and NdT_{DM} model ages of 2.17-2.28 Ga, whereas the Moderna types show similar values of $\epsilon\text{Nd}_{1.81\text{ Ga}}$ (-0.44 to -1.47) and NdT_{DM} model ages (2.17-2.28 Ga) (**table 2, Fig. 3**).

In general, all granitoids of SUAD has dominantly Rhyacian NdT_{DM} model ages and low to moderate negative and, locally, quite positive ϵNd values, including subordinated Siderian NdT_{DM} model ages associated to the much more negative ϵNd values. This picture contrasts with the Martins Pereira and Serra Dourada isotopic Nd patterns in the NUAD, characterized by Siderian (locally Neoproterozoic) NdT_{DM} model ages and highest negative ϵNd values.

Pb on leached feldspars

In this Pb isotope study, the NUAD is represented by the 1.97 Ga Martins Pereira granitoid rocks and 1.90 Ga lenses of leucogranites, which yielded high Pb initial ratios, mainly the $^{207}\text{Pb}/^{204}\text{Pb}$ (15.70 to 15.57), which overlap those of the SUAD granitoids Pb composition (**table 2**). In the SUAD, the Caroebe and Igarapé Azul granitoids show different behavior, although both exhibit $^{207}\text{Pb}/^{206}\text{Pb}$ ratios above of the upper crust evolution curve in the Plumbotectonic model (**Fig. 4**; Doe and Zartman, 1979, Zartman and Doe, 1981). Contrasting with the relatively more scattered pattern of the Igarapé Azul granites ($^{206}\text{Pb}/^{204}\text{Pb}$: 16.62 to 15.87; $^{207}\text{Pb}/^{204}\text{Pb}$: 15.65 to 15.42; $^{208}\text{Pb}/^{204}\text{Pb}$: 36.18 to 35.59), the Caroebe Granite shows the less radiogenic types and more homogeneous Pb initial ratios range ($^{206}\text{Pb}/^{204}\text{Pb}$: 16.41 to 15.90; $^{207}\text{Pb}/^{204}\text{Pb}$: 15.54; $^{208}\text{Pb}/^{204}\text{Pb}$: 36.09 to 35.49).

In summary, all studied granitoids show Pb radiogenic patterns, exhibiting $^{207}\text{Pb}/^{204}\text{Pb}$ (15.70-15.42), $^{206}\text{Pb}/^{204}\text{Pb}$ (16.87-15.87) and $^{208}\text{Pb}/^{204}\text{Pb}$ (36.18-35.49) initial ratios and they plots generally above of the upper crust evolution curve in the Zartman and Doe (1981) model. This behavior contrast with the Pb initial ratios of DM (Rehkamper and Hofmann, 1997), lower crust average (Rudnick and Goldstein 1990) and EM II present-day reservoirs and pointed for dominant crustal-derived reservoir contributions for the Martins Pereira, Caroebe and Igarapé Azul granitoids with no mantle-derived lead. Only one sample (MA-101) shows $^{207}\text{Pb}/^{206}\text{Pb}$ isotope ratios near to the orogen global growth curve and the EMII and lower crust fields (**Fig. 4**; Doe and Zartman, 1979, Zartman and Doe, 1981). In this same diagram, the granitoids samples also show much more low Pb ratios than southwestern of United States of America

basalts (SWUSAB), these last considered as a paleoproterozoic mantle reservoir (~1.8 Ga) similar to actual EMII reservoir (Kempton *et al.*, 1991, Greenough and Kyser, 2003).

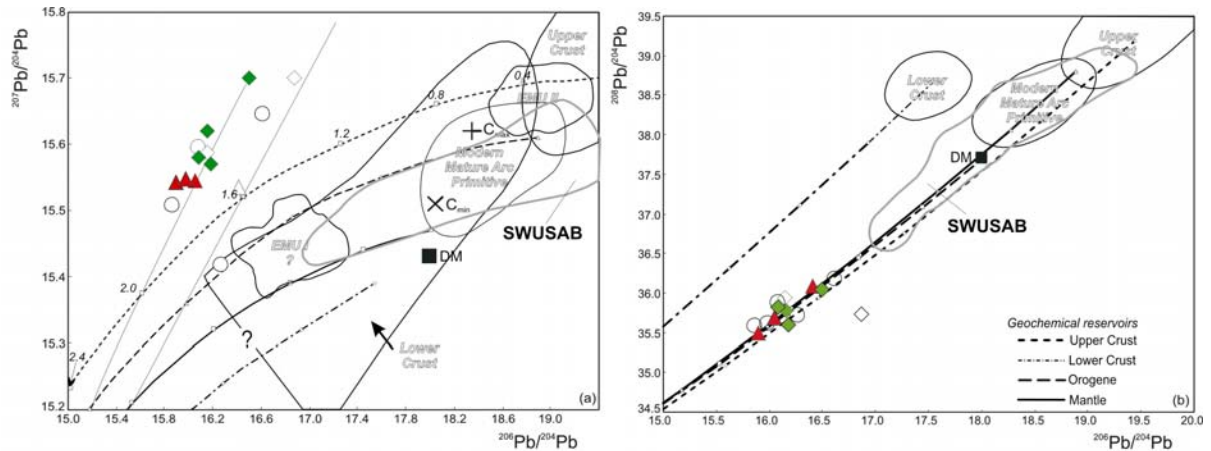


Fig 4. Plots of Pb isotopic compositions of leached feldspars from Martins Pereira, Caroebe and Igarapé Azul granitoids: (a) $^{207}\text{Pb}/^{204}\text{Pb}$ vs. $^{206}\text{Pb}/^{204}\text{Pb}$; (b) $^{208}\text{Pb}/^{204}\text{Pb}$ vs. $^{206}\text{Pb}/^{204}\text{Pb}$. The lead-isotope evolution curves are from Plumbotectonic model (version II) of Zartman and Doe (1981) and represent the isotopic composition of mantle, orogen, upper and lower crust reservoirs along the time. Other reservoirs fields are plotted for comparison, such as DM (Rehkamper and Hofmann, 1997), EMI and EMII (Zindler and Hart, 1986), mature arc primitive (Zartman and Doe, 1981) and continental crust (maximum and minimum average; Rudnick and Goldstein, 1990). Proterozoic enriched mantle reservoir of the southwestern United States of America basalts (SWUSAB, Kempton *et al.*, 1991 in Greenough and Kyser, 2003) are also plotted. Tick marks in the each curve indicate progressively older time in 0.4 b.y increments. Symbols as in fig.3.

DISCUSSION

Nd isotope signatures of the Ventuari-Tapajós (or Tapajós-Parima), Maroni-Itacaiúnas (or Transamazon) and Central Amazonian (or Amazon) Geochronological Provinces and the their boundaries in the Southeastern Roraima

In the Nd isotope system, the Sm-Nd model ages (T_{DM}) are currently used in crustal evolution analysis of a given terrain. Normally, these ages are related to the evolution of the mantle during geologic time, admitting episodes of fractioning associated to the extraction of basaltic magmas. This implies in the residual material generation within the mantle sources becoming enriched gradually in Sm (higher Sm/Nd ratio), but depleted in incompatible elements.

However, the T_{DM} ages must be interpreted very carefully (*e.g.* Arndt and Goldstein, 1987). Natural variations in mantle material are demonstrated by the existence of geochemically distinct reservoirs (DMM, HIMU, EMI, EMII, etc.), including also the possibilities of mixtures between such different reservoirs and crustal sources (Zindler and Hart, 1986). In this sense, the depleted mantle model is employed as a reasonable first approximation. Oceanic lithosphere has been produced throughout geologic time and recycling back to the mantle along B-subduction zones, but part of its material differentiates and remains near the surface of the Earth as continental crust.

Thus, the T_{DM} ages have been considered to be “crust-formation ages”, since they are obtained calculating the time when a given sample had an isotopic composition identical to the depleted mantle, presumed to be its “ultimate source”. But this is true when only a short time elapsed between the

formation of the mantle-derived magma and the final emplacement of the differentiated material in the continental crust (este parentese está confuso) and the Sm/Nd ratio of the sample was not modified by subsequent geological events. According to Arndt and Goldstein (1987), such assumptions may be valid only in a limited number of cases, with the Sm-Nd systematic generally providing an estimate of the average time that the material in the sample has been resident in the continental crust.

In the Archean Central Amazonian (or Amazon) Province (**Fig. 1**), only in the Carajás Block expressive Nd data is available, contrasting with other areas, such as Iricoumé-Mapuera-Trombetas (Guyana Shield) and Irixi-Xingu (Central Brazil Shield) regions, which the isotope data are very scarce. This province is also understood from two different point-of-views. The first model (Tassinari and Macambira 1999, 2004) argue that this region is characterized by a "hidden" basement (>2.5 Ga), inferred by the Nd_{DM} model ages (3.0-2.5 Ga) and negative ϵNd values from widespread younger intrusive granites and volcanics (1.88-1.81 Ga). Archean rocks crop out in the SE portion (Carajás Block), showing 3.04-2.73 Ga Nd_{DM} model ages range (Sato and Tassinari 1997, Dall'Agnol *et al.*, 1999) and ϵNd with +4.55 to -0.54 (**table 3; Fig. 5**). The second hypothesis (Santos *et al.*, 2000, 2004) does not recognize an older basement in the Iricoumé-Mapuera and Irixi-Xingu regions and pointed out a domain of 1.88-1.70 Ga rocks based on the U-Pb ages of the younger granites and volcanic rocks (underplating setting), although the range of the Nd_{DM} model ages (2.85-2.41 Ga) and ϵNd (+1.52 to -14.39) also indicate older sialic crustal sources (Santos *et al.*, 2000).

Archean terranes are also observed in the Central Amapá and Imataca (Venezuela) regions, considered as dominantly Rhyacian domains (**table 3 and Fig. 1**). For the granitic-granulitic association in the Central Amapá, the crystallization (2.90-2.58 Ga) and Nd_{DM} model (3.42-2.92 Ga) ages reinforce an Archean origin (**Fig. 5**). In the Imataca region, the rocks are Transamazonian in age (ca. 2.0 Ga), but keep several records about their Archean origin (Nd_{DM} model ages: 3.91-2.71 Ga) (Tassinari *et al.*, 2004). In the Maroni-Itacaiúnas (or Transamazon) Province, Rhyacian crust occurs mainly in the easternmost region of the Guyana Shield, such as French Guyana (e.g. Avelar *et al.*, 2003; Delor *et al.*, 2003). Based on the available Nd data (**table 3; Fig. 5**) this is roughly subdivided in the northern and southern areas. The southeastern of French Guyana (near to the Brazilian Amapá State boundary) is dominated by 2.16-2.10 Ga granitic-migmatitic rocks with 2.58-2.24 Ga Nd_{DM} model ages range and ϵNd varying from +1.74 to -2.24 . The northern area is characterized by 2.16-2.13 Ga granite-greenstone terrain with juvenile signature (Nd_{DM} model age: 2.29-2.19 Ga and ϵNd : +3.60 to +1.63).

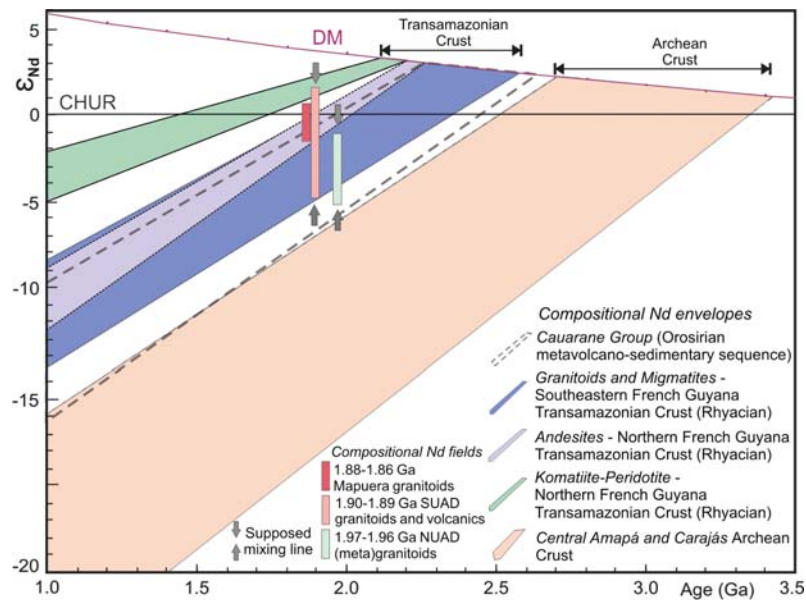


Fig 5. ϵ_{Nd} vs. time diagram showing Nd evolution of rock associations from Cauarane Group, Archean (Carajás and Central Amapá) and Transamazonian (French Guyana) terranes. The SUAD and NUAD sample fields are also plotted. For discussions and references see respectively text and tables. Symbols as in fig.3.

In the Central Brazil Shield, a juvenile origin is also suggested for the Ventuari-Tapajós (or Tapajós-Parima) Province based mainly in Sm-Nd data from the Tapajós domain (**table 3, Fig. 5**). This domain is represented by two main magmatic events (2.05-1.96 Ga and 1.90-1.87 Ga) showing 2.44-2.09 Ga NdT_{DM} model ages and ϵ_{Nd} yielding +2.22 to -4.16 range (Sato and Tassinari, 1997; Santos *et al.*, 2000). On the other hand, in the region near to the boundary of Central Amazonian Province, Lamarão *et al.* (2005) argue that the Nd signature of the granitoids and volcanic rocks are not compatible with a mantle-derived origin. As shown in the **table 3**, they yielded similar NdT_{DM} model ages (2.46-2.28 Ga) in comparison of the other authors, but the ϵ_{Nd} are widespread negatives (-1.01 to -5.19). This different Nd pattern could be related to geographical differences, where the juvenile rocks are dominant in the westernmost areas of Tapajós Domain (Orogenic Domain, 2.05-1.96 Ga) and the crustal sources are most common in the easternmost areas (Post-orogenic Domain; 1.90-1.89 Ga), nearly to the Central Amazonian Province boundary.

The scenario pointed out by Lamarão *et al.* (2005) for the Tapajós domain is similar to the Uatumã-Anauá domain in SE Roraima and except for two samples tentatively correlated to the Água Branca Suite (“post orogenic” domain), which yielded positive $\epsilon_{Nd_{1.89 Ga}}$ (**Table 3**, Sato and Tassinari, 1997), all SE Roraima region does not show suggestive data of mantle-derived magmas, including the correspondent “orogenic” domain. Santos *et al.* (2006) revisited the Tapajós-Parima and Central Amazonian boundary in the Guyana Shield, and proposed that it would be located to the east of study area, in the NW Pará State (**Fig. 1b**). Probably, all SE Roraima is included in the Ventuari-Tapajós (or

Tapajós-Parima) Province, with older provinces such Maroni-Itacaiúnas (or Transamazon) and Central Amazonian as sources of magmatism in the UAD.

Crustal formation and constraints of sources based on integrated use of the Pb-Nd isotopes: Martins Pereira, Igarapé Azul and Caroebe granitoids examples

In general, Nd and Pb data are seen separately, however, these two systems combined on one diagram (using ϵNd and $^{207}\text{Pb}/^{204}\text{Pb}$) permit a more comprehensive assessment of possible sources of the plutonic rocks, especially granitoids. The Martins Pereira, Igarapé Azul and Caroebe granitoids have been taken as example, searching to estimate the most suitable source(s) based on the Nd and Pb integrated analysis. Although contrasting with Nd data, the Pb isotopic data from potential sources are not available, such as rocks of Cauarane Group, Anauá Complex (exposed basement) and Amazonian Central and Transamazonian crusts (unexposed basement).

In this sense, the integrated use of another isotope system (initial Pb ratios) in the special interpretative diagrams, associated with Sm-Nd methodology and supported by previous geochronological data, it allow a more comprehensive evaluation about of origin of the granitoids under investigation. Therefore, these isotope tools furnish important constraints about the discussion of “juvenile” derivation, formed by mantle-continental crust differentiation, “reworked” origin by melting of previously crustal protoliths, or reflecting mixing of material derived from the mantle at different times (Arndt and Goldstein, 1987).

In relation to the Pb system, Tomascak *et al.* (2005) argued that $^{207}\text{Pb}/^{204}\text{Pb}$ ratio is a more powerful tracer of these components than $^{206}\text{Pb}/^{204}\text{Pb}$, mainly in areas where magmatic source components have significant time integrated differences in U/Pb, such as Martins Pereira granitoids. The $^{206}\text{Pb}/^{204}\text{Pb}$ could vary considerably in mantle and crustal materials in response to small changes in U/Pb, which changes may be unrelated to the nature of source materials.

However, in southeastern Roraima, only recently reasonable number of Nd isotopes data are available (Costa, 2005; CPRM unpubl.) and Pb isotopic data do not exist, making it difficult the determination of potential sources and crustal signatures. Despite of this scarce data, Serra Dourada and Martins Pereira granitoids show Nd and Pb signatures that confirm a crustal origin based on the Orosirian to Rhyacian metavolcano-sedimentary sequence and Archean mixing sources (see Fig. 5 and Nd and Pb isotope results).

For the Martins Pereira granitoids, the continental sources are older than those of the Caroebe and Igarapé Azul ones. The restricted 1980-1967 Ma crystallization ages of Martins Pereira granitoids and the low to moderate negative $\epsilon\text{Nd}_{1.97\text{ Ga}}$ values (-0.92 to -4.74), high $^{207}\text{Pb}/^{204}\text{Pb}$ and relatively high NdT_{DM} model ages (2.33-2.67 Ga), suggest dominantly remelting of Neoproterozoic sources and local addition of

Transamazonian sources. The same is true for the S-type Serra Dourada granites that pointed out older metasedimentary sources, as recorded in the Cauarane sequence. In the Caroebe and Igarapé Azul granitoids these isotope results furnish important constraints about the Arndt and Goldstein (1987) discussion, involving a “juvenile” derivation (mantle-continental crust differentiation), “reworked” origin (remelting of previously crustal protoliths) or mixing of material derived from the mantle at different times.

For the studied granitoids of southeastern Roraima, the crystallization ages and NdT_{DM} model ages are not concordant (or slightly discordant). Furthermore, positive (or slightly negative) ϵNd values and low $^{207}Pb/^{204}Pb$ initial ratios are absent and also preclude derivation from primitive mantle sources only for this magmatism. Hence, three hypothesis are provided to explain the origin of the parental magmas: (1) mixture of mantle-derived magmas or juvenile crust (Transamazonic) with subordinate liquids derived from radiogenic crust (Archean); (2) derivation from an enriched mantle; (3) derivation from remelting of slightly older radiogenic crust (Transamazonian), which implies a dominantly crustal source for the parental magmas.

A mixing origin from Transamazonian komatiites-peridotites of greenstone belt sequence (depleted source) and Archean sialic basement (enriched source) is a good hypothesis of work based on the Nd isotopes. However, the elemental contents of these rocks, in particular the compatible elements, are not consistent with a significant input of mantle material. The mantle-crust mixing scenario is also less likely than derivation from a single (or multi) crustal source (*e.g.* lower crust and juvenile crust). This picture is corroborated by data dispersion in samples from Martins Pereira, Caroebe and Igarapé Azul granitoids data at ϵNd and SiO_2 plot (**Fig. 6a**), including the absence of trends between compatible element contents and Nd isotopes (**Fig. 6b**) and their non-primary nature (**Fig. 6c**).

A derivation from an enriched mantle based on the Nd signatures is suggested by some authors for the high-K (slightly shoshonitic) calc-alkaline rocks in the Tapajós domain (*e.g.* Vasquez *et al.*, 1999) and could be a suitable model for the Caroebe and Água Branca granites in SE Roraima. The slightly negative ϵNd values and NdT_{DM} model ages of ca. 2.25 Ga for the 1.90 Ga andesites and gabros of the Tapajós domain are interpreted as crustal enrichment or contamination of the subcontinental lithospheric mantle. The mantle contamination by crustal material is also a work hypothesis for Caroebe and Igarapé Azul granites origin, maybe indirectly related to the subduction process of the Anauá Arc through the time. Several mantle geochemical reservoirs are plotted in the **fig. 7**, including present-day (EMI and EMII) and Proterozoic (SWUSAB) enriched mantle examples, however all analyzed granitoid samples show lower $^{143}Nd/^{144}Nd$ and $^{206}Pb/^{204}Pb$ ratios. Only two samples (Igarapé Azul and Caroebe granites) have been plotted near to the field of EM1 reservoir boundary (**Fig. 4a**).

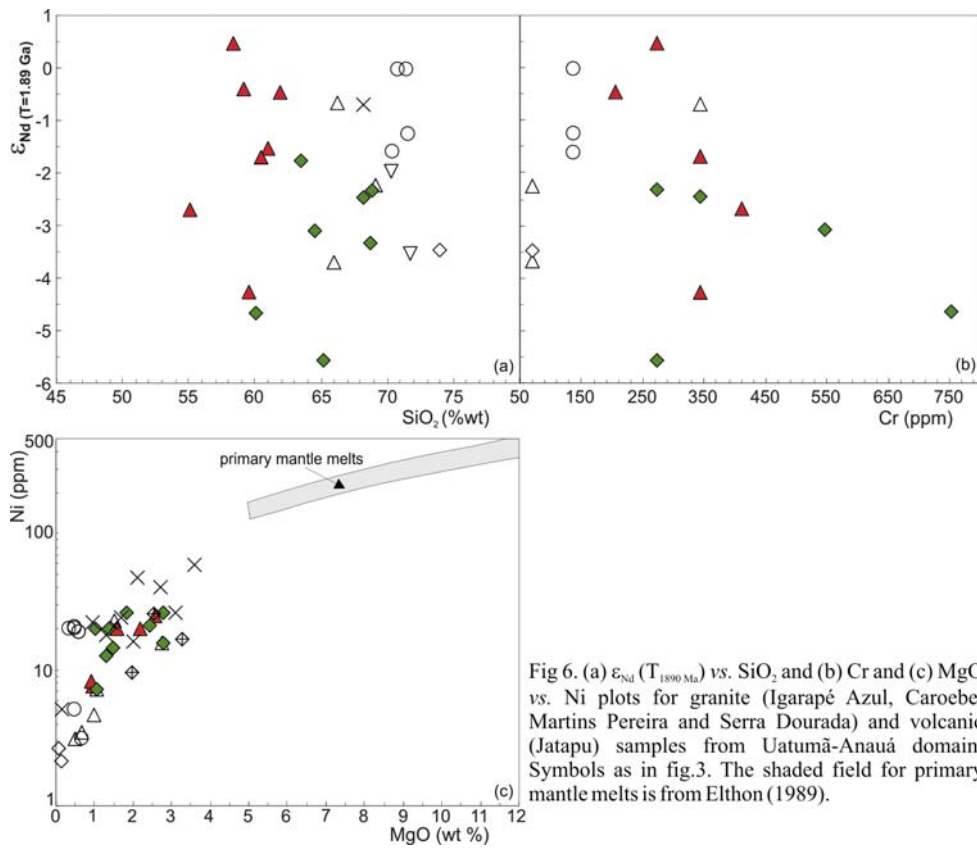


Fig 6. (a) $\epsilon_{Nd}(T_{1.890\text{ Ma}})$ vs. SiO_2 and (b) Cr and (c) MgO vs. Ni plots for granite (Igarapé Azul, Caroebe, Martins Pereira and Serra Dourada) and volcanic (Jatapu) samples from Uatumã-Anauá domain. Symbols as in fig.3. The shaded field for primary mantle melts is from Elthon (1989).

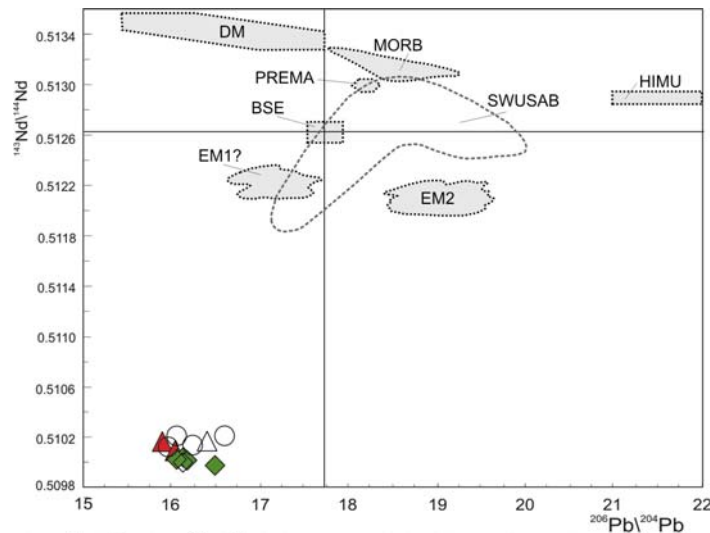


Fig 7. $^{143}\text{Nd}/^{144}\text{Nd}_0$ vs. $^{206}\text{Pb}/^{204}\text{Pb}_0$ isotope correlation diagram for Martins Pereira (1.97 Ga), Caroebe and Igarapé Azul (1.89 Ga) granitoids samples. The mantle geochemical reservoirs are extracted from Zindler and Hart (1986) and the $^{206}\text{Pb}/^{204}\text{Pb}$ of BSE was taken from Allegre *et al.* (1988). Proterozoic enriched mantle reservoir of the Southwestern United States of America basalts (SWUSAB, Kempton *et al.*, 1991 in Greenough and Kyser, 2003) are also plotted for comparison. Symbols and captions as in figs 3 and 4.

In contrast, Nd and Pb data indicate that the parental magmas of these granites were produced mainly by reworking/remelting of Paleoproterozoic crust and very locally by Archean sialic sources. Two crustal potential sources, with different isotopic contents, are selected for comparison: (i) Cauarane Group

rocks of Northern Uatumã-Anauá Domain (back-arc basin related to the Anauá arc?), and (ii) Transamazonian andesites and granite-migmatitic rocks from French Guyana.

The metavolcano-sedimentary (Cauarane Group) rock samples present similar Nd_{DM} model ages (2.27-2.64 Ga) and ϵNd values (+0.21 to -5.40, at 1.97 Ga) of Caroebe and Igarapé Azul granites at 1.89 Ga times. The protholiths of the Cauarane Group also can be subdivided into 2 types in relation to Nd isotopic data: (a) sedimentary and (b) volcanic origin (**table 3**). The first exhibits radiogenic Nd signatures ($\epsilon Nd_{2.07 Ga}$ -1.12 to -4.16) and much higher Nd_{DM} model ages (2.41-2.64 Ga), contrasting with the less radiogenic Nd contents ($\epsilon Nd_{2.07 Ga}$ +0.35 to +1.23) and lower Nd_{DM} model ages (2.27-2.32 Ga) of the second ones (**table 2**).

The Caroebe and Igarapé Azul granitoids show dominantly negative (-1.31 to -4.37) $\epsilon Nd_{1.89 Ga}$, with only locally slightly positive and negative values (+0.37 to -0.59). These least Nd radiogenic types exhibit also the lowest Nd_{DM} model ages (2.16-2.24 Ga), showing the same Nd isotope composition of the Transamazonian andesites and granite-migmatitic terrane of French Guyana in the 1.89 Ga times (**Fig. 3**). This feature suggests that these rocks (e.g. andesites or metatonalites) could be suitable sources for the Caroebe and Igarapé Azul granites, in agreement with the petrogenetic models for the high-K calc-alkaline granites (Roberts and Clements, 1989).

The most Nd radiogenic values yielded by Caroebe and Igarapé Azul granitoids show high Nd_{DM} model ages (2.23-2.47 Ga). This characteristic could indicate progressive input of older “enriched” material, such as Cauarane metasedimentary rocks, Martins Pereira granitoids and/or Archean basement sources to the original melt produced by partial melting of Transamazonian “depleted” source (**Fig. 3**). This hypothesis is reinforced by the geochemical data and by the several 1.97-1.96 Ga inherited ages founded in the Caroebe (Alto Alegre facies) and mainly in the Igarapé Azul granites (**table 1**). In this last type are also observed biotite-rich gneissic enclaves with 1.96 Ga, negative $\epsilon Nd_{1.89 Ga}$ (-1.95 and -3.52) and higher T_{DM} model age (2.51-2.72 Ga).

Thus the lowest $^{207}Pb/^{204}Pb$ and locally high- ϵNd source component of Caroebe and Igarapé Azul magmas, including local Pb and Nd isotopic heterogeneity, are interpreted as having a dominantly crustal derivation. The granitoids origin is probably related to the remelting of the Transamazonian more depleted source (andesites, metatonalites and amphibolites?) and addition of crustal material (e.g. Cauarane Group and Martins Pereira granitoids). According to Tomascak *et al.* (2005), it is likely that mantle heat was required to produce large-scale melting of the mafic to intermediate, metaigneous lower crust, even if compelling evidence for mantle material involvement is lacking.

An outline of geodynamic evolution of central portion of Guyana Shield at the Orosirian times

The whole-rock Nd isotope and previous geochronological data (Costa, 2005, Lamarão *et al.*, 2005, CPRM unpubl., this study), pointed out for the similarities between the Uatumã-Anauá (Guyana

Shield) and Tapajós (Brazil Central Shield) domains and both belong probably to the same province (Ventuari-Tapajós or Tapajós-Parima) and has been experienced the same tectonic evolution.

According to Lamarão *et al.* (2002), the Tapajós domain records global scale accretionary processes related to the formation of the Atlantica supercontinent in the early Orosirian times (2.04-1.96 Ga, Lamarão *et al.*, 2002, Santos *et al.*, 2000, 2004), followed by a 1.90-1.87 Ga intracontinental taphrogenetic event. The tectonic setting of the Tapajós domain is considered thus transitional, in time and space, between a subduction-related setting, involving the generation of a magmatic arc, and a stable continental block affected dominantly by vertical and extensional tectonics. The main example of calc-alkaline granitoids generated in post-collisional and extensional setting is related to Basin-and-Range province in the SW of USA (e.g. Hawkesworth *et al.*, 1995, Coleman and Walker 1992).

In contrast, Santos *et al.* (2000, 2004) included these 1.90-1.87 Ga granitoids (except Maloquinha Granite) and coeval volcanic rocks in the arc-related orogenic setting (Tropas Orogeny). These authors pointed out that the Tropas Orogeny has started with the arc island Tropas magmatism (1898-1893 Ma), followed by formation of the Parauari continental arc magmatism (1893-1879 Ma). The A-type Maloquinha granitoids are quite younger (1882-1870 Ma) and were included in the post orogenic setting, despite of the emplacement event overlap in the time (within errors limits) the Parauari magmatism. Others Paleoproterozoic terranes in the world also comprise 1.9-1.8 Ga calc-alkaline granitoids, sometimes with associated coeval volcanics, such as in northern Australia (Hooper and Lamboo Complexes, e.g. Page, 1988, Griffin *et al.*, 2000), northern United States (Trans-Hudson orogenic belt, e.g. Dumphy and Ludden, 1998; St-Onge *et al.*, 1999), Sweden and Finland (Svecofennian Orogen, e.g. Billström and Weihed, 1996; Lahtinen and Huhma, 1997). All these orogens have their geological scenario reasonably well understood, including several isotopic, geochemical data and petroctectonic assemblage compatible with the arc-island or arc-continental tectonic setting (e.g. turbidite and ophiolites sequences), contrasting with the majority of Amazonian Craton provinces, including the Tapajós domain.

The Nd and Pb isotope data presented here show that the addition of mantle-derived magmas, if really it occurred, was probably very limited in the Uatumã-Anauá domain, although over a wide orogenic area, most granites may be accounted for a binary mixture between a recycled crustal component and a depleted mantle-like component (differentiated Island Arc-type magmas?). But the isotope pattern showed by UAD granitoids is better explained by the melting of older crust (recycling) than by a mantle-crust mixing or a juvenile and arc-related origin. Thus, the regional crustal melting was the dominant magmatic process in this region and this older crust could comprehend important isotopic heterogeneities (e.g. Transamazonian granite-greenstone terranes, metavolcano-sedimentary sequences, and local Archean TTG terranes), resulting in variable $Nd_{T_{DM}}$ and ϵ_{Nd} values.

For the NUAD (**Fig. 8a**), a primitive arc is admitted (Anauá Complex, 2.03 Ga), although it crops out as inliers in the northeastern area and only few isotopic analyses are available (Faria *et al.*, 2002). The granitic rocks studied in the NUAD probably correspond to the late continental arc (Martins Pereira, 1.97 Ga) to early collisional (Serra Dourada, 1.96 Ga) transitional setting (**Fig. 8b**), generated from anatexis of older continental sources (Transamazonian to locally Archean in age). This accretionary model is in agreement with those of Lamarão *et al.* (2002) and Santos *et al.* (2000, 2004) for the Tapajós domain. Lamarão *et al.* (2005) pointed out an Andean-type magmatic arc setting, where the magmas could be modified by interaction with crust, but they also discard a juvenile origin. Alternatively, these authors consider that the 2.0 Ga high-K calc-alkaline magma types are resulted of remelting of an older Paleoproterozoic juvenile arc with a small contribution from Archean sialic sources in the post- to late-orogenic setting, placing in doubt even though the existence of a subduction zone.

In the SUAD, the 1.90-1.89 Ga granitoids and volcanic rocks show isotopic data a little more heterogeneous, but in general sense also exhibit an isotopic continental crust pattern (multicrustal sources). This feature associated to the dominantly Rhyacian NdT_{DM} ages is in agreement with the petrogenetic model based on the melting of tonalites, andesites and/or amphibolites sources, such as those observed in the Transamazonian granite-greenstone terranes (juvenile sources). These magmas could be locally contaminated by the metavolcano-sedimentary sequences or minor Archean sources. Different from NUAD evolution, no ophiolites sequences (or ocean crust) remnants and sedimentation arc-related, including no metamorphism and deformation, are recorded in the SUAD. Thus, following the Lamarão *et al.* (2005) hypothesis for the Tapajós domain, the 1.90-1.89 Ga granitoids studied in SUAD have been attributed to large scale taphrogenesis marking the break up of a large Paleoproterozoic continent driven by underplating mechanism (**Fig. 8c**). Derivation of the original magmas from remelting of crustal sources older than ca. 1.9 Ga and their association with a continental-scale extensional event are consistent with the geological, geochemical and Pb-Nd isotopic data.

CONCLUSIONS

The relatively high NdT_{DM} model ages and the negative $\epsilon_{Nd(T)}$ values observed in the southeast of Roraima preclude an exclusive derivation from primitive (depleted) mantle sources. The isotopic data discussed herein, indicate that the magma sources for the granitoids can be better explained as dominantly Paleoproterozoic (Rhyacian) with limited Archean crustal contributions (e.g. Igarapé Azul and Caroebe granitoids) or by Siderian to Archean sialic sources and negligible crustal Paleoproterozoic contributions (e.g. Serra Dourada and Martins Pereira granitoids).

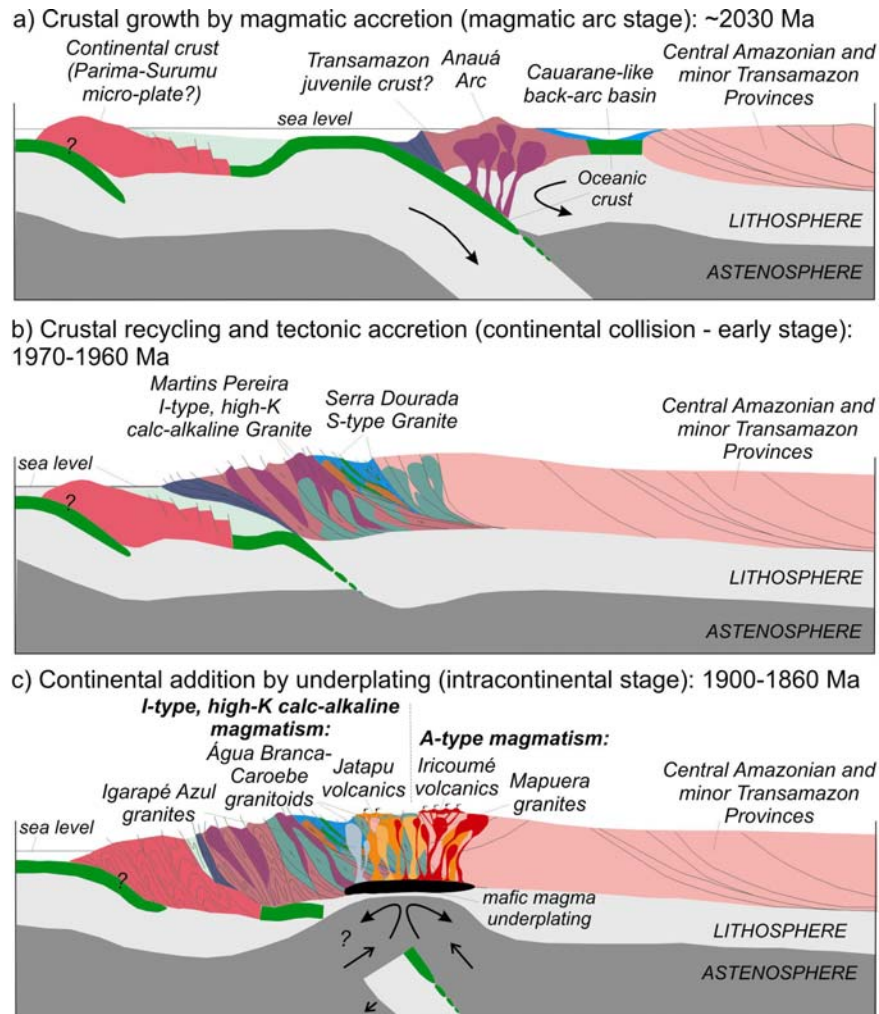


Fig. 8. Schematic paleotectonic model for the Orosirian in the Uatumã-Anauá Domain, southeastern Roraima, central Guyana Shield. (a) In the northern area (NUAD), at ~2030 Ma oceanic crust subducts at the western margin of the continental or oceanic plate. Melting of the subducted oceanic crust generate TTG magmas and fluids that ascent to the overlying mantle wedge and lower crust (Anauá Complex), enclosing ultramafic to mafic xenoliths. Back-arc basin are associated to this environment and produce graywackes, arkoses and locally MORB basalts (Cauarane-like sequences); (b) At 1970-1960 Ma the Anauá arc collides with Central Amazonian and Transamazon (or Maroni-Itacaiúnas) Provinces in the westside. This collision produce by partial melting crustal S-type granites (Serra Dourada) and several magma pulses of high-K calc-alkaline granitoids (Martins Pereira). In more advanced collisional stage (1.94-1.92 Ga?) blocks located to east could be collided with the Anauá Arc. In the boundaries (suture zone?) thrust sheets of granulites are locally exposed at middle-upper crust levels; (c) After convergent dominant process (arc and collisional stages) in early Orosirian times, a major distensional event is dominant in the southern area (SUAD) at 1900-1860 Ma interval. In this stage happen the slab rupture and break-off, including upward asthenosphere migration and magma mafic underplating at the mantle-crust boundary. The lower crustal rocks melt yielding felsic magmas. Different degrees of interaction these magmas with others pre-existing crustal rocks will result in the Água Branca, Caroebe, Igarapé Azul and Mapuera granitoids, including locally charnockitoids and coeval volcanism (Jatapu and Iricoumé).

In the NUAD, the S-type (ca. 1.96 Ga, Serra Dourada) and older high-K calc-alkaline ca. 1.97 Ga, Martins Pereira) granitoids could be related to the early stages of collisional phase after the Anauá arc amalgamation with older crustal sialic basement (Central Amazonian and Maroni-Itacaiúnas provinces) with Rhyacian to Archean age.

The absence of remnants of oceanic crust and arc basin related sequences in the SUAD suggests that Igarapé Azul and Caroebe high-K calc-alkaline granitoids (1.90-1.89 Ga) and Mapuera A-type

granites (ca. 1.87 Ga) were produced in the post-orogenic setting related to an extensional tectonic driven by underplating mafic magma process from dominant depleted (e.g. andesites, tonalites, amphibolites) and/or enriched (e.g. paraderived rocks) crustal sources, both Rhyacian in age (Maroni-Itacaiúnas or Transamazon provinces). This model contrasts with arc-related hypothesis of Santos *et al.* (2000), however, field detailed mapping, structural and metamorphic analyses, including much more laboratory data, are necessary for a construction of a more realistic model in the central segment of Guyana Shield.

The geochronological and isotope similarities between the Uatumã-Anauá and Tapajós domains suggest that both belong to the same province (Ventuari-Tapajós or Tapajós-Parima) and these constraints show that not all the province necessarily possess a juvenile origin, but in contrast (at least in the Southeast of Roraima) rocks of crustal origin dominate. The similarities are related especially to the crystallization age range of the main granitic events: (i) 2.03-1.96 Ga (Orogenic Domain) and 1.90-1.88 Ga (Post-orogenic Domain). However, the absence of granulitic-charnockitic rocks and the paucity of S-type granites in the Tapajós domain point out that the collisional setting was less important in the Tapajós region if compared to the Uatumã-Anauá domain. Furthermore, isotopic data suggesting Archean crust sources (Lamarão *et al.*, 2005) are more limited in Tapajós domain.

ACKNOWLEDGMENTS

Special thanks to the colleagues of CPRM (Geological Survey of Brazil), Pará-Iso (UFPA) and LMTG (Pierre Sabaté University, Toulouse, France) for geological discussions and helpful during isotopic analysis. The authors are also grateful to CPRM-Geological Survey of Brazil for the research grants and FINEP (CT-Mineral 01/2001 Project), CAPES (BEX 1041-05-3) and Pará-Iso for support of laboratorial works.

REFERENCES

- Allegre, C.J., Lewin, E., Dupré, B. 1988. A Coherent Crust Mantle Model for the Uranium Thorium Lead Isotopic System. *Chemical Geology* 70 (3), 211-234.
- Almeida M.E., Fraga L.M.B., Macambira M.J.B. 1997. New geochronological data of calc-alkaline granitoids of Roraima State, Brazil. In: IG/USP, South-American Symp. on Isotope Geology, 1, Ext. Abst., p.34-37.
- Almeida M.E., Macambira M.J.B. 2003. Aspectos geológicos e litoquímicos dos granitóides cálcio-alcálicos Paleoproterozóicos do sudeste de Roraima. In: SBGq, Cong. Brasil. Geol., 9, Anais, p. 775-778 (in portuguese).
- Almeida, M.E., Macambira, M.J.B. Geology, Petrography and Mineralizations of Paleoproterozoic Granitoids from Uatumã-Anauá Domain (Guyana Shield), Southeast of Roraima State, Brazil. *Revista Brasileira de Geociências*. submitted.

- Almeida, M.E., Macambira, M.J.B., Faria, M.S.G. de. 2002. A Granitogênese Paleoproterozóica do Sul de Roraima. In: SBG, Congresso Brasileiro de Geologia., 41, Anais, p 434 (in portuguese).
- Almeida, M.E., Macambira, M.J.B., Oliveira, E.C. Geochemistry and Zircon Geochronology of the I-type High-K Calc-alkaline and S-Type Granitoids from Southeast of Roraima State, Brazil: Orosirian Magmatism Evidence (1.97-1.96 Ga) in central portion of Guyana Shield. *Precambrian Research* submitted. (Almeida *et al*, submitted. a)
- Almeida, M.E., Macambira, M.J.B., Galarza-Toro, M.A., Santos, L.S. Evidence of the Widespread 1.90-1.89 Ga I-type, high-K calc-alkaline magmatism in Southeast of Roraima State, Brazil (central portion of Guyana Shield) based on Geochemistry and Zircon Geochronology. *Lithos* submitted (Almeida *et al.*, submitted b)
- Almeida, M.E., Macambira, M.J.B., Valente, S. de C. New geological and single-zircon Pb evaporation data from the Central Guyana Domain in the southeast of Roraima State, Brazil: tectonic implications for the central portion of the Guyana Shield. *Journal of South-American Earth Science* submitted (Almeida *et al.*, submitted c)
- Arndt, N.T., Goldstein, S.L. 1987. Use and abuse of crust-formation ages. *Geology* 15 : 893–895.
- Avelar, V.G. de, Lafon, J.M., Delor, C., Guerrot, C., Lahondère, D. 2003. Archean crustal remnants in the easternmost part of the Guiana Shield: Pb-Pb and Sm-Nd geochronological evidence for Mesoarchean versus Neoproterozoic signatures. *Géologie de la France* 2-3-4, 83-99.
- Avelar, V.G., Lafon, J.M., Correia, F.C., Jr., Macambira, E.M.B. 1999. O magmatismo Arqueano da região de Tucumã-Província Mineral de Carajás: novos resultados geocronológicos. *Rev. Bras. Geoc.* 29, 453-460 (in Portuguese).
- Billström, K., Weihed, P. 1996. Age and provenance of host rocks and ores in the Palaeoproterozoic Skellefte district, northern Sweden. *Econ. Geol.* 91, 1054–1072.
- Coleman, D.S., Walker, J.D. 1992. Generation of juvenile granitic crust during continental extension: *Journal of Geophysical Research* 92, 11011-11024.
- Cordani, U.G., Tassinari, C.C.G., Teixeira, W., Basei, M.A.S., Kawashita, K. 1979. Evolução tectônica da Amazônia com base nos dados geocronológicos. In: Congresso Geológico Chileno, 2, 1979, Arica, Anais, v.4, p.177-148 (in portuguese).
- Costa, S. dos S. 2005. Análise integrada dos dados geofísicos, geológicos e de sensoriamento remoto do Cinturão Guiana Central e áreas adjacentes do estado de Roraima. Doctoral thesis, Unicamp, São Paulo. 157 p (unpublished).
- Costi, H.T., Dall'Agnol, R., Moura, C.A.V. 2000. Geology and Pb-Pb geochronology of Paleoproterozoic volcanic and granitic rocks of the Pitinga Province, Amazonian craton, northern Brazil. *Intern. Geol. Rev.* 42, 832-849.

- CPRM. 2000. Programa Levantamentos Geológicos Básicos do Brasil. Caracarái, Folhas NA.20-Z-B e NA.20-Z-D (integrais), NA.20-Z-A, NA.21-Y-A, NA.20-Z-C e NA.21-Y-C (parciais). Escala 1:500.000. Estado de Roraima. Superintendência Regional de Manaus, 157 p. CD-ROM. (in portuguese, abstract in english)
- CPRM. 2003. Programa Levantamentos Geológicos Básicos do Brasil. Geologia, Tectônica e Recursos Minerais do Brasil: Sistema de Informações Geográficas - SIG. Rio de Janeiro : CPRM , 2003. Mapas Escala 1:2.500.000. 4 CDs ROM. (in portuguese, abstract in english)
- CPRM. 2005. Programa Levantamentos Geológicos Básicos do Brasil. Escala 1:1000.000. Mapa Geológico do Brasil. 41 mapas Brasília, MME. CD-ROM. (in portuguese)
- CPRM. 2006. Programa Levantamentos Geológicos Básicos do Brasil. Escala 1:1000.000. Mapa Geológico do Estado do Amazonas. Manaus, MME. Text and CD-ROM. (in portuguese)
- Cumming, G.L., Richards, J.R. 1975. Ore Pb-isotope ratios in a continuously changing Earth. *Earth Planet. Sci. Lett.* 28, 155-171.
- Dall'Agnol, R., Råmo, O.T., Magalhães, M.S. de, Macambira, M.J.B. 1999. Petrology of the anorogenic, oxidised Jamon and Musa granites, Amazonian Craton: implications for the genesis of Proterozoic A-type granites. *Lithos* 46, 431–462
- De Paolo, D.J. 1988. Neodymium Isotope Geochemistry, Springer-Verlag. 187 pp
- Delor, C., Lahondère, D., Egal, E., Lafon, J.-M., Cocherie, A., Guerrot, C., Rossi, P., Truffert, C., Théveniaut, H., Phillips, D., Avelar, V.G. de. 2003. Transamazonian crustal growth and reworking as revealed by the 1:500,000-scale geological map of French Guiana (2nd edition). *Géologie de la France* 2-3-4, 5-57.
- Doe, B.R. 1970. Pb Isotopes. Springer, Berlim.
- Doe, B.R., Zartman, R.E. 1979. Plumbotectonics: the Deposits, H.L. Bames, Editor, Second Edition, pages Phanerozoic; in *Geochemistry of Hydrothermal Ore* 22-70; John Wiley and Sons, New York.
- Dunphy, J.M., Ludden, J.N. 1998. Petrological and geochemical characteristics of a Paleoproterozoic magmatic arc (Narsajuaq Terrane, Ungawa Orogen, Canada) and comparisons to Superior Province granitoids. *Precamb. Res.* 91, 109-142.
- Elthon, D. 1989. Pressure origin of primary mid-ocean ridge basalts. In: Saunders, A.D., Norry, M.J. (Eds.), *Magmatism in the Ocean Basins*. Geological Society Special Publication no. 42. Geological Society, London, pp. 125-136.
- Faria, M.S.G. de, Santos, J.O.S. dos, Luzardo, R., Hartmann, L.A., McNaughton, N.J. 2002. The oldest island arc of Roraima State, Brazil – 2.03 Ga: zircon SHRIMP U-Pb geochronology of Anauá Complex. In: SBG, Congresso Brasileiro de Geologia, 41, Anais, p. 306.

- Fraga, L.M.B. 2002. A Associação Anortosito–Mangerito–Granito Rapakivi (AMG) do Cinturão Guiana Central, Roraima e Suas Encaixantes Paleoproterozóicas: Evolução Estrutural, Geocronologia e Petrologia. CPGG, UFPA, Tese de Doutorado. 386p (inédito) (in portuguese).
- Fuck, R.A., Pimentel, M.M., Machado, N., Daoud, W.K. 1993. Idade U-Pb do Granito Madeira, Pitinga (AM). In: Congresso Brasileiro de Geoquímica, 4., Brasília, 1993. Volume de Resumos Expandidos. Brasília, SBGq, p.246-249. (in portuguese).
- Greenough, J.D., Kyser, T.K. 2003. Contrasting Archean and Proterozoic lithospheric mantle: isotopic evidence from the Shonkin Sag sill (Montana). *Contrib. Mineral. Petrol.* **145**, 169–181
- Griffin, T.J., Page, R.W., Sheppard, S., Tyler, I.M. 2000. Palaeoproterozoic post-collisional, high-K felsic igneous rocks from the Kimberley region of northwestern Australia. *Precamb. Res.* 101, 1–23.
- Gruau, G., Martin, H., Lévêque, B., Capdevilla, R. 1985. Rb-Sr and Sm-Nd geochronology of Lower Proterozoic granite-greenstone terrains in French Guyane, South America. *Precamb. Res.* 30, 63-80.
- Hawkesworth, C. J., Turner, S., Gallagher, Hunter, A., Bradshaw, T., Rogers, N. 1995. Calc-alkaline magmatism, lithospheric thinning and extension in the Basin and Range. *J. Geophys. Res.* 100 (B7), 10271-10286
- Heier, K.S., Palmer, P.D., Taylor, S.R. 1967. Comment on the Pb distribution in southern Norwegian Precambrian alkali feldspars. *Nor. Geol. Tidskr.* 47, 189.
- Hemming, S.R., McDaniel, D.K., McLennan, S.M., Hanson, G.N. 1996. Pb isotope constraints on the provenance and diagenesis of detrital feldspars from the Sudbury Basin, Canada. *Earth Planet. Sci. Lett.* 142, 501-512.
- Hogan, J. P., Sinha, A. K. 1991. The effect of accessory on the redistribution of lead isotopes during crustal model. *Geochim. Cosmochim. Acta* 55, 335-348.
- Housh, T., Bowring, S.A. 1991. Lead isotopic heterogeneities within alkali feldspars: implications for the determination of initial lead isotopic compositions. *Geochim. Cosmochim. Acta* 55, 2309-2316.
- Huhma, H., 1986. Sm–Nd, U–Pb and Pb–Pb isotopic evidence for the origin of the early Proterozoic Svecokarelian crust in Finland. *Geol. Surv. Finland Bull.* 337, 48p.
- Kempton, P.D., Fitton, J.G., Hawkesworth, C.J., Ormerod, D.S. 1991. Isotopic and trace element constraints on the composition and evolution of the lithosphere beneath southwestern United States. *J. Geophys. Res.* **96**, 13713–13735
- Lahtinen, R., Huhma, H. 1997. Isotopic and geochemical constraints on the evolution of the 1.93-1.79 Ga Svecofennian crust and mantle in Finland. *Precamb. Res.* 82, 13-34.
- Lamarão, C.N., Dall’Agnol, R., Lafon, J.M., Lima, E.F. 2002. Geology, geochemistry and Pb–Pb zircon geochronology of the Paleoproterozoic magmatism of Vila Riozinho, Tapajós gold province, Amazonian craton, Brazil. *Precamb. Res.* 119 (1-4), 189–223.

- Lamarão, C.N., Dall’Agnol, R., Pimentel, M.M. 2005. Nd isotopic composition of Paleoproterozoic volcanic and granitoid rocks of Vila Riozinho: implications for the crustal evolution of the Tapajós gold province, Amazon craton. *J. South Am. Earth Sci.* 18, 277–292.
- Leite, A. da S.S., Dall’Agnol, R., Macambira, M.J.B., Althoff, F.J. 2004. Geologia e geocronologia dos granitóides arqueanos da região de Xinguara-PA e suas implicações na evolução do terreno granito-greenstone de Rio Maria, Cráton Amazônico. *Rev. Bras. Geoc.* 34(4), 447-458.
- Lenharo S.L.R. 1998. Evolução magmatica e modelo metalogenetico dos granitos mineralizados da regioao de Pitinga, Amazonas, Brasil. Universidade de São Paulo, Tese de Doutorado, São Paulo, 290 p.
- Ludwig, K.R., Silver, L.T., 1977. Lead-isotope inhomogeneity in Precambrian igneous K-feldspars. *Geochim. Cosmochim. Acta* 41(10), 1457-1471.
- Macambira, M.J.B., Almeida, M.E., Santos, L.S. 2002. Idade de Zircão das Vulcânicas Iricoumé do Sudeste de Roraima: contribuição para a redefinição do Supergrupo Uatumã. In: SBG, Simpósio Sobre Vulcanismo Ambientes Associados, 2, Anais, p.22 (in portuguese).
- Macambira, M.J.B., Lancelot, J.R. 1996. Time constraints for the formation of the Archean Rio Maria crust, southeastern Amazonian craton, Brazil. *Intern. Geol. Rev.* 38, 1134–1142.
- McCulloch, M.T., Woodhead, J.D. 1993. Lead isotopic evidence for deep crustal-scale fluid transport during granite petrogenesis. *Geochim. Cosmochim. Acta* 57, 659-674.
- Nironen, M. 1997. The Svecofennian Orogen: a tectonic model. *Precamb. Res.* 86, 21–44.
- Oliveira, M.J.R.; Almeida, M.E.; Luzardo, R., Faria, M.S.G. de. 1996. Litogeoquímica da Suíte Intrusiva Água Branca - SE de Roraima. Congr. Brasil. de Geol., 39, Salvador, 1996. Anais... Salvador, Bahia, SBG, v.2, p. 213-216 (in portuguese).
- Page, R.W., 1988. Geochronology of early to middle Proterozoic fold belts in northern Australia: a review. *Precamb. Res.* 40/41, 1–20.
- Patterson, C.;Tatsumoto, M. 1964. The significance of lead isotopes in detrital feldspar with respect to chemical differentiation within the earth’s mantle, *Geochim. Cosmochim. Acta* 28, 1-22.
- Pimentel, M.M., Machado, N. 1994. Geocronologia U–Pb dos terrenos granito–greenstone de Rio Maria, Para’. 38th Congr. Bras. Geol., 1, São Paulo, pp. 390–391.
- Rehkamper, M., Hofmann, A.W. 1997. Recycled ocean crust and sediment in Indian Ocean MORB. *Earth Planet. Sci. Lett.* 147 (1-4), 93-106.
- Reis, N.J., Fraga, L.M.B., Faria, M.S.G. de, Almeida, M.E. 2003. Geologia do Estado de Roraima. Géologie de la France, 2-3-4, 71-84. Abstract in english (in portuguese).
- Rudnick, R.L., Goldstein, S.L. 1990. The Pb isotopic composition of lower crustal xenoliths and the evolution of lower crustal Pb. *Earth Planet. Sci. Lett.* 98, 192-207.

- Santos J.O.S. dos, Silva L.C., Faria M.S.G. de, Macambira, M.J.B. 1997. Pb-Pb single crystal, evaporation isotopic study on the post-tectonic, sub-alkalic, A-type Moderna granite, Mapuera intrusive suite, State of Roraima, northern Brazil. In: Symposium of Granites and Associated Mineralizations, 2. Extended Abstract and Program. Salvador, Brasil: p. 273-275.
- Santos J.O.S. dos, Hartmann L.A., Gaudette H.E., Groves D.I., McNaughton N.J., Fletcher I.R. 2000. A new understanding of the provinces of the Amazon Craton based on integration of field mapping and U-Pb and Sm-Nd geochronology: *Gondwana Research* 3 (4), 453-488.
- Santos J.O.S. dos; Faria M.S.G.; Hartmann L.H.; McNaughton N.J.; Fletcher I.R. 2001a. Oldest charnockitic magmatism in the Amazon craton: zircon U-Pb SHRIMP geochronology of the Jaburu charnockite, southern Roraima, Brazil. In: SBG\Norte, Simp. Geol. Amaz, 7, CD-ROM (in portuguese).
- Santos, J.O.S. dos, Groves, D.I., Hartmann, L.A., McNaughton, N.J., Moura, M.B. 2001b. Gold deposits of the Tapajós and Alta Floresta domains, Tapajós–Parima orogenic belt, Amazon Craton, Brazil. *Mineralium Deposita* 36, 278–299.
- Santos, J.O.S. dos, Faria, M.S.G. de, Hartmann, L.A., McNaughton, N.J. 2002. Significant presence of the Tapajós-Parima Orogenic Belt in the Roraima region, Amazon Craton based on SHRIMP U-Pb zircon geochronology. In: SBG, Congresso Brasileiro de Geologia, 51, João Pessoa, Anais... p.336.
- Santos, J.O.S. dos, Reis, N.J., Chemale, F., Hartmann, L.A., Pinheiro, S. da S., McNaughton, N.J. 2003. Paleoproterozoic Evolution of Northwestern Roraima State – Absence of Archean Crust, Based on U-Pb and Sm-Nd Isotopic Evidence. In: Simposyum of South-American on Isotope Geology, 4, Pucon, Chile.
- Santos, J.O.S. dos, Van Breemen, O.B., Groves, D.I., Hartmann, L. A., Almeida, M.E., McNaughton, N.J., Fletcher, I.R. 2004. Timing and evolution of multiple Paleoproterozoic magmatic arcs in the Tapajós Domain, Amazon Craton: constraints from SHRIMP and TIMS zircon, baddeleyite and titanite U–Pb geochronology. *Precamb. Res.* 131 (10), 73-109.
- Santos, J.O.S. dos, Hartmann, L.A., Faria, M.S.G. de, Riker, S.R.L., Souza, M.M. de, Almeida, M.E., McNaughton, N.J. 2006. A Compartimentação do Cráton Amazonas em Províncias: Avanços ocorridos no período 2000-2006. In: SBG, Simpósio de Geologia da Amazônia, 9, Belém, CD-ROM.
- Sato, K., Siga Jr., O. 2002. Rapid growth of continental crust between 2.2 to 1.8 Ga in the South American Platform: integrated Australian, European, North American and SW USA crustal evolution study. *Gondwana Research* 5, 165–173.
- Sato, K., Tassinari, C.C.G. 1997. Principais eventos de acreção continental no Cráton Amazônico baseados em idade-modelo Sm–Nd, calculada em evoluções de estágio único e estágio duplo, in:

- Costa, M.L.C., Angélica, R.S. (Eds.), Contribuições à Geologia da Amazônia. Sociedade Brasileira de Geologia, Belém, Brazil, 1, pp. 91–142.
- Sinha, A.K. 1969. Removal of radiogenic lead from potassium feldspars by volatilization. *Earth Planet. Sci. Lett.* 7, 109-115.
- Stacey, J.S., Kramers, J.D. 1975. Approximation of terrestrial lead isotope evolution by a two-stage model. *Earth Planet. Sci. Lett.*, 26, 207-221.
- St-Onge, M.R., Lucas, S.B., Scott, D.J., Wodicka, N., 1999. Upper and lower plate juxtaposition, deformation and metamorphism during crustal convergence, Trans-Hudson Orogen (Quebec-Baffin segment), Canada. *Precambrian Res.* 93, 27–49.
- Tassinari, C.C.G. 1996. O Mapa Geocronológico do Cráton Amazônico no Brasil: revisão dos dados isotópicos. Tese de Livre docência, Instituto de Geociências da Universidade de São Paulo. 139p. (in portuguese).
- Tassinari, C.C.G., Macambira, M.J.B. 1999. Geochronological Provinces of the Amazonian Craton. *Episodes* 22 (3): 174-182.
- Tassinari, C.C.G., Macambira, M.J.B. 2004. A Evolução Tectônica do Cráton Amazônico. In: Mantesso-Neto, V., Bartoreli, A., Carneiro, C.D.R., Brito-Neves, B.B. de (eds), Geologia do Continente Sul-Americano - Evolução da Obra de Fernando Flávio Marques de Almeida, São Paulo, Ed. Beca, p. 471-485. Abstract in english (in portuguese).
- Tassinari, C.G.C., Munhá, J.M.U., Teixeira, W., Palácios, T., Nutman, A.P., Sosa, C.S., Santos, A.P., Calado, B.O. 2004. The Imataca Complex, NW Amazonian Craton, Venezuela: Crustal evolution and integration of geochronological and petrological cooling histories. *Episodes* 27 (1), 1-12.
- Teixeira, W., Tassinari, C.C.G., Cordani, U.G., Kawashita, K. 1989. A review of the Geochronology of the Amazonian Craton tectonic implications. *Precamb. Res.* 42, 213-227.
- Tomascak, P.B. 1995. The petrogenesis of granitic rocks in southwestern Maine. PhD Thesis, University of Maryland, College Park, MD.
- Tomascak, P.B.; Brown, M.; Solar, G.S.; Beckera, H.J.; Centorbi, H.J., Tian, J. 2005. Source contributions to Devonian granite magmatism near the Laurentian border, New Hampshire and Western Maine, USA. *Lithos* 80, 75– 99.
- Väisänen, M., Mänttari, I. Hölttä, P. 2002. Svecofennian magmatic and metamorphic evolution in southwestern Finland as revealed by U-Pb zircon SIMS geochronology. *Precamb. Res.* 116, 111-127.
- Valério, C.S. 2006. Magmatismo Paleoproterozóico do extremo sul do Escudo das Guianas, município de Presidente Figueiredo (AM): geologia, geoquímica e geocronologia Pb-Pb em zircão. Universidade Federal do Amazonas, Dissertação de Mestrado, Manaus, ?p. (in portuguese).

- Valério, C.S., Souza, V.S., Macambira, M.J.B., Milliotti, C.A., Carvalho, A.S. 2005. Geoquímica e idade Pb-Pb de zircão do Grupo Iricoumé na região da borda norte da bacia do Amazonas, município de Presidente Figueiredo (AM). In: SBG, Simp. Vulc. Amaz. Amb. Assoc., 3, Anais, p.47-52.
- Wyborn, L.A. 1988. Petrology, geochemistry and origin of a major Australian 1880–1840 Ma felsic volcano-plutonic suite, a model for intracontinental felsic magma generation. *Precamb. Res.* 40/41, 37–60.
- Zartman, R. E., Haines, S. 1988. The plumbotectonic model for Pb isotopic systematics among major terrestrial reservoirs – a case for bi-directional transport. *Geochim. Cosmochim. Acta* 52, 1327–1339.
- Zartman, R.E., Doe, B.R. 1981. Plumbotectonics - the model. *Tectonophysics* 75, 135-162.
- Zindler, A, Hart, S. 1986. Chemical geodynamics. *Am. Rev. Earth Planet. Sci.* 5(14), 493-571.

Table 1. Summary of previous geochronological data from Uatumã-Anauá domain.

| Sample code | Rock Type | Lithostratigraphic Unit | Crystallization age (Ma) | Reference | Method | Inherited age (Ma) | Reference | Method | obs |
|-------------------------------------|---------------------------|---------------------------------|--------------------------|---------------------------------|--------|--------------------|---------------------------------|--------|--|
| <i>Northern Uatumã-Anauá Domain</i> | | | | | | | | | |
| MA-246C2 | Leucogranite | Pods and lenses of leucogranite | 1906 ± 5 zi | Almeida <i>et al.</i> (Subm. a) | C | 1959 ± 5 zi | Almeida <i>et al.</i> (Subm. a) | C | Martins Pereira |
| | | | | | | 1997 ± 8 zi | Almeida <i>et al.</i> (Subm. a) | C | Anauá Arc? |
| | | | | | | 2128 ± 3 zi | Almeida <i>et al.</i> (Subm. a) | C | Early Transamazonian |
| | | | | | | 2354 ± 6 zi | Almeida <i>et al.</i> (Subm. a) | C | Siderian |
| MF-156 | Monzogranite | S-type Serra Dourada Granite | 1948 ± 11 zi | Almeida <i>et al.</i> (Subm. a) | C | 2138 ± 11 zi | Almeida <i>et al.</i> (Subm. a) | C | Early Transamazonian |
| | | | 1962 ± 6 zi | Almeida <i>et al.</i> (Subm. a) | D | | | | |
| MF-132A | Metamonzogranite | Martins Pereira Granite | 1938 ± 17 zi | Almeida <i>et al.</i> (1997) | B | | | | |
| NR-017 | Metamonzogranite | Martins Pereira Granite | 1960 ± 21 zi | Almeida <i>et al.</i> (1997) | B | | | | |
| MA-007A | Metamonzogranite | Martins Pereira Granite | 1971 ± 2 zi | Almeida <i>et al.</i> (Subm. a) | C | | | | |
| MF-132A | Metamonzogranite | Martins Pereira Granite | 1972 ± 7 zi | CPRM (2003) | F | | | | |
| MA-061A | Mylonitic granodiorite | Martins Pereira Granite | 1973 ± 2 zi | Almeida <i>et al.</i> (Subm. a) | C | | | | |
| MA-172A | Monzogranite | Martins Pereira Granite | 1975 ± 5 zi | Almeida <i>et al.</i> (Subm. a) | C | | | | |
| | Metatonalite (MF-075) | Anauá Complex | 2028 ± 9 zi | Faria <i>et al.</i> (2002) | F | | | | |
| <i>Southern Uatumã-Anauá Domain</i> | | | | | | | | | |
| - | Água Boa Granite | Madeira Suite | 1679 ± 60 wr | Macambira <i>et al.</i> (1987) | A | | | | $^{87}\text{Sr}/^{86}\text{Sr}_o = 0.7113$ |
| - | Madeira Granite | Madeira Suite | 1691 ± 64 wr | Macambira <i>et al.</i> (1987) | A | | | | $^{87}\text{Sr}/^{86}\text{Sr}_o = 0.7062$ |
| - | Água Boa Granite | Madeira Suite | 1794 ± 19 zi | Lenharo (1998) | D | | | | |
| MJ-59A | Moderna Granite | Madeira Suite | 1814 ± 27 zi | Santos <i>et al.</i> (1997b) | B | | | | |
| - | Madeira Granite | Madeira Suite | 1815 ± 5 zi | Lenharo (1998) | D | | | | |
| - | Madeira Granite | Madeira Suite | 1817 ± 2 zi | Costi <i>et al.</i> (2000) | C | | | | |
| - | Madeira Granite | Madeira Suite | 1822 ± 1 zi | Costi <i>et al.</i> (2000) | C | | | | |
| - | Madeira Granite | Madeira Suite | 1824 ± 2 zi | Costi <i>et al.</i> (2000) | C | | | | |
| - | Europa Granite | Madeira Suite | 1829 ± 1 zi | Costi <i>et al.</i> (2000) | C | | | | |
| - | Madeira Granite | Madeira Suite | 1834 ± 6 zi | Fuck <i>et al.</i> (1993) | D | | | | |
| - | Pitinga Mine Granite | Mapuera Suite | 1861 ± 20 zi | Lenharo (2001) | F | | | | |
| - | Pitinga Mine Granite | Mapuera Suite | 1864 ± 13 zi | Lenharo (2001) | F | | | | |
| - | Pitinga Mine Granite | Mapuera Suite | 1865 ± 15 zi | CPRM (2003) | F | | | | |
| MF-17 | Meretxa Mylonitic Granite | Mapuera Suite? | 1869 ± 10 zi | CPRM (2003) | F | | | | |
| JO-05 | Weathered gneiss | Mapuera Suite? | 1871 ± 11 zi | CPRM (2003) | F | | | | |
| km 199 | Abonari Syenogranite | Mapuera Suite | 1871 ± 5 zi | CPRM (2003) | F | | | | |
| JO-07 | Weathered granitoid | Mapuera Suite? | 1879 ± 2 zi | Santos (2002) | F | | | | |
| JO-06 | Weathered granitoid | Mapuera Suite? | 1880 ± 3 zi | Santos (2002) | F | | | | |
| MA-226 | Murauá Granite | Mapuera Suite | 1871 ± 5 zi | Almeida <i>et al.</i> (Subm. b) | C | 1888 ± 3 zi | Almeida <i>et al.</i> (Subm. b) | C | Caroebe? |

Table 1 (continued)

| Sample code | Rock Type | Lithostratigraphic Unit | Crystallization age (Ma) | Reference | Method | Inherited age (Ma) | Reference | Method | obs |
|-------------|---|---|--------------------------|---------------------------------|--------|--------------------|---------------------------------|--------|---|
| - | São Gabriel Granite | Mapuera Suite? | 1889 ± 2 zi | Valério (2006) | C | 2359 ± 7 zi | Almeida <i>et al.</i> (Subm. b) | C | Siderian |
| MA-186A | Monzogranite | Igarapé Azul Granite. Saramandaia Facies | 1889 ± 3 zi | Almeida <i>et al.</i> (Subm. b) | C | 1972 ± 3 zi | Almeida <i>et al.</i> (Subm. b) | C | Martins Pereira |
| MA-201B | Granitic veins in biotite-bearing enclave | Igarapé Azul Granite. Vila Catarina Facies | 1891 ± 3 zi | Almeida <i>et al.</i> (Subm. b) | C | 1967 ± 6 zi | Almeida <i>et al.</i> (Subm. b) | C | Martins Pereira |
| MA-147A | Monzogranite | Igarapé Azul Granite. Cinco Estrelas Facies | 1891 ± 6 zi | Almeida <i>et al.</i> (Subm. b) | C | 1964 ± 4 zi | Almeida <i>et al.</i> (Subm. b) | C | Martins Pereira |
| MA-186A | Monzogranite | Igarapé Azul Granite. Saramandaia Facies | 1913 ± 4 zi | Almeida <i>et al.</i> (Subm. b) | C | | | | |
| MA-198 | Enderbite | Santa Maria Enderbite | 1891 ± 1 zi | Almeida <i>et al.</i> (Subm. b) | C | | | | |
| - | Biotite mylonitized granite | Água Branca Suite | 1890 ± 2 zi | Valério (2006) | C | | | | |
| MA-53A | Monzogranite | Caroebe Granite. Alto Alegre Facies (Água Branca Suite) | 1891 ± 2 zi | Almeida <i>et al.</i> (Subm. b) | C | 1963 ± 4 zi | Almeida <i>et al.</i> (Subm. b) | C | Martins Pereira |
| MF-68A | Quartz Monzodiorite | Igarapé Dias Quartz Monzodiorite (Água Branca Suite) | 1891 ± 6 zi | CPRM (2003) | F | | | | |
| - | Biotite porphyritic granite | Água Branca Suite | 1895 ± 6 zi | Valério (2006) | C | | | | |
| MA-121 | Quartz Monzodiorite | Caroebe Granite. Jaburuzinho Facies (Água Branca Suite) | 1898 ± 2 zi | Almeida <i>et al.</i> (Subm. b) | C | | | | |
| - | Biotite-hornblende mylonitized granite | Água Branca Suite | 1898 ± 3 zi | Valério (2006) | C | | | | |
| HM-181 | Monzogranite (type-area) | Água Branca Granite (Água Branca Suite) | 1901 ± 5 zi | Almeida <i>et al.</i> (Subm. b) | C | 2142 ± 10 zi | Almeida <i>et al.</i> (Subm. b) | C | Early Transamazonian |
| - | - | Northwestern of Pará (Água Branca Suite) | 1910 ± 23 wr | Jorge-João <i>et al.</i> (1985) | A | | | | $^{87}\text{Sr}/^{86}\text{Sr}_0 = 0.70225$ |
| - | Epizonal Rhyolite | Iricoumé Volcanics | 1883 ± 4 zi | Valério <i>et al.</i> (2005) | C | | | | |
| PHR-06 | Rhyolite (Pitinga region) | Iricoumé Volcanics | 1888 ± 3 zi | Costi <i>et al.</i> (2000) | C | | | | |
| MA-209 | Porphyry Dacite (Jatapu River) | Jatapu Volcanics | 1893 ± 2 zi | Macambira <i>et al.</i> (2002) | C | | | | |
| MA-208 | Andesite (Jatapu River) | Jatapu Volcanics | 1893 ± 4 zi | Almeida <i>et al.</i> (Subm. b) | C | 1966 ± 3 zi | Almeida <i>et al.</i> (Subm. b) | C | Martins Pereira |
| MF-34 | Canoas Rhyodacite | Iricoumé Volcanics | 1896 ± 7 zi | CPRM (2003) | F | | | | |

Notes: A. Rb-Sr isochron. B. Pb-evaporation on single filament; C. Pb-evaporation on double filament; D. U-Pb ID-TIMS; E. U-Pb LA-MC-ICP-MS; F. U-Pb SHRIMP. Abbreviations: wr. whole-rock. zi. zircon.

Table 2. Sm-Nd (whole rock) and Pb (leached feldspars) isotopic data of Uatumã-Anauá Domain in south central Guyana Shield.

| Province | Domain | Sample | Rock type | T _{erist} (Ma) | Ref. | Sm (ppm) | Nd (ppm) | Sm/Nd | ¹⁴⁷ Sm/ ¹⁴⁴ Nd | 1σ (10 ⁻⁷) | ¹⁴³ Nd/ ¹⁴⁴ Nd | 1σ (10 ⁻⁶) | eNd ₍₀₎ | eNd _(t) | T _(DM) | Ref. | Pb ²⁰⁶ / _{Pb²⁰⁴} | 1σ (10 ⁻²) | Pb ²⁰⁷ / _{Pb²⁰⁴} | 1σ (10 ⁻²) | Pb ²⁰⁸ / _{Pb²⁰⁴} | 1σ (10 ⁻²) | Ref. | |
|---|--------|---------------------------|-----------|----------------------------|------|----------|----------|-------|--------------------------------------|------------------------|--------------------------------------|------------------------|--------------------|--------------------|-------------------|------|---|------------------------|---|------------------------|---|------------------------|------|------------|
| 1 | 2 | <i>Moderna Granitoids</i> | | | | | | | | | | | | | | | | | | | | | | |
| VT | KSB | UA | MF-103 | Alaskite | 1810 | G, e.a. | 7.02 | 39.61 | 0.18 | 0.10713 | - | 0.511549 | - | -21.24 | -0.44 | 2.14 | CPRM unpubl. | - | - | - | - | - | - | |
| VT | KSB | UA | CA-03 | Syenogranite | 1810 | G, e.a. | 12.15 | 68.53 | 0.18 | 0.10718 | - | 0.511497 | 9 | -22.26 | -1.47 | 2.22 | CPRM unpubl. | - | - | - | - | - | - | |
| VT | TP | UA | MF-33B | Monzogranite protomylonite | 1810 | G, e.a. | 4.69 | 30.53 | 0.15 | 0.09289 | - | 0.511280 | - | -26.49 | -2.39 | 2.23 | CPRM unpubl. | - | - | - | - | - | - | |
| <i>Mapuera Granitoids</i> | | | | | | | | | | | | | | | | | | | | | | | | |
| VT | TP | SUA | MF-04 | Granophyre | 1871 | D, e.a. | 9.28 | 51.30 | 0.18 | 0.10931 | - | 0.511596 | 15 | -20.33 | 0.66 | 2.12 | CPRM unpubl. | - | - | - | - | - | - | |
| VT | TP | SUA | MF-03 | Granite | 1871 | D, e.a. | 8.83 | 51.87 | 0.17 | 0.10290 | - | 0.511481 | 11 | -22.57 | -0.04 | 2.15 | CPRM unpubl. | - | - | - | - | - | - | |
| VT | TP | SUA | KM 199 | Hornblende granite | 1871 | D, e.a. | 15.97 | 93.45 | 0.17 | 0.10332 | - | 0.511474 | 20 | -22.71 | -0.28 | 2.17 | CPRM unpubl. | - | - | - | - | - | - | |
| MI | TP | UA | SC-19 | Granite | 1871 | D, e.a. | 15.25 | 97.30 | 0.16 | 0.09470 | - | 0.511353 | 5 | -25.07 | -0.56 | 2.17 | Costa (2005) | - | - | - | - | - | - | |
| TP | TP | UA | SC-95 | Hornblende-biotite granite | 1871 | D, e.a. | 8.55 | 45.35 | 0.19 | 0.11390 | - | 0.511556 | 6 | -21.11 | -1.22 | 2.28 | Costa (2005) | - | - | - | - | - | - | |
| <i>Igarapé Azul Granite</i> | | | | | | | | | | | | | | | | | | | | | | | | |
| VT | TP | SUA | MA-147A | Monzogranite | 1889 | B | 10.53 | 71.95 | 0.15 | 0.08850 | 10 | 0.511292 | 4 | -26.30 | -0.02 | 2.14 | This study | 16.08 | 2 | 15.59 | 2 | 35.88 | 6 | This study |
| VT | TP | SUA | MF-6A | Leucogranodiorite | 1890 | B, e.a. | 4.76 | 30.72 | 0.15 | 0.09362 | - | 0.511354 | 13 | -25.00 | -0.04 | 2.15 | CPRM unpubl. | 16.62 | 4 | 15.65 | 4 | 36.18 | 12 | This study |
| VT | TP | SUA | MA-201A | Monzogranite | 1890 | B | 6.95 | 39.27 | 0.18 | 0.10705 | 4 | 0.511458 | 4 | -23.00 | -1.27 | 2.27 | This study | 16.27 | 5 | 15.42 | 4 | 35.71 | 12 | This study |
| TP | TP | SUA | SC-91* | Granite | 1889 | B, e.a. | 3.23 | 24.85 | 0.13 | 0.07860 | - | 0.511136 | 9 | -29.30 | -0.67 | 2.28 | mod. Costa (2005) | - | - | - | - | - | - | - |
| VT | TP | SUA | MA-186A | Monzogranite | 1890 | B | 7.60 | 44.45 | 0.17 | 0.10329 | 5 | 0.511394 | 7 | -24.30 | -1.61 | 2.28 | This study | 15.98 | 1 | 15.54 | 1 | 35.61 | 4 | This study |
| VT | TP | SUA | MA-187 | Monzogranite | - | - | - | - | - | - | - | - | - | - | - | - | - | 15.87 | 1 | 15.51 | 2 | 35.59 | 5 | This study |
| <i>Caroebe Granite (Alto Alegre facies)</i> | | | | | | | | | | | | | | | | | | | | | | | | |
| TP | TP | SUA | MA-53A | Granodiorite | 1891 | B | 3.94 | 29.16 | 0.14 | 0.08176 | 3 | 0.511173 | 5 | -28.60 | -0.68 | 2.17 | This study | 16.41 | 7 | 15.54 | 7 | 36.09 | 18 | This study |
| TP | TP | SUA | SC-97 | Monzogranite | 1891 | B, e.a. | 2.88 | 19.48 | 0.15 | 0.08930 | - | 0.511233 | 6 | -27.41 | -1.34 | 2.22 | Costa (2005) | - | - | - | - | - | - | - |
| TP | TP | SUA | MA-276 | Granodiorite | 1891 | B, e.a. | 6.25 | 45.50 | 0.14 | 0.08310 | 6 | 0.511110 | 6 | -29.80 | -2.24 | 2.26 | This study | - | - | - | - | - | - | - |
| VT | TP | SUA | SC-104 | Granodiorite | 1891 | B, e.a. | 6.03 | 34.21 | 0.18 | 0.10660 | - | 0.511384 | 7 | -24.46 | -2.60 | 2.37 | Costa (2005) | - | - | - | - | - | - | - |
| VT | TP | SUA | MA-144A | Granodiorite | 1891 | B, e.a. | 4.84 | 30.10 | 0.16 | 0.09715 | 6 | 0.511211 | 19 | -27.80 | -3.69 | 2.41 | This study | - | - | - | - | - | - | - |
| <i>Caroebe Granite (Jaburuzinho facies)</i> | | | | | | | | | | | | | | | | | | | | | | | | |
| CA | TP | SUA | MA-53C | Tonalite | 1898 | B, e.a. | 5.95 | 32.10 | 0.19 | 0.11211 | 7 | 0.511605 | 10 | -20.20 | 0.46 | 2.16 | This study | - | - | - | - | - | - | - |
| CA | TP | SUA | MA-121 | Quartz monzodiorite | 1898 | B | 8.02 | 55.82 | 0.14 | 0.08685 | 12 | 0.511243 | 3 | -27.20 | -0.45 | 2.17 | This study | 15.90 | 1 | 15.54 | 2 | 35.49 | 5 | This study |
| VT | TP | SUA | MA-144B | Diorite | 1898 | B, e.a. | 11.43 | 65.95 | 0.17 | 0.10476 | 10 | 0.511466 | 5 | -22.90 | -0.46 | 2.21 | This study | - | - | - | - | - | - | - |
| VT | TP | SUA | SC-215 | Monzogranite | 1898 | B, e.a. | 6.54 | 38.61 | 0.17 | 0.10240 | - | 0.511436 | 6 | -23.45 | -0.47 | 2.21 | Costa (2005) | - | - | - | - | - | - | - |

Table 2 (continued)

| Province | Tectonic Domain | Sample | Rock type | T _{crst} (Ma) | Ref. | Sm (ppm) | Nd (ppm) | Sm/Nd | ¹⁴⁷ Sm/ ¹⁴⁴ Nd | 1σ (10 ⁻⁷) | ¹⁴³ Nd/ ¹⁴⁴ Nd | 1σ (10 ⁻⁶) | eNd ₍₀₎ | eNd _(t) | T _(DM) | Ref. | Pb ²⁰⁶ /Pb ²⁰⁴ | 1σ (10 ⁻²) | Pb ²⁰⁷ /Pb ²⁰⁴ | 1σ (10 ⁻²) | Pb ²⁰⁸ /Pb ²⁰⁴ | 1σ (10 ⁻²) | Ref. | |
|--|-----------------|--------|-----------|-----------------------------|------|----------|----------|------------|--------------------------------------|------------------------|--------------------------------------|------------------------|--------------------|--------------------|-------------------|------|--------------------------------------|------------------------|--------------------------------------|------------------------|--------------------------------------|------------------------|------|------------|
| VT | KSB | SUA | MF-68A | Quartz monzodiorite | 1891 | D | 9.95 | 52.35 | 0.19 | 0.11492 | - | 0.511600 | 11 | -20.25 | -0.40 | 2.23 | CPRM unpubl. | - | - | - | - | - | - | |
| CA | TP | SUA | MA-53B | Quartz monzonite | 1898 | B, e.a. | 3.96 | 22.81 | 0.17 | 0.10502 | 4 | 0.511415 | 5 | -23.90 | -1.53 | 2.29 | This study | - | - | - | - | - | - | |
| VT | TP | SUA | MA-112 | Monzogranite | 1898 | B, e.a. | 9.04 | 53.40 | 0.17 | 0.10231 | 9 | 0.511373 | 7 | -24.70 | -1.69 | 2.29 | This study | - | - | - | - | - | - | |
| VT | TP | SUA | MF-26A | Monzogranite protomylonite | 1900 | B, e.a. | 7.62 | 50.02 | 0.15 | 0.09205 | - | 0.511225 | - | -27.56 | -2.05 | 2.29 | CPRM unpubl. | - | - | - | - | - | - | |
| VT | TP | SUA | MA-178B | Quartz monzodiorite | 1898 | B, e.a. | 10.32 | 69.66 | 0.15 | 0.08953 | 11 | 0.511162 | 25 | -28.79 | -2.69 | 2.32 | This study | 16.05 | 1 | 15.54 | 2 | 35.69 | 5 | This study |
| VT | TP | SUA | MA-103 | Granodiorite | 1898 | B, e.a. | 6.65 | 40.29 | 0.17 | 0.09975 | 5 | 0.511209 | 17 | -27.90 | -4.27 | 2.47 | This study | - | - | - | - | - | - | |
| <i>Caroebe Granite?</i> | | | | | | | | | | | | | | | | | | | | | | | | |
| VT | TP | SUA | PT 25* | Granite | 1891 | B, e.a. | 6.29 | 31.87 | 0.20 | 0.11932 | 104 | 0.511758 | 27 | -17.17 | 1.62 | 2.11 | mod. Sato and Tassinari (1997) | - | - | - | - | - | - | |
| VT | TP | SUA | PT 26* | Granodiorite | 1891 | B, e.a. | 4.44 | 38.28 | 0.12 | 0.07016 | 72 | 0.511081 | 33 | -30.37 | 0.33 | 2.21 | mod. Sato and Tassinari (1997) | - | - | - | - | - | - | |
| <i>Água Branca Granite</i> | | | | | | | | | | | | | | | | | | | | | | | | |
| VT | TP | SUA | HM-181 | Granodiorite | 1901 | B | 6.45 | 38.28 | 0.17 | 0.10183 | 5 | 0.511298 | 8 | -26.10 | -3.00 | 2.39 | This study | - | - | - | - | - | - | |
| <i>Igarapé Tamararé Charnockite</i> | | | | | | | | | | | | | | | | | | | | | | | | |
| VT | KSB | SUA | MF-28 | Charnockite | 1890 | B, e.a. | 7.88 | 43.89 | 0.18 | 0.10861 | - | 0.511526 | 8 | -21.69 | -0.32 | 2.21 | CPRM unpubl. | - | - | - | - | - | - | |
| <i>Iricoumé and Jatapu Volcanic rocks</i> | | | | | | | | | | | | | | | | | | | | | | | | |
| CA | TP | SUA | PHR-06 | Rhyolite | 1888 | C | 9.77 | 55.65 | 0.18 | 0.10620 | - | 0.511500 | - | -22.20 | -0.27 | 2.19 | Costi (2000) | - | - | - | - | - | - | |
| VT | TP | SUA | MF-144A | Dacite porphyry | 1893 | F, e.a. | 5.46 | 33.52 | 0.16 | 0.09850 | - | 0.511379 | - | -24.56 | -0.70 | 2.21 | CPRM unpubl. | - | - | - | - | - | - | |
| VT | TP | SUA | MF-01 | ? | 1896 | D, e.a. | 8.78 | 45.80 | 0.19 | 0.11595 | - | 0.511625 | 9 | -19.76 | -0.14 | 2.22 | CPRM unpubl. | - | - | - | - | - | - | |
| CA | TP | SUA | MF-34 | Hornblende-biotite andesite | 1893 | F, e.a. | 8.27 | 50.93 | 0.16 | 0.09817 | - | 0.511337 | 19 | -25.38 | -1.44 | 2.26 | CPRM unpubl. | - | - | - | - | - | - | |
| TP | TP | SUA | SC-90 | Rhyodacite | 1893 | F, e.a. | 4.33 | 27.85 | 0.16 | 0.09400 | - | 0.511269 | 6 | -26.71 | -1.76 | 2.27 | Costa (2005) | - | - | - | - | - | - | |
| TP | TP | SUA | NR-29A | ? | 1893 | F, e.a. | 26.55 | 158.4 3 | 0.17 | 0.10132 | - | 0.511365 | - | -24.83 | -1.66 | 2.28 | CPRM unpubl. | - | - | - | - | - | - | |
| <i>Leucogranites (pods and lenses)</i> | | | | | | | | | | | | | | | | | | | | | | | | |
| VT | TP | NUA | MA-07B | Leuco-syenogranite | 1906 | B | 2.68 | 17.88 | 0.15 | 0.09066 | 4 | 0.511127 | 11 | -29.50 | -3.48 | 2.38 | This study | 16.15 | 2 | 15.59 | 2 | 35.95 | 6 | This study |
| VT | TP | NUA | MA-46B | Leuco-monzogranite | - | - | - | - | - | - | - | - | - | - | - | - | - | 16.87 | 1 | 15.70 | 2 | 35.74 | 5 | This study |
| <i>Enclaves (biotite-bearing gneisses)</i> | | | | | | | | | | | | | | | | | | | | | | | | |
| VT | TP | SUA | MA-213B* | Quartz monzodiorite | 1973 | B, e.a. | 12.26 | 55.73 | 0.22 | 0.13307 | 5 | 0.51166 | 6 | -19.10 | -2.92 | 2.51 | This study | - | - | - | - | - | - | |
| VT | TP | SUA | MA-201B* | Quartz diorite | 1967 | B | 41.72 | 159.7 9 | 0.26 | 0.15719 | 128 | 0.51183 | 7 | -15.70 | -5.93 | 2.72 | This study | - | - | - | - | - | - | |
| <i>Serra Dourada Granite</i> | | | | | | | | | | | | | | | | | | | | | | | | |

Table 2 (continued)

| Province | Tectonic Domain | Sample | Rock type | T _{crst} (Ma) | Ref. | Sm (ppm) | Nd (ppm) | Sm/Nd | ¹⁴⁷ Sm/ ¹⁴⁴ Nd | 1σ (10 ⁻⁷) | ¹⁴³ Nd/ ¹⁴⁴ Nd | 1σ (10 ⁻⁶) | eNd ₍₀₎ | eNd _(t) | T _(DM) | Ref. | Pb ²⁰⁶ /Pb ²⁰⁴ | 1σ (10 ⁻²) | Pb ²⁰⁷ /Pb ²⁰⁴ | 1σ (10 ⁻²) | Pb ²⁰⁸ /Pb ²⁰⁴ | 1σ (10 ⁻²) | Ref. | |
|--------------------------------|-----------------|--------|-----------|-------------------------------|------|----------|----------|-------|--------------------------------------|------------------------|--------------------------------------|------------------------|--------------------|--------------------|-------------------|------|--------------------------------------|------------------------|--------------------------------------|------------------------|--------------------------------------|------------------------|------|------------|
| VT | TP | NUA | MF-156 | Syenogranite with cordierite | 1962 | A | 4.84 | 24.50 | 0.20 | 0.11990 | - | 0.51158 | 18 | -20.70 | -3.19 | 2.38 | CPRM unpubl. | - | - | - | - | - | - | - |
| VT | TP | NUA | MF-151 | Monzogranite with muscovite | 1962 | A, e.a. | 9.14 | 45.45 | 0.20 | 0.12124 | - | 0.51152 | 16 | -21.81 | -4.34 | 2.53 | CPRM unpubl. | - | - | - | - | - | - | - |
| <i>Martins Pereira Granite</i> | | | | | | | | | | | | | | | | | | | | | | | | |
| VT | TP | NUA | NR-18 | Meta-monzogranite | 1973 | A, e.a. | 6.69 | 43.08 | 0.16 | 0.09385 | - | 0.51122 | 9 | -27.74 | -1.74 | 2.33 | CPRM unpubl. | - | - | - | - | - | - | - |
| VT | KSB | NUA | TP-01 | Monzogranite | 1973 | A, e.a. | 10.17 | 56.21 | 0.18 | 0.10939 | - | 0.51145 | 11 | -23.19 | -3.20 | 2.34 | CPRM unpubl. | - | - | - | - | - | - | - |
| VT | TP | NUA | MF-11A | Granodiorite | 1973 | A, e.a. | 6.92 | 35.21 | 0.20 | 0.11884 | - | 0.51158 | 14 | -20.64 | -0.92 | 2.36 | CPRM unpubl. | 16.50 | 1 | 15.70 | 2 | 36.04 | 5 | This study |
| VT | TP | NUA | MA-61A | Mylonite granodioritic | 1973 | A | 10.91 | 58.19 | 0.19 | 0.11335 | 5 | 0.51148 | 9 | -22.50 | -1.42 | 2.38 | This study | 16.18 | 3 | 15.57 | 3 | 35.59 | 8 | This study |
| VT | TP | NUA | MA-07A | Meta-monzogranite | 1971 | A | 12.55 | 68.74 | 0.18 | 0.11037 | 10 | 0.51144 | 6 | -23.40 | -1.55 | 2.38 | This study | 16.09 | 2 | 15.58 | 2 | 35.82 | 7 | This study |
| VT | KSB | NUA | MA-246C1 | Meta-tonalite | 1973 | A, e.a. | 9.81 | 53.44 | 0.18 | 0.11098 | 8 | 0.51141 | 6 | -23.90 | -2.17 | 2.43 | This study | 16.15 | 1 | 15.62 | 1 | 35.77 | 4 | This study |
| VT | TP | NUA | MF-132A* | Meta-monzogranite | 1972 | D | 6.68 | 31.57 | 0.21 | 0.12793 | - | 0.51161 | - | -20.05 | -2.67 | 2.49 | CPRM unpubl. | - | - | - | - | - | - | - |
| VT | TP | NUA | MA-07C* | Epidote-biotite meta-tonalite | 1973 | A, e.a. | 11.69 | 55.99 | 0.21 | 0.12622 | 10 | 0.51152 | 5 | -21.70 | -3.89 | 2.58 | This study | - | - | - | - | - | - | - |
| VT | TP | NUA | MA-172A | Monzogranite | 1975 | A | 17.87 | 97.09 | 0.18 | 0.11130 | 8 | 0.51129 | 3 | -26.40 | -4.74 | 2.64 | This study | - | - | - | - | - | - | - |
| <i>Anauá Complex</i> | | | | | | | | | | | | | | | | | | | | | | | | |
| VT | TP | NUA | MF-126C | Meta-tonalite | 2028 | E, e.a. | 6.91 | 36.46 | 0.19 | 0.11465 | - | 0.51153 | - | -21.56 | -0.19 | 2.33 | Faria <i>et al.</i> (2002) mod. | - | - | - | - | - | - | - |
| VT | TP | NUA | SC-101* | Orthogneiss | 2028 | E, e.a. | 6.08 | 48.33 | 0.13 | 0.07600 | - | 0.51091 | 12 | -33.63 | -2.21 | 2.50 | Costa (2005) | - | - | - | - | - | - | - |

Nd T_{DM} ages are calculated using the model of DePaolo (1981) for Nd evolution of the depleted mantle. Obs: e.a. estimated age; *highly fractionated samples. showing 0.125 < ¹⁴⁷Sm/¹⁴⁴Nd < 0.08. has been recalculated based on Nd evolution by double-stage. Geochronological Provinces: 1. Tassinari and Macambira (2004); 2. Santos *et al.* (2006); KSB. K' Mudku Shear Belt; VT-TP. Ventuari-Tapajós (or Tapajós-Parima); MI. Maroni-ItaTPiúnas; TP. Central Amazonian. Domain: UA – Uatumã-Anauá (SUA - Southern; NUA - Northern). Crystalization ages (References): A. Almeida *et al.* (subm. a); B. Almeida *et al.* (subm. b); C. Costi *et al.* (2000); D. CPRM (2003); E. Faria *et al.* (2002); F. Macambira *et al.* (2003); G. Santos *et al.* (1997).

Table 3. Some Sm-Nd (whole rock) isotopic data of Ventuari-Tapajós (or Tapajós-Parima), Maroni-ItaTPiúnas (or Transamazonic) and Central Amazonian Provinces.

| Provinces | Tectonic Domain | Sample | Rock type | T _{cris} (Ma) | Ref. | Sm (ppm) | Nd (ppm) | Sm/Nd | f(Sm/Nd) | ¹⁴⁷ Sm/ ¹⁴⁴ Nd | ¹⁴³ Nd/ ¹⁴⁴ Nd | 1σ (10 ⁻⁶) | εNd ₍₀₎ | εNd _(t) | T _(DM) | Ref. | |
|--|-----------------|---|-----------|-----------------------------------|------|----------|----------|--------|----------|--------------------------------------|--------------------------------------|------------------------|--------------------|--------------------|-------------------|------|-----------------------------------|
| 1 | 2 | <i>Basement rocks (Carajás Archean TTG terrane)</i> | | | | | | | | | | | | | | | |
| TP | CI | C | 246 | Mogno Trondhjemite? | 2871 | I, e.a. | 1.99 | 13.70 | 0.15 | -0.55 | 0.08804 | 0.510810 | - | -35.66 | +4.55 | 2.73 | mod. of Sato and Tassinari (1997) |
| TP | CI | C | 245 | Granodiorite (Mogno Trondhjemite) | 2871 | I, e.a. | 3.61 | 22.63 | 0.16 | -0.51 | 0.09646 | 0.510862 | - | -34.64 | +2.43 | 2.86 | mod. of Sato and Tassinari (1997) |
| TP | CI | C | MJ 08 | Arco Verde Tonalite | 2957 | H | 2.55 | 18.60 | 0.14 | -0.58 | 0.08272 | 0.510515 | 12 | -41.41 | +2.02 | 2.97 | Dall'Agnol <i>et al.</i> (1999) |
| TP | CI | C | HRM 284 | Rio Maria Granodiorite | 2874 | C | 3.06 | 18.60 | 0.16 | -0.50 | 0.09932 | 0.510834 | 9 | -35.19 | +0.86 | 2.98 | Dall'Agnol <i>et al.</i> (1999) |
| TP | CI | C | 161 | Tonalite (Xingu Complex) | 2974 | A, e.a. | 1.18 | 7.92 | 0.15 | -0.54 | 0.08972 | 0.510641 | - | -38.96 | +0.32 | 2.98 | mod. of Sato and Tassinari (1997) |
| TP | CI | C | 243 | Granodiorite (Xinguara Granite) | 2865 | G, e.a. | 3.81 | 23.81 | 0.16 | -0.60 | 0.07838 | 0.510393 | - | -43.79 | -0.14 | 3.02 | mod. of Sato and Tassinari (1997) |
| TP | CI | C | 160 | Gneiss (Mogno Trondhjemite) | 2871 | I, e.a. | 5.55 | 50.24 | 0.11 | -0.66 | 0.06684 | 0.510149 | - | -48.55 | -0.54 | 3.03 | mod. of Sato and Tassinari (1997) |
| TP | CI | C | Z 509B | Rio Maria Granodiorite | 2874 | C | 5.89 | 29.26 | 0.20 | -0.39 | 0.12160 | 0.511235 | 15 | -27.37 | +0.43 | 3.03 | Dall'Agnol <i>et al.</i> (1999) |
| TP | CI | C | 244 | Granodiorite (Mogno Trondhjemite) | 2871 | I, e.a. | 3.18 | 17.85 | 0.18 | -0.45 | 0.10763 | 0.510956 | - | -32.81 | +0.12 | 3.04 | mod. of Sato and Tassinari (1997) |
| <i>Imataca terrane</i> | | | | | | | | | | | | | | | | | |
| MI | CI | I | V4 | ? | 2000 | e.a. | 19.60 | 107.53 | 0.18 | -0.44 | 0.11020 | 0.511218 | 13 | -27.70 | -5.51 | 2.71 | Tassinari <i>et al.</i> (2004) |
| MI | CI | I | V2 | ? | 2000 | e.a. | 13.30 | 101.65 | 0.13 | -0.60 | 0.07910 | 0.510654 | 11 | -38.70 | -8.54 | 2.73 | Tassinari <i>et al.</i> (2004) |
| MI | CI | I | V8 | ? | 2000 | e.a. | 1.74 | 8.91 | 0.20 | -0.40 | 0.11830 | 0.511345 | 18 | -25.22 | -5.11 | 2.74 | Tassinari <i>et al.</i> (2004) |
| MI | CI | I | V6 | ? | 2000 | e.a. | 5.52 | 17.73 | 0.31 | -0.04 | 0.18810 | 0.512041 | 10 | -11.65 | -9.48 | 2.98 | Tassinari <i>et al.</i> (2004) |
| MI | CI | I | V5 | ? | 2000 | e.a. | 4.71 | 18.80 | 0.25 | -0.23 | 0.15130 | 0.511778 | 11 | -16.78 | -5.14 | 3.16 | Tassinari <i>et al.</i> (2004) |
| MI | CI | I | V3 | ? | 2000 | e.a. | 2.66 | 10.66 | 0.25 | -0.23 | 0.15080 | 0.511705 | 30 | -18.20 | -6.44 | 3.33 | Tassinari <i>et al.</i> (2004) |
| MI | CI | I | V1 | ? | 2000 | e.a. | 4.95 | 20.29 | 0.24 | -0.25 | 0.14740 | 0.511575 | 12 | -20.74 | -8.12 | 3.47 | Tassinari <i>et al.</i> (2004) |
| MI | CI | I | V7 | ? | 2000 | e.a. | 5.18 | 19.29 | 0.27 | -0.17 | 0.16230 | 0.511789 | 18 | -16.56 | -7.77 | 3.91 | Tassinari <i>et al.</i> (2004) |
| <i>Granitic-Granulitic rocks (Central Amapá Archean terrane)</i> | | | | | | | | | | | | | | | | | |
| MI | T | A | TP13B | Felsic Granulite | 2580 | e.a. | 3.33 | 24.60 | 0.14 | -0.58 | 0.08190 | 0.510544 | 8 | -40.85 | -2.76 | 2.92 | Avelar <i>et al.</i> (2003) |
| MI | T | A | TP17A | Tonalitic orthogneiss | 2850 | e.a. | 1.72 | 11.16 | 0.15 | -0.53 | 0.09340 | 0.510747 | 16 | -36.89 | +1.03 | 2.94 | Avelar <i>et al.</i> (2003) |
| MI | T | A | TP19B | Tonalitic orthogneiss | 2850 | e.a. | 3.10 | 17.12 | 0.18 | -0.45 | 0.10850 | 0.511026 | 6 | -31.45 | +0.93 | 2.96 | Avelar <i>et al.</i> (2003) |
| MI | T | A | BA14A | Felsic Granulite | 2600 | e.a. | 1.93 | 14.40 | 0.13 | -0.58 | 0.08100 | 0.510420 | 5 | -43.27 | -5.20 | 3.09 | Avelar <i>et al.</i> (2003) |
| MI | T | A | Sm03/80.4 | Gneiss | - | - | 4.54 | 27.76 | 0.16 | -0.50 | 0.09890 | 0.510737 | 8 | -37.08 | - | 3.10 | Pimentel <i>et al.</i> (1992) |
| MI | T | A | EG18 | Granite | 2900 | e.a. | 7.14 | 52.17 | 0.14 | -0.56 | 0.08280 | 0.510443 | 18 | -42.82 | -2.01 | 3.18 | Sato and Tassinari (1997) |
| MI | T | A | Sm03/72.5 | Gneiss | - | - | 4.95 | 24.63 | 0.20 | -0.38 | 0.12160 | 0.511128 | 7 | -29.46 | - | 3.22 | Pimentel <i>et al.</i> (1992) |
| MI | T | A | Sm03/52.0 | Gneiss | - | - | 2.37 | 13.77 | 0.17 | -0.47 | 0.10410 | 0.510752 | 5 | -36.79 | - | 3.23 | Pimentel <i>et al.</i> (1992) |
| MI | T | A | TP13A | Garnet-bearing granulite | 2580 | e.a. | 4.11 | 22.00 | 0.19 | -0.43 | 0.11300 | 0.510909 | 6 | -33.73 | -5.98 | 3.28 | Avelar <i>et al.</i> (2003) |
| MI | T | A | Sm03/87.2 | Gneiss | - | - | 3.61 | 17.67 | 0.20 | -0.37 | 0.12350 | 0.511071 | 10 | -30.57 | - | 3.40 | Pimentel <i>et al.</i> (1992) |
| MI | T | A | EG02 | Tonalite | 2900 | e.a. | 7.18 | 46.68 | 0.15 | -0.50 | 0.08740 | 0.510508 | 32 | -41.55 | -5.06 | 3.42 | Sato and Tassinari (1997) |
| <i>Granitic-Migmatitic rocks (Southeastern French Guyana)</i> | | | | | | | | | | | | | | | | | |
| MI | T | FG | B85 | Migmatitic granodiorite | 2100 | e.a. | 11.40 | 61.80 | 0.18 | -0.44 | 0.11110 | 0.511543 | 5 | -21.36 | +1.74 | 2.24 | Avelar <i>et al.</i> (2003) |
| MI | T | FG | B25A | Granite | 2100 | e.a. | 5.84 | 34.40 | 0.17 | -0.48 | 0.10260 | 0.511417 | 4 | -23.82 | +1.57 | 2.24 | Avelar <i>et al.</i> (2003) |
| MI | T | FG | B107 | Tonalite | 2130 | e.a. | 4.72 | 21.90 | 0.22 | -0.34 | 0.13030 | 0.511777 | 6 | -16.80 | +1.38 | 2.32 | Avelar <i>et al.</i> (2003) |
| MI | T | FG | B64A | Granodiorite | 2160 | e.a. | 6.57 | 32.20 | 0.20 | -0.37 | 0.12320 | 0.511653 | 6 | -19.21 | +1.19 | 2.35 | Avelar <i>et al.</i> (2003) |
| MI | T | FG | B34 | Granite | 2100 | e.a. | 0.96 | 5.98 | 0.16 | -0.51 | 0.09690 | 0.511241 | 3 | -27.25 | -0.33 | 2.36 | Avelar <i>et al.</i> (2003) |
| MI | T | FG | B20 | Migmatitic paragneiss | 2100 | e.a. | 12.30 | 83.40 | 0.15 | -0.55 | 0.08920 | 0.511084 | 4 | -30.31 | -1.32 | 2.41 | Avelar <i>et al.</i> (2003) |

Table 3 (Continued)

| Provinces | Tectonic Domain | Sample | Rock type | T _{crst} (Ma) | Ref. | Sm (ppm) | Nd (ppm) | Sm/Nd | f(Sm/Nd) | ¹⁴⁷ Sm/ ¹⁴⁴ Nd | ¹⁴³ Nd/ ¹⁴⁴ Nd | 1σ (10 ⁻⁶) | εNd ₍₀₎ | εNd _(t) | T _(DM) | Ref. | |
|--|-----------------|--------|-----------|--------------------------|------|----------|----------|--------|----------|--------------------------------------|--------------------------------------|------------------------|--------------------|--------------------|-------------------|------|------------------------------------|
| MI | T | FG | B68A | Garnet-bearing granulite | 2100 | e.a. | 3.23 | 17.53 | 0.18 | -0.43 | 0.11130 | 0.511405 | 6 | -24.05 | -1.02 | 2.45 | Avelar <i>et al.</i> (2003) |
| MI | T | FG | B99B | Granite | 2100 | e.a. | 3.06 | 17.30 | 0.18 | -0.45 | 0.10730 | 0.511256 | 3 | -26.96 | -2.86 | 2.58 | Avelar <i>et al.</i> (2003) |
| <i>Greenstone Belt Sequence (Northern French Guyana)</i> | | | | | | | | | | | | | | | | | |
| MI | T | FG | T160* | Komatiite Peridotitic | 2155 | D, e.a. | 1.81 | 6.84 | 0.26 | -0.19 | 0.16010 | 0.512302 | 28 | -6.55 | +3.60 | 2.19 | mod. of Gruau <i>et al.</i> (1985) |
| MI | T | FG | T100* | Komatiite Peridotitic | 2155 | D, e.a. | 1.66 | 6.54 | 0.25 | -0.22 | 0.15310 | 0.512182 | 38 | -8.90 | +3.19 | 2.22 | mod. of Gruau <i>et al.</i> (1985) |
| MI | T | FG | T188* | Komatiite Peridotitic | 2155 | D, e.a. | 2.54 | 10.54 | 0.24 | -0.26 | 0.14570 | 0.512070 | 30 | -11.08 | +3.06 | 2.22 | mod. of Gruau <i>et al.</i> (1985) |
| MI | T | FG | T111* | Komatiite Peridotitic | 2155 | D, e.a. | 1.88 | 7.45 | 0.25 | -0.23 | 0.15240 | 0.512162 | 19 | -9.29 | +3.00 | 2.23 | mod. of Gruau <i>et al.</i> (1985) |
| MI | T | FG | L200 | Andesite | 2131 | D, e.a. | 4.69 | 27.65 | 0.17 | -0.48 | 0.10260 | 0.511440 | 16 | -23.37 | +2.41 | 2.21 | mod. of Gruau <i>et al.</i> (1985) |
| MI | T | FG | L365 | Andesite | 2131 | D, e.a. | 4.16 | 20.04 | 0.21 | -0.36 | 0.12550 | 0.511722 | 55 | -17.87 | +1.63 | 2.29 | mod. of Gruau <i>et al.</i> (1985) |
| <i>Mafic and intermediate rocks</i> | | | | | | | | | | | | | | | | | |
| VT | TP | T | JO-69 | Ingarana Gabbro | 1900 | J | 2.26 | 12.61 | 0.18 | -0.58 | 0.10830 | 0.511500 | - | -22.20 | -0.64 | 2.24 | Santos <i>et al.</i> (2000) |
| VT | TP | T | JO-66 | Mamoal Metandesite | 1900 | J | 22.59 | 164.34 | 0.14 | -0.45 | 0.08310 | 0.511100 | - | -30.00 | -2.31 | 2.28 | Santos <i>et al.</i> (2000) |
| <i>Young S.Jorge Granite</i> | | | | | | | | | | | | | | | | | |
| VT | TP | T | RCR 72 | Quartz monzonite | 1891 | F, e.a. | 2.64 | 18.99 | 0.14 | -0.57 | 0.08400 | 0.511063 | - | -30.72 | -3.38 | 2.34 | Lamarão <i>et al.</i> (2005) |
| VT | TP | T | F 09/10 | Monzogranite | 1891 | F | 7.07 | 49.83 | 0.14 | -0.56 | 0.08580 | 0.510993 | - | -32.09 | -5.19 | 2.46 | Lamarão <i>et al.</i> (2005) |
| <i>Older S.Jorge Granite</i> | | | | | | | | | | | | | | | | | |
| VT | TP | T | CMM 103 | Quartz monzonite | 1981 | F, e.a. | 6.00 | 41.67 | 0.14 | -0.56 | 0.08700 | 0.511156 | - | -28.91 | -1.01 | 2.28 | Lamarão <i>et al.</i> (2005) |
| VT | TP | T | RCR 59 | Granite porphyry | 1981 | F, e.a. | 7.48 | 50.96 | 0.15 | -0.55 | 0.08880 | 0.511145 | - | -29.12 | -1.69 | 2.33 | Lamarão <i>et al.</i> (2005) |
| VT | TP | T | RCR 27A | Monzogranite | 1981 | F | 13.94 | 89.96 | 0.15 | -0.52 | 0.09370 | 0.511206 | - | -27.93 | -1.74 | 2.34 | Lamarão <i>et al.</i> (2005) |
| VT | TP | T | RCR 35 | Monzogranite | 1983 | F | 7.67 | 49.08 | 0.16 | -0.52 | 0.09450 | 0.511168 | - | -28.68 | -2.67 | 2.41 | Lamarão <i>et al.</i> (2005) |
| VT | TP | T | RCR 58 | Quartz monzodiorite | 1981 | F, e.a. | 5.89 | 33.05 | 0.18 | -0.45 | 0.10770 | 0.511360 | - | -24.93 | -2.30 | 2.43 | Lamarão <i>et al.</i> (2005) |
| <i>Granites and Volcanic rocks</i> | | | | | | | | | | | | | | | | | |
| VT | TP | T | MA 5 | CrepORIZÃO Tonalite? | 1960 | e.a. | 9.02 | 45.12 | 0.20 | -0.39 | 0.12088 | 0.511773 | 33 | -16.87 | +2.22 | 2.09 | mod. of Sato and Tassinari (1997) |
| VT | TP | T | MA 13 | CrepORIZÃO Tonalite? | 1960 | e.a. | 9.37 | 46.34 | 0.20 | -0.38 | 0.12217 | 0.511749 | 26 | -17.34 | +1.42 | 2.16 | mod. of Sato and Tassinari (1997) |
| VT | TP | T | CR 9 | ? | - | - | 10.41 | 67.36 | 0.15 | -0.52 | 0.09346 | 0.511281 | 18 | -26.47 | - | 2.24 | mod. of Sato and Tassinari (1997) |
| VT | TP | T | PT 29 3 | Iriri Rhyolite? | 1890 | e.a. | 6.31 | 39.10 | 0.16 | -0.50 | 0.09751 | 0.511192 | 23 | -28.21 | -4.16 | 2.44 | mod. of Sato and Tassinari (1997) |
| <i>Pedra Pintada Suite</i> | | | | | | | | | | | | | | | | | |
| MI | TP | S | SC-51 | Granite porphyry | 1958 | B, e.a. | 6.91 | 38.24 | 0.18 | -0.44 | 0.10920 | 0.511511 | 6 | -21.98 | +0.01 | 2.24 | mod. of Costa (2005) |
| MI | TP | S | SC-222 | Granite porphyry | 1958 | B, e.a. | 7.38 | 42.06 | 0.18 | -0.46 | 0.10610 | 0.511455 | 10 | -23.08 | -0.30 | 2.26 | mod. of Costa (2005) |
| MI | TP | S | SC-67 | Biotite granite | 1958 | B, e.a. | 2.91 | 20.07 | 0.14 | -0.56 | 0.08750 | 0.511172 | 6 | -28.60 | -1.15 | 2.27 | mod. of Costa (2005) |
| <i>Surumu Group</i> | | | | | | | | | | | | | | | | | |
| MI | TP | S | SC-83b | Rhyodacite | 1984 | L, e.a. | 6.76 | 32.13 | 0.21 | -0.35 | 0.12720 | 0.511818 | 11 | -16.00 | +1.72 | 2.16 | mod. of Costa (2005) |
| MI | TP | S | SC-50 | Dacite | 1984 | L, e.a. | 7.64 | 39.79 | 0.19 | -0.41 | 0.11620 | 0.511646 | 13 | -19.35 | +1.16 | 2.19 | mod. of Costa (2005) |
| MI | TP | S | SC-166 | Rhyodacite | 1984 | L, e.a. | 8.39 | 46.91 | 0.18 | -0.45 | 0.10810 | 0.511505 | 5 | -22.10 | +0.47 | 2.23 | mod. of Costa (2005) |
| MI | TP | S | SC-46 | Rhyodacite | 1984 | L, e.a. | 5.86 | 34.55 | 0.17 | -0.48 | 0.10260 | 0.511396 | 8 | -24.23 | -0.26 | 2.27 | mod. of Costa (2005) |
| MI | TP | S | SC-53b | Rhyodacite | 1984 | L, e.a. | 9.61 | 52.88 | 0.18 | -0.44 | 0.10990 | 0.511369 | 15 | -24.75 | -2.65 | 2.47 | mod. of Costa (2005) |
| <i>Jauaperi Complex</i> | | | | | | | | | | | | | | | | | |
| VT | TP | CG? | MF-20 | Granitic Gneiss | 1869 | K, e.a. | 2.64 | 20.63 | 0.13 | -0.61 | 0.07741 | 0.511244 | 19 | -27.19 | +1.54 | 2.02 | CPRM unpubl. |
| VT | TP | CG? | MF-18 | Hornblende augen gneiss | 1869 | K, e.a. | 16.54 | 90.23 | 0.18 | -0.44 | 0.11085 | 0.511617 | 7 | -19.92 | +0.76 | 2.12 | CPRM unpubl. |
| VT | TP | CG? | MF-17 | Hornblende gneiss | 1869 | K, e.a. | 9.72 | 53.51 | 0.18 | -0.44 | 0.10977 | 0.511567 | 7 | -20.89 | +0.04 | 2.17 | CPRM unpubl. |

Table 3 (Continued)

| Provinces | Tectonic Domain | Sample | Rock type | T _{crst} (Ma) | Ref. | Sm (ppm) | Nd (ppm) | Sm/Nd | f(Sm/Nd) | ¹⁴⁷ Sm/ ¹⁴⁴ Nd | ¹⁴³ Nd/ ¹⁴⁴ Nd | 1σ (10 ⁻⁶) | εNd ₍₀₎ | εNd _(t) | T _(DM) | Ref. | |
|--|-----------------|--------|-----------|--|------|----------|----------|-------|----------|--------------------------------------|--------------------------------------|------------------------|--------------------|--------------------|-------------------|------|----------------------|
| <i>Serra da Prata Suite</i> | | | | | | | | | | | | | | | | | |
| MI | KSB | CG | LF-63A | Hypersthene-quartz syenite | 1934 | E | 6.58 | 35.59 | 0.18 | -0.43 | 0.11180 | 0.511657 | - | -19.14 | +1.95 | 2.08 | Fraga (2002) |
| MI | KSB | CG | LF-26 | Charnockitoid | 1934 | E, e.a. | 9.00 | 41.17 | 0.22 | -0.41 | 0.11535 | 0.511630 | - | -19.02 | +1.19 | 2.14 | Fraga (2002) |
| MI | KSB | CG | SC-33 | Deformed granite | 1934 | E, e.a. | 8.47 | 45.72 | 0.19 | -0.44 | 0.11100 | 0.511599 | 6 | -20.27 | +1.02 | 2.15 | mod. of Costa (2005) |
| MI | KSB | CG | LF-10E | Charnockitoid | 1934 | E, e.a. | 7.25 | 36.76 | 0.20 | -0.39 | 0.11923 | 0.511686 | - | -18.57 | +0.67 | 2.19 | Fraga (2002) |
| MI | KSB | CG | SC-210* | Mafic granulite | 1934 | E, e.a. | 8.16 | 31.72 | 0.26 | -0.21 | 0.15560 | 0.512160 | 5 | -9.32 | +0.89 | 2.20 | mod. of Costa (2005) |
| MI | KSB | CG | SC-212* | Clinopyroxene granodiorite | 1934 | E, e.a. | 3.54 | 16.73 | 0.21 | -0.35 | 0.12780 | 0.511754 | 22 | -17.24 | -0.14 | 2.28 | mod. of Costa (2005) |
| <i>Barauana Granulite</i> | | | | | | | | | | | | | | | | | |
| VT | KSB | CG | MF-40A | Granulite charnockitic | 1938 | B, e.a. | 6.63 | 36.81 | 0.18 | -0.45 | 0.10883 | 0.511590 | - | -20.44 | +1.43 | 2.12 | CPRM unpubl. |
| VT | KSB | CG | SR-LF-6A | Granulite | 1938 | B, | 9.71 | 51.82 | 0.19 | -0.42 | 0.11329 | 0.511622 | - | -19.82 | +0.94 | 2.16 | CPRM unpubl. |
| VT | KSB | CG | NR-31 | Granulite | 1938 | B, e.a. | 4.65 | 32.27 | 0.14 | -0.56 | 0.08714 | 0.511245 | - | -27.17 | +0.09 | 2.17 | CPRM unpubl. |
| VT | KSB | CG | MF-106B | Granulite charnockitic | 1938 | B, e.a. | 9.05 | 52.40 | 0.17 | -0.47 | 0.10442 | 0.511483 | - | -22.53 | +0.43 | 2.18 | CPRM unpubl. |
| <i>Rio Urubu Complex</i> | | | | | | | | | | | | | | | | | |
| MI | KSB | CG | LF-06A | Igarapé Branco hornblende-biotite gneiss | 1937 | E | 14.00 | 68.09 | 0.21 | -0.37 | 0.12431 | 0.511841 | - | -15.55 | +2.47 | 2.05 | Fraga (2002) |
| MI | KSB | CG | LF-08 | Miracelia biotite-hornblende metagranite | 1935 | E | 8.04 | 45.83 | 0.18 | -0.46 | 0.10604 | 0.511585 | - | -20.54 | +1.99 | 2.07 | Fraga (2002) |
| MI | KSB | CG | SC-14a* | Biotite granite | 1937 | E, e.a. | 2.44 | 9.38 | 0.26 | -0.20 | 0.15740 | 0.512252 | 24 | -7.53 | +2.26 | 2.11 | mod. of Costa (2005) |
| MI | KSB | CG | SC-09 | Granite porphyry | 1937 | E, e.a. | 9.28 | 55.04 | 0.17 | -0.48 | 0.10190 | 0.511465 | 5 | -22.88 | +0.71 | 2.16 | mod. of Costa (2005) |
| MI | KSB | CG | MF-71 | Biotite gneiss | 1937 | E, e.a. | 10.52 | 65.80 | 0.16 | -0.51 | 0.09669 | 0.511391 | 11 | -24.33 | +0.55 | 2.16 | CPRM unpubl. |
| MI | KSB | CG | SC-01 | Leucogranite | 1937 | E, e.a. | 8.44 | 58.30 | 0.14 | -0.56 | 0.08750 | 0.511253 | 10 | -27.02 | +0.15 | 2.17 | mod. of Costa (2005) |
| MI | KSB | CG | MF-108 | Biotite gneiss | 1937 | E, e.a. | 13.36 | 76.16 | 0.18 | -0.46 | 0.10602 | 0.511513 | 21 | -21.95 | +0.61 | 2.17 | CPRM unpubl. |
| MI | KSB | CG | SC-180b | Amphibolite | 1937 | E, e.a. | 10.62 | 63.04 | 0.17 | -0.48 | 0.10190 | 0.511451 | 6 | -23.15 | +0.44 | 2.18 | mod. of Costa (2005) |
| MI | KSB | CG | SC-14c* | Hornblende gabbro-norite | 1937 | E, e.a. | 2.52 | 9.60 | 0.26 | -0.19 | 0.15880 | 0.512219 | 11 | -8.17 | +1.26 | 2.18 | mod. of Costa (2005) |
| MI | KSB | CG | SC-157 | Leucogranite | 1937 | E, e.a. | 10.99 | 56.49 | 0.19 | -0.40 | 0.11760 | 0.511642 | 9 | -19.43 | +0.25 | 2.23 | mod. of Costa (2005) |
| MI | KSB | CG | SC-40b | Biotite granite | 1937 | E, e.a. | 3.86 | 20.14 | 0.19 | -0.41 | 0.11580 | 0.511562 | 48 | -20.99 | -0.86 | 2.31 | mod. of Costa (2005) |
| MI | KSB | CG | SC-89 | Gneiss | 1937 | E, e.a. | 6.28 | 40.67 | 0.15 | -0.53 | 0.09340 | 0.511229 | 9 | -27.49 | -1.79 | 2.31 | mod. of Costa (2005) |
| <i>Caurane Group and rocks related</i> | | | | | | | | | | | | | | | | | |
| MI | TP | CG | SC-04 | Gneiss | 2074 | B, e.a. | 4.24 | 23.00 | 0.18 | -0.43 | 0.11140 | 0.511523 | 9 | -21.75 | +0.98 | 2.27 | mod. of Costa (2005) |
| MI | KSB | CG | SC-170a | Biotite gneiss | 2074 | B, e.a. | 2.86 | 14.23 | 0.20 | -0.38 | 0.12150 | 0.511674 | 9 | -18.80 | +1.23 | 2.27 | mod. of Costa (2005) |
| MI | KSB | CG | SC-37 | Gneiss | 2074 | B, e.a. | 8.53 | 47.39 | 0.18 | -0.45 | 0.10890 | 0.511457 | 6 | -23.04 | +0.35 | 2.32 | mod. of Costa (2005) |
| MI | TP | CG | SC-58 | Garnet gneiss | 2074 | B, e.a. | 4.69 | 27.87 | 0.17 | -0.48 | 0.10180 | 0.511285 | 7 | -26.39 | -1.12 | 2.41 | mod. of Costa (2005) |
| MI | TP | CG | SC-49 | Paragneiss | 2074 | B, e.a. | 6.07 | 34.83 | 0.17 | -0.46 | 0.10530 | 0.511305 | 6 | -26.00 | -1.66 | 2.46 | mod. of Costa (2005) |
| MI | KSB | CG | SC-61a | Garnet gneiss | 2074 | B, e.a. | 6.66 | 38.07 | 0.17 | -0.46 | 0.10570 | 0.511183 | 10 | -28.38 | -4.16 | 2.64 | mod. of Costa (2005) |

Nd T_{DM} ages are calculated using the model of DePaolo (1981) for Nd evolution of the depleted mantle.

*highly fractionated samples. showing $0.125 < ^{147}\text{Sm}/^{144}\text{Nd} < 0.09$ and $-0.60 < f(\text{Sm}/\text{Nd}) < -0.35$ (Sato and Siga Jr. 2002). has been recalculated based on Nd evolution by double-stage (Sato and Tassinari, 1997).

Geochronological Provinces: 1. Tassinari and Macambira (2004); 2. Santos *et al.* (2000); KSB. K' Mudku Shear Belt; VT-TP. Ventuari-Tapajós (or Tapajós-Parima); MI-T - Maroni-ItaPíúnas (or Transamazonic); CA. Central Amazonian. *Domains:* CG. Central Guyana; S. Surumu; T. Tapajós; C. Carajás; FG. French Guyana
Crystalization ages (References): e.a. estimated age; A. Avelar *et al.* (1999); B. CPRM (2003); C. Dall'Agnol *et al.* (1999); D. Delor *et al.* (2003); E. Fraga (2002); F. Lamarão *et al.* (2002); G. Leite *et al.* (2004); H. Macambira and Lancelot (1996); I. Pimentel and Machado (1994); J. Santos *et al.* (2000); K. Santos *et al.* (2002); L. Santos *et al.* (2003)

Table 4. Summary of geological characteristics of the UAD granitoids

| Units | Anauá Complex | Martins Pereira Granite | Serra Dourada Granite | Caroebe and Água Branca Granites | Igarapé Azul Granite |
|------------------------------------|---|---|--|--|---|
| <i>Age</i> | 2028 Ma | 1975-1971 Ma | 1962 Ma | 1901-1891 Ma | 1891-1889 Ma |
| <i>Inheritances</i> | - | 2042 Ma? | 2138 Ma | 1963 Ma; 2142 Ma | 1972-1964 Ma |
| <i>Composition</i> | Meta-tonalites and minor metagranites and meta-diorites | Granodiorites to monzogranites, locally tonalites | Monzogranites to syenogranites, rarely granodiorites | Diorites to monzogranites | (Leuco)granodiorites to (leuco)monzogranites, rarely quartz monzonites and syenogranites |
| <i>Trends</i> | Calc-alkaline Tonalitic-Trondjemitic? | Calc-alkaline Granodioritic (Chilean-type) | Granites of crustal origin field | Calc-alkaline Granodioritic (Peru to Sierra Nevada-types) | Granites of crustal origin field |
| <i>Outcrop style</i> | Basement inliers | Large batholith intruding Anauá Complex rocks | Discrete batholith in association with meta-volcanosedimentary rocks | Large batholith intruding older units | Discrete batholith and small bodies intruding older units |
| <i>Deformation</i> | Well-foliated to weakly foliated, locally with compositional layering | Range in deformational style from well-foliated to massive | Massive to weakly foliated | Massive to foliated (local shear zones) | Massive to foliated (local shear zones) |
| <i>Enclaves</i> | Meta-mafic to meta-ultramafic | Meta-diorites to meta-tonalites (predominate) and paragneiss (scarce) | Not observed | Mafic microgranular | Biotite-bearing tonalite to quartz diorite (surmicaceous); meta-granodiorite; paragneisses and biotite porphyritic diorite-tonalite |
| <i>Geochemical signature</i> | Metaluminous, TTG-like, I-type, calc-alkaline, medium-K, moderate negative Nb and negative to positive Sr-Ti anomalies; low LILE and LREE fractionated ($La_n/Yb_n = 3.6-8.0$); discrete positive Eu anomaly ($Eu_n/Eu^* = 0.78-1.15$) and low HREE ($< 5x$ chondrite) | Metaluminous to peraluminous, I-type, calc-alkaline, high-K, variable but high LILE and REE contents, moderate to pronounced negative P-Ti anomalies and fractionated LREE patterns ($La_n/Yb_n = 4.6-52.9$); negative Eu anomalies ($Eu_n/Eu^* = 0.38-0.74$) | Peraluminous, normal S-type, high-SiO ₂ , low-CaO, moderate to high negative Sr, Ti, Ba and Nb anomalies, moderate fractionated LREE pattern ($La_n/Yb_n = 23.4-28.2$) and moderate to pronounced negative Eu anomalies ($Eu_n/Eu^* = 0.29-0.47$) | Metaluminous, I-type, calc-alkaline, high-K, moderate to high CaO, negative Ti and Ta-Nb anomalies; moderate fractionated LREE pattern ($La_n/Yb_n = 8.6-29.3$); negative to low positive Eu anomalies ($Eu_n/Eu^* = 0.52-1.32$) | Metaluminous to peraluminous, I-type, calc-alkaline, high-K, high-SiO ₂ , moderate to low CaO, negative Sr, Ti, P and Ta-Nb anomalies, moderate to high fractionated LREE pattern ($La_n/Yb_n = 8.7-70.0$) and low to pronounced negative Eu anomalies ($Eu_n/Eu^* = 0.36-0.86$) |
| <i>Nd</i> | -2.21 to -0.19 | -4.74 to -0.92 | -4.34 to -3.19 | -2.05 to +0.46 (local -4.27 to -2.60) | -1.61 to -0.02 |
| <i>Nd T_{DM}</i> | 2.50-2.33 Ga | 2.64-2.33 Ga | 2.53-2.38 Ga | 2.29-2.17 Ga (local 2.47-2.32 Ga) | 2.28-2.14 Ga |
| <i>Pb initial</i> | - | 15.70-15.57 | - | 15.54 | 15.65-15.42 |
| <i>Magma sources</i> | Mantle-derived: generation of (depleted) mantle magma melts under high pressure in the garnet stability field (?) and pre-existing older crustal fragment as basement | Crustally-derived: generation of crustal melts by partial melting of amphibolitic, andesitic and/or tonalitic sources and local input of metavolcano-sedimentary older basement | Crustally-derived: generation of crustal melts by partial melting of metavolcano-sedimentary older basement under moderate pressures (cordierite stability field) | Crustally-derived: generation of crustal melts by partial melting of amphibolitic, andesitic and/or tonalitic (juvenile) sources | Multiple crustal sources: generation of crustal melts by partial melting of amphibolitic, andesitic and/or tonalitic (juvenile) sources; metavolcano-sedimentary basement and Martins Pereira older granitic intrusion (sialic) |
| <i>Tapajós Domain correlations</i> | Cuiú-Cuiú Complex | Creporizão Suite | Small leucogranite bodies in the Cuiú-Cuiú Complex? | Tropas and Parauari granitoids | ? |

5. CONCLUSÕES GERAIS

Os novos dados geológicos, petrográficos, geoquímicos, isotópicos e geocronológicos apresentados no decorrer deste trabalho, rediscutidos e integrados com os dados disponíveis na literatura, permitiram avanços do ponto de vista litoestratigráfico e petrológico acerca dos granitóides do setor centro-sul do Escudo das Guianas, particularmente do sudeste de Roraima. Apesar disso, este significativo acervo de dados é ainda insuficiente para delinear hipóteses por demais conclusivas. Mesmo porque algumas regiões vizinhas, entre elas estão, por exemplo, as áreas estaduais limítrofes entre Amazonas-Roraima e Roraima-Pará e a divisa Brasil-Guiana as quais constituem importantes peças neste quebra-cabeça geológico, carecem enormemente de informações geológicas básicas. A seguir serão listadas as principais conclusões a partir dos resultados obtidos nos granitóides dos domínios tectono-estratigráficos Guiana Central e Uatumã-Anauá, com ênfase neste último.

5.1. DOMÍNIO GÜIANA CENTRAL

- a) O Domínio Guiana Central, junto ao limite (materializado pelo sistema de falha do Itã) do Domínio Uatumã-Anauá, apresenta dois grupos distintos de rochas ortometamórficas. O primeiro é constituído por ortognaisses granulíticos (1942 ± 7 Ma) polideformados e metamorfizados em alto grau, sendo correlacionáveis aos charnoquitóides sintectônicos da Suíte Serra da Prata (1943-1933 Ma). Estes destoam dos milonitos (1889 ± 4 Ma) e granitos foliados (1724 ± 14 Ma) os quais, além de serem mais jovens, exibem apenas uma fase de deformação normalmente associada a amplas zonas de cisalhamento NE-SW, em baixo a médio grau (preservando muitas vezes suas características ígneas como por exemplo fluxo magmático). Milonitos e meta-granitóides mais antigos (1938-1932 Ma) também são descritos em outros setores do Domínio Guiana Central, sendo agrupados na Suíte Metamórfica (ou Complexo) Rio Urubu;
- b) A idade de 1724 ± 14 Ma obtida em granitóide sintectônico (associada a idades Ar-Ar de outros autores) confirma ainda a possibilidade da existência de um episódio tectonicamente ativo entre 1,94-1,93 Ga e 1,20 Ga. Além disso, granitóides com características petrográficas e idade (1889 ± 4 Ma) similares ao do Granito Caroebe, indica que estes intrudem o embasamento do Domínio Guiana Central;

- c) Estes dados materializam uma ampla variedade de protólitos ígneos que, aliada às diferentes e complexas relações metamórfico-estruturais, dificultam o empilhamento estratigráfico das unidades do Domínio Guiana Central. Sugere-se a red denominação da Suíte Metamórfica Rio Urubu para Complexo, de modo a agrupar numa mesma unidade tal diversidade de litótipos (ígneos e metamórficos), de padrões estruturais (polifásico vs. monofásico) e de grau metamórfico (baixo a alto grau).

5.2. DOMÍNIO UATUMÃ-ANAUÁ

5.2.1. Setor Norte

- a) Além do conjunto representado pela associação TTG Anauá e pelas seqüências metavulcanossedimentares do tipo Cauarane, pouco investigado neste trabalho e que materializa muito provavelmente um sistema de arco, o setor norte do Domínio Uatumã-Anauá apresenta os (meta)granitos Martins Pereira e Serra Dourada como as unidades ígneas de maior abrangência territorial. A única mineralização de ouro explorada comercialmente está hospedada nestes granitóides (garimpo Anauá);
- b) O Granito Martins Pereira constitui uma massa batolítica composta por monzogranitos, granodioritos e raramente por tonalitos (*trend* cálcio-alcálico granodiorítico, similar aos tipos chilenos), com textura em geral porfirítica e normalmente afetados por deformação heterogênea penetrativa de escala regional, associada às zonas de cisalhamento destrais de direção ENE-WSW. Quimicamente são rochas cálcio-alcálicas, metaluminosas a peraluminosas e de alto-K, exibindo enriquecimento em LILE (K, U e Th, por exemplo) e ETR;
- c) A utilização de diagramas de variação (lineares), de petrologia experimental, aliado aos dados isotópicos do Nd e Pb, sugerem para o Granito Martins Pereira uma origem a partir da fusão parcial de fontes crustais anfibolíticas e/ou tonalíticas (ϵ_{Nd} -0,92 a -1,55, T_{DM} 2,38-2,33 Ga) com localizada contribuição de metagrauvacas (ϵ_{Nd} -2,37 a -4,74, T_{DM} 2,64-2,43 Ga) e idades supostamente arqueanas (e/ou siderianas?) a riacianas (transamazônicas), gerando idades-modelo T_{DM} mistas. Xenólitos de rochas anfibolíticas e paragnáissicas, apesar de raros, podem ser encontrados no Granito Martins Pereira. Datações em zircão (evaporação de Pb) indicam também um intervalo de cristalização curto e restrito entre 1975 e 1971 Ma para este magmatismo;

- d) O Granito Serra Dourada constitui um batólito de menor expressão e é composto essencialmente por monzogranitos e sienogranitos à muscovita, cordierita e sillimanita. Ocupam o campo dos granitos de fusão crustal no diagrama QAP e apresentam quimismo peraluminoso similar aos granitos tipo S normais. Embora em menor grau, também se mostram afetados por deformação heterogênea penetrativa de escala regional;
- e) Dados petrográficos (mineralogia aluminosa), geoquímicos (caráter peraluminoso) e isotópicos (ϵ_{Nd} -3,19 a -4,34, T_{DM} 2,53-2,38 Ga) obtidos no Granito Serra Dourada sugerem fortemente uma origem a partir da fusão parcial de metagrauvacas, também indicando proveniência de fontes com idades supostamente arqueanas (e/ou siderianas?). Muito embora as idades ao redor de 2,38 Ga possam ser provocadas por local contribuição de fontes riacianas (transamazônica), produzindo ao menos localmente idades-modelo T_{DM} mistas (vide Granito Martins Pereira). Datações em zircão (evaporação de Pb) do Serra Dourada indicam cristalização ao redor de 1962 ± 6 Ma, em acordo com dados obtidos em zircão por U-Pb SHRIMP (1969 ± 4 Ma) em outro granito tipo S existente no Domínio Güiana Central, sendo, portanto, ligeiramente mais jovens que os granitóides tipo I, cálcio-alcálicos de alto-K Martins Pereira;
- f) Lentes e bolsões de leucogranitos ocorrem subconcordantes aos planos de foliação dos metagranitóides Martins Pereira, podendo ser resultado da fusão parcial deste último durante evento gerador dos granitóides da porção sul em torno de 1900 Ma (vide discussão abaixo). A idade de cristalização obtida em zircão pelo método de evaporação de Pb é de 1906 ± 4 Ma e pelo menos quatro conjuntos de idades herdadas foram também detectadas: i) 1959 ± 5 Ma (Granito Martins Pereira?); ii) 1997 ± 8 Ma (Arco Anauá?); iii) 2134 ± 15 Ma (crosta Transamazônica) e iv) 2354 ± 6 Ma (Crosta Amazônia Central);
- g) Os dados disponíveis para o conjunto petrotectônico do setor norte do Domínio Uatumã-Anauá permite a elaboração preliminar de uma proposta evolutiva baseada inicialmente num modelo acrescionário em 2,03 Ga (sistema de arco magmático Anauá e bacias associadas) com subsequente colisão entre blocos crustais (orógeno colisional). Esta colisão teve início entre 1,97-1,96 (granitóides Martins Pereira e Serra Dourada) e evoluiu ao longo tempo, culminando mais a norte com a geração dos granulitos e ortognaisses do cinturão Güiana Central entre 1,94-1,93 Ga. Eventos tectono-metamórficos recorrentes

podem ter afetado este bloco (agora amalgamado) ao longo do Proterozóico (p.ex. ~1,72 Ga e ~1,20 Ga) ;

- h) Modelo evolutivo similar envolvendo a geração de um arco primitivo em torno de 2,00 Ga (arco Cuiú-Cuiú) é adotado igualmente no domínio Tapajós (parte sul do Cráton Amazônico, Escudo Brasil Central), embora alguns autores (e.g. Santos *et al.*, 2004) admitam ainda um segundo arco (continental) ao redor de 1,96 Ga (arco Creporizão). Apesar disso, o estágio acrescionário parece não ter evoluído para um estágio colisional de modo significativo na região supracitada, em função da ocorrência restrita de granitos tipo S e ausência de rochas granulíticas.

5.2.2. Setor Sul

- a) A porção sul, ao contrário da porção norte, não registra efeitos deformacionais significativos, exceto por zonas de cisalhamento destrais muito localizadas (p.ex. Sistema de Falhas do Jauaperi). As principais anisotropias dizem respeito às estruturas de fluxo magmático representadas por enclaves e megacristais preferencialmente alinhados, observados na maioria dos corpos graníticos. Dominam neste setor os granitos Caroebe e Igarapé Azul, além de rochas vulcânicas co-genéticas (Jatapu), charnoquitóides (Santa Maria e Igarapé Tamandaré) e granitos tipo A (Moderna e Mapuera). As duas ocorrências minerais mais importantes deste setor estão assentadas (columbita-tantalita em aluvião) ou hospedadas (pegmatitos com ametista), respectivamente, nos granitóides Igarapé Azul e Moderna;
- b) O Granito Igarapé Azul está dividido em três fácies principais (Vila Catarina, Saramandaia e Cinco Estrelas) e é composto essencialmente por monzogranitos com baixo conteúdo de minerais máficos que se encontram em geral hidrotermalizados. Estes granitóides ocupam no diagrama QAP o campo dos granitos crustais e quimicamente são rochas cálcio-alcálicas com alto-K, ricas em SiO₂ e ligeiramente peraluminosas, exibindo enriquecimento em LILE e padrões variados de ETR. São caracterizados ainda por uma ampla gama de enclaves: 1) ricos em biotita (surmicáceos); 2) meta-granítico (Martins Pereira); 3) paragnaisses (tipo Cauarane); 4) microgranulares tonalítico-granodioríticos.;
- c) O Granito Caroebe apresenta volume de máficos superior (8-48%) e aspecto mosqueado que o distingue do Granito Igarapé Azul. Além disso, duas fácies distintas foram cartografadas tendo como base a presença de biotita acompanhada (fácies Jaburuzinho) ou

não (fácies Alto Alegre) por hornblenda. A primeira fácies é caracterizada por um aspecto mosqueado mais acentuado, em geral com textura equigranular, e tipos que variam de quartzo dioritos a monzogranitos. A segunda apresenta tipos monzograníticos a granodioríticos em geral porfíricos, com caráter geoquímico similar ao dos granitóides Igarapé Azul, muito embora não apresentem efeitos hidrotermais significativos. Em termos geoquímicos o Granito Caroebe apresenta envelope composicional mais amplo de ETR e elementos traços, mostrando conteúdos mais baixos de Rb e K e localmente elevados de Ba, Th, U (LILE) e Nd, P, Hf, Zr e Sm (HSFE);

- d) As idades de zircão pelo método de evaporação de Pb apontam idade de cristalização entre 1891-1889 Ma para os granitóides Igarapé Azul e heranças entre 1972-1964 Ma, estas últimas muito próximas das idades de cristalização obtidas nos granitóides Martins Pereira. Idade de cristalização (1891 ± 2 Ma) e heranças (1963 ± 4 Ma) similares são observadas também na fácies Alto Alegre do Granito Caroebe. O Enderbitto Santo Maria (1891 ± 1 Ma) e as vulcânicas dacíticas e andesíticas Jatapu (1893 ± 5 Ma, herança de 1966 ± 3 Ma) demonstram fazer parte desse mesmo evento magmático. A fácies Jaburuzinho (1895 ± 2 Ma) e o Granito Água Branca (1901 ± 5 Ma) em sua área tipo apontam idades de cristalização ligeiramente mais antigas e, apesar de heranças em torno de 1,97 Ga não terem sido observadas, resquícios transamazônicos foram registrados localmente (2142 ± 10 Ma). O Granito Murauá, provável representante do magmatismo Mapuera (tipo A) na região, apresenta idade mais jovens (1871 ± 5 Ma) e duas populações herdadas (1888 ± 3 Ma e 2359 ± 7 Ma);
- e) Os diagramas geoquímicos de variação e de petrologia experimental, em conjunto com o conteúdo isotópico do Nd e Pb, indicam que os granitos Igarapé Azul, Caroebe e Água Branca podem ter uma origem comum a partir da fusão parcial de fontes crustais anfibolíticas e/ou tonalíticas-andesíticas com progressiva e variável contribuição de fontes metassedimentares (grauvacas) e talvez das próprias rochas encaixantes (Martins Pereira). A contribuição de fontes crustais predominantemente transamazônicas são mais evidentes no Granito Igarapé Azul (ϵ_{Nd} -0,02 a -1,61, T_{DM} 2,28-2,14 Ga), nas fácies Alto Alegre (ϵ_{Nd} -0,68 a -2,24, T_{DM} 2,26-2,17 Ga) e Jaburuzinho (ϵ_{Nd} +0,46 a -2,69, T_{DM} 2,32-2,16 Ga), além das rochas vulcânicas Jatapu (ϵ_{Nd} -0,70 a -1,76, T_{DM} 2,28-2,21 Ga), embora localmente, incluindo a área-tipo do Granito Água Branca, ocorram idades siderianas (ϵ_{Nd}

-2,60 a -4,27, T_{DM} 2,47-2,37 Ga), indicando a presença subordinada de fontes mais antigas;

- f) Associação granítica cálcio-alcálica similar e contemporânea existente no domínio Tapajós tem sido interpretada por alguns autores como originada em ambiente de margem ativa, controlado por subducção, muitas vezes desenvolvidos em vários estágios, representados pelos arcos Tropas (1,90 Ga) e Parauari (1,88 Ga). Entretanto, no setor sul do DUA, além da ausência de sucessões meta-vulcanossedimentares e/ou remanescentes de crosta oceânica (sequência ofiolítica?) contemporâneas à geração de um provável arco magmático em 1,90 Ga e a falta de indícios de metamorfismo e deformação, dificulta a vinculação dos granitóides cálcio-alcálicos do sul do DUA a um ambiente de subducção clássica (tipo-B). Nesse sentido, a assinatura geoquímica dos granitóides estaria muito mais vinculada às características das fontes do que propriamente ao ambiente geotectônico;
- g) Portanto a proposta evolutiva aqui apresentada tem como base a ascensão local da astenosfera (*slab break-off* e delaminação ou atuação de plumas mantélicas?) produzindo magmas basálticos que estacionariam na base da crosta inferior, provocando a fusão desta e gerando um amplo volume de magmas. Estes últimos ao interagir com o restante da crosta dariam origem a uma diversidade de tipos graníticos (em diferentes condições de pressão de H_2O) entre 1,90 (granitos tipo I) e 1,87 Ga (granitos tipo A). Este modelo pós-colisional, baseado num mecanismo controlado por *underplating*, também é proposto no domínio Tapajós como alternativa a origem acrescionária descrita anteriormente.

Apesar dos dados apresentados contribuírem com o aumento do acervo referente à porção central do Escudo das Guianas, evidentemente as conclusões expostas aqui não têm a pretensão do caráter definitivo. Muito pelo contrário, reconhece-se a necessidade de investigação mais aprofundada, sobretudo do ponto de vista geoquímico-isotópico visando apoiar estudos petrológicos e evolutivos, associados a estudos metamórfico-estruturais.

Além disso, a ausência de mapeamento geológico sistemático nas áreas vizinhas (p.ex. fronteira Brasil-Guiana, limites estaduais Amazonas-Pará-Roraima) dificulta enormemente uma correlação em escala regional, impedindo um melhor entendimento e extrapolação do modelo proposto (p.ex. dinâmica e geometria) e sua conexão com o modelo de Províncias Geocronológicas (Província Ventuari-Tapajós ou Tapajós-Parima).

REFERÊNCIAS

- ALMEIDA, M.E. & MACAMBIRA, M.J.B. 2003. Aspectos geológicos e litoquímicos dos granitóides cálcio-alcálicos Paleoproterozóicos do sudeste de Roraima. *In: CONGRESSO BRASILEIRO DE GEOQUÍMICA, 9, Anais...*, SBGq, p. 775-778.
- ALMEIDA, M.E.; FRAGA, L.M.B.; MACAMBIRA, M.J.B. 1997. New geochronological data of calc-alkaline granitoids of Roraima State, Brazil. *In: SOUTH-AMERICAN SYMPOSIUM ON ISOTOPE GEOLOGY, 1, Extended Abstract, IG/USP, p.34-37.*
- ALMEIDA, M.E.; MACAMBIRA M.J.B., FARIA M.S.G. de. 2002. A Granitogênese Paleoproterozóica do Sul de Roraima. *In: CONGRESSO BRASILEIRO DE GEOLOGIA, 41, Anais...*, SBG, p 434.
- ARANTES, J.L.; MANDETTA. P. 1970. *Relatório preliminar de viagem de reconhecimento geológico dos rios Auaris, Parima, Aracaçá e Urariquera*. Rio de Janeiro, DNPM, Relatório 55. 34p.
- ARAÚJO NETO, H.; MOREIRA, H.L. 1976. *Projeto Estanho do Abonari*. Manaus, Convênio DNPM/CPRM, Relatório Final. 2v.
- BARTLETT, J.M.; DOUGHERTY-PAGE, J.S.; HARRIS, N.B.W.; HAWKESWORTH, C.J.; SANTOSH, M. 1998. The application of single zircon evaporation and model Nd ages to the interpretation of polymetamorphic terrains: an example from the Proterozoic mobile belt of south India. *Contributions to Mineralogy and Petrology*, **131**: 181-195.
- BONFIM, L.F.C.; RAMGRAB, G.E.; UCHÔA, I.B.; MEDEIROS, J.B. DE; VIÉGAS FILHO, J. DE R.; MANDETTA, P.; KUYUMJIAN, R.M., PINHEIRO, S. DA S. 1974. *Projeto Roraima*. Manaus, DNPM/CPRM, Relatório Final, vol. IA-D e II.
- BRAUN, O.P.G. 1973. *Projeto Roraima, 2ª Fase; Levantamento geológico integrado: Relatório de mapeamento preliminar ao milionésimo, correspondente à "Fotointerpretação Preliminar"*. Manaus, DNPM/CPRM, 218p., il.
- BROWN, M., 2001. From microscope to mountain belt: 150 years of petrology and its contribution to understanding geodynamics, particularly the tectonics of orogens: *Journal of Geodynamics*, **32** : 115–164.
- BROWN, M. & DALLMEYER, R.D. 1996. Rapid Variscan exhumation and role of magma in core complex formation: Southern Brittany metamorphic belt, France. *Journal of Metamorphic Geology*, **14** : 361–379.

- CORDANI, U.G. & BRITO NEVES, B.B. 1982. The Geologic Evolution of South America During the Archean and Early Proterozoic. *Revista Brasileira de Geociências*, **12** (1-3) : 78-88.
- COSTI, H.T., DALL'AGNOL, R., MOURA, C.A.V. 2000. Geology and Pb-Pb geochronology of Paleoproterozoic volcanic and granitic rocks of the Pitinga Province, Amazonian craton, northern Brazil. *International Geology Review*, **42** : 832-849.
- COSTI, H.T., SANTIAGO, A.F., PINHEIRO, S. DA S. 1984. *Projeto Uatumã-Jatapu*. Manaus, CPRM, Relatório Final. 133p.
- CPRM. 1999. *Programa Levantamentos Geológicos Básicos do Brasil. Roraima Central, Folhas NA.20-X-B e NA.20-X-D (integrais), NA.20-X-A, NA.20-X-C, NA.21-V-A e NA.21-V-C (parciais). Escala 1:500.000. Estado de Roraima*. Manaus, CPRM, 166 p. (em CD-ROM).
- CPRM. 2000a. *Programa Levantamentos Geológicos Básicos do Brasil. Caracará, Folhas NA.20-Z-B e NA.20-Z-D (integrais), NA.20-Z-A, NA.21-Y-A, NA.20-Z-C e NA.21-Y-C (parciais). Escala 1:500.000. Estado de Roraima*. Manaus, CPRM, 157 p. (em CD-ROM).
- CPRM. 2000b. *Programa Levantamentos Geológicos Básicos do Brasil. Província Mineral do Tapajós, Folha SB.21-V-D (Vila Mamãe Anã). Escala 1:250.000. Estados do Amazonas e Pará*. Manaus, CPRM, 157 p. (em CD-ROM).
- CPRM. 2003. *Programa Levantamentos Geológicos Básicos do Brasil. Geologia, Tectônica e Recursos Minerais do Brasil: sistema de informações geográficas - SIG*. Rio de Janeiro, CPRM, Mapas. Escala 1:2.500.000. (em 4 CDs-ROM)
- CPRM. 2004. *Programa Levantamentos Geológicos Básicos do Brasil. Escala 1:1000.000. Mapa Geológico do Brasil - 41 mapas*. Brasília, CPRM-MME. (em CD-ROM).
- CPRM. 2006. *Programa Integração, Atualização e Difusão de Dados da Geologia do Brasil: Subprograma Mapas Geológicos Estaduais. Geologia e Recursos Minerais do Estado do Amazonas*. Manaus, CPRM/CIAM-AM, 2006. Escala 1:1.000.000. Texto explicativo, 148p. (em CD-ROM).
- ELLIS, D.J. 1987. Origin and evolution of granulites in normal and thickened crusts: *Geology*, **15** : 167-170.
- FARIA M.S.G.DE, LUZARDO R., PINHEIRO S. DA S. 1999. Litoquímica e petrogênese do Granito Igarapé Azul. In: SIMPÓSIO DE GEOLOGIA DA AMAZÔNIA, 6, *Anais...*, SBG, p. 577-580.

- FRAGA, L.M.B. 2002. *A Associação Anortosito–Mangerito–Granito Rapakivi (AMG) do Cinturão Güiana Central, Roraima e Suas Encaixantes Paleoproterozóicas: Evolução Estrutural, Geocronologia e Petrologia*. Belém, Universidade Federal do Pará, Centro de Geociências, Pós-Graduação em Geoquímica e Petrologia. 386p. (Tese de Doutorado)
- GAUDETTE, H.E.; OLSZEWSKI, W.J. JR.; SANTOS, J.O.S. DOS. 1996. Geochronology of Precambrian rocks from the northern part of Güiana Shield, State of Roraima, Brazil. *Journal of South American Earth Sciences*, **9**: 183-195.
- GAUDETTE, H.E.; LAFON, J.M.; MACAMBIRA, M.J.B.; MOURA, C.A.V; SCHELLER, T. 1998. Comparison of single-filament Pb evaporation/ionization zircon ages with conventional U-Pb results: examples from the Precambrian of Brazil. *Journal of South American Earth Sciences*, **11**: 351-363.
- GIBBS, A.K. & BARRON, C.N. 1993. *The geology of the Guyana Shield*. Oxford University Press, Oxford, N. York, 245 p.
- HASUI, Y.; HARALYI., N.L.E.; SCHOBENHAUS F°, C. 1984. Elementos geofísicos e geológicos da região amazônica: subsídios para o modelo geotectônico. In: SYMPOSIUM AMAZONICO, 2, Manaus. *Anais...*, SBG, v. 1, pp. 129-148.
- HOUSH, T. & BOWRING, S.A. 1991. Lead isotopic heterogeneities within alkali feldspars: implications for the determination of initial lead isotopic compositions. *Geochimica et Cosmochimica Acta*, **55** : 2309-2316.
- KOBER, B. 1986. Whole grain evaporation for $^{207}\text{Pb}/^{206}\text{Pb}$ age investigations on single zircons using a double filament source. *Contributions to Mineralogy and Petrology*, **93** : 82-490.
- KOBER, B. 1987. Single-grain evaporation combined with Pb+ emitter bedding for $^{207}\text{Pb}/^{206}\text{Pb}$ investigations using thermal ion mass spectrometry, and implications for zirconology. *Contributions to Mineralogy and Petrology*, **96** : 63-71.
- KROGH, T.E. 1973. A low contamination method for hydrothermal decomposition of zircons and extraction of U and Pb for isotopic age determinations. *Geochimica et Cosmochimica Acta*, **37**: 485-494.
- KRYMSKY, R. 2002. *Metodologia de análise de U-Pb em mono zircão com traçador ^{235}U - ^{205}Pb* . Belém, Universidade Federal do Pará, Laboratório de Geologia Isotópica. 7p.
- LAMARÃO, C.N.; DALL'AGNOL, R.; LAFON, J.-M.; LIMA, E.F. 2002. Geology, geochemistry and Pb–Pb zircon geochronology of the Paleoproterozoic magmatism of Vila

- Riozinho, Tapajós gold province, Amazonian craton, Brazil. *Precambrian Research*, **119** (1-4) : 189–223.
- LUDWIG, K.R. 1993. PBDAT. *A computer program for processing Pb-U-Th isotope data*. Version 1.24. USGS Open File Report, 88-542. 34 p.
- LUDWIG, K.R. 2001. *User' s manual for Isoplot / ExVersion 2.49. A geochronological toolkit for Microsoft Excel*. Berkeley Geochronology Center, Berkeley, CA, USA, 59 p. (Spec. Pub., 1a).
- LUDWIG, K.R. & SILVER, L.T. 1977. Lead-isotope inhomogeneity in Precambrian igneous K-feldspars. *Geochimica et Cosmochimica Acta*, **41**(10) : 1457-1471.
- MACAMBIRA, M.J.B. & SCHELLER, T. 1994. Estudo comparativo entre métodos geocronológicos aplicados em zircões: o caso do Granodiorito Rio Maria. In: SIMPÓSIO DE GEOLOGIA DA AMAZÔNIA, 4, Belém, *Boletim de Resumos Expandidos...*, SBG, p. 343-346.
- MACAMBIRA, M.J.B.; ALMEIDA, M.E.; SANTOS, L.S. 2002. Idade de Zircão das Vulcânicas Iricoumé do Sudeste de Roraima: contribuição para a redefinição do Supergrupo Uatumã. In: SIMPÓSIO SOBRE VULCANISMO E AMBIENTES ASSOCIADOS, 2, *Anais...*, SBG, p. 22.
- MELO, A.F.F. DE; SANTOS, A.J.; CUNHA, M.T.P.; CAMPOS, M.J., D'ANTONA, R.J. DE G. 1978. *Projeto Molibdênio em Roraima*. Relatório Final. Manaus. DNPM/CPRM, v. 1A-B.
- MONTALVÃO, R.G.M.; MUNIZ, C.M.; ISSLER, R.S.; DALL'AGNOL, R.; LIMA, M.I.C.; FERNANDES, P.E.C.A.; SILVA, G.G. 1975. *Folha NA.20-Boa Vista e parte das folhas NA.21-Tumucumaque, NB.20-Roraima e NB.21; Geologia* Projeto RADAMBRASIL, Rio de Janeiro, MME, DNPM. (Levantamento de Recursos Minerais, 8).
- MUNIZ, C.M. & DALL'AGNOL, R. 1974. Geologia do território brasileiro nas folhas Boa Vista (NA.200, Roraima (NB.20/21) e parte da folha Tumucumaque (NA.21). In: CONGRESSO BRASILEIRO DE GEOLOGIA, 28, Porto Alegre, *Anais...*, SBG, v.4. p.247-267.
- OLIVEIRA, E.C. 2002. *Implantação do método sm-nd em minerais metamórficos e sua aplicação em rochas da região central do Amapá, sudeste do Escudo das Guianas*. Belém, Universidade Federal do Pará, Centro de Geociências, Pós-Graduação em Geoquímica e Petrologia. 100p. (Dissertação de Mestrado)

- OLIVEIRA, M.J.R.; ALMEIDA, M.E.; LUZARDO, R.; FARIA, M.S.G. DE. 1996. Litogeoquímica da Suíte Intrusiva Água Branca - SE de Roraima. *In: CONGRESSO BRASILEIRO DE GEOLOGIA*, 39, Salvador, *Anais...*, SBG, v.2, p. 213-216.
- PAIVA, G. 1929. *Valle do Rio Negro: physiografia e geologia*. Rio de Janeiro, SGM, 40, 62p.
- PARRISH, R.R. 1987. An improved micro-capsule for zircon dissolution in U-Pb geochronology. *Chemical Geology*, **66**: 99-102.
- PINHEIRO, S. DA S.; NUNES, A.C.B.; COSTI, H.; YAMAGUTY, H.S.; FARACO, M.T.L.; REIS, N.J.; MENEZES, R.G. DE; RIKER, S.R.L.; WILDNER, W. 1981. *Projeto Catrimã ni-Uraricoera*. Relatório de Progresso. Manaus, DNPM/CPRM, Vol.II-B.
- PINHEIRO, S. DA S.; REIS, N.J.; COSTI, H.T. 1990. *Projeto Caburai*. Relatório Final. Manaus, DNPM/CPRM, 91p.
- RAMGRAB, G.E. & DAMIÃO, R.N. 1970. *Reconhecimento geológico dos rios Anauá e Barauana*, Relatório Inédito. Boa Vista, DNPM, 40 p.
- RAMGRAB, G.E.; BOMFIM, L.F.C., MANDETTA, P. 1972. *Projeto Roraima. 2a. Fase*. Relatório Final. Manaus, DNPM/CPRM, 38 p.
- REIS, N.R. & FRAGA, L.M.B. 1996. Vulcanismo Surumu - Estado de Roraima: Caracterização de seu comportamento químico à luz de novos dados. *In: CONGRESSO BRASILEIRO DE GEOLOGIA*, 39, Salvador, *Anais...*, SBG, v. 2, p. 88- 90.
- REIS, N.J.; FRAGA, L.M.; FARIA, M.S.G. DE; ALMEIDA, M.E. 2003. Geologia do Estado de Roraima. *Géologie de la France*, **2-3**: 71-84.
- SANTOS, J.O.S. DOS; MOREIRA, A.S.; PESSOA, M.R.; OLIVEIRA, J.R. DE; MALOUF, R.F.; VEIGA JR., J.P.; NASCIMENTO, J.O. DO. 1974. *Projeto Norte da Amazônia, Domínio Baixo Rio Negro; Geologia da Folha NA.20-Z*. Relatório Final, Manaus, DNPM/CPRM, v.III A.
- Santos J.O.S. dos, Silva L.C., Faria M.S.G. de, Macambira, M.J.B. 1997. Pb-Pb single crystal, evaporation isotopic study on the post-tectonic, sub-alkalic, A-type Moderna granite, Mapuera intrusive suite, State of Roraima, northern Brazil. *In: SYMPOSIUM OF GRANITES AND ASSOCIATED MINERALIZATIONS*, 2, Salvador, *Extended Abstract...*, SBG, p.273-275.
- SANTOS, J.O.S. DOS; HARTMANN, L.A.; GAUDETTE, H.E.; GROVES, D.I.; MCNAUGHTON, N.J.; FLETCHER, I.R. 2000. A new understanding of the provinces of the

- Amazon Craton based on integration of field mapping and U-Pb and Sm-Nd geochronology. *Gondwana Research*, **3** (4) : 453-488.
- SANTOS, J.O.S. DOS, VAN BREEMEN, O.B., GROVES, D.I., HARTMANN, L. A., ALMEIDA, M.E., MCNAUGHTON, N.J., FLETCHER, I.R. 2004. Timing and evolution of multiple Paleoproterozoic magmatic arcs in the Tapajós Domain, Amazon Craton: constraints from SHRIMP and TIMS zircon, baddeleyite and titanite U–Pb geochronology. *Precamb. Res.*, **131** (10) : 73-109.
- SANTOS, J.O.S. DOS; HARTMANN, L.A.; FARIA, M.S.G. DE; RIKER, S.R.L.; SOUZA, M.M. DE; ALMEIDA, M.E.; MCNAUGHTON, N.J. 2006a. A Compartimentação do Cráton Amazonas em Províncias: Avanços ocorridos no período 2000-2006. In: SIMPÓSIO DE GEOLOGIA DA AMAZÔNIA, 9, Belém, *Anais...*, SBG. (em CD-ROM).
- SANTOS, J.O.S. DOS; FARIA, M.S.G. DE; RIKER, S.R.L.; SOUZA, M.M. DE; HARTMANN, L.A.; ALMEIDA, M.E., MCNAUGHTON, N.J.; FLETCHER, I.R. 2006b. A faixa colisional K'Mudku (idade Grenvilliana) no norte do Cráton Amazonas: reflexo intracontinental do Orógeno Sunsás na margem ocidental do cráton. In: SIMPÓSIO DE GEOLOGIA DA AMAZÔNIA, 9, Belém, *Anais...*, SBG. (em CD-ROM).
- SARDINHA, A.S. 1999. *Petrografia do Granito Igarapé Azul, Sudeste do Estado de Roraima*. Belém, Centro de Geociências, Universidade Federal do Pará, 32p. (Trabalho de Conclusão de Curso)
- SATO, K. & TASSINARI, C.C.G. 1997. Principais eventos de acreção continental no Cráton Amazônico baseados em idade-modelo Sm–Nd, calculada em evoluções de estágio único e estágio duplo. In: COSTA, M.L.C. & ANGÉLICA, R.S. (Coord.), *Contribuições à Geologia da Amazônia*. Belém, FINEP/SBGNO, p. 91–142.
- SENA COSTA, J.B. & HASUI, Y. 1997. Evolução Geológica da Amazônia. In: COSTA, M.L.C. & ANGÉLICA, R.S. (Coord.), *Contribuições à Geologia da Amazônia* Belém, FINEP/SBGNO, p. 15-90.
- SÖDERLUND, U. 1996. Conventional U-Pb dating vs. single-zircon Pb evaporation dating of complex zircons from a pegmatite in the high-grade gneisses of southwestern Sweden. *Lithos*, **38** : 93-105.
- STACEY, J.S. & KRAMERS, J.D. 1975. Approximation of terrestrial lead isotope evolution by a two-stage model. *Earth and Planetary Science Letters*, **26** : 207-221.

- STEIGER, R.H. & JAGER, J. 1977. Convention of the use of decay constants in geo- and cosmochronology. *Earth and Planetary Science Letters*, **36** : 359-362.
- TASSINARI, C.C.G. & MACAMBIRA M.J.B. 1999. Geochronological Provinces of the Amazonian Craton. *Episodes*, **22** (3) : 174-182.
- TASSINARI, C.C.G. & MACAMBIRA M.J.B. 2004. A Evolução Tectônica do Cráton Amazônico. In: MANTESSO-NETO, V., BARTORELI, A., CARNEIRO, C.D.R. BRITONEVES, B.B. de (Coord.), *Geologia do Continente Sul-Americano - Evolução da Obra de Fernando Flávio Marques de Almeida*, São Paulo, Ed. Beca, p. 471-485.
- VALÉRIO, C.S. 2006. *Magmatismo Paleoproterozóico do extremo sul do Escudo das Guianas, município de Presidente Figueiredo (AM): geologia, geoquímica e geocronologia Pb-Pb em zircão*. Manaus, Universidade Federal do Amazonas, Programa de Pós-Graduação em Geociências. (Dissertação de Mestrado)
- VANDERHAEGHE, O.; LEDRU, D.; THIÉBLEMONT, D.; EGAL, E.; COCHERIE, A.; TEGYEY, M.; MILÉSI, J.P. 1998. Contrasting mechanisms of crustal growth. Geodynamic evolution of the Paleoproterozoic granite-greenstone belts of French Guiana. *Precambrian Research*, **92**, 165-193.
- VASQUEZ, M.V.; RICCI, P.S.F.; KLEIN, E.L. 2002. Granitóides pós-colisionais da porção leste da Província Tapajós. In: KLEIN, E.L., VASQUEZ, M.L., ROSA-COSTA, L.T. (Coord.), *Contribuições à Geologia da Amazônia* vol. 3, Belém, SBG-NO, p. 63-83.
- VEIGA JR., J.P.; NUNES, A.C.B.; SOUZA, E.C. DE; SANTOS, J.O.S. DOS; AMARAL, J.E.; PESSOA, M.R.; SOUZA, S.A. DE S. 1979. *Projeto Sulfetos do Uatumã*. Relatório Final, Manaus, DNPM/CPRM, 6 v.

ANEXO 1

Mapa de Estações Geológicas

ANEXO 2
Mapa Geológico